UNDERSTANDING THE ROLE OF N-METHYLOLACRYLAMIDE (NMA) DISTRIBUTION IN POLY(VINYL ACETATE) LATEX ADHESIVES

by

Nicole Robitaille Brown

A Dissertation submitted to the Faculty of
Virginia Polytechnic Institute and State University
in partial fulfillment of the requirements for the degree of

Doctor of Philosophy

in

Wood Science and Forest Products

Approved by:

Dr. Charles E. Frazier
(Co-Chair)

Dr. Joseph R. Loferski
(Co-Chair)

Dr. Frederick A. Kamke

Dr. Harry W. Gibson

Dr. John G. Dillard

December 11, 2003
Blacksburg, Virginia

Keywords: N-methylolacrylamide, NMA, poly(vinyl acetate), PVAc, wood adhesives, ^{13}C-NMA, ^{15}N-NMA, ^{13}C ^{15}N-NMA, fracture mechanics, durability, monomer distribution, emulsion polymerization, solution NMR

N-METHYLOLACRYLAMIDE (NMA) DISTRIBUTION AND PERFORMANCE IN POLY(VINYL ACETATE) LATEX ADHESIVES

N.R. Brown

C.E. Frazier, Co-chair

J.R. Loferski, Co-chair

Wood Science and Forest Products

ABSTRACT

This work addresses the distribution of N-methylolacrylamide (NMA) units in crosslinking poly(vinyl acetate) (PVAc) adhesives. In this case, distribution refers to the three potential locations of polymerized NMA units in a latex: the water-phase, the surface of polymer particles, and the core of the polymer particles. The objective is to identify the distribution of NMA in three latices and to determine whether NMA distribution correlates with durability related performance. NMA distribution was studied via a series of variable temperature solution NMR experiments, while the durability-related performance was studied via mode I fracture mechanics tests.

Studying the distribution of NMA required the use of isotopically labeled NMA. Both ^{15}N-NMA and ^{13}C, ^{15}N-NMA were synthesized. Three NMA/vinyl acetate (VAc) latices were prepared. The NMA feed strategy was varied during each of the three emulsion copolymerizations. Latex characterization methods including differential scanning calorimetry (DSC), rheometry, particle size analysis, and scanning electron microscopy (SEM) were used to study the three latices.

The solution NMR method to identify NMA distribution was performed on untreated latices and on washed latices. Washing techniques included membrane dialysis and centrifugation. Results revealed that the three latices had different NMA distributions, and that the distributions were related to the expected differences in microstructure. Latex 3 had ~ 80% core-NMA, while

Latex 2 had ~ 80% surface-NMA. Latex 1 had a high proportion of surface-NMA (~60%), but also had the highest proportion of water-phase NMA (~ 20%). This high proportion of water-phase NMA could be responsible for the unique morphology Latex 1 exhibited in SEM studies.

Mode I opening fracture mechanics studies were used to study adhesive performance. Specimens were analyzed after exposure to accelerated aging treatments. Latex 2 and Latex 3 exhibited very similar results, despite having very different NMA distributions. All three latices showed good durability related performance. In Latex 2 and Latex 3, the critical strain energy release rates (G_c) after accelerated aging treatments were statistically the same as the G_c of the control specimens. The most interesting finding was that the Latex 1 G_c values were significantly *higher* after accelerated aging. Latex 1 also had the highest proportion of water-phase NMA. Bondline images and SEM micrographs both indicated that the integrity of Latex 1 was least affected by the accelerated aging treatments.

ACKNOWLEDGEMENTS

The work presented in this dissertation could never have been accomplished without the support, encouragement, and guidance of my family, friends, coworkers, and advisors. During these six years, I have learned a lot about wood and polymer chemistry. I have also learned a lot about myself, and the many blessings of this life. I am grateful for all of the discoveries along this road, and thank each of you for what you have shared with me.

Dr. Chip Frazier served as co-chair of my advisory committee and has given me every opportunity to excel. He has been an outstanding role model for me. His enthusiasm in the classroom, laboratory, and over Hokie football are contagious! Dr. Frazier, thank you for continually challenging me and encouraging me to persevere. I am truly grateful that I had the opportunity to be one of your students.

I appreciate the many contributions of my other committee members, including committee co-chair Dr. Joe Loferski, Dr. Wolfgang Glasser, Dr. John Dillard, and Dr. Harry Gibson. I would also like to thank Dr. Fred Kamke for his willingness to serve as a substitute for Dr. Glasser while he is on sabbatical. Dr. Rick Davis, and the other CASS faculty members and students also provided valuable insights regarding this project. Tom Glass provided a great deal of assistance with the NMR experiments. Thank you, Tom, for the time and efforts you devoted to helping me. David Berry graciously provided access to the particle size analyzer, while Steve McCartney completed the SEM studies. Mr. Chuck Shuster and Michele Tobbe (Franklin International) both devoted a significant amount of time towards training me on their polymerization techniques, and towards answering questions as they arose. I am grateful for your involvement in this project. I would also like to acknowledge the continual support provided by departmental staff members, including: Debbie, Angie, Sharon, Rick, Kenny, David, Butch, and Carlile. This project was funded through the USDA National Needs Fellowship Program, and through the Center for Adhesive and Sealant Science (CASS). I would like to thank Linda and Tammy Jo at CASS for all of their assistance over the years.

As a graduate student in the Wood Science and Forest Products Department, I had the opportunity to become friends with people from all around the globe. I would like to thank Dr. Geza Ifju, former Department Head, for his commitment to such a diverse student population. I

would also like to thank Sylvie, Klemen, Milan, and Balazs for their friendship. Marie-Pierre Laborie and Elena Kultikova—we have shared many hours of studying, working, eating and laughing. Thank you both so much for your friendship! Many people have come and gone during my "stay" in the wood adhesion group. It was a great adventure to work with such an intelligent, witty, and well-rounded group of individuals. Rob, Marie, Dan, Mike, Jerone, Jun, Das, Romain, Brian, Darren, Joe, Leslie, Subi, Nanjian, and Scott (an honorary group member)—I really enjoyed working with each of you. Thank you for your friendship and companionship as well as your physical contributions to this work.

Lastly, I would like to thank my family for their love, support, encouragement, and prayers. My parents and brothers have always been there for me, and have cheered me on every step of the way. I thank God for each of you every day! Steve, you are my best friend. On so many occasions you have given selflessly of your time and energy so I could devote myself to this task. Your encouragement and love has meant more to me than you will ever know.

TABLE OF CONTENTS

LIST OF TABLES

LIST OF FIGURES

Chapter 1: Introduction

N-methylolacrylamide (NMA), has been used in water borne formulations with many different applications, including: fabric coatings, textile finishes, binders, paper coatings, and adhesives (Bufkin and Grawe 1978). Including NMA in these formulations (typically in the range of 3 to 7 weight percent) increased tensile strength, impact resistance, wet and dry abrasion resistance, peel strength, chemical and water resistance, heat resistance, and gloss (Bufkin and Grawe 1978).

Figure 1-1 illustrates the crosslinking reactions of NMA with itself and with other hydroxyl functionalities. Two NMA units (or an NMA unit and a hydroxyl group) can undergo a condensation reaction to form methylene ether crosslinks. These crosslinks are unstable, and can release formaldehyde to form methylene bridges. Crosslinking of NMA can be achieved by thermal curing or by catalysis with acids or bases. Thermal curing is more efficient and generally gives better physical properties (Bufkin and Grawe 1978).

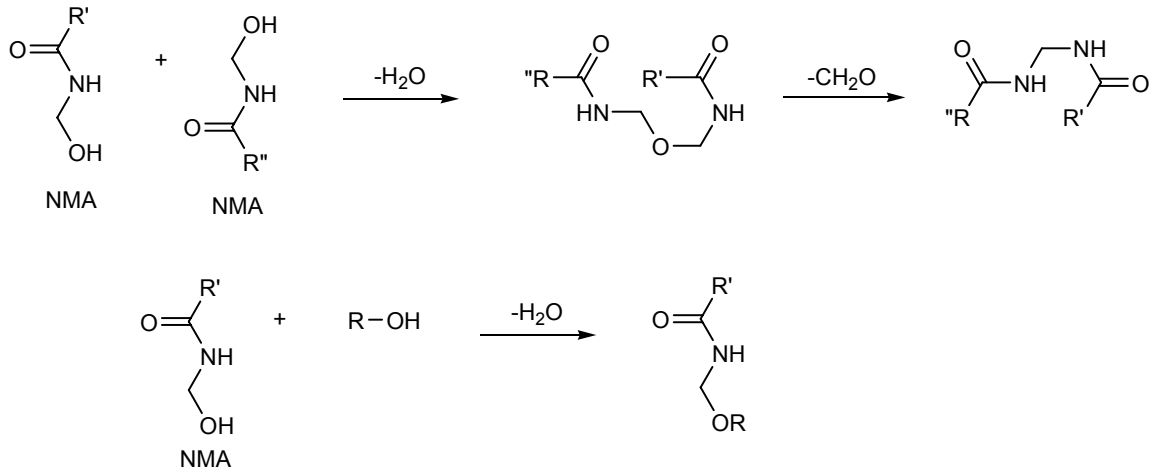

Figure 1-1: Potential crosslinking schemes for NMA-NMA, and NMA-hydroxyl crosslinks.

Prior to the development and use of NMA/vinyl acetate (VAc) adhesives, many interior grade wood products were bonded with homopolymeric poly(vinyl acetate) (PVAc) latex adhesives. These joints were susceptible to moisture-induced failures. Unlike phenol formaldehyde and isocyanate resin adhesives, poly(vinyl acetate) is thermoplastic. It flows when exposed to excess heat, or sustained loading. In addition, the hydrophilic nature of the colloid stabilizer absorbs water, so the system is

moisture sensitive. The advent of NMA/VAc systems and their application to wood products resulted in noticeable improvements in durability, presumably due to the crosslinking afforded by NMA (Armour 1962), (Goldberg and Jasinski 1967), (Armour 1969). Today, NMA/VAc adhesive compositions remain much the same as the initial formulations. These adhesives continue to be utilized in the wood industry for bonding wooden components of furniture, doors, and windows. It is somewhat surprising to learn that even after 40 years of commercial use, very little is understood regarding the durability-related performance of this system. The motivation for this work is to obtain a better understanding of the role of NMA in the performance of PVAc latex adhesives.

1.1 NMA: Considerations Relating to Durability

One of the key components in gaining an understanding of the role of NMA in NMA/VAc systems is detecting the location of polymerized NMA with respect to the latex polymer particles. Three separate NMA locations will be considered: 1.) the water phase of the latex; 2.) the surface of the particles; and 3.) within the core of the particles. A simplistic representation identifying the three possible locations of NMA in the adhesive is illustrated in Figure 1-2. Since NMA units may be present in each of the areas, the term "relative distribution" will be used to indicate the location of NMA units in the latex.

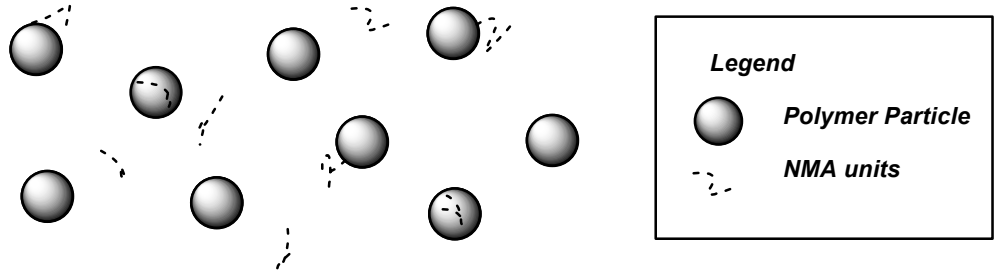

Figure 1-2: Diagram showing possible NMA locations with respect to the latex particles.

It is important to note that in Figure 1-2, only homopolymeric NMA is illustrated. This oversimplification is presented only for convenience. In reality, NMA units may exist as homopolymeric chains, but they may also be incorporated in either random or blocky segments along a PVAc chain. Since NMA and VAc have very different reactivity ratios, 2.4 to 0.45, respectively (Niyazova and Kulagina 1972), the means by which the more reactive NMA monomer is added will dictate the copolymer composition. Both a vinyl acetate radical and a NMA radical will preferentially

add NMA. In a latex, the microstructure will influence the distribution of compounds in each of the three phases because NMA is much more hydrophilic than vinyl acetate.

The relative distribution of NMA is an important aspect of this investigation because it is a parameter which could have significant effects on durability. Consider the film formation process that latices undergo as they dry, depicted in Figure 1-3. All latex products undergo some degree of film formation as they dry. Initially, water evaporates, bringing the particles closer (A to B). As water continues to evaporate (if the particle shells are not too rigid) the particles deform into a tightly packed hexagonal film (B to C). Depending on the nature of the polymer and the temperature, polymer chains can interdiffuse to varying extents (D through F). If the temperature of the system is above the minimum film formation temperature, then a completely coalesced film is formed, and no particle boundaries are evident. When interdiffusion of polymer chains is limited by temperature or by a rigid shell, the film formation process cannot proceed to completion. In some cases, films remain between stages B and C, where all water has evaporated, but hexagonal packing is limited.

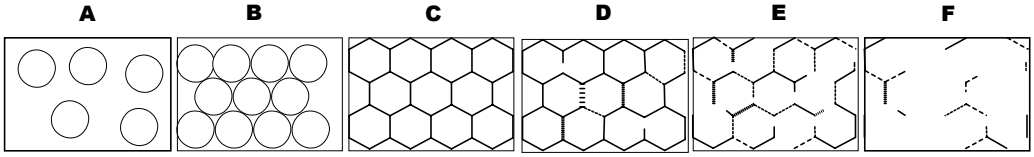

Figure 1-3: Simplistic sketch of the film formation process which occurs in latices as they dry.

In cases of incomplete film coalescence (stages C, D, and E of Figure 1-3), the formation of inter-particle crosslinks could improve the mechanical integrity of the film, thereby enhancing durability. For such inter-particle crosslinks to occur, a significant proportion of NMA should be present near the particle surfaces. On the other hand, if most NMA units were trapped in the core of the polymer particles, then the integrity of the dry film might be poor because nothing is present to stabilize the boundaries between particles.

Another example illustrating the importance of detecting NMA distribution is the fate of water-phase NMA and its role in promoting durability. Any NMA in the water phase of the latex could easily achieve significant penetration into wood and react with wood polymers. This reaction with wood may enhance bond properties, perhaps through reinforcement and/or through dimensional

stabilization.

While it is clear that NMA distribution may have some effect on durability, little work has been done to establish correlations between testing results and NMA distribution in the latex. This dissertation will describe the methods used to study NMA distribution, and investigate any correlation between NMA distribution and the durability related performance of the adhesives.

1.2 Objectives

Overall, the goal is to elucidate the molecular aspects of performance in poly(VAc/NMA) systems by focusing on the role of NMA. This will be accomplished by focusing on two main objectives:

1. Determining the distribution of NMA within the latex, and
2. Evaluating the durability related performance of the adhesives to determine any correlations between NMA distribution and performance.

1.3 Overview of the Experimental Approach

1.3.1 Objective 1: Determining the distribution of NMA

Very little NMA (less than 5% w/w on vinyl acetate) is present in these adhesives. To detect a signal from NMA units in a solution NMR experiment, isotopically enriched NMA was necessary. These products are not commercially available; therefore, they were synthesized in the laboratory. The syntheses of ^{13}C-NMA, ^{15}N-NMA, and ^{13}C, ^{15}N-NMA are the foci of Chapter 3.

To evaluate whether NMA distribution correlates with performance, several latices were prepared. NMA was fed into the reactor in different ways to achieve different copolymer compositions, and different NMA distributions. The emulsion copolymerization reactions and the characterization of the three adhesives via differential scanning calorimetry, particle size analysis, rheological studies, and scanning electron microscopy are presented in Chapter 4.

A variable temperature solution NMR method was applied to determine the distribution of NMA in the latex. This method was adapted from the work of Bonardi *et al.* (Bonardi, Christou et al.

1991), and is based on the mobility of the polymer at various temperatures. This method and its results are the focus of Chapter 5.

1.3.2 Objective 2: Evaluating the durability related performance of the latices via fracture mechanics

A number of prior studies have indicated that mode I fracture tests are a very sensitive probe of the wood-adhesive bond line. Species effects have been determined (Malmberg 2003), as have effects due to different degrees of cure (Gagliano and Frazier 2001), different accelerated aging treatments (Zheng 2002), and different surface pre-treatments (Sernek 2002). For this reason, fracture studies were selected to probe the durability related performance of the latex adhesives. These studies are included in Chapter 6.

1.4 Other Aspects of this Work

A literature review of the emulsion polymerization of vinyl acetate is included in Chapter 2. In this chapter, the references are presented in the form of footnotes. Details regarding the application of solution NMR to study NMA distribution will be postponed until Chapter 5. Background on the fracture mechanics approach is given in Chapter 6.

1.5 References

Armour, W. B. (1962). N-Methylolacrylamide -Vinyl Acetate Copolymer Emulsions. U.S.Patent.

Armour, W. B. (1969). Water Resistant Poly(vinyl acetate) Adhesive Compositions. U.S. Patent.

Bonardi, C., P. H. Christou, et al. (1991). "Acrylic Latexes Functionalized by N-Methylolacrylamide and Crosslinked Films from these Latexes." New Polymeric Materials **2**(4): 295-.

Bufkin, B. G. and J. R. Grawe (1978). "Survey of the Applications, Properties, and Technology of Crosslinking Emulsions, Part I." Journal of Coatings Technology **50**(641): 41-55.

Gagliano, J. M. and C. E. Frazier (2001). "Improvements in the Fracture Cleavage Testing of Adhesively-Bonded Wood." Wood and Fiber Science **3**(3): 377-385.

Goldberg, A. I. and V. Jasinski (1967). N-Methylolacrylamide-Vinyl Acetate Copolymer Emulsions Containing Poly(vinyl alcohol). U.S. Patent.

Malmberg, M. (2003). Species Dependence of pMDI/Wood Adhesion. Wood Science and Forest Products. Blacksburg, Virginia Polytechnic Institute and State University.

Niyazova, Z. M. and T. G. Kulagina (1972). "Copolymerization of N-alkylolacrylamides with vinyl acetate in a suspension." Sin. Vysokomol. Soedin.: 14-17.

Schmidt, R. G. (1998). Aspects of Wood Adhesion: Applications of ^{13}C CP/MAS NMR and Fracture Testing. Wood Science and Forest Products. Blacksburg, Virginia Polytechnic Institute and State University**:** 150.

Sernek, M. (2002). Comparative Analysis of Inactivated Wood Surfaces. Wood Science and Forest Products. Blacksburg, Virginia Polytechnic Institute and State University**:** 193.

Zheng, J. (2002). Studies of PF Resole/Isocyanate Hybrid Adhesives. Wood Science and Forest Products. Blacksburg, Virginia Polytechnic Institute and State University**:** 198.

Chapter 2: Literature Review on Emulsion Polymerization

Although emulsion techniques have been widely adopted, the field of emulsion polymerization is often considered, even by specialists, to be more of an "art" than a science.[1] Consider some of the opening remarks of an article written by Sudol, Daniels, and El-Aasser.[2]

> "The word *chaos* has been used to describe physical behavior which is macroscopically unpredictable in detail despite knowledge of the physics of individual events which are a subset of this behavior…. In some ways, emulsion polymerization can be viewed as *chaotic*. The fate of a single species, such as a monomer molecule, is not predictable. At best, some estimate of its probability of reacting and becoming a part of a polymer particle can be made. But which particle, where in the particle, at what position in a polymer chain, these cannot be predicted."

The nature of the science behind emulsion polymerization is very complex, and even though it has been the subject of a great deal of research, much remains to be learned. Preparing a review of the extensive amount of literature that exists in this area is a daunting task, and has been the focus of more than a few books. It is feasible, therefore, that this review will contain only the highlights of the literature in the area, and that a few noteworthy aspects of emulsion polymerization will be selected for discussion. Particular emphasis will be given to the emulsion polymerization of vinyl acetate, which, as a relatively polar monomer, exhibits unique behavior.

Included in this review are sections on: the background of free radical polymerizations, descriptions for basic terms and topics of emulsion polymerization, the historical development of heterogeneous polymerization (with emphasis on emulsions), the emulsion polymerization of vinyl acetate, a brief overview of copolymerizations with vinyl acetate, and a few notes regarding characterization methods for latices. In preparing this review, three textbooks were particularly useful. These included Blackley's *Emulsion Polymerization;* [3] one edited by the team of Lovell and El-Aasser, which is entitled *Emulsion Polymerization and Emulsion Polymers;* [4] and *Vinyl Acetate Emulsion Polymerization and Copolymerization with Acrylic Monomers*, by H. Yildirim Erbil.[5]

2.1 Free Radical Polymerizations

Emulsion polymerization is one of many types of free radical polymerization. To begin, a review of the basic mechanisms of free radical addition (or chain) polymerization will be given.

---

[1] Sudol, E.D., Daniels, E.S., and El-Aasser, M.S., "Overview of Emulsion Polymerization" in *Polymer Latexes: Preparation, Characterization, and Applications*. ACS Symposium Series #492. E.D. Sudol, E.S. Daniels, and M.S. El-Aasser, Eds. ACS: Washington, 1992.
[2] Ibid.
[3] Blackley, D.C. *Emulsion Polymerization: Theory and Practice*. Applied Science Publishers: London, 1975.
[4] *Emulsion Polymerization and Emulsion Polymers*. P.A. Lovell and M.S. El-Aasser, Eds. Wiley: Chichester, 1997.
[5] Erbil, H.Y. *Vinyl Acetate Emulsion Polymerization and Copolymerization with Acrylic Monomers*. CRC: Boca Raton, 2000.

2.1.1 Initiation

Polymerization begins shortly after a water-soluble initiator is added to the system. The initiator functions by breaking down or reacting to produce primary free radicals. These radicals then quickly react with monomer to create a monomer radical, which is also known as an active center. Generally, the formation of primary free radicals, R^* is much slower than their reaction with monomer. Therefore, the activation of the initiator is the rate determining step in the initiation process.[6]

In general, initiators used in emulsion polymerization can be categorized as either being dissociative or redox initiators. Dissociative initiators often contain a weak bond which can undergo homolytic cleavage when some small amount of energy is input to the system. For example, peroxide molecules dissociate thermally (thermolysis); whereas other molecules may require ultraviolet light (photolysis) to produce two free radicals. Redox initiators function by the transfer of a single electron between pair participants, also resulting in the formation of a free radical species.

The Formation of Primary Free Radicals

There are two components of the initiation process. In the first stage, primary free radical species are formed. Later, these primary free radicals react with monomer to produce monomer radicals.

Dissociative Initiation

Thermolysis

In thermolysis, heat is used to break a bond that is generally weak. Although all bonds undergo homolytic cleavage if heated to sufficient temperatures, there are a few bonds which cleave more readily near ambient conditions, usually highly polar bonds between two electronegative elements. Perhaps the most common example is the oxygen-oxygen bond in peroxides, which has a bond dissociation energy of 143 kJ/mol.[7] As a reference, a typical carbon-carbon bond dissociation energy is 344 kJ/mol.[8] Another relatively weak bond which can be cleaved at rather low temperatures is the carbon-nitrogen bond of an azo compound, which has an average bond dissociation energy of ~200 kJ/mol.[9]

---

[6] Lovell, P.A., "Free Radical Polymerization" in *Emulsion Polymerization and Emulsion Polymers*. P.A. Lovell and M.S. El-Aasser, Eds. Wiley: Chichester, 1997.

[7] Tinoco, I., Jr., K. Sauer, and J.C. Wang. *Physical Chemistry Principles and Applications in Biological Sciences*. Prentice Hall: New Jersey, 1995.

[8] Ibid.

[9] Isaacs, N.S. *Physical Organic Chemistry*. 2nd Ed. Longman Scientific and Technical: Essex, 1995.

The most general representation of initiation by thermolysis is:

$$I \xrightarrow{k_i} 2R* \qquad (2\text{-}1)$$

where I is a molecule of initiator which can break down into two primary free radicals, $R*$. A common example of an initiator that undergoes thermolysis is benzoyl peroxide, as shown in Figure 2-1:.[10]

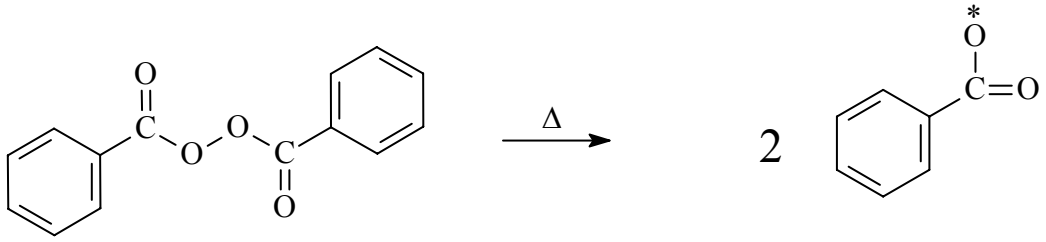

Figure 2-1: Thermolysis of the initiator benzoyl peroxide.

Photolysis

Photolysis is similar to thermolysis in that energy is required for homolytic cleavage to occur. However, in photolysis light energy is absorbed, so the initiator molecule must contain a suitable chromophore. A common example of a class of molecules which undergo photolysis are ketones, which have an n->π* transition in the ultraviolet region.[11] Absorption of light energy leads to the cleavage of the C-CO bond, and produces acyl and alkyl radicals.[12]

Assuming, once again, that the initiator breaks down into two free radicals, as shown in Equation (2-1), and also assuming that the required light intensity for bond cleavage is very small as compared to the intensity of the incident light, then the following equation can be used to describe the rate of initiation for photolysis:[13]

$$R_i = 2I_0[I]\varepsilon\phi \qquad (2\text{-}2)$$

where I_0 is the intensity of the incident light, [I] is the concentration of the initiator, ϕ is the quantum yield (which is the analogous quantity in photochemical terms to the initiator efficiency, f), and ε is the molar absorptivity of the initiator.

[10] Lovell, P.A., "Free Radical Polymerization" in *Emulsion Polymerization and Emulsion Polymers*. P.A. Lovell and M.S. El-Aasser, Eds. Wiley: Chichester, 1997.
[11] Isaacs, N.S. *Physical Organic Chemistry*. 2nd Ed. Longman Scientific and Technical: Essex, 1995.
[12] Ibid.
[13] Lovell, P.A., "Free Radical Polymerization" in *Emulsion Polymerization and Emulsion Polymers*. P.A. Lovell, and M.S. El-Aasser, Eds. Wiley: Chichester, 1997.

Redox Initiation

Redox initiators function by donating or receiving an electron to or from a pair participant, also forming free radical species. The difference in redox potentials (ΔE) between the two participants will govern the thermodynamic feasibility of the reaction. Unlike dissociative initiators, redox initiators do not require heat or light to react. Therefore, it is often advantageous to use redox initiation systems where polymerization conditions require low temperature. Expressions for R_i cannot be generalized for redox reactions since they are specific to a given initiating system. As an example, Lovell[14] considers the redox reaction of cumyl hydroperoxide with a ferrous ion, shown in Figure 2-2.

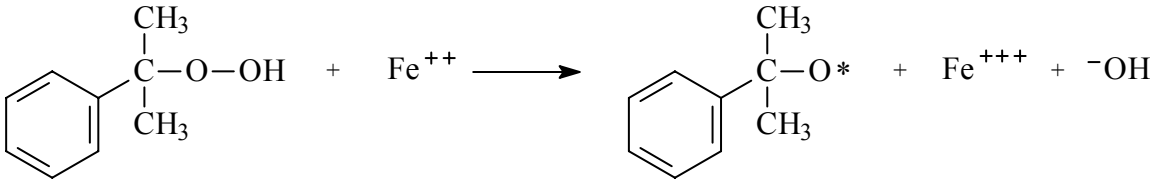

Figure 2-2: Redox initiation for cumyl peroxide and iron (II) ion.

An example of both a dissociative and a redox initiator is potassium persulfate ($K_2S_2O_8$), which is one of the most common initiators used in emulsion polymerization.[15] Under heat, homolytic cleavage results, while in the presence of sodium bisulfite ($Na_2S_2O_6$), a redox reaction can occur.

The Reaction of Primary Free Radicals with Monomer

The second step in the initiation process occurs when the primary free radical, generated by either thermolysis, photolysis, or a redox reaction, attacks the monomer. This is a regioselective process, meaning that it is influenced by the orientation of the monomer species.[16] For vinyl monomers, this step is shown in Figure 2-3, where *R** represents the primary free radical that is generated in the first initiation step.[17]

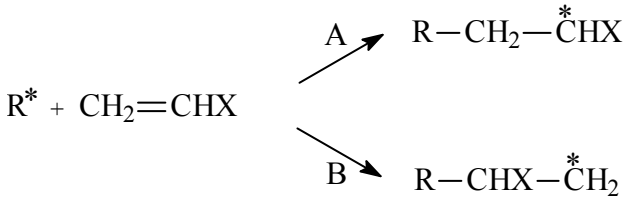

Figure 2-3: Regioselectivity of the initiation process.

For most vinyl systems, this reaction occurs through pathway A because steric effects can hinder the approach of the primary free radical in pathway B. In addition, resonance stabilization is

[14] Lovell, P.A., "Free Radical Polymerization" in *Emulsion Polymerization and Emulsion Polymers*. P.A. Lovell and M.S. El-Aasser, Eds. Wiley: Chichester, 1997.
[15] Ibid.
[16] McMurray, J. *Organic Chemistry*. 3rd Ed. Brooks/Cole: Pacific Grove, 1992.
[17] Lovell, P.A., "Free Radical Polymerization" in *Emulsion Polymerization and Emulsion Polymers*. P.A. Lovell, and M.S. El-Aasser, Eds. Wiley: Chichester, 1997.

often available through the pendant group (represented by X), which delocalizes the high energy free radical that is produced. Since the primary free radicals carry no charge, inductive stabilization does not play a role in the regioselectivity.

Another important consideration is that not all primary free radicals will complete the second step of the initiation process. Some radicals recombine and others are consumed in side reactions, as shown later, in Figure 2-7. This process is referred to as induced decomposition, and is particularly important for peroxides.[18]

2.1.2 Propagation

Addition of monomer units to the monomer radical, or active center, builds the molecular weight of the polymer through a process known as propagation. During this stage of the polymerization, monomer units add to the growing chain in rapid succession. According to Lovell,[19] the time required for the addition of one monomer unit to the growing chain is one millisecond, which would indicate that thousands of additions could occur over a period of several seconds. Propagation reactions are also thought to occur at a constant rate, given that the concentration of monomer in the reaction loci has reached some equilibrium.

Depending on the nature of the monomer, propagation can either occur in a head-to-tail or head-to-head fashion. Due to the steric and electronic effects of the pendant side group (X), the reaction usually proceeds in head-to-tail fashion, particularly for more bulky side groups. However, it is not uncommon to find occasional head-to-head linkages. In fact, it will soon be shown that termination by combination results in a head-to-head configuration. A diagram showing both head-to-head and head-to-tail addition is provided in

Figure **2-4**, which is a representation of what is shown in the text of Lovell.[20]

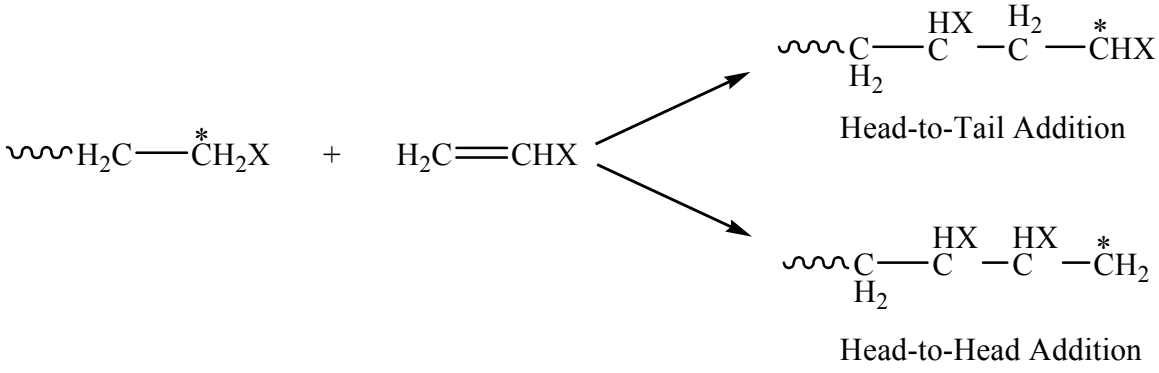

Figure 2-4: Possible addition configurations.

[18] Lovell, P.A., "Free Radical Polymerization" in *Emulsion Polymerization and Emulsion Polymers*. P.A. Lovell, and M.S. El-Aasser, Eds. Wiley: Chichester, 1997.
[19] Ibid.
[20] Ibid.

2.1.3 Termination

During polymerization, certain reactions occur which consume the free radical at the active center, thereby preventing any further propagation. This is referred to as termination, and it can occur by several different mechanisms. The chemical nature of the monomer and the polymerization system are the primary characteristics which influence the type of termination.[21] For example, styrene polymerizations terminate mostly by combination, methyl methacrylate active centers usually terminate via disproportionation (above 60° C). Chain transfer reactions terminate an active center, but polymerization continues through the formation of a new active center. Therfore, chain transfer is not a true termination reaction. However, it will be included in this section. Vinyl acetate polymerizations involve a significant amount of chain transfer.[22]

Combination

The simplest of the termination reactions is combination, where two active centers combine to form a covalent bond. Termination by combination usually results in the formation of a head-to-head sequence, as shown in Figure 2-5.[23] The polymer molecule will also have initiator fragments at both ends of the chain, which are represented in this case by *R*.

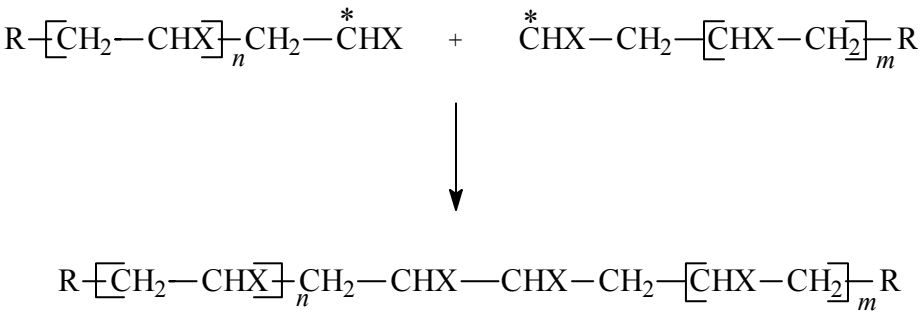

Figure 2-5: Termination by combination.

Disproportionation

Disproportionation involves the removal of a hydrogen atom from a growing chain, by another growing chain. This results in two terminated polymer molecules, one of which has an unsaturated end group. Each of the polymeric molecules, after reacting, will have initiator fragments at one end. Disproportionation is illustrated in Figure 2-6; once again, this representation closely mimics that which is provided by Lovell.[24]

---

[21] Ibid.
[22] Ibid.
[23] Lovell, P.A., "Free Radical Polymerization" in *Emulsion Polymerization and Emulsion Polymers*. P.A. Lovell, and M.S. El-Aasser, Eds. Wiley: Chichester, 1997.
[24] Ibid.

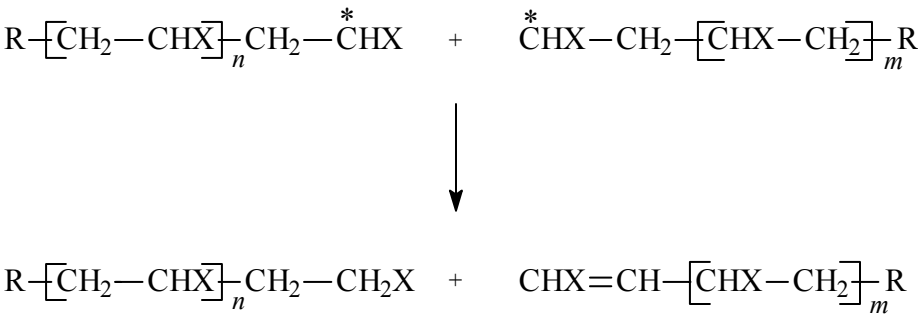

Figure 2-6: Termination by disproportionation.

Chain Transfer

Chain transfer reactions change the locus of the active center. Since polymerization can still occur at the newly formed active center, the rate of polymerization remains relatively unaffected. The molecular weight and the degree of branching in the chains will, however, be impacted. It is also important to recognize that any molecule present in the system can participate in a chain transfer mechanism.[25] Growing polymer chains can undergo chain transfer to monomer, solvent, and polymer. In addition, intramolecular chain transfer reactions are also possible, leading to the formation of long branches.[26] Some common chain transfer reactions will be shown. The following figures are all representations of what is presented in the text of Lovell.[27]

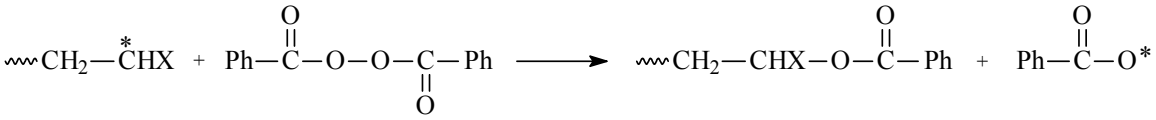

Figure 2-7: Chain transfer to initiator, and induced decomposition of the initiator.

[25] Lovell, P.A., "Free Radical Polymerization" in *Emulsion Polymerization and Emulsion Polymers*. P.A. Lovell, and M.S. El-Aasser, Eds. Wiley: Chichester, 1997.
[26] Ibid.
[27] Ibid.

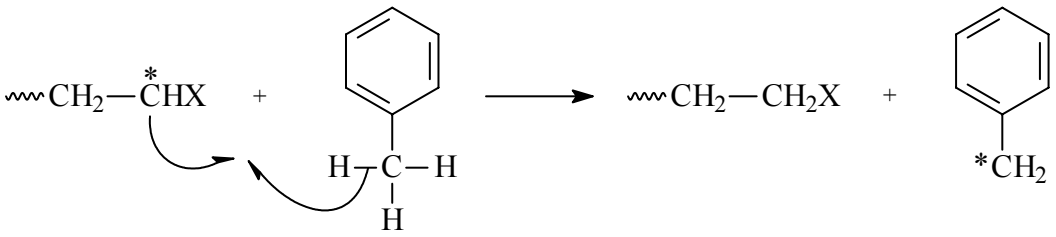

Figure 2-8: Chain transfer to solvent (toluene).

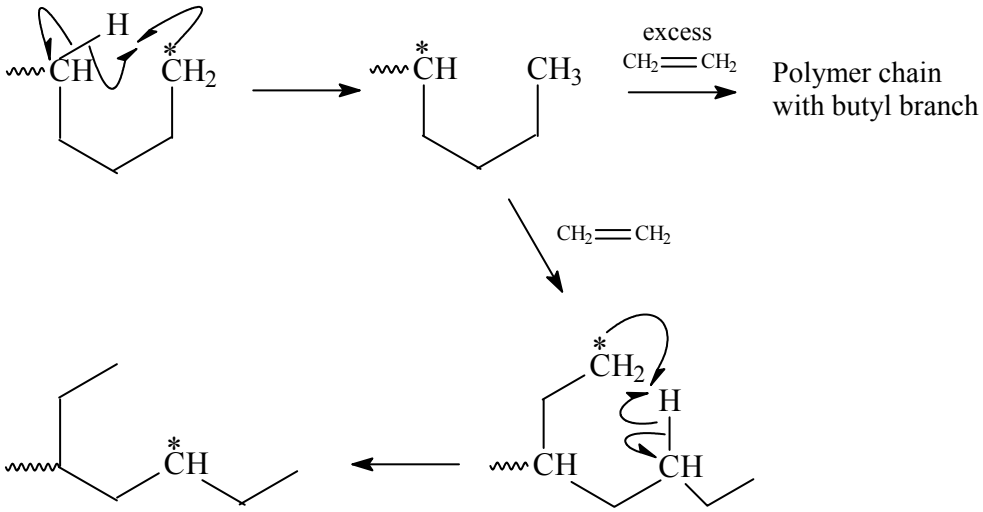

Figure 2-9: Intramolecular chain transfer that commonly occurs in polyethylene. This is also called "back-biting" and leads to short chain branches.

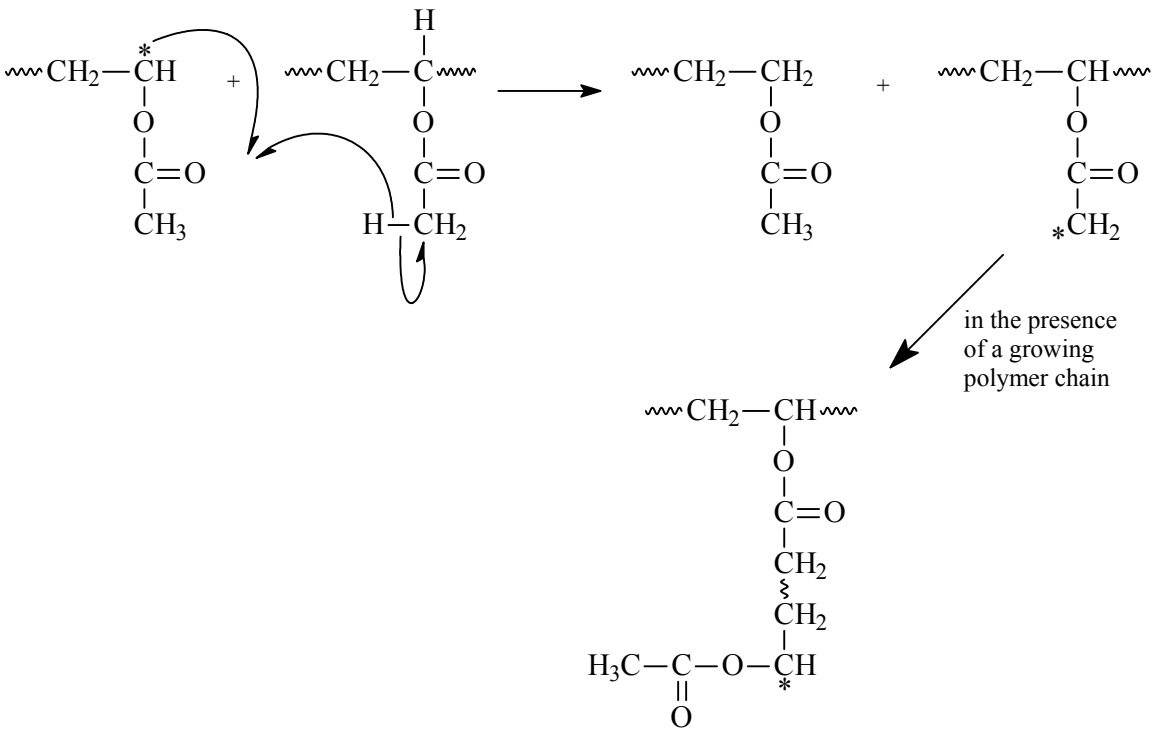

Figure 2-10: Intermolecular chain transfer in vinyl acetate. This is an important mechanism that leads to long chain branching.

2.1.4 Kinetics of Free Radical Polymerizations

Having viewed the previous reactions, it becomes clear that a more precise understanding of the rate at which monomer is consumed and converted to polymer is valuable. Assuming that the rate of propagation of a growing chain is independent of chain length, the following relationship can be written to express the rate of polymerization, R_p:[28]

$$R_p = -\frac{d[M]}{dt} = k_1[R^*][M] + k_p[M^*][M] \quad (2\text{-}3)$$

which simplifies (since the amount of monomer consumed in propagation is much greater than the amount in initiation) to:[29]

$$R_p = k_p[M^*][M] \quad (2\text{-}4)$$

[28] Lovell, P.A., "Free Radical Polymerization" in *Emulsion Polymerization and Emulsion Polymers*. P.A. Lovell, and M.S. El-Aasser, Eds. Wiley: Chichester, 1997.
[29] Ibid.

While this equation is generally true in all cases, it is more practical to eliminate the unknown quantity [M*] and replace it with measurable quantities. A general expression for the rate of change of [M*] can be written by considering the rates of initiation and termination.[30]

$$\frac{d[M^*]}{dt} = R_i - 2k_t[M^*][M^*] = R_i - 2k_t[M^*]^2 \qquad (2\text{-}5)$$

Assuming steady state conditions for the rate of change of monomer radicals (i.e. $d[M^*]/dt = 0$), then substituting into the general expression in (2-4), gives Equation (2-6), which is a general expression for the rate of polymerization in a free radical polymerization.[31]

$$R_p = k_p\left(\frac{R_i}{2k_t}\right)^{\frac{1}{2}}[M] \qquad (2\text{-}6)$$

2.1.5 Homogeneous Free Radical Polymerization

Homogeneous polymerizations include cases where both the monomer and resulting polymer are miscible in the reaction medium. Although this review is primarily concerned with the heterogeneous case of emulsion polymerization, it is advantageous to discuss other polymerization techniques and to point out the advantages and the shortcomings of such methods.

Bulk Polymerization

In a bulk polymerization, no solvents or diluents are added to the reactor. The monomer is polymerized in itself, following the addition of a monomer-soluble initiator. This is the simplest kind of free radical polymerization, as no additional compounds are added to generate any impurities. However, the high concentration of monomer that is available allows molecular weight to build very quickly, causing several problems. The first of the problems is temperature control. Because the polymerization reaction is exothermic, the temperature of the reactor climbs very quickly as the chain propagates. The increased temperature leads to more favorable conditions for polymerization, as molecules have greater energy to overcome the activation energy barrier. Thus, the reaction rate continually increases. Another problem is that the stirring often becomes inefficient, and sometimes impossible, due to the increasing viscosity of the system. When these temperature and viscosity effects occur simultaneously, autoacceleration often results. Autoacceleration, which is also known as the Trommsdorff-Norrish effect, or the gel effect, is an observed increase in the rate of reaction due to the decreasing occurrence of termination events. This phenomenon is easily visualized by considering a very viscous system, where growing chain ends lose their ability to find and collide with other active centers.

[30] Ibid.
[31] Lovell, P.A., "Free Radical Polymerization" in *Emulsion Polymerization and Emulsion Polymers*. P.A. Lovell, and M.S. El-Aasser, Eds. Wiley: Chichester, 1997.

Autoacceleration makes thermal control even more difficult to achieve, and often leads to a runaway reaction since small, mobile monomer molecules are both plentiful and capable of finding and reacting with active centers.[32] To avoid this phenomenon, bulk polymerizations are often stopped at relatively low conversion. This means that excess monomer must be stripped from the system prior to use.

Solution Polymerization

Adding a solvent alleviates many of the problems that are typically encountered in bulk polymerizations, and allows the reaction to proceed to higher conversions. The viscosity of the system is decreased, stirring becomes relatively easy, and heat transfer is more efficient, so the occurrence of autoacceleration decreases. Most of these effects are due to the reduced concentration of monomer in the system, which in turn reduces the rate of polymerization. However, solution polymerizations have several problems. First, chain transfer to solvent can limit molecular weight. Another considerable drawback is that at some point, if pure polymer is required, then the solvent must be removed from the system. For this reason, solution polymerizations tend to be utilized only in cases when the end use of the polymer requires it to remain in solution.

2.1.6 Heterogeneous Free Radical Polymerizations

Heterogeneous polymerizations involve a dispersion of monomer(s) and/or resulting polymer in an immiscible liquid.[33] Usually, one of these components is water, leading to the common terminology of oil in water (o/w) and water in oil (w/o) polymerizations, where the first component is the dispersed phase and the second is the dispersing medium. Most monomers are relatively hydrophobic, so heterogeneous polymerization in that case would involve an o/w system. However, water-soluble polymers, such as acrylamide, are commonly polymerized in a w/o system.

Advantages of Heterogeneous Polymerization

Today, heterogeneous polymerization techniques are a very commonplace means of producing high molecular weight polymers. Compared to more traditional methods of polymerization (bulk and solution polymerizations), heterogeneous polymerization offers several unique advantages.[34]

Initially, solution polymerizations found favor over bulk reactions because they eliminated the problems associated with heat removal, high viscosities, and the risk of autoacceleration. However, solution polymerizations had some inherent problems as well, including the use of a suitable solvent for the monomer/polymer system. Perhaps the most significant reason for the widespread shift to heterogeneous polymerization has been the environmental push to reduce the use of toxic solvents. In heterogeneous polymerizations, water is the most common medium, and, in addition to being environmentally friendly, it is both inexpensive and readily available.

---

[32] Arshady, R. 1992. *Colloid and Polymer Science*. 270, 717.
[33] Arshady, R. 1992. *Colloid and Polymer Science*. 270, 717.
[34] Thompson, M.W. "Types of Polymerization" in *Polymer Colloids.* R. Buscall, T. Corner, and J.F. Stageman, Eds. Elsevier: London, 1985.

A second advantage for heterogeneous polymerizations is that heat evolution during the polymerization is more easily managed due to the high specific heat of water (the medium). In essence, emulsion and suspension polymerizations allow bulk polymerizations to occur inside microcapsules. Water's ability to efficiently remove heat during the reaction dramatically decreases the autoacceleration effect, which is an improvement over bulk polymerizations. There is also no need for a solvent since the viscosity of the system is relatively low, therefore minimizing chain transfer to solvent.

Also, polymer produced via emulsion polymerization can often be used as is; there is no need for further processing such as precipitation, which is sometimes required following solution polymerizations. Emulsion polymerization is just one of several types of heterogeneous polymerization. Two other common types of heterogeneous polymerizations are suspension and dispersion polymerizations. Unfortunately, in some of the literature these terms are used interchangeably, while other authors are careful to differentiate between the various classes. Clearly, the lack of a common nomenclature for heterogeneous polymerizations has led to a great deal of confusion. For this reason, a description of the classes of heterogeneous polymerizations and terminology will follow.

Classes of Heterogeneous Free Radical Polymerization

Many authors have offered their own criteria for distinctions between classes of heterogeneous polymerizations, but no set of terms has been accepted as common nomenclature. In reviewing the literature, the most thorough system of categorization has been proposed by Arshady,[35] who considers the initial state of the polymerization mixture, the kinetics of polymerization, the mechanism of particle formation, and the shape and size of the final polymer particles in his classification system. In addition to the three classes of heterogeneous polymerizations that are most easily confused in the literature (i.e. suspension, dispersion, and emulsion polymerizations), Arshady adds a fourth—precipitation polymerization. Other authors consider only the size of the resulting particle as the distinguishing criteria. Below, each class will be briefly discussed. As indicated by Arshady, in many cases, a particular heterogeneous polymerization may be multimodal--for example, it may exhibit characteristics of both suspension and emulsion polymerizations.

Emulsion Polymerization

In classical emulsion polymerizations, both the initial state of the mixture and the loci of polymerization are difficult to describe. The monomer is not soluble (that is, it is *scarcely* soluble) in the dispersing medium, but the initiator is soluble. Surfactants or other stabilizers, commonly called emulsifiers, aid the dispersion of monomer in the media as it partitions (under agitation) into one of three locations: 1.) monomer droplets (usually 1-10 μm in diameter); 2.) micelles (usually 50 – 100 Å) or 3.) the media (usually this represents a small amount of monomer—for example, at 70°C, only 4 g. of styrene is soluble in one liter of water). Initiator molecules, being soluble in the water phase, can only activate monomer that is present in the water phase or in micelles. Over time, short chain oligoradicals develop into higher molecular weight polymer chains. Although the initial locus of emulsion polymerization depends largely

[35] Arshady, R. 1992. *Colloid and Polymer Science*. 270, 717.

upon the solubility of the monomer in the media, it is widely accepted that most of the polymerization reaction occurs in surfactant or colloid stabilized polymer particles.

According to Arshady, particles from emulsions typically range from 50 – 300 nm in size, although he does acknowledge that the size is highly dependent upon the polymerization conditions.[36] Other authors concede that the particle size obtained from emulsion polymerizations can exceed 1 μm. For emulsions, particle size is independent of the size of the monomer droplets, since the monomer droplet is not the loci of polymerization. Instead, particle size is dependent on the rate of particle nucleation (which is proportional to the rate of polymerization). Therefore, the amount of monomer that is soluble in the medium, the emulsifier concentration, the salt concentration, and the polymerization temperature (higher temperatures leads to smaller particles) all influence particle size in emulsion polymerizations.[37]

Suspension Polymerization

In suspension polymerizations neither the monomer nor the initiator is soluble in the medium; however, the initiator is soluble in the monomer. Under stirring, tiny droplets of monomer become dispersed throughout the medium, and since the initiator is soluble in the monomer phase, the monomer "microdroplets" are rapidly converted through what may be called a micro-bulk polymerization, into polymer "microbeads".[38,39] Often, the polymerization requires the use of protective colloids or suspending agents to minimize coalescence of individual monomer droplets, particularly due to the tackiness of the polymer particles that have been plasticized by monomer.[40] Suspension polymerizations are also frequently referred to as "pearl" and "bead" polymerizations.[41]

Particle sizes from suspension polymerization vary from 100 nm – 2 mm, although for vinyl monomers the polymerization usually produces larger particles, ranging from 20 um – 2 mm.[42] Dawkins states that the particle size for suspensions typically ranges from 10 μm to 5 mm.[43] Particle size control is achieved by manipulating the size of the monomer droplets. Equation 2-7 shows the variables that influence $\bar{d}$, the average particle size.[44] In the equation, k is a parameter describing the design of the reactor, the type of stirrer, and the self-stabilization of the system (thus is highly dependent on the system), D_v is the diameter of the vessel, D_s the diameter of the stirrer, R the volume ratio between the droplet phase and the medium, η_d and η_m the viscosities of the droplet and medium phases, γ the interfacial tension, and [S] the concentration of the stabilizer.

[36] Ibid.
[37] Ibid.
[38] Ibid.
[39] Blackley, D.C. *Emulsion Polymerization: Theory and Practice*. Applied Science Publishers: London, 1975.
[40] Blackley, D.C. *Emulsion Polymerization: Theory and Practice*. Applied Science Publishers: London, 1975.
[41] Dawkins, J.V. "Aqueous Suspension Polymerizations" in *Comprehensive Polymer Science*, Volume 4, Chapter 14. G. Allen and J.C. Bevington, Eds. Pergamon: Oxford, 1989.
[42] Arshady, R. 1992. *Colloid and Polymer Science*. 270, 717.
[43] Dawkins, J.V. "Aqueous Suspension Polymerizations" in *Comprehensive Polymer Science*, Volume 4, Chapter 14. G. Allen and J.C. Bevington, Eds. Pergamon: Oxford, 1989.
[44] Arshady, R. 1992. *Colloid and Polymer Science*. 270, 717.

$$\bar{d} \equiv k\left(\frac{D_v \cdot R \cdot \eta_d \cdot \gamma}{D_s \cdot N \cdot \eta_m \cdot [S]}\right) \quad (2\text{-}7)$$

The morphology of the polymer particles is dependent upon the degree to which the monomer swells the polymer. If the polymer swells in the monomer, the surface of the polymer particles is regular and smooth (as occurs for polystyrene and polymethyl methacrylate); if it does not, the surface of the particles is irregular and porous, as in polyvinyl chloride and polyacrylonitrile.[45] For applications like ion exchange resins and polymer supports, an irregular or porous morphology is desired. This can be encouraged through the use of appropriate monomer diluents.

Kinetics in suspension polymerizations are very similar to bulk polymerizations, except in the presence of a monomer-soluble diluent. In that case, the kinetics more closely resemble that of a solution polymerization.[46]

Dispersion Polymerization

Dispersion polymerizations begin like solution polymerizations, as both the monomer and initiator are soluble in the medium, resulting in what is initially a homogeneous system. However, the polymer that is produced is insoluble in the medium, which quickly leads to phase separation and particle nucleation. As the particles are swollen by the medium and/or monomer, polymerization ensues within the particles.

Particle sizes for this class of polymerization range from 0.1-10 μm, (1-15 μm, according to Cawse[47]), and the particles can easily coagulate if they are not stabilized properly (see Precipitation Polymerization, below).[48] Temperature, the concentration of the monomer, initiator, and stabilizer, and the solvency of the medium all influence particle size.[49] For dispersion polymerizations, the most suitable stabilizers are colloid stabilizers, which consist of polymers having some solubility in the medium but also some affinity for the particles.

Precipitation Polymerization

Precipitation polymerization is very similar to dispersion polymerization with the exception that the polymer that forms is not swelled by the medium, and thus, precipitates from solution. The result is continuous nucleation and coagulation of polymer particles, which continually builds larger, and larger particles. In these cases, the particle size distribution is fairly broad and the particles are irregularly shaped.[50]

---

[45] Ibid.
[46] Ibid.
[47] Cawse, J.L. "Dispersion Polymerization" in *Emulsion Polymerization and Emulsion Polymers*, P.A. Lovell and M.S. El-Aasser, Eds. Wiley and Sons: New York, 1997.
[48] Arshady, R. 1992. *Colloid and Polymer Science*. 270, 717.
[49] Ibid.
[50] Arshady, R. 1992. *Colloid and Polymer Science*. 270, 717.

2.2 Basic Terms and Principles Related to Emulsion Polymerization

While it has been well established that three separate phases of matter exist, and that homogeneous solutions between those phases also exist, it was not until the middle of the 19th century that it became clear that some intermediate class of materials existed. Within this group, one material is finely dispersed in another component, but not to the extent that it is molecularly dissolved, as in a homogeneous solution. When the heterogeneities reach domains greater than or equal to one nanometer, they deviate significantly from homogeneous solutions. Everett[51] refers to these systems as "microheterogeneous systems", where the heterogeneity is on the scale of 1 to 1000 nanometers. It is this realm that is characteristic of colloids.

2.2.1 Colloids

Although most are unfamiliar with the term, people observe and use colloids on a daily basis. Common examples include fogs, mists, smokes, milk, paints, muds, and jellies. Even from the beginning, Man was quick to observe and to make use of colloidal phenomena. To quote D.H. Everett: [52]

> "Perhaps the oldest record of a colloidal phenomenon is that of the deposition of silt at river mouths mentioned in the Babylonian Creation myth—which, incidentally, was inscribed on tablets of clay, themselves an example of a colloidal material—while the Book of Genesis refers to clouds and the fall of rain. But early Man must also have been familiar with many other colloidal phenomena, such as the effect of walking on wet sand and the treachery of quicksands. He soon exploited them in the preparation of butter, cheese, and yoghurt and in the making of bread. His early technology, too, often depended on colloids and their properties: the making of bricks, the extraction of glue from bones, and the preparation of inks and pigments are a few examples. Indeed, there can have been few aspects of his domestic life that were independent of the behavior of colloids, either of natural occurrence or prepared by him."

Awareness of such systems came as early as 1774, when Macquer printed in his Dictionary of Chemistry that he suspected alchemists had used some type of finely divided gold to create both potable gold (the "Elixir of Life") and Purple of Cassius, which was used to make ruby glass.[53] Scientific investigations into colloidal behavior began in 1845, when Selmi experimented and created "demulsions" of sulfur and silver halides, and these investigations were furthered in 1856, with Faraday's study on colloidal gold.[54] In 1861, the term "colloid" was used to denote adhesive particles which diffused only very slowly through porous membranes.[55] Since that time, the term has been extended far beyond adhesive solutions to describe a wide array of materials. According to Fitch,[56] colloids refer to "a dispersion of fine particles in a fluid medium."

Progress in studying colloidal phenomena has been comparatively slow due to the difficulties encountered in producing materials that can be characterized well, and give reproducible

[51] Everett, D.H. *Basic Principles of Colloid Science*. Royal Society of Chemistry: London, 1988.
[52] Ibid.
[53] Ibid.
[54] Ibid.
[55] Ibid.
[56] Fitch, R.M. *Polymer Colloids: A Comprehensive Introduction*. Academic Press: San Diego, 1997.

behavior. Perhaps Hedges[57] says it best: 'To some the word *colloidal* conjures up visions of things indefinite in shape, indefinite in chemical composition and physical properties, fickle in chemical deportment, things infilterable and generally unmanageable.'

2.2.2 Latex

Another term that is frequently found in the literature pertaining to emulsion polymerization is the word "latex". In Webster's, [58] this word is defined in two different ways:

> 1.) a milky usually white fluid that is produced by cells of various seed plants (as of the milkweed, spurge, and poppy families) and is the source of rubber, gutta-percha, chicle, and balata; and 2.) a water emulsion of a synthetic rubber or plastic obtained by polymerization and used especially in coatings (as paint) and adhesives.

The most important natural latex is that from *Hevea brasiliensis*. This species, which was originally found in the Amazon basin of Brazil, was later transplanted successfully in Malaysia and Indonesia.[59] Its product is a colloidal suspension of rubber particles which are stabilized by protein.[60] The latex from the *Hevea brasiliensis* tree will be referred to as "natural" latex. Colloidal suspensions of synthetic polymers came to be known as synthetic latexes, or synthetic latices. In this paper, natural latices are not of great interest, so the word "latex" will be used to describe synthetic latices.

2.2.3 The Role of Surfactants

Surfactants are molecules containing a non-polar "tail" (usually consisting of a hydrocarbon chain) and a polar "head" fragment. Their amphiphilic characteristics allow associations of molecules which lower the surface free energy of the system. In a typical oil in water system, surfactants play several important roles. First, they lower the surface free energy of water. Second, they aid in the emulsification of monomer by stabilizing monomer droplets which are formed through agitation. Third, they form micelles, which become the "meeting place" for oil-soluble monomer molecules and water-soluble initiators. In a similar fashion, surfactants also aid in the stabilization of polymer particles in the aqueous phase, protecting the particles from coagulation and flocculation.

Early in the literature, surfactants (also known as detergents) were recognized for having significant solubilization effects. McBain[61], one of the pioneers in the area of detergent action, defined solubilization as "the spontaneous passage of molecules of a substance insoluble in water into a dilute aqueous solution of a detergent to form a thermodynamically stable solution." In other words, when a monomer is solubilized, it no longer exists as a separate phase. This has

---

[57] Everett, D.H. *Basic Principles of Colloid Science*. Royal Society of Chemistry: London, 1988.
[58] *Merriam-Webster's Collegiate Dictionary*. Springfield: Merriam-Webster, Inc., 1993.
[59] Bovey, F.A., I.M. Kolthoff, A.I. Medalia, and E.J. Meehan. *Emulsion Polymerization*. Interscience: New York, 1955.
[60] Ibid.
[61] McBain, J.W. *Advances in Colloid Science*. E.O. Kraemer, Ed. Interscience: New York, 1942.

been demonstrated in experiments where the vapor pressure of various hydrocarbons was found to decrease upon dispersion in a detergent solution. Increases to the representative vapor pressures of the hydrocarbons only occurred when the limits of solubility were exceeded, i.e., when a separate hydrocarbon phase existed.[62] Solubilization occurs in solutions where the detergent concentration is slightly above the CMC, and therefore relies on micellar action.[63]

According to McBain,[64] there are three important classes of detergent molecules: 1. anion-active, 2. cation-active, and 3. non-electrolytic (these correspond with the current nomenclature of anionic, cationic and nonionic surfactants). Within the broader category of detergents were the "soaps", or anionic surfactants. This class of amphiphilic molecules is the most widely used in current emulsion polymerization techniques.[65] Common examples of soaps include stearate, palmitate, oleate, and organic sulfates, carboxylates, and sulfonates.[66] Cationic surfactants are less common, but include alkyl ammonium halides and alkyl-substituted pyridinium halides.[67] Finally, polyglycerol esters of fatty acids or condensation products of ethylene oxide and other compounds compose the nonionic surfactants, which can be utilized over a wide range of pH.[68, 69]

Physicochemical Properties of Surfactants and the CMC

Generally, at low concentrations, the addition of surfactants does not have a notable effect on the physicochemical properties of a solution. However, if the amount of surfactant added reaches or exceeds some limiting value, the properties of the solution (including the osmotic coefficient, electrical conductivity, ion activities, viscosity, and surface tension) are markedly influenced. This limiting concentration is known as the CMC, or critical micelle concentration. Below this concentration, all surfactant is molecularly dissolved in the dispersing media, and thus, has no effect on properties. However, at or above the CMC, surfactant molecules associate, forming a colloidal particle known as a micelle (see Figure 2-11). Although micelles exhibit some aspects of colloidal behavior, they are also capable of disassociating if the concentration of surfactant molecules in solution drops below the CMC. This association and dissociation phenomena is completely reversible, and depends solely on the concentration of surfactant in the solution.

In the 1960s, research done by Shinoda et al.[70] on a number of different detergent solutions lead to the development of an equation which allows predictions of the CMC for a given surfactant based upon the length of its hydrocarbon chain. In general:

---

[62] Ibid.
[63] Ibid.
[64] McBain, J.W. *Advances in Colloid Science*. E.O. Kraemer, Ed. Interscience: New York, 1942.
[65] Bovey, F.A., I.M. Kolthoff, A.I. Medalia, and E.J. Meehan. *Emulsion Polymerization*. Interscience: New York, 1955.
[66] Ibid.
[67] Ibid.
[68] Ibid.
[69] Erbil, H.Y. *Vinyl Acetate Emulsion Polymerization and Copolymerization with Acrylic Monomers*. CRC: Boca Raton, 2000.
[70] Shinoda, K., T. Nakagawa, B. Tamamushi, and T. Isemura. *Colloidal Surfactants: Some Physico-Chemical Properties*. Academic: New York, 1963.

$$\log_{10}[CMC] = ABn \qquad (2\text{-}8)$$

where A is a constant with a value of approximately 1.70 for most anionic and cationic surfactants, B is also a constant with a value of approximately 0.292 and n represents the number of atoms in the hydrocarbon chain of the surfactant.[71]

The Structure of Micelles

Even at the time that Bovey et al.'s [72] textbook was published, the structure of micelles was not clear. Early X-ray evidence by several authors[73,74] indicated that laminar (or lamellar) micelles were predominant, and McBain was a large proponent for this theory. However, others, including Hartley,[75] believed that spherical arrangements were more likely. It is now widely accepted that micelles adopt a spherical conformation, which has a smaller surface area and therefore a lower surface free energy.

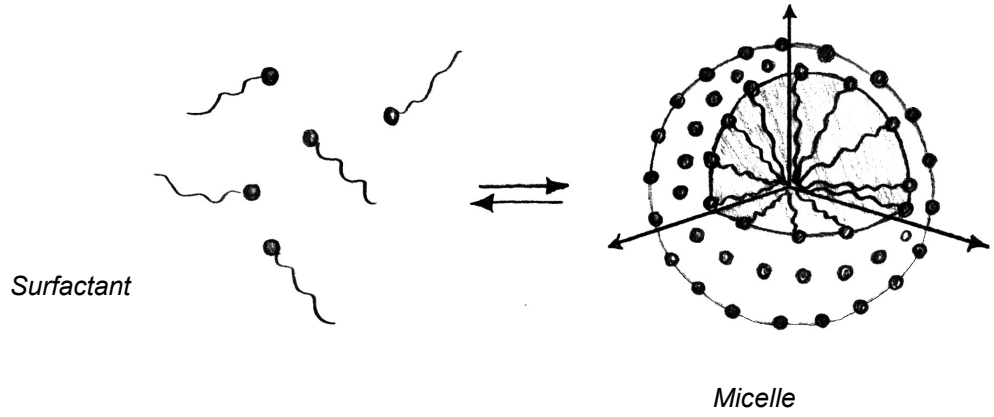

Figure 2-11: Schematic representation of micellization, similar to that depicted in the text of Hiemenz.[76] At the left are the surfactant molecules having a hydrophilic head (circular) and a hydrophobic tail. The right hand side of the equilibrium shows a cutaway section of a micelle which shows the hydrophilic tails of the surfactant molecules oriented towards the center of the sphere.

Amount of surfactant

The amount of surfactant added has very important implications. It will control both the number and size of the polymer particles and will also influence the kinetics of the polymerization. For emulsion polymerizations, the amount of soap used must exceed the critical micelle

[71] Ibid.
[72] Bovey, F.A., I.M. Kolthoff, A.I. Medalia, and E.J. Meehan. *Emulsion Polymerization*. Interscience: New York, 1955.
[73] Harkins, W.D., R.W. Mattoon, and M.L. Corrin. 1946. *Journal of Colloid Science*. 1, 105.
[74] Mattoon R.W., R.S. Stearns, and W.D. Harkins. 1948. *Journal of Chemical Physics*. 16, 64.
[75] Hartley, G.S. 1938. *Journal of the Chemical Society*. 1968.
[76] Hiemenz, P.C. *Polymer Chemistry: The Basic Concepts*. Marcel Dekker: New York, 1984.

concentration (CMC). This is due to the initial effects that are observed when a detergent is added to water. To minimize the interfacial tension, soap molecules that are dissolved in the media orient themselves preferentially at the air-water interface to minimize the surface free energy, γ, of the system. Only after the interface has been stabilized are the additional soap molecules free to form micelles within the medium. Erbil [77] points out that while some polymerizations have been completed with soap concentrations as little as 10 times the CMC, more appropriate concentrations are 50 and 100 times the CMC.

2.2.4 Stability

Another important aspect of colloidal systems is the stability of the dispersions. Potential energy diagrams are illustrative in demonstrating the thermodynamics of particle stabilization and destabilization phenomena. Consider the case where two particles are in relatively close proximity to one another. Both attractive and repulsive forces act on those particles, which are separated by some distance, *r*. The fate of the particles and their response to the forces acting on them can be evaluated by considering the sum of the attractive and repulsive components present at particular distances of separation, *r*.

Attractive Forces

Attractive forces between non-polar molecules were first discovered by van der Waals in 1873.[78] Later, London developed an understanding of such forces, which are in most cases referred to as "dispersion forces". Since this terminology could easily lead to confusion in the colloidal regime, the forces will instead be referred to as London forces. The sum of these forces has lead to Equations (2-9) and (2-10) which represent the attractive nature of two particles as they approach one another. (In the equations, *r* represents the distance of separation between the two particles.) Equation (2-10) assumes that reversibly separating these particles requires work, and that the work required must be equal in magnitude to the of the sum of the attractive forces over the distances of *r* to ∞.

$$F_{att} = \frac{-A}{r^7} \qquad (2\text{-}9)$$

$$\Delta G_{att} = \frac{-A'}{r^6} \qquad (2\text{-}10)$$

According to Equations (2-9) and (2-10), where *A* and *A'* are constants, as the particles move closer together (*r* decreases) the free energy becomes increasingly negative, favoring further attraction. This phenomena is illustrated in Figure 2-12 in a representation which was taken from Shaw's text and slightly modified.

---

[77] Erbil, H.Y. *Vinyl Acetate Emulsion Polymerization and Copolymerization with Acrylic Monomers*. CRC: Boca Raton, 2000.

[78] Shaw, D.J. *Introduction to Colloid and Surface Chemistry*. Butterworth-Heinemann: Oxford, 1992.

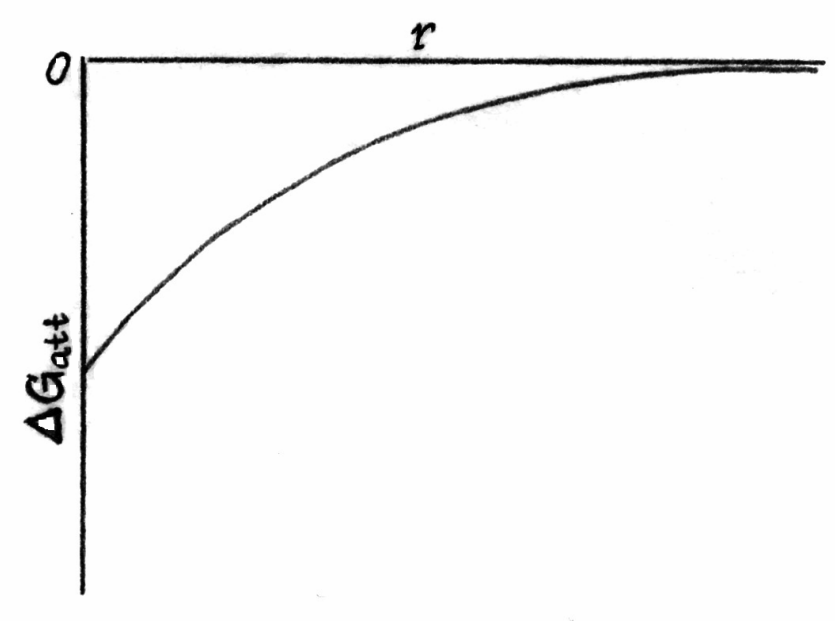

Figure 2-12: Illustration of the attractive component of the free energy (normalized by the surface areas of the particles) as a function of the distance of separation, r, between particles. Similar to the representation given in the text of Shaw. [79]

Repulsive Forces

However, when the particles become increasingly close, their electron clouds interact and repulsive phenomena are observed. This became known as the Born repulsion, and is represented in Equations (2-11) and (2-12).[80]

$$F_{rep} = Be^{-ar} \qquad (2\text{-}11)$$

$$\Delta G_{rep} = \frac{B'}{r^{12}} \qquad (2\text{-}12)$$

In this case, *B* and *B'* are constants, as is *a*, and *r* remains the distance of separation. Therefore, as the particles reach some small distance of separation *r*, the free energy becomes quite large and positive, and therefore, the particles remain separated. This is illustrated in Figure *2-13* which was adapted from the text of Shaw.

[79] Ibid.
[80] Shaw, D.J. *Introduction to Colloid and Surface Chemistry*. Butterworth-Heinemann: Oxford, 1992.

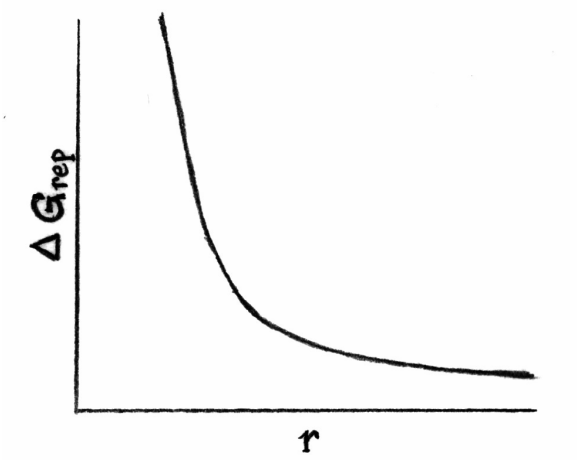

Figure 2-13: Diagram showing the repulsive component of the free energy curve as two particles approach one another. Similar to the representation in the text of Shaw. 81

The Lennard Jones potential describes the sum of the attractive and repulsive components of the free energy. Combining equations (2-10) and (2-12):[82]

$$\Delta G_{tot} = \Delta G_{rep} + \Delta G_{att} = \frac{B'}{r^{12}} - \frac{A'}{r^{6}} \quad (2\text{-}13)$$

Usually, the constants *B*' and *A*' are replaced by factors which describe the system in better detail. These are ε_{min}, the depth of the potential well, and r_0, the distance of particle separation where the potential reaches zero. These substitutions into Equation (2-13) lead to Equation (2-14).[83]

$$\Delta G_{tot} = 4\varepsilon_{\min}\left[\left(\frac{r_0}{r}\right)^{12} - \left(\frac{r_0}{r}\right)^{6}\right] \quad (2\text{-}14)$$

Both ε_{min} and r_0 can be seen in Figure 2-14, which shows various free energy curves for different systems. Notice that there is a primary repulsive energy barrier which particles must overcome before they may move closer together. This barrier can be engineered through the use of various stabilizers and surfactant materials. Systems showing potential energy diagrams similar to these have some stability. However, changes in the temperature of the system may impart enough energy for the particles to surpass the energy barrier and become unstable.

[81] Ibid.
[82] Ibid.
[83] Shaw, D.J. *Introduction to Colloid and Surface Chemistry*. Butterworth-Heinemann: Oxford, 1992.

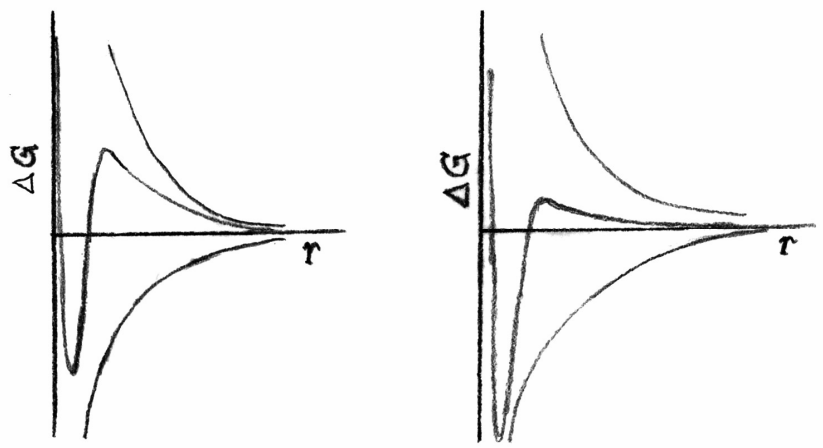

Figure 2-14: Total free energy curves, showing the combination of attractive and repulsive components for different systems. Representation is similar to that exhibited in the text of Shaw.[84]

Flocculation and Coagulation

Due to problems with stability, dispersed particles may come into contact and stick together to form aggregates. In some cases, gravity may then cause these aggregates to fall out of solution. Two processes describe the formation of aggregates: flocculation and coagulation. Coagulation generally refers to an irreversible phenomenon, whereas flocculation is reversible.[85] Furthermore, coagulation generally indicates denser aggregates, which form coagulum, whereas flocculation results in a more open aggregate, known as a floc.[86] Flocs may or may not separate out of solution whereas coagula generally do. Typical processes used to separate aggregates out of a colloidal dispersion are referred to as sedimentation and creaming. Creaming is used when the aggregates are less dense than the medium whereas sedimentation occurs when the aggregates are more dense.

The degree of coagulation that would occur in when two particles come into contact would depend on the tackiness of the polymer particles and the glass transition temperature of the polymer. If the polymer particles are above T_g, then it is likely that Brownian motion would allow the polymer chains to interdiffuse and the particles would coagulate to form one large particle. However, below T_g or for polymers having less tack, flocculation is more likely.

This discussion of stabilization in colloids is very brief, and leaves out detailed descriptions of other important surface and electrostatic phenomena at the particle surface. Most notably, particles in solution are heavily influenced by the presence of adsorbed ionic species (sometimes from initiator fragments), by the ionization of surfactant molecules that leads to charge development at the particle surface and by steric effects of polymeric stabilizers. Therefore, a more appropriate qualitative representation for ΔG of the system would be that which is shown in Equation (2-15).[87]

---

[84] Ibid.
[85] Everett, D.H. *Basic Principles of Colloid Science*. Royal Society of Chemistry: London, 1988.
[86] Ibid.
[87] Shaw, D.J. *Introduction to Colloid and Surface Chemistry*. Butterworth-Heinemann: Oxford, 1992.

$$\Delta G_{tot} = \Delta G_{att}\left(van\ der\ Waals\ or London\ \ forces\right) + \Delta G_{rep}\left(electron\ cloud\right) + \Delta G_{rep}\left(electrostatic\right) + \Delta G_{rep}\left(steric\right) + \Delta G\left(other\ effects\right) \quad (2\text{-}15)$$

2.2.5 Film Formation in Latices

During the emulsion polymerization process and throughout the latex's shelf life, particle stabilization is of great importance. The selection of the appropriate type and quantity of stabilizer is a key component of the formulation to prevent particle coagulation or flocculation. Yet, when these systems are applied, the particles must overcome the repulsive nature of the stabilizers to form a continuous coalesced film. This very complex process will be briefly discussed in this section of the paper.

The film formation process begins when water evaporates, causing the latex particles to pack more closely. Once the particles have packed into an ordered regime, they gradually begin to deform. Finally, the polymer chains that had previously been restricted to the interior domain of the particles interdiffuse to form a continuous film. Certain conditions must exist in order for the film formation process to reach completion.

Understanding the terminology related to film formation has been complicated by authors who use the same terms to describe different processes. Many authors refer to different "stages" of film formation, defining stage I to correspond (roughly) with the evaporation of water, stage II with particle deformation, and stage III with interdiffusion. Other authors[88, 89] consider only two stages, while a few believe the system to be a latex until it goes through a single event which then transforms it into a film.[90]

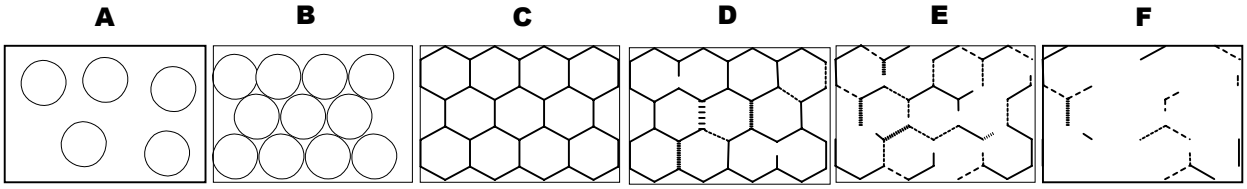

Figure 2-15: Diagrammatic representation of film formation. Steps A-E represent various changes occurring in the film morphology with time.

A similar problem exists regarding the minimum filming temperature (MFT), which is also commonly referred to as the minimum film-formation temperature (MFFT). The MFT, according to Eckersley and Rudin[91], is "the minimum temperature at which a cast latex becomes continuous and clear. Below this critical temperature, the dry latex is opaque and powdery." Winnik, Wang, and Haley[92] rely on a similar definition, but provide an additional criterion called the "crack point", which is the minimum temperature that the latex forms a crack-free film

[88] Dillon, R.E., E.B. Bradford, and R.D Andrews, Jr. 1953. *Industrial and Engineering Chemistry*. 45, 728.
[89] Yoyutskii, S.S. 1958. *Journal of Polymer Science*. 32, 528.
[90] Keddie, J.L. 1997. *Materials Science and Engineering*. 21, 101.
[91] Eckersley, S.T., and A. Rudin. 1990. *Journal of Coatings Technology*. 62, 89.
[92] Winnik, M.A., Y. Wang, and F. Haley. 1992. *Journal of Coatings Technology*. 64, 51.

(Winnik [93] refers to this as the "crack-point MFT"). An additional criterion is also put forth by Winnik:[94] the "knife-point MFT", which is the minimum temperature that the latex shows mechanical toughness. Usually the optical MFT and the crack-point MFT are almost identical. The knife-point MFT, however, is often higher, as complete interdiffusion is required for the development of mechanical toughness. Understanding the MFT of a latex is still of great importance today, as it indicates the lowest temperature that a latex can successfully be applied; however, as recently as 1992, it was still being called "an ill-defined concept." [95]

A number of different factors affect the extent of the film formation process in a given system. Some processes tend to drive film formation whereas others resist it. The driving forces favoring particle deformation are still under rigorous debate; however, several authors consider capillary forces, polymer surface tension (in the case of dry polymer particles), and polymer-water interfacial tension as being important. Viscoelastic resistance competes with these driving forces.

In general, the film formation process for latices is very complex. Mechanisms for the processes involved are relatively unclear at this point. Two recent reviews [96,97] on the subject give excellent detail on mechanistic theories and experimental techniques to examine film formation.

2.2.6 Batch, Semi-Batch and Continuous Processes

Batch, semi-batch, and continuous processes are the three most common industrial techiniques used in emulsion polymerizations. In a batch reaction, all of the ingredients are added to the polymerization vessel at the beginning of the reaction. In a semi-batch (also known as semicontinuous or delayed addition polymerization) process, the monomer, which may or may not be emulsified, and some or all of the other ingredients are added gradually to the stirred polymerization reactor. Finally, in a continuous process, one or more reactors are utilized, and new reactants are added continuously as product continually overflows from one vessel to another.

2.3 The Historical Development of Heterogeneous Polymerization

Polymerizations of olefins were first observed as early as 1838, when bulk polymerizations were completed in the presence of either heat, light, or some catalyst. [98, 99, 100] Heterogeneous polymerization attempts began much later, and will be the focus of this chapter.

2.3.1 Synthetic Rubber

Initial efforts towards heterogeneous polymerization strategies can be credited towards attempts to produce a synthetic version of natural rubber, the product of *Hevea brasiliensis*, which has the

[93] Winnik, M.A. 1997. *Current Opinions in Colloid and Interface Science*. 2, 192.
[94] Ibid.
[95] Dobler, F., T. Pith, M. Lambla, and Y. Holl. 1992. *Journal of Colloid and Interface Science*. 152, 12.
[96] Keddie, J.L. 1997. *Materials Science and Engineering*. 21, 101.
[97] Steward, P.A., J. Hearn, and M.C. Wilkinson. 2000. *Advances in Colloid and Interface Science*. 86, 195.
[98] Hohenstein, W.P. and H. Mark. 1946. *Journal of Polymer Science*. 1, 2, 127.
[99] Regnault, F. 1828. *Annales de Chimie et de Physique.* 69, 157.
[100] Mark, H. and R. Raff, in *High Polymeric Reactions* (High Polymer Series, Vol. III). Interscience: New York, 1941.

morphology of a latex.[101,102] Seeking to produce a synthetic version of the valuable natural resource, many researchers focused their efforts on polymerization conditions that mimicked those occurring in plants; thereby avoiding high temperature and pressure reactions, and metallic catalysts. Initial patents in the area were obtained in 1909–1912 by Hoffman and Delbrück, [103] who used materials such as egg white, gelatin, starch, flour, and blood serum as colloidal stabilizers during polymerizations of diene monomers. No initiator was added in those experiments; in fact, free radicals were only produced by the dissociation of oxygen, therefore their methods required weeks to form high molecular weight polymer. Klatte and Rollet [104] and Gottlob [105] incorporated the use of continuous stirring and oxygen-liberating compounds to speed up the polymerization process.

In 1929, the first patent for the production of synthetic rubber was granted to R. P. Dinsmore, [106] an employee of the Goodyear Tire and Rubber Company, who disclosed:

> "by treating the basic unsaturated hydrocarbon from which the rubber is to be produced with an emulsifying agent so as to break up the hydrocarbon into definite globules, a product much superior to any synthetic rubber heretofore produced is obtained."

Dinsmore's polymerization technique did not include initiator, thus continuing the trend of extremely slow polymerizations; however, for the first time, the product could be vulcanized with sulfur (just like natural rubber) to impart superior performance.[107] Initiators were introduced to the field in patents awarded to Luther and Heuck [108] in 1927 and 1932.

Styrene-butadiene emulsion copolymers (commonly known as Buna S rubbers) were patented in 1933 by the German team of Tschunker and Bock,[109] and soon thereafter butadiene-acrylonitrile emulsion copolymers (Buna N rubbers) were developed. At that time, Germany was leading the way in synthetic rubber production, but the advent of war in Europe in September of 1939 brought an end to U.S. cooperation with Germany. In May of 1940, as France fell to the Third Reich, the U.S. Government realized the potential for shortages of natural rubber, a vital resource, and implemented aggressive strategies to bolster the production of synthetic rubbers by forming the Office of the Rubber Reserve Program of World War II.[110] R.F. Dunbrook[111] describes the contribution of that group in this way:

---

[101] Hohenstein, W.P. and H. Mark. 1946. *Journal of Polymer Science*. 1, 2, 127.
[102] Bovey, F.A., I.M. Kolthoff, A.I. Medalia, and E.J. Meehan. *Emulsion Polymerization*. Interscience: New York, 1955.
[103] Hoffman, F. and K. Delbrück. German Patents (1909) 250,690; (1912) 254,672; (1912) 255,129.
[104] Klatte, F. and A. Rollet. German Patent (1914) 281,688.
[105] Gottlob, K. U.S. Patent (1915) 1,149,577.
[106] Dinsmore R.P. British Patent (1927) 297,050. U.S. Patent (1929) 1,732,795.
[107] Blackley, D.C. *Emulsion Polymerization: Theory and Practice*. Applied Science Publishers: London, 1975.
[108] Luther, M. and C. Heuck. German Patent (1927) 558,890. U.S. Patent (1928) 1,864,073. *Chemical Abstracts* (1932) 26,4505. U.S. Patent (1927) 1,860,681. *Chemical Abstracts* (1932) 26, 3804; U.S. Patent (1932) 1,864,078.
[109] Tschunker, E. and W. Bock. German Patent (1933) 570,980. U.S. Patent (1933) 1,938,731.
[110] Vanderhoff, J.W., M.S. El-Aasser. "Introduction" in *Emulsion Polymerization of Vinyl Acetate*. J.W. Vanderhoff and M.S. El-Aasser, Eds. Applied Science: London, 1981.
[111] Dunbrook, R.F. "Historical Review" in *Synthetic Rubber*. G.S. Whitby, C.C. Davis, and R.F. Dunbrook, Eds. Wiley: New York, 1954.

> "The war, in necessitating the immediate production of synthetic rubber and constituent materials on a vastly accelerated and expanded scale, also made it necessary to insure that the best qualities of product should be secured and that the best processes suited to available raw materials should be rapidly advanced to an efficient and commercial state. It was necessary to accomplish in less than two years a swift expansion of the small synthetic-rubber industry to the status of a great and going essential industry, and to condense into that brief time technical and commercial developments which under normal circumstances might easily have taken twenty years or more. It was recognized that it was necessary to provide for a full and effective interchange of technical information among those private organizations having useful knowledge and experience in the various portions of the field, and also to provide a supporting framework of patent protection…"

The cooperation between industrial scientists that began when Congress implemented the U.S. Rubber Program allowed a surge in the production of rubber, and also led to a significant number of publications in the scientific literature, which had previously been scant.[112] Vanderhoff and El-Aasser[113] cite the Rubber Reserve Program (also called the Rubber Reserve Company[114]) with the "first coherent account" of the mechanism in emulsion polymerization.

The efforts of scientists working in the Rubber Program, in addition to bolstering the understanding of emulsion polymerization, also helped tremendously with the war effort. When the supply of natural rubber was compromised by Japan's occupation of Malaysia in 1942, synthetic rubber plants in the U.S. were able to increase their production more than ten fold, providing a crucial source of raw material for the U.S. during WWII.[115]

After the war, British and U.S. subcommisions were formed to identify technological developments occurring in Germany during the war. Disclosed in both the BIOS (British Intelligence Objectives Subcommission) and the US' FIAT (Field Intelligence Agency Technical) reports were the developments that had occurred in the emulsion polymerization of vinyl acetate.[116] In 1948, soon after the information contained in those reports was released, England became a producer of synthetic latex paints made from vinyl acetate.[117] Emulsion technology in the U.S. remained focused in synthetic rubbers for some time, but gradually branched outward into other monomers.

2.3.2 Classical Theories for the Mechanism of Emulsion Polymerization

Since emulsion polymerizations proceed in separate loci, the kinetics of the reaction are much different than in bulk and solution polymerizations. Emulsion polymerizations are faster than

---

[112] Hohenstein, W.P. and H. Mark. 1946. *Journal of Polymer Science*. 1, 2, 127.
[113] Vanderhoff, J.W., M.S. El-Aasser. "Introduction" in *Emulsion Polymerization of Vinyl Acetate.* J.W. Vanderhoff and M.S. El-Aasser, Eds. Applied Science: London, 1981.
[114] Bovey, F.A., I.M. Kolthoff, A.I. Medalia, and E.J. Meehan. *Emulsion Polymerization*. Interscience: New York, 1955.
[115] Dunbrook, R.F. "Historical Review" in *Synthetic Rubber*, Whitby, G.S., Davis, C.C., and Dunbrook, R.F., Eds., Wiley: New York, 1954.
[116] Dunn, A.S. "The Polymerization of Aqueous Solutions of Vinyl Acetate" in *Emulsion Polymerization of Vinyl Acetate*. J.W. Vanderhoff and M.S. El-Aasser, Eds. Applied Science: London 1981.
[117] Dunn, A.S. "The Polymerization of Aqueous Solutions of Vinyl Acetate" in *Emulsion Polymerization of Vinyl Acetate*. J.W. Vanderhoff and M.S. El-Aasser, Eds. Applied Science: London 1981.

their homogeneous counterparts, and yield polymers having much higher molecular weights. The major issues in emulsion polymerization, according to El-Aasser and Sudol,[118] involve:

> "the understanding of the processes by which latex particles form and grow, which includes the evolution of particle size (or particle number) and size distribution, the development of molar mass and molar mass distribution, and the polymerization rate profile during the course of the polymerization and how these are influenced by the basic polymerization parameters such as monomer(s), surfactant(s) type and concentration, initiator type and concentration, temperature, and mode and rate of monomer addition."

The evolution of the theory of emulsion polymerization will be presented up to the Smith-Ewart theory, which became one of the most important fundamental contributions to the field. Following the Smith-Ewart theory, brief notes will be included regarding more recent developments to emulsion theory. Later, in Chapter 5, particular attention will be focused on the emulsion polymerization of vinyl acetate.

Initial Philosophies

Although Dinsmore[119] and Luther and Heuck[120] had carried out the first true emulsion polymerizations (since they were in the presence of emulsifiers) in 1927, no authors proposed mechanisms for those polymerizations until more than 10 years had passed. According to Bovey et al.,[121] early work in the area led to independent conclusions that the latex particles were formed when the suspended droplets of monomer were initiated and polymerized in the oil phase. While this is true for suspension polymerization, it was later discovered that emulsion polymerizations proceed by a different mechanism.

Fikentsher

Fikentscher, an employee of I.G. Farbenindustrie in Ludwigshafen, proposed the then controversial notion that emulsion polymerization begins in the water phase; not in the monomer droplets. He based his theory on experimental observations of a two phase system where methyl methacrylate floated on an aqueous solution containing both soap and initiator.[122] Over time, the aqueous solution became cloudy and at the same time the volume of the monomer layer was decreasing. He reasoned that the cloudiness was due to the formation of latex particles in the aqueous phase.[123] Others argued that interfacial polymerization was occurring.

---

[118] El-Aasser, M.S. and E.D. Sudol. "Features of Emulsion Polymerization" in *Emulsion Polymerization and Emulsion Polymers*. J.W. Vanderhoff and M.S. El-Aasser, Eds. Wiley: New York, 1997.
[119] Dinsmore R.P. British Patent (1927) 297,050; U.S. Patent (1929) 1,732,795.
[120] Luther, M. and C. Heuck. German Patent (1927) 558,890. U.S. Patent (1928) 1,864,073. *Chemical Abstracts* (1932) 26,4505. U.S. Patent (1927) 1,860,681. *Chemical Abstracts* (1932) 26, 3804; U.S. Patent (1932) 1,864,078.
[121] Bovey, F.A., I.M. Kolthoff, A.I. Medalia, and E.J. Meehan. *Emulsion Polymerization*. Interscience: New York, 1955.
[122] Erbil, H.Y. *Vinyl Acetate Emulsion Polymerization and Copolymerization with Acrylic Monomers*. CRC: Boca Raton, 2000.
[123] Erbil, H.Y. *Vinyl Acetate Emulsion Polymerization and Copolymerization with Acrylic Monomers*. CRC: Boca Raton, 2000.

In 1938, Fikentscher published an article in *Angewante Chemie*[124] that discussed his observations and ideas regarding emulsion polymerization. A rough translation of the first paragraph of that paper is provided in Blackley's [125] text:

> 'On the basis of experimental evidence, we incline to the opinion that in emulsion polymerizations it is not, as is frequently assumed, the part of the vinyl compound as droplets, but it is the part dissolved in the water of the emulsion which is polymerized, and this is continually replenished from the emulsified liquid droplets, and therefore throughout the whole polymerization remains constant as long as such droplets are present.'

Unfortunately, Fikentsher was not very specific when he concluded that polymerization began in the "water phase". More specifically, it was unclear whether his notion of the water phase included micelles, or if he was referring to polymerization of monomer soluble in the aqueous phase. Due to this ambiguity, Harkins is granted credit for publishing the first viable representation for emulsion polymerization. However, as will be discussed in Chapter 5, Fikentsher's description is accurate for monomers having greater solubility in water, such as vinyl acetate.

Experimental Support for the Polymerization Not Occurring in the Monomer Droplets

One year after Fikentsher's work was published, Gee, Davies, and Melville[126] published their work on the polymerization of butadiene vapor over aqueous hydrogen peroxide. They concluded that polymerization occurred both at the interface of the dispersed monomer droplets and in the aqueous phase. However, the conditions employed were far different than those typical of emulsion polymerization.

In his article, Mark[127] cites discussions he had between 1935 and 1938 with a team of German scientists regarding the locus of emulsion polymerization. One of those scientists was Fitkentsher, whose ideas were discussed above. However, another scientist, Valko, had "considered it as highly probable that the monomer, solubilized in the micelles of the soap solution, was most favorably exposed to the action of a water-soluble catalyst and, therefore, might be considered as the principal site of the reaction."[128] Unfortunately, Valko never published these ideas.

In 1945, Price and Adams[129] observed that the reaction rate had an apparent zero order dependence on monomer concentration, leading them to the conclusion that polymerization

---

[124] Fikentsher, H. 1938. *Angewandte Chemie*. 51, 443.
[125] Blackley, D.C. *Emulsion Polymerization: Theory and Practice*. Applied Science Publishers: London, 1975.
[126] Gee, G., C.B. Davies, and W.H. Melville. 1939. *Transactions of the Faraday Society*. 35, 1298.
[127] Hohenstein, W.P. and H. Mark. 1946. *Journal of Polymer Science*. 1, 2, 127.
[128] Hohenstein, W.P. and H. Mark. 1946. *Journal of Polymer Science*. 1, 2, 127.
[129] Price, C.C., and C.E. Adams. 1945. *Journal of the American Chemical Society*. 67, 1674.

occurred in a medium of constant monomer concentration. This shifted their focus from the monomer droplet to the water phase as the primary locus of polymerization. However, their conception of the water phase was also ill-defined. Furthermore, as Corrin[130] later points out, the solubility of monomer in an aqueous soap solution changes with the soap concentration, which led to some errors in their work.

Fryling and Harrington,[131] in 1944, presented work which supported emulsion polymerizations beginning in soap micelles then later shifting to monomer-swollen polymer particles. Independently, Harkins had also been acquiring results that led him to believe the same micellar mechanism. In fact, Harkins had reported his results to the Office of the Rubber Reserve two years before Fryling and Harrington's work was published, but war-time secrecy restrictions prevented him from publishing his theories until 1945.[132] Harkins' theories will be described later in greater detail, as they offer the first thorough depiction of the mechanism of emulsion polymerization.

It should also be pointed out that a number of other contributions to the field were offered between 1910 to 1945. An excellent review of those developments is included in two reviews by Hohenstein and Mark.[133, 134]

Montroll's Phenomenological Theory

In 1945, Elliot Montroll submitted a paper which attempted to provide a mathematical basis for experimental observations of styrene emulsion polymerizations.[135] His "phenomenological theory" was one of the first to attempt to provide a mathematical basis for the complicated processes that participate in the kinetics of emulsion polymerization.

In his work, Montroll accounts for the inhibition period observed at the beginning of the reaction and also for changes in monomer droplet size with soap concentration. His theory also describes the initial increases in the reaction rate which lead up to steady state conditions.[136] Despite these noteworthy contributions, his theory has been largely ignored due to the assumptions he employed for his work:[137]

> "Since the catalysts used in styrene polymerization are generally inorganic salts insoluble in styrene, it is highly improbable that the reaction could occur inside the styrene globules. If the reaction zone were in the aqueous phase, the rate should be independent of total interface surface, which does not seem to be

[130] Corrin, M.L. 1947. *Journal of Polymer Science*. 2, 3, 257.
[131] Fryling, C.F. and E.W. Harrington. 1944. *Industrial and Engineering Chemistry.* 36, 114.
[132] Bovey, F.A., I.M. Kolthoff, A.I. Medalia, and E.J. Meehan. *Emulsion Polymerization*. Interscience: New York, 1955.
[133] Hohenstein, W.P. and H. Mark. 1946. *Journal of Polymer Science*, 1, 2, 127.
[134] Hohenstein, W.P. and H. Mark. 1946. *Journal of Polymer Science.* 1, 6, 549.
[135] Montroll, E.W. 1945. *Journal of Chemical Physics*. 13, 8, 337.
[136] Blackley, D.C. *Emulsion Polymerization: Theory and Practice*. Applied Science Publishers: London, 1975.
[137] Ibid.

> the case. When the reaction zone is at the water-styrene interface, the change in volume of a styrene globule is proportional to the surface area of the globule, or $dV/dt = -4 \pi k r^2$, where k is the proportionality constant. Since the sphere volume is given by $V = 4 \pi r^3/3$, this leads to $dr/dt = -k$, and the radius diminishes at a constant rate. This law of disappearance of monomer was observed (microscopically) in soap solutions of many organic liquids, including styrene, by Vinograd, Fong, and Sawyer. In this paper we shall consider only those reactions which occur at the interface."

Montroll's work was based on polymerization at the interface of the styrene droplet and the water phase. The argument that he presented above explained that the interface was the only reasonable locus of polymerization considering the results found by Vinograd, Fong, and Sawyer. [138] In their research, Vinograd, Fong, and Sawyer found that the diameters of oil droplets submerged in soap solutions decreased linearly with time until 99% of the oil droplets had been depleted. Unfortunately for Montroll, the diffusion process for oils in soap solutions is quite complex, and the results obtained by Vinograd, Fong, and Sawyer were not representative of all types of oil droplets in different media. Harkins and Stearns[139] later repeated Vinograd, Fong, and Sawyer's[140] experiment with ethylbenzene (instead of styrene) and found that the rate of disappearance of monomer droplets actually increased with time. After Harkins discussed this discrepancy with Debye, some expressions were developed which show that the diffusion process of oil droplets in soap solutions depend on both the diffusion constant and the thickness of the diffusion layer.[141] Montroll's argument for interfacial polymerization was therefore obsolete.

Furthermore, Montroll was incorrect to disregard the aqueous phase as a possible reaction locale. He based this reasoning on prior observations that showed: 1. that the soap concentration influenced monomer droplet size, (i.e. more soap lead to smaller droplets) and 2. that monomer droplet size influenced the polymerization rate (i.e. smaller droplets polymerized more quickly).[142] By dismissing the aqueous phase, Montroll showed that he did not consider the diffusion processes which allow oil droplets to migrate through the water phase and into micelles or polymer particles.[143]

Harkins' Theory

Harkins is widely credited with one of the most important contributions to the field, as he developed the first thorough and viable qualitative theory of emulsion polymerization. Many later theories, including the Smith-Ewart theory, are based on the phenomena that he proposes. His ideas are presented in several different publications.[144, 145, 146]

---

[138] Vinograd, J.R., L.L. Fong, and W.M. Sawyer. 1944. *Abstracts of Papers of the American Chemical Society*. 108, September 13, page 3E.
[139] Harkins, W.D. and R.S. Stearns. 1946. *Journal of Chemical Physics*. 14, 215.
[140] Vinograd, J.R., L.L. Fong, and W.M. Sawyer. 1944. *Abstracts of Papers of the American Chemical Society*. 108, September 13, page 3E.
[141] Harkins, W.D. 1950. *Journal of Polymer Science*. 5, 2, 217.
[142] Blackley, D.C. *Emulsion Polymerization: Theory and Practice*. Applied Science Publishers: London, 1975.
[143] Ibid.
[144] Harkins, W.D. 1945. *Journal of Chemical Physics*. 13, 9, 381.
[145] Harkins, W.D. 1946. *Journal of Chemical Physics*. 14, 47.

The theory, as presented in the articles, becomes increasingly correct with each subsequent article. Initially, in both of the letters, it is clear that Harkins believed that the monomer droplets were important loci for initiation. He later reversed that conclusion. In a similar manner, he developed his ideas regarding the morphology of micelles as new data became available. He initially discussed laminar micelles and later acknowledged that at the concentrations of soap present in emulsion polymerization, it is more likely that the micelles assume a spherical shape. For the purposes in this review, the ideas which will be discussed are those which he discusses in his last, and most detailed publication. Harkins' theory is based on styrene emulsion polymerization, and therefore can only represent a qualitative description of the polymerization of very hydrophobic or "ideal" monomers, such as styrene and butadiene.

An Overview of the Harkins' System

Perhaps the best way to envision the emulsion system is pictorially. Three different diagrammatic representations (
Figure 2-16,
Figure 2-17, and Figure 2-18) of the emulsion system are given. These have been taken from representations included in the work of Cowie,[147] Barton and Capek,[148] and Sudol. [149]

Micelles

At the time that his letters were published, the morphology of micelles was somewhat in question. According to X-ray analyses done by Harkins, [150, 151] Harkins, Mattoon, and Corrin, [152] and McBain, [153] micelles had a lamellar structure. However, the multi-layer structures of micelles which were initially proposed by the aforementioned researchers later fell from acceptance[154] due to further work by Harkins, Mattoon, Stearns and Corrin[155, 156] and discussions of that work with Debye. Debye and Harkins,[157] and Staudinger [158] agreed (independently) that micelles exist as individual (not multi-layered), spherical structures.

Harkins was the first to recognize that hydrophobic monomer could diffuse into micelles and be solubilized there. He suggested that micelles were an important meeting place for the solubilized monomer, and the initiator.

---

[146] Harkins, W.D. 1947. *Journal of the American Chemical Society*. 69, 1428.
[147] Cowie, J.M.G. *Polymers: Chemistry and Physics of Modern Materials*, 2nd Ed. Chapman and Hall: New York, 1991.
[148] Barton, J. and I. Capek. *Radical Polymerization in Disperse Systems*. T.J. Kemp, Translation Ed. Horwood: New York, 1994.
[149] Sudol, E.D. "Overview of Emulsion Polymerization" in *Polymer Latexes: Preparation, Characterization, and Applications*. ACS Symposium Series #492. E.S. Daniels, E.D. Sudol, M.S. El-Aasser, Eds. ACS: Washington, 1992.
[150] Harkins, W.D. 1945. *Journal of Chemical Physics*. 13, 381.
[151] Harkins, W.D. 1946. *Journal of Chemical Physics*. 14, 47.
[152] Harkins, W.D., R.W. Mattoon, and M.L. Corrin. 1946. *Journal of Colloid Science*. 1, 105.
[153] McBain, J.W. 1942. *Advances in Colloid Science*. 1, 99.
[154] Staudinger, J.J.P. 1948. *Chemistry and Industry*. 563.
[155] Mattoon, R.W., R.S. Stearns, and W.D. Harkins. 1947. *Journal of Chemical Physics*. 15, 209.
[156] Harkins, W.D., R.W. Mattoon, and M.L. Corrin. 1946. *Journal of the American Chemical Society*. 68, 220.
[157] Harkins, W.D. 1947. *Journal of the American Chemical Society*. 69, 1428.
[158] Staudinger, J.J.P. 1948. *Chemistry and Industry*. 563.

Monomer Droplets

In emulsion polymerization, agitation is used to create two phases. Monomer, being hydrophobic and generally insoluble in water is divided into spherical particles, which are stabilized by surfactant or some other emulsifier or stabilizer. These monomer droplets are much larger than the micelles. Measuring 10,000 angstroms in diameter, the monomer droplets are roughly 200 times the size of a micelle.[159] According to Erbil,[160] only about 1% of the total amount of monomer will initially be solubilized in the micelles. This solubilization leads to swelling of the micelles, which initially measure 40-50 angstroms in diameter, and swell to 60–100 angstroms.[161]

For Harkins' theory, it is important to note that monomer that is soluble in the water phase is ignored. This is a fair approximation for hydrophobic monomers. Only 0.04% of styrene can be dissolved by water.[162]

Water Phase

Technically, the micelles are included in Harkins' description of the water phase, but because they are of great importance in the polymerization, they will be considered separately. Otherwise, the water phase contains only water and molecules that are dissolved in it.

Initiator

The initiator is a water-soluble molecule which breaks down into free radicals, as described earlier.

[159] Erbil, H.Y. *Vinyl Acetate Emulsion Polymerization and Copolymerization with Acrylic Monomers*. CRC: Boca Raton, 2000.
[160] Ibid.
[161] Ibid.
[162] Erbil, H.Y. *Vinyl Acetate Emulsion Polymerization and Copolymerization with Acrylic Monomers*. CRC: Boca Raton, 2000.

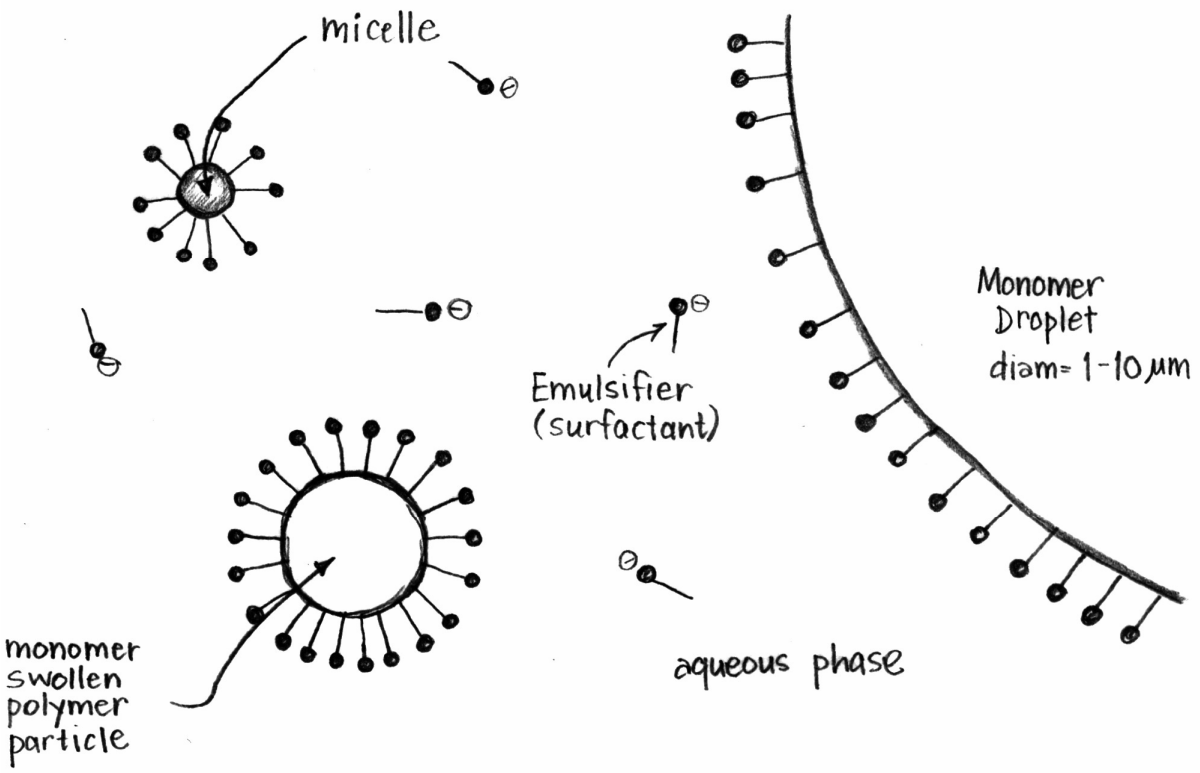

Figure 2-16: An illustration depicting Cowie's vision of the emulsion system.[163]

[163] Cowie, J.M.G. *Polymers: Chemistry and Physics of Modern Materials*, 2nd Ed. Chapman and Hall: New York, 1991.

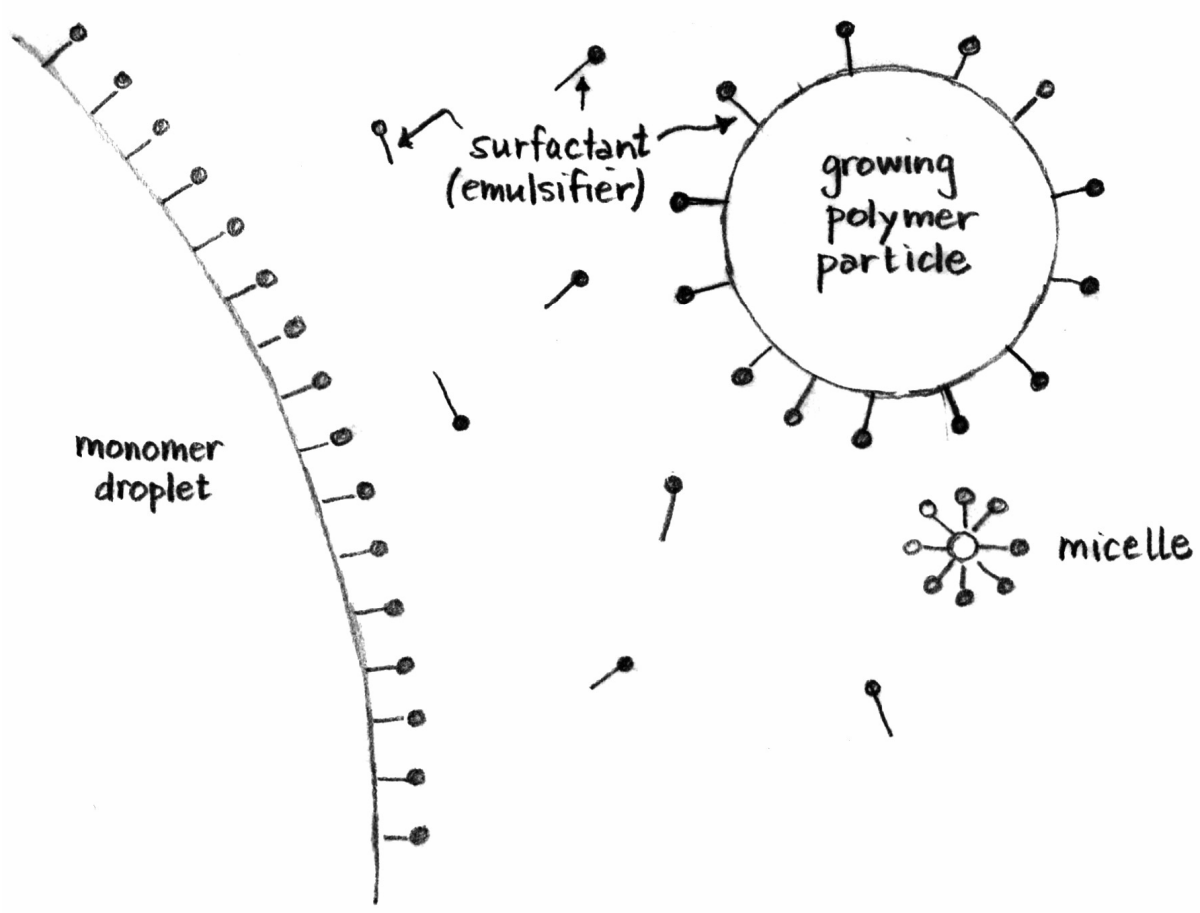

Figure 2-17: An illustration representing Barton and Capek's vision of the emulsion system.[164]

[164] J. Barton and I. Capek. *Radical Polymerization in Disperse Systems*. T.J. Kemp, Translation Ed. Horwood: New York, 1994.

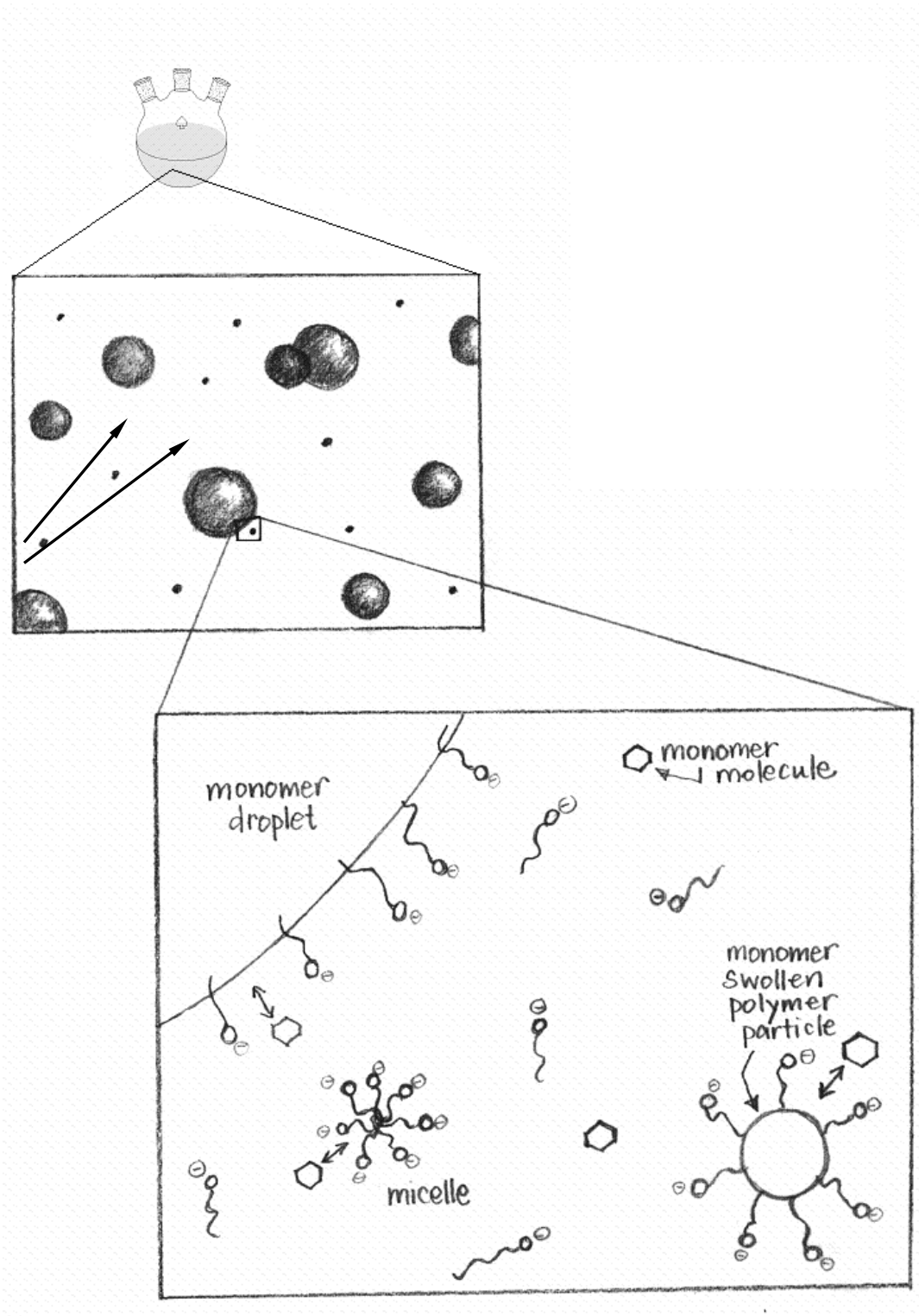

Figure 2-18: An illustration representing Sudol's vision of an emulsion system.[165]

[165] Sudol, E.D. "Overview of Emulsion Polymerization" in *Polymer Latexes: Preparation, Characterization, and Applications*. ACS Symposium Series #492. E.S. Daniels, E.D. Sudol, M.S. El-Aasser, Eds. ACS: Washington, 1992.

The Initial Locus of Polymerization

Prior to his work, two theories existed regarding the initial locus of polymerization in emulsions:

1. The monomer droplet itself polymerizes at the interface (as put forth by Montroll)
2. Initiation occurs in the "aqueous phase", like Fikentsher had earlier proposed. However, Fikentsher did not define the aqueous phase very clearly.

Harkins agreed with Fikentscher's hypothesis that the locus of polymerization is in the aqueous phase, however, he goes one step further, saying that the precise location of initiation is in soap micelles. This notion was based on titrations of the aqueous phase with increasing polymer conversion. Harkins[166] noted that soap disappeared from the aqueous phase with increasing conversion:

> "These facts suggested to the writer that an early locus of polymerization is in the soap micelles and that this is shifted to the polymer particles as the yield increases."

Harkins states that polymerization begins in the monomer-swollen micelle when a free radical enters. It quickly reacts with monomer to produce a monomer radical. Within the micelle, the monomer radical continues to propagate by reacting with more and more monomer molecules. Meanwhile, the supply of monomer is continually replenished via diffusion from the surfactant stabilized monomer droplets, allowing the chain reaction to continue, and polymer molecules form. Once initiation begins, the molecular weight of the polymer begins to grow very rapidly.

The Shift in Polymerization Locus and the Disappearance of Micelles

At some point, the polymer chain becomes so large that it outgrows the micelle, and is "ejected". It then requires additional emulsifier, surfactant, or stabilizer to hold it in solution, so it adsorbs soap from the water phase. As this process occurs for many polymer chains, the soap concentration in the water phase falls below its critical micelle concentration (CMC). To remedy the problem, inactive micelles, (those in which no initiation or growth is occurring) readily disassociate in solution, allowing soap to be adsorbed to support growing, monomer-swollen polymer particles. At about 10-20% conversion, depending on the system, all of the soap that had been in micelles is either adsorbed by polymer particles, or has dissolved in the water phase, so that no micelles remain. (It is interesting to note that at this point, the reduced amount of molecularly dissolved soap has effectively raised the surface tension of water, implying that agitation is necessary to prevent the coalescence of polymer particles.[167])

According to his theory, monomer continues to diffuse from the monomer droplets (which are gradually decreasing in size) to either the micelles or the polymer particles for quite some time (until conversion is very high).

The Swelling of the Polymer Particles by Monomer

Most monomers are good solvents for their polymer. Flory-Huggins theory describes the thermodynamic driving force for swelling of polymers by a suitable solvent. The free energy of

[166] Harkins, W.D. 1947. *Journal of the American Chemical Society*. 69, 1428.
[167] Ibid.

mixing, ΔG_{mix}, has both enthalpic (H) and entropic (S) components, as shown in Equation(2-16).[168]

$$\Delta G_{mix} = \Delta H_{mix} - T\,\Delta S_{mix} \quad (2\text{-}16)$$

In small particles, polymer – solvent mixing is described by the following relation:

$$\ln \phi_m = \left(\frac{1}{j} - 1\right)\phi_p - \chi\,\phi_p^2 - \frac{2\,\overline{V}_m\,\gamma}{R\,T\,r_p} \quad (2\text{-}17)$$

where ϕ_m and ϕ_p represent the volume fraction of monomer and polymer, j represents the degree of polymerization, χ represents the Flory-Huggins interaction parameter between polymer and monomer, V_m is the partial molar volume of the monomer, γ is the interfacial tension between the particle and the medium, and r_p is the radius of the polymer particle. In Equation (2-17), the last term represents the resistance to swelling as the radius of the particle decreases. As the particle becomes smaller, there is less surface area, and therefore, the volume fraction of monomer that swells the polymer, ϕ_m, decreases. Also, when the interfacial tension is higher, the polymer will not swell as much.

During the polymerization, the rate of diffusion of monomer into the polymer particles is usually very fast as compared to the rate of monomer consumption. Therefore, the polymer particles are essentially fully swollen at all times (until the monomer droplets are depleted).

The Disappearance of the Monomer Droplets

Finally, at around 50 – 85% conversion, all of the monomer droplets are depleted, leaving only a small quantity of monomer in the polymer particles.

Summarizing the Developments of Harkins' Theory

The essential features of Harkins' micellar model are well-stated by Barton and Capek:[169]

- An appreciable amount of the soap/surfactant/emulsifier exists in the form of micelles
- The principle locus of polymerization is the monomer-swollen micelle (early stages) and the monomer-swollen polymer particle (later stages).
- Monomer droplets serve as reservoirs; negligible quantities of polymer are formed in the emulsified monomer droplets.
- Growth of the polymer particles results in particles with larger surface area. This growth occurs via consumption of monomer which continually diffuses

168

169 Barton, J. and I. Capek. *Radical Polymerization in Disperse Systems*. T.J. Kemp, Translation Ed. Horwood: New York, 1994.

from the monomer droplets, through the water phase, and into the polymer particles.

- The growing polymer particles continually adsorb soap/surfactant/emulsifier from the water phase, leading to the disappearance of micelles at relatively low conversion.
- Monomer droplets eventually disappear as they are depleted, usually at intermediate conversions.
- The rate of polymerization is proportional to the initial concentration of soap/surfactant/emulsifier.
-

Comments on Harkins' Theory

Generally, Harkins' theory is regarded to be true for "ideal" cases.[170] Monomers that are insoluble in the polymerization medium, which is usually water, are considered to be ideal. The best examples of ideal monomers are styrene and butadiene. Harkins' theory does not account for cases where the monomer is somewhat water-soluble. For these monomers, some initiation and propagation can both occur in the aqueous media, thereby diminishing the importance of micelles as the meeting place for monomer and initiator in Harkins' theory. This mechanism is known as homogeneous nucleation, and will be discussed later.

The second criterion of ideality that Harkins does not consider is that the polymer must be miscible in its monomer in all proportions.[171] Exceptions to that condition include acrylonitrile, vinyl chloride, and vinylidene chloride. For these monomers, polymerization initially proceeds as Harkins describes. The deviation occurs when the monomer is not able to swell the stabilized polymer particles that have formed. This essentially limits polymerization to monomer which can adsorb to particles' surfaces, thereby limiting the available concentration of monomer which results in a drastic decrease in the polymerization rate. Since the monomer is not used up as quickly, it remains in large, unstable droplets. These droplets coalesce into even larger droplets which further limit the rate of reaction, as diffusion limited by the lower surface area. Eventually, the polymer particles do grow in size, and as they become larger, collisions with the large monomer droplets become more likely. Collisions serve to disperse the monomer and promote diffusion and adsorption, thereby increasing the reaction rate for a short period of time.

Contemporaries of Smith and Ewart

Before the theory of Smith and Ewart (1948) is explained, two theories proposed by their contemporaries will be noted. The first is that of Corrin[172] (1947), and the second is that of Haward,[173] published in 1949. Both authors note the similarities between the rate of polymerization observed for styrene emulsion polymerization and that in the bulk.

---

[170] Duck, E.W. "Emulsion Polymerization" in *Encyclopedia of Polymer Science and Technology*, Volume 5. Wiley: New York, 1966.
[171] Ibid.
[172] Corrin, M.L. 1947. *Journal of Polymer Science*. 2, 3, 257.
[173] Haward, R.N. 1949. *Journal of Polymer Science*. 4, 273.

Corrin's Theory

Corrin investigated the kinetics of styrene emulsion polymerization during the period when polymerization occurs predominantly in the polymer particles. That is, he studied the kinetics after the micelles had been depleted, and thus, the nucleation of new particles was not considered. This stage of the reaction can be divided into two different components. In the first, monomer droplets exist as a separate phase, and in the second, the monomer droplets have been depleted so that any monomer present is likely found in the polymer particles. Corrin treats the second case as a bulk phenomenon, proposing the rate of monomer consumption to be:

$$\frac{-d[M]}{dt} = k[M]^{\frac{3}{2}} \quad (2\text{-}18)$$

where k is a constant, and $[M]$ is the monomer concentration at some time, t. Integration between t and t_o (the time at which the separate monomer phase just disappears) gives:

$$\frac{1}{\sqrt{[M]}} - \frac{1}{\sqrt{[M_0]}} = \frac{k}{2}(t - t_0) \qquad (2\text{-}19)$$

where $[M_0]$ is the concentration of monomer at time t_0. Substituting for the percent conversion, Y, where $[M]=(100\text{-}Y)/Y$, we obtain:

$$t = t_0 + \frac{2}{k}\left\{\sqrt{\left(\frac{Y}{100-Y}\right)} - \sqrt{\left(\frac{Y_0}{100-Y_0}\right)}\right\} \qquad (2\text{-}20)$$

Equation 4-5 indicates that a plot of t versus the square root of (Y /(100-Y) should be linear. According to Corrin's experimental data, the plot is linear, indicating his theory was correct. Furthermore, the slope of that line gives k, the rate constant.

Corrin also develops some equations to represent the kinetics of the emulsion polymerization between the time when micelles disappear to the time when the separate monomer phase disappears. For the sake of brevity, this development will not be described. His theoretical predictions again fit experimental data quite nicely. However, Blackley[174] argues that the theoretical basis for those equations was not clearly presented, and his own attempts to provide the theoretical derivation fail. In general, Corrin's contributions were largely overshadowed by the developments presented in the Smith-Ewart theory, which provide kinetic expressions for the rate of polymerization over all ranges of conversion.

[174] Blackley, D.C. *Emulsion Polymerization: Theory and Practice*. Applied Science Publishers: London, 1975.

Haward's Theory

In 1949, just after Smith and Ewart's theory had been published, Haward[175] put forward a paper suggesting that the rate of polymerization in discrete systems is similar to that observed in bulk polymerizations, but is impacted by "compartmentalization". To develop this idea of compartmentalization, Haward defines a "critical drop" which is the dimension of a spherical volume of monomer which contains only one active center. According to his calculations for various monomers, the critical drop size ranges from 0.1 - 1 μm, which corresponds to colloidal dimensions. Therefore, according to Haward, [176] compartmentalization of the active center into droplets should be expected to affect the kinetics of the reaction:

> "Clearly a polymerization system dependent on a bimolecular termination process cannot be indefinitely subdivided without causing drastic alterations in the mode and character of the reactions."

Under bulk conditions, the rate of termination is much lower than that of propagation. In a typical bulk polymerization, the rate of termination is presented in Equation (2-21).

$$R_{t\ bulk} = 2\,k_t\left[M^*\right]^2 \qquad (2\text{-}21)$$

However, the termination process changes profoundly when the reaction is limited to a small volume. When a growing polymer radical is compartmentalized, the concentration of the growing radical is relatively high. Thus, when a second radical enters the small chamber, it takes very little time for it to "find" the growing radical and to terminate. The lifetime of radicals are expressed by Haward as τ. In essence, the first radical lives until a second radical enters. Termination occurs instantaneously, so the lifetime of the second radical inside of the particle is neglected. Small particles only contain one or zero radicals, leading to "zero-one" kinetics.

If ρ_a, the rate of entry of radicals into the particles, is high then the average number of radicals per particle, n, is ½. This is approximately true for ideal monomers, where chain transfer processes are insignificant, and termination is only due to combination. (Later it was discovered that for other monomers where chain transfer does occur, this transfer reaction provides a means for a radical to "escape" from the particle, which influences kinetics.)

The rate of growth of a radical was found to be equal to the expression in Equation (2-22) for the case of compartmentalization.

$$r_p = k_p\left[M\right]_p \qquad (2\text{-}22)$$

In the expression, k_p is the rate constant of propagation and $[M]_p$ is the equilibrium concentration of the monomer swelling the latex particle. Allowing N to represent the number of latex particles per unit volume of the aqueous phase, the rate of polymerization per unit of water is expressed in Equation (2-23), where N_A is Avogadro's number.

[175] Haward, R.N. 1949. *Journal of Polymer Science*. 4, 273
[176] Ibid.

$$R_p = \frac{\bar{n}\, N\, k_p \left[M\right]_p}{N_A} \qquad (2\text{-}23)$$

Similar to Smith and Ewart, Haward considered several different "cases" for active center compartmentalization. In the simplest case, the particle volumes are small and one active center exists per drop. Active centers can then diffuse into the drops and terminate within the drops thereby influencing the kinetics of the polymerization.

Several interesting results come out of Haward's theory, which are also seen in the Smith-Ewart theory:

1. at any time, approximately one half of the droplets contain an active center while the other half do not
2. the overall rate of polymerization increases proportionally to the number of droplets present, and
3. the degree of polymerization increases proportionally to the number of droplets present.

Haward bases his theory on the observations of several authors, but he does not clearly define the mechanism(s) causing the compartmentalization effect or how it differs from a viscosity effect (also known as "diffusion control") which had been shown[177, 178, 179] to limit the rate of termination during polymerizations involving discrete particles:[180]

> "diffusion control can operate in the same way as the compartmentalization effect in emulsion polymerization, and it is not easy to distinguish between the two processes."

Furthermore, the compartmentalization effect is based on the kinetics of a bulk polymerization, thereby limiting its applicability to emulsions. Most notably, as Blackley[181] points out, Haward's theory does not offer a means of calculating the degree of compartmentalization for emulsions, nor does it show how compartmentalization impacts the individual rate constants for free-radical polymerizations. The Smith-Ewart theory seems to incorporate many of these principles while providing direct applicability to emulsions and also indicating how various steps in the free radical polymerization will be impacted.

---

[177] Norrish, R.G.W. and R. R. Smith. 1945. *Nature*. 156, 661.
[178] Melville, H.W. 1946. *Nature*. 158, 553.
[179] Haward, R.N. 1948. *Journal of Polymer Science*. 3, 10.
[180] Haward, R.N. 1949. *Journal of Polymer Science*. 4, 273.
[181] Blackley, D.C. *Emulsion Polymerization: Theory and Practice*. Applied Science Publishers: London, 1975.

Smith-Ewart Theory

Being perhaps the most noted theory of emulsion polymerization, Smith and Ewart's contributions warrant a detailed discussion. In their work, Smith and Ewart consider the kinetics of free radical polymerization in attempts to provide a rational explanation for the high molecular weight that can be produced over relatively short time periods in emulsion polymerization.

The basis for Smith and Ewart's work is primarily that of Harkins, and the "ideal" emulsion system. Several of the criteria for ideality were already discussed in Harkins' theory; however, Smith and Ewart,[182, 183] along with Haward,[184] introduced more specific conditions for their "ideal" polymerizations. These are well stated by Erbil: [185]

- The monomer is completely insoluble in water
- Initiator is only soluble in water (completely insoluble in monomer)
- No inhibitors are present
- No retarders or chain-transfer agents are present
- Colloidal stabilizers and electrolytes have no effect on kinetics, and
- Agitation rate is constant throughout the polymerization

Smith and Ewart, like Harkins, assume that the initiation of a polymer chain occurs in the monomer-swollen micelles (although they do differentiate between a micelle and a particle by stating that once initiation occurs the micelle has been "lost" and a polymer particle has been "gained"). In addition, they assume that the monomer-swollen polymer particles are stabilized by adsorbed soap, and that as they continue to grow, they adsorb more and more soap.

Differentiating their work from that of Harkins is the inclusion of the concept that the amount of free radicals generated by the initiator is in excess, and that free radicals could diffuse into and out of various polymer particles over the course of the reaction. Their approach to gaining an understanding of emulsion polymerization kinetics is to first determine the rate of polymerization that occurs in an individual monomer-swollen polymer particle and then to determine how many such particles exist. The overall rate is then expressed by the product of those two quantities. Equation (2-23), shown previously in Harkins work, was derived by Smith and Ewart in greater detail than by Harkins, and has actually become known as the "Smith-Ewart equation."

In determining the rate of polymerization in a single polymer particle, three simplifying cases were developed, all of which include a number of relevant factors, such as: the rate of formation of free radicals, the rate of escape of free radicals from polymer particles, rates of termination of free radicals in the polymer particles and the aqueous phase, and the rate of polymerization of a free radical in a polymer particle. The three different cases relate to the average number of free radicals present in each per polymer particle. In Case I, the number is much less than one, in Case II, the number is approximately one half, and in Case III the number is close to one.

---

[182] Smith, W.V. and R.H. Ewart. 1948. *Journal of Chemical Physics*. 16(6), 592.
[183] Smith, W.V. 1948. *Journal of the American Chemical Society*. 70(11), 365; 1949. *Journal of the American Chemical Society*. 71, 4077.
[184] Haward, R.N. 1949. *Journal of Polymer Science*. 4, 273.
[185] Erbil, H.Y. *Vinyl Acetate Emulsion Polymerization and Copolymerization with Acrylic Monomers*. CRC: Boca Raton, 2000.

Derivations for each of the three cases are presented in the Appendix. The derivation results showing the rate of polymerization for each of the three cases is given below.

Rate of Polymerization, Average Lifetime of a Particle

Case I: Termination in the Polymer Particle

$$\frac{dM}{dt} = \frac{k_p\,[M]\,\rho\,v}{k_o\,a} = k_p\,[M]\sqrt{\frac{R_{tp}\,N\,v}{2\,k_o\,a}} = k_p\,[M]\sqrt{\frac{R_{tp}\,V}{2\,k_o\,a}} \qquad (2\text{-}24)$$

$$T = \frac{n_1}{\frac{2\,\rho^2\,v}{k_o\,N\,a}} = \frac{N}{2\,\rho} = \sqrt{\frac{V}{2\,k_o\,a\,R_{tp}}} \qquad (2\text{-}25)$$

Case I: Termination in the Aqueous Phase

$$\frac{dM}{dt} = k_p\,[M]\;V\,\alpha\sqrt{\frac{R_{ta}}{2\,k_{ta}}} \qquad (2\text{-}26)$$

$$T = \frac{c_p\,V}{2\,k_{ta}\,c_w{}^2} = \frac{a\,V}{2\,k_{ta}\,c_w} = \frac{a\,V}{\sqrt{2\,k_{ta}\,R_{ta}}} \qquad (2\text{-}27)$$

Case II:

$$\frac{dM}{dt} = \frac{k_p\,[M]\,N}{2} \qquad (2\text{-}28)$$

$$T = \frac{N}{\rho} \qquad (2\text{-}29)$$

Case III:

$$\frac{dM}{dt} = k_p\,[M]\,N\,n = k_p[M]\sqrt{\frac{\rho\,N\,v}{2\,k_t}} = k_p\,[M]\sqrt{\frac{\rho\,V}{2\,k_t}} \qquad (2\text{-}30)$$

$$T = \frac{n}{\frac{2\,k_t\,n^2}{v}} = \sqrt{\frac{N\,v}{2\,k_t\,\rho}} = \sqrt{\frac{V}{2\,k_t\,\rho}} \qquad (2\text{-}31)$$

In addition to deriving rate equations in great detail for three different conditions, Smith and Ewart also derived relationships to calculate upper and lower limits for the total number of polymer particles, *N*.

Too Many Loci:

$$N \cong 0.53\, \mu^{\frac{-2}{5}}\, a_s\, \rho^{\frac{2}{5}}\, S^{\frac{3}{5}} \qquad (2\text{-}32)$$

Too Few Loci:

$$N = 0.370\, \mu^{\frac{-2}{5}}\, a_s^{\frac{3}{5}}\, \rho^{\frac{2}{5}}\, S^{\frac{3}{5}} \quad (2\text{-}33)$$

Conclusions about the Smith-Ewart Theory

Considering the expressions Smith and Ewart developed for *N*, shown in Equations (2-32) and (2-33) it is notable that the difference between the two extremes (*N* being either too high or too low) is surprisingly small, and is limited to the leading constant. Substitution of these results back into the appropriate rate of polymerization equation (by appropriate it is meant that one of the three different cases that was developed, either Case I, II or III should be selected depending on conditions) would replace the numerical constants of 0.37 or 0.53 with a coefficient χ, where χ has values between 0.37 and 0.53.

Of the greatest interest is Case II, as the results of these calculations were consistent with the experimental observations of the emulsion polymerization of styrene. Considering then the Case II results, shown in Equation (2-28), and the results of the derivations for *N* discussed above, the overall rate of polymerization predicted by Smith and Ewart would be:

$$\frac{dM}{dt} = \frac{k_p[M]N}{2} = \frac{\chi}{2} k_p[M]\mu^{\frac{-2}{5}} a_s^{\frac{3}{5}} \rho^{\frac{2}{5}} S^{\frac{3}{5}} \qquad (2\text{-}34)$$

where k_p is the rate constant for propagation, [*M*] is the monomer concentration at the polymerization locus, χ is a constant having values between 0.37 and 0.53, μ is the rate of growth of particles during nucleation (assumed to be constant), a_s is the area that a unit mass of soap occupies (constant for a certain soap), ρ is the rate at which radicals enter micelles or particles, and *S* is the total mass of surfactant (fixed for a given polymerization).

From this expression, one can conclude that the steady state rate of polymerization should be:[186]

- Zero order with respect to the concentration of monomer.
- 2/5 order with respect to initial initiator concentration

[186] Blackley, D.C. *Emulsion Polymerization: Theory and Practice*. Applied Science Publishers: London, 1975.

- 3/5 order with respect to the concentration of the soap, and when the rate of polymerization is considered per unit mass of soap, then the rate should be inversely proportional to the $2/5^{th}$ power of the concentration of the soap.

These predictions for rate dependencies were later verified independently by Bartholome et al.[187] for styrene, but discrepancies were noted for other monomers.

In their theory, Smith and Ewart neglected to consider the effect of electrolyte and the valence of counterions, both of which can influence the number of particles, *N*, and lead to deviations in certain experimental conditions.[188,189] Furthermore, they made some incorrect assumptions about a_s, the area of an emulsifier molecule at the polymer-water interface. They assumed that it would be the same as it is for the air-water interface and that it would be unaffected by the presence of monomers or other swelling agents. These assumptions were later found to be incorrect.[190]

Discussion and Later Developments of the Smith-Ewart Theory

Stockmayer,[191] in 1957, offered alternative solutions to Smith and Ewart's recursion formula, thereby allowing the distribution of radicals among particles to be calculated for particles of intermediate size. Previously the solution had only been given for either large or small particles. His solution is only valid in cases where the steady state assumption applies (i.e. during Interval II). Kaichi[192] gives an approximate solution to the problem before a steady state condition applies (Interval I).

Like Stockmayer,[193] O'Toole[194] presents alternative expressions for the distribution of radicals per particle where it is assumed that radicals can leave the particles, but he presents the derivations in greater detail. Furthermore, he comments that while the solutions that both he and Stockmayer attain are mathematically correct, they are meaningless in a physical sense unless one can assume that radicals are exchanged with the aqueous phase. O'Toole also follows Haward's[195] derivations and extends them to conditions that are more physically applicable, attaining similar conclusions.

Parts et al.[196] developed theories, based on the work of Smith and Ewart, to explain the nucleation of polymer particles and at the same time, the disappearance of micelles. They derived a rate expression which reaches a maximum when the micelles disappear from solution, a phenomena also found by Parts and Moore,[197] and Vanderhoff.[198,199] Parts et al. also

[187] Bartholome, E., H. Gerrens, R. Herbeck, and H.M Weit. 1956. *Zeitschrift fuerElektrochemie*. 60, 334.
[188] Dunn, A.S., and Z.F. Said. 1982. *Polymer*, 23, 1172.
[189] Blackely, D.C. and A.R.D. Sebastian. 1989. *British Polymer Journal*. 21, 313.
[190] Piirma, I. and S.R. Chen. 1980. *Journal of Colloid and Interface Science*. 74, 90.
[191] Stockmayer, W.H. 1957. *Journal of Polymer Science*. 24, 314.
[192] Kaichi, S. 1956. *Bulletin. Chemical Society of Japan*. 29, 241.
[193] Stockmayer, W.H. 1957. *Journal of Polymer Science*. 24, 314.
[194] O'Toole, J.T. 1965. *Journal of Applied Polymer Science*. 9, 1291.
[195] Haward, R.N. 1949. *Journal of Polymer Science*. 4, 273.
[196] Parts, A.G., D.E. Moore, and J.G. Watterson. 1965. *Makromolekulare Chemie.* 89, 156.
[197] Parts, A.G. and D.E. Moore. 1962. *Journal of Oil Colour Chemists' Association*. 45, 648.

introduced the parameter γ, an arbitrary factor by which the partitioning of radicals into micelles is reduced. Since polymer particles are unaffected by γ, its inclusion signifies increasing numbers of radicals entering growing polymer particles, thereby reducing the number of growing particles and increasing the number of dormant particles to meet Smith-Ewart's Case II criterion (½ of the particles are growing, ½ are "dead" or dormant).

Napper and Parts[200] investigated both the Smith-Ewart theory and the work of Stockmayer and developed equations for the instantaneous rate of polymerization at any stage of the reaction.

Ugelstad et al. [201] offered contributions to O'Toole and Stockmayer's work by assuming that, in addition to radicals being able to leave the particles, they can also re-enter. They provide derivations useful for calculating the average number of radicals per particle and also provide simplified expressions when this number is low.[202]

Gardon's Theory

Some of the most notable improvements to the Smith-Ewart theory were provided by Gardon in 1968-1971.[203, 204, 205] First, he thoroughly reviewed the Smith-Ewart theory and confirmed most of its findings. Then he proposed that the radicals entered the particles through collisions (with the particle) instead of diffusion, which had been postulated by Smith and Ewart. Gardon divided the polymerization into three different "stages". Stage one corresponds to the period of particle nucleation, which abruptly ends before stage two commences. During stage two, the monomer still exists in a dispersed phase, separate from the particles, and finally, in stage three the monomer is no longer present as a separate dispersed phase. Therefore, during stage three, polymerization involves only the monomer that is present in the monomer-swollen particles.

Theoretically, Gardon defined three new parameters, K, R, and S where K is the volume growth rate of the particle, R is the number of radicals (per second) produced by decomposition of the initiator (per unit of aqueous phase), and S is the total area that a surfactant molecule occupies in a monolayer at the polymer-water interface. Equations defining each of the parameters is given in Equation Scheme (2-35).

---

[198] Vanderhoff, B.M.E. *Symposium on Polymerization and Polycondensation Processes*, *Advances in Chemistry Series,* Volume 34. American Chemical Society: Washington, D.C., 1962.
[199] Parts, A.G., D.E. Moore, and J.G. Watterson. 1965. *Makromol. Chem*. 89 156.
[200] Napper, D.H. and A.G. Parts. 1962. *Journal of Polymer Science*. 61,113.
[201] Ugelstad, J., P.C. Mork, and J.O. Aasen. 1967. *Journal of Polymer Science*. A-1, 5, 2281.
[202] Ibid.
[203] Gardon, J.L., 1968. *Journal of Polymer Science*. A-1, 6(3), 623, 648, 665, and 687.
[204] Gardon, J.L., 1968. *Journal of Polymer Science*. A-1, 6(9), 2853, and 2859.
[205] Gardon, J.L., 1971. *Journal of Polymer Science*. A-1, 9, 2763.

$$K = \frac{dr^3}{dt} = \frac{\frac{3}{4}\frac{k_p}{N_A}\frac{\rho_m}{\rho_p}\phi_m}{1-\phi_m}$$

$$R = 2N_A k_d [I] \qquad (2\text{-}35)$$

$$S = N_A A_s \left([E] - [E_{CMC}]\right)$$

In this scheme, r is the particle radius, k_p is the rate constant for the propagation of monomer, N_A is Avogadro's number, r_m and r_p are the densities of monomer and polymer, ϕ_m is the volume fraction of monomer in the swollen polymer particle, $[I]$ is the concentration of initiator, A_s is the interfacial area occupied by one molecule of soap at the polymer-water interface, E is the concentration of surfactant, and the subscript $_{CMC}$ indicates the critical micelle concentration.

Gardon used those terms to define the number of latex particles, N as:

$$N = 0.208 S^{\frac{3}{5}} \left(\frac{R}{K}\right)^{\frac{2}{5}} \qquad (2\text{-}36)$$

He then assumed that the average number of active radicals per particle was approximately one half (analogous to Case II of Smith-Ewart theory), and obtained an expression for the rate of polymerization, as shown in Equation (2-37):

$$R_p = \frac{k_p N [M]_p}{2N_A} \quad (2\text{-}37)$$

where M_p is the equilibrium concentration of monomer in the swollen polymer particles. Gardon also provided derivations for the root mean cube radius and the average molar mass of polymer produced in stage two of the polymerization. Results are shown in Equation (2-38). In the first equation, m/w is the mass ratio of monomer to water.

$$r_{rmc} = 1.05 \left(\frac{m}{w}\right)^{\frac{1}{3}} \left(\frac{\rho_w}{\rho_p}\right)^{\frac{1}{3}} \frac{1}{S^{\frac{1}{5}}} \left(\frac{K}{R}\right)^{\frac{2}{15}}$$

$$M_n = \frac{k_p \phi_m N \rho_m}{R} \qquad (2\text{-}38)$$

Gardon also published some selected values for these parameters (*K*, *R*, *S*) for various monomers. Experiments run by Dunn and Al-Shahib [206] initially verified Gardon's work, but later Dunn suggested that Gardon's work may have only seemed correct due to a "compensation of errors."[207] The collision (Gardon) vs. diffusion (Smith and Ewart) theory for the mechanism of radical entry has been debated with no clear result prevailing. As examples of this continuing debate, Fitch and Shih [208] found that the diffusion theory fit their data more appropriately whereas Kao et al. [209] found the opposite.

2.3.3 Particle Nucleation Mechanisms in Emulsion Polymerization

Micellar Nucleation

The micellar nucleation model is that which was initially envisioned by Harkins and later developed mathematically by Smith and Ewart. Derivations showing the development of the Smith-Ewart model are included in the Appendix of this chapter.

Several problems have been found with this model of nucleation, as it is presented in the Smith-Ewart theory. These are noted by Hansen and Ugelstad:[210]

1. Polymer particles are formed even if no surfactant (micelles) is present, indicating it cannot be the sole means of nucleation;
2. Smith-Ewart theory predicts that the number of particles will be twice what has been found experimentally;
3. Monomers having greater solubility in water do not fit the predicted results; and
4. Smith-Ewart theory predicts a maximum in the polymerization rate at the end of the nucleation period, and this phenomena has not been observed experimentally.

Developments in the literature which noted these discrepancies led to the development of other nucleation models. One of these was the homogeneous nucleation model. In 1971, Fitch and Tsai [211] were the first to develop mathematical representations of the model.

Homogeneous Nucleation

In homogeneous nucleation, the active center, which is formed through the dissociation or reaction of the initiator, reacts with water-soluble monomer in the aqueous phase. Eventually, the oligomeric chain reaches some critical molecular weight, where it phase separates from the water and forms a particle. This process is depicted Figure 2-19, which appears in the text of Fitch.[212]

---

[206] Dunn, A.S. and W.A. Al-Shahib. 1978. *British Polymer Journal*. 10, 137.
[207] Dunn, A.S. "Harkins, Smith-Ewart and Related Theories" in *Emulsion Polymerization and Emulsion Polymers*. P.A. Lovell, M.S. El-Aasser, Eds. Wiley: Chichester, 1997.
[208] Fitch, R.M. and L. Shih. 1975. *Progress in Colloid and Polymer Science*. 56, 1.
[209] Kao, C.I., D.P. Grundlach, and R.T. Nelsen. 1984. *Journal of Polymer Science, Polymer Chemistry*. 22, 3499.
[210] Hansen, F.K. and J. Ugelstad. "Particle Formation Mechanisms" in *Emulsion Polymerization*. I. Piirma, Ed. Academic Press: New York, 1982.
[211] Fitch, R.M and C.H. Tsai. In *Polymer Colloids, Proceedings*. R.M. Fitch, Ed. Plenum Press: New York, 1971.
[212] Fitch, R.M. 1997. *Polymer Colloids: A Comprehensive Introduction*. R.M. Fitch, Ed. Academic Press: San Diego, 1997.

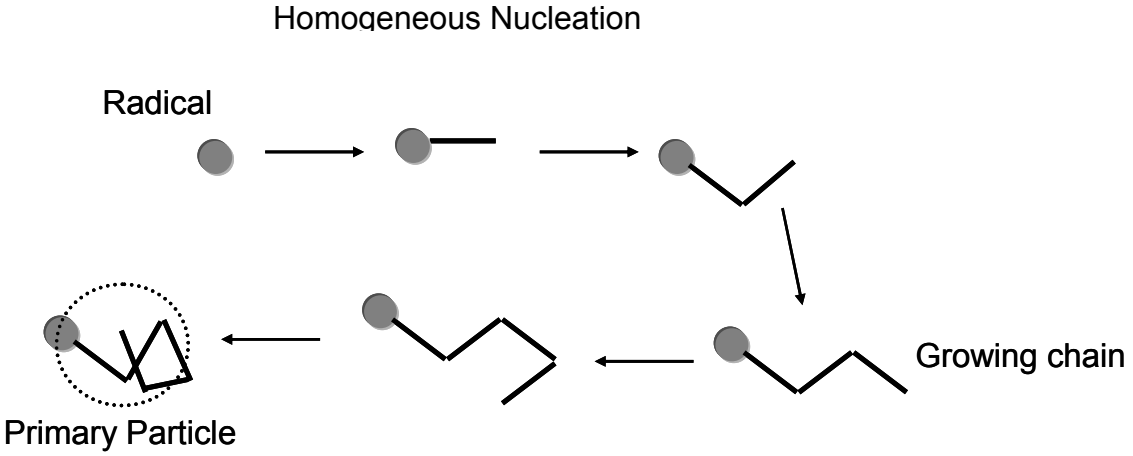

Figure 2-19: The circular group represents the initiator fragment and the other line segments indicate bonds between repeat units. Eventually, the oligomer precipitates and forms a new polymer particle. Figure similar to that in the text of Fitch.

The formation of this second phase (the particle) requires some additional free energy, as a new interface has been formed. The required amount of energy is given in Equation (2-39):[213]

$$\Delta G_s = 4\,\pi\, r^2\, \gamma_{pw} \qquad (2\text{-}39)$$

where γ_{pw} represents the interfacial tension between the polymer and water and r is the radius of the particle. In order for spontaneous nucleation to occur, this energy, ΔG_s, must be supplied by phenonema occurring in the solution.[214] In this case, it is supplied by the increase in free energy due to the association of hydrophobic parts of the growing chain, where g_v represents the free energy of condensation per unit volume.[215]

$$\Delta G_c = -\frac{4}{3}\pi\, r^3\, g_v \qquad (2\text{-}40)$$

The overall free energy of the system is then represented by the sum of Equations (2-39) and (2-40).[216]

$$\Delta G = \Delta G_s + \Delta G_c \quad (2\text{-}41)$$

When the chain is very small, then r is small, and G_s dominates; however, as the chain grows, G_c becomes more important and results in spontaneous particle formation. For polymer colloids, the polymer-water interfacial energy is usually not very high, and the presence of surfactants further decreases the interfacial energy.

---

[213] Fitch, R.M. 1997. *Polymer Colloids: A Comprehensive Introduction*. R.M. Fitch, Ed. Academic Press: San Diego, 1997.
[214] Ibid.
[215] Ibid.
[216] Ibid.

Evidence to support homogeneous nucleation has been documented in the works of Priest,[217] Alexander and Napper,[218] Nomura et al.,[219] and Barrett.[220] Furthermore, Fitch and Tsai,[221] Goodall et al.,[222] and Chen and Piirma[223] all measured the molecular weight of the oligomers produced during homogeneous nucleation and found that they ranged from 1 to 70 repeat units.

The development of the homogeneous nucleation model solves the first discrepancy which was noted for the Smith-Ewart theory. That is, it explains how the nucleation of polymer particles can occur when no surfactant molecules or micelles are present. Even in cases where micelles are present, it is believed that homogenous nucleation is important, especially for monomers with higher water solubility.

Droplet Nucleation

Although droplet nucleation is not generally regarded as having great importance in emulsion polymerizations, Hansen and Ugelstad[224] found that it is important in cases where the monomer droplets have a high relative surface area (i.e., for very small monomer droplets). A discussion by Fitch[225] summarizes the likelihood of droplet nucleation:

> "In true 'emulsion polymerization' oligoradicals of course can be captured by monomer droplets and start polymerization therein, but ordinarily this is negligible because of statistical considerations: there will be on the order of 10^{11} monomer droplets and 10^{17} polymer particles per liter, 1000000 times as many. Thus a free radical in the aqueous phase is essentially completely surrounded by polymer particles and can hardly 'see' any monomer drops. But there is clearly a finite probability that some polymerization will occur in the monomer phase, and this can cause problems in practical manufacturing situations. For example, as the monomer droplets are consumed by diffusion to polymer particles and polymerization therein, the polymer residue in the monomer droplets will remain as insoluble, amorphous material often considered erroneously as 'coagulum.' "

Droplet nucleation plays an important role for polymerizations where high agitation speeds and good surfactants are utilized. In fact, Hansen and Ugelstad[226] point out that in some cases, it may be the sole mechanism of nucleation. In essence, droplet nucleation seems to be a minisuspension polymerization occurring with a water-soluble initiator, however, the correct term for this phenomenon is "miniemulsion polymerization." Particles produced from miniemulsion polymerizations are generally *larger* than traditional emulsion polymerization

[217] Priest, W.J. 1952. *Journal of Physical Chemistry*. 56, 1077.
[218] Alexander, A.E. and D.H. Napper. 1971. *Progress in Polymer Science*. 3, 145.
[219] Nomura, M., M. Harada, W. Eguchi, and S. Nagata. 1975. *Polymer Preprints*. American Chemical Society, Division of Polymer Chemistry. 16, 217.
[220] Barrett, K.E.J. *Dispersion Polymerization in Organic Media*. Wiley: New York, 1975.
[221] Fitch, R.M and C.H. Tsai. In *Polymer Colloids, Proceedings*. R.M. Fitch, Ed. Plenum Press: New York, 1971.
[222] Goodall, A.R., M.C. Wilkinson, and J. Hearn. 1975. *Progress in Colloid and Interface Science*. 53, 327.
[223] Chen, C-Y., and I. Piirma. 1980. *Journal of Polymer Science, Polymer Chemistry*. 18, 1979.
[224] Hansen, F.K. and J. Ugelstad. "Particle Formation Mechanisms" in *Emulsion Polymerization*. I. Piirma, Ed. Academic Press: New York, 1982.
[225] Fitch, R.M. *Polymer Colloids: A Comprehensive Introduction*. Academic Press: San Diego, 1997.
[226] Hansen, F.K. and J. Ugelsad. 1979. *Journal of Polymer Science, Polymer Chemistry*. 17, 3069.

particles, and have different molecular weight distributions. Smith-Ewart Case III kinetics generally apply to miniemulsions.[227]

Theories Supporting Homogeneous Nucleation

Fitch-Tsai Theory

Fitch and Tsai were the first to quantitatively express the theory of homogeneous nucleation for emulsion polymerization. They proposed that the rate of particle formation would be equal to the rate of radical formation less some factor, *b*, which accounts for a reduction in rate due to termination, aggregation, or other reactions which consume the active radical. This is a relatively good assumption, since the decomposition or reaction of the initiator is the rate limiting step in the initiation process.

$$\left(\frac{dN}{dt}\right)_0 = b\, R_{i\,w} \quad (2\text{-}42)$$

In Equation (2-42), N is the number of particles generated per liter and the subscript 0 indicates that this expression represents initial conditions. The rate of generation of free radicals, depending on the initiator, is approximately 10^{15} radicals generated per liter per second, and therefore, the rate of generation of particles is approximately the same. In a matter of seconds, 10^{15} particles are produced per liter. New radical chains continue to grow in the aqueous phase, as additional initiator creates new primary free radicals. However, second generation particles have a different environment than their predecessors. Now a number of particles exist and the oligomeric chains which are growing in the aqueous phase generally have some ionic, or polar head group as well as a hydrophobic tail. Therefore, the oligomers could function as surfactants and stabilize the polymer particles which are already present.

Each time an oligomer adsorbs onto a growing polymer particle, acting as a surfactant, Fitch and Tsai's equation which predicts the number of polymer particles must be modified by R_c, the overall rate of oligoradical capture by particles.

$$\left(\frac{dN}{dt}\right)_0 = b\, R_{i\,w} - R_c \qquad (2\text{-}43)$$

Figure 2-20, which appears in the text of Fitch,[228] illustrates the relatively sharp initial increase in the number of particles formed. However, the sudden plateau indicates that the particles capture oligoradicals relatively efficiently in styrene emulsion polymerizations.

[227] Fitch, R.M. *Polymer Colloids: A Comprehensive Introduction*. Academic Press: San Diego, 1997.
[228] Fitch, R.M. *Polymer Colloids: A Comprehensive Introduction*. Academic Press: San Diego, 1997.

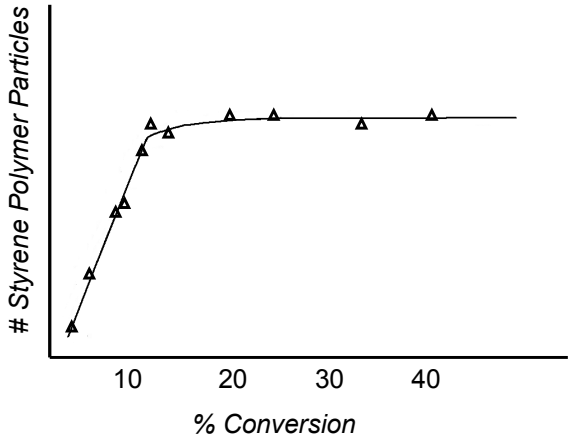

Figure 2-20: Number of particles as a function of conversion in styrene emulsion polymerization. The number of particles levels off around 10% conversion. Similar to the diagram included in the text of Fitch.[229]

The case for methyl methacrylate, also taken from Fitch's text,[230] is very different, as seen in Figure 2-21. In this case, Brownian motion of the monomer-swollen particles is leading to collisions, and fusion of two individual particles into one more highly charged particle. This is illustrated in Figure 2-22, taken from the text of Fitch.[231]

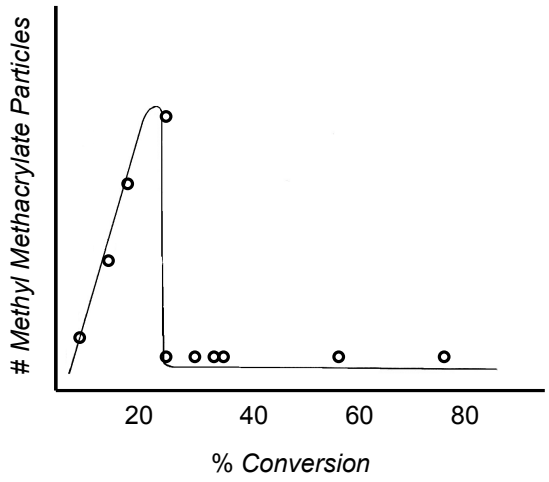

Figure 2-21: Number of particles as a function of conversion in methyl methacrylate emulsion polymerization. After a sharp peak, the number of particles drops dramatically. Similar to the diagram in the text of Fitch.[232]

[229] Ibid.
[230] Fitch, R.M. *Polymer Colloids: A Comprehensive Introduction*. Academic Press: San Diego, 1997.
[231] Ibid.
[232] Ibid.

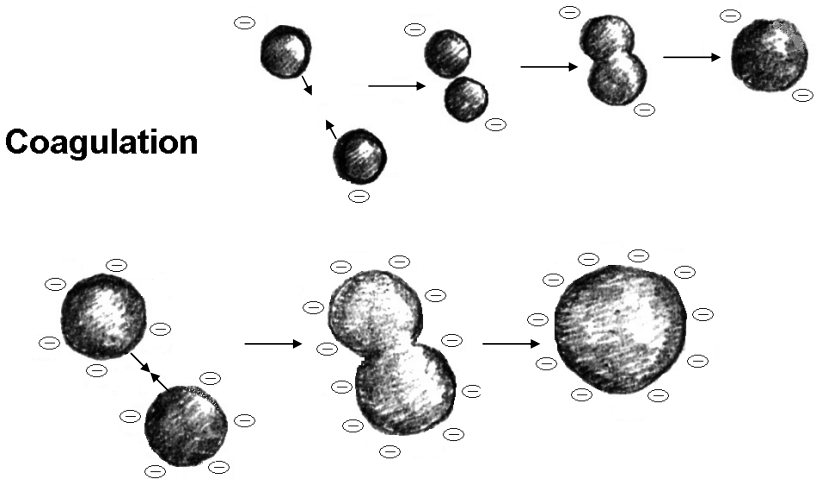

Figure 2-22: Flocculation and fusion (coalescence) of charged particles as a result of Brownian motion. The resulting particles are larger and have higher surface charge densities. Similar to that shown in the text of Fitch.[233]

Coagulation, represented by R_f, reduces the number of particles that exist during emulsion polymerization. Equation (2-44) is the complete Fitch-Tsai Equation.

$$\left(\frac{dN}{dt}\right)_0 = b\,R_{i\,w} - R_c - R_f \quad \text{(2-44)}$$

Hansen and Ugelstad [234, 235] made further contributions to the homogeneous nucleation model of Fitch and Tsai. Their developments related the expressions for the number of polymer particles more directly to the rates of polymerization. For the sake of brevity, derivations of the Hansen-Ugelstad developments will not be included.

It is important to consider that when a polymerization begins by homogeneous nucleation, the second generation of growing oligomers could participate in the emulsion in a number of different ways. They could:

1. Be absorbed into a micelle
2. Be absorbed into a monomer droplet
3. Be absorbed into a polymer particle which already exists
4. Continue to propagate in the water phase
5. Terminate in the water phase
6. Precipitate out of the water phase
7. Associate with other oligomers or with surfactants (if present) to form a micelle

[233] Ibid.
[234] Hansen, F.K, and J. Ugelstad. 1978. *Journal of Polymer Science, Polymer Chemistry*. 17, 1953; 17, 3033.
[235] Hansen, F.K, and J. Ugelstad. 1978. *Journal of Polymer Science, Polymer Chemistry*. 16, 3047; 17, 3069.

Many of the mechanistic developments in emulsion polymerization after the development of the Fitch-Tsai and Hansen-Ugelstad models describe the various fates of the growing oligomer radicals. Important considerations for vinyl acetate will be discussed later.

2.3.4 Other Considerations which Influence Kinetics

Electrolyte Concentration

The use of ionic initiators, such as ammonium or potassium peroxides or persulfates, change the ionic strength of the aqueous phase, and thereby influence the reaction in a number of ways. Unfortunately, this effect has been "widely overlooked".[236] Effects of increasing the ionic content of the water phase include: decreased critical micelle concentrations (CMCs), larger micelles, more solubilization of monomer in the water phase, increased adsorption of emulsifier on the polymer particle surfaces, and (as a result of the increased adsorption), the surface charge density increases. Furthermore, the diffuse portion of the electrical double layer can become compressed, which can promote coalescence and large particle sizes.

Non-Ionic Emulsifiers

Non-ionic emulsifiers are generally high molecular weight and provide stabilization through a steric mechanism, whereas low molecular weight emulsifiers function through an electrostatic mechanism. Due to the differences in the nature of these two types of emulsifiers, differences can be exhibited in the polymerization. Most importantly, anionic emulsifiers have many more micelles in the water phase than non-ionic emulsifiers. In addition, the micelles are much smaller for ionic emulsifiers. This results in non-ionic emulsifiers having both fewer and larger particles than their ionic counterparts. The CMCs for the ionic and non-ionic emulsifiers are also very different. For non-ionic emulsifiers, the CMC is much lower, and micelles have a much higher molecular weight, while the reverse is true for ionic emulsifiers.

The Structure of the Emulsifier

As the length of the alkyl chain in the emulsifier increases, several interesting effects are observed. First, the area that the emulsifier molecule occupies on the polymer particle surface, a_s, decreases.[237] Recalling the Smith-Ewart theory, it is clear that changes in a_s are important because a_s is inversely proportional to the number of particles, N, in the system (N scales with $a_s^{3/5}$). Knowing that N is directly proportional to the polymerization rate, we can predict that as the length of the alkyl chain increases, N should decrease, and therefore, R_p should likewise decrease. However, experimental observations noted the opposite effect.[238,239]

The increases seen in N and R_p were due to the lower CMC that is characteristic of longer alkyl chain surfactants. When the same concentration of soap A and soap B are used in an emulsion,

---

[236] Dunn, A.S. "Harkins, Smith-Ewart and Related Theories" in *Emulsion Polymerization and Emulsion Polymers*. P.A. Lovell and M.S. El-Aasser, Eds. Wiley: Chichester, 1997.
[237] Erbil, H.Y. *Vinyl Acetate Emulsion Polymerization and Copolymerization with Acrylic Monomers*. CRC: Boca Raton, 2000.
[238] Dunn, A.S. "Harkins, Smith-Ewart and Related Theories" in *Emulsion Polymerization and Emulsion Polymers*. P.A. Lovell and M.S. El-Aasser, Eds. Wiley: Chichester, 1997.
[239] Dunn, A.S. and W.A. Al-Shahib. 1978. *British Polymer Journal*. 10, 137.

and B has a longer alkyl chain than A, then B will have a higher concentration of micelles than A, and therefore, will have more polymer particles nucleated and a higher overall rate of polymerization. If the concentration of micellar emulsifier is kept constant, then the two different emulsifiers can produce the same number of particles with the same particle size distribution.[240]

Duration of Interval I: Its Dependence on Monomer Solubilization

As more monomer is solubilized in micelles, the duration of Interval I decreases. Emulsifiers that have a longer alkyl chain form larger micelles, which then solubilize more monomer, thereby decreasing the time spent in Interval I.

Effect of Monomer to Water Ratio

Several important issues must be considered in the determination of the ratio of the weight of monomer as compared to that of water. The aqueous medium is an important aspect of the system as it provides viscosity control, and, due to its high specific heat, also acts as a heat sink. Interestingly, it has also been found that this ratio can, in some circumstances, influence the rate of polymerization. (Smith and Ewart proposed that this monomer to water ratio should have no influence on either the rate of polymerization or the number of polymer particles formed, however, experimental results have proven otherwise.[241])

If the amount of water, the concentration of emulsifier, and the relative concentration of initiator (on water) are held constant while the amount of monomer is increased, larger particles are formed. Also, more monomer droplets (or larger droplets) will require additional stabilization from emulsifier, which will decrease the number of micelles present. During polymerization, the polymer particles will also swell to accommodate more monomer. This promotes the likelihood that more radicals will be present in the polymer particles, changing from the usual Smith-Ewart Case II behavior to Case III. Under these conditions, instability and flocculation can easily result if the concentration of emulsifier is too low.

The other condition is that the amount of monomer is low related to the water (and emulsifier) content. This leads to the case where many small particles are formed.[242, 243] From Smith-Ewart theory, it is clear that increasing the number of latex particles would have the direct result of increasing the polymerization rate. Incidentally, this condition is a useful means of synthesizing seed particles which "eliminate the oscillations otherwise experienced during the startup of continuous stirred-tank reactors for emulsion polymerization".[244, 245, 246]

---

[240] Ibid.

[241] Erbil, H.Y. *Vinyl Acetate Emulsion Polymerization and Copolymerization with Acrylic Monomers*. CRC: Boca Raton, 2000.

[242] Chatterjee, S.P., N. Banerjee, and R.S. Konar. 1979. *Journal of Polymer Science, Polymer Chemistry*. 17, 2193.

[243] Nomura, M. and M. Harada. "On the Optimal Reactor Type and Operation For Continuous Emulsion Polymerization" in *Emulsion Polymers and Emulsion Polymerization*. D.R. Bassett and A.E. Hamielec, Eds. ACS Symposium Series, Volume 165. Washington D.C., 1981.

[244] Erbil, H.Y. *Vinyl Acetate Emulsion Polymerization and Copolymerization with Acrylic Monomers*. CRC: Boca Raton, 2000.

Effect of Temperature

Smith-Ewart and other models which assume ideal conditions include a constraint of constant temperature. Increases in temperature result in overall rate increases in the polymerization, and lower molecular weights. More specifically, Erbil[247] cites the following results of increased temperature:

- Increased rate of initiation, and therefore, higher concentrations of free radicals
- Increased number of micelles in solution, and therefore more polymer particles
- Increased rate of diffusion of monomer to micelles/particles, and higher concentrations of monomer in those locations, and finally
- Increased rate of radicals diffusing into the particles.

While increased rates of polymerization may seem positive, there are also several side effects that Erbil[248] points out:

- Greater risk of instability (pre-flocculation, coagulation, etc.)
- Greater risks of producing cross-linked, branched, or gelled polymers
- Changes in structure and molecular weight distribution, and
- Different efficiencies of chain transfer agents (if applicable).

Effect of Agitation

Some polymerization systems are more highly affected by agitation than others. In general, it can be said that enough agitation is necessary to break up the monomer into droplets. However, excessive agitation would lead to higher amounts of shear and thus, would induce flocculation or coagulation. Signs of excessive agitation include coagulum on the stirrer, the baffles (if present), and on the walls of the reaction vessel (all of which signal a loss in yield). On the other hand, inefficient stirring promotes a rather slimy product, since the monomer phase was not sufficiently dispersed into droplets.[249]

The Smith-Ewart theory assumes constant agitation. High stirring speeds will result in deviations from predicted behavior. Specifically, the rate of polymerization will increase and the molecular weight of polymer produced will decrease, as increased agitation promotes monomer diffusion. Changes in the stirring speed could also influence the efficiency of chain transfer agents.[250]

---

[245] Nomura, M. and M. Harada. "On the Optimal Reactor Type and Operation For Continuous Emulsion Polymerization" in *Emulsion Polymers and Emulsion Polymerization*. D.R. Bassett and A.E. Hamielec, Eds. ACS Symposium Series, Volume 165. Washington D.C., 1981.
[246] Poehlein, G.W., W. Dubner, and H.C. Lee. 1982. *British Polymer Journal*. 14, 143.
[247] Erbil, H.Y. *Vinyl Acetate Emulsion Polymerization and Copolymerization with Acrylic Monomers*. CRC: Boca Raton, 2000.
[248] Ibid.
[249] Ibid.
[250] Ibid.

Of course, speed is not the only element to consider in the agitation process. Different stirring geometries and reactor geometries can promote or disturb the agitation process as well, and must be taken into consideration.

Effect of Conversion

During polymerization, many polymers exhibit behavior that is not predicted by the Smith-Ewart theory at high (>80%) conversion. These deviations may include: coagulation, latex instability, gelled or branched polymer, and altered copolymer composition. Styrene-butadiene copolymers and butadiene homopolymers are two examples of such systems. To prevent these effects, "shortstop agents" such as hydroquinone, phenylhydrazine, sodium polysulfide, and sodium dimethyldithiocarbamate are added to keep the reaction below 100% conversion, thereby producing a polymer having more desirable properties.[251]

Trommsdorf or Gel-Effect

The Trommsdorf or gel-effect occurs in the polymer particles as they attain higher molecular weights, and thus, higher viscosities. Under very viscous conditions, the rate of termination decreases, and the radical concentration inside polymer particles increases above predicted, ideal conditions. The result is very high molecular weight polymer, which could also be highly branched or cross-linked. In methyl methacrylate emulsion polymerizations, this effect is evident even at relatively low conversions.[252]

2.3.5 Appendix: Smith Ewart Derivations

In developing an understanding of the derivation behind these equations, the text of Blackley[253] was a notable resource. In fact, the derivations presented follow Blackley's text closely, with few exceptions. The derivation is also explained by Smith and Ewart[254] in their article.

The Three Cases

Case I

The Case I condition is one in which the number of free radicals per polymer particle is very low. This implies that many of the particles contain no radical at all, a situation that occurs when the rate of diffusion of free radicals out of the particle is much greater than their rate of entry. Equation (2-45) is the mathematical representation of such a condition.

$$\frac{\rho}{N} << k_o \frac{a}{v} \qquad (2\text{-}45)$$

where:

- ρ is the rate of entry of radicals into the polymerization loci (or polymer particles)

[251] Erbil, H.Y. *Vinyl Acetate Emulsion Polymerization and Copolymerization with Acrylic Monomers*. CRC: Boca Raton, 2000.
[252] Ibid.
[253] Blackley, D.C. *Emulsion Polymerization: Theory and Practice*. Applied Science Publishers: London, 1975.
[254] Smith, W.V. and R.H. Ewart. 1948. *Journal of Chemical Physics*. 16, 6, 592.

- N is the number of loci
- k_o is the rate coefficient for diffusion out of the particle
- a is the surface area of the particle, and
- v is the volume of the particle.

Rate of Polymerization

Recurrence Relationships. Smith and Ewart base their polymerization kinetics on recurrence relationships which describe the number of radicals that are present in a polymer particle. To develop these recurrence relationships, they must account for several possible processes:

- The transfer of radicals (by diffusion) from the aqueous phase to the polymer particle. For a single particle, this can be expressed as ρ/N, as in Equation (2-45).
- The transfer of radicals from the polymer particle back to the aqueous phase. This is written as $k_o\, a(i/v)$, where k_o, a, and v are described above for Equation (2-45) and i is the number of radicals in the polymer particle.
- The loss of radicals by combination. This is written as $2k_t\, i\, [(i\text{-}1)/v]$ where k_t is the rate constant for combination.

Now, if n_o, n_1, n_2, …, n_i, … represent the number of particles containing (0, 1, 2, …, i, …) radicals, then the rate of formation of particles containing t radicals is given by Equation (2-46).

$$n_{i-1}\,\frac{\rho}{N} + n_{i+1}\; k_o\; a\,\frac{i+1}{v} + n_{i+2}\; k_t\,\frac{(i+2)(i+1)}{v} \qquad (2\text{-}46)$$

Similarly, the rate of loss of particles containing i radicals is:

$$n_i\,\frac{\rho}{N} + n_i\; k_o\; a\,\frac{i}{v} + n_i\; k_t\,\frac{i(i-1)}{v} \qquad (2\text{-}47)$$

Assuming that the number of loci remains constant throughout the polymerization, then the two expressions can be equated and solved for the number of particles containing a certain number of radicals (i.e., n_o, n_1, n_2, etc.). This expression has become known as the Smith-Ewart recurrence equation. It provides useful solutions to each of the different Cases. For Case I, the only recurrence relationship that is appropriate is the steady state solution for polymer particles containing one radical, (where $n_i = n_1$).

$$n_1 k_o\,\frac{a}{v} = n_o\,\frac{\rho}{N} \qquad (2\text{-}48)$$

Since, in Case I most particles do not contain a radical, a substitution of $n_o \cong N$ is allowed in Equation (2-48), giving a simplified expression for the number of particles containing a radical.

$$n_1 \cong \frac{\rho v}{k_o a} \qquad (2\text{-}49)$$

The rate of polymerization, R_p, can then be considered as the rate of change of monomer concentration per particle multiplied by the number of polymer particles, as illustrated in Equation (2-50):

$$R_p = \frac{d[M]}{dt} * n_1 = k_p[M] * n_1 \qquad (2\text{-}50)$$

where:

- $d[M]/dt$ is the change in the concentration of monomer inside the polymer particle over time, and
- k_p is the rate constant of the polymerization process.

Substituting from Equation (2-49), we obtain an overall rate expression, shown in Equation (2-51).

$$R_p \cong k_p [M] * \frac{\rho v}{k_o a} \qquad (2\text{-}51)$$

In addition, n_1 can also be expressed as $c_p V$, where:

- c_p is the concentration of radicals in the particle (per unit volume) and
- V is the total volume of dispersed polymer (per unit of the aqueous phase).

Therefore, an alternate expression for the rate of polymerization, obtained by substitution into Equation (2-50), gives the result shown in Equation (2-52).

$$R_p \cong k_p [M] * c_p V \qquad (2\text{-}52)$$

Termination Kinetics

But the propagation kinetics do not tell the whole story in themselves; also of interest is the termination behavior of the radicals. According to Smith and Ewart, radicals can be terminated either in the aqueous phase or in the polymer particles, which makes derivations a bit more complex as two separate cases for termination must be considered.

Termination in the Aqueous Phase. Let us consider termination in the aqueous phase first. Assuming that the concentration of radicals in the aqueous phase is at some steady state concentration, c_w, Smith and Ewart write that the rate of termination of radicals per unit volume in the aqueous phase, R_{ta}, is equal to the following:

$$R_{ta} = 2\, k_{ta}\, c_w^{\,2} \qquad (2\text{-}53)$$

where k_{ta} is the rate constant for termination in the aqueous phase. Rearranging, we find the following expression for c_w:

$$c_w = \sqrt{\frac{R_{ta}}{2\, k_{ta}}} \qquad (2\text{-}54)$$

Furthermore, if some partition function called α exists, which separates radicals between the polymer particles and the aqueous phase, then:

$$c_p = \alpha \sqrt{\frac{R_{ta}}{2\, k_{ta}}} \qquad (2\text{-}55)$$

Now having an expression for c_p which is based on termination in the aqueous phase, we can learn more about the overall rate of polymerization by substituting Equation (2-55) back into Equation (2-52), giving:

$$\frac{dM}{dt} = k_p\, [M]\; V\, \alpha \sqrt{\frac{R_{ta}}{2\, k_{ta}}} \qquad (2\text{-}56)$$

We can also calculate the average lifetime of a radical in the polymer particle, T. Given that termination occurs in the aqueous phase and also that few polymer particles contain a free radical at any one instant, T can be expressed as the number of polymer particles containing a free radical, n_1, divided by the rate of termination of the radical in the aqueous phase, R_{ta}.

$$T = \frac{c_p\, V}{2\, k_{ta}\, c_w^{\,2}} = \frac{a\, V}{2\, k_{ta}\, c_w} = \frac{a\, V}{\sqrt{2\, k_{ta}\, R_{ta}}} \qquad (2\text{-}57)$$

Therefore, according to Smith and Ewart's Case I derivation where termination occurs in the aqueous phase, both the rate of polymerization and the average lifetime of a growing polymer particle are independent of particle size, but dependent on the volume of the particles.

Termination in the polymer particle. The alternative to termination in the aqueous phase is termination in the polymer particles. Assuming that the rate of termination is rapid compared to

the rate of time for radicals to enter the polymer particle, we can write that the rate of termination is just two times the rate of radical entry into active particles.

$$R_{tp} = \frac{2\, n_1\, \rho}{N} = \frac{2\, \rho^2\, v}{k_o\, N\, a} \qquad (2\text{-}58)$$

If the concentration of radicals is at steady state, then:

$$\rho = \sqrt{\frac{R_{tp}\, k_o\, N\, a}{2\, v}} \qquad (2\text{-}59)$$

and, from Equation (2-51) and substitution from Equation (2-59), the overall rate of polymerization can be expressed as:

$$\frac{dM}{dt} = \frac{k_p\, [M]\, \rho\, v}{k_o\, a} = k_p\, [M] \sqrt{\frac{R_{tp}\, N\, v}{2\, k_o\, a}} = k_p\, [M] \sqrt{\frac{R_{tp}\, V}{2\, k_o\, a}} \qquad (2\text{-}60)$$

and the average lifetime of growing radicals when termination occurs in the particle is approximately n_1 over R_{tp}, as shown in Equation (2-61).

$$T = \frac{n_1}{\frac{2\, \rho^2\, v}{k_o\, N\, a}} = \frac{N}{2\, \rho} = \sqrt{\frac{V}{2\, k_o\, a\, R_{tp}}} \qquad (2\text{-}61)$$

Deciding which termination mechanism applies. It is clear that the final expressions derived for both the overall rate of polymerization (Equations (2-56) and (2-60)) and the average lifetime of a growing radical (Equations (2-57) and (2-61)) depend on the mechanism of termination. Therefore, Smith and Ewart developed a criterion for deciding whether termination in the aqueous phase or the polymer particles was more likely occurring. This criterion was based on the assumption that the entrance of a free radical is given by the rate of diffusion of radicals (diffusion rate constant, D) from an infinite medium having a concentration of radicals, c_w, into a particle of radius r having zero concentration of radicals. Mathematically, this simplifying assumption is expressed in Equation (2-62).

$$\frac{\rho}{n} = 4\, \pi\, D\, r\, c_w \qquad (2\text{-}62)$$

Now, the expressions developed for termination in both the polymer particle and the aqueous phase must be recalled and compared to the previous expression. Considering termination which occurred in the polymer particles, as described in Equation (2-58), a few simple mathematical manipulations can be made to allow comparison. First, Equation (2-58) must be multiplied through by *N*/*N*, and rearranged to give:

$$R_{tp} = \left(\frac{2\,N\,v}{k_o\,a}\right)\left(\frac{\rho}{N}\right)^2 \qquad (2\text{-}63)$$

Then, substituting V for $N\,v$, and $4\,\pi\,D\,r\,c_w$ for ρ/N, we obtain:

$$\frac{2\,V}{k_o\,a}(4\,\pi\,D\,r\,c_w)^2 \qquad (2\text{-}64)$$

This result must then be compared with the rate of termination for the aqueous phase, as provided in Equation (2-56), and the larger of the rates must predominate. In the equations shown in Scheme (2-65), it is shown that if k_{ta} is greater than the expression developed for termination in the polymer particle then termination must occur in the aqueous phase.

$$\begin{aligned} 2\,k_{ta}\,c_w^{\,2} &>> \frac{2\,V}{k_o\,a}(4\,\pi\,D\,r\,c_w)^2 \\ k_{ta} &>> \frac{V}{k_o\,a}(4\,\pi\,D\,r)^2 \qquad (2\text{-}65) \\ k_{ta} &>> \frac{4\,\pi\,D^2\,V}{k_o} \end{aligned}$$

Case II

Case II of the Smith-Ewart theory involves two simplifying assumptions:

1. There is no mechanism for a free radical to leave a polymer particle, instead, it must remain in that polymer particle until it is terminated.
2. Once a second radical enters a polymer particle, termination occurs relatively quickly (as compared to the time between successive free radical entries).

This allows one to surmise that at any given point during emulsion polymerization, approximately one half of the polymer particles contain an active free radical and the other half do not. Smith and Ewart point out that this case seems to be true for the emulsion polymerization of styrene. Mathematically, the case that half of the particles contain a radical while the other half do not can be expressed by:

$$k_o \frac{a}{v} << \frac{\rho}{N} < \frac{k_t}{v} \qquad (2\text{-}66)$$

Rate of Polymerization

Recurrence Relationships to Determine R_p. Solution of the recursion relationships for the condition with $k_o = 0$ and the term β being sufficiently large, where β is defined as:

$$\beta = \frac{k_t N}{v \rho} \qquad (2\text{-}67)$$

gives a very simple expression for the rate of polymerization per unit of water phase.

$$\frac{dM}{dt} = \frac{k_p [M] N}{2} \qquad (2\text{-}68)$$

According to Blackley's[255] interpretation, *dM/dt* (where there are no brackets around the *M*) signifies "the rate of conversion of monomer to polymer expressed as number of monomer molecules converted per second in unit volume of aqueous phase."

Termination Kinetics

The average lifetime of a radical, *T*, is derived rather easily. Since termination occurs rapidly upon the entry of a subsequent radical, the lifetime of the particle can be defined as the number of particles in the system, *N*, divided by the total number of radicals that enter per unit time, ρ. Smith and Ewart add a factor of ½ to this quantity, which appears, according to Blackley,[256] to be an error.

$$T = \frac{N}{\rho} \qquad (2\text{-}69)$$

Smith and Ewart point out that these conditions and results help to explain the high rates and high molecular weights that are characteristic of emulsion polymerizations. Since there are many particles present, *N*, and half of them contain active radicals (this is exceptionally higher than the typical concentration of radicals in other oil phase polymerizations), it seems reasonable that the polymerization would occur much more rapidly. Secondly, from Equation (2-69), it can be reasoned that increasing the number of particles would promote longer lifetimes for free radicals, which would result in greater amounts of monomer consumed per radical in emulsions.

[255] Blackley, D.C. *Emulsion Polymerization: Theory and Practice*. Applied Science Publishers: London, 1975.
[256] Ibid.

Case III

In Case III it is assumed that the radicals enter the polymer particles much more rapidly then they are consumed by termination. Mathematically, this can be expressed as:

$$\frac{\rho}{N} >> \frac{k_t}{v} \qquad (2\text{-}70)$$

The next assumption is that a true system can be approximated by a system in which all of the polymer particles contain the same number of free radicals; which may be accurate when the concentration of radicals is very high. This assumption allows Equation (2-71) to describe the steady state condition.

$$\frac{\rho}{N} = 2\,k_t\,\frac{n^2}{v}$$
$$n = \sqrt{\left(\frac{\rho\, v}{2\,k_t\,N}\right)} \qquad (2\text{-}71)$$

Rate of Polymerization

The overall rate of polymerization is then given by:

$$\frac{dM}{dt} = k_p\,[M]\,N\,n = k_p[M]\sqrt{\frac{\rho\,N\,v}{2\,k_t}} = k_p\,[M]\sqrt{\frac{\rho\,V}{2\,k_t}} \qquad (2\text{-}72)$$

Termination Kinetics

Also, the average lifetime of a radical is given by the ratio of the number of radicals per particle and the rate of combination of the radicals.

$$T = \frac{n}{\frac{2\,k_t\,n^2}{v}} = \sqrt{\frac{N\,v}{2\,k_t\,\rho}} = \sqrt{\frac{V}{2\,k_t\,\rho}} \qquad (2\text{-}73)$$

Deriving the Number of Loci, N

To this point, equations describing polymerization kinetics have been given for a single particle in each of the three simplifying cases. The task that remains is to derive equations for the total number of particles present so that the overall rate of polymerization for the system can be calculated.

For this component of their work, Smith and Ewart only consider the number of loci after the micelles disappear from solution, implying that all the "loci" must be polymer particles. In addition, several other simplifying assumptions are made:[257, 258]

1. Soap is almost exclusively present in the form of micelles in the initial stages (soap that is dissolved in the water phase or is adsorbed onto the monomer droplets) is ignored.

2. As polymerization occurs, the total mass of soap that is being considered, S, is distributed between the micelles, S_m and the polymer particles, S_p, and although the distribution changes as polymerization continues, the total amount of soap, S, is always equal to the sum of the amount in micelles and that on the polymer particles.

3. The interfacial area of a gram of soap, a_s, is the same for soap micelles and polymer particles, that is, until the micelles disassociate. Therefore, if the variables A, A_m, and A_p, represent the total interfacial area, the interfacial area of micelles, and the interfacial area of particles, respectively, then:

$$\frac{A}{S} = \frac{A_m}{S_m} = \frac{A_p}{S_p} = a_s \qquad (2\text{-}74)$$

Providing a direct means of calculating N would be quite difficult, so Smith and Ewart again make some simplifying assumptions and look at limiting cases. The additional assumptions that are made are as follows:[259, 260]

1. During the nucleation of loci, the ratio of monomer to polymer remains constant. (This is generally regarded as valid when the monomer droplets exist as a separate phase, which is the case if sufficient surfactant is used, however, in his text, Blackley gives a detailed discussion of this assumption).[261]

2. The rate of polymerization within a single particle is constant during this stage, which, given assumption 4, should be true.

Considering these additional two assumptions, one can conclude that the rate of growth of a particle (dv/dt) is constant (denoted by μ); and is therefore independent of size.

---

[257] Blackley, D.C. *Emulsion Polymerization: Theory and Practice*. Applied Science Publishers: London, 1975.
[258] Smith, W.V. and R.H. Ewart. 1948. *Journal of Chemical Physics*. 16, 6, 592.
[259] Blackley, D.C. *Emulsion Polymerization: Theory and Practice*. Applied Science Publishers: London, 1975.
[260] Smith, W.V. and R.H. Ewart. 1948. *Journal of Chemical Physics*. 16, 6, 592.
[261] Blackley, D.C. *Emulsion Polymerization: Theory and Practice*. Applied Science Publishers: London, 1975.

Two Limiting Cases for *N*

Two limiting cases exist for the calculation of *N*. In the first case, the number of polymer particles calculated is too high, because it is based on the assumption that as long as micelles are present, they will capture all the radicals. Obviously, over time, radicals will, in addition to entering micelles, enter the polymer particles, which would and result in termination. Not all micelles will be nucleated in reality, and thus *N* is overestimated. The other extreme results in the calculation of too few particles. In this case the preliminary assumption is that a given interfacial area will have the same effectiveness in capturing free radicals, regardless of the size or curvature of the particle that it composes.

Calculations for Too Many Loci

To begin, equations for the volume, *v*, and the surface area, a_s, are developed as a function of time. Several important times to be considered are:

- t^* the time between the start of the reaction and the disappearance of micelles
- τ the time when a particle is first initiated, and
- t time between τ and t^*.

Equations for volume as a function of time will then be transformed into equations for surface area using the well-known facts that, for spherical particles, $v = 4/3\ \pi\ r^2$ and $a = 4\ \pi\ r^2$, where *r* is the radius of the particle.

$$v(\tau,t) = v_o + \mu(t-\tau) \qquad (2\text{-}75)$$

In Equation (2-75), μ is the constant denoting the rate of growth of a particle and v_o is the initial volume of the particle. Using the aforementioned geometric relationships, one easily obtains a solution for *a* where θ is $(36\ \pi\ \mu^2)^{1/3}$.

$$a(\tau,t) = \sqrt[3]{36\ \pi\ \mu^2\ (t-\tau)^2}$$
$$a(\tau,t) = \theta\ (t-\tau)^{\frac{2}{3}} \qquad (2\text{-}76)$$

Now the aggregate surface area of the particles must be calculated. This will be the sum of all of the individual interfacial areas over some given time. Particles initiated at time $\tau+\delta\tau$, (there will be $\rho\ \delta\tau$ of these), all have a surface area of $a(\tau, t)$ at time *t*. Therefore, their total contribution to the interfacial area would be $\rho\ a\ (\tau, t)\ \delta\tau$. Summing over time and giving the aggregate interfacial area the symbol $A_p(t)$, then:

$$A_p(t) = \int_0^t \rho\ a(\tau,t)\,d\tau = \int_0^t \rho\ \theta(t-\tau)^{\frac{2}{3}}\,d\tau = \frac{3}{5}\ \rho\ \theta\ t^{\frac{5}{3}} \qquad (2\text{-}77)$$

At time t^*, when all the micelles disappear, $A_p(t^*)$ must equal A which must in turn equal a_s, which leads to the following conclusions:

$$\frac{3}{5}\rho\,\theta\,t^{*\frac{5}{3}} = a_s\,S$$

$$t^* = \left(\frac{5\,a_s\,S}{3\,\rho\,\theta}\right)^{\frac{3}{5}}$$

$$N = \rho\,t^* = \rho^{\frac{2}{5}}\left(\frac{5\,a_s\,S}{3\,\theta}\right)^{\frac{3}{5}} \qquad \text{(2-78)}$$

$$N \cong 0.53\,\mu^{\frac{-2}{5}}\,a_s\,\rho^{\frac{2}{5}}\,S^{\frac{3}{5}}$$

The equations in Scheme (2-78) give an expression for the total number of paticles, N, according to this derivation method. Smith and Ewart acknowledge that this is an overestimate.

Calculation for too few loci

The calculation for too few loci is rather extensive, and shall be presented in a very limited fashion. The initial assumptions the rate of creation of new nuclei is given by:

$$\frac{dN}{dt} = \rho\frac{A_m}{A} \qquad \text{(2-79)}$$

and the use of Equation (2-64) gives:

$$\frac{dN}{dt} = \rho - \frac{\rho\,A_p}{a_s\,S} \qquad \text{(2-80)}$$

In steps similar to those used in the development of Equation (2-67), the individual contribution to interfacial area can be summed over time as shown in the following integral:

$$A_p(t) = \int_0^t \theta(t-\tau)^{\frac{2}{3}}\,\frac{dN}{dt}\,d\tau \qquad \text{(2-81)}$$

Then, substitution into Equation (2-80) gives:

$$\frac{dN}{dt} = \rho - \frac{\rho\,\theta}{a_s\,S}\int_0^t \theta(t-\tau)^{\frac{2}{3}}\,\frac{dN}{dt}\,d\tau \qquad \text{(2-82)}$$

which is known as a Volterra equation of the second kind, and thereby requires a special solution. After some rigorous calculations, the final answer for this case is obtained.

$$N = 0.370\ \mu^{\frac{-2}{5}}\ a_s^{\frac{3}{5}}\ \rho^{\frac{2}{5}}\ S^{\frac{3}{5}} \qquad (2\text{-}83)$$

2.4 Emulsion Homopolymerization of Vinyl Acetate

2.4.1 Important Considerations

Vinyl acetate exhibits very different behavior than styrene and other ideal monomers and therefore, does not follow Smith-Ewart Case II theory. One of the most important differences between vinyl acetate and other monomers is that it is much more water-soluble. Furthermore, it has a high heat of polymerization, 21 ± 0.5 kcal/mol[262], which has introduced some problems of maintaining control during the reaction, even in emulsion polymerization. After it polymerizes for some time at the azeotropic temperature of 65-66°C (for the vinyl acetate/water system), the reaction becomes exothermic, and if not properly controlled, will boil and foam, causing destabilization of the system.[263] Vinyl acetate also has a much higher chain transfer constant than other common monomers. During the polymerization, chain transfer drastically slows the rate of polymerization and leads to excessive branching, which has important effects on the performance of the latex.[264]

2.4.2 Common Ingredients and Their Properties

Monomer

The structure of vinyl acetate is shown in Figure 2-23. Klatte[265] was the first to recognize vinyl acetate. It was a by-product from his work in preparing ethylidene diacetate. From 1920 to 1930, the reaction of liquid acetic acid with acetylene to produce the monomer were optimized in Canada.[266] Just prior to World War II, a gas-phase process was designed which utilized the same reagents.[267] Vinyl acetate was produced on a large scale in Germany during World War II.[268]

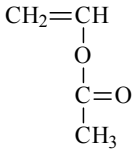

Figure 2-23: Structure of vinyl acetate monomer.

[262] Joshi, R.M. 1963. *Makromolekulare Chemie*. 66, 114.
[263] Erbil, H.Y. *Vinyl Acetate Emulsion Polymerization and Copolymerization with Acrylic Monomers*. CRC: Boca Raton, 2000.
[264] Ibid.
[265] Klatte, F. U.S. Patent (1914) 1, 084, 581; Chemical Abstracts (1914) 8, 991.
[266] Leonard, E.C. "Vinyl Acetate" in *Vinyl and Diene Monomers, Part I*. E.C. Leonard, Ed. Wiley: New York, 1970.
[267] Ibid.
[268] Ibid.

An inhibitor, usually hydroquinone or diphenylamine, is added to the monomer before shipping to prevent polymerization. The inhibitors are easily removed via distillation. It should be noted that copper or brass fittings in vessels containing vinyl acetate could introduce impurities which could affect the polymerization rate.[269] Aluminum, stainless steel, and glass-lined equipment is suitable for storing and handling the monomer.[270]

Properties of Vinyl Acetate Monomer

The table below is taken from the text of Leonard,[271] and gives some useful properties of vinyl acetate monomer. Not included here are the tables Leonard also provides for the viscosity and boiling point of vinyl acetate at different temperatures, as well as the boiling point and composition of azeotropes containing vinyl acetate. All references are through Leonard's text.

Table 2-1: Selected properties of vinyl acetate monomer

Property	Value	Conditions	Reference
Boiling Point	72.5°C	1 atm	[272]
Freezing Point	-100.2°C	1 atm	[273]
Critical Pressure	22.4 atm		[274]
Coefficient of cubical expansion	1.52×10^{-3}	20 – 40°C	[275]
Viscosity	0.432 cP	20°C	[276]
Refractive index	1.3952		[277]
Specific Gravity	0.9338	20°C	[278]
Surface Tension	23.95		[279]
Reid Vapor Pressure	3.7 dynes/cm	20°C	[280]
Solubility of Monomer in Water	2.5g/100g water 2.1g/100g water	20°C 50°C	[281]
Solubility of Water in Monomer	0.1g/100g vinyl acetate 1.7g/100g vinyl acetate	20°C 66°C	[282]
Flash Point	23°F	Open cup method	[283]
Autoignition Temp	427°C		[284]

[269] Ibid.
[270] Ibid.
[271] Leonard, E.C. "Vinyl Acetate" in *Vinyl and Diene Monomers, Part I*. E.C. Leonard, Ed. Wiley: New York, 1970.
[272] The Borden Chemical Company. "Vinyl Acetate Monomer," Technical Data Sheet.
[273] Dollivar, M.A., T.L. Gresham, G.B. Kistiakowsky, E.A. Smith, and W.E. Vaughn. 1938. *Journal of the American Chemical Society*. 60, 440.
[274] The Borden Chemical Company. "Vinyl Acetate Monomer," Technical Data Sheet.
[275] Celanese Corporation of America. Technical Bulletin S-56-2.
[276] Ibid.
[277] Ibid.
[278] Ibid.
[279] Ibid.
[280] Ibid.
[281] Shaw, T.P.G. "Vinyl Acetate," in *Encyclopedia of Chemical Technology*, Volume 14. Interscience: New York, 1955.
[282] Ibid.
[283] Celanese Corporation of America. Technical Bulletin S-56-2.

Weight (lb/gal)	7.78	20°C	[285]
Heat of Vaporization	90.6 cal/g	72.7°C	[286]
Specific Heat Vapor Liquid	 0.26 cal/g 0.46 0.48 .505	 20°C 60°C 100°C	[287]
Heat of Formation	-28.3 kcal	From ethylene, acetic acid	[288]
Heat of Hydrogenation	-31.120 ± .06 cal/mol		[289]
Heat of Combustion	495 kg cal/mol		[290]
Dielectric Constant	5.8	25°C	[291]
Dipole Moment	1.75 Debye units		[292]

Chemical Reactions of the Monomer

Hydrolysis

The hydrolysis of vinyl acetate has been studied in great detail and, according to Erbil[293], it has been the subject of several reviews.[294,295] When vinyl acetate is hydrolyzed, it produces acetic acid and vinyl alcohol, which then tautomerizes to form acetaldehyde.[296] First studied in 1927,[297] the hydrolysis reaction has been found to proceed rapidly under extreme pH, both acidic and basic. The rate of the reaction, in aqueous media, reaches a minimum at a pH of 4.44,[298] and in general, acidic conditions lead to much slower reaction rates than basic conditions. Mercury ions,[299] and, in acidic conditions, palladium chloride[300] have been found to catalyze the reaction.

Addition

Addition to the double bond of vinyl acetate is possible through hydrogenation, or by the addition of halogens or hydrogen-halogen compounds. In fact, the addition of bromine (in the presence of sodium acetate and acetic anhydride) is one of the classical means to identify residual monomer content after polymerization.[301,302] The hydrogenation reaction produces ethyl

[284] Ibid.
[285] Ibid.
[286] Ibid.
[287] Celanese Corporation of America. Technical Bulletin S-56-2.
[288] The Borden Chemical Company. "Vinyl Acetate Monomer," Technical Data Sheet.
[289] Ibid.
[290] Ibid.
[291] Air Reduction Company, Inc. "Airco Vinyl Acetate Monomer," Murray Hill, N.J, 1964.
[292] Lee, S. 1940. *Journal. Society of the Chemical Industry of Japan*. 43, Supplemental Binding 190-191.
[293] Erbil, H.Y. *Vinyl Acetate Emulsion Polymerization and Copolymerization with Acrylic Monomers*. CRC: Boca Raton, 2000.
[294] Rekasheva, A.F. *Russian Chemical Reviews,* (1968) 37, 1009.
[295] Lee, S. and H. Kawakami. 1940. *Journal. Society of the Chemical Industry of Japan*. 43, 228.
[296] Cordiero, C.F. "Vinyl Polymers (Vinyl Acetate)" in *Encyclopedia of Chemical Technology*, Volume 24. J.I. Kroschwitz, and M. How-Grant, Eds. Wiley: New York, 1994.
[297] Skrabal, A. and A. Zachroka. 1927. *Manatshefte*. 48, 459.
[298] Morrison, G.O., and T.P.G. Shaw. 1933. *Transactions of the Electrochemical Society*. 63, 425.
[299] Kiprianova, L.A., and A.F. Rekasheva. 1964. *Doklady Akademii Nauk SSSR*. 154, 423.
[300] Smidt, J. 1959. *Angewandte Chemie*. 71, 176.
[301] Gross, H. 1963. *Praktische Chemie*. 21, 99.
[302] Gross, H. 1965. *Chemische Berichte*. 98, 1673.

acetate when 5% platinum is added.[303] α–haloethyl acetates are produced by the addition of hydrogen bromide or hydrogen chloride.[304] Esters can be formed by the addition of certain carboxylic acids,[305] and sulfides[306, 307] are synthesized after benzyl mercaptan and mercaptoethanol add to the double bond. Leonard[308] states that the following materials or classes of chemicals also add to vinyl acetate:

1-2 Addition:
1.) Hydrogen Cyanide
2.) Halogens
3.) Mercaptans
4.) Halocarbons
5.) Amines
6.) α-Chloroethers
7.) Silanes
8.) Substituted "methylenes"

Cycloaddition:
1.) Tetrafluoroethylene
2.) Benzonitrile Oxide
3.) "Benzyne"
4.) Salicylic Acid
5.) Acetaldehyde

Oxidation

Oxidation of vinyl acetate in an inert solvent proceeds very slowly, much more slowly than for styrene, in the presence of a free radical source. In hydrogen peroxide, it has been found that vinyl acetate forms glycol aldehyde[309,310] and adducts of oxygen[311,312,313,314,315] have occurred under various conditions.

Transesterification

In an acidic medium, and in the presence of mercuric salts, transesterification reactions proceed with vinyl acetate to produce acetic acid and a vinyl carboxylate derivative.[316] Vinyl acetate also reacts with alcohols to produce vinyl ethers,[317] and succinimide and phthalimide esters can also be prepared.[318] A catalyst for these reactions is palladium (II) chloride, when in the presence of sodium or lithium chloride.[319]

---

[303] Dolliver, M.A., T.L. Gresham, G.B. Kistiakowsky, E.A. Smith, and W.E. Vaughan. 1938. *Journal of the American Chemical Society*. 6, 440.
[304] Moffett, E. 1934. *Journal of the American Chemical Society*. 56, 2009.
[305] Erbil, H.Y. *Vinyl Acetate Emulsion Polymerization and Copolymerization with Acrylic Monomers*. CRC: Boca Raton, 2000.
[306] Rueggeberg, W.H., J. Chernack, I.M. Rose, and E.E. Reid. 1948. *Journal of the American Chemical Society*. 70, 2292.
[307] Szabo, J.L. and E.T. Stiller. 1948. *Journal of the American Chemical Society*. 70, 3367.
[308] Leonard, E.C. "Vinyl Acetate" in *Vinyl and Diene Monomers, Part I*. E.C. Leonard, Ed. Wiley: New York, 1970.
[309] Milas, N.A., S. Sussman, and H.S. Mason. 1939. *Journal of the American Chemical Society*. 61, 1844.
[310] Langman, I., A.F. McKay, and G.F. Wright. 1949. *Journal of Organic Chemistry*. 14, 550.
[311] Mayo, F.R., A.A. Miller, G.A. Russell. 1958. *Journal of the American Chemical Society*. 80, 2500.
[312] Barnes, C.E., R.M. Elofson, and G.D. Jones. 1950. *Journal of the American Chemical Society*. 72, 210.
[313] Schmitz, E. and O. Brede. 1970. *Journal fuer Praktische Chemie*. 312, 43.
[314] Gorton, B.S. and J. A. Reeder. 1962. *Journal of Organic Chemistry*. 27, 2920.
[315] Frostick, F.C., B. Phillips, and P.S. Starcher. 1959. *Journal of the American Chemical Society*. 81, 3350.
[316] Erbil, H.Y. *Vinyl Acetate Emulsion Polymerization and Copolymerization with Acrylic Monomers*. CRC: Boca Raton, 2000.
[317] Adelman, R.L. 1953. *Journal of the American Chemical Society*. 75, 2678.
[318] Adelman, R.L. U.S. Patent (1951) 2,550,449.
[319] Sabel, A., J. Smidt, R. Jira, and H. Prigge. 1969. *Chemische Berichte*. 102, 2939.

Reaction with Paraformaldehyde

It has been found that paraformaldehyde reacts with vinyl acetate as well. This reaction produces acrolein and acetic acid.[320,321]

Decomposition

At 360°C, vinyl acetate begins to decompose.[322] It does not polymerize, however, at that temperature. Pyrolysis occurs at 500°C, which liberates β-ketoaldoses, acetic acid, acetylene, propylene, ketene, acetaldehyde, carbon monoxide, carbon dioxide and dimethylketene.[323]

Emulsifiers

Emulsifiers are extremely important in the emulsion polymerization system; Dunn[324] outlines the five most important functions.

- They act to stabilize the monomer droplets in an emulsion form (i.e., the droplets act as a reservoir to supply the growing polymer particles with additional monomer), or can act as the locus of polymerization if the monomer emulsions are comparable in size to monomer-swollen micelles, as in the case of miniemulsion polymerization.
- They serve to solubilize monomer within surfactant micelles.
- They stabilize the formed latex particles as well as the particles which continue to grow during polymerization.
- They act to solubilize polymer.
- They serve as the site for the nucleation of particles.
- They act as chain transfer agents or retarders.

In the emulsion polymerization of vinyl acetate, nonionic and anionic surfactants are widely used, sometimes in conjunction with each other and sometimes with a protective colloid. These types are particularly successful because they are more compatible with the negatively charged persulfate initiator fragments that stabilize poly(vinyl acetate) particles.[325] Only 0.05 to 2.0 % of the total weight of the reactants (0.1 to 4.0% by weight of monomer) is comprised of surfactants.[326] Cationic and zwitterionic emulsifiers are not used in the emulsion polymerization of vinyl acetate.

---

[320] Walker, J.F. U.S. Patent (1949) 2,473,989.
[321] Sieglitz A. and O. Horn. Chemical Abstracts (1952) 46, 3497. (through #310)
[322] Harkness, J.B., G.B. Kistiakowsky, and W.H. Meas. 1937. *Journal of Chemical Physics*. 5, 632.
[323] Allan, R.J.P., R.L. Froman, and P.D. Richtie. 1955. *Journal of the Chemical Society*. 2717.
[324] Dunn, A.S. "Effects of the Choice of Emulsifier in Emulsion Polymerization" in *Emulsion Polymerization.* I. Pirrma, Ed. Academic Press: New York, 1982.
[325] Erbil, H.Y. *Vinyl Acetate Emulsion Polymerization and Copolymerization with Acrylic Monomers*. CRC: Boca Raton, 2000.
[326] Ibid.

Anionic Emulsifiers

These are molecules with a hydrophilic, negatively charged end group. The presence of the charged group provides stability in the presence of electrolytes and at different pH's. Hydrophobic portions of the surfactants are also important, as they influence the interfacial energy and the critical micelle concentration. Common examples of anionic emulsifiers include molecules having sulfate, sulfonate, sulfosuccinate, or phosphate groups, such as:[327]

- Sodium lauryl (dodecyl) sulfate
- Sodium dodecylbenzene sulfonate
- Sodium dioctyl sulfosuccinate, and
- Nonyl phenol ethoxy phosphate ester.

Nonionic Emulsifiers

Unlike anionic emulsifiers, nonionics generally produce particles having relatively large particle sizes.[328] These compounds are characterized by cloud point determination.[329] Common examples of nonionic emulsifiers include: ethylene oxide additives to alkyl aryl phenols (like nonylphenol polyoxyethylene glycol and octylphenol polyoxyethylene glycol), ethylene oxide additives to straight chain primary alcohols, and polyethylene oxide-polypropylene oxide-polyethylene oxide triblock copolymers.[330]

Protective Colloids

Water-soluble polymers are often employed in emulsion polymerizations to enhance the stability of the latex particles by preventing particle coalescence. A protective colloid is able to deter coalescence via a steric mechanism. To function in this manner, part of the colloid must be anchored or well adsorbed on the particle surface while the remainder juts out into the aqueous phase. In some cases, these stabilizers can be engineered to provide certain morphologies, such as a comb-like structure, to provide the desired stability.

Non-ionic polymer that functions as a protective colloid provides not only good freeze-thaw stability, but also electrolytic stability.[331] However, there are also several disadvantages to using colloid stabilizers, and therefore, their inclusion is generally limited in the formulation from 1 to 5 wt% in solution.[332] Common disadvantages include:[333]

- They are not as effective at controlling particle size as conventional surfactants
- Latex films that include them are inherently sensitive to water, and

[327] Ibid.
[328] Erbil, H.Y. *Vinyl Acetate Emulsion Polymerization and Copolymerization with Acrylic Monomers*. CRC: Boca Raton, 2000.
[329] Ibid.
[330] Ibid.
[331] Ibid.
[332] Ibid.
[333] Ibid.

- Their presence is generally limited to the surface of the particles, and therefore, may cause haziness in films.

Some examples of protective colloids include: poly(vinyl alcohol), hydroxyethyl cellulose, poly(vinyl pyrrolidone), block copolymers of poly(ethylene oxide) and poly(propylene oxide), poly(acrylic acid), poly(methacrylic acid), polystyrene-block-poly(ethylene oxide) and poly(diisobutylene/maleic anhydride).[334]

Poly(vinyl alcohol)

Formed by the hydrolysis of poly(vinyl acetate), this polymer exists in several grades for use in polymerizations of vinyl acetate. Partially hydrolyzed poly(vinyl alcohol) (87-89% hydroxyl groups) is the grade which is most commonly used[335] in industrial emulsion polymerizations (these give better stability), although fully hydrolyzed (98-99 mol%) and an intermediate grade (93-97%) are also available.[336] Properties of the alcohol are highly dependent on both degree of hydrolysis and molecular weight. If the degree of hydrolysis is kept constant, increasing the molecular weight results in increased tensile strength, increased water and solvent resistance, and increased adhesive strength of the resultant film.[337] Similarly, if the molecular weight is kept constant and the degree of hydrolysis is increased, the water and solvent resistance increases, as does the crystallinity, the tensile strength, and the tack.[338] During its synthesis, both the degree of hydrolysis and the molecular weight can be controlled, allowing good selection of properties.

Poly(vinyl alcohol) is usually purchased as a solid and is dissolved to form an aqueous solution. These solutions are stable, but must include a biocide to prevent rust contamination and microbial growth.[339] Sodium nitrate (0.05-0.20 wt%) can be added to prevent rust while formaldehyde has been found to be an excellent biocide at concentrations as low as 500 ppm.[340]

Chemical Reactions

Generally, poly(vinyl alcohol) reacts like many other secondary polyhydric alcohols.[341] Common reactions that poly(vinyl alcohol)s undergo are:[342]

- Forming polyvinyl acetals and aldehydes
- Crosslinking (with glyoxal, with urea-formaldehyde or melamine-formaldehyde if ammonium sulfate or ammonium chloride is present).

[334] Ibid.
[335] Warson, H. 1983. *Chemistry and Industry*. 21, 220.
[336] Erbil, H.Y. *Vinyl Acetate Emulsion Polymerization and Copolymerization with Acrylic Monomers*. CRC: Boca Raton, 2000.
[337] Erbil, H.Y. *Vinyl Acetate Emulsion Polymerization and Copolymerization with Acrylic Monomers*. CRC: Boca Raton, 2000.
[338] Ibid.
[339] Ibid.
[340] Ibid.
[341] Ibid.
[342] Ibid.

- Complexation with borax or boric acid. This results in gelation which successfully limits penetration into porous substrates.

Hydroxyethyl Cellulose

Hydroxyethyl cellulose is also widely used as a colloid stabilizer. It is synthesized by grafting 1.8 to 2.5 (on average) moles of ethylene glycol on each anhydroglucose unit in cellulose. The result is a non-ionic polymer that is extremely tolerant of different electrolytic and pH conditions, but susceptible to microbial attack.[343] Hydroxyethyl cellulose is also widely used for rheology control.[344] It is available in different molecular weight grades.

Initiators

The general classes of initiators were discussed earlier in this review. At this point, some of the systems that are commonly used in the emulsion polymerization of vinyl acetate will be discussed.

Thermal Dissociating Initiators

Persulfates

Potassium, sodium, and ammonium persulfates are the most commonly used initiators for the emulsion polymerization of vinyl acetate.[345] They are generally used from 50°-90°C, and cleave homolytically to produce two free radicals.[346] Persulfates are highly water-soluble and are insoluble in vinyl acetate monomer, thereby leading to initiation in the aqueous phase.[347] Sulfate ion radicals are also capable of reacting with water to yield bisulfate ions and hydroxide radicals.[348] Whether the hydroxide or the sulfate ion radical initiates the vinyl acetate chain, the end unit will be highly hydrophilic, leading to good stability in the water phase. It should also be noted that these initiators decompose under acidic conditions without generating free radicals.[349]

Peroxides

Hydrogen peroxide and others are both soluble in the water phase and in the swollen polymer particles.[350] This could lead to some changes in the mechanism of initiation, which will be discussed in greater detail in a later section. Hydroperoxides can also react with water to form hydroxy radicals and other oxygenated radical fragments. [351]

Others

In rare cases, water-soluble derivatives of AIBN (azobisisobutryronirile) such as 4,4'-azobis-4-cyanopentanoic acid and disodium 2,2'-azobis-2-cyanopropane-1-sulfonate have been used in

[343] Ibid.
[344] Ibid.
[345] Ibid.
[346] Erbil, H.Y. *Vinyl Acetate Emulsion Polymerization and Copolymerization with Acrylic Monomers*. CRC: Boca Raton, 2000.
[347] Ibid.
[348] Ibid.
[349] Ibid.
[350] Ibid.
[351] Ibid.

vinyl acetate emulsion polymerizations.[352] Although AIBN itself is a good free radical initiator, it is not water-soluble, and thus, cannot be used in emulsion polymerizations.

Redox Initiators

Redox initiators are sometimes advantageous because they require much less energy to produce free radicals than thermally dissociating initiators (10 kcal/mol vs. 30-35 kcal/mol).[353] This means that the polymerization can be initiated at much lower temperatures. The reaction occurs by an electron transfer between a primary initiator precursor and a reducing agent, which donates the electron. The active initiator is then a free radical or a free radical ion. Systems commonly used in the initiation of vinyl acetate include, (as shown in the text of Erbil):[354]

Persulfate-Bisulfite:

$$S_2O_8^{-2} + HSO_3^{-1} \rightarrow SO_4^{*\ -1} + SO_3^{*\ -1} + HSO_4^{-1}$$

Persulfate-Thiosulfate:

$$S_2O_8^{-2} + 2\ S_2O_3^{-2} \rightarrow 2\ SO_4^{*\ -1} + S_4O_6^{-2}$$

Persulfate-Formaldehyde Sulfoxylate

$$S_2O_8^{-2} + HOCH_2SO_2^{-1} + OH^{\ -1} \rightarrow 2\ SO_3^{*\ -1}\ (HCHO) + H_2O$$

Peroxide-Formaldehyde Sulfoxylate

$$2\ H_2O_2 + HOCH_2SO_2^{-1} \rightarrow 2\ HO^* + HOCH_2SO_3^{-1} + H_2O$$

Peroxide-Metallic Ion (reduced state)

$$H_2O_2 + Fe^{+2} \rightarrow HO^* + OH^{\ -} + Fe^{+3}$$

Persulfate-Metallic Ion (reduced state)

$$S_2O_8^{-2} + Fe^{+2} \rightarrow SO_4^{*\ -1} + SO_4^{*\ -2} + Fe^{+3}$$

Other Methods of Initiation

High energy radiation has also been found to generate free radicals *in situ* (such as hydroxy radicals) and was found to be successful in vinyl acetate polymerizations.[355] Sources of the radiation include ultrasonic methods, as well as gamma radiation and electron bombardment. Newer developments in the area include grafting of either monomer or polymer chains to introduce chemical modifications to the substrate polymer.[356]

[352] Ibid.
[353] Ibid.
[354] Ibid.
[355] Erbil, H.Y. *Vinyl Acetate Emulsion Polymerization and Copolymerization with Acrylic Monomers*. CRC: Boca Raton, 2000.
[356] Ibid.

Water

Deionized water is preferred in industrial emulsion polymerization.[357] The most common deionization process involves passing the water through successive anion and cation exchange tubes, although reverse osmosis and distillation can also be used to purify the water.[358] Common impurities in water are minerals such as calcium and magnesium (which give "hardness" to water)[359] as well as organic and gas impurities. Cation and anion exchange tubes remove chloride, sulfate, nitrate, nitrite, fluoride, phosphate and borate anions as well as the aforementioned cations, plus sodium and potassium.[360] Removal of magnesium and calcium is especially important because they could otherwise influence particle size and stability.[361]

Most organics that are present in water are in very low quantities, and thus, are often neglected.[362] However, the dissolved oxygen content has an important influence on polymerization kinetics as oxygen is a free radical scavenger, and thus a polymerization inhibitor. If the polymerization reactor is not purged with ample nitrogen before the reaction, the presence of dissolved oxygen results in a significant delay in the onset of polymerization.

As mentioned previously, water has a very important role in heat transfer during the polymerization. It also aids in viscosity control. Reaction kinetics are influenced by the ratio of monomer to water that is selected. Generally, the highest monomer to water ratio which allows the highest rates of polymerization while still providing adequate viscosity control and heat transfer is selected.[363]

Buffers

Premature crosslinking, hydrolysis, changes in the decomposition rate of the initiator, and changes in the charge on surfactants are all effects that can be caused by changes in pH. The addition of a buffer, such as sodium bicarbonate, will help to alleviate these effects. However, since buffers are salts, they can impact the colloidal stability and the particle size of the latex.[364]

Plasticizers and Coalescing Aids

Often, additives are necessary to ensure that the film formation process progresses to completion in a relatively short period of time. In addition, in many cases, the film formation temperature of poly(vinyl acetate) latices is too high for certain applications. To achieve a homogeneous film at lower temperatures, and therefore, better performance at those lower temperatures, plasticizers or

---

[357] Klein, A. and E.S. Daniels. "Formulation Coponents" in *Emulsion Polymerization and Emulsion Polymers*. P.A. Lovell and M.S. El-Aasser, Eds. Wiley: New York, 1997.
[358] Ibid.
[359] Smart, R.B. and K.H. Mancy, in *Kirk Othmer Concise Encyclopedia of Chemical Technology*, M. Grayson, Ed. Wiley: New York, 1985. (through #359)
[360] Erbil, H.Y. *Vinyl Acetate Emulsion Polymerization and Copolymerization with Acrylic Monomers*. CRC: Boca Raton, 2000.
[361] Ibid.
[362] Ibid.
[363] Erbil, H.Y. *Vinyl Acetate Emulsion Polymerization and Copolymerization with Acrylic Monomers*. CRC: Boca Raton, 2000.
[364] Klein, A. and E.S. Daniels. "Formulation Concepts" in *Emulsion Polymerization and Emulsion Polymers.* P.A. Lowell and M.S. El-Aasser, Eds. Wiley: Chichester, 1997.

coalescing agents are postadded to the latex. While these materials both result in lower MFTs (minimum filming temperatures), they function somewhat differently. Plasticizers remain in the film for a much longer time, ultimately impacting the T_g of the system (reducing it), and its modulus (reducing it), whereas coalescing agents have much lower molecular weights, and evaporate after film formation has occurred. Coalescing agents then have the desirable property of restoring the T_g of the polymer to its initial level, plus they do not reduce the modulus of the final system.[365] Common examples of coalescing agents include glycols, esters of carbitol, 2-butoxyethanol, and 2,2,4-trimethyl-1,3-pentanediol monisobutyrate.[366] Plasticizers include dibutyl phthalate and tricresyl phosphate.[367]

Biocides/Fungicides

In previous years, the presence of residual monomer was sufficiently high to combat infestations of microbes.[368] However, this is no longer the case, and often, bio and fungicides must be added to extend the useful lifetime of a product. The selection of the appropriate chemical additive depends on the type of microbe that is present. More generally, the following types of chemicals have found use in this area: phenolics, halogen compounds, quaternary ammonium compounds, metal derivatives, amines, alkanol amines, nitro derivatives, anilides, organosulfur and sulfur nitrogen compounds.[369]

Antifoaming Agents

Due to the presence of surfactants, the use of antifoaming agents is sometimes required to prevent excessive entrapment of air in poly(vinyl acetate) adhesives. This is particularly true for emulsions containing poly(vinyl alcohol).[370] Although many antifoaming agents are proprietary, Erbil[371] speculates that they "are believed to contain aliphatic solvents, silicone oils, and possibly heavy metal soaps." For poly(vinyl alcohol), it is believed that silicone agents are the most effective, but they also have a significant drawback in that they may decrease wettability.[372] Furthermore, these agents are not long lasting.[373] Non-silicone agents composed of octyl alcohol and tributyl phosphate are just as effective as the silicone agents, and are recommended for use.[374] Generally 0.01 to 0.05% (on aqueous solution) is added to the formulation.[375]

Chain Transfer Agents

To regulate the molar mass or its distribution, a chain transfer agent, such as a mercaptan, carbon tetrachloride, or chloroform, may be added during the polymerization.[376] The chain transfer

---

[365] Erbil, H.Y. *Vinyl Acetate Emulsion Polymerization and Copolymerization with Acrylic Monomers*. CRC: Boca Raton, 2000.
[366] Ibid.
[367] Ibid.
[368] Ibid.
[369] Klein, A. and E.S. Daniels. "Formulation Concepts" in *Emulsion Polymerization and Emulsion Polymers.* P.A. Lowell and M.S. El-Aasser, Eds. Wiley: Chichester, 1997.
[370]
[371] Erbil, H.Y. *Vinyl Acetate Emulsion Polymerization and Copolymerization with Acrylic Monomers*. CRC: Boca Raton, 2000.
[372] Ibid.
[373] Ibid.
[374] Ibid.
[375] Ibid.
[376] Ibid.

constant for a given additive can be found in the Polymer Handbook,[377] or in other publications. However, the addition of a chain transfer agent may also impact the rate of polymerization.[378] In certain formulations, some ingredients may have the propensity to act as a chain transfer agent.[379]

Retarders

Retarders are used to aid in the rate control of the polymerization reaction. In particular, they are useful to prevent the excessive build up of heat that can occur with polymerization. Common chemicals that are added to slow down the reaction include some vinyl monomers, ortho-nitrophenol, conjugated dienes and trienes.[380] All of these function by producing less reactive monomer radicals, or active centers, and when used in excess they may become inhibitors, and prevent further polymerization.[381]

Antioxidants and UV Stabilizers

Essentially, antioxidants and UV stabilizers are free radical scavengers that are added to the system to preserve its integrity. Over time, free radicals can be generated by homolytic bond cleavage, and if those free radicals are not consumed, they can induce further chain scission reactions, thereby reducing the effective molecular weight of the system. Typical stabilizers that are added to prevent UV degradation include: 2-hydroxybenzophenone; phenyl salicylate; 1,3,5-tris(2;-hydroxyphenyl)triazine; and 2-(hydroxyphenyl)benzotriazole.[382] A list of antioxidants that are commonly used can be found in the literature.[383]

2.4.3 Polymerization Techniques and Conditions

Typically, the polymerization of vinyl acetate results in high molecular weight, crosslinked or highly branched chains. These branches and crosslinks have long been recognized as having important effects on the properties and performance of poly(vinyl acetate). The literature reveals that the branching of poly(vinyl acetate) occurs largely through the acetate group, and it occurs due to chain transfer to monomer and polymer.[384] Developments in the literature regarding these phenomena will be discussed in greater detail later. The polymerization of vinyl acetate is also very sensitive to impurities.[385] Even in very low concentrations, impurities such as

---

[377] Berger, K.C. and G. Brandrup. "Transfer Constants to Monomer, Polymer, Catalyst, Solvent, and Additive in Free Radial Polymerization" in *Polymer Handbook, 3rd Ed.* J. Brandrup and E.H. Immergut, Eds. Wiley-Interscience: New York, 1989.

[378] Erbil, H.Y. *Vinyl Acetate Emulsion Polymerization and Copolymerization with Acrylic Monomers*. CRC: Boca Raton, 2000.

[379] Klein, A. and E.S. Daniels. "Formulation Concepts" in *Emulsion Polymerization and Emulsion Polymers.* P.A. Lowell and M.S. El-Aasser, Eds. Wiley: Chichester, 1997.

[380] Erbil, H.Y. *Vinyl Acetate Emulsion Polymerization and Copolymerization with Acrylic Monomers*. CRC: Boca Raton, 2000.

[381] Ibid.

[382] Ibid.

[383] Hoy, K.L. 1973. *Journal of Paint Technology*. 45(579), 51.

[384] Erbil, H.Y. *Vinyl Acetate Emulsion Polymerization and Copolymerization with Acrylic Monomers*. CRC: Boca Raton, 2000.

[385] Leonard, E.C. "Vinyl Acetate" in *Vinyl and Diene Monomers, Part I*. E.C. Leonard, Ed. Wiley: New York, 1970.

crotonaldehyde, acetaldehyde, and mono-and divinylacetylene all retard the polymerization of vinyl acetate.[386] Acrylonitrile and styrene have a similar retarding effect.[387]

Although vinyl acetate is capable of being polymerized via bulk, solution, emulsion and suspension polymerizations, emulsion polymerization is favored industrially.[388] Bulk polymerization is problematic due to insolubilization of the polymer that results from poor heat removal and from increased branching at high polymer/monomer ratios.[389] In general, the bulk reaction is difficult to control. Solution polymerizations are carried out when poly(vinyl acetate) is required as a solution, or when it is to be converted into poly(vinyl alcohol). Behind emulsion polymerization, suspension polymerization is the second most popular means of polymerizing vinyl acetate. The main end use of the suspension is also the production of poly(vinyl alcohol).[390]

2.4.4 Properties of Poly(vinyl acetate)

As expected, properties of poly(vinyl acetate) vary with molecular weight. Materials can range from gum-like to leather-like.[391] The main applications of poly(vinyl acetate) include: latex paints, adhesives, binders for pigmented paper coatings, textiles, and the synthesis of poly(vinyl alcohol), polyvinyl butyral, and polyvinyl formal.[392] A table including some important properties of poly(vinyl acetate) is included, based on that found in the Polymer Handbook (references provided are all from the Polymer Handbook):[393]

Table 2-2: Selected properties of poly(vinyl acetate)

Property	Value	Conditions	References
Absorption of water	3-6%	at 20°C for 144 hrs.	[394]
Coefficient of thermal expansion: cubic	6.7×10^{-4}		[395, 396]
Compressibility	18×10^{-6}	Glassy state	[397]
Decomposition Temperature	150°C		[398]
Thermal Degradation	$T^{1/2} = 269$°C	$T^{1/2}$ is the temp. where the polymer loses 1/2 its weight when heated in vac.for 30 min.	[399]

[386] Ibid.
[387] Ibid.
[388] Ibid.
[389] Erbil, H.Y. *Vinyl Acetate Emulsion Polymerization and Copolymerization with Acrylic Monomers*. CRC: Boca Raton, 2000.
[390] Ibid.
[391] Leonard, E.C. "Vinyl Acetate" in *Vinyl and Diene Monomers, Part I*. E.C. Leonard, Ed. Wiley: New York, 1970.
[392] Ibid.
[393] *Polymer Handbook, 3rd Ed*. J. Brandrup, E.H. Immergut, Eds. Wiley: New York, 1989.
[394] Schildknecht, C.E. *Vinyl and Related Polymers*. Wiley: New York, 1952.
[395] Mowilith, Polyvinylacetat, Farbwerke Hoechst AG, Frankfurt, 1969.
[396] Saito, S. 1963. *Kolloid Zeitschrift*. 189, 116.
[397] Martynyuk, M.M., V.K. Semenchenko. 1964. *Kolloid Zhurnal*. 26, 83.
[398] Mowilith, Polyvinylacetat, Farbwerke Hoechst AG, Frankfurt, 1969.
[399] Van Krevelen, D.W. *Properties of Polymers*. Elsevier: New York, 1976.

Density	1.191 1.19 1.17 1.11 1.05	20°C 25°C 50°C 120°C 200°C	400, 401, 402
Dielectric Constant	3.5 8.3	50°C, 2x10^3 Hz 150°C, 2x10^{3}Hz	403
Elongation at Break	10-20%	20°C, 20% RH	404
Glass Transition Temperature	28-31		405
Heat Capacity	1.465 kJ/kg	30°C	406
Heat of Polymerization	87.5 kJ/mol		407, 408
Index of Refraction Index of Refraction, cont'd	1.4669 1.4657 1.4600 1.4480 1.4317	20.7°C 30.8°C 52.1°C 80°C 142°C	409
Interfacial Tension	14.5 mN/m 8.4 mN/m 9.9 mN/m 4.2 mN/m	20°C, polyethylene 20°C, polydimethylsiloxane 20°C, polyisobutene 20°C, polystyrene	410 411 412 413
Modulus of Elasticity	1274-2255 MPa	ASTM-D-256	414
Molar Volume	74.25 cm^3/mol	25°C	415
Softening Temperature	35-50°C		416
Solubility	Soluble in: benzyl alcohol, diacetone alcohol, 95% ethanol, methanol, acetaldehyde, furfural, aniline, pyridine, carbon tetrachloride, chloroform, chlorobenzene, benzene, dichloroethylene acetic acid, trichloroethylene, n-		417

[400] Shaw, T.P.G. *Encyclopedia of Chemical Technology*, Volume 14. Interscience: New York, 1955.
[401] Lindemann, M.K. *Encyclopedia of Polymer Science and Technology,* Volume 15. Interscience: New York, 1971.
[402] Schildknecht, C.E. Vinyl and Related Polymers. Wiley: New York, 1952.
[403] Thurn, H., K. Wolf. 1956. *Kolloid Zeitschrift*. 148, 16.
[404] Hacobi, H.R. *Ullmans Encyklopaedie der Technischen Chemie*, Volume 11, 3rd Ed. Urban & Schwarzenberg: Munich, 1960.
[405] Saito, S. 1963. *Kolloid Zeitschrift*. 189, 116.
[406] Wilski, H. 1966. *Kolloid Zeitschrift*. 210, 37.
[407] Joshi, R.M. 1963. *Makromolekulare Chemie*. 66, 114.
[408] Joshi, R.M. 1962. *Journal of Polymer Science*. 56, 313.
[409] Broens, O., F.H. Mueller. 1955. *Kolloid Zeitschrift*. 140, 121.
[410] Wu, S. 1969. *Journal of Colloid and Interface Science*. 31, 153.
[411] Wu, S. 1971. *Journal of Polymer Science, Part C*. 34, 19.
[412] Wu, S. 1969. *Journal of Colloid and Interface Science*. 31, 153.
[413] Wu, S. 1971. *Journal of Polymer Science, Part C*. 34, 19.
[414] Hacobi, H.R. *Ullmans Encyklopaedie der Technischen Chemie*, Volume 11, 3rd Ed. Urban & Schwarzenberg: Munich, 1960.
[415] Ahmad, H., M. Yassen. 1979. *Polymer Engineering and Science*. 19, 858.
[416] Schmieder, K., K. Wolf. 1953. *Kolloid Zeitschrift*. 134, 149.
[417] Blaikie, K.G. and T.P.G. Shaw, "Poly(vinyl acetate) Solid Resins," in *Encyclopedia of Chemical Technology*, Volume 4. Interscience: New York, 1955. (through #393)

	butyl actetate, acetone, ethyl acetate, isopropyl acetate, methyl or ethyl Cellusolve, dioxane, toluene, methyl ethyl ketone, nitrobenzene, nitromethane, liquid sulfur dioxide, and pine oil.		
Solubility Parameters	18.6 - 19.9 $(MPa)^{1/2}$		418, 419, 420, 421
Radius of Gyration (unperturbed)	0.107 A^2 mol/g	Linear PVAc	422
Specific Volume	0.841 L/kg		423
Surface Resistance	$5x10^{-11}$ Ω/cm^3		424
Surface Tension	36.5 mN/m 28.6mN/m 27.9 mN/m 25.9 mN/m	20°C 140°C 150°C 180°C	425, 426, 427
Tensile Strength	29.4- 49.0	20°C	428
Thermal Conductivity	0.159 W/(m K)		429

2.4.5 The Mechanism of the Emulsion Polymerization of Vinyl Acetate—Historical Developments

Early Developments

Klatte and Rollet[430] were the first to patent the synthesis of poly(vinyl acetate), however, they abandoned the product, finding it "too soft" for use as a plastic.[431] Some understanding of the mechanism of vinyl acetate polymerization was later developed by Staudinger,[432] and in 1929, the resin was commercially produced by Shawinigan Chemicals Ltd. in Canada. However, at that time very little was understood about the emulsion polymerization mechanism.

[418] Daoust, H., M. Rinfret. 1952. *Journal of Colloid Science*. 7, 11.
[419] Managaraj, D., S. Patra, P.C. Roy, S.K. Bhatnagar. 1965. *Makromolekulare Chemie*. 84, 225.
[420] Small, P.A. 1953. *Journal of Applied Chemistry*. 3, 71.
[421] Allen, G. 1961. *Polymer*, 2, 375.
[422] Chan, R.K.S., C. Worman. 1972. *Polymer Engineering and Science*. 12, 437.
[423] Tager, A.A., A.A. Askadskii, M.V. Tsilipotkina. 1975. *Vysokomolekulyarnye Soedineniya, Seria A*. 17, 1346.
[424] Mowilith, Polyvinylacetat, Farbwerke Hoechst AG, Frankfurt, 1969, p. 214-215.
[425] Cho, H.G., S.C. Yoon, M.S. Jhon. 1982. *Journal of Polymer Science, Polymer Chemistry Ed*. 20, 1247.
[426] Hong, K.M., J. Noolandi. 1981. *Macromolecules*. 14, 1229.
[427] Gaines Jr., G.L. 1972. *Polymer Engineering and Science*. 12, 1.
[428] Shaw, T.P.G. *Encyclopedia of Chemical Technology,* Volume 14. Interscience: New York, 1955.
[429] Ibid.
[430] Klatte, F. and A. Rollett. German Patent (1913) 281, 687 (through #432).
[431] Leonard, E.C. "Vinyl Acetate" in *Vinyl and Diene Monomers*, High Polymer Series, Volume 14. E.C. Leonard, Ed. Wiley: New York, 1970.
[432] Staudinger, H. , K. Frey, and W. Starck. 1927. *Chemische Berichte*. 60B, 1782; Chemical Abstracts (1928) 22, 215.

Mechanistic Studies

In general, it is well documented throughout the literature that the emulsion polymerization of vinyl acetate does not correlate well with the predictions of the Smith-Ewart theory. This is believed to be due to the polarity and higher water solubility of the vinyl acetate molecule (2.8% is soluble at 60°C as compared to 0.054% for styrene).[433] Most authors believe that this higher water-solubility leads to homogeneous nucleation.

The solubility of vinyl acetate has also lead to other interesting deviations from the Smith-Ewart theory. First, it has been observed and widely documented that the monomer droplets are depleted at very low conversion, as low as 14% to 20%. This leads to highly swollen particles and micelles early in the polymerization, and ultimately, to much larger latex particles (0.2 – 1 μm).[434] During the polymerization, it has also been hypothesized that the particles, on average, hold more than one radical.[435] In addition, the number of growing particles was found to decrease as conversion increased, up to a limit of about 20% conversion, where an equilibrium was attained. This equilibrium is caused by destruction of particles (via coagulation) and the nucleation of new particles, which can form when the precipitating chain adsorbs emulsifier.[436] Other findings that have been well documented have been that the overall rate of polymerization:[437]

- is relatively constant from 20 to 80 % conversion
- scales with the concentration of initiator raised to a power ranging from 0 – 0.25
- scales with the number of particles raised to the power 0.2, and
- is independent of the concentration of monomer in the particles.[438]

It should also be pointed out here that many contradictory findings are published in the literature regarding the emulsion polymerization of vinyl acetate. This is particularly true for mechanistic debates concerning particle nucleation during the polymerization. A good deal of this confusion stems from authors comparing results to other published works, where different experimental conditions were utilized. However, in some cases, very similar systems were used and the results were inconsistent.

---

[433] Dunn, A.S. "Polymerization of Aqueous Solutions of Vinyl Acetate" in *Emulsion Polymerization of Vinyl Acetate.* M.S. El-Aasser and J.W. Vanderhoff, Eds. Applied Science: London, 1981.
[434] Erbil, H.Y. *Vinyl Acetate Emulsion Polymerization and Copolymerization with Acrylic Monomers*. CRC: Boca Raton, 2000.
[435] Ibid.
[436] Ibid.
[437] Ibid.
[438] Ibid.

1952—Priest [439]

The first real mechanistic study of the emulsion polymerization of vinyl acetate came in 1952, when Priest published his results. One of the systems Priest studied included no surfactant. He therefore confirmed that emulsion polymerizations can proceed via a mechanism other than Harkins' micellar means. In that experiment he observed how certain variables affected the particle size of self-stabilized poly(vinyl acetate) latices.

Priest also examined latices stabilized by surfactant and added stabilizers. He argued that the decrease in the number of particles that is observed throughout the reaction can be explained by coagulation. Higher concentrations of emulsifier resulted in decreased particle size, due to a reduction in the occurrence of coagulation.

1960--Patsiga, Litt, and Stannett [440]

In 1960, Patsiga, Litt and Stannett suggested that the emulsion polymerization of vinyl acetate proceeds mostly in the water phase when "true surfactants" such as sodium lauryl sulfate were used. Different results had been found for polymeric stabilizers, and these results will be discussed later. Experimental evidence was based on comparisons of the emulsion polymerization of vinyl acetate and that of styrene, both completed in the presence of seed particles. Patsiga, Litt, and Stannett found that at 15-20% conversion, all of the monomer had partitioned between the water phase and the polymer particles.

Like Priest,[441] Patsiga, Litt and Stannett supported the homogeneous nucleation mechanism. However, they also believed that chain transfer to monomer could occur, thereby producing a monomer radical which could diffuse back into the water phase and polymerize there. In addition, Patsiga, Litt and Stannett supported the hypothesis that the polymer particles acted as reservoirs for monomer, constantly releasing monomer into the water phase. They concluded that the constant rate of polymerization that has been observed from ~ 20 – 80 % conversion is due to the polymerization occurring, for the most part, in the water phase. A constant concentration of monomer exists in the water phase until about 85% conversion, when the latex particles no longer supply monomer. As a result of their work, they concluded: "It was found that the Smith-Ewart kinetics were inapplicable to the vinyl acetate system."[442]

1962--Okamura and Motoyama [443]

The work of Okamura and Motoyama, published in 1962, strongly agrees with the results presented by Patsiga, Litt and Stannett.[444] They also developed some simple expressions to compare the chain transfer and retardation effects of surfactant (in this case, polyethylene oxide dodecyl ether) on vinyl acetate radicals as compared to those of styrene. In this study, they concluded that:

[439] Priest, W.J. 1952. *Journal of Physical Chemistry*. 56, 1077.
[440] Patsiga, R., M. Litt, and V. Stannett. 1960. *Journal of Physical Chemistry*. 64, 801.
[441] Priest, W.J. 1952. *Journal of Physical Chemistry*. 56, 1077.
[442] Ibid.
[443] Okamura, S. and T. Motoyama. 1962. *Journal of Polymer Science*. 58, 221.
[444] Patsiga, R., M. Litt, and V. Stannett. 1960. *Journal of Physical Chemistry*. 64, 801.

1. the solubility of vinyl acetate in water (2.5%, which is 100 times the solubility of styrene) introduces important deviations to Smith-Ewart behavior, and that
2. the effects of surfactant on chain transfer and retardation cannot be ignored for vinyl acetate polymerizations.

1962--Napper and Parts [445, 446]

Also in 1962, Napper and Parts published their findings on the kinetic behavior of vinyl acetate polymerizations. In their first paper, no emulsifier was added, but the work was carried out in the presence of a buffer at 40°C and a stable latex was produced. The rate of polymerization was monitored during the reaction in a dilatometer, and assuming that the monomer concentration in the particles remained constant over the bulk of the reaction, the kinetics were found to resemble Smith-Ewart Case III behavior, where more than one radical exists per particle.

Results also suggested that polymerization occurred primarily in the particle, which is in contrast to the findings of Patsiga, Litt, and Stannett, [447] and of Okamura and Motoyama;[448] however, this study was carried out in the *absence* of emulsifier and stabilizers while the others' were completed in the presence of surfactant. Napper and Parts also found that the number of latex particles remained constant after the initial stages of the reaction, that the propagation constant that was calculated closely resembled that for bulk polymerizations, and that the termination constant was similar to that for very viscous systems.

In a subsequent paper, Napper and Parts investigated the changes in the polymerization when small amounts (less than that required to reach the CMC) of anionic, non-ionic, and cationic surfactants were added. Results showed that the non-ionic surfactant led to conditions similar to that when no surfactant was added, the anionic surfactant led to smaller particle sizes and accelerated rates of polymerization and the cationic surfactant led to larger particle sizes and slower polymerization. In addition, the length of the hydrophobic component of the surfactant molecule was altered to determine its effect on the reaction. The results noted that the length of the cationic surfactants exhibited no effect on the reaction rate, whereas the length of the hydrocarbon chain in anionic surfactants showed some evidence of rate dependence. All effects were explained by considering the surface charges of the particle and how the surfactant interacted with those charges.

1964--Elgood, Gulbekian and Kinsler [449]

In 1964, Elgood, Gulbekian and Kinsler found that different formulations yielded differing results when polymerized in a semi-continuous (they consider it to be continuous, but that definition is not consistent with the current terminology) fashion. In these polymerizations, 90% of the monomer, emulsifier, and initiator were fed into the reactor over a two-hour period. The two formulations they studied were very similar, having only slight differences in the concentration of initiator and surfactant. They found that the number of polymer particles

[445] Napper, D.H. and A.G. Parts. 1962. *Journal of Polymer Science*. 61, 113.
[446] Napper, D.H. and A.G. Parts. 1962. *Journal of Polymer Science*. 61, 127.
[447] Patsiga, R., M. Litt, and V. Stannett. 1960. *Journal of Physical Chemistry*. 64, 801.
[448] Okamura, S. and T. Motoyama. 1962. *Journal of Polymer Science*. 58, 221.
[449] Elgood, B.G., E.V. Gulbekian, and D. Kinsler. 1964. *Journal of Polymer Science, Part B, Polymer Letters*. 2, 257.

decreased over the course of the reaction in one case (Case B) and in the other case (Case A), the number of particles only decreased until conversions of 25% were attained. Interestingly, they found that for Case A, the particle surface area increased throughout the polymerization, whereas for Case B, it remained constant after 25% conversion has been attained. The number of particles they calculated was roughly equivalent to the results found by Priest[450] and French.[451] They encouraged the theory that the particle surface area seemed to be the parameter which scaled most closely with the rate of polymerization.

1969—Netschey, Napper, and Alexander [452]

In 1969, Netschey, Napper and Alexander published their findings on the effect of seed stabilization mechanisms on the rate of polymerization during the first 10% of conversion. They found that particles stabilized by both an electrostatic and a steric (polyethylene oxide) mechanism retarded the rate of polymerization. Particles having only a steric stabilizer polymerized twice as fast as the system with both stabilizing mechanisms, and the system that incorporated only an electrostatic stabilizer proceeded with the fastest rate of polymerization, approximately 4 times the rate of polymerization for the combination of both the steric and electrostatic mechanisms.

The suggested reason for the findings was the varying rates of diffusion of the oligomer radicals into the stabilized particles. According to the authors, the rate of diffusion was significantly hindered by the presence of the steric stabilizer, and is less impacted by the electrostatic repulsion that is encountered between the oligomer chain and the electrostatically stabilized particle. The authors also point out that the findings of O'Donnell, Mesrobian, and Woodward;[453] French;[454] Patsiga, Litt, and Stannett;[455] Elgood, Gulbekian and Kinsler;[456] and Gulbekian[457] are "suspect" because they failed to consider these mechanisms.

1970—Litt, Patsiga, and Stannett [458]

In a model proposed in 1970, Litt, Patsiga, and Stannett consider the importance of polymerization variables on the polymerization mechanism. They extend their previously proposed model to account for behavior exhibited by more complex systems (for example, those which include salt or are seeded). They propose that polymerization proceeds in the aqueous phase to a greater extent than previously considered. This is because the polymer absorbs soap molecules and become a polyelectrolyte. Essentially, polymerization continues until the degree of polymerization reaches 50-300 units. At that point, the polyelectrolyte is swept up into a particle. Their view on termination is also different than had previously been considered. Termination was widely considered to be due to an aqueous radical being swept into the particle.

---

[450] Priest, W.J. 1952. *Journal of Physical Chemistry*. 56, 1077.
[451] French, D.M. 1958. *Journal of Polymer Science*. 32, 395.
[452] Netschey, A., D.H. Napper, and A.E. Alexander. 1969. *Journal of Polymer Science, Part B, Polymer Letters.* 7, 329.
[453] O'Donnell, J.T, R.B. Mesrobian, and A.E. Woodward. 1958. *Journal of Polymer Science*. 28, 171.
[454] French, D.M. 1958. *Journal of Polymer Science*. 32, 395.
[455] Patsiga, R., M. Litt, and V. Stannett. 1960. *Journal of Physical Chemistry*. 64, 801.
[456] Elgood, B.G., E.V. Gulbekian, and D. Kinsler. 1964. *Journal of Polymer Science, Part B, Polymer Letters*. 2, 257.
[457] Gulbekian, E.V. 1968. *Journal of Polymer Science*, A-1. 6, 2265.
[458] Litt, M., R. Patsiga, and V. Stannett. 1970. *Journal of Polymer Science, A-1*. 8, 3607.

Litt, Patisga, and Stannett here propose the formation of a cyclic species (a butyrolactonyl radical) and hypothesize that its collision with an aqueous polymer radical is the primary means of termination for emulsions having low ionic strengths.

1971—Harriott [459]

In 1971, Harriott developed a model to explain the kinetics of the emulsion polymerization of vinyl acetate. He assumed that radical concentrations reach some equilibrium distribution between the water phase and the polymer particles, which is similar to the assumption for Smith-Ewart Case I kinetics. His equations predicted that the rate of polymerization:

1. scaled with monomer concentration to the first power (experimentally, many observations showed the rate of polymerization to be independent of monomer concentration);
2. scaled with initiator concentration to the 0.5 power (experimentally, the rate scaled with initiator concentration from the 0.5 to the 1.0 powers), and
3. scaled with the volume of the polymer particles to the 0.5 power (experimentally, the rate scaled to the 0.35 power)

1971—Harada et al. [460]

Harada et al. also developed a mathematical representation for the kinetics of the polymerization. Their expressions were based on finding *n*, the average number of radicals per particle. They accomplished this by a recursion formula which included diffusion constants for radicals in both the water and the polymer phases. Although the model works well up to 30% conversion, it fails thereafter, so a semi-empirical correction factor is included. Like Harriott's[461] model, Harada et al.'s result failed to explain the dependency of the rate on the initiator concentration above the power 0.5.

1973—Elgood and Gulbekian [462]

Redox initiators were investigated in Elgood and Gulbekian's 1973 article. During the polymerization, which was carried out at 50°C, the pH was found to decrease from 3.5 to about 2.2. The authors found that the maximum rate of polymerization could not be achieved unless the pH was modified through the addition of alkali.

1973—Friis and Nyhagen [463]

Friis and Nyhagen also contributed several noteworthy papers in 1973 and 1975. They note the non-classical behavior of vinyl acetate, and offer that it is mainly due to high chain transfer to monomer and also high water solubility of the monomer. They pointed out two widely accepted features of the polymerization of vinyl acetate: 1. the rate of polymerization and its constancy up to conversions of ~85%, and 2. that the separate monomer phase disappears at or before 30% conversion.

---

[459] Harriott, P. 1971. *Journal of Polymer Science, A-1*. 9, 1153.
[460] Harada, M., M. Nomura, W. Eguchi, and S. Nagata. 1971. *Journal of Chemical Engineering (Japan)*. 4,1,54.
[461] Harriott, P. 1971. *Journal of Polymer Science, A-1*. 9, 1153.
[462] Elgood, B.G. and E.V. Gulbekian. 1973. *British Polymer Journal*. 5, 249.
[463] Friis, N. and L. Nyhagen. 1973. *Journal of Applied Polymer Science*. 17, 2311.

Their objective was to elucidate the mechanism of the polymerization, which in the literature had remained somewhat controversial. Previously, the group of Stannett, Litt and Patsiga,[464] as well as the individual work of Gershberg[465] offered that the water phase was an important locus of polymerization. However, the hypothesis of water-phase polymerization does not "fit" with the unusually high rates of polymerization that are observed in emulsion polymerization. Gershberg also recognized this quandary, and to make his theory work, he assumed an unusually low termination rate, which was later found to be inconsistent with results. Later, the team of Stannett, Klein, and Litt[466] developed another theory, proposing that the escape of radicals from the polymer particles was an important part of emulsion polymerization for vinyl acetate. Nomura, Harada, Nakagawara, Eguchi, and Nagata[467] did some collective work in this area, as did Harriott.[468] However, the contributions of the three independent groups were rather contradictory.

Friss and Nyhagen completed batch polymerizations of vinyl acetate with potassium persulfate as an initiator and with sodium lauryl sulfate as a surfactant. They examined the effect of the emulsifier concentration on the rate of polymerization and found:

1. that the emulsifier concentration had little effect on the initiation rate, (the dependence was to the 0.12 power, whereas for styrene this dependence was to the 0.6 power);
2. that the number of particles increased with the emulsifier concentration, $N \sim [E]^{0.5}$, (Smith-Ewart theory predicts to the 0.6 power);
3. that the polymerization proceeds at a rate roughly equal to $[N]^{0.25}$ (which agrees with the results of Litt[469]), and
4. that the viscosity was independent of the emulsifier concentration and the particle number, which agreed with work by O'Neill[470].

They also studied the effects of changing the initiator concentration. They found that the rate is proportional to $[I]^{0.5}$, which agrees with the findings of Dunn and Taylor,[471] Gershberg,[472] and with Ugelstad,[473] but contradicts the findings of Litt[474] and Vanzo.[475] Adding initiator at different conversions also lead to interesting results. The polymerization rate always increased when initiator was added. It was also found that the ratio of rate of polymerization after addition of initiator with the rate before addition was proportional to the square root of the ratio of the

[464] Litt, M., R. Patsiga and V. Stannett. 1970. *Journal of Polymer Science, A-1*. 8, 3607.
[465] Gershberg, D. Paper presented at the Joint Meeting of A.I.Ch.E. and I.Ch.E. London, June 14, 1965.
[466] Stannett, V., A. Klein, and M. Litt. 1975. *British Polymer Journal*. 7, 139.
[467] Nomura, M., M. Harada, K. Nakagawara, W. Eguchi, and S. Nagata. 1971. *Journal of Chemical Engineering (Japan)*. 4, 2, 160.
[468] Harriott, P. 1971. *Journal of Polymer Science, A-1*. 9, 1153.
[469] Litt, M., R. Patsiga, and V. Stannett. 1970. *Journal of Polymer Science, A-1*. 8, 3607.
[470] O'Neill, T., J. Pinkava, and J. Hoigne. Paper presented at the 3rd Symposium on Radiation Chemistry. Tihany, Hungary, May 10-15, 1971.
[471] Dunn, A.S. and P.A. Taylor. 1965. *Makromolekulare Chemie*. 83, 207.
[472] Gershberg, D. Paper presented at the Joint Meeting of A.I.Ch.E. and I.Ch.E. London, June 14, 1965.
[473] Ugelstad, J. and P.C. Mork. 1971. *British Polymer Journal*. 2, 31.
[474] Litt, M., R. Patsiga, and V. Stannett. 1970. *Journal of Polymer Science, A-1*. 8, 3607.
[475] Vanzo, E. Ph.D. Thesis. State University of New York, College of Forestry at Syracuse University. Syracuse, New York, 1962.

initiator concentration after addition over the initiator concentration prior to addition. This result was previously noted by Ugelstad, who studied vinyl chloride polymerizations. The initiator concentration was found to have no effect on the number of polymer particles, which is a stark contrast to the Smith Ewart theory, which predicted a dependence of $N \sim [I]^{0.4}$. The number of polymer particles was also found to be constant between 10 and 100% conversion, which was previously observed by Napper and Parts.[476] Viscosity was independent of initiator concentration, suggesting that it is molecular weight controlled and influenced by transfer to monomer and polymer.

Friis and Nyhagen also studied the effect of electrolyte, but in fact, found no effect. This was different than the results of Litt,[477] where the presence of potassium phosphate buffer was found to increase the rate of polymerization and to reduce the rate dependence on the initiator.

Finally, Friis and Nyhagen proposed a model for the polymerization which is based largely on the model of Ugelstad,[478] which had been developed for the emulsion polymerization of vinyl chloride. In summary, the findings of Friis and Nyhagen offer the important result that the emulsion polymerization of vinyl acetate has many similarities to that of vinyl chloride. The model that they propose, which has slight deviations from that proposed by Ugelstad for vinyl chloride, finds excellent agreement with the results of Nomura,[479] but disagrees with the findings of Litt.[480]

1975—Friis and Hameilec [481]

Later, Friis published another paper, this time with Hameilec. The focus of this second paper was to explore the kinetics of the polymerization reaction and determine which factors control molecular weight and then to derive expressions to predict molecular weight averages and branching densities. In this paper, comparisons are also made with vinyl chloride systems. For polyvinyl chloride, the polydispersity is approximately equal to 2, and the molecular weight distribution in bulk or suspension polymerization is not significantly different than for the emulsion polymerization. However, for poly(vinyl acetate), this is not the case. Emulsion polymerizations of vinyl acetate result in very high polydispersity ratios, indicating that the polymer is highly branched. The polydispersity ratio obtained from emulsion polymerization is much higher than that for bulk polymerizations for vinyl acetate. In the paper, it is postulated that transfer to monomer, and polymer, as well as terminal double bond polymerization all occur and influence molecular weight for vinyl acetate emulsion polymerizations. In fact, the authors go so far as to say that the ordinary termination reactions are "unimportant" because the transfer processes occur so readily. They also found that molecular weight was independent of [*I*], [*E*], *N*, and particle size.

[476] Napper, D.H. and A.G. Parts. 1962. *Journal of Polymer Science*. 61, 113.
[477] Litt, M., R. Patsiga, and V. Stannett. 1970. *Journal of Polymer Science, A-1*. 8, 3607.
[478] Ugelstad, J. and P.C. Mork. 1971. *British Polymer Journal*. 2, 31.
[479] Nomura, M., M. Harada, K. Nakagawara, W. Eguchi, and S. Nagata. 1971. *Journal of Chemical Engineering (Japan)*. 4, 2, 160.
[480] Litt, M., R. Patsiga and V. Stannett. 1970. *Journal of Polymer Science, A-1*. 8, 3607.
[481] Friis, N. and A.E. Hamielec. 1975. *Journal of Applied Polymer Science*. 19, 97.

1975—Stannett, Klein, and Litt [482]

In their 1975 article, Stannett, Klein and Litt offer a summary of the findings which have found consensus in the literature and also provide an argument for the most feasible model for vinyl acetate polymerization. Among the consensus findings mentioned were:

1. The rate of polymerization is zero order from 20 – 85% conversion.
2. The number of particles is independent of conversion above 20% conversion.
3. The rate of polymerization scales with the number of particles to the 0.2 power.
4. The rate of polymerization increases when fresh initiator is added, even after the number of particles has reached a constant value, and after the monomer droplets have been depleted.
5. The rate of polymerization has a very slight dependence on the concentration of emulsifier. (The maximum dependence noted was to the 0.25 power)
6. Similar molecular weights have been obtained, and it was widely held that chain transfer to monomer was important.

At the time, issues that were still being disputed were both the rate and the particle number dependence on the concentration of initiator, and also the mechanism of the polymerization. To that point, four models had been developed to describe the polymerization: that of Harriott,[483] Harada et al.,[484] Friis and Nyhagen,[485] and these authors. All of the theories were similar in some respects: they only considered polymerization after 10 or 20% conversion where there was no separate monomer phase, they allow for the entry, escape, and re-entry of radicals, and they assumed that the number of particles containing radicals was very low. Stannett, Klein and Litt[486] state that their model is the best because it accounts for the range in rate dependence seen on the initiator concentration. They propose that the wide range in experimental observations for rate dependence on initiator concentration is due to electrostatic effects. The weakness in their model is that they fail to incorporate radical exit at high conversion.

1978—Bataille, P. B., T. Van, and Q.B. Pham [487]

These authors studied the semicontinuous polymerization of vinyl acetate. Over the course of the polymerization, Bataille, Van, and Pham found that particles were continuously being nucleated. Older particles ended up being much larger than their more recently formed counterparts. Therefore, the semicontinuous addition technique was found to have a broadening effect on the particle size distribution. They proposed that both homogeneous and micellar mechanisms were important in the polymerization, that the polymerization was first order, and that a linear increase in the rate of polymerization was observed with an increase in particle number .

[482] Stannett, V., A. Klein, and M. Litt. 1975. *British Polymer Journal*. 7, 139.
[483] Harriott, P. 1971. *Journal of Polymer Science, A-1*. 9, 1153.
[484] Harada, M., M. Nomura, W. Eguchi, and S. Nagata. 1971. *Journal of Chemical Engineering (Japan)*. 4, 1, 54.
[485] Friis, N. and L. Nyhagen. 1973. *Journal of Applied Polymer Science*. 17, 2311.
[486] Stannett, V., A. Klein, and M. Litt. 1975. *British Polymer Journal*. 7, 139.
[487] Bataille, P., B.T. Van, and Q.B. Pham. 1978. *Journal of Applied Polymer Science*. 22, 3145.

Similar to the findings of Elgood, Gulbekian and Kinsler,[488] these authors also found that the rate of polymerization increased linearly with increasing surface area of the latex particles.

1979—Zollars [489]

Zollars also tried to develop a model for the kinetics of vinyl acetate polymerization. He showed that the length of the hydrophobic portion of the emulsifying molecule had no effect on the polymerization rate. This was opposite the findings of Netschey, Napper and Alexander.[490] Zollars commented that the discrepancy was due to the extremely low monomer concentration that the other team utilized in their study. Apparently Netschey, Napper, and Alexander carried out experiments in concentrations where all of the monomer was soluble in the water phase, which led to different findings.

Furthermore, Zollars accounts for changes in the particle number with initiator concentration, and criticizes the work of Litt[491] and Friis,[492] who did not consider the impact of the initiator concentration on particle number.

1981—Chang, Litt, and Nomura [493]

These authors examined a number of different parameters and their impact on the polymerization rate. Among the variables being studied were changes in: particle concentration, the nature and concentration of the emulsifier, the initiator concentration, the ionic strength, and the volume of monomer. They found that the rate of polymerization was roughly independent of monomer concentration from 20 to 85% conversion, and that the number of particles was independent of conversion in unseeded systems (above 30% conversion). Furthermore, they found that the polymerization rate depended on the number of particles to the 0.2 power and on the emulsifier concentration to the 0.25 power. Lastly, they added that while chain transfer was an important factor in determining the molecular weight, all of the other variables which were studied had no effect on molecular weight.

1983—Warson [494]

Warson provides an excellent article on the industrial aspects of the polymerization. He emphasizes that industrial emulsion polymerizations have unique complications. Reproducibility of the properties of the latices (especially with respect to the solids content, particle size distribution, viscosity, molecular weight, and residual monomer content) had to be maintained within set limits to sell the products; yet was difficult to attain. Furthermore, the geometries of the reaction vessel and stirrer were noted to have important effects on the polymerization.

---

[488] Elgood, B.G., E.V. Gulbekian, and D. Kinsler. 1964. *Journal of Polymer Science, Part B, Polymer Letters*. 2, 257.
[489] Zollars, R.L. 1979. *Journal of Applied Polymer Science.* 24, 1353.
[490] Netschey, A., D.H. Napper, and A.E. Alexander. 1969. *Journal of Polymer Science, Part B, Polymer Letters.* 7, 329.
[491] Litt, M., R. Patsiga, and V. Stannett. 1970. *Journal of Polymer Science, A-1*. 8, 3607.
[492] Friis, N. and L. Nyhagen. 1973. *Journal of Applied Polymer Science*. 17, 2311.
[493] Chang, K.H.S., M. H. Litt, and M. Nomura. "The Reinvestigation of Vinyl Acetate Emulsion Polymerization" in *Emulsion Polymerization of Vinyl Acetate*. M.S. El-Aasser, J.W. Vanderhoff, Eds. Applied Science: London, 1981.
[494] Warson, H. 1983. *Chemistry and Industry*. 21, 220.

Warson also observed that reactions that had been successful on the lab scale often failed for no evident reason during scale-up; resulting in precipitation.

1983—Triveldi et al. [495]

These authors conducted a study to investigate the effect of changing the monomer to water ratio on the rate of polymerization. They concluded that the rate increased, and the molecular weight decreased, with increasing monomer to water ratios. Their data seemed to support the model of Harriott.

1987—Bataille, Bourassa and Payette [496]

In 1987, the effect of metallic salts on the emulsion polymerization of vinyl acetate (when initiated by potassium persulfate and stabilized by sodium lauryl sulfate) was investigated by Bataille, Bourassa and Payette. The parameters that were examined included molecular weight, conversion, and the rate of polymerization. Silver ions decreased the induction time, and led to a gradual increase in molecular weight up to 80% conversion, then a very sharp increase. Cobalt had no effect on the rate of polymerization, but led to longer induction times. Copper led to limited conversion and lower molecular weights. Iron cations seemed to have no negative effect, but it was noted that they could scavenge sulfate anions. Sulfate and chloride anions led to shorter induction times, while nitrate ions increased the induction time.

The authors also performed the same experiments with a non-ionic surfactant, and found slightly different results. Under these conditions, only copper was found to be somewhat of an inhibitor. The use of a salt always led to higher global conversion than the same conditions without a salt. Silver led to a higher rate of polymerization.

The authors concluded that the non-ionic surfactant led to better results because it favored the polymerization occurring within the polymer particles. That is, there was not as great of an electrostatic barrier for the oligoradicals (formed by homogeneous nucleation) to enter the stabilized polymer particles.

1991—Hergeth, Lebek, Kakuschke, Schmiltzler [497]

According to homogeneous nucleation, short chain oligomers form at the beginning of the polymerization. These authors set out to characterize those oligomers and to determine whether or not they formed micelles during the polymerization. They concluded that the oligomers are produced and that they associate and form micelles.

1993—Brooks and Wang [498]

The work of Brooks and Wang begins with a brief review of the developments and theories important in the emulsion polymerization of vinyl acetate. Then the authors describe their study of the emulsifier-free emulsion polymerization of vinyl acetate, initiated by potassium persulfate. Their goal was to investigate the effect of seed on the polymerization reaction. The authors

[495] Triveldi, M.K., K.R. Rajagopal, and S.N. Joshi. 1983. *Journal of Polymer Science, Polymer Chemistry Ed*. 21, 2011.
[496] Bataille, P., H. Bourassa and A. Payette. 1987. *Journal of Coatings Technology*. 59, 753, 71.
[497] Hergeth, W.D., W. Lebek, R. Kakuschke, K. Schmutzler. 1991. *Makromolekulare Chemie*. 32, 2265.
[498] Brooks, B.W. and J. Wang. 1993. *Polymer*. 34, 1, 119.

found that the rate of polymerization was independent of the monomer to polymer ratio, but that stable new particles formed when the ratio was high. They also found that at high stirring speeds, the rate of polymerization was reduced.

1994—Tobita [499]

Tobita et al. developed a simulation method to predict the kinetics of long chain branching in vinyl acetate systems. His model seems promising in fitting experimental data.

1996—DeBruyn, Gilbert, and Ballard [500]

In vinyl acetate emulsion polymerization, the rate of polymerization remains fairly constant in interval III, whereas for other monomers, the rate generally decreases since the amount of monomer is being depleted. A possible explanation for this is the balancing effect between the decreasing concentration of monomer in the particles and the longer lifetimes of the radicals. Radical exit was monitored by gamma-radiolysis and it was found that as radicals exited, the rate of polymerization slowed; thereby confirming the authors' hypothesis.

1998—Britton, Heatley, and Lovell [501]

Noting the significant effects that branching has on the viscosity and mechanical properties of the polymeric system, these authors studied the mechanism of branching by ^{13}C NMR. The authors give evidence for chain transfer where the abstraction of a hydrogen atom occurs primarily from the methyl group.

Effects of Polymeric Stabilizers

Pluronic™ (block copolymer of propylene oxide and ethylene oxide)

1958—French [502]

French completed a study similar to that of Priest[503] in 1958, but used Pluronic™ (block copolymers of propylene oxide and ethylene oxide) as the emulsifying agent. The polymerization was a batch polymerization of vinyl acetate completed at 65° to 70° C, and resulted in the following observations:

- the number of polymer particles remained constant in the polymerization, above 20% conversion,
- monomer- swollen polymer particles achieve their maximum diameter at 13.5% conversion,
- monomer droplets disappeared below 15% conversion,
- the surface area of the particles was proportional to the concentration of emulsifier, and

[499] Tobita, H. 1994. *Polymer*. 35, 3032.
[500] DeBruyn, H., R.G. Gilbert, and M.J. Ballard. 1996. *Macromolecules*. 29, 8666.
[501] Britton, D., F. Heatley, and P.A. Lovell. 1998. *Macromolecules*. 31, 2828.
[502] French, D.M. 1958. *Journal of Polymer Science*. 32, 395.
[503] Priest, W.J. 1952. *Journal of Physical Chemistry*. 56, 1077.

- the number of particles and the surface area of the particles, normalized by the amount of emulsifying agent, was much lower in the case of vinyl acetate polymerization than that for styrene polymerization.

French advocates the micellar mechanism, as opposed to the solution polymerization proposed by Priest, and finds results that correspond well to the predicted values from the Smith-Ewart theory (the number of polymer particles scales with soap concentration to the 3/5 power). The only difference noted between the vinyl acetate polymerization and that of styrene was that the water-solubility of vinyl acetate resulted in disappearance of monomer droplets much earlier (<15 % conversion) than that for styrene (> 30 % conversion).

1968—Gulbekian [504]

Gulbekian, in 1968, published another paper (in addition to French's) regarding the emulsion polymerization of vinyl acetate in the presence of Pluronic™. He completed the polymerization in a semi-continuous manner, and found that the surfactant concentration determined the particle size (it relates to the area the surfactant molecule can adequately stabilize), and that the surfactant to monomer ratio is also directly proportional to the particle surface area. For this system, he also observed that the rate of polymerization was found to be proportional to the amount of monomer soluble in the water phase, and therefore, Gulbekian concedes that the major locus of polymerization is in the water phase.

Poly(vinyl alcohol) and Hydroxyethyl cellulose

1958--O'Donnell, Mesrobian, and Woodward [505]

O'Donnell, Mesrobian, and Woodward published the first study which used poly(vinyl alcohol) as a colloid stabilizer in 1958. They reaffirmed Smith-Ewart behavior with respect to 1. rate dependence on the concentration of initiator, and 2. the polymerization rate being independent of monomer concentration; however, they found a differing result for the rate dependence on the emulsifier concentration. According to Smith and Ewart[506], the rate should scale with the concentration of emulsifier to the 2/5 power. O'Donnell, Mesrobian and Woodward instead found that the rate scaled with the concentration of emulsifier to the 0.7 power, and could offer no explanation for the increased rate dependence, except to suggest that polymeric emulsifiers behaved differently. They noted that poly(vinyl alcohol) in water (from 1% to 10%) maintained a surface tension of 44.8 dynes/cm.

1970—Noro [507]

In his studies, Noro found that the chemical structure of the poly(vinyl alcohol) had a profound impact on the properties of the emulsion. When the poly(vinyl alcohol) was synthesized by acid hydrolysis it was not a good stabilizer for the emulsion, however, reacetylated poly(vinyl alcohol) provided fair stability. Fully hydrolyzed poly(vinyl alcohol) was found to improve water resistance, however, it diminished the freeze-thaw stability of the system. Ultimately,

[504] Gulbekian, E.V. 1968. *Journal of Polymer Science*, A-1. 6, 2265.
[505] O'Donnell, J.T, R.B. Mesrobian, and A.E. Woodward. 1958. *Journal of Polymer Science*. 28, 171.
[506] Smith, W.V. and R.H. Ewart. 1948. *Journal of Chemical Physics*. 16, 592.
[507] Noro, K. 1970. *British Polymer Journal*. 2, 128.

Noro found that the viscosity, freeze-thaw stability, particle size, and stability were all impacted by the fine chemical structure of the alcohol.

1973—Gulbekian and Reynolds [508]

In 1973 Gulbekian and Reynolds published a chapter that surveyed the use of poly(vinyl alcohol) as a colloid stabilizer. They found that maximum conversion and minimum precipitate resulted with poly(vinyl alcohol) that was between 82.6 and 91.5 % hydrolyzed. They also noted that persulfate initiators could oxidatively degrade the poly(vinyl alcohol).

1980--Donescu et al. [509]

In their paper, Donescu et al. evaluated the emulsion polymerization of vinyl acetate when initiated by potassium persulfate stabilized with hydroxyethyl cellulose. They found that the rate of polymerization increased with 1. higher initial monomer concentrations, 2. higher initiator concentrations, and 3. higher hydroxyethyl cellulose concentrations. Two interesting findings in their work were that potassium persulfate induced oxidative degradation of the hydroxyethyl cellulose and that there was evidence of grafting.

1981—Dunn [510]

Dunn also offered some interesting notes about the effects of poly(vinyl alcohol) in the emulsion polymerization of vinyl acetate. He states that the 88% hydrolyzed polymer is the prime choice for emulsion polymerization, and cites work which shows that the remaining 12% of acetate groups are found in short blocks along the length of the chain.

During the polymerization reaction, the presence of poly(vinyl alcohol) was found to dramatically slow the emulsion polymerization of vinyl acetate. Anionic surfactants, by comparison, are much more effective in diminishing the particle size, and also have a minimal effect on the rate of polymerization. Finally, increased adsorption of colloid stabilizer was found to decrease particle size, but increase viscosity.

1983—Warson [511]

Warson provided some industrial background on the usage of poly(vinyl alcohol) stabilizers in emulsion polymerizations. His experience was that poly(vinyl alcohol) having broad molecular weight distribution generally provided greater stability to a latex. Typically, 88% hydrolyzed poly(vinyl alcohol) is used in the emulsion polymerization of vinyl acetate, but variations in the molecular structure introduce changes to the latex. When the polymerization is completed semicontinuously, poly(vinyl acetate) has a tendency to graft onto poly(vinyl alcohol), which sometimes leads to instability. To remedy this problem, additional non-ionic surfactant is added to the formulation. Replacing one type of alcohol with another can result in a product which is completely unstable.

---

[508] Gulbekian, E.V., and G.E. Reynolds. "Poly(vinyl alcohol) in Emulsion Polymerization" in *Poly(vinyl alcohol): Properties and Applications*. C.A. Finch, Ed. Wiley: London, 1973.
[509] Donescu, D., I. Deaconescu, K. Gosa, M. Mazare, and I. Gavat. 1980. *Revue Roumaine de Chimie*. 25, 7, 975.
[510] Dunn, A.S. "Polymerization of Aqueous Solutions of Vinyl Acetate" in *Emulsion Polymerization of Vinyl Acetate.* M.S. El-Aasser and J.W. Vanderhoff, Eds. Applied Science: London, 1981.
[511] Warson, H. 1983. *Chemistry and Industry*. 21, 220.

1985—Donescu [512]

In this article, Donescu utilized poly(vinyl alcohol) in conjunction with cetyl alcohol ethoxylated with ethylene oxide as a protective colloid. He found that greater stability was exhibited for this system in comparison to a simple poly(vinyl alcohol). He also found that the poly(vinyl alcohol) increased the dissociation constant for the potassium persulfate initiator. In general, the conclusion was that the behavior of the system was very complex. Both the particle number and the conversion were found to vary over the course of the reaction. Furthermore, the stirring rate and the distribution of the co-emulsifier were thought to influence the conversion behavior and the structure of the latex.

1993—Donescu, Ciupitoiu, Gosa and Languri [513]

These authors found that the semicontinuous polymerization of poly(vinyl acetate) in the presence of poly(vinyl alcohol) resulted in a hydrated shell. This hydrated shell contained bound water, which acted as a true plasticizer for the system.

1994—Lepizzera and Hamielec [514]

In 1994, Lepizzera and Hamielec used two different molecular weights of 88% hydrolyzed poly(vinyl alcohol) to determine their effects on particle nucleation. In the absence of the alcohol, no new particles were formed, whereas in the presence of the alcohol, new particles were formed and a bimodal particle size distribution resulted. Of the two different molecular weights, more particles were nucleated with the higher molecular weight alcohol. The suspected mechanism involved precipitation of poly(vinyl acetate)-co-vinyl alcohol chains.

2.4.6 Practical Ways to Achieve Desired Properties

Erbil,[515] in his text, provides very brief notes on how to manipulate a polymerization to achieve changes in the following characteristics. These segments were taken from his text.

To Change the Particle Size

Changing the following parameters will result in larger particle size:[516]

1. Decrease the concentrations of emulsifier or protective colloid
2. Decrease the rate of addition of the emulsifier or protective colloid
3. Decrease the initiator content
4. Decrease the rate of addition of the initiator
5. Decrease the temperature of the polymerization

---

[512] Donescu, D., K. Gosa, and A. Ciupitoiu. 1985. Journal of Macromolecular Science-Chemistry. A22, 931.; A22, 941.
[513] Donescu, D., A. Ciupitoiu, K. Gosa, and I. Languri. 1993. *Revue Roumaine de Chimie*. 38, 12, 1441.
[514] Lepizzera, S.M. and A.E. Hamielec. 1994. *Macromolecular Chemistry and Physics*. 195, 3103.
[515] Erbil, H.Y. *Vinyl Acetate Emulsion Polymerization and Copolymerization with Acrylic Monomers*. CRC: Boca Raton, 2000.
[516] Erbil, H.Y. *Vinyl Acetate Emulsion Polymerization and Copolymerization with Acrylic Monomers*. CRC: Boca Raton, 2000.

Alternatively, to form smaller particles, the following recommendations are given:[517]

1. Increase concentration of emulsifier and protective colloid
2. Increase the concentration of initiator
3. Feed the monomer more slowly
4. Increase the temperature of the polymerization
5. Increase the monomer to water ratio

Molecular Weight

To increase molecular weight: [518]

1. Do not use chain transfer agents
2. Decrease the temperature of the polymerization
3. Use redox initiators at lower temperatures
4. Decrease the concentration of initiator
5. Increase the initial charge of monomer to 15-20%
6. Increase the rate of addition of monomer

Viscosity

To increase viscosity:[519]

1. Decrease particle size
2. Increase the concentration of emulsifier and protective colloid
3. Increase the solids concentration
4. Increase the temperature during the polymerization

Stability

To promote stability:[520]

1. Use sufficient concentration of emulsifier
2. Keep the pH within normal range
3. Avoid electrolytes when stabilization is achieved electrostatically
4. Avoid low molecular weight alcohols, which could desorb steric stabilizers from the particle surface
5. Remain at moderate temperatures
6. Avoid high speed agitation or excessive shear, which could strip the stabilizers from the particle surface.

---

[517] Ibid.
[518] Ibid.
[519] Ibid.
[520] Erbil, H.Y. *Vinyl Acetate Emulsion Polymerization and Copolymerization with Acrylic Monomers*. CRC: Boca Raton, 2000.

2.5 Emulsion Copolymerization of Vinyl Acetate

2.5.1 Introduction to Copolymerization

Copolymerization affords the unique opportunity of tailoring a polymer to have properties reflecting the constituent monomers. Over the years, hundreds of monomers have been copolymerized with vinyl acetate. [521] Since some of the major applications of poly(vinyl acetate) latices include paints and adhesives, many monomers have been used in attempts to improve the adhesion and water sensitivity of the polymer while lowering its T_g. [522] Two of the most important commercial copolymers are the copolymers of vinyl acetate with vinyl chloride (flexible sheeting and molded compounds) and with ethylene (hot melt adhesives, as well as other applications). This chapter will provide a very brief overview of the development of free radical copolymerization theory and an equally brief segment on common monomers that are copolymerized with vinyl acetate. The text of Bovey *et al*[523] and of Leonard[524] covered these topics in greater detail.

2.5.2 Historical Developments

Summaries of early empirical work on free radical copolymerization reactions have been published by Mayo and Walling,[525] Alfrey,[526] and Meyer.[527] Perhaps the first published account that attempted to describe the mechanism of copolymerization was published by Dostal.[528] Soon thereafter, Norrish and Brookman[529] offered contributions on the copolymerization of styrene and methyl methacrylate. Wall[530] presented a very insightful article in 1941, suggesting that the composition of a copolymer was a function of the relative reactivities of the monomer radicals. The advances put forth by Mayo and Lewis,[531] Alfrey and Goldfinger,[532] and futher contributions of Wall[533] have led to a solid fundamental understanding of copolymerization mechanisms. The "copolymer equation" is discussed by each of the aforementioned authors, and is considered to be the basis for understanding copolymerization mechanisms. This will be presented below, according to the agreed conventions.[534]

---

[521] Leonard, E.C. "Vinyl Acetate" in *Vinyl and Diene Monomers, Part I*. E.C. Leonard, Ed. Wiley: New York, 1970.
[522] Ibid.
[523] Bovey, F.A., I.M. Kolthoff, A.I. Medalia, and E.J. Meehan. *Emulsion Polymerization*, High Polymer Series Volume 9. H. Mark, C.S. Marvel, H.W. Melville, and G.S. Whitby, Eds. Interscience: New York, 1955.
[524] Leonard, E.C. "Vinyl Acetate" in *Vinyl and Diene Monomers, Part I*. E.C. Leonard, Ed. Wiley: New York, 1970.
[525] Mayo, F.R. and C. Walling. 1950. *Chemical Reviews*. 46, 191; (through #525)
[526] Alfrey Jr., T., J.J. Bohrer, and H. Mark. *Copolymerization*. Interscience: New York, 1952. (through # 525)
[527] Meyer, K.H. *Natural and Synthetic High Polymers*. Interscience: New York, 1950 (through #525)
[528] Dostal, H. 1936. *Monatshefte fuer Chemie*. 69, 424. (through #525)
[529] Norrish, R.W.G, and E.F. Brookman. 1939. *Proceedings of the Royal Society of London*. A171, 147. (through #525)
[530] Wall, F.T. 1941. *Journal of the American Chemical Society*. 63, 1862. (through #525)
[531] Mayo, F.R. and F.M. Lewis. 1944. *Journal of the American Chemical Society*. 66, 1594. (and later references)
[532] Alfrey, Jr. T. and G. Goldfinger. 1944. *Journal of Chemical Physics*. 12, 205.
[533] Wall, F.T. 1944. *Journal of the American Chemical Society*. 66, 2050.
[534] Alfrey, Jr. T., F.R. Mayo, and F.T. Wall. 1946. *Journal of Polymer Science*. 1, 581.

2.5.3 The Copolymer Equation

Given that two different monomers, M_1 and M_2 are present and are capable of reacting with a free radical to form an active center, the following four reactions can occur.

$$\begin{aligned} M_1^* + M_1 &\xrightarrow{k_{11}} M_1^* \\ M_1^* + M_2 &\xrightarrow{k_{12}} M_2^* \\ M_2^* + M_1 &\xrightarrow{k_{21}} M_1^* \\ M_2^* + M_2 &\xrightarrow{k_{22}} M_2^* \end{aligned} \qquad (2\text{-}84)$$

In Equation (2-84), *k* refers to the rate constant of the particular reaction, and the asterisk denotes the radical-bearing active center at the end of the growing chain. The rates, in this case, are assumed to depend only on the nature of the active center. This assumption is known as the "terminal" model. Others have investigated the effect that the penultimate unit may have. However, results have shown that those previous units only influence the kinetics in a limited number of conditions. The rate constants are also said to be independent of chain length, which is a valid assumption, except in cases of very short chains.[535]

From the equations shown in (2-84), it follows that the rate of consumption of monomers M_1 and M_2 can be described by the equations in (2-85).

$$\begin{aligned} \frac{-d[M_1]}{dt} &= k_{11}\left[M_1^*\right][M_1] + k_{21}\left[M_2^*\right][M_1] \\ \frac{-d[M_2]}{dt} &= k_{12}\left[M_1^*\right][M_2] + k_{22}\left[M_2^*\right][M_2] \end{aligned} \qquad (2\text{-}85)$$

Considering the composition alone (i.e., ignoring the rates), the equations in (2-85) lead to Equation (2-86).

$$\frac{d[M_1]}{d[M_2]} = \frac{k_{11}\left[M_1^*\right][M_1] + k_{21}\left[M_2^*\right][M_1]}{k_{12}\left[M_1^*\right][M_2] + k_{22}\left[M_2^*\right][M_2]} \qquad (2\text{-}86)$$

Then, assuming that steady state conditions exist, the following equation is obtained.:

$$k_{21}\left[M_2^*\right][M_1] = k_{12}\left[M_1^*\right][M_2] \qquad (2\text{-}87)$$

In Equation (2-88), r_1 and r_2 are referred to as the reactivity ratios of the monomers. These parameters illustrate whether the respective monomer would rather react with the same monomer or the opposing monomer. Higher values of *r* indicate that the monomer prefers to react with itself instead of the opposing monomer. This leads to blocky structures. When the reactivity

[535] Mayo, F.R. 1948. *Journal of the American Chemical Society*. 70, 3689.

ratio is close to zero, the monomer has an equal preference for adding a like substituent or the other comonomer. This leads to alternating copolymers.

$$\frac{d[M_1]}{d[M_2]} = \frac{[M_1]}{[M_2]} \times \frac{r_1[M_1]+[M_2]}{[M_1]+r_2[M_2]} \qquad (2\text{-}88)$$

$$r_1 = \frac{k_{11}}{k_{12}}$$

$$r_2 = \frac{k_{22}}{k_{21}}$$

An "ideal" copolymer is defined for cases where the product of r_1 and r_2 equals unity. In this special case, the rate for addition is constant. This is relatively rare. The product of most monomer reactivity ratios is less than one.

2.5.4 Effects of Comonomer Addition Rates

Rate Control

The maximum rate of polymerization in emulsions can only be attained when the polymer particles are completely swollen, that is, when the maximum concentration of monomer exists in the particles. In semicontinuous polymerizations, then feed rate, F, is of prime importance. If the feed rate is too high, then the monomer concentration in the reactor is greater than the amount of monomer the particles can hold. This leads to the formation of additional monomer droplets, and is commonly referred to as a "flooded" condition. In this case, semicontinuous polymerization essentially becomes a batch polymerization.

The opposite extreme occurs when the feed rate is too low. In this case, the polymerization is "starved" because the particles are not completely swollen with monomer. Industrially, starved conditions are used to control the rate of polymerization and the composition of copolymers (discussed below).

It is important to note that monomers can partition differently during the reaction due to thermodynamics. Understanding the partitioning that occurs between the water phase, the monomer droplets and the polymer particles requires a thorough understanding of interaction parameters and interfacial tensions, which are both difficult to measure during the polymerization.

Composition Control

When a polymerization is in a monomer-starved state, it is generally true that the instantaneous conversion of comonomers is very high (> 90%). Therefore, controlling the feed of one comonomer allows different distributions of that monomer to be achieved in the copolymer.

Bassett and Hoy[536] developed a technique known as "power feeding" which allows controlled composition drift. Furthermore, core-shell structures can be created through manipulation of the comonomer feed.

Despite the many advantages of monomer-starved conditions, there are also some concerns. First, the lower feed rate gives rise to slower copolymerization rates, which lead to higher molecular weights. Secondly, online monitoring of the copolymer composition or residual monomer cannot be done accurately, since these analyses require time, and the composition is constantly changing.

2.5.5 Important Vinyl Acetate Copolymers

Since vinyl acetate is widely used as an adhesive, paint, and as a constituent of textile coatings, most copolymerizations are completed so as to reduce the glass transition temperature of the product. However, vinyl acetate systems have many other applications. Therefore, vinyl acetate has been copolymerized with hundreds of different kinds of monomers.[537] Here we will briefly note a few of the more important copolymers, as presented in the text of Leonard.[538]

Copolymers with Unsaturated Hydrocarbons

Ethylene

Copolymers of vinyl acetate and ethylene are widely used as hot melt adhesives. The incorporation of ethylene allows the T_g to drop significantly, depending on the mole fraction added. Typically the mole fraction of ethylene is varied from 25 to 80%. Since ethylene is a gas, the use of high pressure is required during the copolymerization.

Others

Propylene, isobutylene, cyclopentadiene, and even styrene can be polymerized with vinyl acetate. The copolymerization with styrene requires the use of an ionic initiator, as styrene can be used as an inhibitor in vinyl acetate polymerization.

Copolymers with Olefinic Halides

Vinyl Chloride

Copolymers of vinyl chloride with vinyl acetate are used in flexible sheeting and films, as well as in molding and extrusion compounds. In fact, 25% of all vinyl acetate resin sales are from copolymers with vinyl chloride. If the vinyl acetate content is less than 10%, then the copolymer can be synthesized via suspension polymerization, which is the typical route for the homopolymerization of vinyl chloride. However, if the vinyl acetate content is greater than 10%, a solution polymerization is conducted.

---

[536] Bassett, D.R. and K.L. Hoy. "Nonuniform Emulsion Polymers: Process Description and Polymer Properties" in Emulsion Polymers and Emulsion Polymerization, ACS Symposium Series #165. D.R. Bassett and A.E. Hamielec, Eds. American Chemical Society: Washington D.C., 1981.

[537] Leonard, E.C. "Vinyl Acetate" in *Vinyl and Diene Monomers, Part I.* E.C. Leonard, Ed. Wiley: New York, 1970.

[538] Ibid.

Other olefinic halides that copolymerize with vinyl acetate include: allyl and methallyl chloride, chloroprene, vinyl fluoride, vinylidene fluoride, tetrafluoroethylene, and many others.

Copolymers with Unsaturated Acids and Esters

Acrylic and Methacrylic Acids and Esters

This class of materials is widely used in paints, adhesives, and textile treating agents. The incorporation of these unsaturated acids and esters provides flexibility to the system, and also provides functional sites which are capable of reacting to improve the durability of the system. Important comonomers for vinyl acetate include acrylic acid, butyl methacrylate, methacrylic acid, methyl acrylate, methyl methacrylate, and others. Erbil's text[539] contains a detailed review of the copolymerization of vinyl acetate with other acrylate monomers.

Various derivatives of maleic and fumaric acids have also been copolymerized with vinyl acetate.

Other Notable Comonomers

Phosphates

Incorporation of phosphate esters provides enhanced fire-resistance to the polymeric system.

Copolymers with monomers containing amide groups

Although vinyl acetate reacts slowly with monomers such as acrylamide, these copolymers are useful, especially in the presence of formaldehyde, as they are capable of crosslinking. Amide containing copolymers can also be crosslinked with toluene diisocyanate. Formulations of vinyl acetate which include a small amount (< 5%) of N-methylolacrylamide are widely used in the furniture industry to bond wood products.

2.6 Common Methods of Characterization for Latices

In preparing these brief notes on characterization methods for latices, the text of Erbil[540] and a chapter by German[541] proved to be excellent resources. Topics included in this discussion will be methods to monitor conversion, molecular weight, particle size, chemical composition, and more.

2.6.1 Conversion During Polymerization

Most of the analyses below are suitable for measuring conversion of homopolymers. Calculating the conversion for copolymers is somewhat more difficult, as partial conversions for each monomer must be determined. Methods like nuclear magnetic resonance (NMR) spectroscopy, infrared spectroscopy (IR), high performance liquid chromatography (HPLC), or titration must

[539] Erbil, H.Y. *Vinyl Acetate Emulsion Polymerization and Copolymerization with Acrylic Monomers*. CRC: Boca Raton, 2000.
[540] Erbil, H.Y. *Vinyl Acetate Emulsion Polymerization and Copolymerization with Acrylic Monomers*. CRC: Boca Raton, 2000.
[541] German, A.L. *et al*. "Latex Polymer Characterization" in *Emulsion Polymerization and Emulsion Polymers*, M.S. El-Aasser and P.A. Lovell, Eds. Wiley: Chichester, 1997.

be used to determine average copolymer composition of the polymer. Alternatively, the precise composition of monomers in the feed must be determined. Another method useful for this task is gas chromatography (GC). Some researchers utilize a GC method with internal standards to directly calculate partial monomer conversions, but according to Erbil,[542] this method is not accurate.

Gravimetric Analysis

The gravimetric analysis for conversion is based on comparing the ratio the solids content of a sample with that which is expected at 100% conversion. In this method, a sample is obtained from the polymerization reactor, and the polymerization reaction is stopped, either by cooling, adding air, or adding a sufficient quantity of inhibitor to the sample. The weight of the sample, and if necessary, the weight of the inhibitor, are recorded. The sample is then dried, and its solids content is determined. By comparing this amount with the amount expected at complete conversion, a relative percentage is obtained.

Gas Chromatography

Either the latex itself[543] or the headspace above the latex (if in equilibrium with the latex) can be sampled and submitted for GC analysis to determine conversion. Quantitative analyses are possible through the inclusion of an internal standard and calculation of the relative response factors of the monomer and the standard. As stated above, Erbil suggests that this is not a suitable method for copolymer conversion. [544]

Ultrasound

Sensors having frequencies between 20 KHz and 100 MHz can be used for the online determination of monomer conversion. The speed of ultrasound waves depend on the relative amounts of the aqueous phase and the polymer particles, thereby allowing a means of calculating conversion.[545, 546]

Dilatometry and Densitometry

The polymerization of monomer into polymer results in a decrease in the partial molar volume of the system. Such a change can be monitored by completing the reaction in a vessel where volume can easily be measured. A simplistic means of this calculation is in a graduated cylinder; however, dilatomers provide more reliable measurements and are more frequently utilized for

---

[542] Erbil, H.Y. *Vinyl Acetate Emulsion Polymerization and Copolymerization with Acrylic Monomers*. CRC: Boca Raton, 2000.
[543] Guyot, A., J. Guillot, C. Graillat, and M.F. Llauro. 1984. *Journal of Macromolecular Science and Chemistry*. A21, 683. (through #543)
[544] Erbil, H.Y. *Vinyl Acetate Emulsion Polymerization and Copolymerization with Acrylic Monomers*. CRC: Boca Raton, 2000.
[545] Morbidelli, M., G. Storti, and A. Siani. in *Polymeric Dispersions: Principles and Applications* (Nato ASI Series Volume 335). J.M. Asua, Ed. Kluwer: Dordrecth, 1997.
[546] Canegallo, S., M. Apostolo, G. Storti, and M. J. Morbidelli. 1995. *Journal of Applied Polymer Science*. 57, 1333. (through #554)

this purpose. In a similar fashion, the change in density which accompanies polymerization can be monitored by Paar digital densitometers[547] or bubble densitometers.[548]

Calorimetry

Another online method that can provide information about conversion is calorimetry. In this case, the reactor is considered a calorimeter, and heat flux is measured throughout the course of the polymerization. Details can be found in the given references [549,550]

Residual Monomer Content

Classically, residual monomer can be detected by GC or via reactions with the unsaturated olefin bond in the monomer. One possible method is to titrate with bromine. Others include the addition of iodine monochloride (which will allow the determination of the iodine number), or the addition of mercury II salts, which can be detected polarographically.[551]

2.6.2 Molecular Weight

Obtaining information about the molecular weight of a polymer can be very valuable, as many properties correlate directly with molecular weight. Many techniques have been developed to characterize the molar mass of polymeric molecules, but all of them require dissolving the polymer in a suitable solvent. Some techniques give information about the number average molecular weight, M_n, others the weight average molecular weight, M_w, and still others give higher averages, such as M_z. Among the various techniques that can be used to determine molecular weight, some measure the mass directly while others rely on indirect methods, requiring calibrations. So-called absolute methods for measuring molar mass are: osmometry, ebullioscopy, cryoscopy, scattering, and ultracentrifugation. Indirect methods include viscometry, size exclusion chromatography, and field-flow fractionation. Some of the more important techniques will be briefly described.

Absolute Methods

Osmometry

Membrane Osmometry. Membrane osmometry gives the number average molar mass (M_n) directly, and is generally effective in determining molecular weights ranging from 50,000 – 500,000 grams per mole.[552] In this technique, a polymeric sample is placed in a membrane and the membrane is immersed in a bath of pure solvent. Solvent molecules, having small molar volumes, are able to pass through the pores of the membrane and do so in an attempt to establish equilibrium. Over time, the concentration of the polymer solution becomes increasingly dilute,

---

[547] Caris, C.H.M., R.P.M. Kuijpers, A.M. vanHerk, and A.L. German. 1990. *Makromolekulare Chemie, Macromolecular Symposia.* 35/36, 535. (through #554)
[548] Schork, F.J. and W.H. Ray. 1983. *Journal of Applied Polymer Science*. 28, 407. (through #554)
[549] Jansson, L., H. Nilsson, C. Silvergren, and B. Tornell. 1987. *Thermochimica Acta*. 118, 97. (through #554)
[550] Moritz, H.U. in *Polymer Reaction Engineering*. K.H. Reichert and W. Geiseler, Eds. VCH: Verlag, 1989. (through #554)
[551] Erbil, H.Y. *Vinyl Acetate Emulsion Polymerization and Copolymerization with Acrylic Monomers*. CRC: Boca Raton, 2000.
[552] German, A.L. *et al*. "Latex Polymer Characterization" in *Emulsion Polymerization and Emulsion Polymers*, M.S. El-Aasser, and P.A. Lovell, Eds. Wiley: Chichester, 1997.

and an osmotic pressure develops. In the limit of infinite dilution, c (the polymer concentration) approaches zero, and the following relation holds:

$$\left(\frac{\pi}{c}\right)_{c\to 0} = \frac{R\,T}{M_n} \quad (2\text{-}89)$$

where π is the osmotic pressure, R is the gas constant, and T is the temperature. M_n is determined by taking several measurements of the osmotic pressure as the polymer concentration drops, and then by extrapolating to zero.[553,554]

Vapor Pressure Osmometry. Vapor pressure osmometery is very similar to membrane osmometry, however, in this technique no membrane is necessary. Here, a drop of the polymer solution and a drop of solvent are placed on two thermistors in an insulated, solvent-saturated chamber. The solvent vapor condenses on the drop of polymer solution causing heat to register on the thermistor. Eventually, the vapor pressure reaches that of the pure solvent. The change in temperature is then related to solution molality, which can be used to compute molar mass. For this experiment, the molecular weight of the sample must be less than 15,000 grams per mole.[555]

Scattering Methods

Several different scattering techniques exist which are useful in determining M_w. These include static light scattering (SLS), small-angle x-ray scattering (SAXS), and small-angle neutron scattering (SANS). In each of these techniques a sample is irradiated with a beam of light at some incident angle to the surface. An analysis of the intensity of the scattered light verses the incident angle gives data regarding the molar mass distribution of the sample. Generally, samples in the range of 10,000 – 10,000,000 grams per mole can be analyzed. For the sake of brevity, further details regarding the scattering procedures will not be given here. Wyatt[556] presents an excellent review of scattering which includes more theoretical background.

Ultracentrifugation

Like the scattering methods, ultracentrifugation allows the analysis of polymers having a wide range of molar masses (1,000 – 1,000,000 grams per mole). It has also been shown to be extremely suitable for heterogeneous samples, such as latices.[557] The theoretical basis for the technique is that polymer molecules, when placed in a centrifugal field, distribute themselves according to molecular weight along the axis that is perpendicular to rotation. By allowing a detector to probe this axis through either interferometry or refraction measurements, molar mass

[553] Young, R.J. and P.A. Lovell. *Introduction to Polymers*. 2nd ed. Chapman and Hall: London, 1991. (through #554)
[554] Billmeyer Jr., F.W. *Textbook of Polymer Science*, 3rd ed. Wiley-Interscience: New York, 1984. (through #556)
[555] German, A.L. *et al*. "Latex Polymer Characterization" in *Emulsion Polymerization and Emulsion Polymers*, M.S. El-Aasser, and P.A. Lovell, Eds. Wiley: Chichester, 1997.
[556] Wyatt, P.J. 1993. *Analytica Chimica Acta*. 272, 1. (through #557)
[557] Springer, J. M.D. Lechner, H. Dautzenberger, and W-M. Kulicke. 1992. *Makromolekulare Chemie, Macromolecular Symposia.* 61, 1. (through #562)

data can be obtained, either through sedimentation equilibrium or sedimentation velocity theories.[558]

Matrix-Assisted Laser Desorption Ionization Mass Spectrometry (MALDI-MS)

MALDI-MS is a relatively new technique for directly measuring molar mass of a sample. It was originally developed for high molecular weight biopolymers, but recently[559] has been applied successfully to synthetic polymers like polymethyl methacrylate, polyethylene glycol and polystyrene. In the experiment, the polymer sample is dissolved in a UV-active matrix. When a UV-laser pulse is applied to the sample matrix, the polymer molecules are ionized, transferred to the gas phase, and accelerated by an electrical field. Over time, the mass spectrum of the sample is recorded by the time of flight (TOF) technique. Generally the technique can be applied to polymers having molar masses up to approximately 200,000 grams per mole.[560] A review of the technique can be found in a recent publication by Creel.[561]

Indirect Measurement Techniques

Viscometry

Viscosity measurements allow indirect calculations of molar mass. In this case, it is the viscosity average molar mass, M_v, which is measured. M_v always takes on values between M_n and M_w, but tends to be closer to M_w. This technique is based on an empirical relationship, which gives a correction factor for calculating molar mass on the basis of intrinsic viscosity, $[\eta]$. Intrinsic viscosity is the limiting value for the reduced viscosity as the concentration of the polymer solution approaches zero. One important empirical relationship that has been established is the Mark-Houwink expression, shown below.

$$[\eta] = K\, M_v^a \qquad (2\text{-}90)$$

In this equation, both K and a are constants, and are known as the Mark-Houwink constants. These parameters have certain values for a given system, and depend on the temperature, the solvent, and the polymer. Viscosity measurements can be accurate over a range of molar masses, from 1,000-10,000,000 grams per mole, but it is noted that corrections to the experimental viscosity may be necessary at the extremes.[562]

Size Exclusion/Gel Permeation Chromatography (SEC) or (GPC)

SEC, also known as GPC, has become one of the most common means of measuring molar mass of polymers. As a relative method, it requires calibrations with polymeric standards having known molecular mass and narrow polydispersity. Preferentially, a sample of the same chemical composition should be used as a standard. However in many cases, a polymer having the same

---

[558] German, A.L. *et al*. "Latex Polymer Characterization" in *Emulsion Polymerization and Emulsion Polymers*, M.S. El-Aasser, and P.A. Lovell, Eds. Wiley: Chichester, 1997.
[559] Bahr, U. A. Deppe,, M. Karas, F. Hillenkamp and U. Siesmann. 1992. *Analytical Chemistry.* 64, 2866. (through #562)
[560] German, A.L. "Latex Polymer Characterization" in *Emulsion Polymerization and Emulsion Polymers*, M.S. El-Aasser, and P.A. Lovell, eds. Wiley: Chichester, 1997.
[561] Creel, H.S. 1993. *Trends in Polymer Science*. 1, 336. (through #562)
[562] German, A.L. "Latex Polymer Characterization" in *Emulsion Polymerization and Emulsion Polymers*, M.S. El-Aasser, and P.A. Lovell, eds. Wiley: Chichester, 1997.

chemical composition as the sample, a known molar mass, and a narrow molecular weight distribution simply is not available. In these cases, a universal calibration must be completed. For the universal calibration, a polymeric standard is selected which has approximately the same hydrodynamic volume as the sample, as similar hydrodynamic volumes would lead to similar elution behaviors.

The principle of the SEC or GPC experiment is based on elution through a chromatogram packed with porous particles. A suitable solvent for the polymer is selected, and is used to prepare a polymer solution of known concentration. When a sample of the polymer solution is injected into the chromatogram, only relatively small molecules will be able to penetrate the holes in the porous column packing material. This results in smaller molecules interacting with many of the porous particles, and thus, they elute very slowly. Larger molecules, on the other hand, elute very quickly, as their size prohibits them from interacting with the porous packing material. This process allows an efficient separation of the chains of various molar masses during the chromatogram run. At the end of the packed column, a detector monitors the concentration of polymer passing by at any given time. Typically, the detector is a refractive index (RI) detector, although others methods are available as well.[563,564] By analyzing the standards under a given set of conditions, a calibration curve can be developed which provides useful data regarding the relationship between molar mass and the elution volume.

Field-Flow Fractionation (FFF)

Field-Flow Fractionation bears similarities to both the ultracentrifugation technique and the SEC/GPC method. For this experiment, a dilute polymer sample is allowed to flow through a narrow tube as a centrifugal force is applied perpendicular to the flow. This creates a gradient within the tube and molecules then align according to their sizes. According to Gunderson,[565] the FFF technique has greater sensitivity than the SEC/GPC technique.

2.6.3 Particle Size Distribution

Many techniques are available to investigate the particle size distribution of a latex, most of which assume that the particles are spherical. Understanding the average particle size and the breadth of the size distribution aids the scientist in developing an understanding of the polymerization kinetics, and also the ultimate performance of the latex, particularly with respect to the viscosity and stability of the polymer. Procedures to determine particle size will be noted briefly here. Most of the techniques require dilution prior to analysis.

[563] Kuo, C-Y. and T. Provder. *Size Exclusion Chromatography for Polymers and Coatings*, ACS Symposium Series, Volume 351. 1987. (through #566)
[564] German, A.L. "Latex Polymer Characterization" in *Emulsion Polymerization and Emulsion Polymers*, M.S. El-Aasser, and P.A. Lovell, eds. Wiley: Chichester, 1997.
[565] Gunderson, J.J. and J. C. Giddings, 1986. *Analytica Chimica Acta.* 189, 1. (through #566)

Microscopy

Optical Microscopy

The biggest problem with using optical microscopy to evaluate particle size in latices is that its resolution is limited to 0.4 μm. Therefore, according to Erbil,[566] latices with particle sizes less than 2 μm are not typically investigated in this manner. In 1938, Lucas[567] found that the use of UV light enhanced the resolving power, but the source had to be adequate for examining the particles. Later, in 1955, dark-field microscopy was invented by Schoon and Phoa,[568] who used a dark-field condenser with a phase-contrast objective. This method also resulted in improved resolving power, and has a useful range of 0.05-0.80 μm.[569]

Theoretically, microscopy allows the particle size to be determined as predicted by the Mie scattering theory, where the particles act as point sources for scattering. Although the method is sensitive to dust contaminations on the microscope slide, much useful information can be obtained, such as the breadth or narrowness of the size distribution, the presence of very large and or agglomerated particles, and the presence of flocs and second generation particles.[570,571,572]

Electron Microscopy

The most typical means of measuring latex particle size and particle size distribution is through the use of electron microscopy. In this technique, an electron source is used to bombard a very dilute sample of latex. Usually, the particles are added on the stage in very dilute concentration, and the stage is examined after the solution has evaporated from the surface. However, there are several problems that can occur during this type of measurement. The first problem is for rubbery latex particles. When these particles dry, they could agglomerate or flatten during the drying process. Therefore, the dimensions which are measured may not be truly representative of the actual dimensions. To remedy this problem, Brown[573] came up with a bromination technique which was useful in hardening the particles, fixing them at a given size. Another problem that arises from this technique is the lack of definitition that is seen in the particle size. This is due to the scattering behavior of latices being very similar to the scattering behavior of the metal substrate. Metal shadow casting of a gold film, approximately 0.8 nm thick around the particles has been used to eliminate this effect. Finally, there is usually a problem with obtaining a representative sample. Since an initial sample of the latex is further diluted, it may be necessary to do a number of analyses to be sure the measurements accurately reflect the particle size distribution of the latex.

---

[566] Erbil, H.Y. *Vinyl Acetate Emulsion Polymerization and Copolymerization with Acrylic Monomers*. CRC: Boca Raton, 2000.
[567] Lucas, F.F. 1938. *Industrial and Engineering Chemistry*. 30, 146; 1942. *Industrial and Engineering Chemistry*. 34, 1371. (through #568)
[568] Schoon, Th. G.F. and K.L. Phoa. 1955. *Journal of Colloid Science*. 10, 226.
[569] Erbil, H.Y. *Vinyl Acetate Emulsion Polymerization and Copolymerization with Acrylic Monomers*. CRC: Boca Raton, 2000.
[570] Collins, E.A., "Measurement of Particle Size and Particle Size Distribution" in *Emulsion Polymerization and Emulsion Polymers*, Lovell, P.A. and El-Aasser, M.S., Eds. Wiley: New York 1997.
[571] Brown, W.E. 1947. *Journal of Applied Physics*, 18, 273. (through #568)
[572] Davidson, J.A. and H.S. Haller. 1955. *Journal of Colloid and Interface Science*. 10, 226.
[573] Brown, W.E. 1947. *Journal of Applied Physics*, 18, 273. (through #568)

In the literature, Priest[574] was the first to use electron microscopy to determine particle size distributions. Later, Klein and Stannett[575] used a freeze drying technique in conjunction with carbon replication to harden the PVAc latex particles. Later Lepizzera and Hamielec[576] disputed the use of electron microscopy for poly(vinyl acetate) latices, citing that the particles shrunk when exposed to the electron beam. They chose to instead use a disc centrifugation method.

Fractional Creaming

The fractional creaming method for determining particle size dates back to 1939.[577] In the 1950's, universal calibration curves were developed which showed the variation of the maximum particle number with the concentration of the creaming agent remaining in the aqueous phase. To determine particle size by fractional creaming, increasing aliquots of a creaming agent such as sodium alginate are added to a series of diluted latex dispersions. The total solids content of each dispersion is adjusted to 2.5%. After the addition of the creaming agent, the dispersion is gently mixed, and allowed to stand at room temperature for 24 to 48 hours. Over this period of time a skin forms, which contains all of the particles above a given "critical" size. The skin is removed and analyzed to determine polymer content, and the concentration of sodium alginate remaining in the aqueous phase is also measured. The difference between the initial latex polymer content and the skin indicates the amount of polymer particles present in the water phase which are below the critical size. A universal calibration curve is used to determine the critical particle size, based on the amount of sodium alginate remaining in the aqueous phase. Careful analysis of all the samples allows a mass distribution curve to be constructed where a known fraction of particles exists in the dispersed phase below the critical dimension.[578]

This method works extremely well for particles having low glass transition temperatures. It is based on the principle that there is some variation of particle size within the dispersion. Eventually, a limiting particle size is attained, such that the addition of more creaming agent results in no significant change.

Soap Titration

Another method for determining particle size is soap titration. In this method, small quantities of surfactant (0.05 – 0.25 M) are added to a dilute (10% solids content) sample of latex. The polymer content in the latex must be known prior to the addition of surfactant. After each addition of surfactant, either the surface tension (via the du Nuoy ring) or the electrical conductance of the latex is measured. A sharp peak in the measurements indicates that the CMC has been reached. Assuming that the particles are spherical, and that any surfactant that is initially present in the system will be replaced by the added surfactant, the diameter of the particles can be determined. Since the CMC for the surfactant is known, the polymer content is known, and the area that each adsorbed surfactant molecule occupies is known, then the "volume-to-surface-area diameter" can be calculated. Generally, the method does not give high

---

[574] Priest, W.J. 1952. *Journal of Physical Chemistry*. 56, 1077.
[575] Klein, A. and V.T. Stannett. "Surface Chemical Effects on Free Radical Capture" in *Emulsion Polymerization of Vinyl Acetate.* M.S. El-Assser and J.W. Vanderhoff, Eds. Applied Science: London, 1981.
[576] Lepizzera, S.M. and A.E. Hamielec. 1994. *Macromolecular Chemistry and Physics*. 195, 3103.
[577] McGavack, J. 1939. *Industrial Engineering and Chemistry.* 31, 1509. (through #580)
[578] Erbil, H.Y. *Vinyl Acetate Emulsion Polymerization and Copolymerization with Acrylic Monomers*. CRC: Boca Raton, 2000.

accuracy, but it is relatively quick to perform. Several articles on the soap titration method have been published by Maron, Elder, and co-workers.[579,580,581]

Light and Scattering Methods

When electromagnetic radiation is passed into a colloidal solution, part of it is transmitted, part is absorbed, and the remainder scatters. Some of the incident energy causes fluctuations in dipoles within the particles. The light that is scattered has the same frequency and wavelength as the incident light, and depends on the size, shape, nature, and concentration of the particles in the dispersion. Small particles exhibit the same scattering intensity in forward and reverse directions, whereas larger particles are impacted by interference which cause more scattering in the forward direction than the reverse. Therefore, by varying the angle of the incident radiation, an accurate picture of particle size can be determined.

Classical Light Scattering

Lord Rayleigh,[582] Mie,[583] and Debye[584] are three of the pioneers in the theory behind light scattering. The subject is very complex, and will not be covered here in great detail. In a light scattering experiment, a beam of unpolarized light is filtered, expanded, collimated, and passed through a dilute dispersion. Both diffracted and transmitted light are collected by an optics system and are focused onto a detector. Large particles scatter at small angles, and small particles scatter at large angles, so typically a series of concentric diffraction rings are obtained. By applying Mie and Fraunhofer theories, the weight average particle size distribution is obtained. This technique is useful in the range of 0.1 to 50 μm. Dunn and Chong[585] and Zollars[586] both used light scattering techniques to measure the particle size distributions of poly(vinyl acetate) latices.

Quasi-Elastic Light Scattering

A number of different techniques are considered in the category of quasi-electric light scattering (QELS). These include photon correlation spectroscopy, dynamic light scattering, laser scattering, light beating spectroscopy and laser Doppler velocimetry. The difference between QELS and classical light scattering is that the time and frequency fluctuations due to Brownian motion of the particles is the basis for QELS, whereas classical light scattering is focused on collecting only information about the average intensity of the scattered light. The diffusivity of the particles is determined by following its frequency and intensity fluctuations, and the diffusion constant is easily related to particle diameter through the Stokes-Einstein equation.

QELS is limited to particles with a particle size between 0.003 – 5 μm. Furthermore, it cannot be used for samples having a multimodal particle size distribution.

---

[579] Maron, S.H., S.E. Elder, and I.N. Ulevitch. 1954. *Journal of Colloid Science*. 9, 89. (through #580)
[580] Maron, S.H., S.E. Elder, and C.J. Moore. 1954. *Journal of Colloid Science*. 9, 104. (through #580)
[581] Maron, S.H. and S.E. Elder. 1954. *Journal of Colloid Science*. 9, 263; 9, 347; and 9, 353. (through #580)
[582] Rayleigh, L. 1871. *Philosophical Magazine*. 41, 107, 274; and 447. (through #580)
[583] Mie, G. 1908. *Annalen der Physik*. 25, 377. (through #580)
[584] Debye, P. 1915. *Annalen der Physik*. 46, 809. (through #580)
[585] Dunn, A.S. and L.C.H. Chong. 1970. *British Polymer Journal*. 2, 49.
[586] Zollars, R.L. 1979. *Journal of Applied Polymer Science*. 24, 1353.

Turbidity

Turbidity measurements are a simpler means of gathering information about the particle size of a latex. For this measurement, a latex sample is diluted enough to eliminate effects of multiple scattering, and placed in an optical cell having known path length (l). Then the ratios of incident (I_0) and transmitted (I) light are detected at a given wavelength by a spectrophotometer. Turbidity (τ) is calculated by the relationship given in Equation (2-91).

$$\tau = \left(\frac{1}{l}\right) \ln\left(\frac{I_0}{I}\right) \quad (2\text{-}91)$$

Semi-empirical relationships [587,588,589,590] allow the particle size distribution to be determined from turbidity results at different wavelengths of incident light. The measurement is very easy to perform. All that is necessary is dilution of the latex and and a UV Spectrometer. Gulbekian,[591] and Kiparissedes, MacGregor, Singh, and Hamielec[592] used this method to determine the average particle size of poly(vinyl acetate) latexes.

Chromatography

Both hydrodynamic and size exclusion chromatography can also be used to determine particle size. These techniques are very similar, with the exception of the porosity of the packing material. For hydrodynamic chromatography, the beads are non-porous, and the method depends on the velocity profile that develops as the dilute polymer solution flows through the packed capillary column. Large particles tend to flow through the center and elute more rapidly whereas smaller particles tend to be near the wall and elute more slowly. A range of particle size from 0.015- 1.50 μm can be analyzed. Care must be taken to ensure calibration of the column, and it should also be noted that the column could become blocked. Size Exclusion Chromatography was described earlier as part of the molecular weight determination tools.

2.6.4 Chemical Composition

Infrared Spectroscopy (IR/FTIR)

Infrared spectroscopy has been widely used to characterize the chemical composition of polymers. It is a relatively quick method, and is able to accommodate a wide variety of samples. Polymer can be dissolved in a solvent and then applied to salt plates, or it could be ground into a fine powder and pressed into a potassium bromate pellet for analysis. One particular study was the determination of the core-shell morphology of poly(vinyl acetate)-polystyrene particles.[593] In that experiment, IR and Raman spectroscopy were able to determine some properties of the interface between the two polymer layers. Generally, the type of IR

[587] Loebel, A.B. 1959. *Industrial Engineering and Chemistry*. 51, 118. (through #580)
[588] Wales, M. 1962. *Journal of Physical Chemistry*. 66, 1768. (through #580)
[589] Gledhill, R.J. 1962. *Journal of Physical Chemistry*. 66, 458. (through #580)
[590] Maron, S.H., P.E. Pierce, and I.N. Ulevitch. 1963. *Journal of Colloid Science*. 18, 470. (through #614)
[591] Gulbekian, E.V. 1968. *Journal of Polymer Science*, *A-1*. 6, 2265.
[592] Kiparissides, C., J. F. MacGregor, S. Singh, and A.E. Hameielec. 1980. *Canadian Journal of Chemical Engineering*. 58, 65.
[593] Hergeth, W-D. and J. Lange. 1991. *Makromolekulare Chemie, Macromolecular Symposium*. 52, 283. (through #566)

spectroscopy used today is Fourier Transform IR, which hastens the analysis, and provides better sensitivity and resolution than traditional IR.[594,595] FTIR is only used in very specific cases on latices. Wang and Poehlein[596] used FTIR and carbon NMR to analyze the composition of oligomers in one latex copolymer system. Real-time FTIR can also have interesting applications to latices. For example, relatively slow processes, like the film formation process, can be monitored, as can a relatively quick curing reaction that may be typical for a UV-curing coating.[597,598]

Attenuated total reflectance FTIR (ATR-FTIR) is a method that relies on the reflectivity of a crystal to transfer radiation to the sample. Since the method is inherently sensitive to materials that strongly absorb IR radiation, films that still contain some water have been studied through this method by Evanson *et al*.[599,600] The surface composition of coalesced films was also studied by ATR-FTIR by Zhao *et al*.[601]

Two other methos include photoacoustic FTIR (PA-FTIR) and reflection/absorption (RA-FTIR). In PA-FTIR, the heat of absorption that occurs as a sample absorbs IR radiation is measured after the heat is released to an inert gas, which is present in the sample chamber. Applications of the PA-FTIR method to latices include Evanson's studies, which were alluded to previously the ATR-FTIR section. RA-FTIR is useful in studying films of varying thickness on metal surfaces.[602,603,604]

Ultraviolet Spectroscopy (UV)

The use of ultraviolet spectroscopy in determining the chemical composition of a polymer is somewhat rare due to the likelihood of finding characteristic, isolated peaks. Nevertheless, both Wojtczak and Switala[605] and Shashidnar *et al* [606] found useful applications for the technique.

Nuclear Magnetic Resonance Spectroscopy (NMR)

Proton and carbon NMR analyses have been very widely used to determine the chemical composition of polymers. Using NMR, even microstructural details can be elucidated. Solution NMR is the preferred technique, and requires that the polymer be either soluble in or swollen by a deuterated solvent, or solvent mixture. An excellent review of the NMR technique and its

[594] Griffiths, P.R. Ed. *Transform Techniques in Chemistry*. Plenum: New York, 1978. (through #566)
[595] Bell, R.J. *Introductory Fourier Transform Spectroscopy*. Academic Press: New York, 1982. (through #566)
[596] Wang, S.T. and G.W. Poehlein. 1993. *Journal of Applied Polymer Science*. 50, 2173; and 1994. 51, 593. (through #566)
[597] Decker, C. and K. Moussa. 1990. *Journal of Polymer Science, Polymer Chemistry Ed*. 28, 3429. (through #566)
[598] Allen, N.S. *et al*. 1991. *Journal of Appled Polymer Science*. 42, 1169. (through #566)
[599] Evanson, K.W. and M.W. Urban. 1991. *Journal of Applied Polymer Science*. 42, 2287. (through #566)
[600] Evanson, K.W., T.A. Thorstenson, and M.W. Urban. 1991. *Journal of Applied Polymer Science*. 42, 2297. (through #566)
[601] Zhao, C.L. *et al.* 1987. *Colloid and Polymer Science*. 265, 823. (through #566)
[602] Francis, S.A. and A.H. Ellison. 1959. *Journal of the Optical Society of America*. 49, 131. (through #566)
[603] Greenler, R.G. 1966. *Journal of Chemical Physics*. 44, 310;and 1969. 50, 1963. (throught #566)
[604] Nguyen, T. and E. Byrd. 1987. *Journal of Coatings Technology*. 59, 39. (through #566)
[605] Wojtczak, Z. and M. Switala. 1986. *Makromolekulare Chemie*. 187, 2427. (through #566)
[606] Shashidnar, G.V. *et al*. 1990. *Journal of Polymer Science, Polymer Letters Ed*. 28, 157. (through #566)

applicability to polymers has been provided by Koenig.[607] Britton, Heatley, and Lovell[608] utilized this method to determine the mechanism of chain transfer in vinyl acetate polymerization.

Pyrolysis Gas Chromatography (PGC)

PGC is useful in determining copolymer composition. This technique involves heating a sample of the copolymer to a high temperature, and then using Gas Chromatography (GC) to monitor the by products of the decomposition. By analyzing individual homopolymers, the approximate composition of the copolymer can be obtained. The advantage of this technique is that only very small samples are necessary, and that the technique offers results very quickly.

2.6.5 Solids Content

An ISO standard[609] exists detailing the procedure for measuring the solids content of rubbery latices. The method is a gravimetric determination after the sample has been dried in a 105°C oven for 2 hours. Before final weighing, the sample is allowed to cool to room temperature in a dessicator.

2.6.6 Density

Either a pyknometer or a hydrometer can be used to measure the density of a latex. This measurement is important for commercial shipping applications. Like most water-based latices, the density of poly(vinyl acetate) is greater than 1 g/cm^3. The polymer handbook[610] reports the density to be 1.191 g/cm^3 at 20°C.

2.6.7 pH

Typically a glass electrode coupled with a saturated calomel electrode are utilized to determine the pH of aqueous latices. An ISO procedure[611] details the exact conditions to be used, and specifies that successive measurements should agree within ± 0.05 units. PH indicator papers can also be used to make rough determinations of pH, but the opacity of the latex can obscure the interpretation of the measurement.[612]

2.6.8 Surface Tension

Polymers' surface free energies cannot be measured directly due to the constraints present in the system. Therefore, indirect methods are required. Generally, contact angles of various liquids on polymer surfaces provide a viable means of learning about the surface energy of a polymer. For such studies, the surface properties of the liquid must be established. Either static

---

[607] Koenig, J.L. *Spectroscopy of Polymers*, ACS Professional Reference Book, American Chemical Society: Washington, DC, 1992.
[608] Britton, D., F. Heatley, and P.A. Lovell. 2000. *Macromolecules*. 33, 5048.
[609] ISO Standard 124-1992: *Rubber Latices-Determination of Total Solids Content*. (through #614)
[610] *Polymer Handbook, 3rd Ed*. J. Brandrup, E.H. Immergut, Eds. Wiley: New York, 1989.
[611] ISO Standard 9760-1986: Rubber Latices-Determination of pH. (through #614).
[612] Erbil, H.Y. *Vinyl Acetate Emulsion Polymerization and Copolymerization with Acrylic Monomers*. CRC: Boca Raton, 2000.

(goniometer, captive bubble, tilting plate, drop dimensions, and Wilhelmy plate methods) or dynamic methods of measuring the contact angle may be used.[613]

2.6.9 Colloidal Stability

Colloidal stability has been measured by adding various quantities of salts to latices and monitoring the time required for coagulum to form. Different applications may require variations of this test. For example, if pH is of concern, then the pH could be altered and the time for destabilization could be measured. The mechanical stability of latices can also be examined in this manner. The sample is simply exposed to some exterior stress and the time to coagulation is recorded.

2.6.10 Coagulum

Coagulum content is specified by passing a diluted sample of the latex through a mesh cloth having openings of 180 ± 10 μm. An ISO procedure[614] provides greater details for the exact experimental conditions. Once the latex has been filtered, the residue on the cloth is washed with a diluted latex, then water, and then is dried to determine the coagulum content. Duplicate measurements should be made, and results should agree within 0.01% by weight.

2.6.11 Mercaptan

Titrations with aqueous iodine solution can be used to detect the amount of n-dodecyl mercaptan in the latex. Ampoteric titrations with silver can also be utilized.[615]

2.6.12 Determining the Branched, Grafted, and Cross-linked Polymer Fractions

Branched and Grafted Material

Both branching and graft polymer content can be determined by GPC. Low-angle light scattering (LALLS) can be used to look at branching as well. Perhaps the best means of distinguishing between grafted and non-grafted materials is to perform selective solvent extractions or precipitations. If material has been grafted onto a polymer backbone which has residual double bonds, then oxidizing agents can be used to cleave the grafted groups.[616]

Cross-Linked Material

The determination of cross-linked material is best achieved through swelling studies, or successive extractions. Cross-linked material will be insoluble in both cases. NMR has also been used to determine crosslinking during polymerization.

---

[613] Ibid.
[614] ISO Standard 706-1985: Determination of Coagulum Content. (through #614).
[615] Bovey, F.A. *et al*. *Emulsion Polymerization*, Vol. 9 in High Polymer Series. Interscience: New York, 1955. (through #614)
[616] Bovey, F.A. *et al*. *Emulsion Polymerization*, Vol. 9 in High Polymer Series. Interscience: New York, 1955.

2.7 References

Adelman, R.L. 1953. *Journal of the American Chemical Society*. 75, 2678.

Adelman, R.L. U.S. Patent (1951) 2,550,449.

Ahmad, H., M. Yassen. 1979. *Polymer Engineering and Science*. 19, 858.

Air Reduction Company, Inc. "Airco Vinyl Acetate Monomer," Murray Hill, N.J, 1964.

Alfrey, Jr. T. and G. Goldfinger. 1944. *Journal of Chemical Physics*. 12, 205.

Alfrey Jr., T., J.J. Bohrer, and H. Mark. *Copolymerization*. Interscience: New York, 1952.

Alfrey, Jr. T., F.R. Mayo, and F.T. Wall. 1946. *Journal of Polymer Science*. 1, 581.

Allan, R.J.P., R.L. Froman, and P.D. Richtie. 1955. *Journal of the Chemical Society*. 2717.

Allen, G. 1961. *Polymer*, 2, 375.

Allen, N.S. *et al*. 1991. *Journal of Appled Polymer Science*. 42, 1169.

Alexander, A.E. and D.H. Napper. 1971. *Progress in Polymer Science*. 3, 145.

Arshady, R. 1992. *Colloid and Polymer Science*. 270, 717.

Bahr, U. A. Deppe, M. Karas, F. Hillenkamp and U. Siesmann. 1992. *Analytical Chemistry*. 64, 2866.

Barnes, C.E., R.M. Elofson, and G.D. Jones. 1950. *Journal of the American Chemical Society*. 72, 210.

Barrett, K.E.J. *Dispersion Polymerization in Organic Media*. Wiley: New York, 1975.

Bartholome, E., H. Gerrens, R. Herbeck, and H.M Weit. 1956. *Zeitschrift fuerElektrochemie*. 60, 334.

Barton, J. and I. Capek. *Radical Polymerization in Disperse Systems*. T.J. Kemp, Translation Ed. Horwood: New York, 1994.

Bassett, D.R. and K.L. Hoy. "Nonuniform Emulsion Polymers: Process Description and Polymer Properties" in *Emulsion Polymers and Emulsion Polymerization*, ACS Symposium Series #165. D.R. Bassett and A.E. Hamielec, Eds. American Chemical Society: Washington D.C., 1981.

Bataille, P., H. Bourassa and A. Payette. 1987. *Journal of Coatings Technology*. 59, 753, 71.

Bataille, P., B.T. Van, and Q.B. Pham. 1978. *Journal of Applied Polymer Science*. 22, 3145.

Bell, R.J. *Introductory Fourier Transform Spectroscopy*. Academic Press: New York, 1982.

Berger, K.C. and G. Brandrup. "Transfer Constants to Monomer, Polymer, Catalyst, Solvent, and Additive in Free Radial Polymerization" in *Polymer Handbook, 3rd Ed.* J. Brandrup and E.H. Immergut, Eds. Wiley-Interscience: New York, 1989.

Billmeyer Jr., F.W. *Textbook of Polymer Science*, 3rd Ed. Wiley-Interscience: New York, 1984.

Blackley, D.C. *Emulsion Polymerization: Theory and Practice*. Applied Science Publishers: London, 1975.

Blackely, D.C. and A.R.D. Sebastian. 1989. *British Polymer Journal*. 21, 313.

Blaikie, K.G. and T.P.G. Shaw, "Poly(vinyl acetate) Solid Resins," in *Encyclopedia of Chemical Technology*, Volume 4. Interscience: New York, 1955.

The Borden Chemical Company. "Vinyl Acetate Monomer," Technical Data Sheet.

Bovey, F.A., I.M. Kolthoff, A.I. Medalia, and E.J. Meehan. *Emulsion Polymerization*. Interscience: New York, 1955.

Britton, D., F. Heatley, and P.A. Lovell. 1998. *Macromolecules*. 31, 2828.

Broens, O., F.H. Mueller. 1955. *Kolloid Zeitschrift*. 140, 121.

Brooks, B.W. and J. Wang. 1993. *Polymer*. 34, 1, 119.

Brown, W.E. 1947. *Journal of Applied Physics*, 18, 273.

Canegallo, S., M. Apostolo, G. Storti, and M. J. Morbidelli. 1995. *Journal of Applied Polymer Science*. 57, 1333.

Caris, C.H.M., R.P.M. Kuijpers, A.M. vanHerk, and A.L. German. 1990. *Makromolekulare Chemie, Macromolecular Symposia.* 35/36, 535.

Cawse, J.L. "Dispersion Polymerization" in *Emulsion Polymerization and Emulsion Polymers*. P.A. Lovell and M.S. El-Aasser, Eds. Wiley and Sons: New York, 1997.

Celanese Corporation of America. Technical Bulletin S-56-2.

Chan, R.K.S., C. Worman. 1972. *Polymer Engineering and Science*. 12, 437.

Chang, K.H.S., M. H. Litt, and M. Nomura. "The Reinvestigation of Vinyl Acetate Emulsion Polymerization" in *Emulsion Polymerization of Vinyl Acetate*. M.S. El-Aasser, J.W. Vanderhoff, Eds. Applied Science: London, 1981.

Chatterjee, S.P., N. Banerjee, and R.S. Konar. 1979. *Journal of Polymer Science, Polymer Chemistry*. 17, 2193.

Chen, C-Y., and I. Piirma. 1980. *Journal of Polymer Science, Polymer Chemistry*. 18, 1979.

Cho, H.G., S.C. Yoon, M.S. Jhon. 1982. *Journal of Polymer Science, Polymer Chemistry Ed*. 20, 1247.

Collins, E.A., "Measurement of Particle Size and Particle Size Distribution" in *Emulsion Polymerization and Emulsion Polymers*, Lovell, P.A. and El-Aasser, M.S., Eds. Wiley: New York 1997.

Cordiero, C.F. "Vinyl Polymers (Vinyl Acetate)" in *Encyclopedia of Chemical Technology*, Volume 24. J.I. Kroschwitz, and M. How-Grant, Eds. Wiley: New York, 1994.

Corrin, M.L. 1947. *Journal of Polymer Science*. 2, 3, 257.

Cowie, J.M.G. *Polymers: Chemistry and Physics of Modern Materials*, 2nd Ed. Chapman and Hall: New York, 1991.

Creel, H.S. 1993. *Trends in Polymer Science*. 1, 336.

Daoust, H., M. Rinfret. 1952. *Journal of Colloid Science*. 7, 11

Davidson, J.A. and H.S. Haller. 1955. *Journal of Colloid and Interface Science*. 10, 226.

Dawkins, J.V. "Aqueous Suspension Polymerizations" in *Comprehensive Polymer Science*, Volume 4, Chapter 14. G. Allen and J.C. Bevington, Eds. Pergamon: Oxford, 1989.

DeBruyn, H., R.G. Gilbert, and M.J. Ballard. 1996. *Macromolecules*. 29, 8666.

Debye, P. 1915. *Annalen der Physik*. 46, 809.

Decker, C. and K. Moussa. 1990. *Journal of Polymer Science, Polymer Chemistry Ed*. 28, 3429.

Dillon, R.E., E.B. Bradford, and R.D Andrews, Jr. 1953. *Industrial and Engineering Chemistry*. 45, 728.

Dinsmore R.P. British Patent. 297,050 (1927); U.S. Patent. 1,732,795 (1929).

Dobler, F., T. Pith, M. Lambla, and Y. Holl. 1992. *Journal of Colloid and Interface Science*. 152, 12.

Dollivar, M.A., T.L. Gresham, G.B. Kistiakowsky, E.A. Smith, and W.E. Vaughn. 1938. *Journal of the American Chemical Society*. 60, 440.

Donescu, D., A. Ciupitoiu, K. Gosa, and I. Languri. 1993. *Revue Roumaine de Chimie*. 38, 12, 1441.

Donescu, D., I. Deaconescu, K. Gosa, M. Mazare, and I. Gavat. 1980. *Revue Roumaine de Chimie*. 25, 7, 975.

Donescu, D., K. Gosa, and A. Ciupitoiu. 1985. *Journal of Macromolecular Science-Chemistry*. A22, 931.; A22, 941.

Dostal, H. 1936. *Monatshefte fuer Chemie*. 69, 424.

Duck, E.W. "Emulsion Polymerization" in *Encyclopedia of Polymer Science and Technology*, Volume 5. Wiley: New York, 1966.

Dunbrook, R.F. "Historical Review" in *Synthetic Rubber*. G.S. Whitby, C.C. Davis, and R.F. Dunbrook, Eds. Wiley: New York, 1954.

Dunn, A.S. "Harkins, Smith-Ewart and Related Theories" in *Emulsion Polymerization and Emulsion Polymers*. P.A. Lovell, M.S. El-Aasser, Eds. Wiley: Chichester, 1997.

Dunn, A.S. in *Emulsion Polymerization.* I. Pirrma, Ed. Academic Press: New York, 1982.

Dunn, A.S. "The Polymerization of Aqueous Solutions of Vinyl Acetate" in *Emulsion Polymerization of Vinyl Acetate*. J.W. Vanderhoff and M.S. El-Aasser, Eds. Applied Science: London 1981.

Dunn, A.S. and W.A. Al-Shahib. 1978. *British Polymer Journal*. 10, 137.

Dunn, A.S. and L.C.H. Chong. 1970. *British Polymer Journal*. 2, 49.

Dunn, A.S., and Z.F. Said. 1982. *Polymer*, 23, 1172.

Dunn, A.S. and P.A. Taylor. 1965. *Makromolekulare Chemie*. 83, 207.

Eckersley, S.T., and A. Rudin. 1990. *Journal of Coatings Technology*. 62, 89.

El-Aasser, M.S. and E.D. Sudol. "Features of Emulsion Polymerization" in *Emulsion Polymerization and Emulsion Polymers*. J.W. Vanderhoff and M.S. El-Aasser, Eds. Wiley: New York, 1997.

Elgood, B.G., E.V. Gulbekian, and D. Kinsler. 1964. *Journal of Polymer Science, Part B, Polymer Letters*. 2, 257.

Elgood, B.G. and E.V. Gulbekian. 1973. *British Polymer Journal*. 5, 249.

Emulsion Polymerization and Emulsion Polymers. Lovell, P.A. and M.S. El-Aasser, Eds. Wiley: Chichester, 1997.

Erbil, H.Y. *Vinyl Acetate Emulsion Polymerization and Copolymerization with Acrylic Monomers*. CRC: Boca Raton, 2000.

Evanson, K.W. and M.W. Urban. 1991. *Journal of Applied Polymer Science*. 42, 2287.

Evanson, K.W., T.A. Thorstenson, and M.W. Urban. 1991. *Journal of Applied Polymer Science*. 42, 2297.

Everett, D.H. *Basic Principles of Colloid Science*. Royal Society of Chemistry: London, 1988.

Fitch, R.M. *Polymer Colloids: A Comprehensive Introduction*. Academic Press: San Diego, 1997.

Fitch, R.M and C.H. Tsai. In *Polymer Colloids, Proceedings*. R.M. Fitch, Ed. Plenum Press: New York, 1971.

Fitch, R.M. and L. Shih. 1975. *Progress in Colloid and Polymer Science*. 56, 1.

Fikentsher, H. 1938. *Angewandte Chemie*. 51, 443.

Francis, S.A. and A.H. Ellison. 1959. *Journal of the Optical Society of America*. 49, 131.

French, D.M. 1958. *Journal of Polymer Science*. 32, 395.

Friis, N. and A.E. Hamielec. 1975. *Journal of Applied Polymer Science*. 19, 97.

Friis, N. and L. Nyhagen. 1973. *Journal of Applied Polymer Science*. 17, 2311.

Frostick, F.C., B. Phillips, and P.S. Starcher. 1959. *Journal of the American Chemical Society*. 81, 3350.

Fryling, C.F. and E.W. Harrington. 1944. *Industrial and Engineering Chemistry*. 36, 114.

Gaines Jr., G.L. 1972. *Polymer Engineering and Science*. 12, 1.

Gardon, J.L., 1968. *Journal of Polymer Science*. A-1, 6(3), 623, 648, 665, and 687.

Gardon, J.L., 1968. *Journal of Polymer Science*. A-1, 6(9), 2853, and 2859.

Gardon, J.L., 1971. *Journal of Polymer Science*. A-1, 9, 2763.

Gee, G., C.B. Davies, and W.H. Melville. 1939. *Transactions of the Faraday Society*. 35, 1298.

Gershberg, D. Paper presented at the Joint Meeting of A.I.Ch.E. and I.Ch.E. London, June 14, 1965.

Gledhill, R.J. 1962. *Journal of Physical Chemistry*. 66, 458

Goodall, A.R., M.C. Wilkinson, and J. Hearn. 1975. *Progress in Colloid and Interface Science*. 53, 327.

Gorton, B.S. and J. A. Reeder. 1962. *Journal of Organic Chemistry*. 27, 2920

Gottlob, K. U.S. Patent. 1,149,577 (1915).

Greenler, R.G. 1966. *Journal of Chemical Physics*. 44, 310;and 1969. 50, 1963.

Griffiths, P.R. Ed. *Transform Techniques in Chemistry*. Plenum: New York, 1978.

Gross, H. 1963. *Praktische Chemie*. 21, 99.

Gross, H. 1965. *Chemische Berichte*. 98, 1673.
Hacobi, H.R. *Ullmans Encyklopaedie der Technischen Chemie*, Volume 11, 3rd Ed. Urban & Schwarzenberg: Munich, 1960.

Gulbekian, E.V. 1968. *Journal of Polymer Science*, A-1. 6, 2265.

Gulbekian, E.V., and G.E. Reynolds. "Poly(vinyl alcohol) in Emulsion Polymerization" in *Poly(vinyl alcohol): Properties and Applications*. C.A. Finch, Ed. Wiley: London, 1973.

Gunderson, J.J. and J. C. Giddings, 1986. *Analytica Chimica Acta.* 189, 1.

Guyot, A., J. Guillot, C. Graillat, and M.F. Llauro. 1984. *Journal of Macromolecular Science and Chemistry*. A21, 683.

Hansen, F.K, and J. Ugelstad. 1978. *Journal of Polymer Science, Polymer Chemistry*. 17, 1953; 17, 3033.

Hansen, F.K, and J. Ugelstad. 1978. *Journal of Polymer Science, Polymer Chemistry*. 16, 3047; 17, 3069.

Hansen, F.K. and J. Ugelsad. 1979. *Journal of Polymer Science, Polymer Chemistry*. 17, 3069.

Hansen, F.K. and J. Ugelstad. "Particle Formation Mechanisms" in *Emulsion Polymerization*. I. Piirma, Ed. Academic Press: New York, 1982.

Harada, M., M. Nomura, W. Eguchi, and S. Nagata. 1971. *Journal of Chemical Engineering (Japan)*. 4,1,54.

Harkins, W.D. 1945. *Journal of Chemical Physics*. 13, 9, 381.

Harkins, W.D., R.W. Mattoon, and M.L. Corrin. 1946. *Journal of Colloid Science*. 1, 105.

Harkins, W.D., R.W. Mattoon, and M.L. Corrin. 1946. *Journal of the American Chemical Society*. 68, 220.

Harkins, W.D. 1946. *Journal of Chemical Physics*. 14, 47.

Harkins, W.D. and R.S. Stearns. 1946. *Journal of Chemical Physics*. 14, 215.

Harkins, W.D. 1947. *Journal of the American Chemical Society*. 69, 1428.

Harkins, W.D. 1950. *Journal of Polymer Science*. 5, 2, 217.

Harkness, J.B., G.B. Kistiakowsky, and W.H. Meas. 1937. *Journal of Chemical Physics*. 5, 632

Harriott, P. 1971. *Journal of Polymer Science, A-1*. 9, 1153.

Hartley, G.S. 1938. *Journal of the Chemical Society*. 1968.

Haward, R.N. 1948. *Journal of Polymer Science*. 3, 10.

Haward, R.N. 1949. *Journal of Polymer Science*. 4, 273.

Hergeth, W.D. and J. Lange. 1991. *Makromolekulare Chemie, Macromolecular Symposium*. 52, 283.

Hergeth, W.D., W. Lebek, R. Kakuschke, K. Schmutzler. 1991. *Makromolekulare Chemie*. 32, 2265.

Hiemenz, P.C. *Polymer Chemistry: The Basic Concepts*. Marcel Dekker: New York, 1984.

Hoffman, F. and K. Delbrück. German Patents: 250,690 (1909); 254,672 (1912); 255,129 (1912).

Hohenstein, W.P. and H. Mark. 1946. *Journal of Polymer Science*. 1, 2, 127.

Hohenstein, W.P. and H. Mark. 1946. *Journal of Polymer Science.* 1, 6, 549.

Hong, K.M., J. Noolandi. 1981. *Macromolecules*. 14, 1229

Hoy, K.L. 1973. *Journal of Paint Technology*. 45(579), 51.

Isaacs, N.S. *Physical Organic Chemistry*. 2nd Ed. Longman Scientific and Technical: Essex, 1995.

ISO Standard 706-1985: *Determination of Coagulum Content*.

ISO Standard 124-1992: *Rubber Latices-Determination of Total Solids Content*.

ISO Standard 9760-1986: *Rubber Latices-Determination of pH*.

Jansson, L., H. Nilsson, C. Silvergren, and B. Tornell. 1987. *Thermochimica Acta*. 118, 97.

Joshi, R.M. 1962. *Journal of Polymer Science*. 56, 313.

Joshi, R.M. 1963. *Makromolekulare Chemie*. 66, 114.

Kaichi, S. 1956. *Bulletin. Chemical Society of Japan*. 29, 241.

Kao, C.I., D.P. Grundlach, and R.T. Nelsen. 1984. *Journal of Polymer Science, Polymer Chemistry*. 22, 3499.

Keddie, J.L. 1997. *Materials Science and Engineering*. 21, 101.

Kiparissides, C., J. F. MacGregor, S. Singh, and A.E. Hameielec. 1980. *Canadian Journal of Chemical Engineering*. 58, 65.

Kiprianova, L.A., and A.F. Rekasheva. 1964. *Doklady Akademii Nauk SSSR*. 154, 423.

Klatte, F. U.S. Patent (1914) 1, 084, 581; Chemical Abstracts (1914) 8, 991.

Klatte, F. and A. Rollet. *German Patent*. 281,688 (1914).

Klein, A. and E.S. Daniels. "Formulation Coponents" in *Emulsion Polymerization and Emulsion Polymers*. P.A. Lovell and M.S. El-Aasser, Eds. Wiley: New York, 1997.

Klein, A. and V.T. Stannett. "Surface Chemical Effects on Free Radical Capture" in *Emulsion Polymerization of Vinyl Acetate.* M.S. El-Assser and J.W. Vanderhoff, Eds. Applied Science: London, 1981.

Koenig, J.L. *Spectroscopy of Polymers*, ACS Professional Reference Book, American Chemical Society: Washington, DC, 1992.

Kuo, C-Y. and T. Provder. *Size Exclusion Chromatography for Polymers and Coatings*, ACS Symposium Series, Volume 351. 1987.

Langman, I., A.F. McKay, and G.F. Wright. 1949. *Journal of Organic Chemistry*. 14, 550.

Lee, S. 1940. *Journal. Society of the Chemical Industry of Japan*. 43, Supplemental Binding 190-191.

Lee, S. and H. Kawakami. 1940. *Journal. Society of the Chemical Industry of Japan*. 43, 228.

Leonard, E.C. "Vinyl Acetate" in *Vinyl and Diene Monomers, Part I*. E.C. Leonard, Ed. Wiley: New York, 1970.

Lepizzera, S.M. and A.E. Hamielec. 1994. *Macromolecular Chemistry and Physics*. 195, 3103.

Lindemann, M.K. *Encyclopedia of Polymer Science and Technology,* Volume 15. Interscience: New York, 1971.

Litt, M., R. Patsiga, and V. Stannett. 1970. *Journal of Polymer Science, A-1*. 8, 3607.

Loebel, A.B. 1959. *Industrial Engineering and Chemistry*. 51, 118.

Lovell, P.A., "Free Radical Polymerization" in *Emulsion Polymerization and Emulsion Polymers*. Lovell, P.A. and M.S. El-Aasser, Eds. Wiley: Chichester, 1997.

Lucas, F.F. 1938. *Industrial and Engineering Chemistry*. 30, 146; 1942. Industrial and Engineering Chemistry. 34, 1371.

Luther, M. and C. Heuck. German Patent. 558,890 (1927); U.S. Patents: 1,860,681 (1927); 1,864,073 (1928); 1,864,078 (1932).

Managaraj, D., S. Patra, P.C. Roy, S.K. Bhatnagar. 1965. *Makromolekulare Chemie*. 84, 225.

Mark, H. and R. Raff, in *High Polymeric Reactions* (High Polymer Series, Vol. III). Interscience: New York, 1941.

Maron, S.H., S.E. Elder, and I.N. Ulevitch. 1954. *Journal of Colloid Science*. 9, 89.

Maron, S.H., S.E. Elder, and C.J. Moore. 1954. *Journal of Colloid Science*. 9, 104.

Maron, S.H. and S.E. Elder. 1954. *Journal of Colloid Science*. 9, 263; 9, 347; and 9, 353.

Maron, S.H., P.E. Pierce, and I.N. Ulevitch. 1963. *Journal of Colloid Science*. 18, 470.

Martynyuk, M.M., V.K. Semenchenko. 1964. *Kolloid Zhurnal*. 26, 83.

Mattoon, R.W., R.S. Stearns, and W.D. Harkins. 1947. *Journal of Chemical Physics*. 15, 209.

Mattoon R.W., R.S. Stearns, and W.D. Harkins. 1948. *Journal of Chemical Physics*. 16, 64.

Mayo, F.R. 1948. *Journal of the American Chemical Society*. 70, 3689.

Mayo, F.R. and F.M. Lewis. 1944. *Journal of the American Chemical Society*. 66, 1594.

Mayo, F.R., A.A. Miller, G.A. Russell. 1958. *Journal of the American Chemical Society*. 80, 2500.

Mayo, F.R. and C. Walling. 1950. *Chemical Reviews*. 46, 191.

McBain, J.W. *Advances in Colloid Science*. E.O. Kraemer, Ed. Interscience: New York, 1942.

McGavack, J. 1939. *Industrial Engineering and Chemistry*. 31, 1509.

McMurray, J. *Organic Chemistry*. 3rd Ed. Brooks/Cole: Pacific Grove, 1992.

Melville, H.W. 1946. *Nature*. 158, 553.

Merriam-Webster's Collegiate Dictionary. Springfield: Merriam-Webster, Inc., 1993.

Meyer, K.H. *Natural and Synthetic High Polymers*. Interscience: New York, 1950

Mie, G. 1908. *Annalen der Physik*. 25, 377.

Milas, N.A., S. Sussman, and H.S. Mason. 1939. *Journal of the American Chemical Society*. 61, 1844.

Moffett, E. 1934. *Journal of the American Chemical Society*. 56, 2009.

Montroll, E.W. 1945. *Journal of Chemical Physics*. 13, 8, 337.

Morbidelli, M., G. Storti, and A. Siani. in *Polymeric Dispersions: Principles and Applications* (Nato ASI Series Volume 335). J.M. Asua, Ed. Kluwer: Dordrecth, 1997.

Moritz, H.U. in *Polymer Reaction Engineering*. K.H. Reichert and W. Geiseler, Eds. VCH: Verlag, 1989.

Morrison, G.O., and T.P.G. Shaw. 1933. *Transactions of the Electrochemical Society*. 63, 425.

Mowilith, Polyvinylacetat, Farbwerke Hoechst AG, Frankfurt, 1969.

Napper, D.H. and A.G. Parts. 1962. *Journal of Polymer Science*. 61, 113.

Napper, D.H. and A.G. Parts. 1962. *Journal of Polymer Science*. 61, 127.

Netschey, A., D.H. Napper, and A.E. Alexander. 1969. *Journal of Polymer Science, Part B, Polymer Letters.* 7, 329.

Nguyen, T. and E. Byrd. 1987. *Journal of Coatings Technology*. 59, 39.

Nomura, M., M. Harada, K. Nakagawara, W. Eguchi, and S. Nagata. 1971. *Journal of Chemical Engineering (Japan)*. 4, 2, 160.

Nomura, M., M. Harada, W. Eguchi, and S. Nagata. 1975. *Polymer Preprints*. American Chemical Society, Division of Polymer Chemistry. 16, 217.

Nomura, M. and M. Harada. "On the Optimal Reactor Type and Operation For Continuous Emulsion Polymerization" in *Emulsion Polymers and Emulsion Polymerization*. D.R. Bassett and A.E. Hamielec, Eds. ACS Symposium Series, Volume 165. Washington D.C., 1981.

Noro, K. 1970. *British Polymer Journal*. 2, 128.

Norrish, R.W.G, and E.F. Brookman. 1939. *Proceedings of the Royal Society of London*. A171, 147.

Norrish, R.G.W. and R. R. Smith. 1945. *Nature*. 156, 661.

O'Donnell, J.T, R.B. Mesrobian, and A.E. Woodward. 1958. *Journal of Polymer Science*. 28, 171.

Okamura, S. and T. Motoyama. 1962. *Journal of Polymer Science*. 58, 221.

O'Neill, T., J. Pinkava, and J. Hoigne. Paper presented at the 3rd Symposium on Radiation Chemistry. Tihany, Hungary, May 10-15, 1971.

O'Toole, J.T. 1965. *Journal of Applied Polymer Science*. 9, 1291.

Parts, A.G. and D.E. Moore. 1962. *Journal of Oil Colour Chemists' Association*. 45, 648.

Parts, A.G., D.E. Moore, and J.G. Watterson. 1965. *Makromolekulare Chemie.* 89, 156.

Patsiga, R., M. Litt, and V. Stannett. 1960. *Journal of Physical Chemistry*. 64, 801.

Piirma, I. and S.R. Chen. 1980. *Journal of Colloid and Interface Science*. 74, 90.

Poehlein, G.W., W. Dubner, and H.C. Lee. 1982. *British Polymer Journal*. 14, 143.

Polymer Handbook, 3rd Ed. J. Brandrup, E.H. Immergut, Eds. Wiley: New York, 1989.

Price, C.C., and C.E. Adams. 1945. *Journal of the American Chemical Society*. 67, 1674.

Priest, W.J. 1952. *Journal of Physical Chemistry*. 56, 1077.

Rayleigh, L. 1871. *Philosophical Magazine*. 41, 107, 274; and 447.

Regnault, F. 1828. *Annales de Chimie et de Physique.* 69, 157.

Rekasheva, A.F. *Russian Chemical Reviews,* (1968) 37, 1009.

Rueggeberg, W.H., J. Chernack, I.M. Rose, and E.E. Reid. 1948. *Journal of the American Chemical Society*. 70, 2292.

Sabel, A., J. Smidt, R. Jira, and H. Prigge. 1969. *Chemische Berichte*. 102, 2939.

Saito, S. 1963. *Kolloid Zeitschrift*. 189, 116.

Schildknecht, C.E. *Vinyl and Related Polymers*. Wiley: New York, 1952.

Schmieder, K., K. Wolf. 1953. *Kolloid Zeitschrift*. 134, 149.

Schmitz, E. and O. Brede. 1970. *Journal fuer Praktische Chemie*. 312, 43.

Schoon, Th. G.F. and K.L. Phoa. 1955. *Journal of Colloid Science*. 10, 226.

Schork, F.J. and W.H. Ray. 1983. *Journal of Applied Polymer Science*. 28, 407.

Shashidnar, G.V. *et al*. 1990. *Journal of Polymer Science, Polymer Letters Ed*. 28, 157.

Shaw, D.J. *Introduction to Colloid and Surface Chemistry*. Butterworth-Heinemann: Oxford, 1992.

Shaw, T.P.G. "Vinyl Acetate," in *Encyclopedia of Chemical Technology*, Volume 14. Interscience: New York, 1955.

Shinoda, K., T. Nakagawa, B. Tamamushi, and T. Isemura. *Colloidal Surfactants: Some Physico-Chemical Properties.* Academic: New York, 1963.

Sieglitz A. and O. Horn. Chemical Abstracts (1952) 46, 3497

Skrabal, A. and A. Zachroka. 1927. *Manatshefte*. 48, 459.

Small, P.A. 1953. *Journal of Applied Chemistry*. 3, 71.

Smart, R.B. and K.H. Mancy, in *Kirk Othmer Concise Encyclopedia of Chemical Technology*, M. Grayson, Ed. Wiley: New York, 1985.

Smidt, J. 1959. *Angewandte Chemie*. 71, 176.

Smith, W.V. 1948. *Journal of the American Chemical Society*. 70(11), 365; 1949. *Journal of the American Chemical Society*. 71, 4077.

Smith, W.V. and R.H. Ewart. 1948. *Journal of Chemical Physics*. 16(6), 592.

Springer, J. M.D. Lechner, H. Dautzenberger, and W-M. Kulicke. 1992. *Makromolekulare Chemie, Macromolecular Symposia.* 61, 1.

Stannett, V., A. Klein, and M. Litt. 1975. *British Polymer Journal*. 7, 139.

Staudinger, J.J.P. 1948. *Chemistry and Industry*. 563.

Staudinger, H. , K. Frey, and W. Starck. 1927. *Chemische Berichte*. 60B, 1782; Chemical Abstracts (1928) 22, 215.

Steward, P.A., J. Hearn, and M.C. Wilkinson. 2000. *Advances in Colloid and Interface Science*. 86, 195.

Stockmayer, W.H. 1957. *Journal of Polymer Science*. 24, 314.

Sudol, E.D., Daniels, E.S., and El-Aasser, M.S., "Overview of Emulsion Polymerization" in *Polymer Latexes: Preparation, Characterization, and Applications*. ACS Symposium Series #492. Sudol, E.D., Daniels, E.S., and El-Aasser, M.S. Eds. ACS: Washington, 1992.

Szabo, J.L. and E.T. Stiller. 1948. *Journal of the American Chemical Society*. 70, 3367

Tager, A.A., A.A. Askadskii, M.V. Tsilipotkina. 1975. *Vysokomolekulyarnye Soedineniya, Seria A*. 17, 1346.

Thompson, M.W. "Types of Polymerization" in *Polymer Colloids.* R. Buscall, T. Corner, and J.F. Stageman, Eds. Elsevier: London, 1985.

Thurn, H., K. Wolf. 1956. *Kolloid Zeitschrift*. 148, 16.

Tinoco, I., Jr., K. Sauer, and J.C. Wang. *Physical Chemistry Principles and Applications in Biological Sciences*. Prentice Hall: New Jersey, 1995.

Tobita, H. 1994. *Polymer*. 35, 3032.

Triveldi, M.K., K.R. Rajagopal, and S.N. Joshi. 1983. *Journal of Polymer Science, Polymer Chemistry Ed*. 21, 2011.

Tschunker, E. and W. Bock. German Patent. 570,980 (1933); U.S. Patent. 1,938,731 (1933).

Ugelstad, J. and P.C. Mork. 1971. *British Polymer Journal*. 2, 31.

Ugelstad, J., P.C. Mork, and J.O. Aasen. 1967. *Journal of Polymer Science*. A-1, 5, 2281.

Van Krevelen, D.W. *Properties of Polymers*. Elsevier: New York, 1976.

Vanderhoff, B.M.E. *Symposium on Polymerization and Polycondensation Processes*, *Advances in Chemistry Series,* Volume 34. American Chemical Society: Washington, D.C., 1962.

Vanderhoff, J.W., M.S. El-Aasser. "Introduction" in *Emulsion Polymerization of Vinyl Acetate*. J.W. Vanderhoff and M.S. El-Aasser, Eds. Applied Science: London, 1981.

Vanzo, E. Ph.D. Thesis. State University of New York, College of Forestry at Syracuse University. Syracuse, New York, 1962.

Vinograd, J.R., L.L. Fong, and W.M. Sawyer. 1944. *Abstracts of Papers of the American Chemical Society*. 108, September 13, page 3E.

Wang, S.T. and G.W. Poehlein. 1993. *Journal of Applied Polymer Science*. 50, 2173; and 1994. 51, 593.

Wales, M. 1962. *Journal of Physical Chemistry*. 66, 1768.

Walker, J.F. U.S. Patent (1949) 2,473,989.

Wall, F.T. 1944. *Journal of the American Chemical Society*. 66, 2050.

Wall, F.T. 1941. *Journal of the American Chemical Society*. 63, 1862.

Wilski, H. 1966. *Kolloid Zeitschrift*. 210, 37.

Winnik, M.A. 1997. *Current Opinions in Colloid and Interface Science*. 2, 192.

Winnik, M.A., Y. Wang, and F. Haley. 1992. *Journal of Coatings Technology*. 64, 51.

Wojtczak, Z. and M. Switala. 1986. *Makromolekulare Chemie*. 187, 2427.

Wu, S. 1969. *Journal of Colloid and Interface Science*. 31, 153.

Wu, S. 1971. *Journal of Polymer Science, Part C*. 34, 19.

Wyatt, P.J. 1993. *Analytica Chimica Acta*. 272, 1.

Young, R.J. and P.A. Lovell. *Introduction to Polymers*. 2nd ed. Chapman and Hall: London, 1991.

Yoyutskii, S.S. 1958. *Journal of Polymer Science*. 32, 528.

Zhao, C.L. *et al.* 1987. *Colloid and Polymer Science*. 265, 823.

Zollars, R.L. 1979. *Journal of Applied Polymer Science*. 24, 1353.

Chapter 3: Synthesis of ^{15}N-NMA and ^{13}C, ^{15}N—NMA

3.1 Introduction

Recall that one of the primary objectives of this work was to identify the partitioning of N-methylolacrylamide (NMA) units with respect to the poly(vinyl acetate) (PVAc) latex particles. In this project the method used to study NMA distribution was nuclear magnetic resonance (NMR) spectroscopy. Since the quantity of NMA in crosslinking poly(vinyl acetate) adhesives is so small (typically less than 5% (w/w) of NMA compared to vinyl acetate), isotopic enrichment was required to evaluate the NMA distribution.

Isotopically enriched NMA is not commercially available. This chapter describes the synthetic methods used to produce ^{13}C-NMA, ^{15}N-NMA and ^{13}C, ^{15}N-NMA, as well as the characterization of these monomers via solution NMR.

3.1.1 Background: Synthesis of NMA and Acrylamide Monomers

The synthesis of NMA is overviewed by Warson (Warson 1990). A common method of preparing NMA is heating acrylamide and either formaldehyde solution or paraformaldehyde to 50° under alkaline conditions. Variations of this method, largely dealing with the choice of solvent, reaction temperature, time, or catalyst, exist in the patent literature. Solvents for the reaction include tetrachloroethylene, ethylene chloride, 1,2-dichloroethane, and water (Feuer and Lynch 1953; Matejicek and Cerny 1986; Warson 1990; Chan, Jhingran et al. 1998). Kinetic studies using sodium hydroxide as a catalyst indicate that the reaction rate increases with temperature and pH, and that the activation energy for the reaction is 24.3 kcal/mol (Warson 1990). Although higher temperatures may increase the reaction rate, caution must be exercised so that polymerization does not occur. For this reason, reaction temperatures typically do not exceed 50°C. Here, isotopically modified reagents were used to produce labeled NMA. Specifically, ^{13}C-NMA, ^{15}N-NMA and ^{13}C, ^{15}N-NMA all were produced. To achieve the ^{15}N label, ^{15}N-acrylamide was a required starting material. This material is not available commercially; therefore, it had to be synthesized.

Synthetic methods for producing acrylamide are reviewed by Carpenter and Davis (Carpenter and Davis 1957). The first reported preparation of acrylamide was published by Moreau and Lynch; they slowly added dry ammonia to a saturated solution of acryloyl chloride in benzene (Moureau and Lynch 1893). Ammonium chloride, the by-product, was removed via filtration after the benzene solution was boiled. Acrylamide flakes precipitated on cooling. Several other authors have produced the monomer in a similar fashion (Jones, Zomlefer et al.; Wojcik, Szymanski et al. 1980). Most industrial synthetic routes proceed from acrylonitrile (Habermann 1991). In one case, acrylonitrile is reacted with hydrogen chloride to form β-chloropropionamide; then hydrogen chloride is eliminated upon treatment with base. Several methods are based upon the hydrolysis of acrylonitrile with sulfuric acid monohydrate. The primary difference among these methods is the means of separating the acrylamide from the sulfuric acid mixture. In this work, the method of Moreau and Lynch was modified slightly to produce acrylamide.

3.2 Experimental

3.2.1 Materials

The following chemicals were purchased and used as received: ethanol (95%, Mallincrodt), tetrahydrofuran (Aldrich, anhydrous, 99.9%), ^{15}N-ammonia (Cambridge Isotope Labs, 98+%), calcium chloride (Fisher, 4 mesh), benzene (Aldrich, anhydrous, 99.8%), 4-methoxyphenol (Aldrich, 99%), carbon tetrachloride (Aldrich, anhydrous, 99.5^{+}%), paraformaldehyde (Aldrich, powder, 95%), sodium ethoxide catalyst (Aldrich, 96%), 4-methoxyphenol (Aldrich, 99%), ethyl acetate (Aldrich, anhydrous, 99.8%), deuterated dimethylsulfoxide (DMSO-d6) (Cambridge Isotope Labs, 99.96%), acrylamide (Aldrich, 99+%), ^{15}N-aniline (Cambridge Isotope Labs, 98%).

Acryloyl chloride (Aldrich, 96%) was distilled over calcium chloride and stored over molecular sieves. ^{13}C-Paraformaldehyde (Cambridge Isotope Labs, ^{13}C 99%) was re-hydrated (method described later) prior to use.

3.2.2 Methods

^{15}N-Acrylamide Synthesis

First, a cold bath was prepared from dry ice pellets and ethanol to achieve a temperature of approximately –78°C. Then the reaction vessel (1000 mL Ace Glass medium pressure glass reactor) was set up, purged with nitrogen gas, and flamed under heavy nitrogen flow.

Approximately 250 mL of tetrahydrofuran (THF) was introduced into the flamed reactor via canula transfer. The reactor was transferred to the cold bath, and allowed to cool under nitrogen pressure. Two equivalents of ^{15}N-ammonia (6.20 L, 0.256 mol) were introduced to the reactor via bubbling through an 18 gauge stainless steel needle. The flow rate of the gas was monitored with a Gilmont® direct-reading flow meter; indicated values for air were multiplied by a correction factor of 1.3 to obtain the flow rate of ammonia. The reactor was then sealed to prevent the escape of ammonia gas.

Acryloyl chloride was distilled over calcium chloride prior to use then sealed under nitrogen and stored in the refrigerator over molecular sieves. One equivalent (10.2 mL, 0.128 mol) of the acid chloride was syringed into the reactor drop-wise under stirring. Upon addition of the acryloyl chloride, the headspace in the reactor became clouded. The colorless ammonia/THF solution gradually became an opaque white mixture and stirring was difficult to maintain as ammonium chloride precipitated. The reaction vessel was kept in the bath for several hours. As the dry ice sublimed, the bath and the reaction vessel gradually warmed to room temperature. Acrylamide was separated from the ammonium chloride precipitate via filtration through a sintered glass funnel. Ammonium chloride was washed (2 x 100 ml THF) to recover additional product. Raw acrylamide (9.15 g, 0.127 moles) was recovered when the combined filtrates were rotovapped and vacuum dried. Yield (99.3%).

To purify the raw product, it was boiled in benzene in the presence of a small amount of inhibitor (4-methoxyphenol, 0.01 g, 0.08 mmol), then filtered through a warm ground glass filter. Large flakes of acrylamide crystals formed upon cooling. The solution was filtered and the recovered crystals were dried under vacuum to obtain 8.27 grams (0.115 moles, 90.5% yield) of ^{15}N-acrylamide. Proton, carbon, and nitrogen NMR spectra of the product are included in the Results

and Discussion section (see Figures 3-4, 3-5, 3-7, 3-8, (^{1}H spectra); 3-10 (^{13}C spectrum); and 3-11 (^{15}N spectrum)).

^{15}N-NMA Synthesis

In a 50 mL round bottom flask, one equivalent (2.46 g, 0.0341 moles) of ^{15}N-acrylamide (synthesized, as described previously) was reacted with a slight excess (1.05-1.1 equivalents, ~1.115g) of paraformaldehyde in carbon tetrachloride (20mL). The contents of the flask were rapidly agitated over a magnetic stirring plate. Sodium ethoxide catalyst (0.025 g, 0.37 mmol) was added to the flask. The mixture was allowed to react at 50°C in the presence of a small amount of inhibitor (4-methoxyphenol, ~0.020g, 0.16 mmol) for 1 hour. During this time, several changes were observed. In the first 5-15 minutes of the reaction, a viscous white layer began to separate from the solution, appearing on top of the organic phase. The layer clarified as the reactants were consumed. After the reaction was complete, the round bottom flask was removed from the heating bath and placed in a freezer (-20°C). The top layer completely solidified over the organic phase after several hours. The bulk of the carbon tetrachloride was removed via pipette, and the remainder was pulled off under vacuum. The product was purified by removing residual paraformaldehyde. First it was ground to a fine powder via mortar and pestle; then it was warmed in ethyl acetate (20mL) in the presence of inhibitor (4-methoxyphenol, ~0.050g, 0.40 mmol). Exposure to temperatures above 60°C was avoided to prevent polymerization. The mixture was filtered through a sintered glass frit. NMA crystals formed as the ethyl acetate solution cooled. Ethyl acetate was filtered off, and the crystals were dried under vacuum. Yield (3.48g, 76.7%). Proton, Carbon, and Nitrogen NMR spectra are included in the Results and Discussion section (see Figures 3-12 through 3-18 (^{1}H spectra); 3-19 and 3-20 (^{13}C spectra); and 3-21 (^{15}N spectra)).

^{13}C, ^{15}N-NMA Synthesis

^{13}C-Paraformaldehyde was rehydrated prior to use in an attempt to decrease its molecular weight. The rehydration was accomplished by sealing the ^{13}C-paraformaldehyde (4.2g) in a glass tube containing distilled water (4.5g) and heating the mixture under constant stirring at 90°C for 24 hours. The product was vacuum dried for 24 hours, then was ground with a mortar and pestle prior to use. Ninety percent of the product was recovered. Some losses were incurred during vacuum drying.

The synthesis of ^{13}C, ^{15}N-NMA proceeded similarly to that described previously for ^{15}N-NMA. One difference was that this reaction, even with the rehydrated paraformaldehyde, required more time. In some cases it took approximately 3 hours for the product layer to become translucent. Product yield was also lower (67%). Proton, carbon, and nitrogen NMR spectra of the product are available in the results and discussion section (see Figures 3-22 and 3-23 (^{1}H spectra); 3-25 and 3-26 (^{13}C spectra); and 3-27 (^{15}N spectra)).

NMR Spectroscopy

NMR spectra were obtained in deuterated dimethyl sulfoxide (DMSO-d6), using either a Varian Unity 400 or a Bruker AMX-2-500 spectrometer.

3.3 Results and Discussion

3.3.1 Initial efforts using ^{13}C-NMA

The NMA methylol carbon was selected for labeling because of the relative ease of this reaction. By reacting acrylamide with commercially available ^{13}C-paraformaldehyde in the presence of base and inhibitor (Figure 3-1), the labeled analogue (^{13}C-NMA) was synthesized.

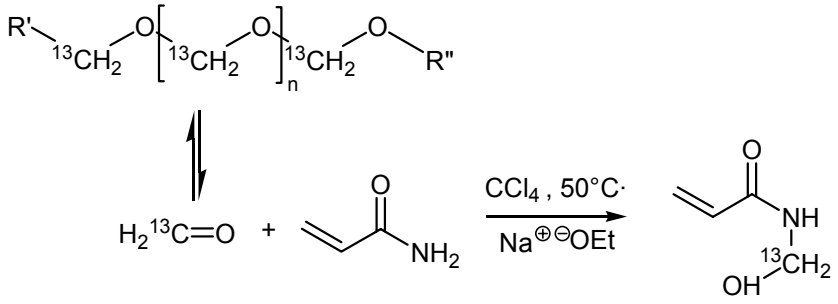

Figure 3-1: Synthesis of ^{13}C-NMA from acrylamide and ^{13}C-paraformaldehyde.

The ^{13}C-NMA was then copolymerized with vinyl acetate and the resulting latex was analyzed by ^{13}C solution NMR spectroscopy in an effort to study the distribution of NMA in the latex. At this point, a potential problem was discovered. Analysis of the supernatant material (obtained

after centrifuging the latex) showed two salient peaks, indicating the presence of two labeled moieties. This spectrum is shown in Figure 3-2. The peak at ~63 ppm corresponds to the labeled NMA methylol group. However, the intensity of the peak at ~82 ppm indicates the presence of an additional ^{13}C-compound.

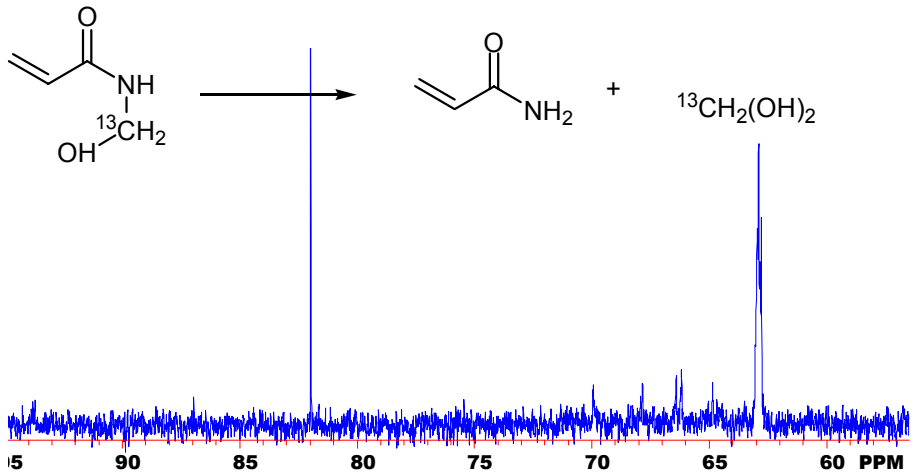

Figure 3-2: Carbon NMR spectrum revealing hydrolysis of ^{13}C-NMA. The reaction scheme indicates the products of this reaction--^{13}C-methylene glycol and unlabeled acrylamide.

This downfield peak (82 ppm) is likely due to ^{13}C-methylene glycol, which is the hydrated form of ^{13}C-formaldehyde (Lauterbur 1957; Le Botlan, Mechin et al. 1983; Schmidt, Laborie et al. 2000). Formaldehyde is released when NMA crosslinks, or when it is hydrolyzed. The evidence of methylene glycol here indicates that the ^{13}C label on the NMA units is being depleted. Therefore, the study of NMA distribution in the latex could be limited when the ^{13}C-methylol carbon is utilized as the tag.

For this reason, the strategy was modified. Instead of labeling the methylol carbon of NMA, the more stable amide nitrogen was labeled with its magnetically active isotope, ^{15}N. Synthetically, a new step was required to produce NMA because ^{15}N-acrylamide is not commercially available. This synthetic procedure is described in the next section.

While the introduction of the ^{15}N label would allow NMA distribution in the latex to be determined, another long-term goal was to study the crosslinking chemistry of the latex. The

^{13}C-methylol label may enable a greater understanding of the ultimate behavior of NMA in the system. For example, if NMA hydrolysis occurs in the latex, then the fate of the liberated methylene glycol would be of interest. Therefore, the ^{13}C label was not completely abandoned. It was decided that one of the three latices would include ^{13}C, ^{15}N-NMA. The other two would only be used for the NMR partitioning analysis, and so required only ^{15}N-NMA.

3.3.2 ^{15}N-Acrylamide Synthesis

The synthetic approach used here for obtaining ^{15}N-acrylamide is similar to the method of Moureau and Lynch (Moureau and Lynch 1893). Moreau produced acrylamide in 80% yield by slowly saturating a solution of acryloyl chloride and benzene with dry ammonia at 10°C. Here, several modifications were made to achieve higher yields. The reaction was conducted in a pressure vessel as a precaution due to the low boiling point (–33°C) of ammonia.

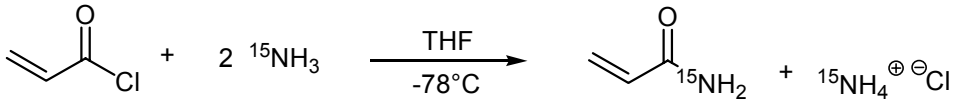

Figure 3-3: Synthesis of ^{15}N-acrylamide.

Stoichiometrically, two equivalents of ^{15}N-ammonia gas were required to produce one equivalent of acrylamide. Figure 3-3 illustrates the reaction scheme. It should be noted here that the synthesis was attempted with a stoichiometric equivalent of many other bases to limit the consumption of ^{15}N-ammonia to one equivalent. These included sodium carbonate, poly(vinyl pyridine), dimethylaminopyridine, trioctylamine, tributylamine, and triethylamine. Of all the bases utilized, triethylamine was the most promising. However, separation and purification of the products from the byproduct hydrochloride salts was difficult and resulted in decreased yields. For this reason, the simpler method of using two equivalents of ^{15}N-ammonia was selected.

Figure 3-4 shows a proton NMR spectrum of unlabeled acrylamide above a proton spectrum of homemade ^{15}N-acrylamide. Enlarged portions of these spectra are shown later in Figure 3-5 through 3-8. The complete proton spectrum can be subdivided into three major regions: 1. the upfield portion of the spectrum (below 5 ppm), which includes the solvent (deuterated dimethylsulfoxide) at 2.5 ppm and residual water at approximately 3.4 ppm; 2. the vinylic

portion of the spectrum (from 5-7 ppm) containing protons attached to the vinylic carbons; and 3. the downfield portion, which corresponds to the 2 amide protons (above 7 ppm).

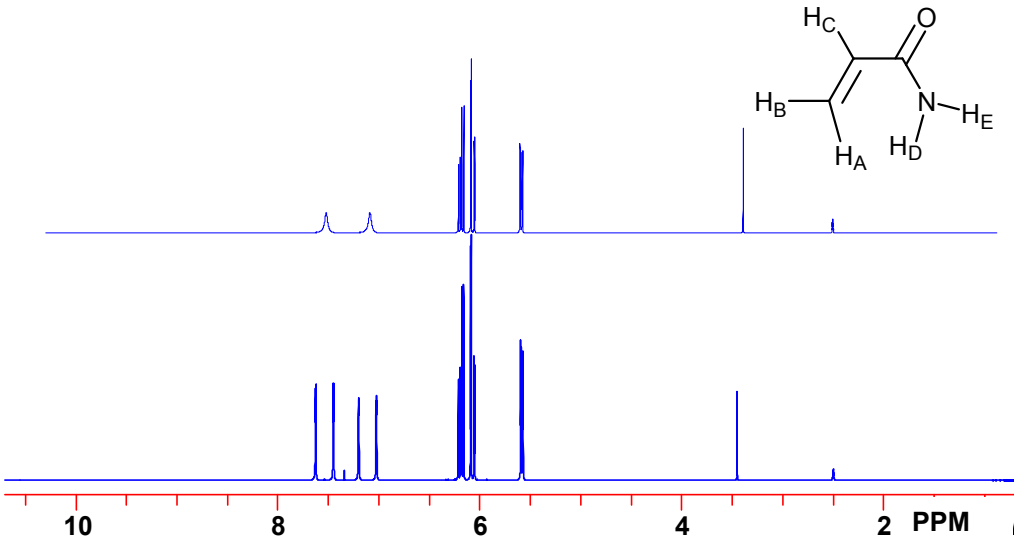

Figure 3-4: Proton NMR spectra of acrylamide (top) and ^{15}N-acrylamide (bottom) in DMSO-d6.

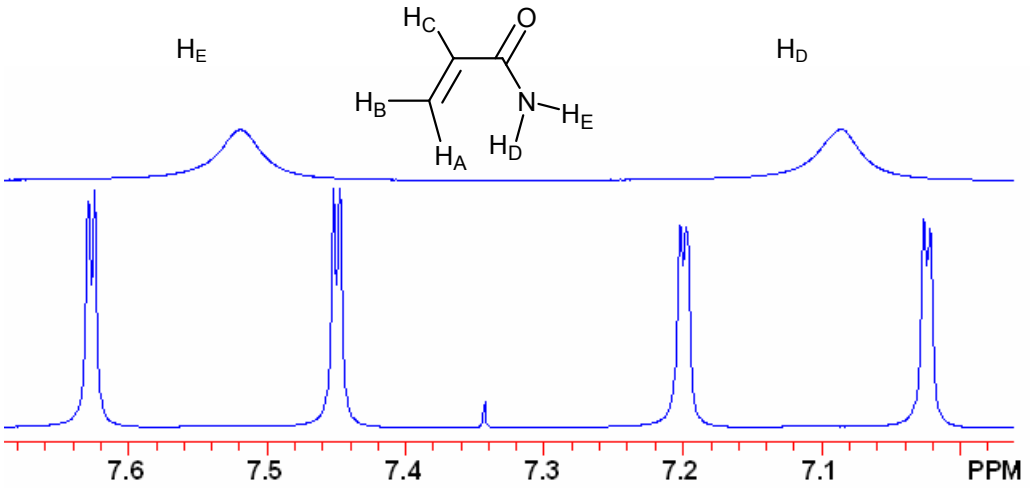

Figure 3-5: Amide region of proton NMR spectra of acrylamide (top) and ^{15}N-acrylamide (bottom). Peaks shown are from protons D and E. The solvent was DMSO-d6.

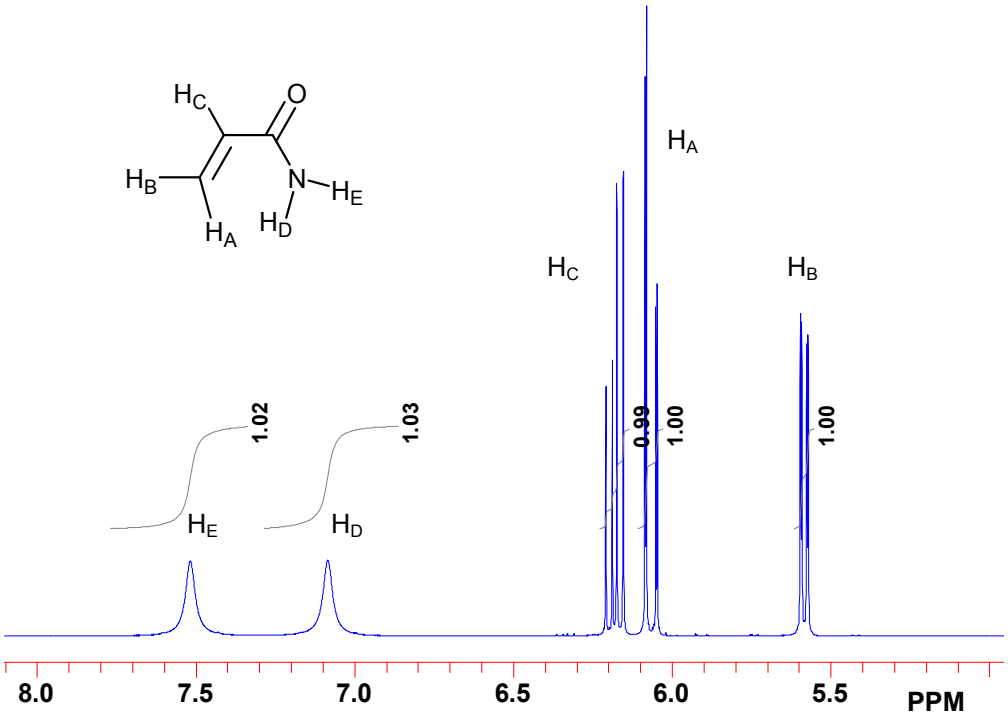

Figure 3-6: Portion of the proton spectrum of unlabeled acrylamide showing peak integrals. Peaks were integrated relative to the vinylic protons from H_B, at ~5.6ppm. The solvent was DMSO-d6.

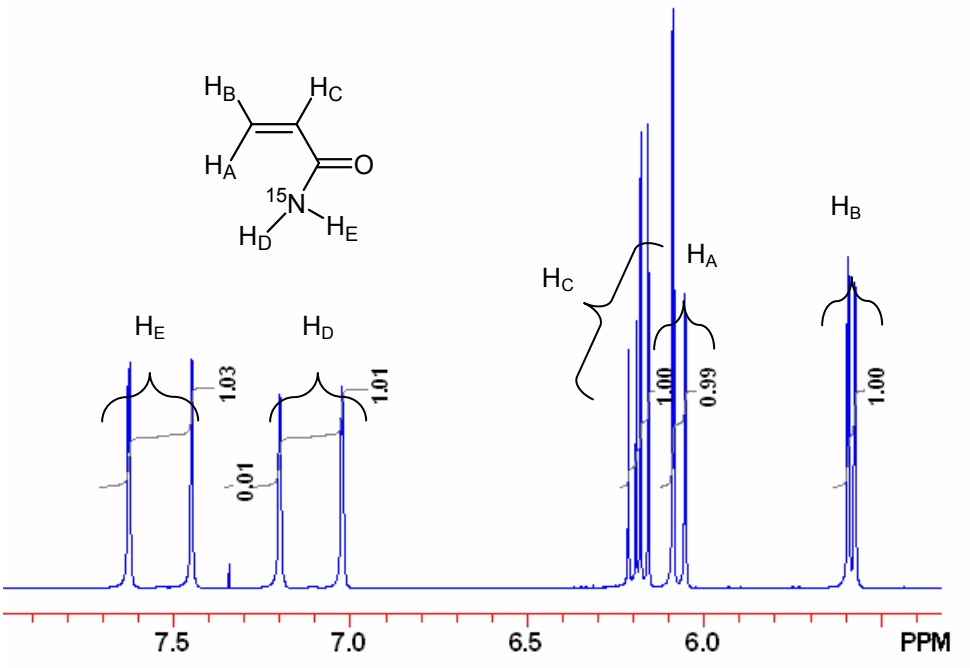

Figure 3-7: Enlarged view of ^{15}N-acrylamide proton spectrum showing integrals. The solvent was DMSO-d6.

Notice in Figure 3-4 that the upper and lower spectra correspond nicely, with few exceptions (also consider enlarged views of the spectra which are available in Figures 3-6 (acrylamide) and 3-7 (^{15}N-acrylamide)). One obvious difference between the labeled and unlabeled spectra exists in the most downfield region (above 6.5 ppm). However, before discussing the discrepancies in the amide region, peak assignments and splitting patterns for the vinylic protons (5.0-6.5 ppm) will be discussed.

Figure 3-8 shows an enlarged view of the vinylic region of ^{15}N-acrylamide. In the spectrum, the four most downfield peaks (6.15-6.22 ppm) correspond to H_C. These peaks appear downfield because of deshielding by the electron withdrawing carbonyl group. Moving upfield, the next doublet of doublets (~ 6.05-6.1 ppm) arises from H_A, which also shares a through space interaction with the electron withdrawing carbonyl group. H_B is the most insulated from the carbonyl group and therefore appears furthest upfield between 5.55 and 5.62 ppm. These peak assignments are confirmed by Chan et al. (Chan, Jhingran et al. 1998).

Figure 3-8 also reveals the through-bond (spin-spin) coupling, or "splitting" observed in the vinyl region of the acrylamide spectrum. Protons H_A, H_B and H_C are non-equivalent, and less than four bonds separate them. Therefore, there is a small interaction between them. This interaction is due to the effect that the spinning proton nucleus has on bonding electrons. In short, it is energetically favorable for a bonding electron to pair its spin with the nearest proton nuclei. The through-bond coupling is indicated by the value of *J*, the coupling constant. *J* depends on several parameters: 1. the nuclei involved, 2. the distance between the two nuclei, 3. the angle of interaction between the two nuclei, and 4. the nuclear spin of the nuclei (Crews, Rodriguez et al. 1998). Protons H_A and H_B are attached to the same atom, and result in a small value of *J*. In this situation, the coupling between H_A and H_B, J_{AB}, is measured to be 2.2 Hz. Proton H_C also interacts with both H_A and H_B. Its orientation with respect to H_A is *trans*, which yields a coupling constant of 17.0 Hz, while its *cis* interaction (with H_B) is measured as 10.1 Hz. The amide protons, H_D and H_E, are too distant to be coupled to the three vinylic protons.

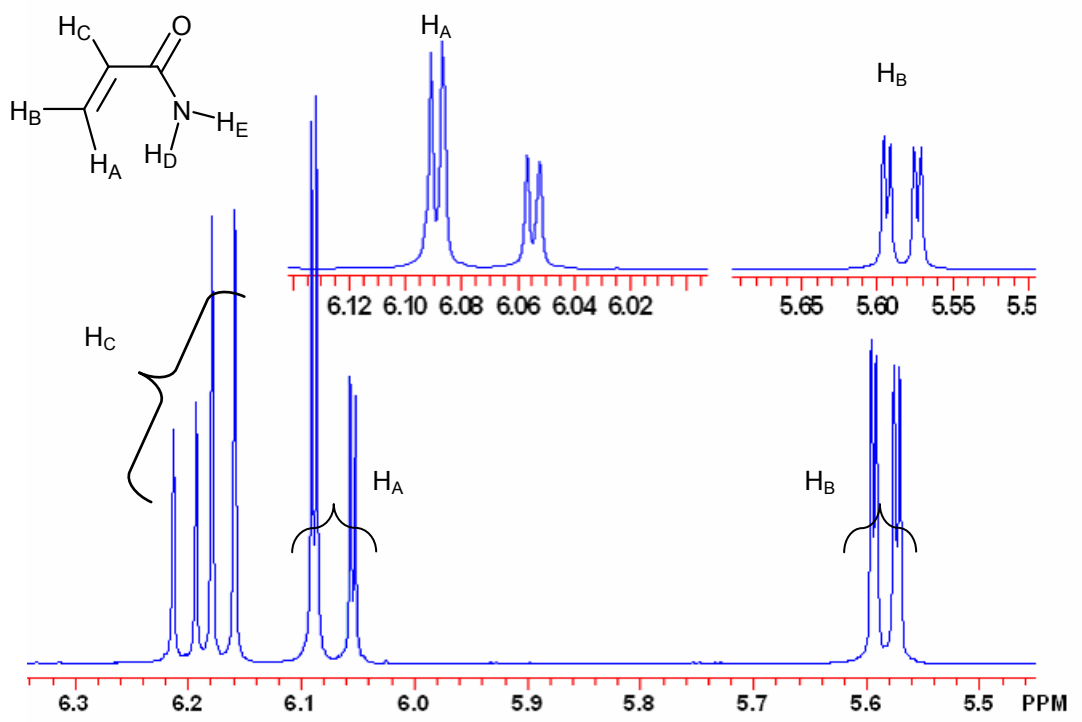

Figure 3-8: Vinylic region of ^{15}N-acrylamide spectrum. The solvent was DMSO-d6.

Recall that the major difference between the proton spectra of the labeled and unlabeled acrylamide (Figure 3-4, enlarged view in Figure 3-5) existed in the most downfield region of the spectrum. While the amide protons appear in the unlabeled spectrum as two broad peaks, four sharp peaks exist for those in ^{15}N-acrylamide. The number of peaks present will be discussed first, then the breadth of the peaks will be considered. In the spectrum of unlabeled acrylamide, one peak exists for each amide proton because they are not equivalent. Here these two protons are bonded to the same nucleus; however, they experience different chemical environments. Amides have an important resonance contribution that imparts significant double bond character between the carbonyl carbon atom and the amide nitrogen (see Figure 3-9). This restricts rotation about the nitrogen carbon bond, and causes the two amide protons to be isolated in different chemical environments. The downfield amide peak is due to the proton that is cis to the oxygen atom (H_E) while the other proton is trans to the same oxygen atom. The through space interaction between H_E and the oxygen atom deshields the proton, causing it to appear further downfield. In the spectrum of ^{15}N-acrylamide, the resonance continues to contribute to the actual structure of the molecule. Therefore, we might expect two amide proton peaks. However, the amide nitrogen here is a spin ½ nucleus. Therefore, each proton exhibits additional splitting

with the ^{15}N nucleus and appears as a doublet of doublets where J_{DE} is measured to be 2.2 Hz and J_{NH} is ~88 Hz. These J values correspond to expected values (Levy and Lichter 1979). Another confirmation of this assessment is to integrate the spectrum and verify that each doublet of doublets corresponds to one proton. Figure 3-6 and Figure 3-7 show the integral values that are obtained for unlabeled and labeled acrylamide, respectively. The signals at approximately 5.6 ppm, which correspond to proton H_B, were defined to give a value of 1. All other values are relative to this integral.

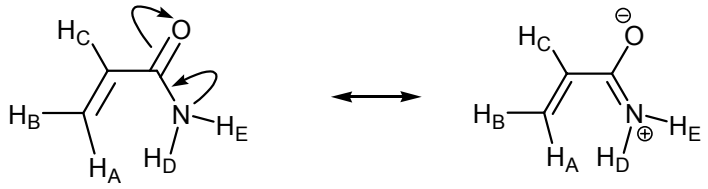

Figure 3-9: One of the resonance structures for acrylamide. Another resonance form that is not shown here is the delocalization of the vinylic double bond. These resonance structures are also important for NMA.

Having explained the number of amide peaks present in the labeled and unlabeled spectra of acrylamide, we now consider the breadth of those peaks. In short, the broader peaks (Figure 3-5) present in the unlabeled spectrum are due to the quadrupolar effect associated with ^{14}N. This phenomenon arises in nuclei having spin quantum numbers greater than ½, all of which exhibit a non-symmetrical nuclear charge distribution. Motion of the unsymmetric nuclear charge creates a fluctuating electric field, also known as an electric quadrupole. For ^{14}N, the magnitude of the quadrupole moment is large enough to influence adjacent nuclei, which is why the amide protons are affected. This fluctuating electric field can induce transitions between spin states, just like the spin-lattice (T_1) mechanism can induce transitions. Because the electric quadrupole provides an additional means of relaxation during the NMR experiment, we see broader peaks. (Faster relaxations during the NMR experiment lead to broader peaks.) When ^{14}N is substituted with the spin ½ nucleus of ^{15}N, the quadrupolar effect is eliminated because spin ½ nuclei have a symmetrical charge distribution. Therefore, the relaxation must once again occur via dipolar interactions (the T_1 mechanism), the result being sharper peaks.

Another difference between the unlabeled and labeled spectra in Figure 3-5 involves slight downfield shifts in the case of the labeled spectrum. The amide proton peaks appear slightly

further downfield. This downfield shift could be due to a change in the resonance frequency due to increased mass, or to differences in sample concentration. The small sharp peak occurring at 7.34 ppm is an impurity due to residual benzene (Silverstein, Bassler et al. 1974). If the vertical scaling of this region of the spectrum is enlarged, two small peaks appear which indicate the presence of unlabeled acrylamide. Integrating these peaks revealed that 3% of the acrylamide was unlabeled. The ammonia gas contained 98% ^{15}N-ammonia.

Figure 3-10 shows the carbon NMR spectrum of ^{15}N-acrylamide. Peaks corresponding to each of the three carbon atoms, plus a multiplet for the deuterated solvent (39.50 ppm), are noted. The carbonyl carbon atom is furthest downfield, occurring at 166.5 ppm. Notice that it is split into a doublet. This confirms the presence of ^{15}N, which is coupled to the carbonyl carbon. The J_{NC} coupling for the carbonyl carbon is 15.5 Hz. Further upfield, the two vinylic carbons are present. The peak further downfield (132 ppm) corresponds to the methine carbon atom. It is shifted downfield due to its proximity to the electron withdrawing carbonyl group. It is also split into a doublet due to the geminal spin coupling with ^{15}N. Here, J_{NC} is 9.3 Hz. The other vinylic carbon (126 ppm) is too far away to experience coupling with the ^{15}N. It remains a singlet. These assessments are in accordance with similar coupling values for ^{15}N (Levy and Lichter 1979).

Finally, in Figure 3-11, the nitrogen spectrum of ^{15}N-acrylamide is presented. Since there is only one nitrogen atom in acrylamide, we expect only one peak. Furthermore, due to the presence of the label, it should be a sharp, well defined peak. This is exactly what is observed. Here the spectrum has been referenced to an external standard, ^{15}N-aniline which has been sealed in a microcapillary tube. The aniline has been shifted to 0 ppm. The ^{15}N-acrylamide peak occurs at just over 50 ppm.

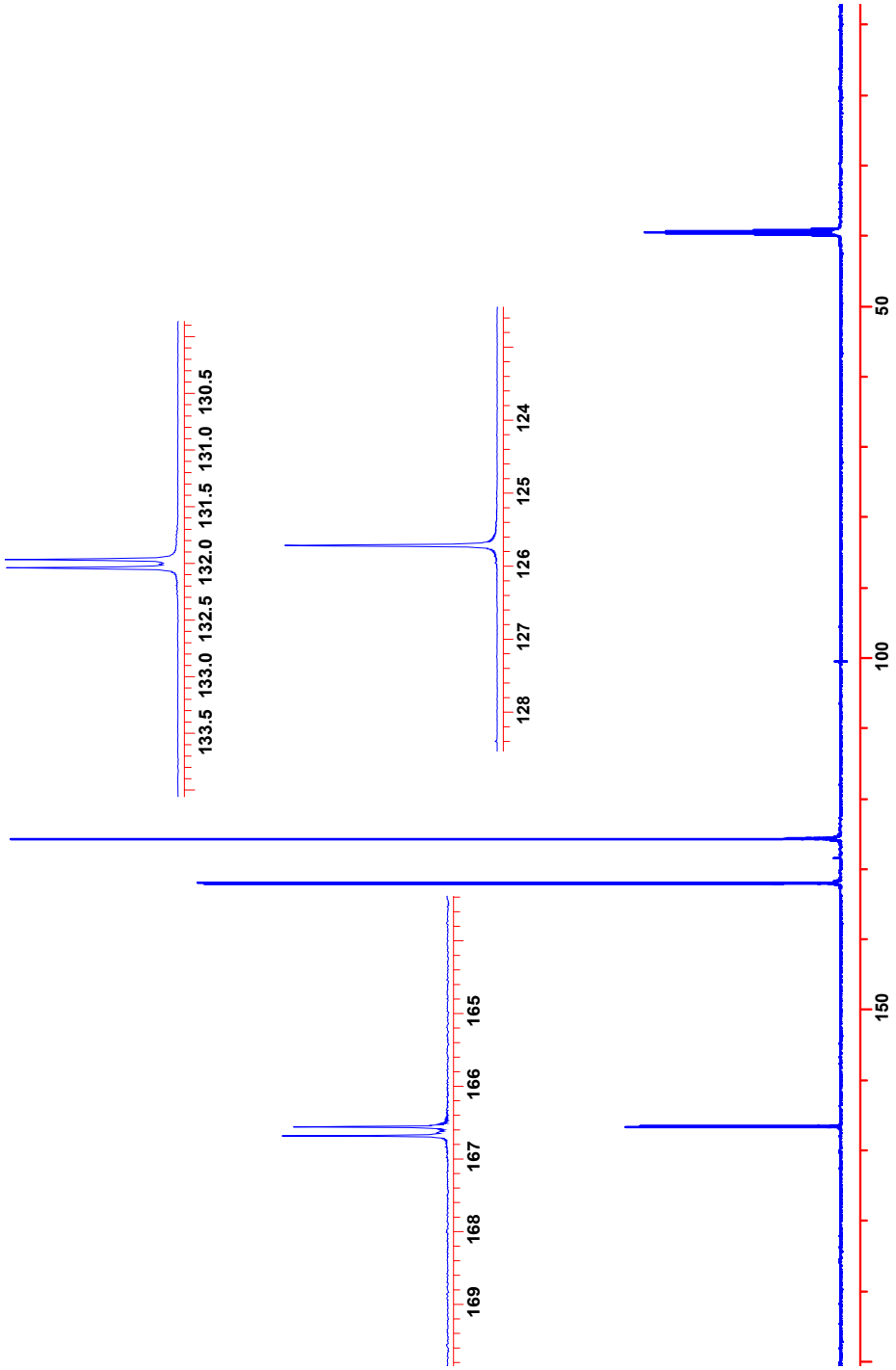

Figure 3-10: Carbon NMR spectrum of ^{15}N-acrylamide in DMSO-d6.

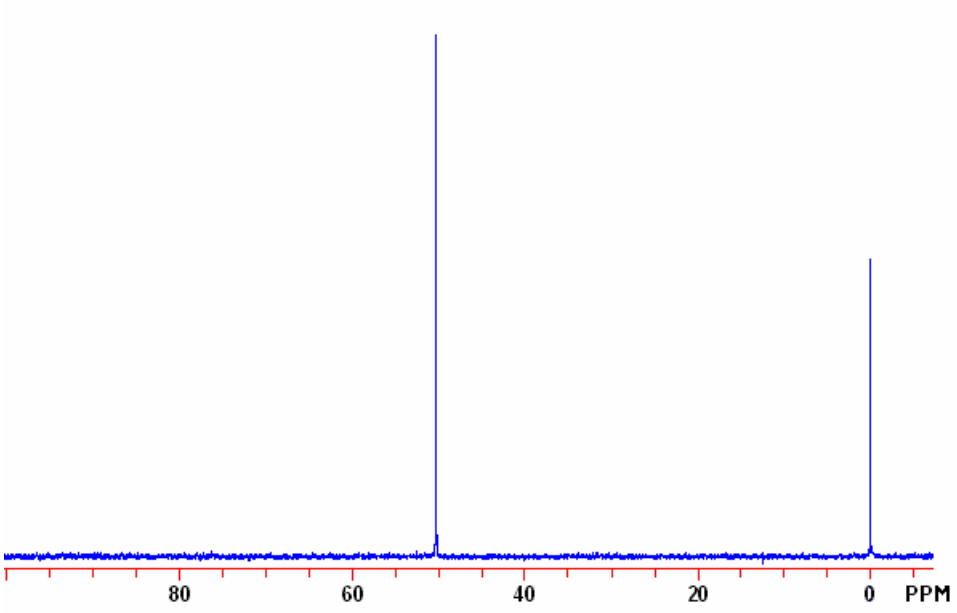

Figure 3-11: Nitrogen NMR spectrum of ^{15}N-acrylamide in DMSO-d6.

3.3.3 ^{15}N-NMA Synthesis

To produce labeled NMA, ^{15}N-acrylamide was reacted with paraformaldehyde. This reaction was conducted in a manner similar to that described by Feuer and Lynch (Feuer and Lynch 1953). It is well known that the reaction of acrylamide and paraformaldehyde proceeds only to limited conversion in good solvents because it is a reversible reaction (Feuer and Lynch 1953; Ugelstad and de Jonge 1957). Therefore, to drive the reaction to completion a poor solvent for the product was utilized. While Feuer and Lynch suggested that 1,2-dichloroethane was the most appropriate solvent for the reaction, this synthesis was conducted in carbon tetrachloride, and yields of 76.7% were obtained.

The proton spectrum of unlabeled NMA is shown above the spectrum of ^{15}N-NMA in Figure 3-12. These spectra look very similar, with the exception of the amide region. Note that in the unlabeled spectrum, there is only one amide peak, whereas in the ^{15}N-NMA spectrum, there is a doublet of triplets. This region of the spectra is enlarged in Figure 3-13. The vinylic region of both NMA spectra (enlarged in Figure 3-14) is more complex than that of acrylamide. Recall that in the proton spectrum of acrylamide, the H_B proton appeared as a doublet of doublets at 5.6 ppm. Here, there are additional signals that partially overlap the

H_B peaks. These new peaks are due to the hydroxyl proton of NMA. Returning to Figure 1-12, the peak at 4.6 ppm is due to the two methylene protons of NMA. They appear as a triplet, as shown in Figure 3-15. The solvent (DMSO-d6) appears at 2.5 ppm, and residual water occurs at 3.3 ppm.

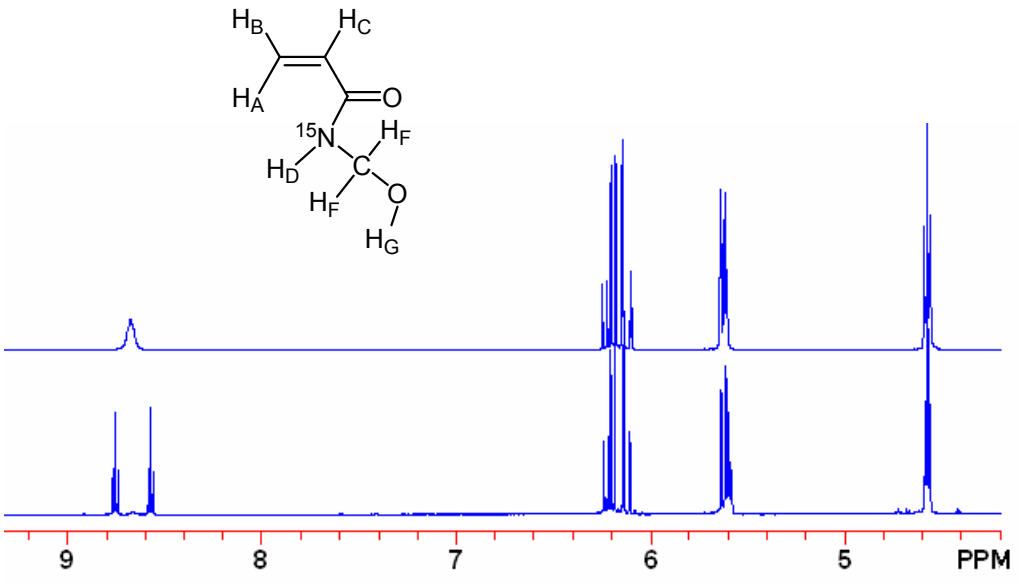

Figure 3-12: Proton spectrum of unlabeled NMA over ^{15}N-NMA. Both spectra collected in DMSO-d6.

The single N-H proton appears as a doublet of triplets for ^{15}N-NMA because of splitting by the ^{15}N nucleus (causing a doublet) and further splitting by the methylene protons, leading to the triplets. Coupling values were: J_{NH} ~91 Hz, and the proton-proton coupling J_{DF} ~ 6.4 Hz. The small peak between the two triplets is due to unlabeled NMA. Integration here reveals that a higher percentage of the NMA is unlabeled (~7%). Recall that only 3% of the ^{15}N-ammonia was unlabeled. The reason for the higher percentage of unlabeled NMA is unclear.

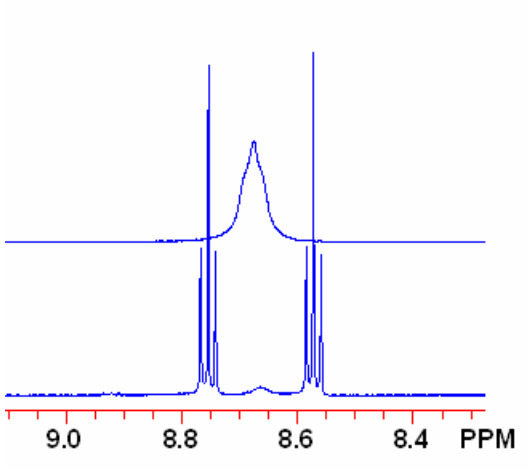

Figure 3-13: Proton spectrum of unlabeled NMA over ^{15}N-NMA, both in DMSO-d6. Amide region.

In the vinylic region, the spectrum appears to be very similar to that exhibited by acrylamide. The primary difference occurs at approximately 5.6 ppm, where a triplet overlaps with the H_B doublet of doublets. This triplet is due to the hydroxylic proton of NMA, which is split by the adjacent CH_2 protons. Often hydroxylic protons do not show coupling because they exchange rapidly with other available protons; however, in DMSO it is possible for hydroxylic protons to show coupling. This is presumably due to hydrogen bonding with the solvent, which limits exchange. Because of the unanticipated coupling exhibited here, a homonuclear two dimensional correlation spectroscopy technique (COSY) was used to confirm coupling assignments with the hydroxyl proton. The sample that was analyzed was ^{13}C, ^{15}N-NMA, which exhibits similar, but more complex splitting patterns. The discussion of the COSY findings, while applicable here, will be discussed in the following section.

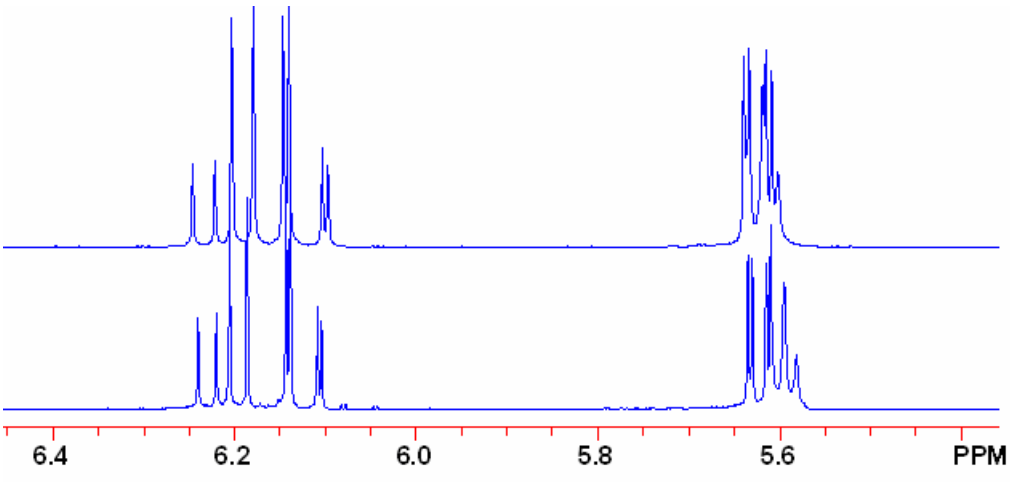

Figure 3-14: Proton spectrum of unlabeled NMA over ^{15}N-NMA, both in DMSO-d6. Vinylic region. Unlabeled spectrum was collected on a 400 MHz instrument, while ^{15}N-NMA spectrum was collected on a 500 MHz instrument.

One way to resolve overlapping peaks is to re-run a sample in an instrument having a higher magnetic field. The upper, unlabeled spectrum was run in a 400MHz instrument, while the lower spectrum (^{15}N-NMA) was run in a 500 MHz instrument. Enlarged views of the region around 5.6 ppm are shown in Figure 3-16 and Figure 3-17.

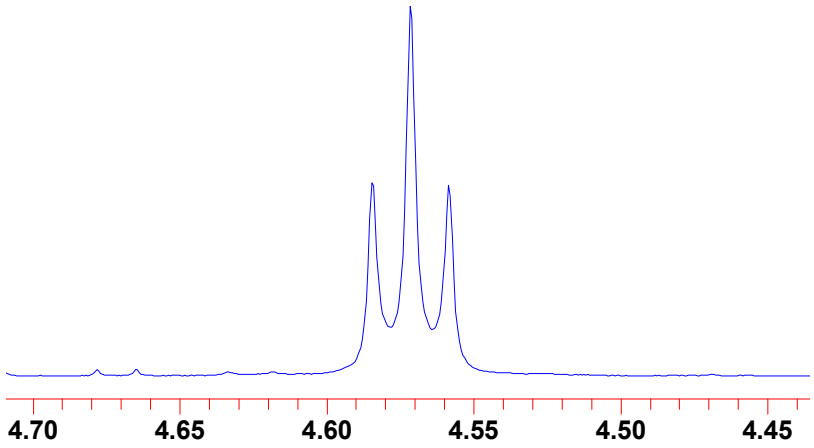

Figure 3-15: Portion of the proton spectrum of ^{15}N-NMA in DMSO-d6. This region shows the triplet from the methylene group.

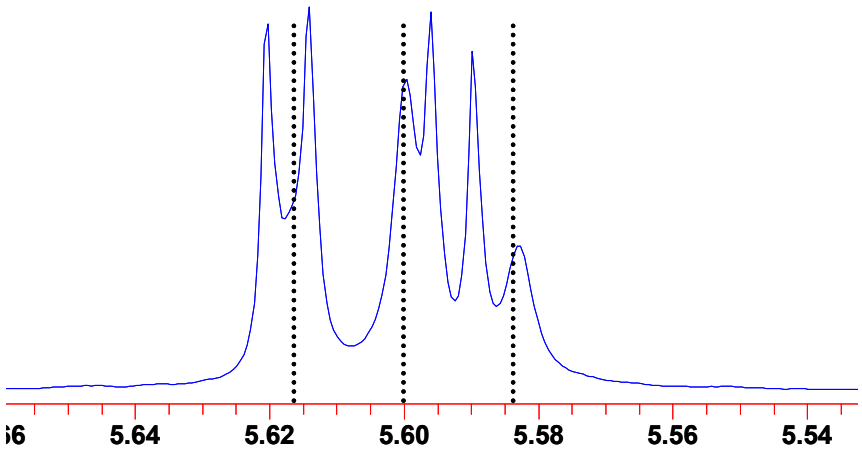

Figure 3-16: Unlabeled NMA, 400 MHz, in DMSO-d6. Dashed lines indicate the three underlying peaks of the hydroxyl proton, which is split into a triplet.

In Figure 3-16 and Figure 3-17, the dashed lines indicate the splitting pattern of the triplet, which has J_{FG} of 6.8 Hz in both spectra. This confirms that the multiplet is a triplet. In the 500 MHz spectrum, there is less overlap, so two of the three triplet peaks are resolved from the H_B proton signals. Since these were two different samples, there could also have been an inadvertent shift due to sample concentration. In other words, the greater peak resolution could have been a function of two things: the increased magnetic field and/or a slight change in chemical shift due to sample concentration.

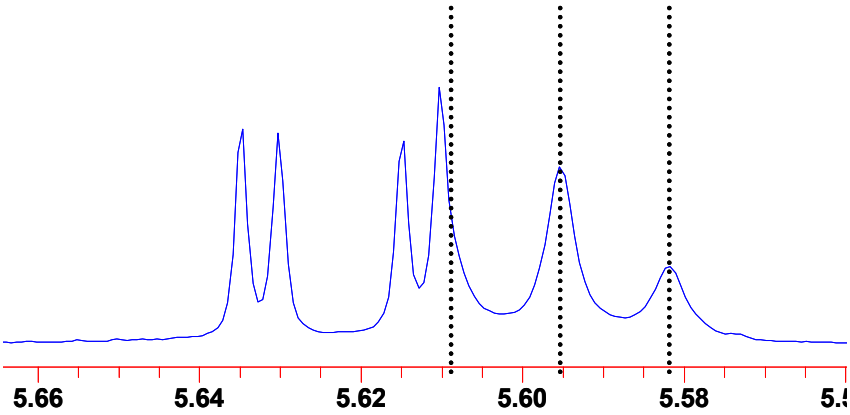

Figure 3-17: ^{15}N-NMA, 500 MHz, in DMSO-d6. Dashed lines indicate the three underlying peaks of the hydroxyl proton, which is split into a triplet.

Returning to the discussion of Figure 3-12, the CH_2 methylol protons at ~ 4.6 ppm are equivalent, and are split by the hydroxyl proton (causing a doublet) J_{FG} ~ 6.8 Hz, and the amide proton (another doublet) J_{FD}~6.4 ppm. Coupling between ^{15}N and the methylene protons is expected to have a coupling constant close to zero, so the splitting may not be obvious. The doublets from the amide proton and the hydroxyl proton are overlapping here to form a pseudo triplet. (This splitting is also confirmed by the COSY technique). Integration of the spectrum (see Figure 1-18) confirms that the peak at ~4.6 corresponds to two protons.

The carbon NMR of unlabeled NMA is shown above the spectrum of ^{15}N-NMA in Figure 3-19. Both the carbonyl carbon (~164 ppm, J_{NC} ~ 15.4 Hz) and the downfield vinyl carbon (~132 ppm, J_{NC} ~ 9.3 Hz) are split by ^{15}N (J_{NC} ~ 9.3 Hz) (see Figure 3-20). The other vinylic carbon (~126 ppm) remains a singlet (is not coupled to ^{15}N). In addition, the CH_2 group is evident at ~62.5 ppm, and it is also split by the neighboring ^{15}N nucleus (J_{NC} ~ 1.1 Hz). Notice also that a small amount of oligomeric formaldehyde is present here, at approximately 86 ppm. The only other peak in the spectrum is due to DMSO-d6, the solvent.

In the nitrogen NMR spectrum (Figure 3-21), three peaks are evident. The peak that is furthest upfield is due to residual ^{15}N-acrylamide (50 ppm). A small impurity appears at 67 ppm. The origin of this signal is unknown. Since it bears the ^{15}N label, it is evident, but the amount is minor. The major peak occurs downfield, and represents the amide nitrogen in ^{15}N-NMA (~75 ppm).

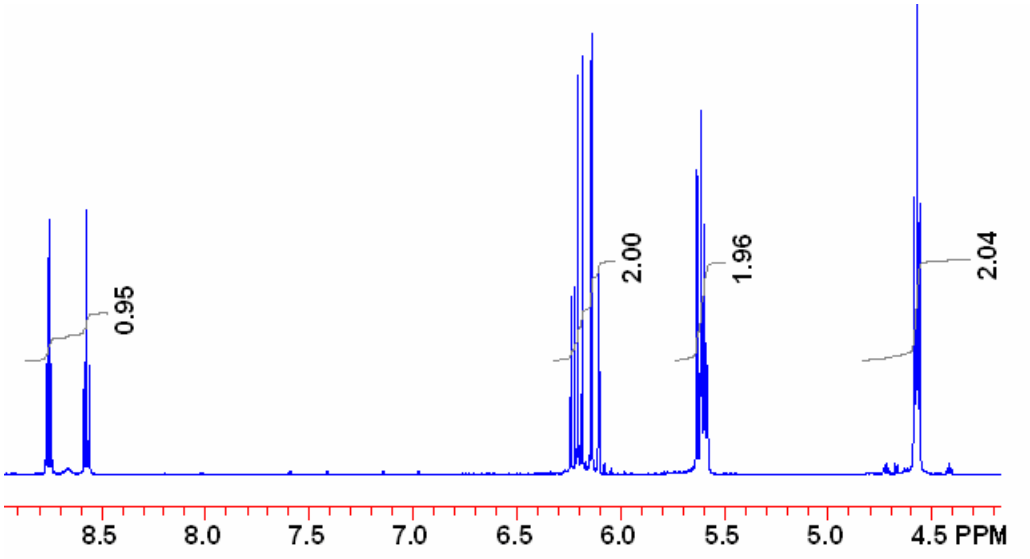

Figure 3-18: Portion of the proton spectrum of ^{15}N-NMA showing integrals. The solvent was DMSO-d6.

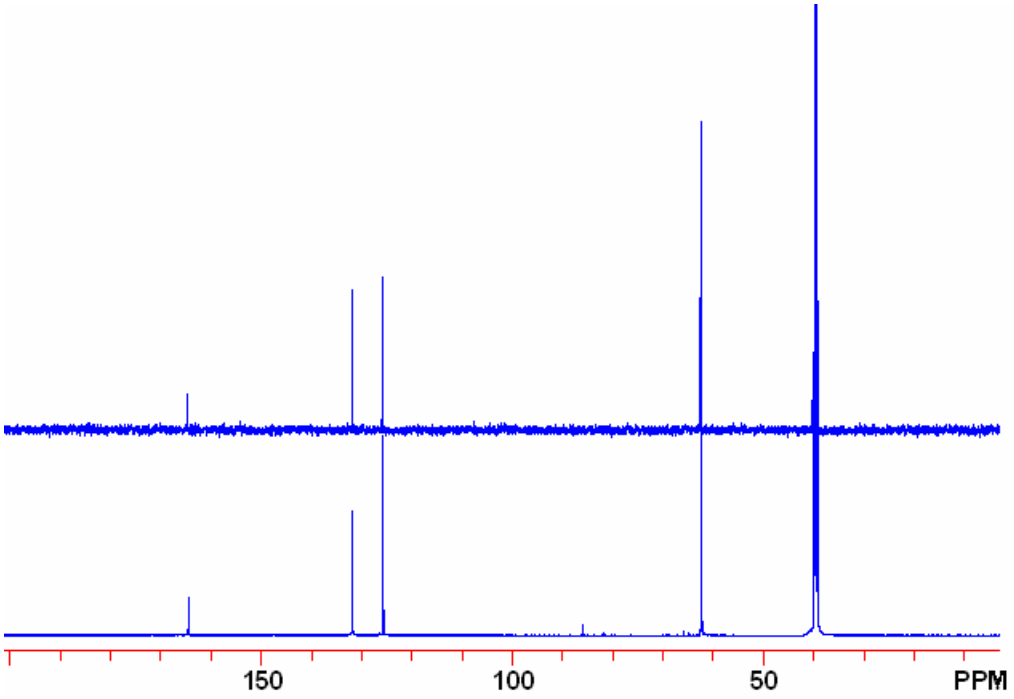

Figure 3-19: Carbon NMR spectrum of unlabeled NMA over ^{15}N-NMA, both in DMSO-d6.

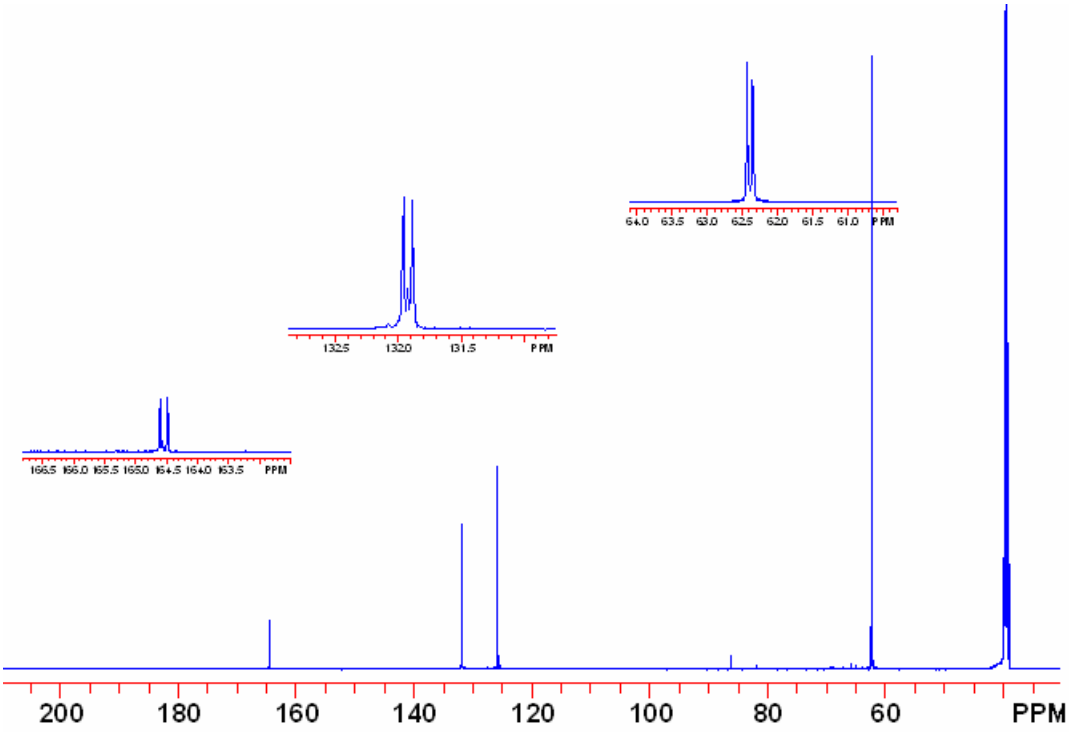

Figure 3-20: Carbon NMR spectrum of ^{15}N-NMA in DMSO-d6.

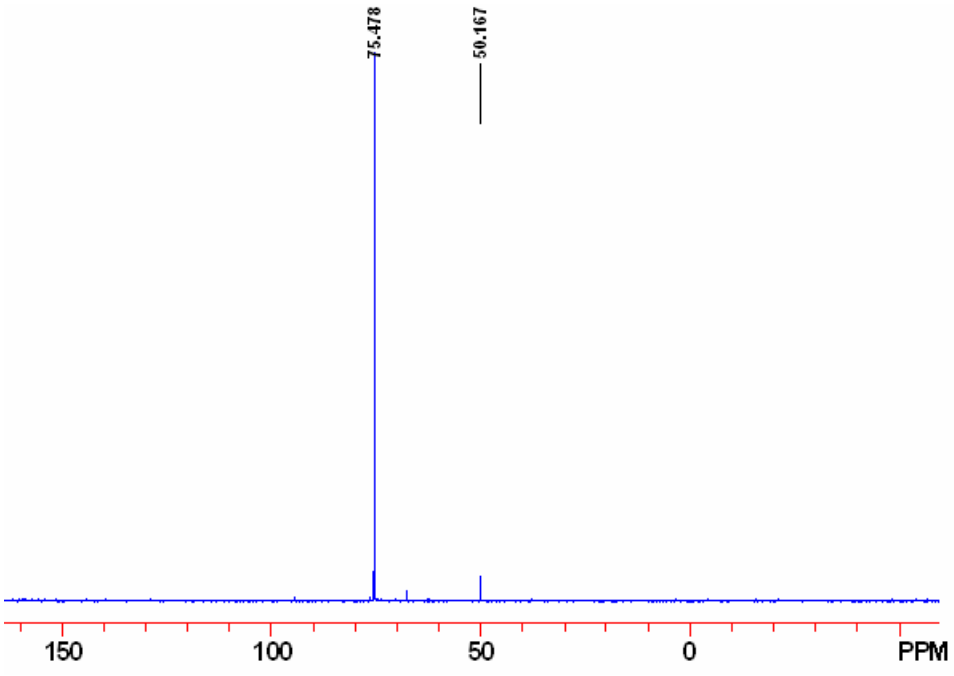

Figure 3-21: Nitrogen NMR spectrum of ^{15}N-NMA in DMSO-d6.

3.3.4 $^{13}C, ^{15}N$-NMA Synthesis

Initial synthetic attempts using ^{13}C-paraformaldehyde proceeded slowly and resulted in poor yields. In fact, the ^{13}C-paraformaldehyde was noticeably less reactive than its unlabeled counterpart. The poorer reactivity was thought to be due to higher molecular weight paraformaldehyde. Therefore, a rehydration step was conducted in an attempt to decrease the molecular weight of the ^{13}C-paraformaldehyde and thereby increase the reaction rate. The alternative, extending the reaction time, was thought to decrease yields because of polymerization of either acrylamide (the reactant) or NMA (the desired product). The molecular weight of the initial ^{13}C-paraformaldehyde was not known, nor was any attempt made to measure it. Similarly, the molecular weight following rehydration was not measured.

The reaction to produce the ^{13}C, ^{15}N-NMA closely followed that described for ^{15}N-NMA, except that rehydrated ^{13}C-paraformaldehyde was used instead of the unlabeled paraformaldehyde. Even after the rehydration was completed, the reaction still required several hours. In future work, the rehydration step would be eliminated. This would conserve an additional 10% of ^{13}C-paraformaldehyde. The reactivity of the ^{13}C-paraformaldehyde may be lower because of an isotope effect, not a molecular weight effect.

The proton NMR spectrum of ^{13}C,^{15}N-NMA is displayed in Figure 3-22. Generally, the spectrum is very similar to that of ^{15}N-NMA. Here there is evidence of ^{15}N-acrylamide (the four small peaks occurring between 6.8 and 8 ppm). This amount is minor (about 5% of the overall product) as indicated by the integrated proton spectrum shown in Figure 3-23. It is either the result of hydrolysis, or is residual acrylamide that was not consumed during the synthetic reaction. The ^{15}N spectrum (refer to Figure 3-27) confirms the presence of ^{15}N-acrylamide (50ppm).

Returning to Figure 3-22, one of the insets shows that the NMA amide peak appears as a doublet of triplets, which is identical to that observed previously for ^{15}N-NMA. The amide region of the spectrum also reveals that a small portion of the product is due to NMA without a ^{15}N label. By integrating this central peak (result not shown) the amount of NMA missing the ^{15}N label is calculated to be approximately 3% of the product. This corresponds closely to the percentage of

unlabeled ammonia in the ^{15}N-ammonia gas (~2%). Recall that a similar proportion of unlabeled acrylamide existed for ^{15}N-acrylamide, and for ^{15}N-NMA.

The vinyl region of the ^{13}C, ^{15}N-NMA proton spectrum also appears very similar to that seen for ^{15}N-NMA, except here the splitting pattern due to the hydroxyl proton (at 5.6 ppm) is more complex. This is due to the additional coupling with ^{13}C. Such coupling could overlap with the triplet previously observed.

Another key difference between the spectra of ^{15}N-NMA and ^{13}C, ^{15}N-NMA is the appearance of the peaks occurring between 4 and 5 ppm. For ^{15}N-NMA this region of the spectrum exhibited a single triplet. Here we see a doublet of triplets due to the interaction of the ^{13}C nucleus with its methylene protons. This coupling is expected to be quite large. There is also a smaller, intermediate triplet. This is likely due to NMA that does not bear the ^{13}C label. According to Figure 3-23, this amount is roughly 5%.

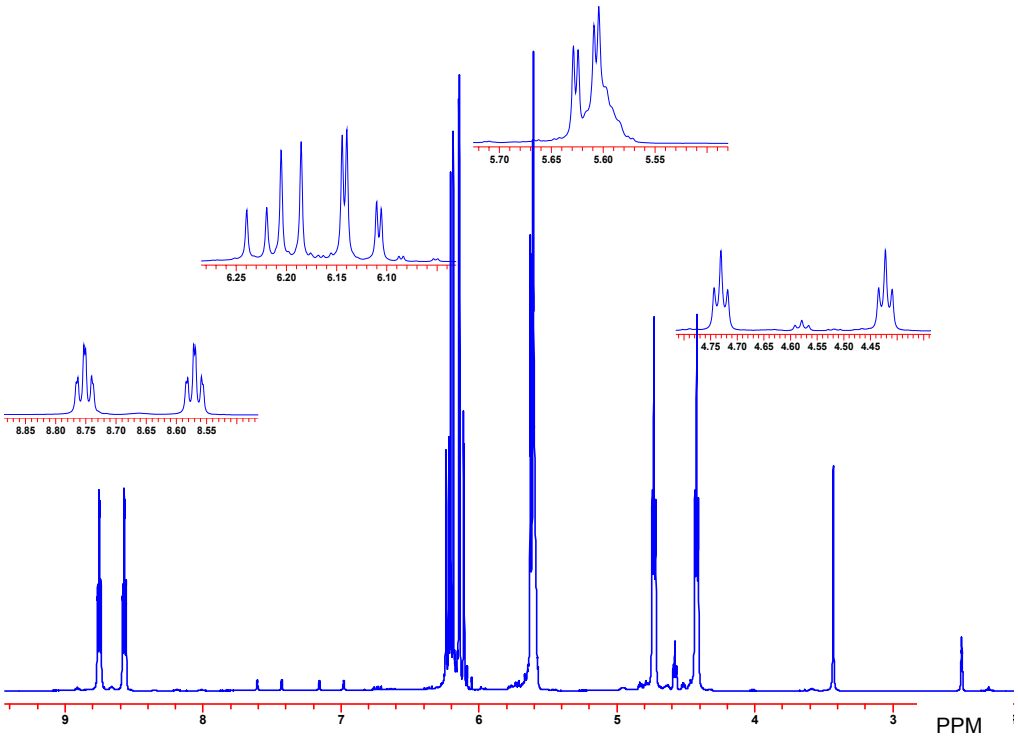

Figure 3-22: Proton NMR spectrum of ^{13}C, ^{15}N-NMA in DMSO-d6.

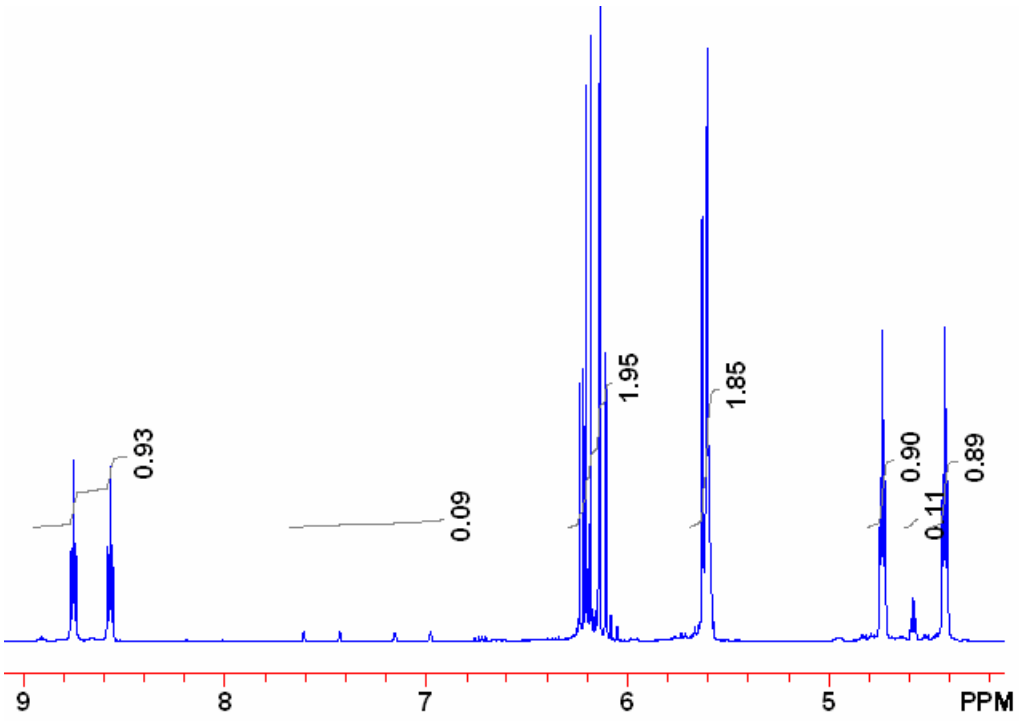

Figure 3-23: Integrated proton spectrum of ^{13}C, ^{15}N-NMA in DMSO-d6. Integral over the complete methylene region (4 to 5 ppm) set to 2.0.

As stated previously, a two dimensional homonuclear correlation spectroscopy (COSY) technique was used to investigate the coupling between protons. The result is shown in Figure 3-24. In a COSY spectrum, the proton spectrum is plotted on both the x and y axes. Coupling between protons is indicated by the presence of cross peaks, which are exhibited here by contours. The diagonal running from the top right to bottom left corners of the figure is not informative, as it indicates that a given peak correlates with itself. To obtain useful information from the COSY spectrum, only peaks on one side of the diagonal are considered. Here we will focus on the lower right corner of the figure, where seven cross peaks are present. First, coupling between the vinylic protons is confirmed by the large peak occurring between protons at 6.1-6.2 ppm and protons at ~5.6 ppm. This is the interaction between protons H_A and H_C (6.1-6.2 ppm) and H_B (~5.6 ppm). Recall that each of these protons splits the others into a doublet, revealing a pattern of doublets of doublets. Of greater interest, though, is the evidence that a proton at 5.6 ppm (the underlying hydroxylic proton) is coupled with protons at both 4.3 and 4.8 ppm, which correspond to the two methylene protons of the ^{13}C-methylol group. Those same methylene protons (4.3 and 4.8 ppm) also couple with the two amide protons occurring at ~8.55

and 8.8 ppm. These couplings confirm the presence of the hydroxyl proton and show that in this case, exchange is not occurring. Coupling between the amide protons and the hydroxylic proton is not evident.

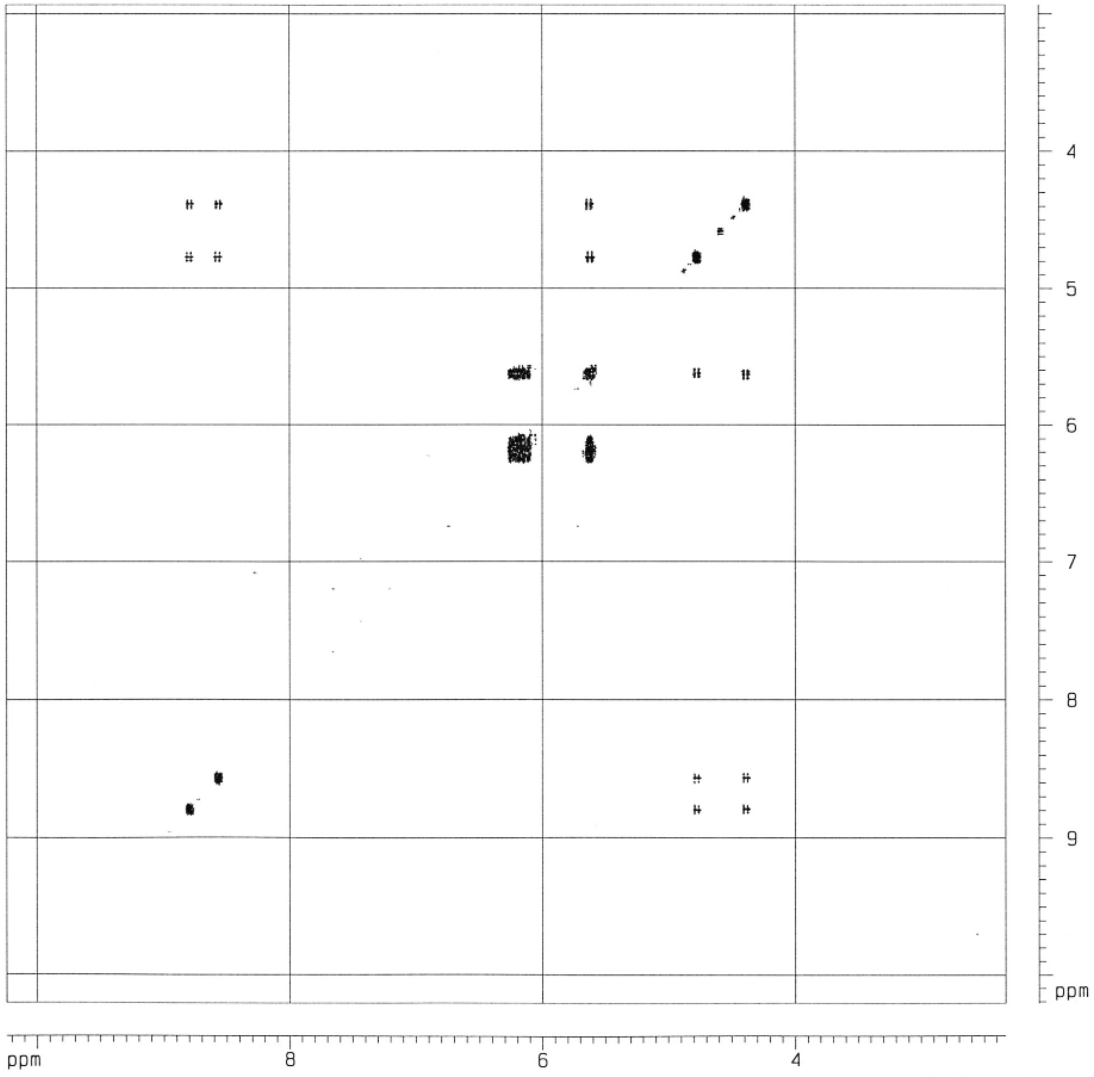

Figure 3-24: Portion of a COSY spectrum of ^{13}C, ^{15}N-NMA in DMSO-d6.

Figure 3-25 contains the carbon spectrum of ^{13}C, ^{15}N-NMA. In the ^{13}C spectrum there should be a peak for each of the vinylic carbons as well as a peak for the carbonyl carbon and the methylol carbon. Additionally, splitting due to the presence of ^{15}N should be observed, just as were present in the carbon spectrum of ^{15}N-acrylamide. The ^{13}C label greatly enhances the signal from the methylol carbon. This is most evident by observing Figure 3-26. In this diagram, the

NMR spectrum has been adjusted so that the methylol carbon peak is at full scale. Notice how the other peaks from the monomer are barely noticeable compared to the labeled signal. The spectrum in Figure 3-25 was plotted by enlarging the vertical scaling for the same spectrum. Here we can see that the carbon peaks correspond to the expected chemical shifts for NMA. We observe a number of signals between 60 and 70 ppm, presumably due to small contaminants from side reactions of ^{13}C-paraformaldehyde and ^{13}C-formaldehyde. Werstler indicated that peaks in this region are associated with hemiformals (Werstler 1986). In Figure 3-26, these peaks are barely evident. The peak at 86 ppm is also due to labeled impurity—an oligomer of ^{13}C-formaldehyde.

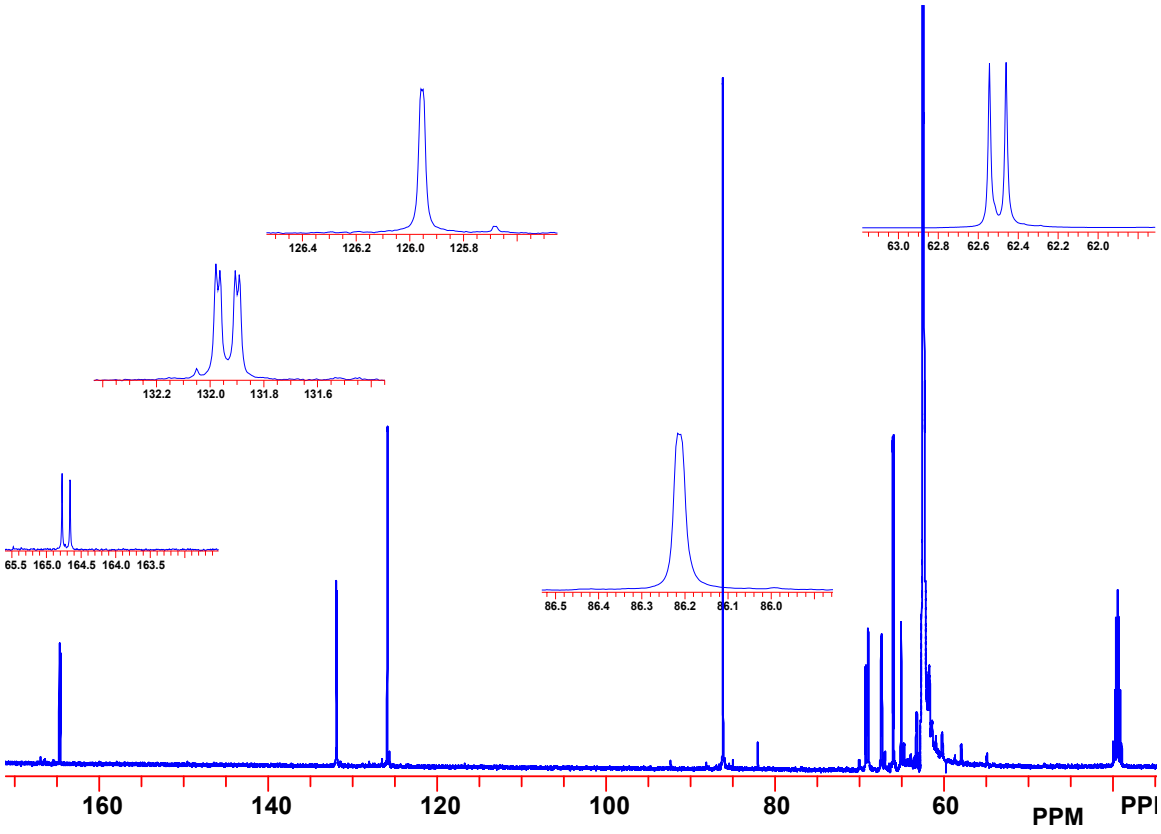

Figure 3-25: Carbon NMR spectrum of ^{13}C, ^{15}N-NMA in DMSO-d6. The spectrum has been enlarged to show the unlabeled carbon peaks.

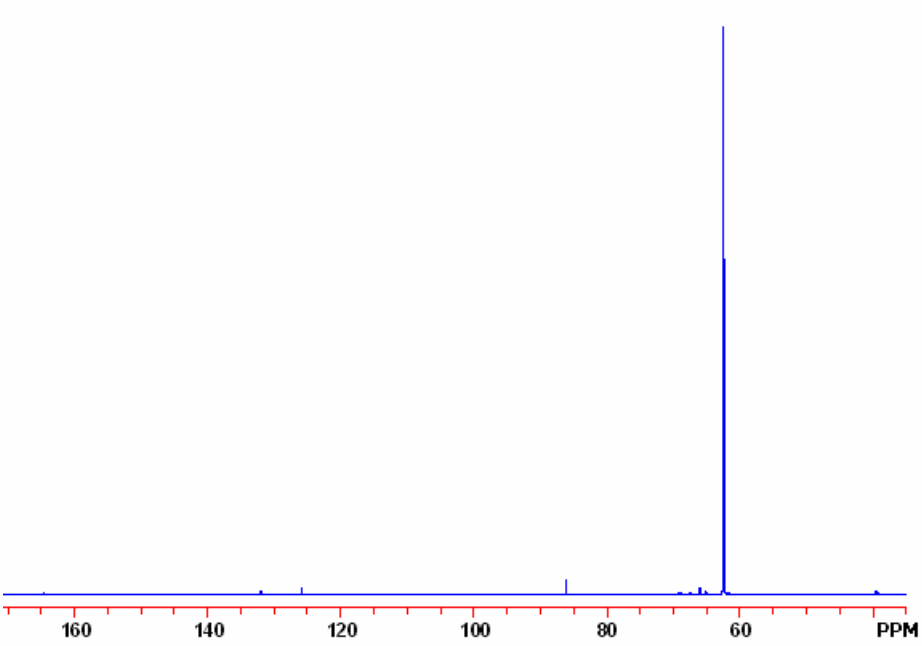

Figure 3-26: Carbon NMR spectrum of ^{13}C, ^{15}N-NMA where the labeled methylol carbon is full scale. The solvent was DMSO-d6.

Finally, the nitrogen spectrum of ^{13}C, ^{15}N-NMA is presented (see Figure 3-27). The expected contribution from NMA at ~ 75 ppm is observed, as well as some residual labeled acrylamide at 50 ppm. A very small peak is also present at approximately 67 ppm. It is not clear what is causing this peak, but it was evident for ^{15}N-NMA as well.

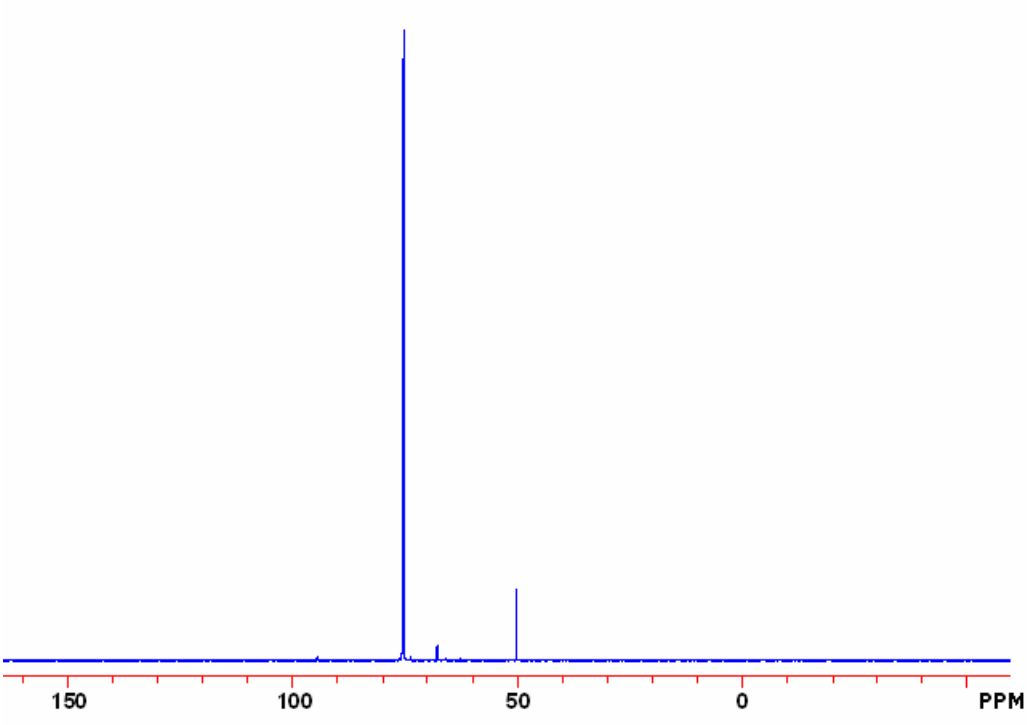

Figure 3-27: Nitrogen NMR spectrum of ^{13}C, ^{15}N-NMA.

3.4 Conclusions

^{13}C-NMA was produced and polymerized with vinyl acetate. Analysis of this product revealed that the ^{13}C-methylol group of NMA was being hydrolyzed, thereby limiting the effectiveness of NMR spectroscopy in detecting NMA units in the latex. For this reason, ^{15}N-NMA was produced. To study crosslinking chemistry, some ^{13}C, ^{15}N-NMA was also produced. NMR spectroscopy shows the purity of the monomers being used, and also indicates coupling between the nuclei.

3.5 Acknowledgements

The author would like to acknowledge the early assistance of Dr. Xiaobing "Joe" Zhou for his ideas towards the development of the synthetic strategy. Also, the assistance of Mr. Tom Glass in the NMR facility was greatly appreciated.

3.6 References

Carpenter, E. L. and H. S. Davis (1957). "Acrylamide. Its Preparation and Properties." Journal of Applied Chemistry **7**: 671-6.

Chan, G. Y. N., A. G. Jhingran, et al. (1998). "Approaches to the controlled formation of network polymers. 1. Synthesis and evaluation of monomers with vinyl differentiation." Polymer **39**(23): 5781-87.

Crews, P., J. Rodriguez, et al. (1998). Organic Structure Analysis. New York, Oxford University Press.

Feuer, H. and U. E. Lynch (1953). "The Synthesis and Reactions of Unsaturated N-Methylolamides." Journal of the American Chemical Society **75**: 5027-9.

Habermann, C. E. (1991). Acrylamide. Encyclopedia of Chemical Technology. New York, John Wiley and Sons. **1:** 251-266.

Jones, G. D., J. Zomlefer, et al. (1944). "Attempted Preparation of Polyvinylamine." Journal of Organic Chemistry **9**: 500-512.

Lauterbur, P. C. (1957). "C13 Nuclear Magnetic Resonance Spectra." Journal of Chemical Physics **26**(1): 217-218.

Le Botlan, D. J., B. G. Mechin, et al. (1983). "Proton and Carbon-13 Nuclear Magnetic Resonance Spectroscopy of Formaldehyde in Water." Analytical Chemistry **55**: 587-91.

Levy, G. C. and R. L. Lichter (1979). Nitrogen-15 Nuclear Magnetic Resonance Spectroscopy. New York, John Wiley and Sons.

Matejicek, A. and J. Cerny (1986). "Synthesis of N-hydroxymethylacrylamide in an Aqueous Solution." Collection Czechoslovak Chem. Commun. **51**: 1656-64.

Moureau, C. and U. E. Lynch (1893). Bull. Soc. Chim. Fr. **3**(9): 417.

Schmidt, R. G., M.-P. Laborie, et al. (2000). "Lab-Scale Synthesis of Isotopically Labeled Formaldehyde for the Production of Formaldehyde-Based Wood Adhesives." Holzforschung **54**(1): 98.

Silverstein, R. M., G. C. Bassler, et al. (1974). Spetrometric Identification of Organic Compounds. New York, John Wiley and Sons.

Ugelstad, J. and J. de Jonge (1957). "A Kinetical Investigation of the Reaction between Amides and Formaldehyde." Recueil des Travaux Chimiques des Pays-Bas **76**: 919-945.

Warson, H. (1990). "Preparation of Derivatives of Acrylamide." Paint and Resin **60**(3): 26-9.

Werstler, D. D. (1986). "Quantitative 13C n.m.r. characterization of aqueous formaldehyde resins: 2. Resorcinol-formaldehyde resins." Polymer **27**: 757-64.

Wojcik, J., S. Szymanski, et al. (1980). "Conformational Analysis of Some Acrylamide Homologues." Bulletin de l'Academie Polonaise Des Sciences. Serie des sciences chimiques. **28**(9-10): 613-619.

Details regarding the synthesis of the latex adhesives are considered proprietary. A chapter describing this work has been omitted to protect the proprietary interests of our collaborators.

Chapter 4: Characterization of Copolymers

This chapter includes characterization studies for three latex adhesives that were synthesized. Factors such as the extent of film formation, or the thermal behavior of the copolymers, their particle size distributions, and their rheological behavior can all impact performance of the adhesive. This chapter will briefly describe the characterization methods and conditions, and will describe the results of the studies.

4.1 Materials and Methods

Adhesive synthesis

Details of the emulsion copolymerization process used to produce the adhesives are proprietary, and cannot be disclosed. The same amount of the co-monomer, NMA, was added to each adhesive. It was added as a 48% solution of NMA in distilled water. In each adhesive, NMA was introduced to the polymerization reactor in different ways. For Latex 1, NMA was incrementally injected into the reactor. For Latex 2, NMA was also injected incrementally, but the injections were delayed—beginning at ~ 50% conversion. For Latex 3, NMA was fed continuously into the reactor.

DSC

Differential Scanning Calorimetry was conducted on a TA Instruments 2920 DSC equipped with MDSC™ and a refrigerated cooling system. A nitrogen purge gas (50mL/minute) was used. Baseline calibration was completed with empty pans, while an indium standard was used to obtain the cell constant and the temperature calibration.

Uncatalyzed and catalyzed latex films were studied. Multibond catalyst (50% aluminum chloride hexahydrate in water, 5 wt.% catalyst was added to a each sample of adhesive) was hand-mixed with a small amount of adhesive just prior to preparing the catalyzed films. Films were cast on a glass plate with a Byrd bar (MCD Industries). Films were carefully lifted from the plate using a razor blade. The thickness of the films was approximately 0.3mm. Uncatalyzed and catalyzed films were analyzed after being stored over calcium sulphate in a desiccator. In addition, some catalyzed films were subjected to accelerated aging exposures, including a boil exposure and an oven treatment. The boil exposure was a 4 hour boil, followed

by oven drying at 104°C for 8 hours. Other catalyzed films were annealed at 104°C for 24 hours. The samples were stored in a desiccator over calcium sulphate until analyzed. A punch was used to obtain samples from the films. The samples were loaded into aluminum pans and sealed. Sample weights ranged from 2 to 4mg. Samples were heated and cooled at a uniform rate of 10°C/minute. A heat-cool-heat method was applied. Data are based on the second heating cycle.

Rheometry

Flow experiments were conducted on an AR1000 TA Instruments Rheometer using a parallel plate geometry. Temperature was held constant at 25°C via the Peltier plate while the shear rate was ramped. A small sample of uncatalyzed adhesive was applied to the center of the Peltier plate, then the plate was lowered into position. Excess adhesive was removed. A bead of silicon oil was applied to seal the sample edge. This provided a barrier that prevented the adhesive from drying out during the experiment. The viscosity of all three latices were examined before and after dilution. Franklin's Titebond® II was also studied. Viscosity readings were verified by testing certified viscosity standards.

Particle Size Analysis

A Horiba LA700 laser scattering particle size distribution analyzer was used. This instrument was equipped with a circulating bath and ultrasonic disruptor. The dispersing phase was a 0.1% solution (w/w) of poly(vinyl alcohol) (Celvol™ 823) in distilled water. Only a very small amount of uncatalyzed latex was necessary (~0.2 grams). The volume of the dispersing phase was approximately 150mL. Additional water or polymer sample was added until the instrument indicated that the turbidity was in the appropriate range. An ultrasonic pre-treatment of 5 minutes was set to ensure that the particles were adequately dispersed just prior to analysis. A polystyrene latex having a known particle size (Duke Scientific) was used to calibrate the instrument.

FE/SEM

A Leo 1550 field emitting scanning electron microscope was also used to study particle size and the extent of film formation. The electron beam was set at 5kV, and the in-lens detector was

used. A variety of samples were analyzed. These included catalyzed and uncatalyzed latex films, as well latices that were applied to wood substrates, then weathered. Catalyzed and uncatalyzed films were prepared on glass plates using a Byrd Bar (MCD Industries). Multibond catalyst (5 wt. %) was added to the sample and was hand-mixed with the latex just before the films were cast. Films were lifted off the glass plates and samples were cut with scissors or punched out. Untreated films were dried at room temperature and stored in a dessicator over calcium sulphate. Annealed films were allowed to dry in a Blue/M oven at 104°C for 24 hours. Boiled films underwent a 4 hour water boil exposure, then were dried at 104°C in the oven for 8 hours.

Each latex was also applied to two yellow-poplar boards in a manner that simulated the preparation of fracture mechanics specimens. The boards had been machined and equilibrated just as the fracture substrates had been treated, and the adhesive loadings on the surface and open times were also identical to those used in the preparation of the fracture specimens (refer to Chapter 6). After a brief consolidation period (5 minutes under a 50lb weight), the bonded sample was opened up and allowed to dry under atmospheric conditions so that an adhesive film remained on both wood substrates. Individual "specimens" (20 mm wide) were cut from the boards on a table saw, then the bondline region of the sample was isolated for analysis by cutting away the bulk of the wood substrate. (This step was necessary to facilitate drying. The SEM analysis requires a vacuum chamber, and the presence of moisture in the wood can result in delays for adequate vacuum to be obtained. For this reason, thinner wood specimens are preferred.) Specimens were then exposed to the different accelerated aging conditions that were applied to the fracture specimens: boil exposure, vacuum soaking, and oven drying (see Chapter 6). All specimens were dried in a Blue/M oven at 104°C for 24 hours. Samples were removed with a punch or with scissors. Care was taken to ensure that the wood samples remained completely dry prior to the analysis. They were stored and transported to the SEM facility in a desiccator under nitrogen and over calcium sulphate.

Film samples were sputter coated with 6nm of gold via a Cressington 208HR sputter coater. Wood samples were sputter coated to a depth of 10.3 nm. Samples were affixed to the stage via two-sided copper tape.

4.2 Results and Discussion

4.2.1 Characterization of the Latices

The properties of the latices were then studied with DSC, Rheometry, Particle Size Analysis, and SEM. NMR analysis of the latices is the subject of Chapter 5.

DSC Studies

The thermal properties of the system were explored using DSC. The glass transition temperatures were very similar among the three latices. This finding is not surprising due to the identical overall composition of the latices. It was hoped that any changes due to crosslinking might be observed via increases in T_gs after catalysis and exposure to the accelerated aging treatments.

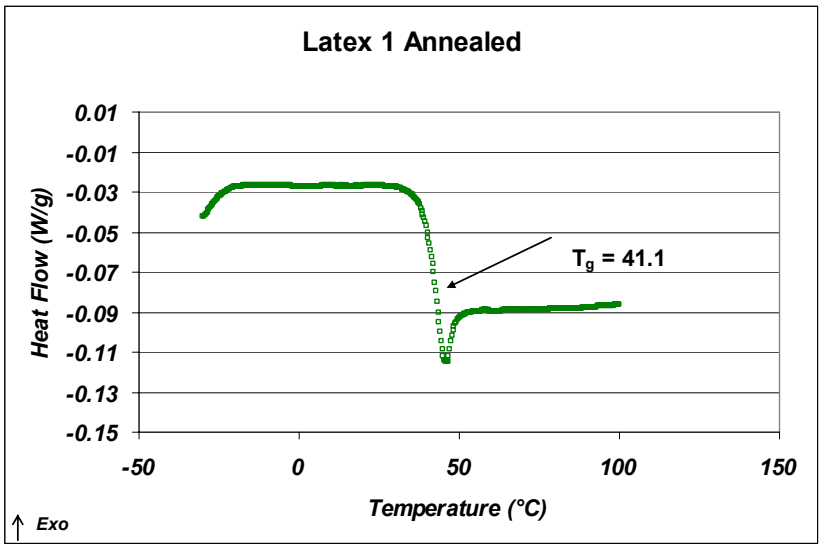

Figure 4-1: Representative DSC thermogram of an annealed Latex film. T_g is defined as the inflection point of the curve.

Individual thermograms are included in the Appendix. Figure 4-1 includes a representative thermogram. Data was analyzed by TA Instruments Universal Analysis Software. T_g was defined as the inflection point of the transition.

Table 4-1 includes the results of the DSC studies. No difference was observed in the behavior of the uncatalyzed and catalyzed films of Latex 1 and 2. For Latex 3, the T_g did increase after

catalysis. Oven drying the films resulted in slight increases in the T_g of Latex 1 and 2, but the increase for Latex 3 was small. The boiling exposure led to the highest T_gs for all three latices. After the films were boiled, they were dried in an oven in a treatment very similar to the annealed film. The result was a slightly higher T_g.

Table 4-1: T_g values according to DSC experiments.

	Latex 1	**Latex 2**	**Latex 3**
T_g (uncatalyzed film)	40.7	40.5	39.8
T_g (catalyzed film)	40.6	40.3	42.0
T_g (annealed catalyzed film)	41.1	40.9	42.1
T_g (boiled catalyzed film)	41.3	41.6	42.4

It is difficult to say whether or not differences observed here are significant. Physical or chemical changes could be responsible for the observed increase in T_g for the boiled films. For example, defoamer or catalyst could be leached out of the system, or acetate groups could be hydrolyzed. Removing small plasticizing molecules would also increase the observed T_g.

Another interesting finding is the slight change observed in Latex 1 T_g between untreated and treated samples. The difference between the T_g of the boiled film and the T_g of the uncatalyzed film was only 0.6°C. For Latex 2, this difference increased to 1°C, and for Latex 3, the difference was 2.7°C. This suggests that the film of Latex 1 is less affected by accelerated aging exposures. It also suggests that something is happening in Latex 3 to cause higher T_gs. The NMA distribution study (discussed in the following chapter) revealed that Latex 3 had predominantly (~80%) core-NMA while Latex 1 and 2 had mostly surface NMA (~60% and ~80%, respectively). The increased T_g for Latex 3 could be due to crosslinking of core-NMA.

Rheology Studies

A simple flow experiment was conducted to examine the differences in viscosity among the latices. During this experiment, the shear rate was ramped over a broad range and the torque required to maintain the shear rate gives information regarding the nature of the samples. Figure 4-2 shows a plot of viscosity versus shear rate for the three latices plus Franklin's Titebond® II.

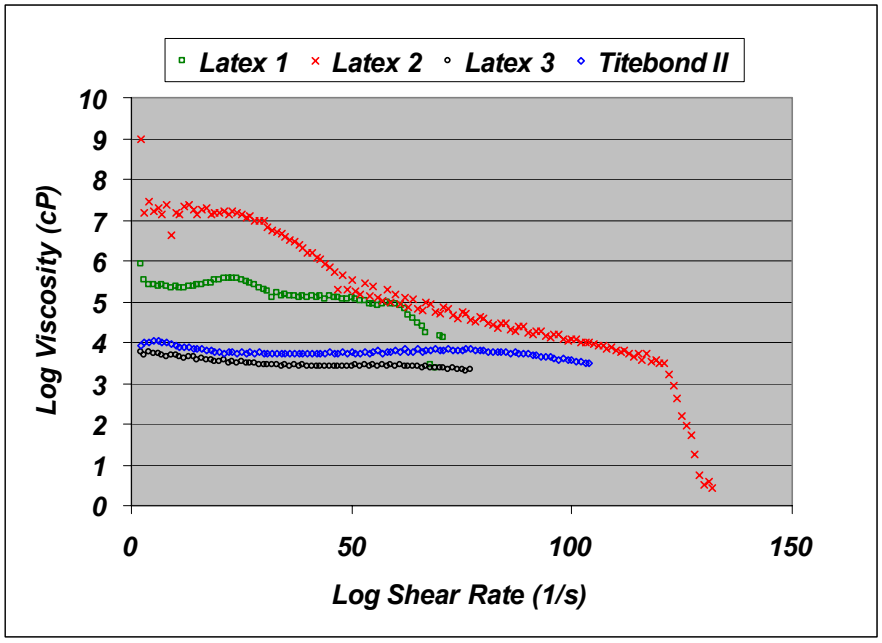

Figure 4-2: Plot of viscosity versus shear rate for Latex 1, Latex 2, Latex 3 and Franklin's Titebond® II.

Latex 3 has very similar rheological behavior to the commercially available product. Latex 1 and Latex 2 exhibit much, much higher viscosities at low shear rates. Viscosity is known to influence adhesive penetration, and therefore can impact the performance of bonded assemblies. For the fracture cleavage studies, a viscosity effect was deemed undesirable. Therefore, the latices were diluted to achieve similar viscosities. After dilution, the viscosity behavior was much more like the behavior of the commercially available product. At lower shear rates, Latex 2 still has a higher viscosity, but it is within an order of magnitude of the other samples.

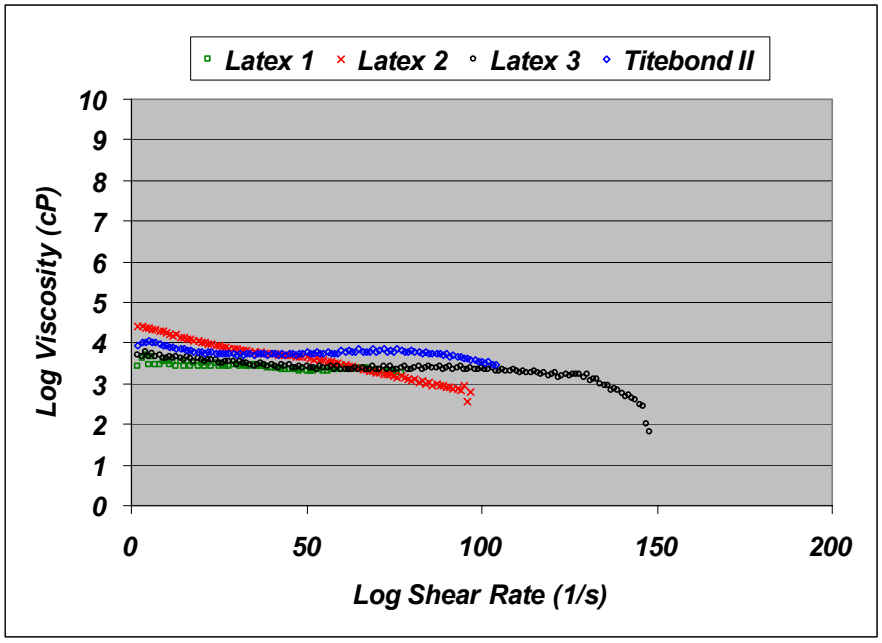

Figure 4-3: Viscosity versus shear rate for Latex 1, Latex 2, Latex 3, and Franklin's Titebond® II after dilution. The Titebond® II was not diluted.

It is interesting to note that none of the latices appear to exhibit Newtonian behavior. Generally, a shear thinning trend is observed with increasing shear rates, indicating that some level of structure within the system is breaking down under higher shear rates.

Another interesting finding is the viscosity peak in some of the samples. An example of this behavior is shown in Figure 4-4, which includes viscosity versus shear rate plots for Franklin's Titebond® II. Here we observe the viscosity peak as the shear rate approaches $10s^{-1}$. This behavior is thought to be due to the formation of aggregates, which are then dispersed at higher shear rates. Initially it was thought that the peak could be due to the latex drying out over time. However, the data here were taken over different ranges of shear rates. If this were a time-dependent phenomenon, as we would expect for drying, then the peak would occur at similar times—not at the same shear rate. The formation of aggregates which are then disrupted is a viable possibility. As the shear rate increases, particle collisions increase. It would be relatively easy for a few entanglements to occur between chains grafted onto particle surfaces if the particles remained in contact for a given time period. However, as the shear rate increases, there is not enough time for entanglements to form.

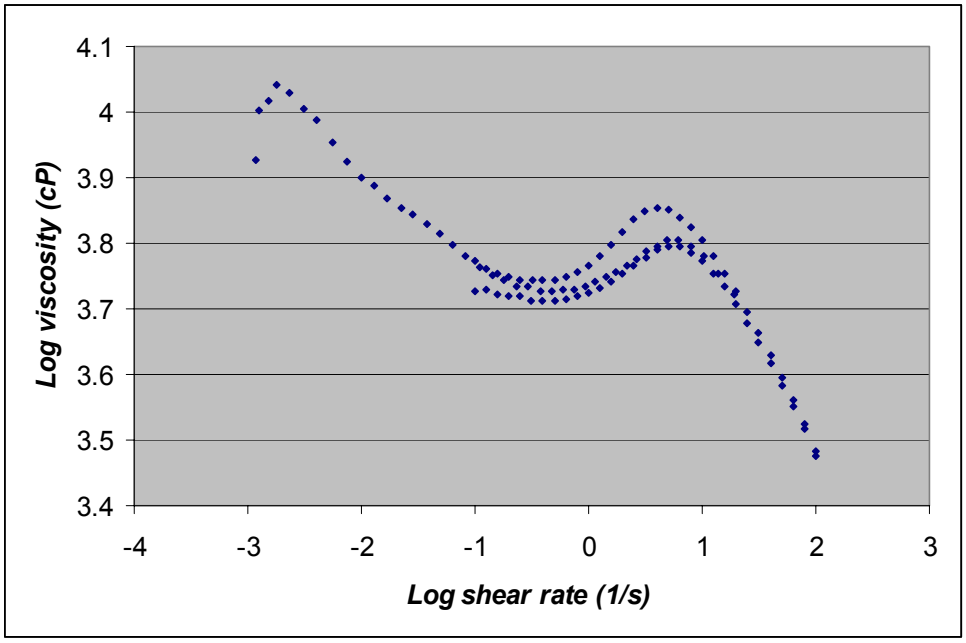

Figure 4-4: Viscosity versus shear rate plots for three rheological flow experiments using Franklin's Titebond® II adhesive.

Similar, but less pronounced peaks were evident in the rheological data for Latex 1 (Figures 4-5 and 4-6) and Latex 3 (Figures 4-9 and 4-10). For Latex 2 no peaks were evident, but a region of the plot did show a change in concavity (Figures 4-7 and 4-8). After dilution, the appearance of the viscosity peak shifted to higher shear rates. In a more dilute system, there is more free space between particles, so it may require higher shear rates before the aggregation effect is observed.

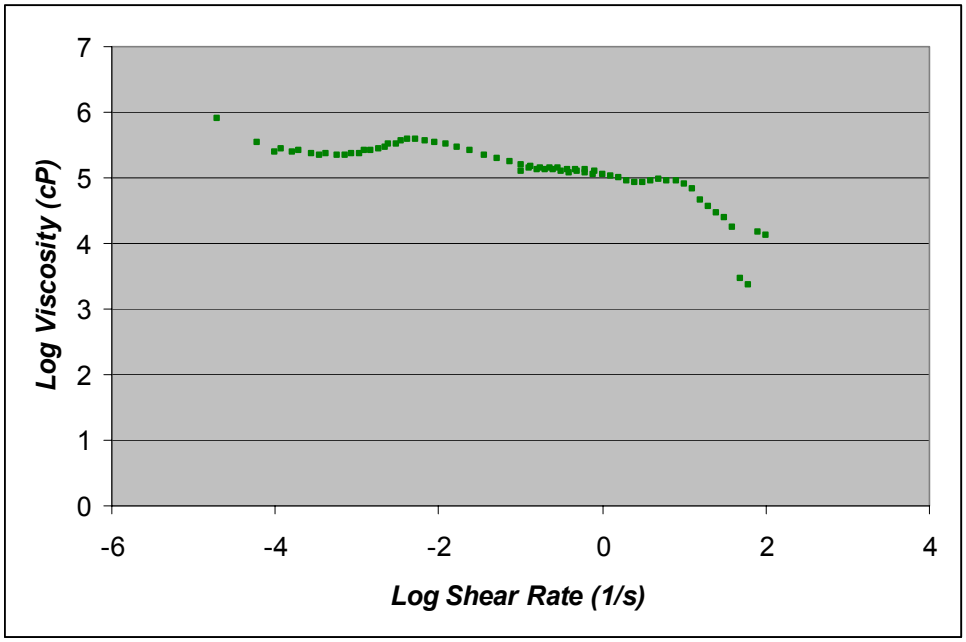

Figure 4-5: Viscosity of Latex 1 before dilution.

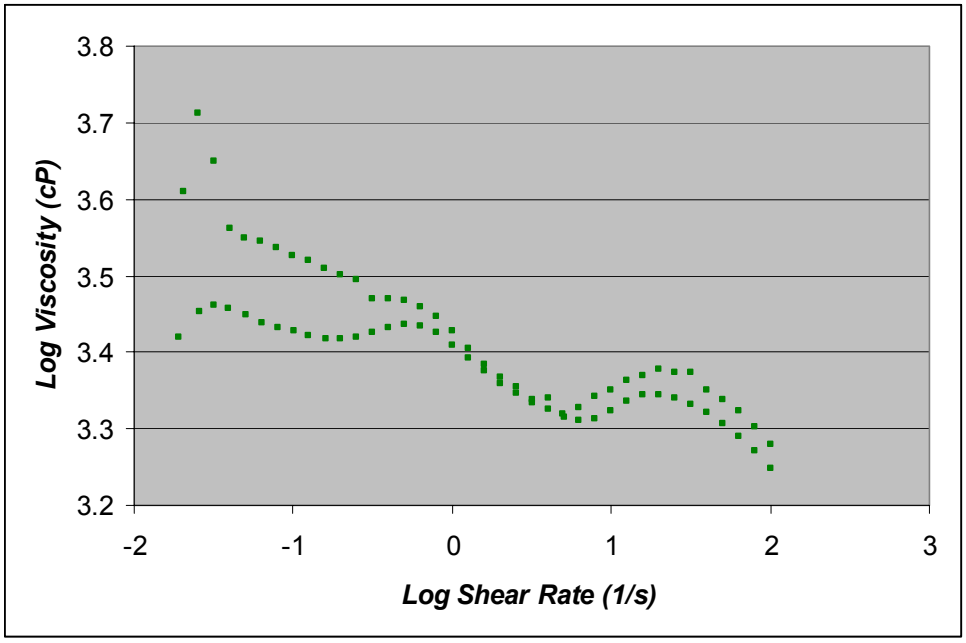

Figure 4-6: Viscosity of Latex 1 after dilution.

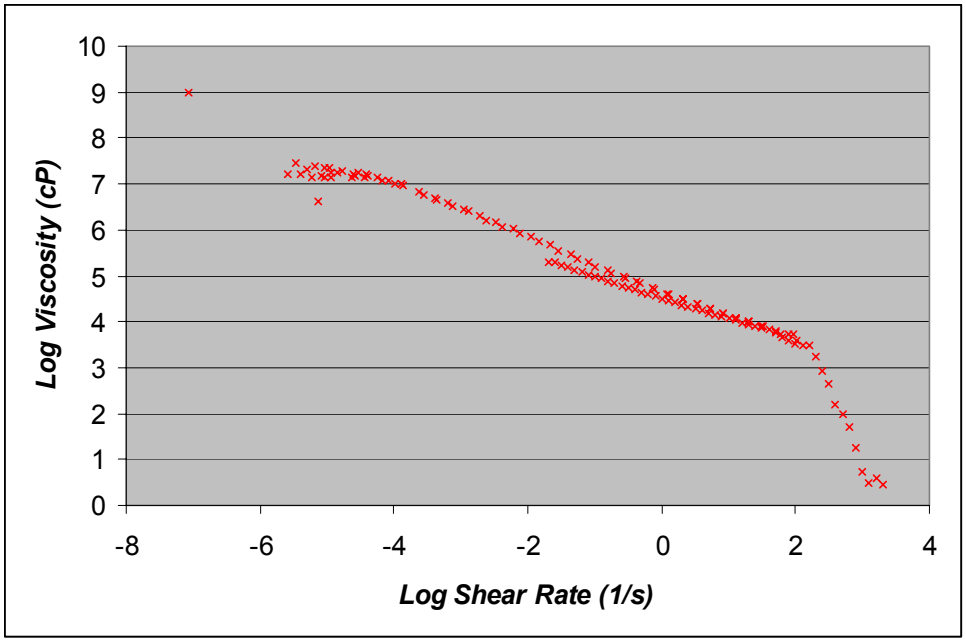

Figure 4-7: Viscosity of Latex 2 before dilution.

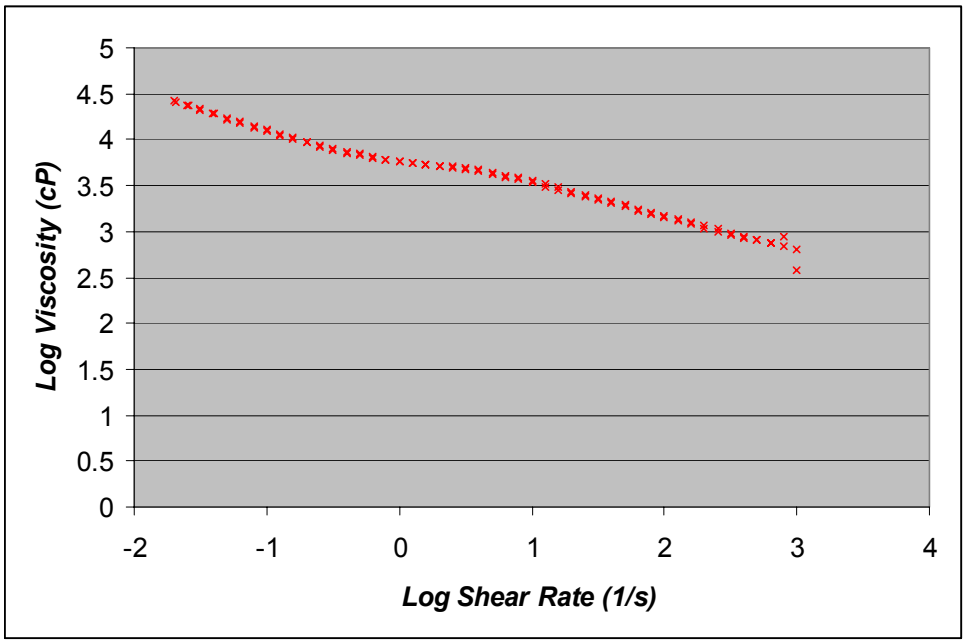

Figure 4-8: Viscosity of Latex 2 after dilution.

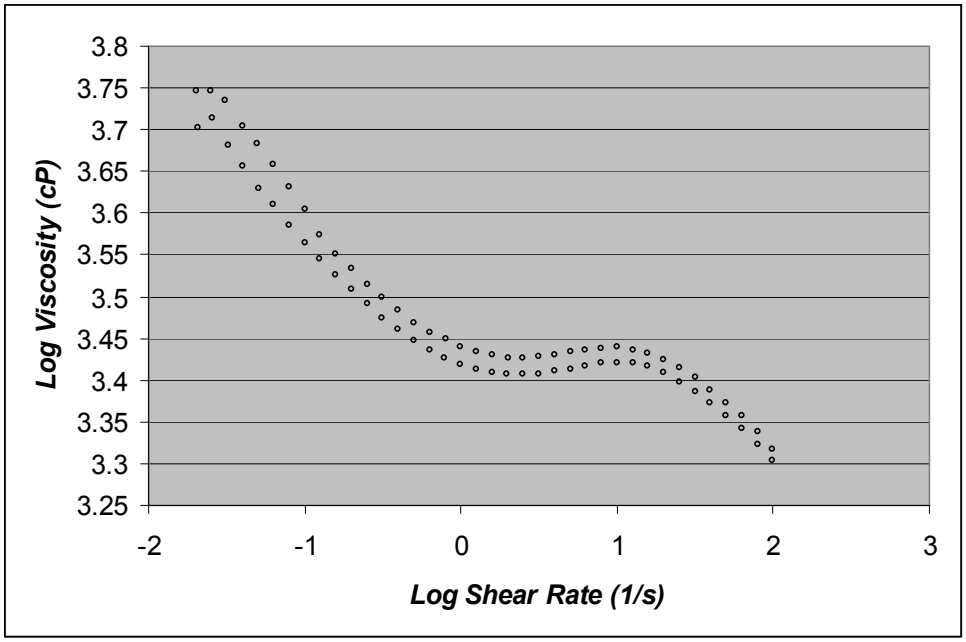

Figure 4-9: Viscosity of Latex 3 before dilution.

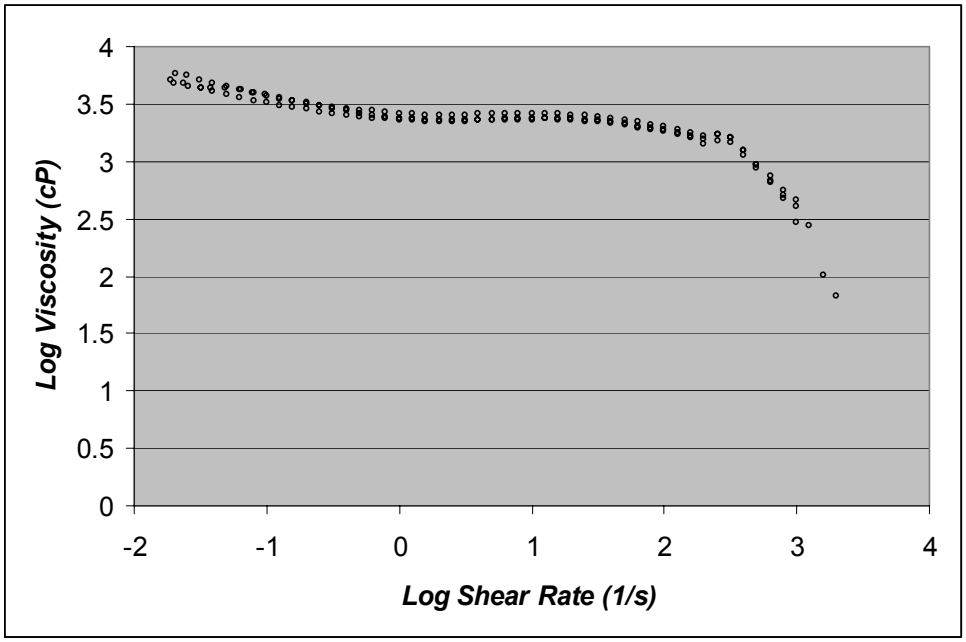

Figure 4-10: Viscosity of Latex 3 after dilution.

To summarize, the viscosity data indicate that Latex 2 is very different from Latex 1, Latex 3, and Franklin's Titebond® II. It has much higher viscosities at lower shear rates. Furthermore, it does not exhibit the same peak in viscosity that is observed in the other systems at increasing shear rates. Latex 1 and 2 initially had very high viscosities, but the dilution decreased the viscosity significantly.

Particle Size Analysis

Another means of evaluating the latices is through the use of a particle size analyzer. The instrument is based on static light scattering, specifically, Mie scattering theory (Griffifths 2002). Here, a polystyrene latex having a certified diameter was evaluated first. The standard latex was analyzed several times. An average particle size distribution was obtained, and is plotted in Figure 4-11. A reference line indicates the certified mean particle size. The distribution is assumed to be normal, so that the mean particle size would correspond with the center of the peak. This indicates that the particle size analyzer was slightly off, requiring a shift of 0.25 microns. The same data is plotted after shifting in Figure 4-12. The particle sizes of the three latices (after correction) are plotted in Figure 4-13. Each latex was analyzed 3 times, and the data plotted represents the average of those three readings.

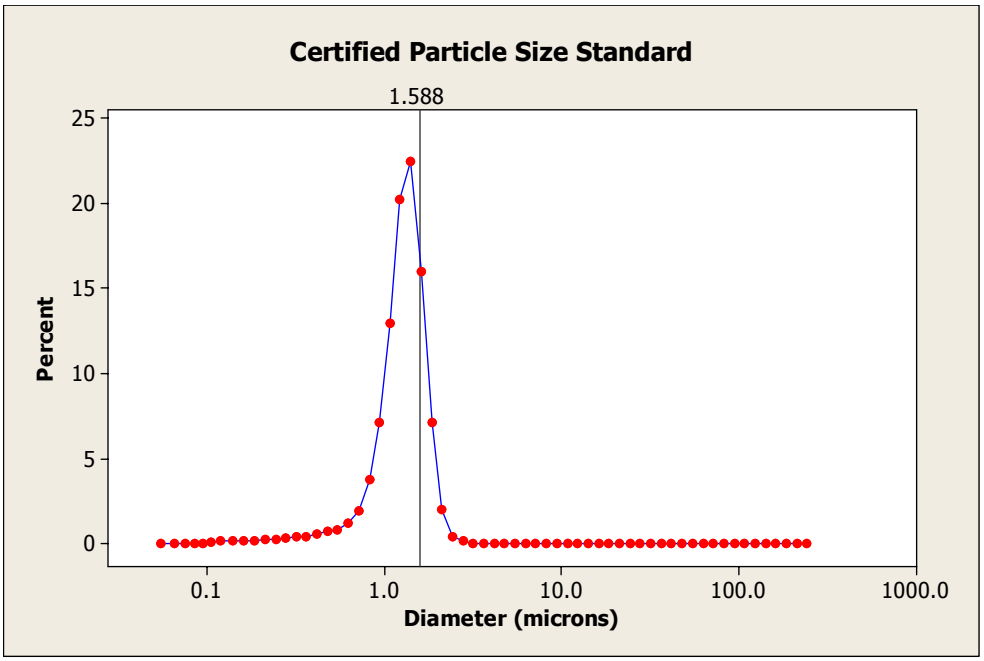

Figure 4-11: Particle size data for a polystyrene latex with known diameter (1.588 microns). The percentage of particles in a given range are indicated by a datapoint at the midpoint of that range.

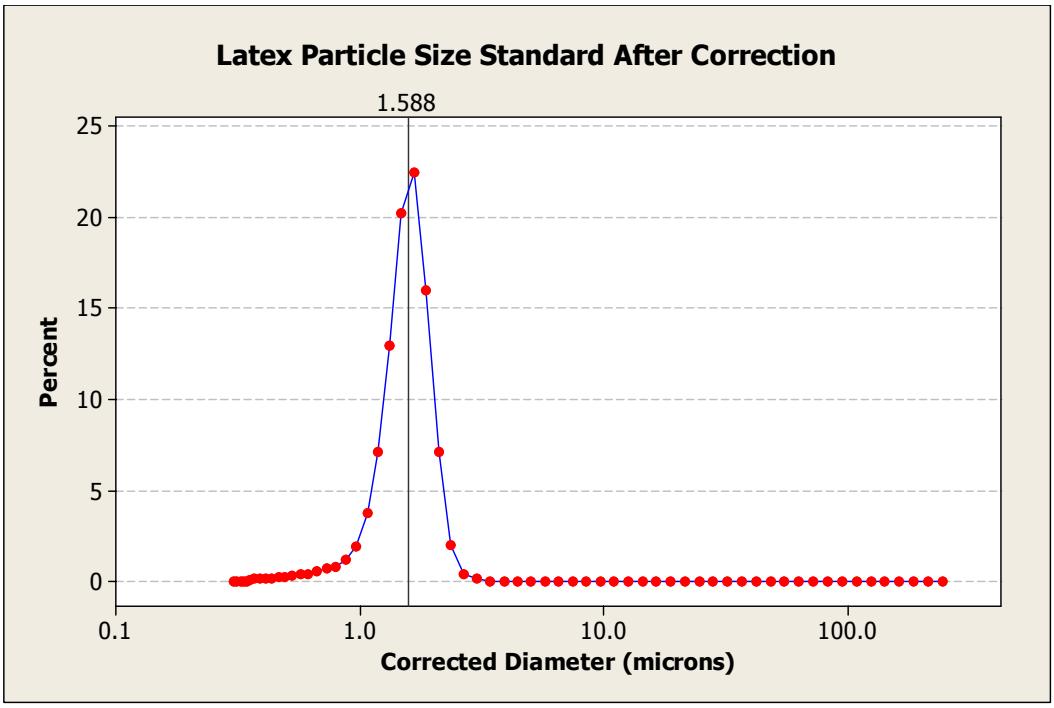

Figure 4-12: Particle size analysis data after the correction is applied.

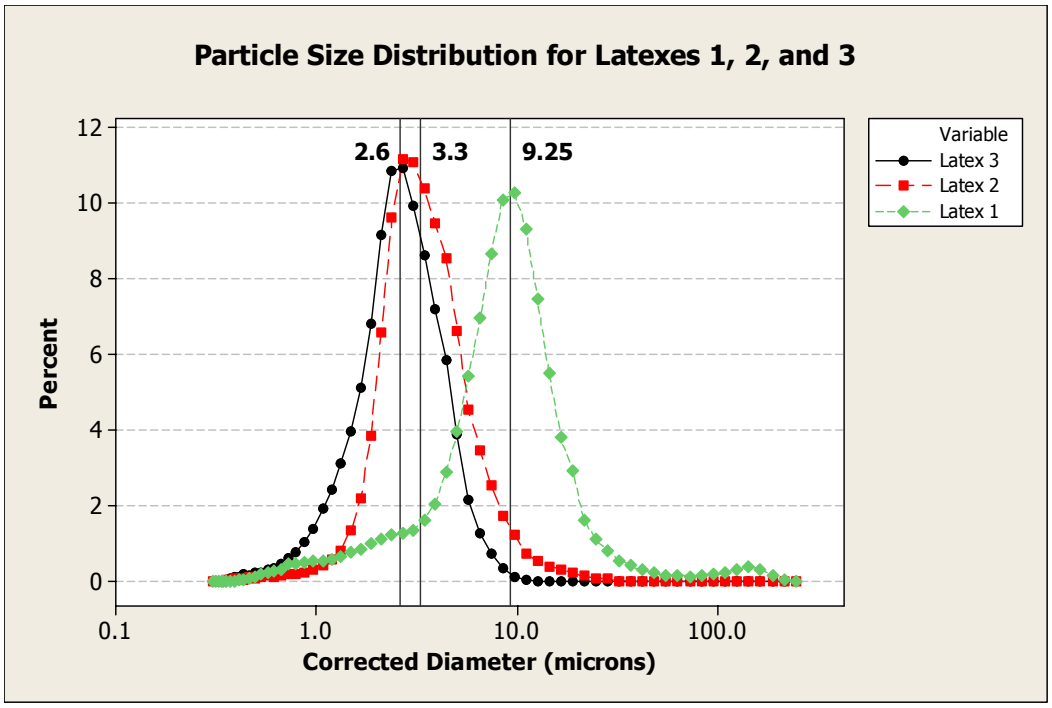

Figure 4-13: Particle size analysis data for Latex 1, Latex 2, and Latex 3.

Of the three latices, Latex 3 had the smallest average particle size (2.6 microns), while Latex 1 was found to have considerably larger particles (9.25 microns). The particles in Latex 2 are of a similar size as those in Latex 3, only they are slightly larger (3.3 microns), on average. The distributions are also noticeably broader than the polystyrene standard. It is evident that Latex 1 does not possess a normally distributed particle size.

SEM

Latex films were also observed via SEM to obtain an indication of particle size, as well as an indication of the coalescence and integrity of the films after exposure to various conditions. Larger SEM micrographs are included in the Appendix at the end of the chapter.

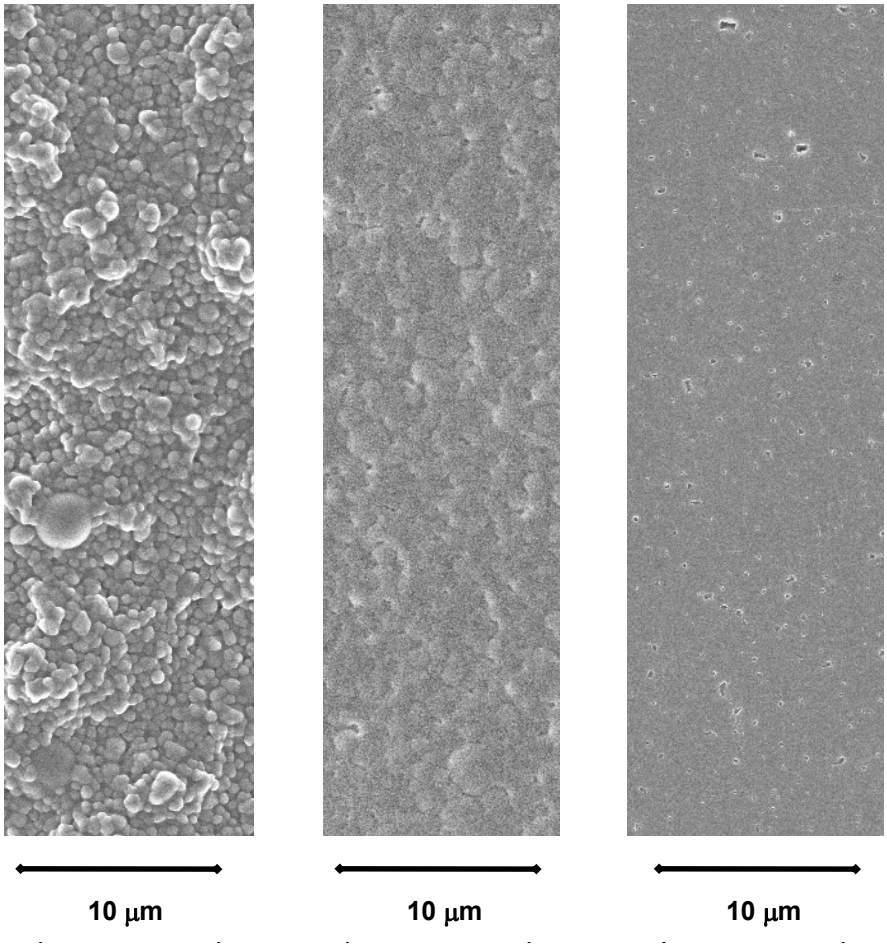

Figure 4-14: SEM Micrographs of uncatalyzed films of Latex 1,2, and 3 (left to right).

In the uncatalyzed films, Latex 1 is distinctly different from both Latex 2 and Latex 3. First, the film appears to have noticeable variations in depth. Some areas appear to contain stacks of particles, while other areas appear as valleys. In Latex 1, the film formation process has not proceeded very far, while Latex 2 shows particle deformation and some evidence of interdiffusion of polymer chains, and Latex 3 shows no evidence of particle boundaries. The small "particles" that are seen for Latex 3 are tiny voids in the film. In Latex 2, some of the particle boundaries remain distinct. For Latex 1, the polymer particles are still very well defined. These results indicate that the particles are clearly different. The minimum film formation temperature (based on these micrographs) appears to be different for the three latices, even though their T_gs (as measured from DSC) were very similar (40.7°C (Latex 1); 40.5°C (Latex 2); and 39.8° C (Latex 3)). The extent of film formation does correspond to the trend in T_gs. One would expect the material with the highest T_g to have the most limited extent of film formation, and the lowest T_g material to exhibit the greatest degree of film formation.

Samples of uncatalyzed latex were also analyzed in a particle size analyzer. The SEM micrographs indicate different particle sizes than the particle size analyzer. Particle size analysis determined that the mean diameter for Latex 2 particles was 3.3 μm. Via SEM, most of the particles appear to have a diameter of between 2.5 and 3 μm, which agrees reasonably well with the particle size analysis result. However, some degree of film formation was achieved in the Latex 2 SEM micrograph. This process may have flattened the particles, thus increasing the apparent particle size. Subsequent figures (Figures 4-15 through 4-19), which all included catalyst, indicate that the particles are much smaller than what was measured by particle size analysis. The catalyzed samples seem to be better suited for particle size analysis work. Discrepancies between the particle size analysis and the SEM results are quite noticeable for Latex 1. The particle size analysis technique indicated an average Latex 1 particle size to be 9.25 μm, while SEM indicates much smaller particles are present. One possibility for this large error could be that the particle size analysis was heavily influenced by the aggregates that are observed in other SEM micrographs (refer to Figures 4-15 through 4-19). In Latex 3, only catalyzed samples can be compared since the uncatalyzed sample has formed a film. Considering Figures 4-15 and 4-16, the particles of Latex 3 appear to be smaller than the 2.6 μm average which was obtained by the particle size analyzer.

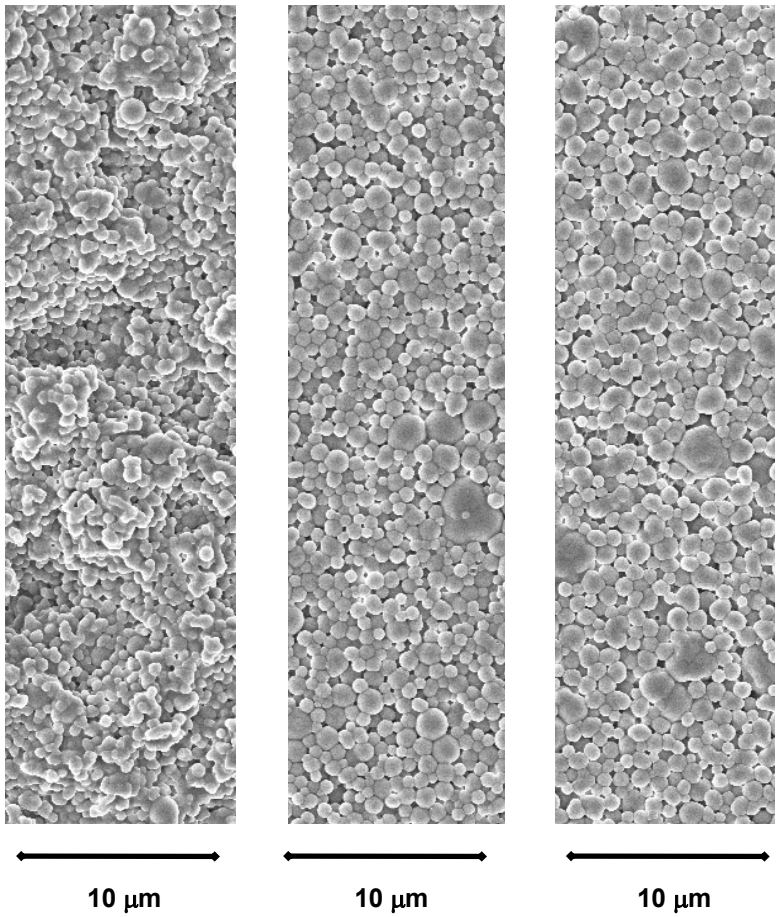

Figure 4-15: SEM Micrographs of catalyzed films of Latex 1,2, and 3 (left to right).

When 5% of the Multibond catalyst is added to the latices before the film is cast, the extent of film formation clearly changes (see Figure 4-15). Latex 1 appears to be similar to the uncatalyzed film. For Latex 2 and 3, catalysis has limited the extent of the film formation process to particle deformation and hexagonal packing. Recall that for uncatalyzed films of these adhesives we saw evidence of particle interdiffusion in Latex 2, and complete film formation for Latex 3.

DSC indicated that the T_gs of the catalyzed and uncatalyzed films of Latex 1 were probably not significantly different (40.7°C and 40.6°, respectively). For Latex 2, the measured T_g's were 40.5°C (uncatalyzed) and 40.3°C (catalyzed). Again, these are probably not statistically different. For Latex 3, the T_g *increased* noticeably after catalysis, from 39.8°C to 42.0°C. This would lead to expected decreases in the extent of film formation, which is observed. Latex 1 continues to have a very different appearance than Latex 2 and Latex 3. The film surface again

shows much more variation in depth. Furthermore, the particles do not appear to be as distinct or as round as the particles in Latex 2 and 3.

When the catalyzed film is poured and allowed to dry, then annealed at 104°C for 24 hours, the appearance of the films change slightly (see Figure 4-16). For Latex 1, indications of an irregular surface (greater depth) are seen. Large aggregates are also present. Individual particles are small and defined, but a thick polymeric coating appears on the surface of the film, particularly around the aggregates. This is not present in the images taken from Latex 2 or Latex 3. In Latex 2, the particles show some indication of beam damage. After bombarding a given region of the sample with the electron beam, the particles began to show signs of surface "buckling". This is consistent with the dimpling observed on the particles in Latex 2. In this film, the particles have come into contact, but there is not much hexagonal packing or particle interdiffusion. Latex 3 appears to be similar to Latex 2, except that there is no indication of beam damage.

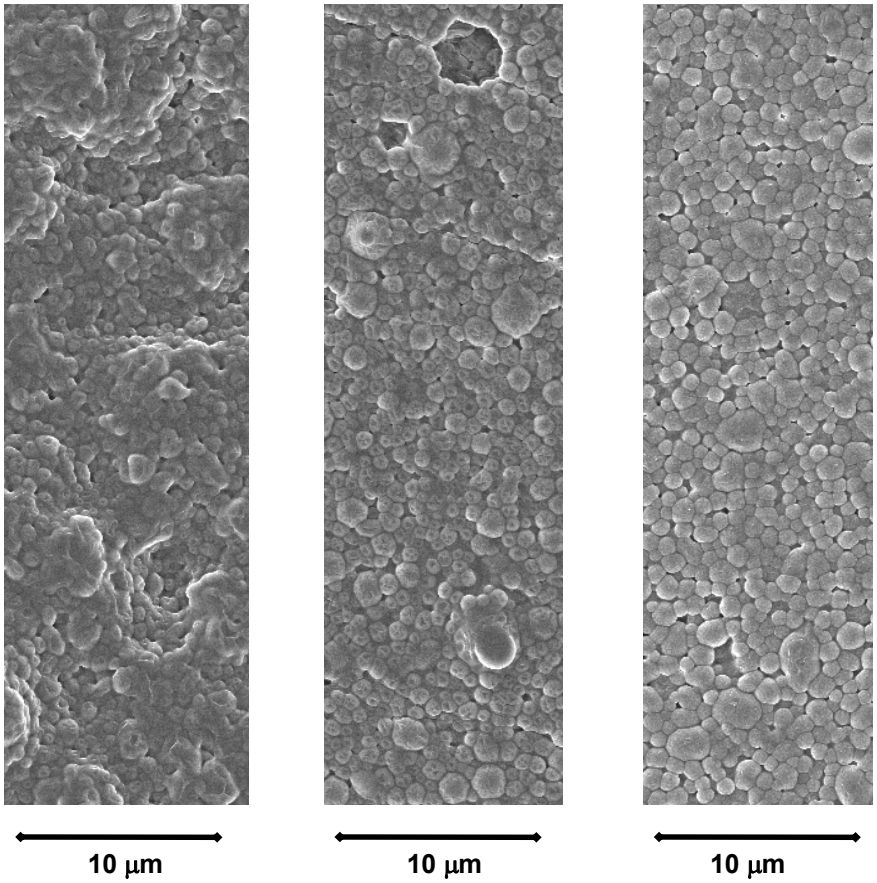

Figure 4-16: SEM Micrographs after catalyzed films of Latex 1,2, and 3 (left to right).after annealing at 104° for 24 hours.

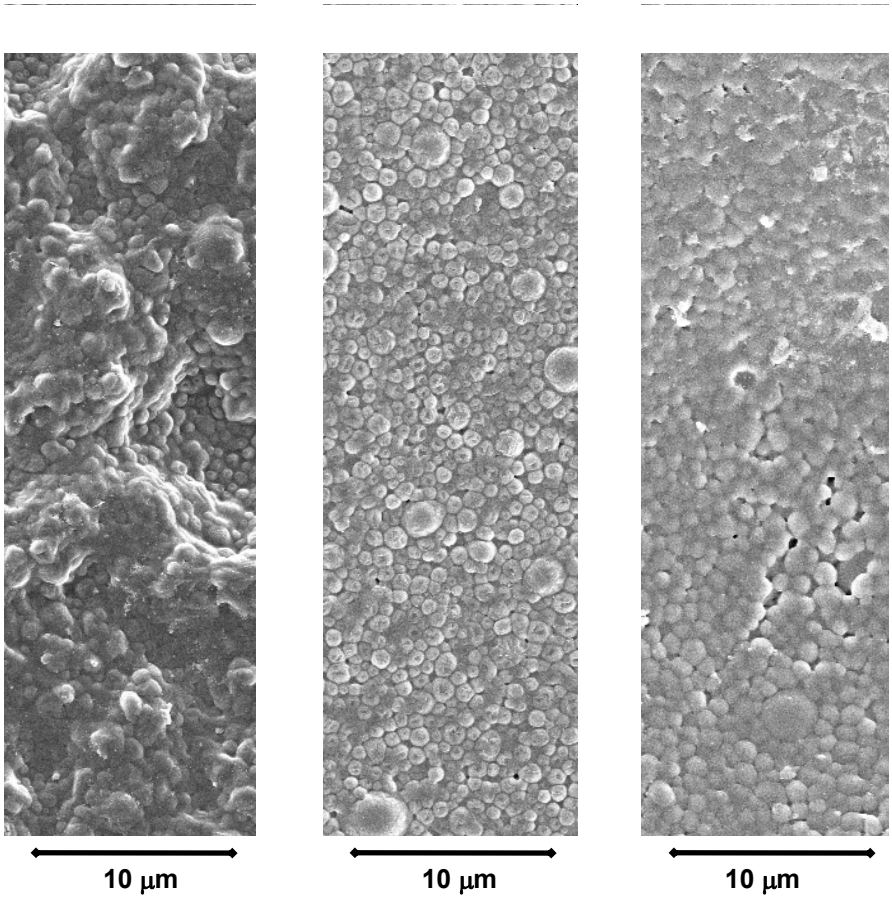

Figure 4-17: SEM Micrographs of Latex 1, Latex 2, and Latex 3 (left to right) on wood. These specimens were subjected to the control treatment, then examined.

In Figures 4-17, 4-18, and 4-19, the latex was applied to wood. These specimens were prepared just as the fracture mechanics specimens were prepared, using catalyzed adhesive. Specimens were exposed to the same control, boil, and vacuum soak treatments that were applied to the fracture specimens (conditions are described more thoroughly in Chapter 6).

Figure 4-17 shows the surfaces after exposure to the control treatment, which was simply oven drying at 104°C until dry. There is little difference between these observations and what was seen in Figure 4-16, which was an SEM image of catalyzed oven-treated films that were cast on glass. For Latex 1, we continue to see indications of an irregular surface (greater depth) and the polymeric matrix around larger aggregates. In Latex 2, the particles again show some indication of beam damage. In this film, the particles have come into contact, but there is not much hexagonal packing or particle interdiffusion. For Latex 3, there is clear evidence of voids in the

film. The particles have achieved a greater degree of packing than those in Latex 2. Also, it is interesting that Latex 3 adhesive on wood seems to have coalesced to a greater extent than the film on glass. Particle boundaries are still present in all three systems.

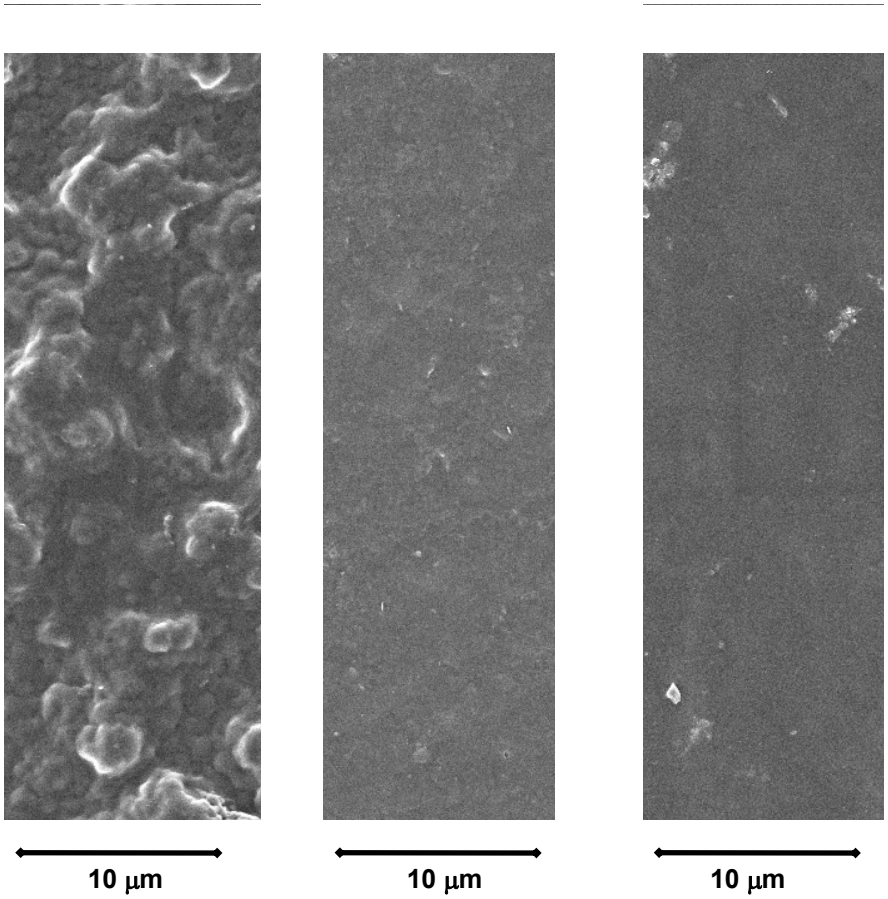

Figure 4-18: SEM Micrographs of Latex 1, Latex 2, and Latex 3 (left to right) on wood. The treated wood specimens were boiled and oven dried (8 hrs. at 104°C) before they were examined.

In Figure 4-18, the latex-coated wood specimens were boiled, and in Figure 4-19 they were vacuum soaked. Again, these accelerated aging treatments were completed to simulate the boiling and vacuum soak exposures that the fracture specimens undergo. Here, the latex surface is directly exposed to the water, whereas in the fracture specimens it is not.

In each case, the films in Latex 2 and 3 show no evidence of latex particle boundaries. In fact, from these figures, there is no evidence of latex present at all. However, latex was evident in

visual observations of the surface prior to SEM studies. Latex 2 and Latex 3 have formed continuous films. Latex 1 is distinctly different than Latex 2 and Latex 3. In both the boil and vacuum soak exposure, there continues to be evidence of distinct particle boundaries in a matrix of polymeric material. The surface still exhibits some roughness, indicating that the accelerated aging treatments had little effect on the integrity of adhesive.

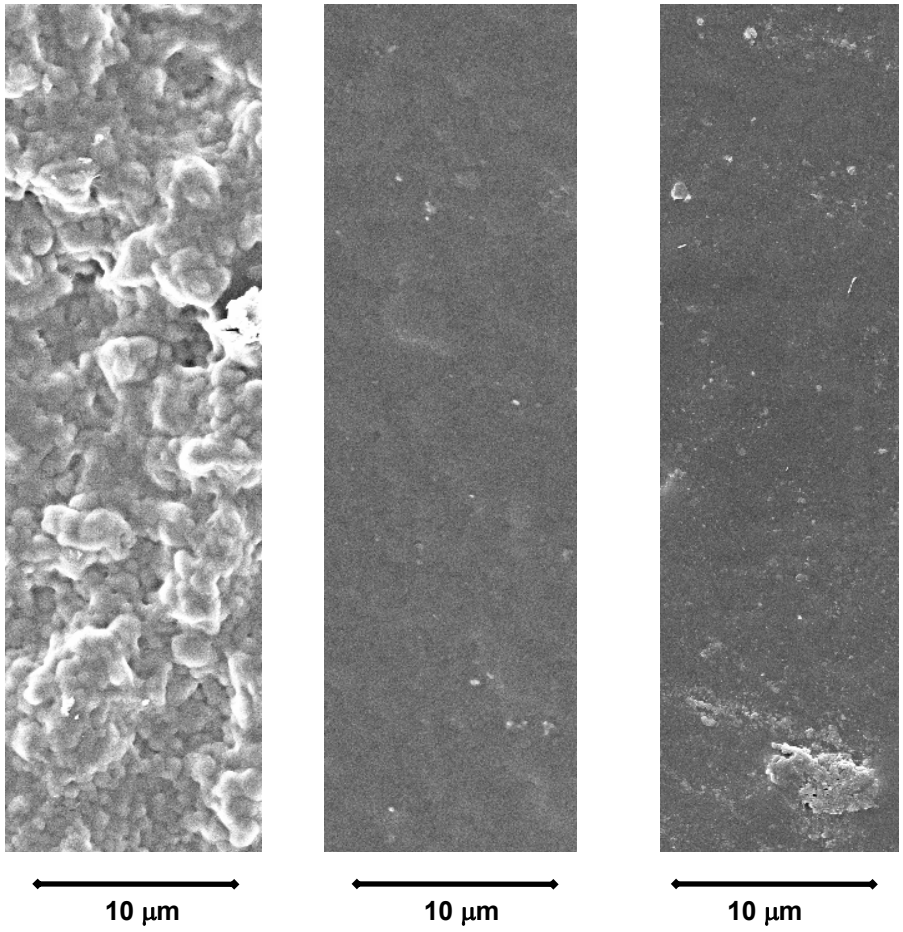

Figure 4-19: SEM Micrographs of Latex 1, Latex 2, and Latex 3 all applied on wood substrates. The specimens were exposed to a vacuum soak, then oven dried before examined.

According to SEM, the particle size difference among the latices is not appreciable. Latex 1 does appear to be more heterogeneous, with a number of small particles and a number of larger aggregates. Also, the stacking of particles into layered structures or aggregates is unique. Latex 2 and 3 seem to be more spherical particles and show less indication of stacking or irregularities in the film surface.

4.3 Conclusions

DSC was used to probe the T_gs of both catalyzed and uncatalyzed films, as well as boiled and oven-treated films. Differences among the adhesives and among the accelerated aging conditions were slight, but did seem to correlate to the extent of film formation in the latex films, as seen in the SEM experiments.

Particle size analysis revealed that Latex 1 had much larger particles (9.25 microns) than Latex 2 (3.3 microns) and Latex 3 (2.6 microns). SEM observations did not correlate with the particle size analysis results. Instead, the micrographs revealed that most of the latexes had similar particle sizes. SEM indicated that aggregates of particles were present in Latex 1 samples. If these aggregates were not disrupted by the ultrasonic treatment, they could have caused the large particle size readings.

SEM also provided interesting evidence of the effect of catalysis and accelerated aging treatments. In general, catalysis seemed to inhibit film formation for all three lattices if no aging treatment was imposed. Latex 1 did not form a continuous film under any circumstances. Instead, it showed indications of surface roughness in the film. Catalyzed samples of Latex 2 and 3 formed continuous films when they were applied to wood substrates and then exposed to an acclerated aging treatment. When similar samples were oven-dried (conditions analogous to the "control" exposure in the fracture testing), the particle boundaries remained intact.

The viscosities of Latex 1 and Latex 2 were initially much higher than that of Latex 3 and of Franklin's Titebond® II. After dilution, all viscosities were within an order of magnitude. An apparent peak in the viscosity was found for Latex 3, Latex 1, and Franklin's product. This is thought to be due to polymer chain entanglement due to collisions and prolonged contact. Higher speeds tended to break up the aggregates and prevented enough time for chain entanglement to occur.

4.4 Acknowledgements

Particle size analysis was conducted through the assistance of Mr. David Berry and Dr. Carlos Suchicital of the Materials Science and Engineering Department. Mr. Steve McCartney

completed the microscopy work, and provided many interesting discussions (over good music!). Thanks to Mr. David Jones for his assistance in preparing the wood specimens.

4.5 References

Erbil, H.Y. (2000). Vinyl Acetate Emulsion Polymerization and Copolymerization with Acrylic Monomers. Boca Raton, CRC Press.

Griffifths, D. (2002). Horiba Information. Personal Communication.

4.6 Appendix

Included here are all of the DSC thermograms, and the SEM micrographs. The caption of each figure provides the relevant details.

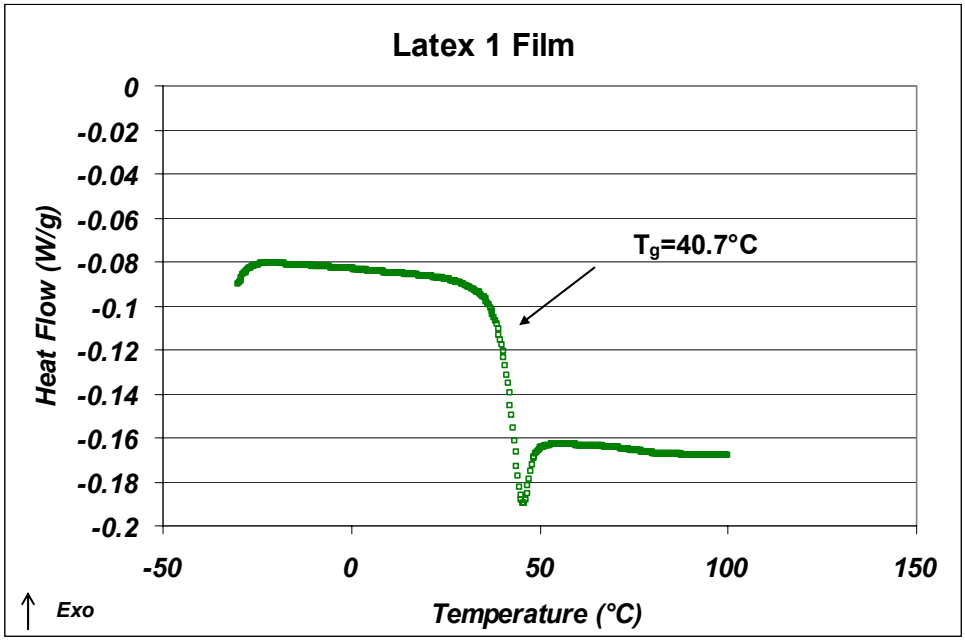

Figure 4-20: DSC Thermogram of a film of Latex 1, without catalyst.

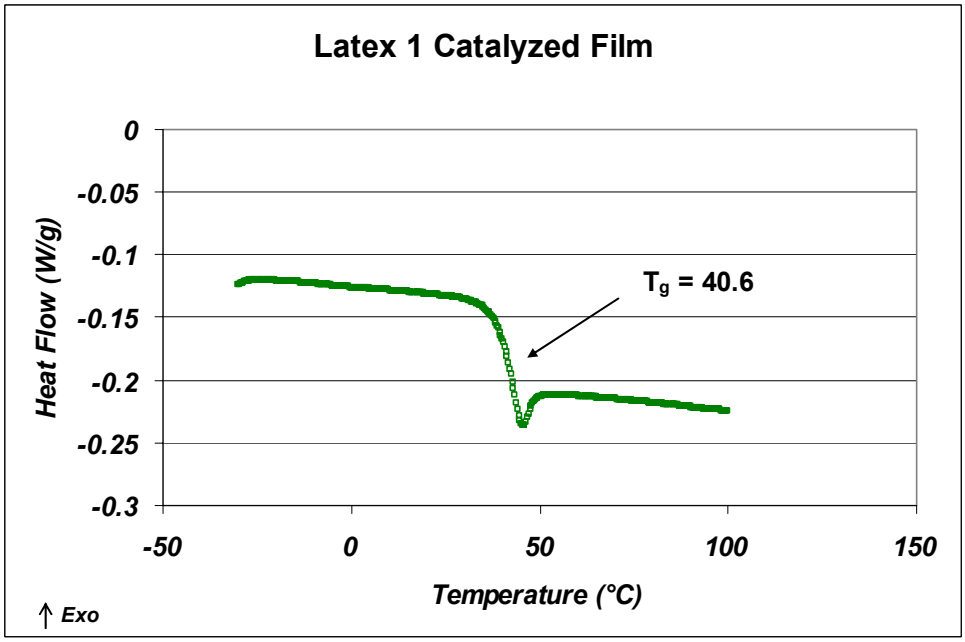

Figure 4-21: DSC Thermogram of a catalyzed film of Latex 1.

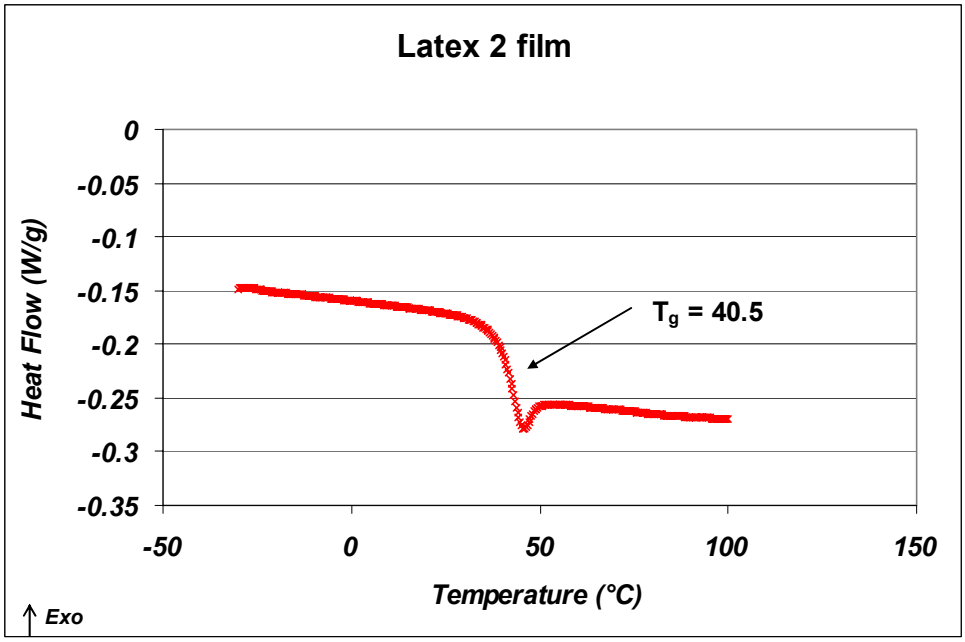

Figure 4-22: DSC Thermogram of a film of Latex 2, without catalyst.

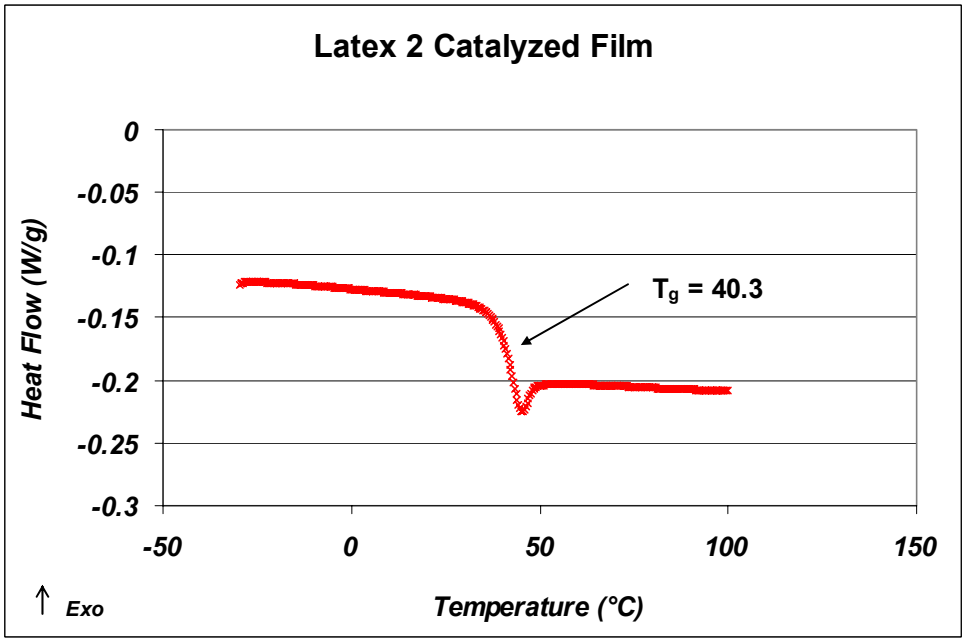

Figure 4-23: DSC Thermogram of a catalyzed film of Latex 2.

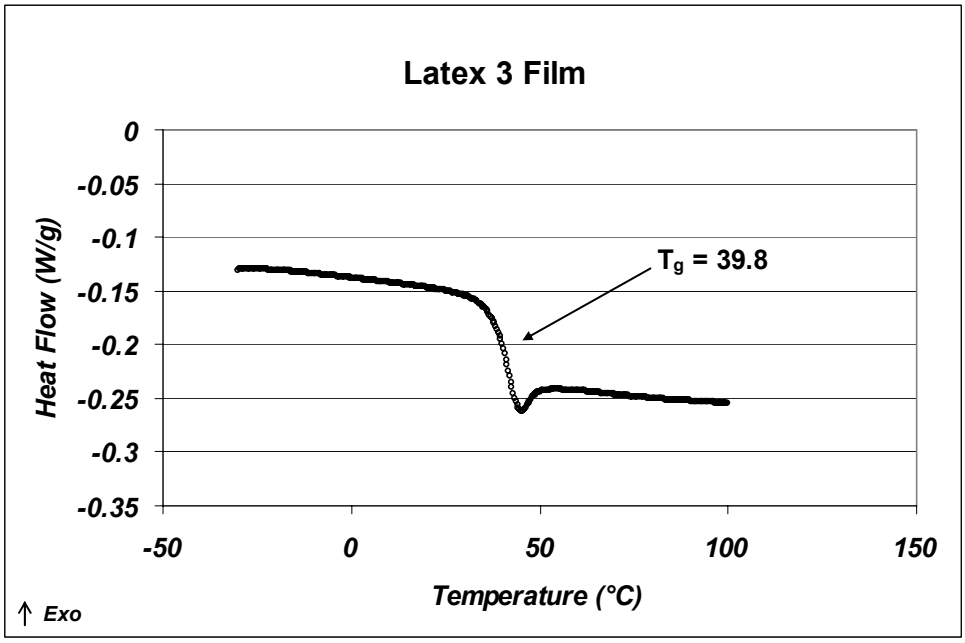

Figure 4-24: DSC Thermogram of a film of Latex 3, without catalyst.

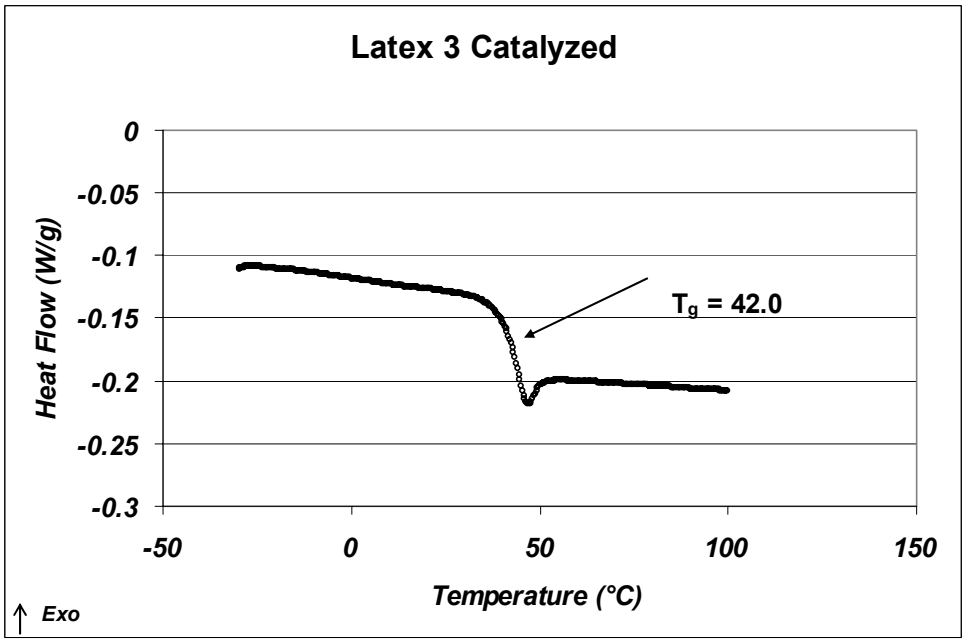

Figure 4-25: DSC Thermogram of a catalyzed film of Latex 3.

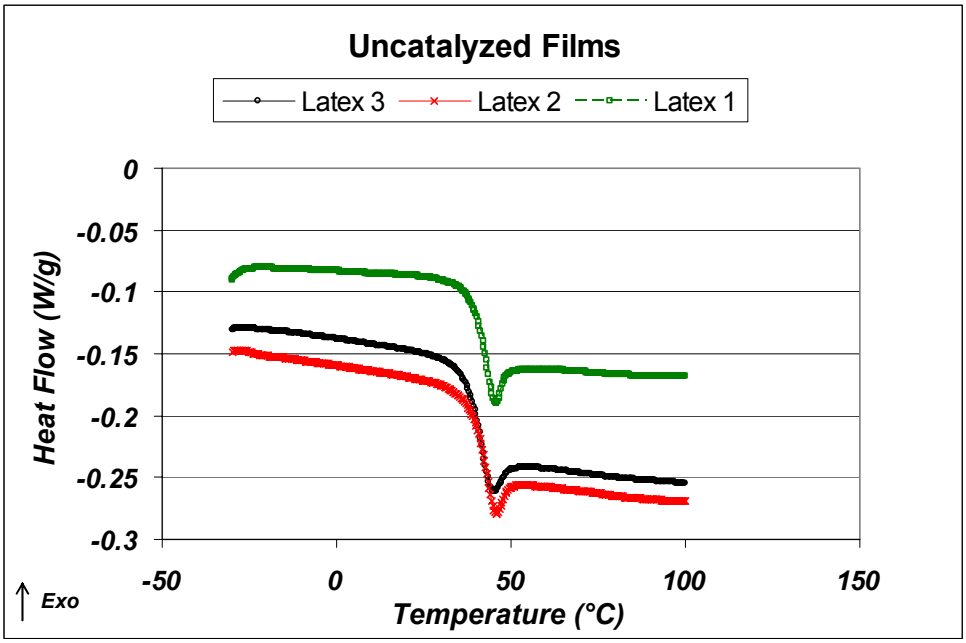

Figure 4-26: DSC Thermogram of a film of all uncatalyzed films.

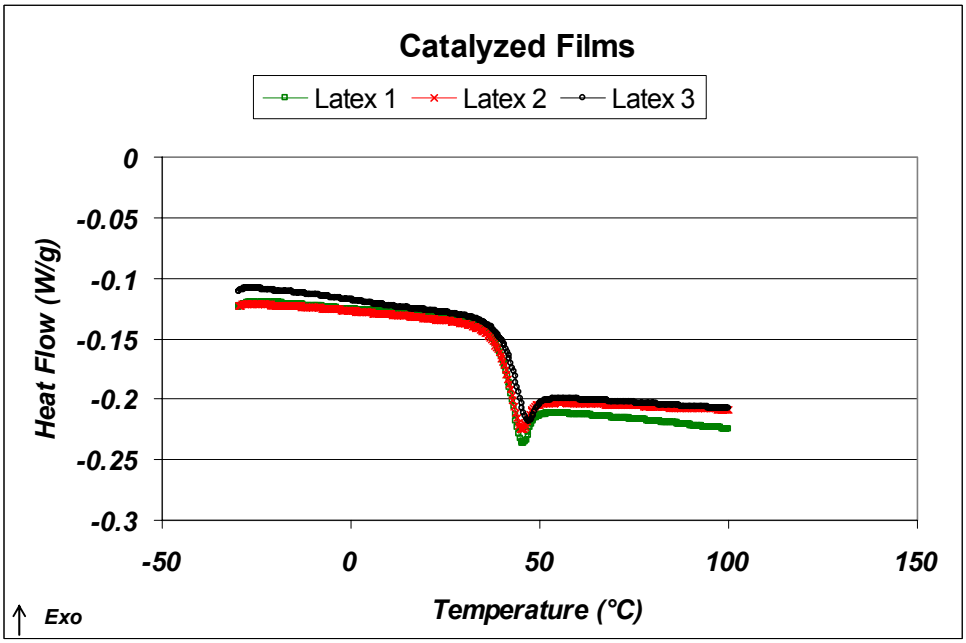

Figure 4-27: DSC Thermogram of all catalyzed films.

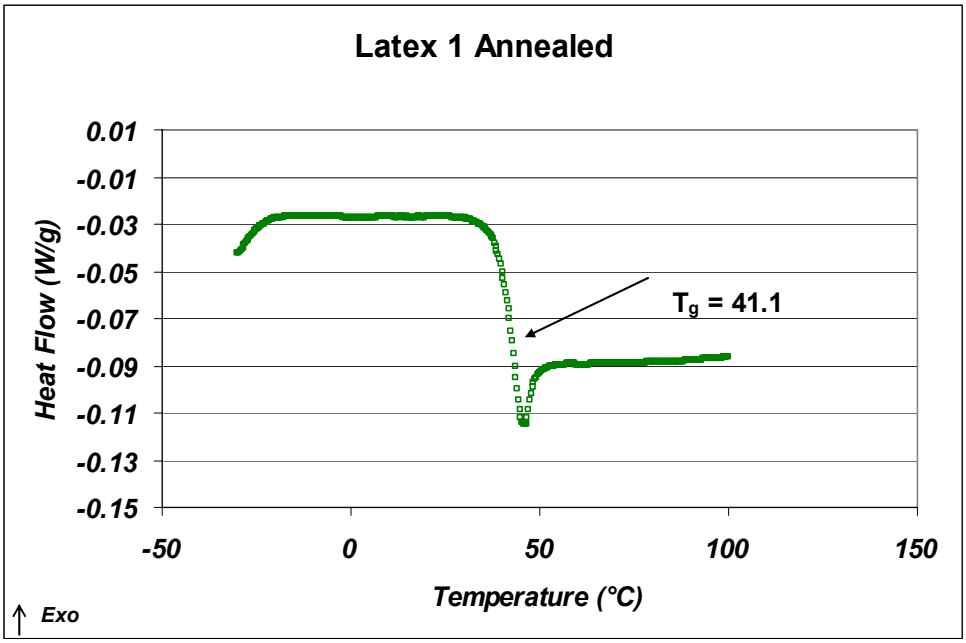

Figure 4-28: DSC Thermogram of a catalyzed film of Latex 1 following annealing at 104°C for 24 hours.

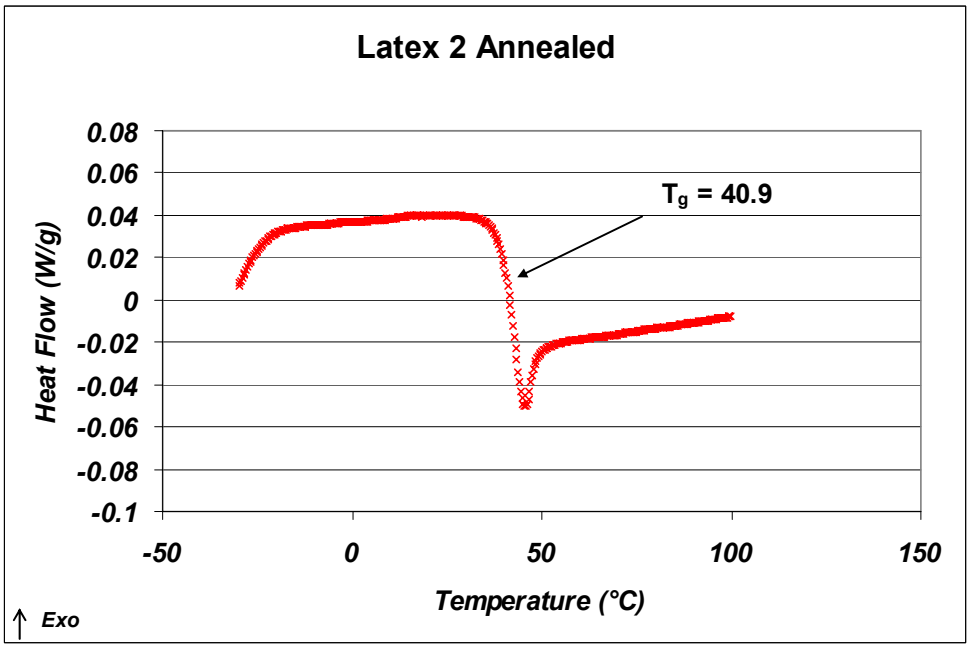

Figure 4-29: DSC Thermogram of a catalyzed film of Latex 2 following annealing at 104°C for 24 hours.

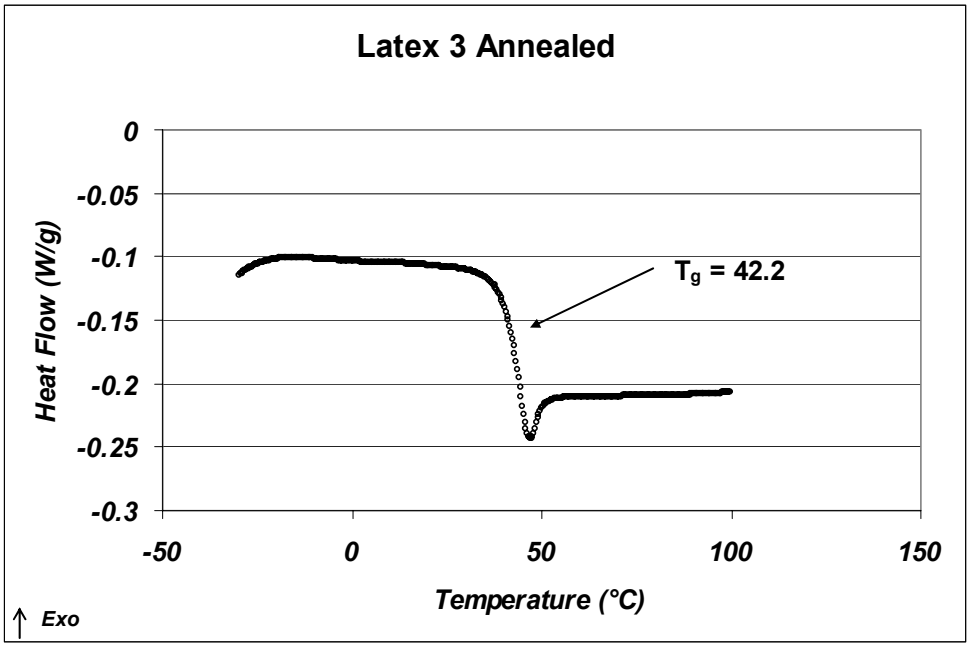

Figure 4-30: DSC Thermogram of a catalyzed film of Latex 3 following annealing at 104°C for 24 hours.

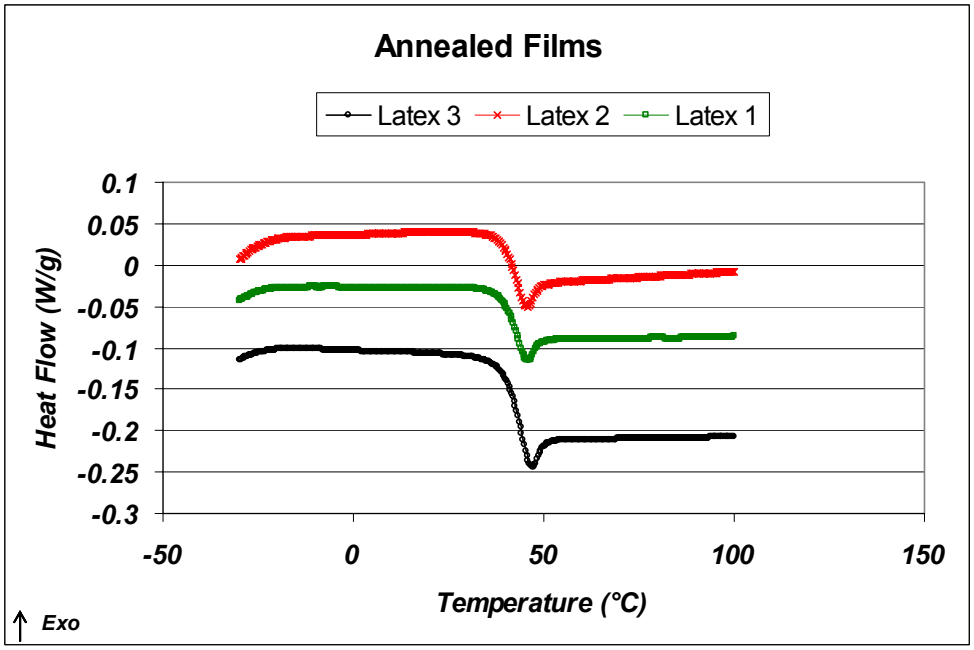

Figure 4-31: DSC Thermogram of catalyzed films from all 3 Latices following annealing at 104°C for 24 hours.

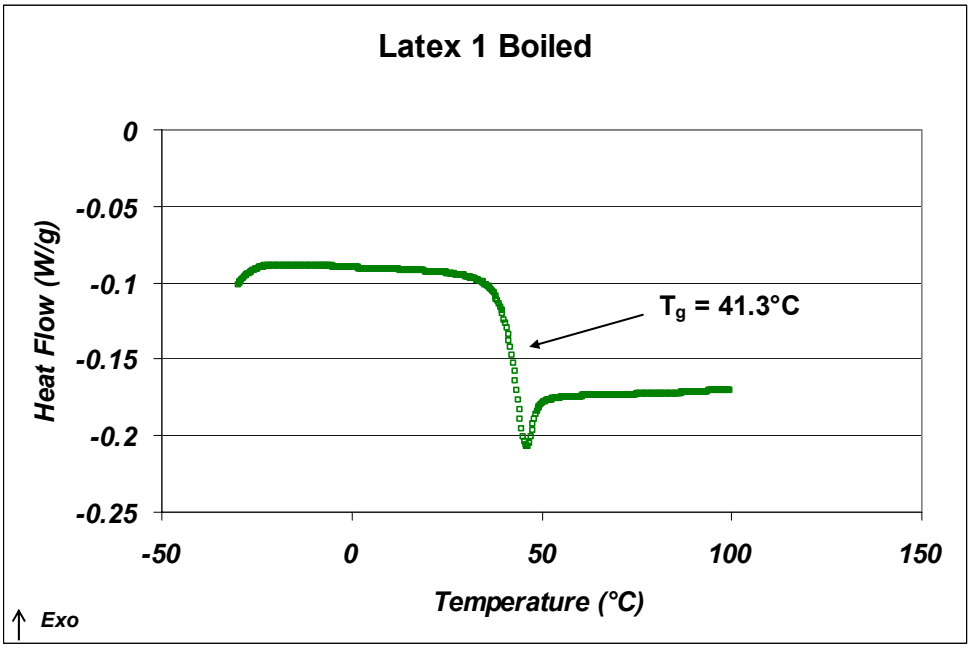

Figure 4-32: DSC Thermogram of a catalyzed film of Latex 1 following boiling and oven drying at 104°C for 8 hours.

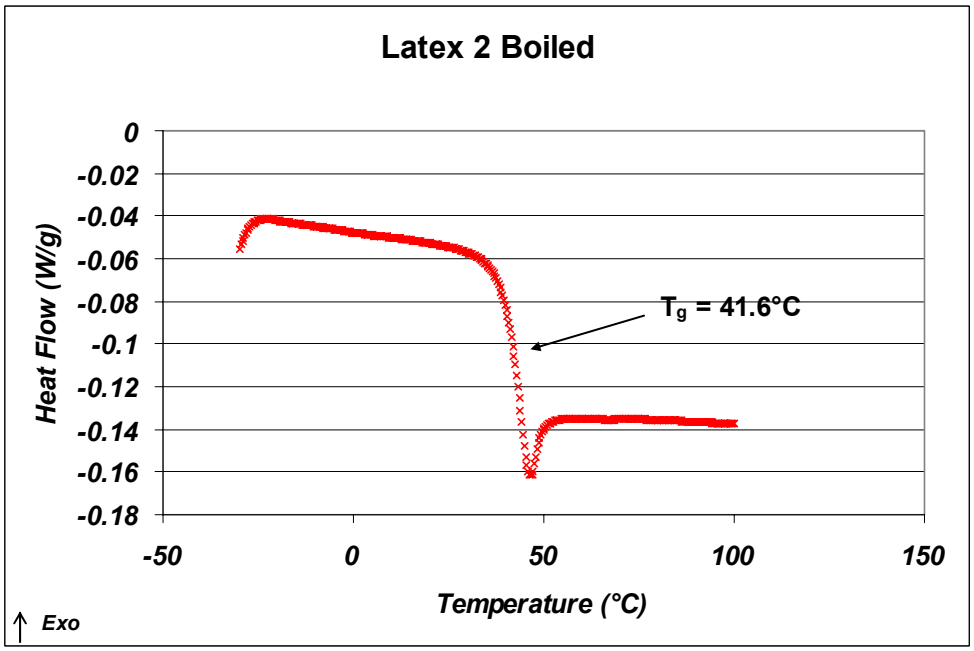

Figure 4-33: DSC Thermogram of a catalyzed film of Latex 2 following boiling and oven drying at 104°C for 8 hours.

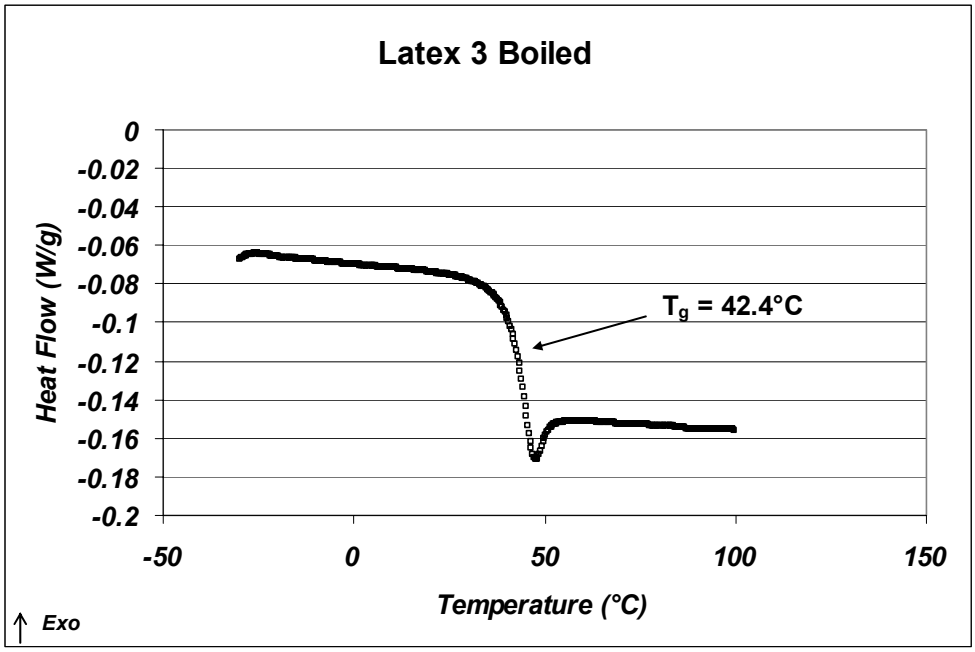

Figure 4-34: DSC Thermogram of a catalyzed film of Latex 3 following boiling and oven drying at 104°C for 8 hours.

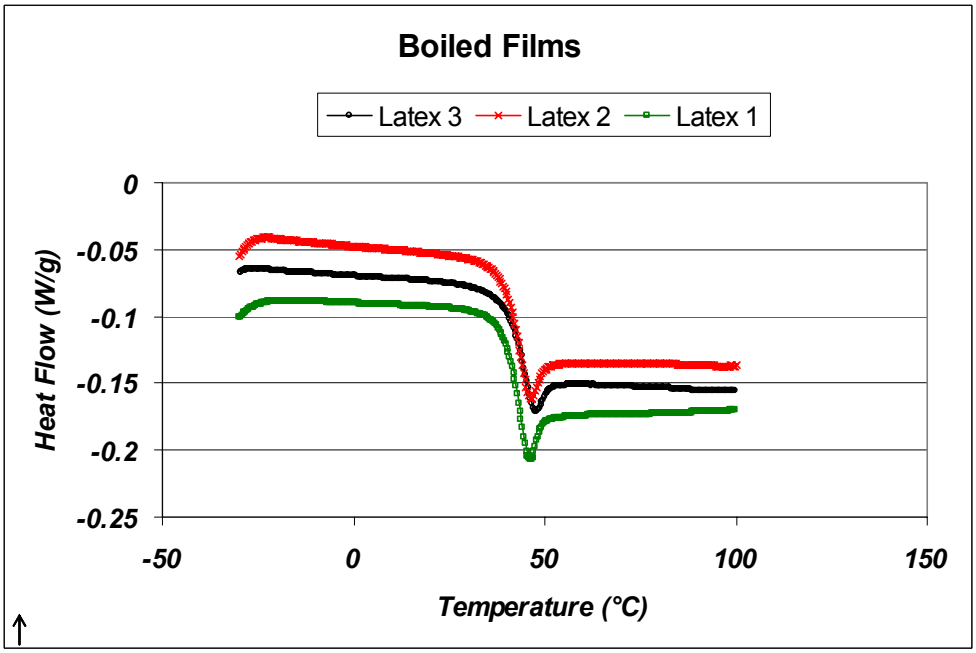

Figure 4-35: DSC Thermogram of catalyzed films of all three Latices following boiling and oven drying at 104°C for 8 hours.

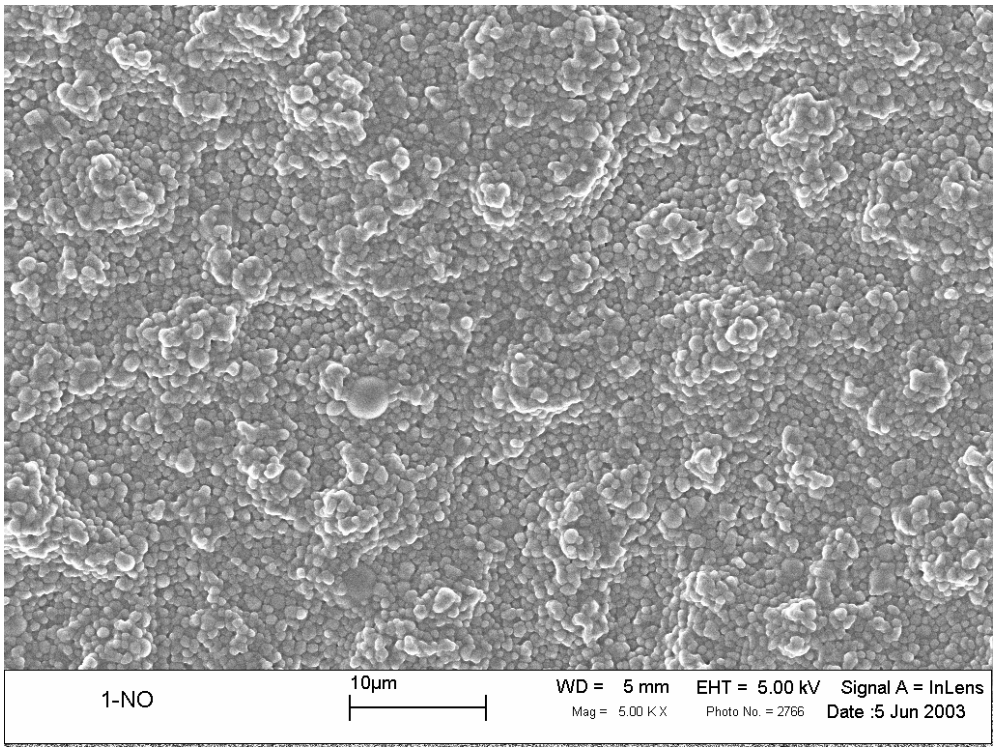

Figure 4-36: Latex 1, Uncatalyzed film, 5000x.

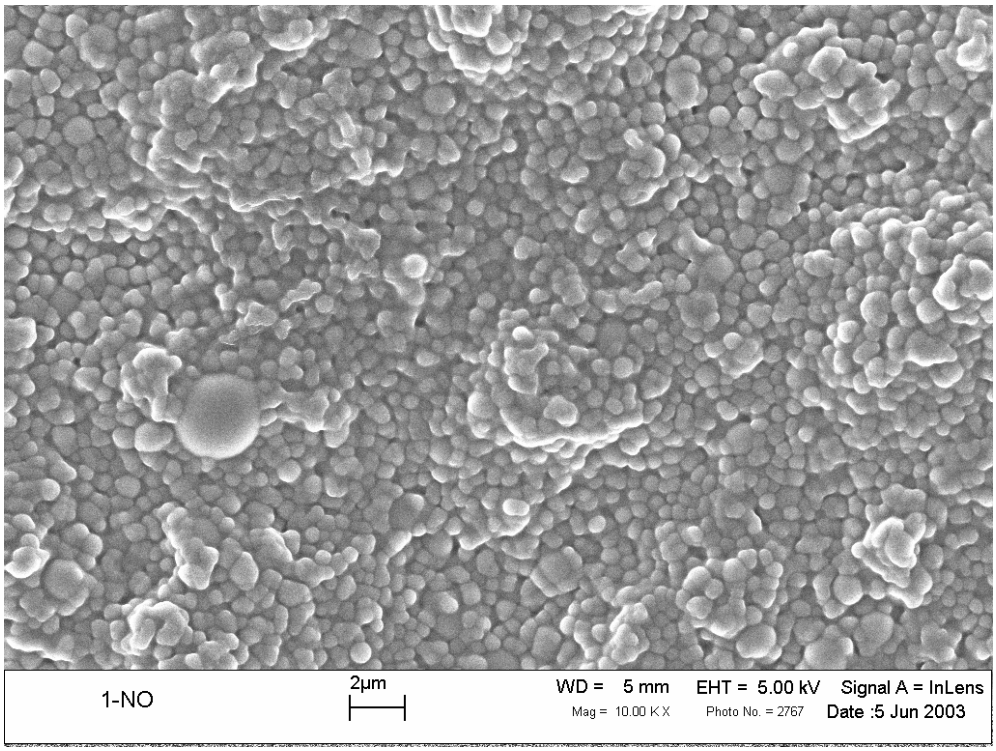

Figure 4-37: Latex 1 Uncatalyzed film, 10,000 x.

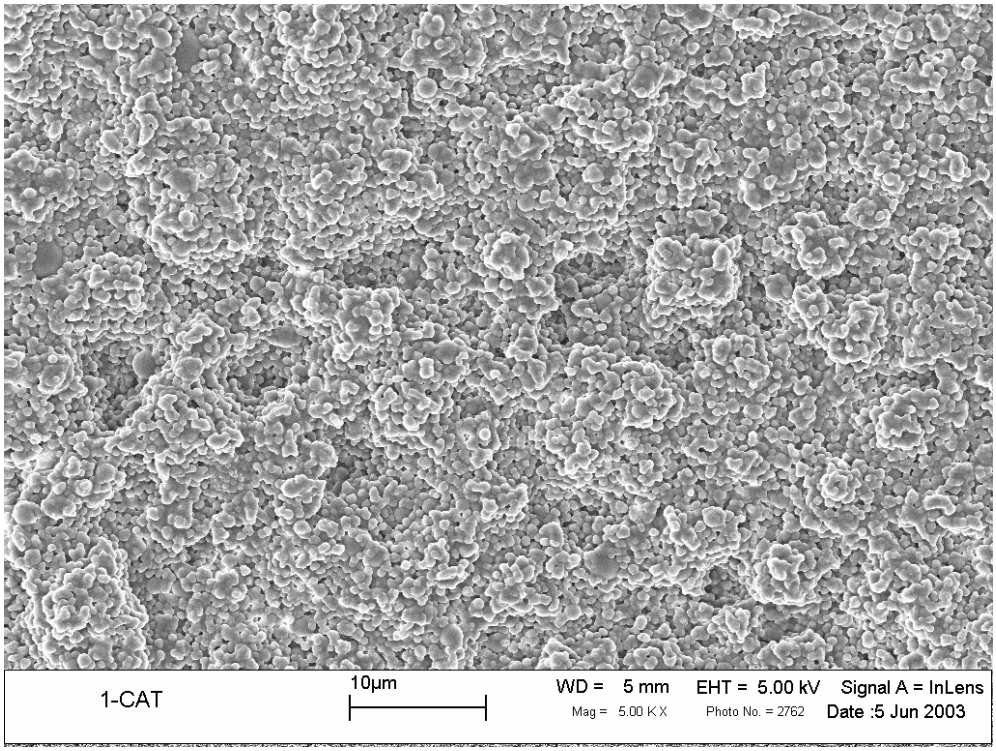

Figure 4-38: Latex 1 catalyzed film, 5% (w/w), 5000 x.

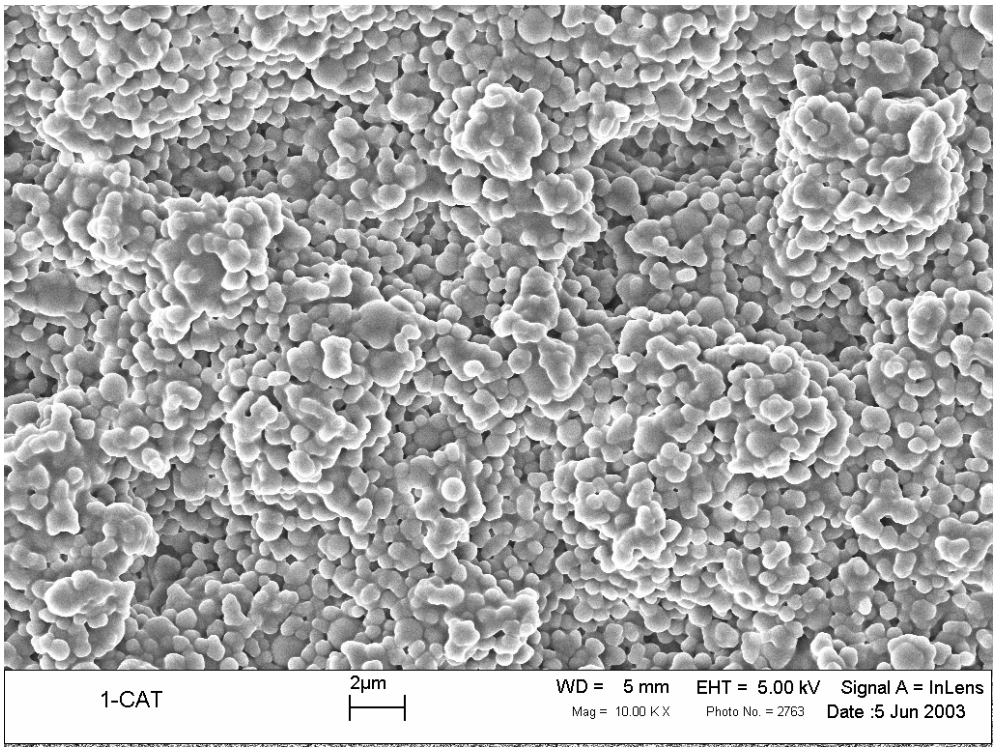

Figure 4-39: Latex 1 catalyzed film, 5% (w/w), 10,000 x.

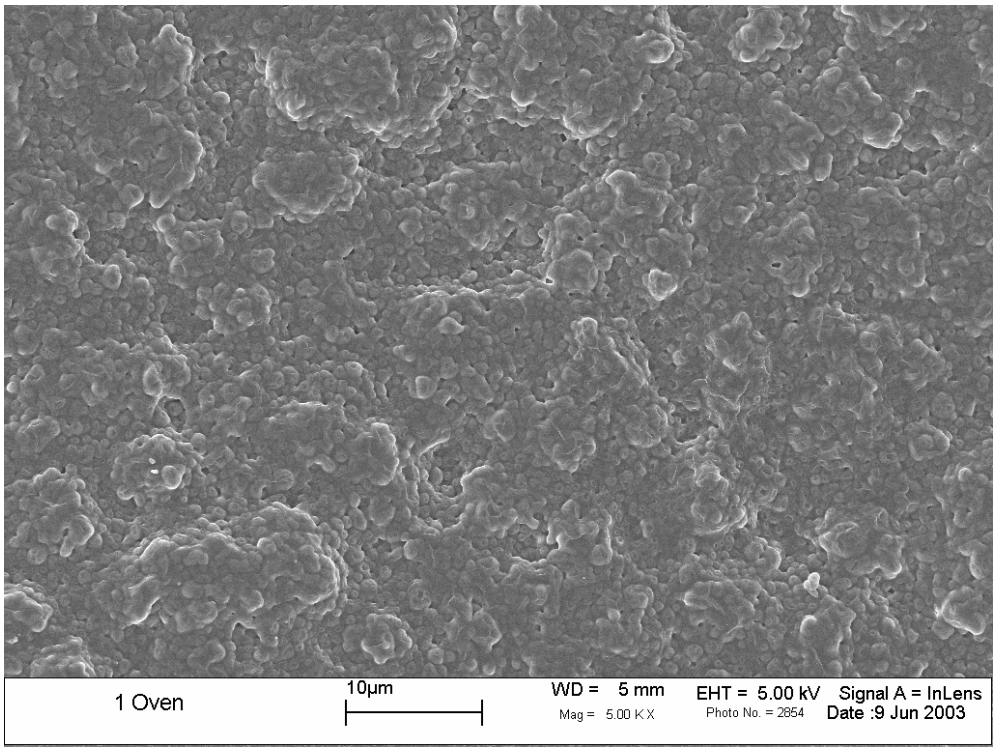

Figure 4-40: Latex 1 catalyzed film (5% w/w), oven dried 24 hrs, 5,000 x.

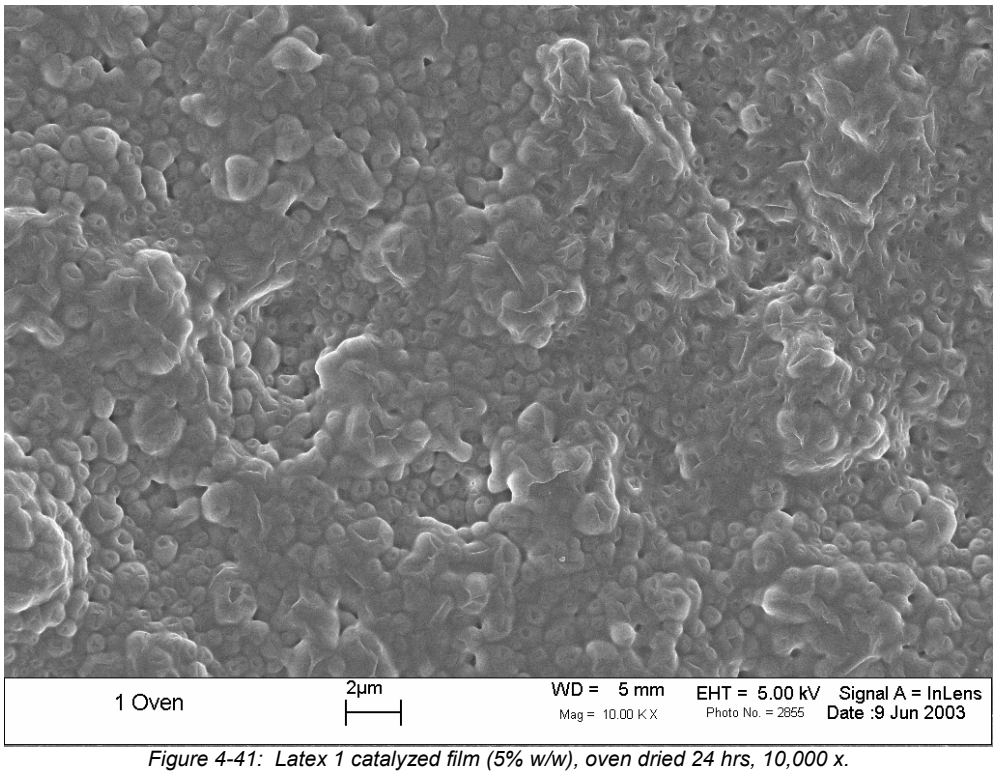

Figure 4-41: Latex 1 catalyzed film (5% w/w), oven dried 24 hrs, 10,000 x.

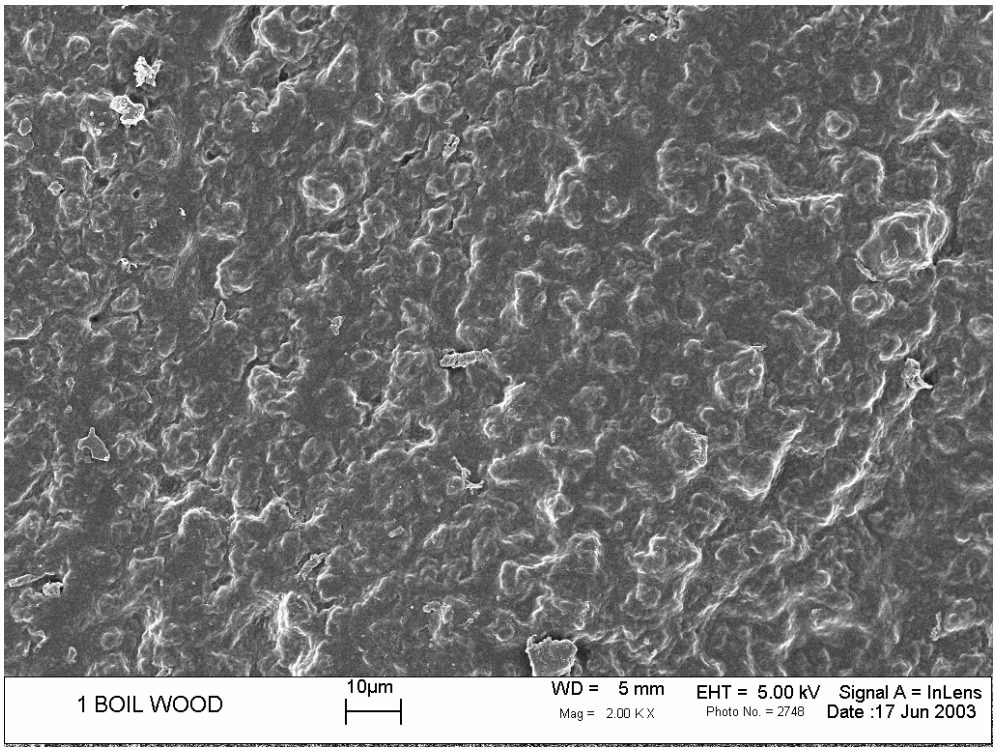

Figure 4-42: Latex 1 catalyzed (5% w/w) applied to wood, boiled 4 hrs, oven dried 24 hrs, 2,000 x.

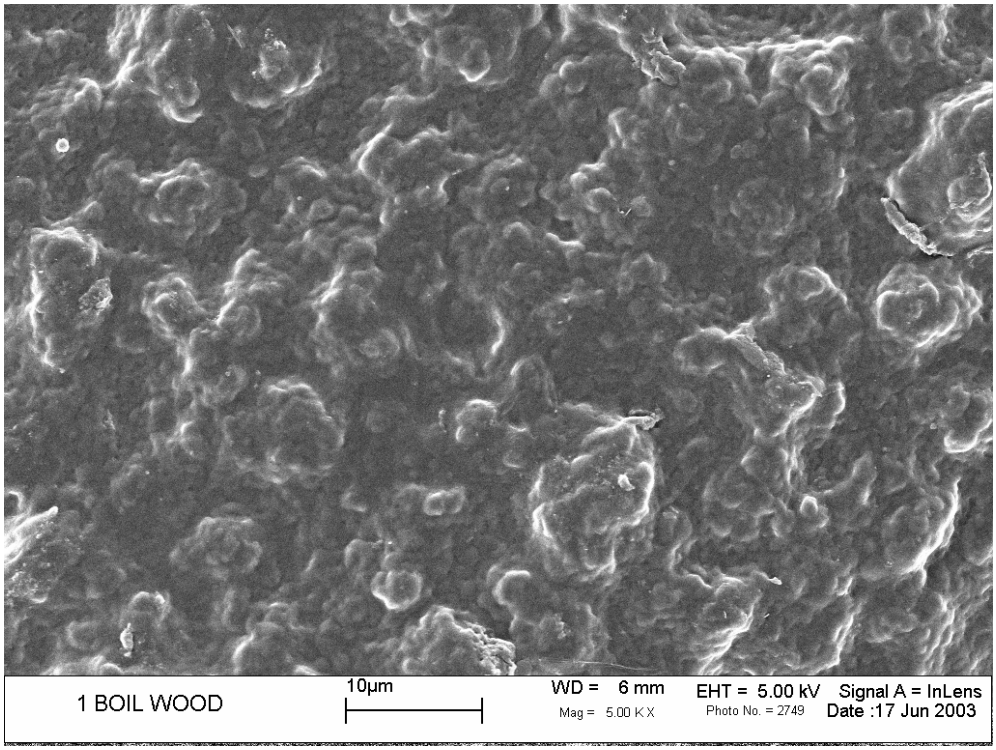

Figure 4-43: Latex 1 catalyzed (5% w/w) applied to wood, boiled 4 hrs, oven dried 24 hrs, 5,000 x.

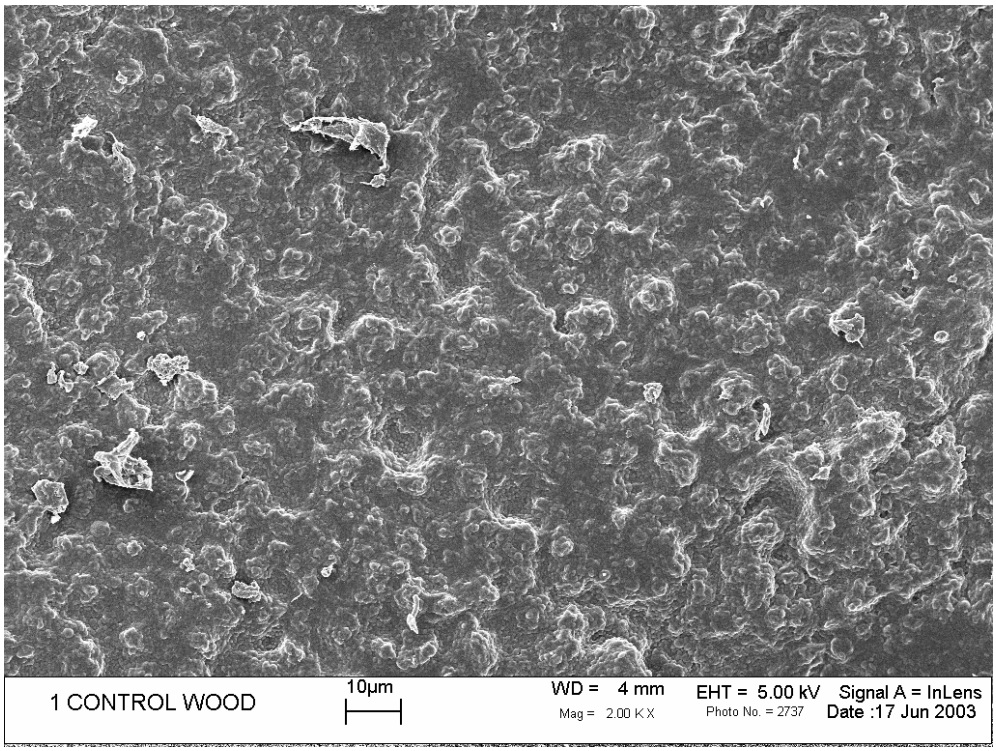

Figure 4-44: Latex 1 catalyzed (5% w/w) applied to wood, oven dried 24 hrs, 2,000 x.

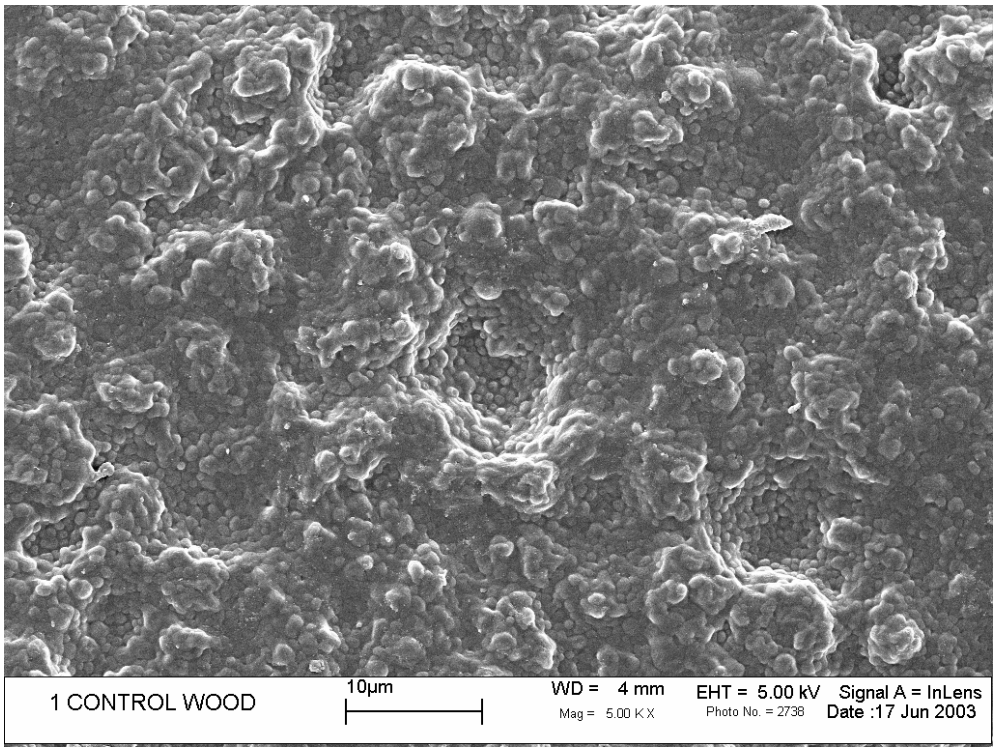

Figure 4-45: Latex 1 catalyzed (5% w/w) applied to wood, oven dried 24 hrs, 5,000 x.

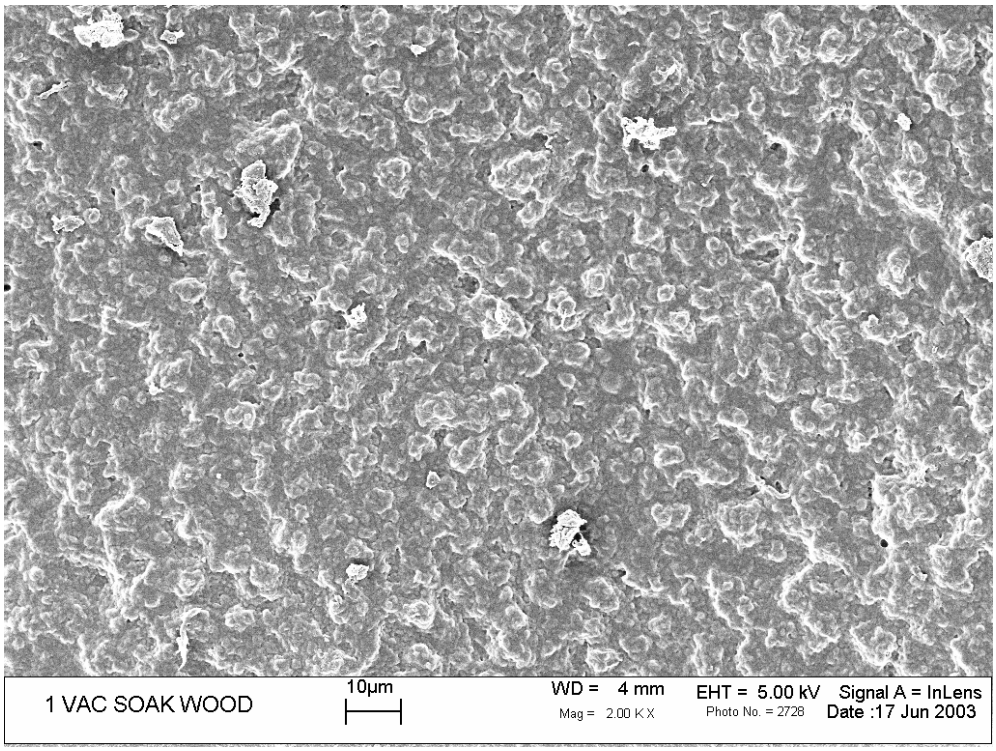

Figure 4-46: Latex 1 catalyzed (5% w/w) applied to wood, vacuum soak 2 hrs, oven dried 24 hrs, 2,000 x.

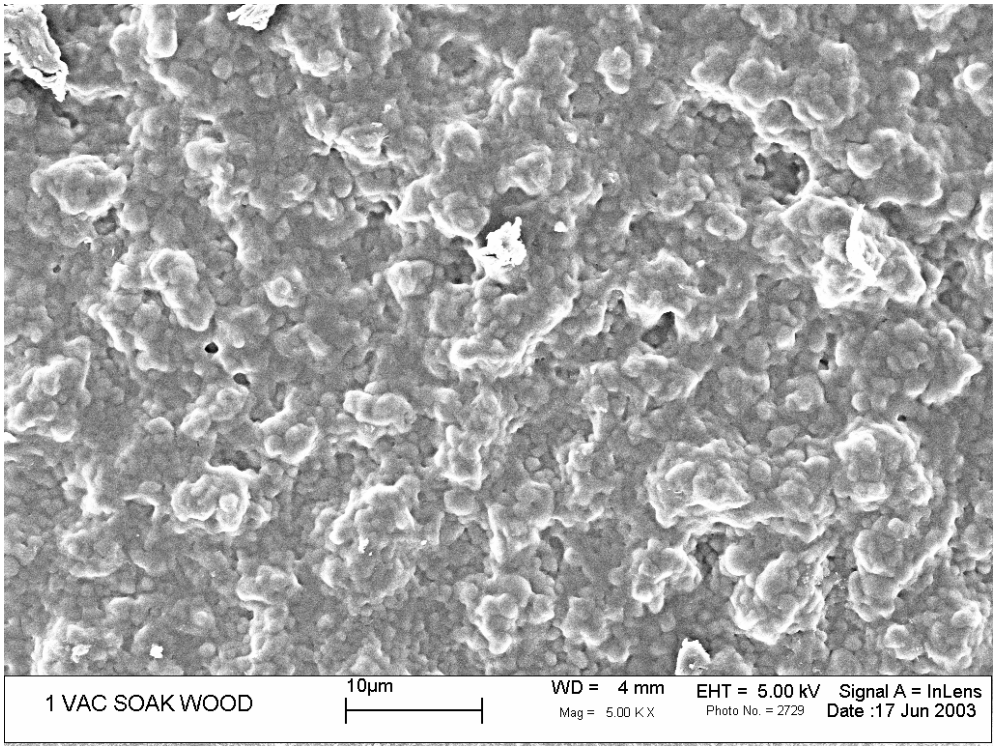

Figure 4-47: Latex 1 catalyzed (5% w/w) applied to wood, vacuum soak 2 hrs, oven dried 24 hrs, 5,000 x.

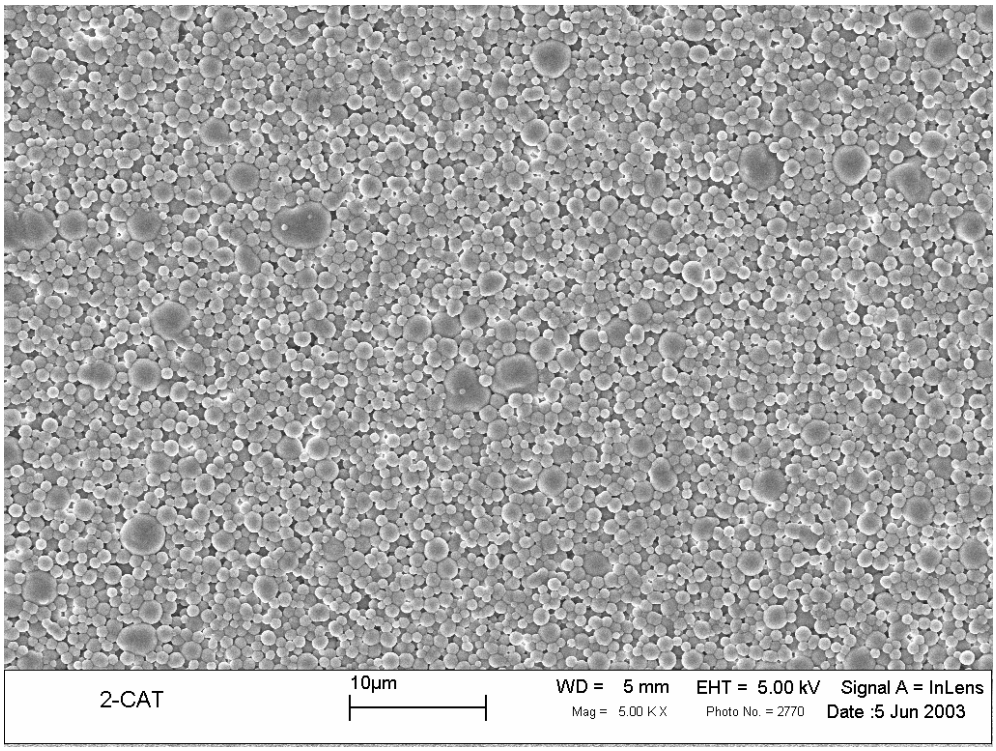

Figure 4-48: Latex 2 catalyzed film (5% w/w), 5,000 x.

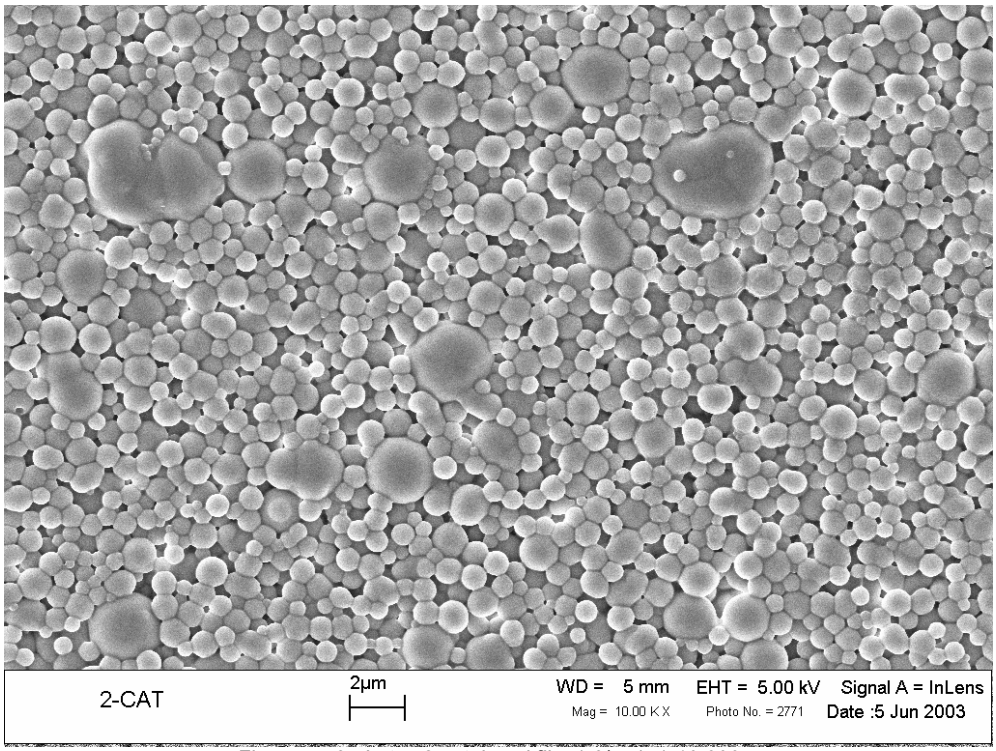

Figure 4-49: Latex 2 catalyzed film (5% w/w,) 10,000 x.

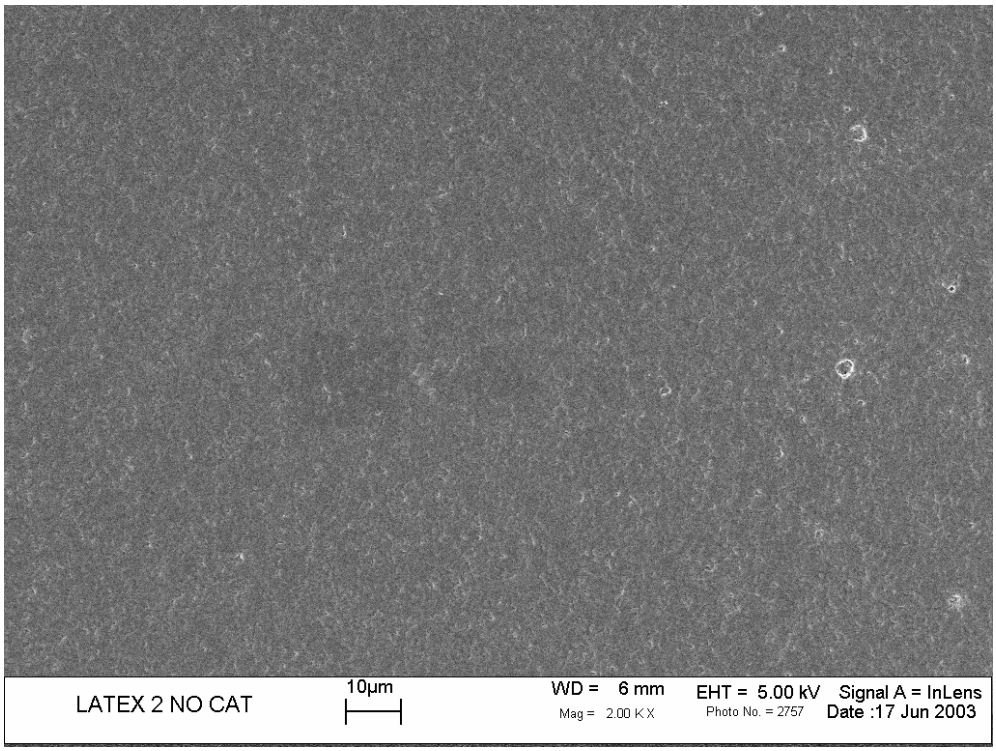

Figure 4-50: Latex 2, uncatalyzed film, 2,000 x.

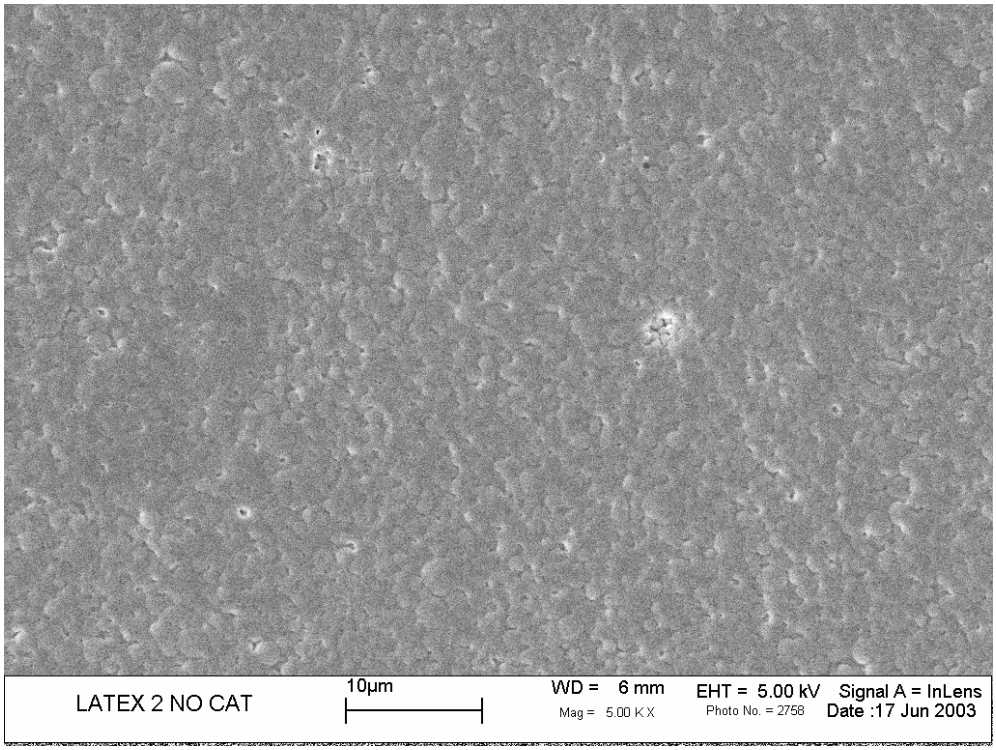

Figure 4-51: Latex 2, uncatalyzed film, 5,000 x.

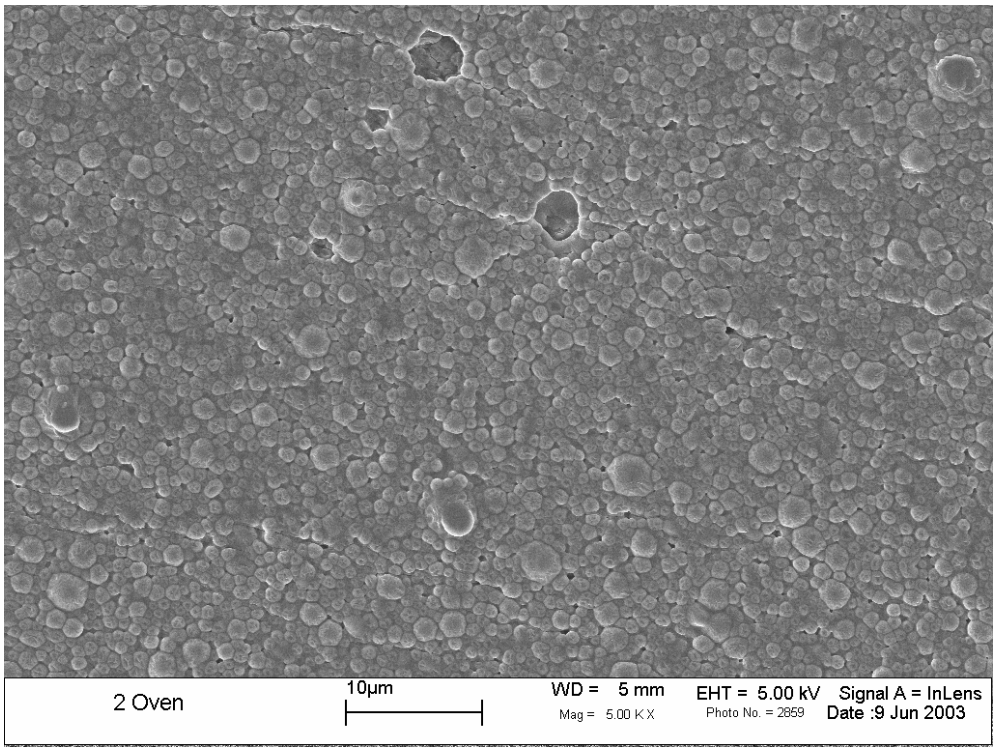

Figure 4-52: Latex 2 catalyzed film (5% w/w), oven dried 8 hrs, 5,000 x.

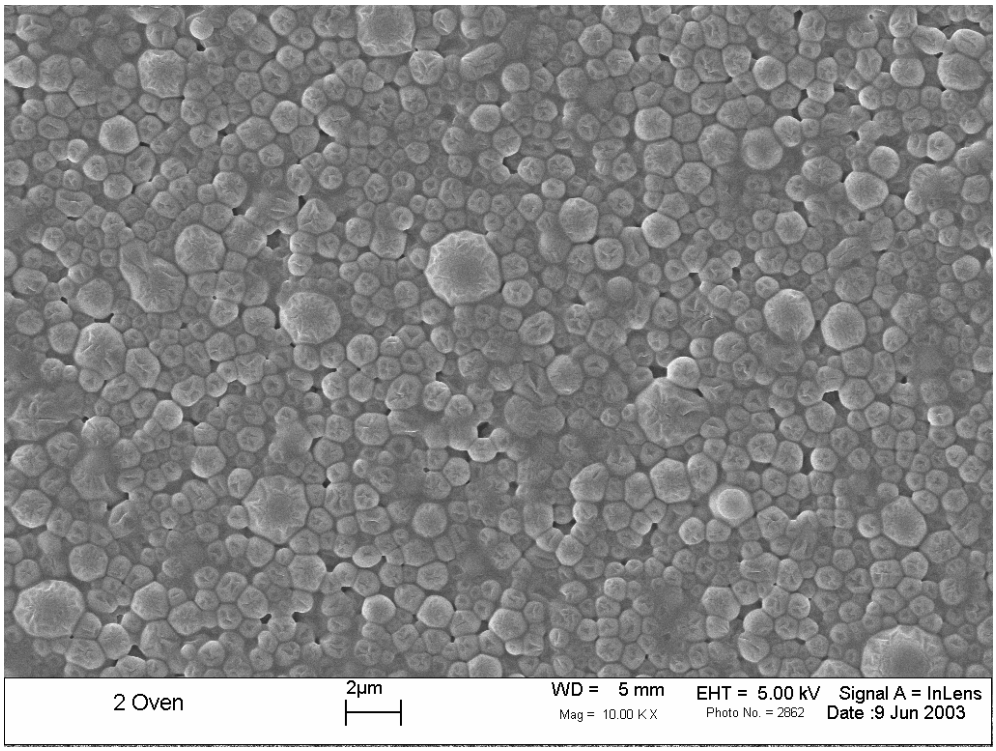

Figure 4-53: Latex 2 catalyzed film (5% w/w), oven dried 8 hrs, 10,000 x.

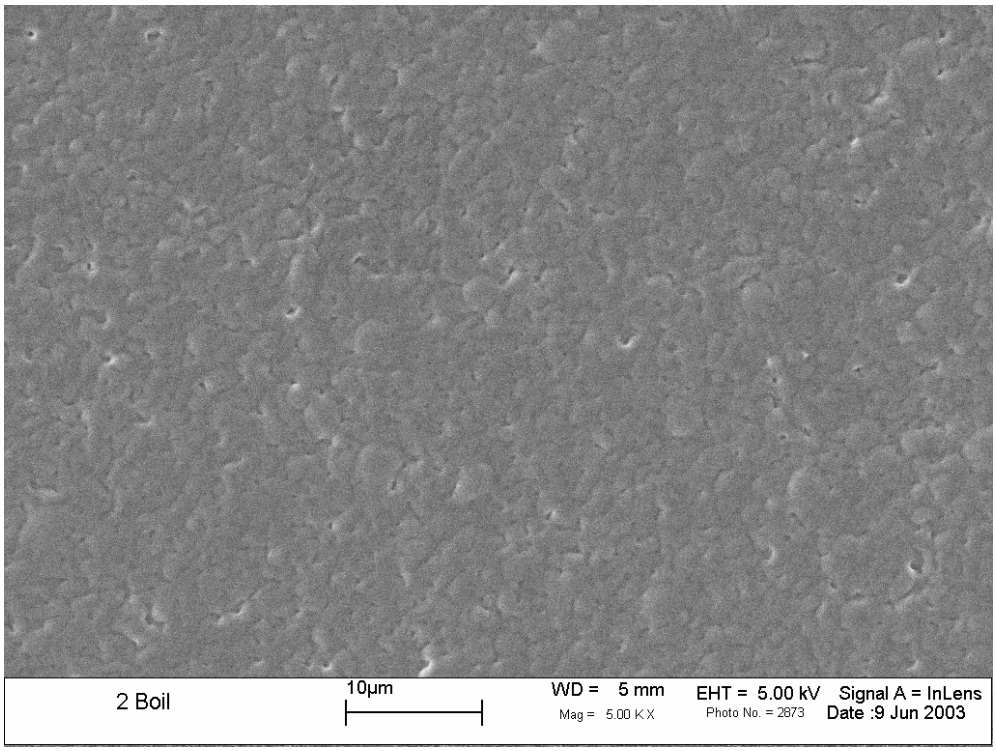

Figure 4-54: Latex 2 catalyzed (5% w/w) applied to wood, boiled 4 hrs, oven dried 24 hrs, 5,000 x.

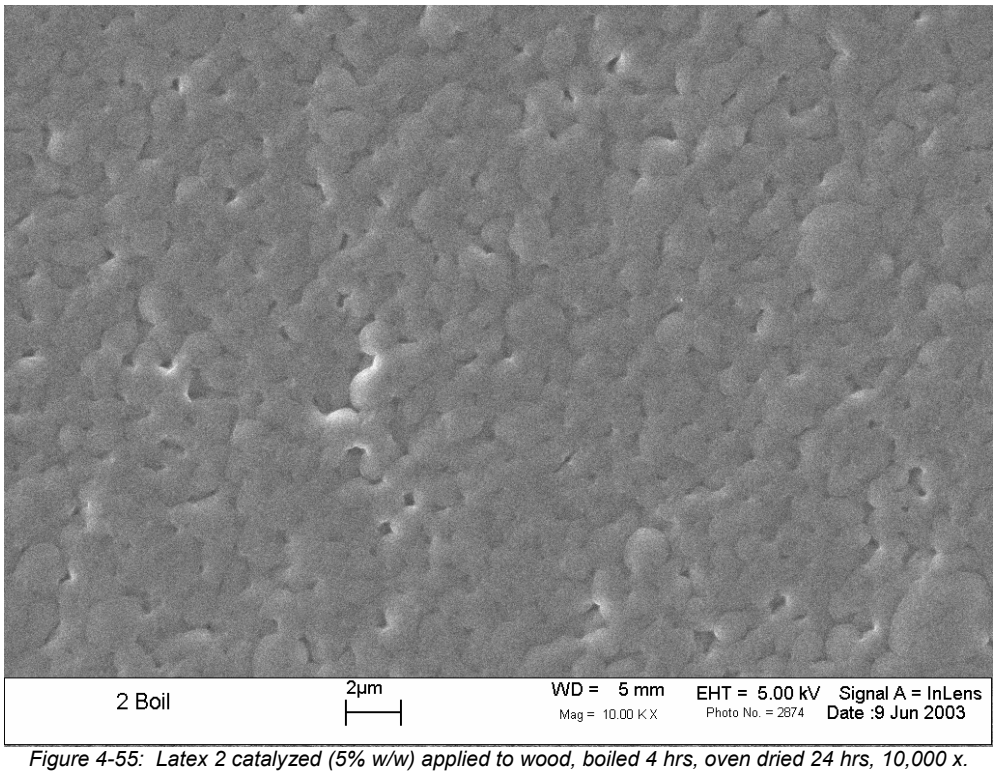

Figure 4-55: Latex 2 catalyzed (5% w/w) applied to wood, boiled 4 hrs, oven dried 24 hrs, 10,000 x.

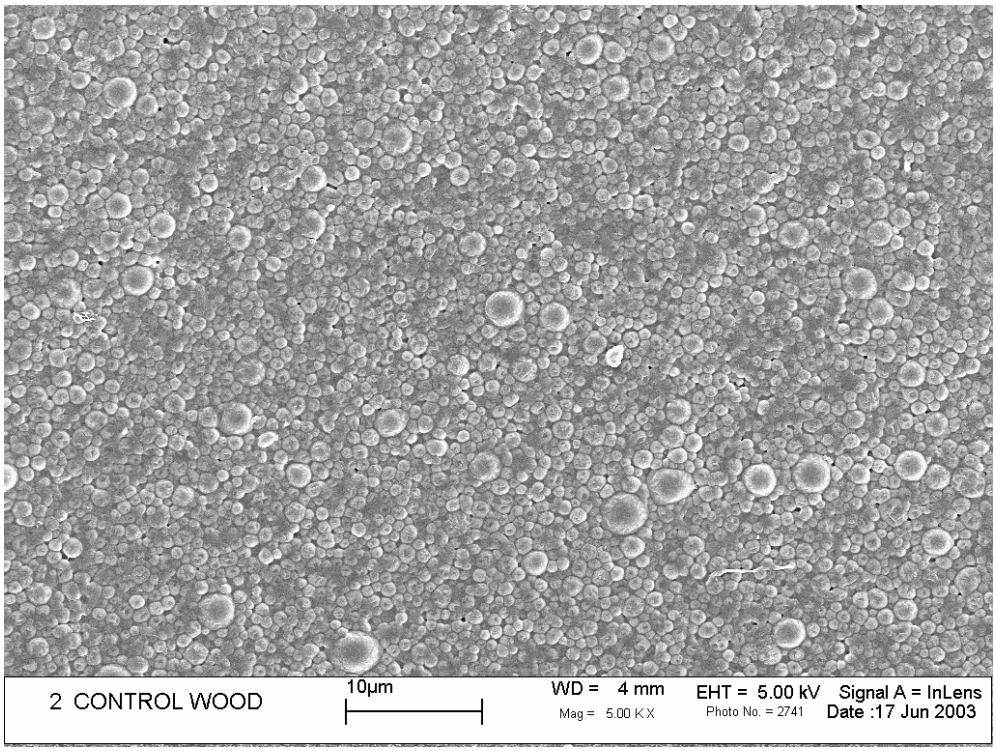

Figure 4-56: Latex 2 catalyzed (5% w/w) applied to wood, oven dried 24hrs, 5,000 x.

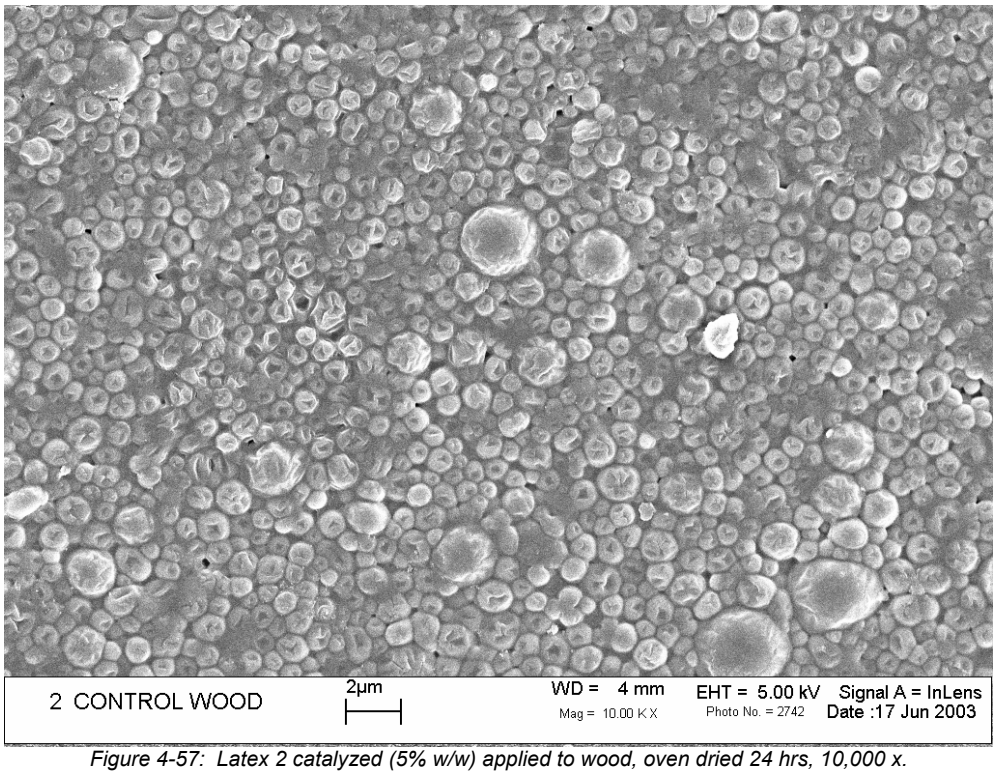

Figure 4-57: Latex 2 catalyzed (5% w/w) applied to wood, oven dried 24 hrs, 10,000 x.

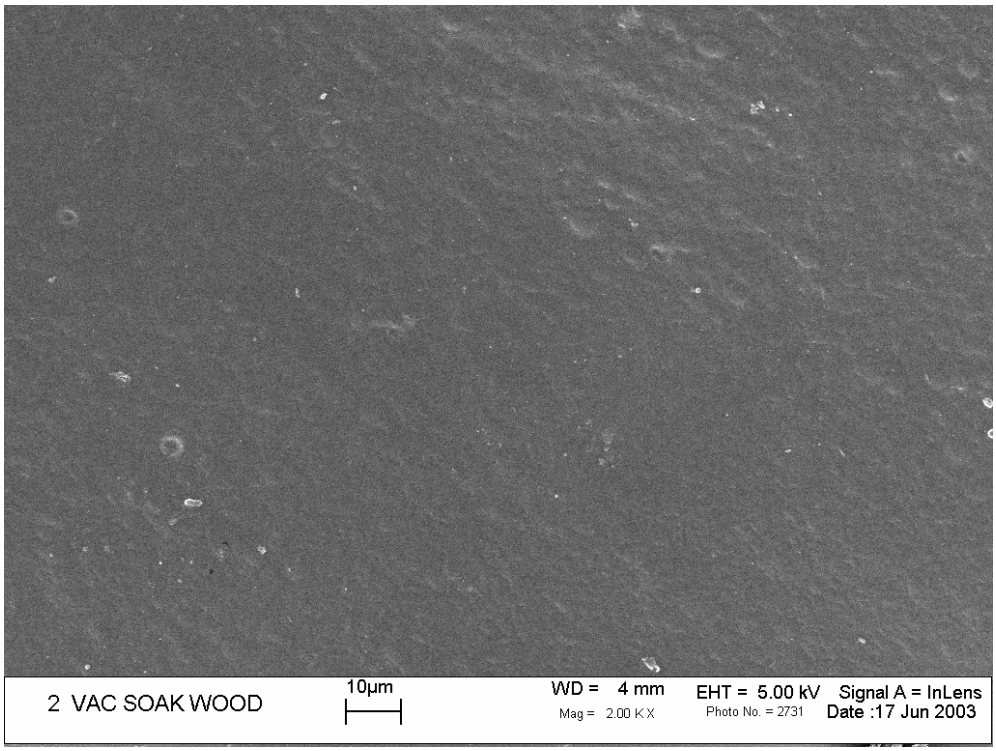

Figure 4-58: Latex 2 catalyzed (5% w/w) applied to wood, vacuum soak 2 hrs, oven dried 24 hrs, 2,000 x.

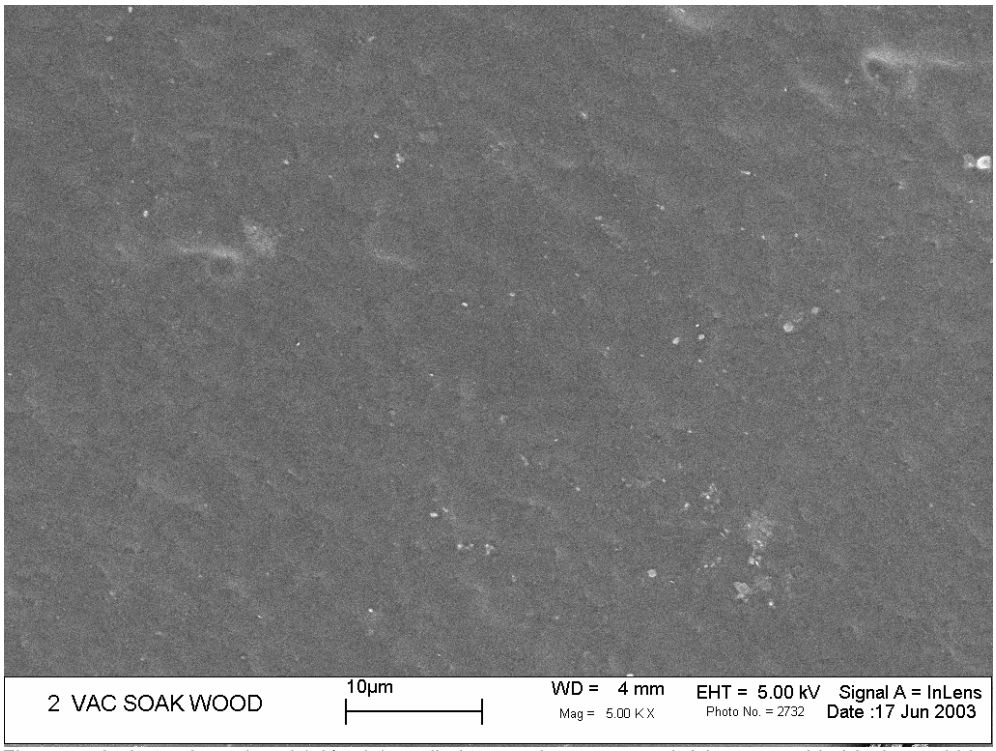

Figure 4-59: Latex 2 catalyzed (5% w/w) applied to wood, vacuum soak 2 hrs, oven dried 24 hrs, 5,000 x.

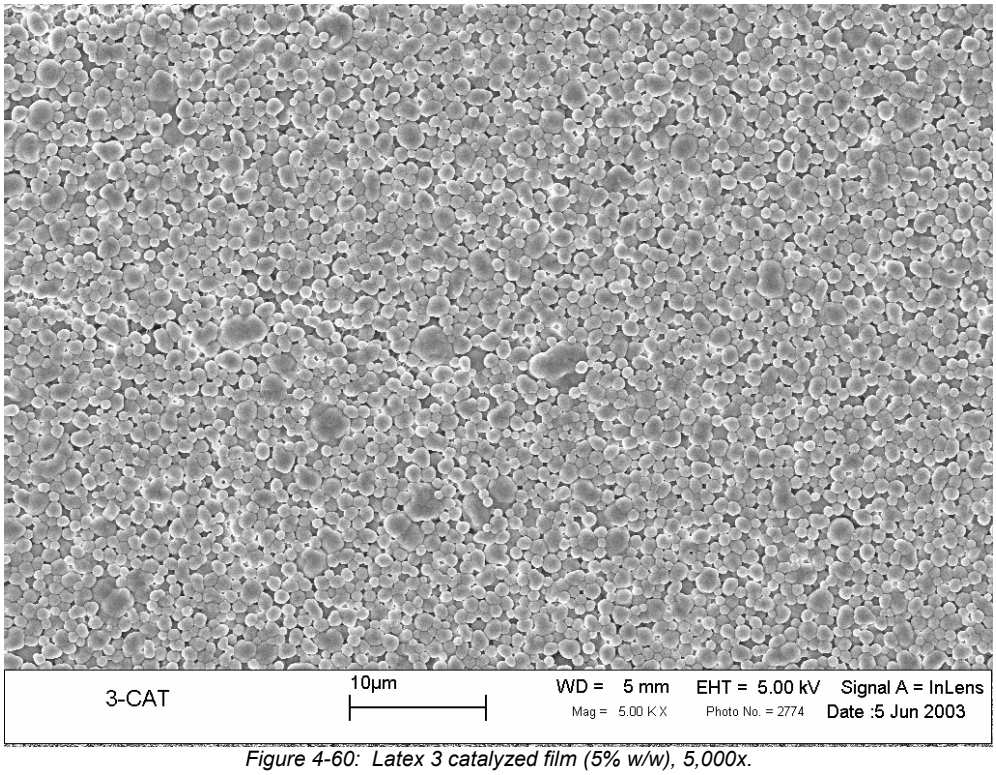

Figure 4-60: Latex 3 catalyzed film (5% w/w), 5,000x.

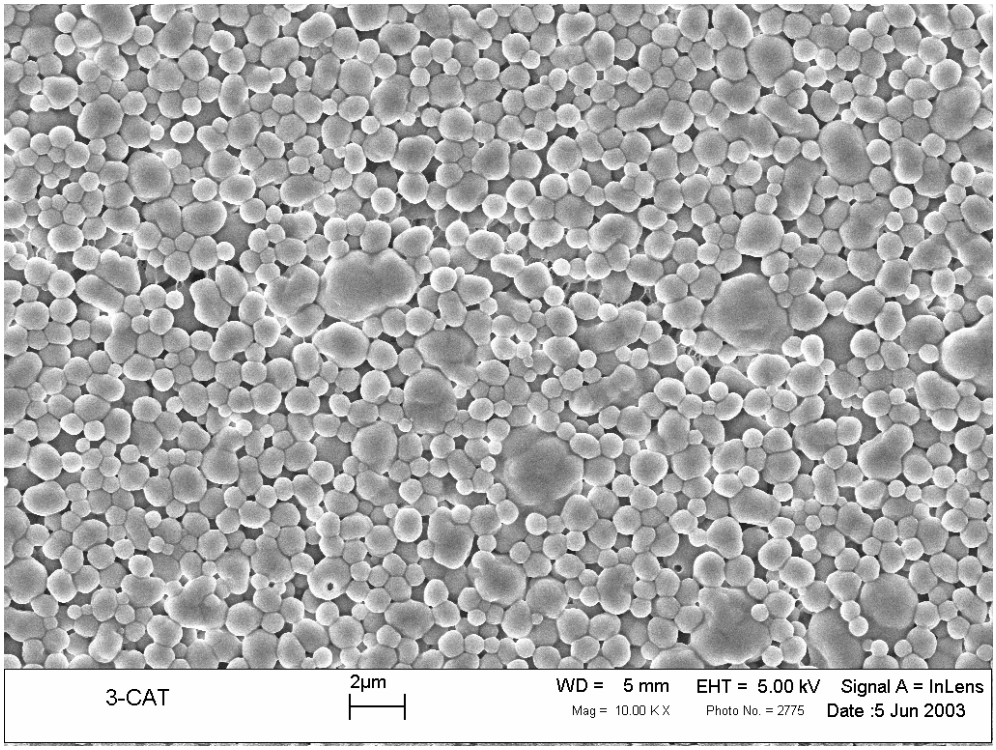

Figure 4-61: Latex 3 catalyzed film (5% w/w), 10,000 x.

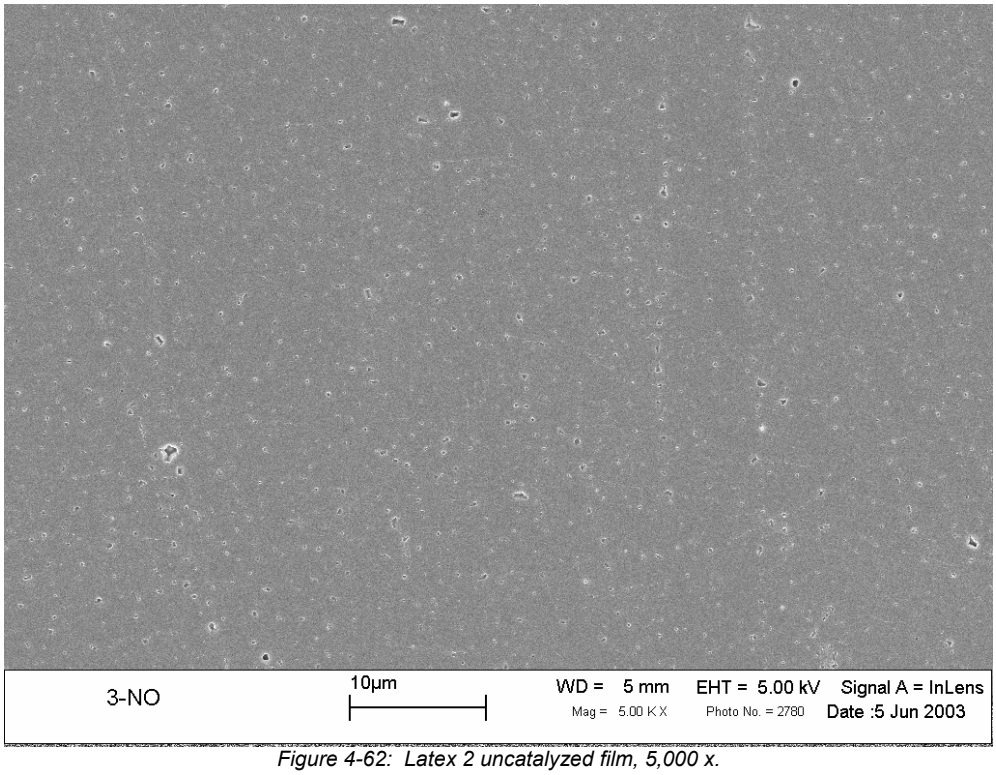

Figure 4-62: Latex 2 uncatalyzed film, 5,000 x.

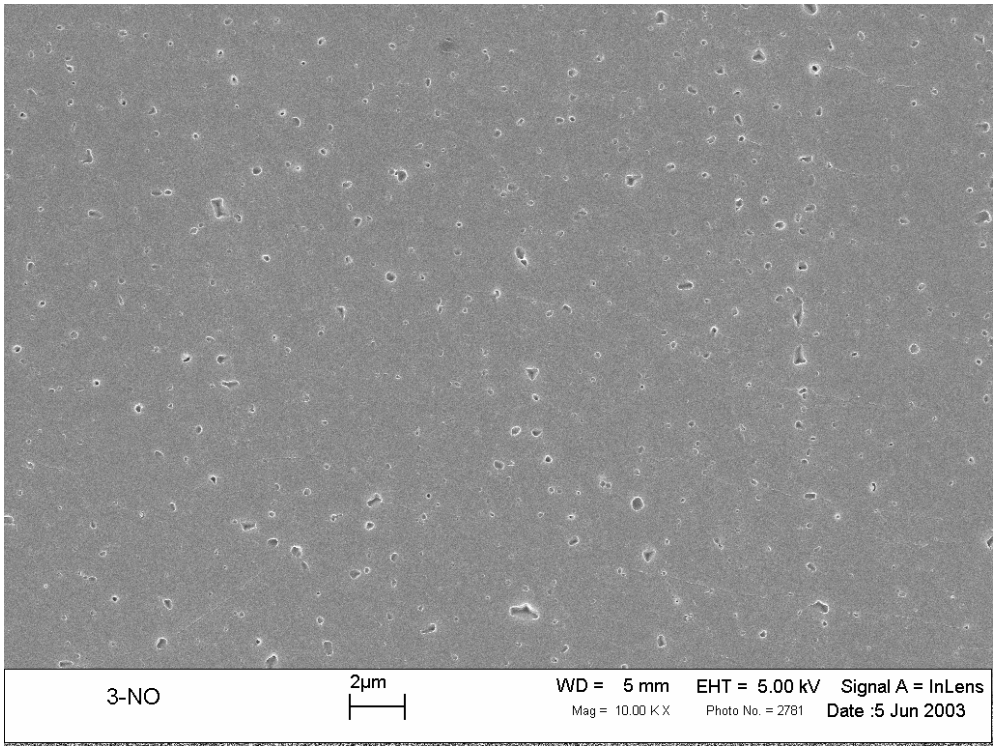

Figure 4-63: Latex 2 uncatalyzed film 10,000 x.

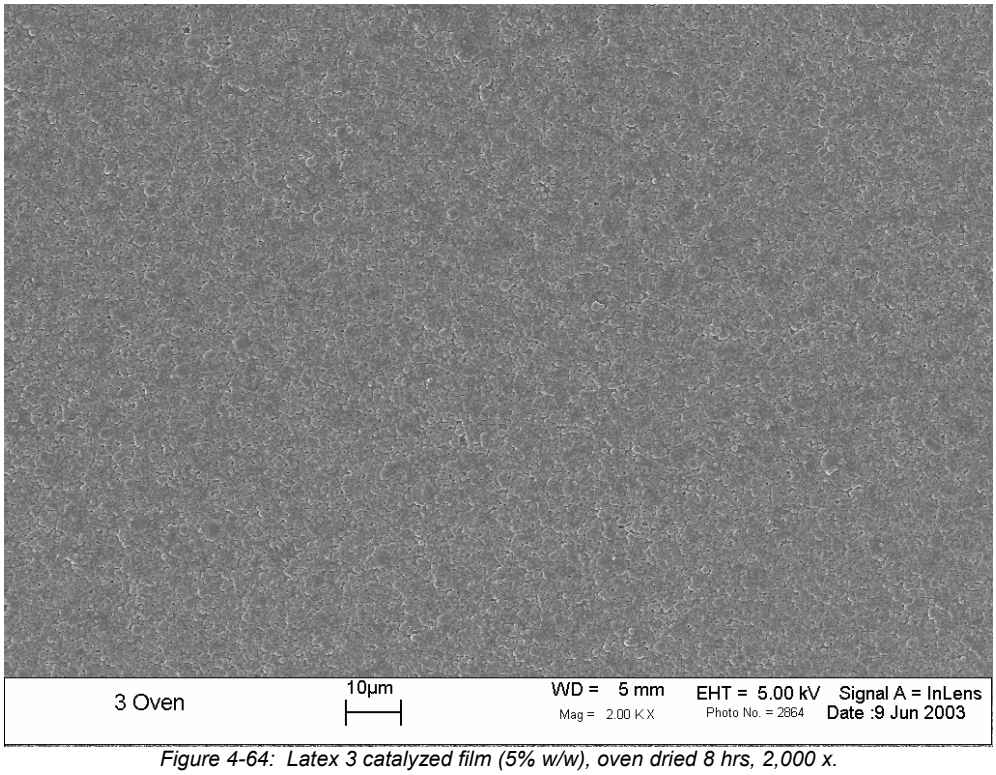

Figure 4-64: Latex 3 catalyzed film (5% w/w), oven dried 8 hrs, 2,000 x.

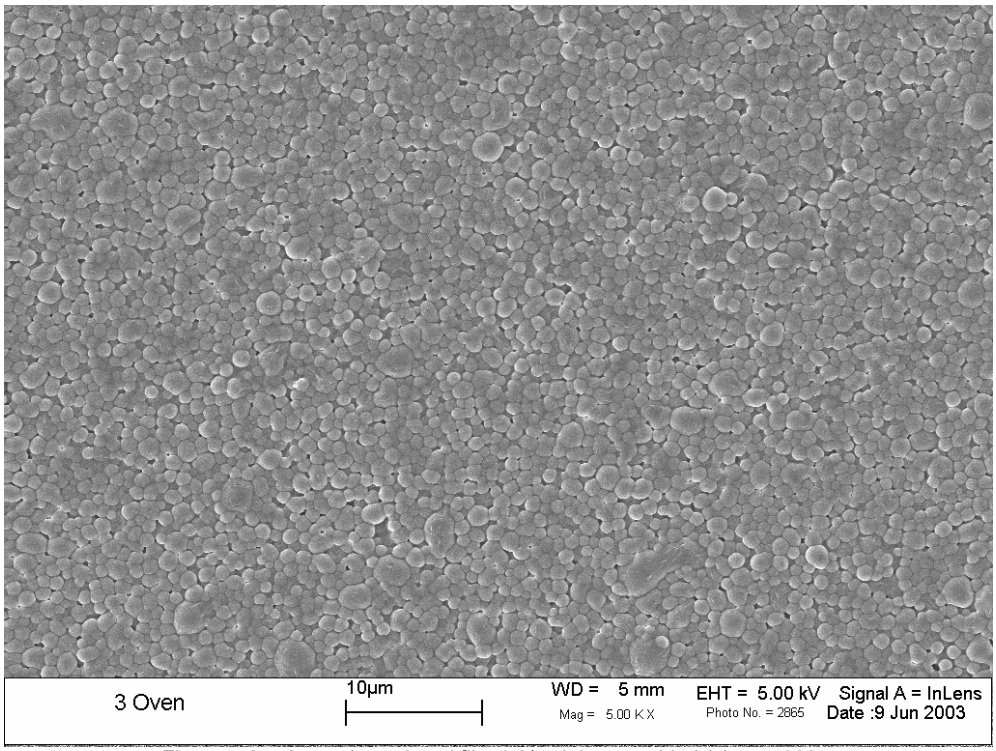

Figure 4-65: Latex 3 catalyzed film (5% w/w), oven dried 8 hrs, 5,000 x.

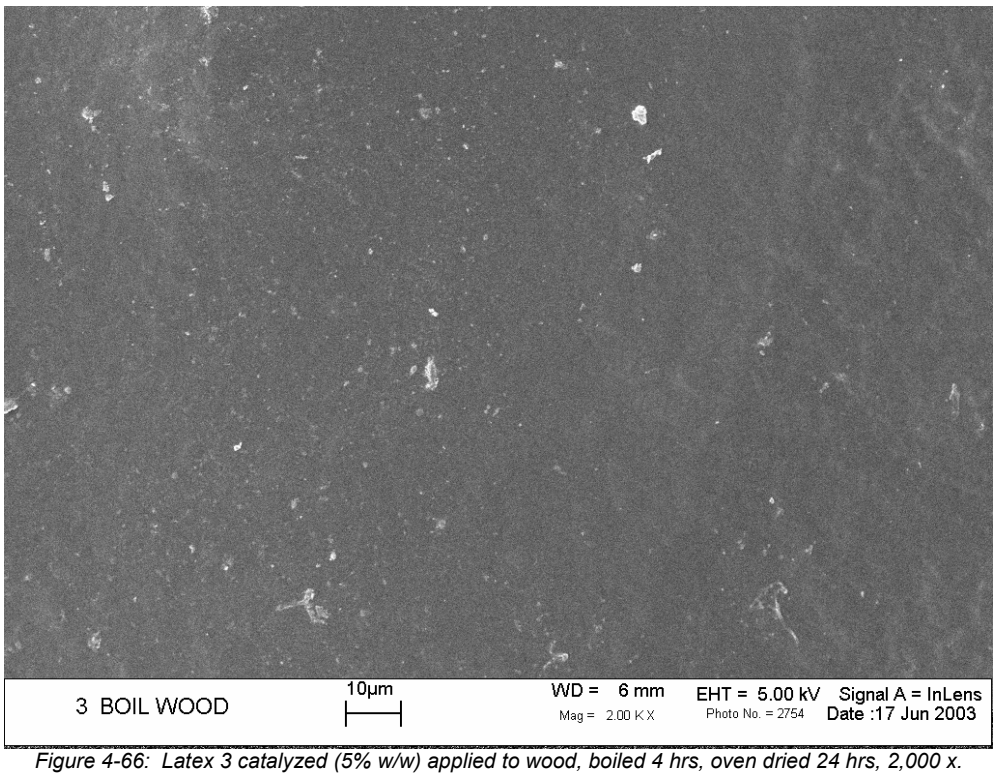

Figure 4-66: Latex 3 catalyzed (5% w/w) applied to wood, boiled 4 hrs, oven dried 24 hrs, 2,000 x.

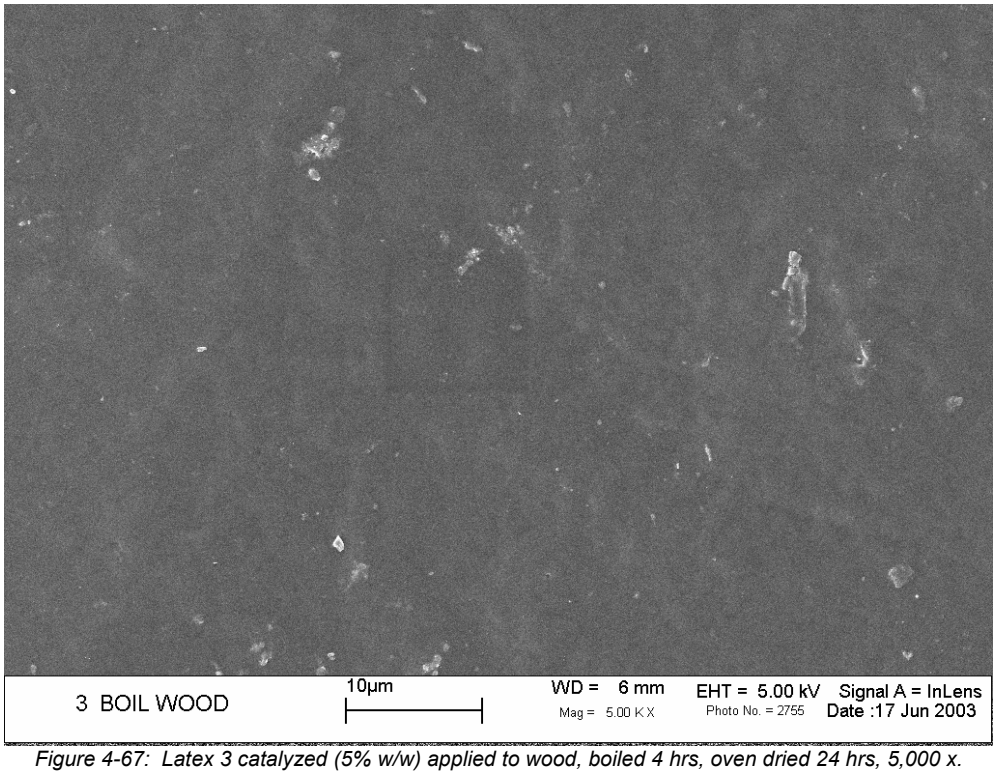

Figure 4-67: Latex 3 catalyzed (5% w/w) applied to wood, boiled 4 hrs, oven dried 24 hrs, 5,000 x.

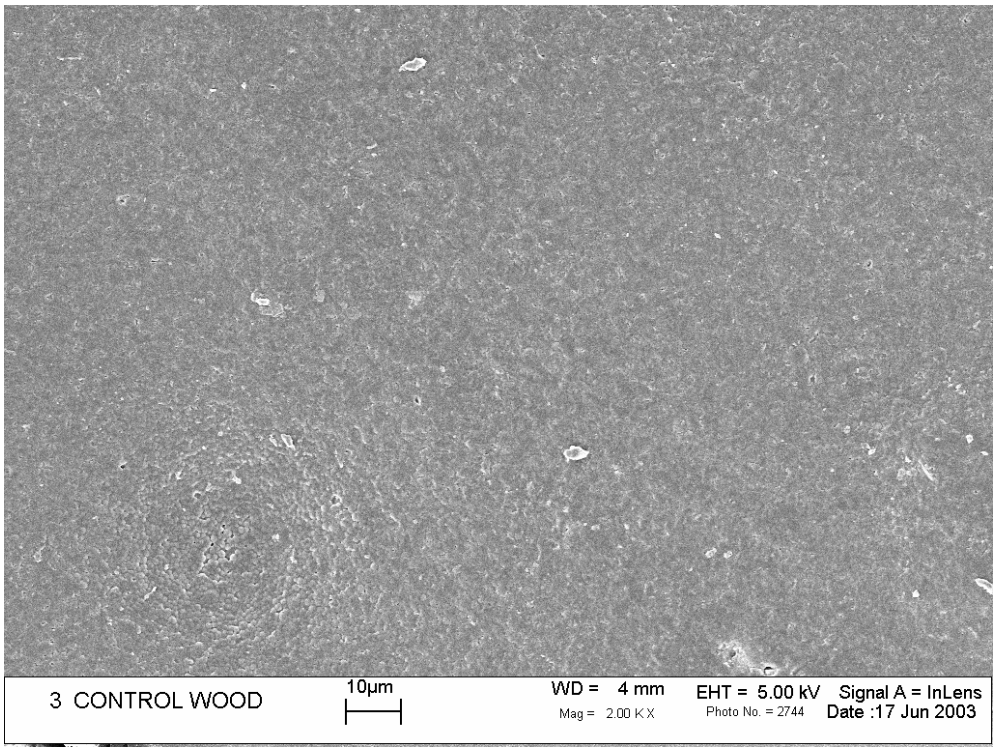

Figure 4-68: Latex 3 catalyzed (5% w/w) applied to wood, oven dried 24 hrs, 2,000 x.

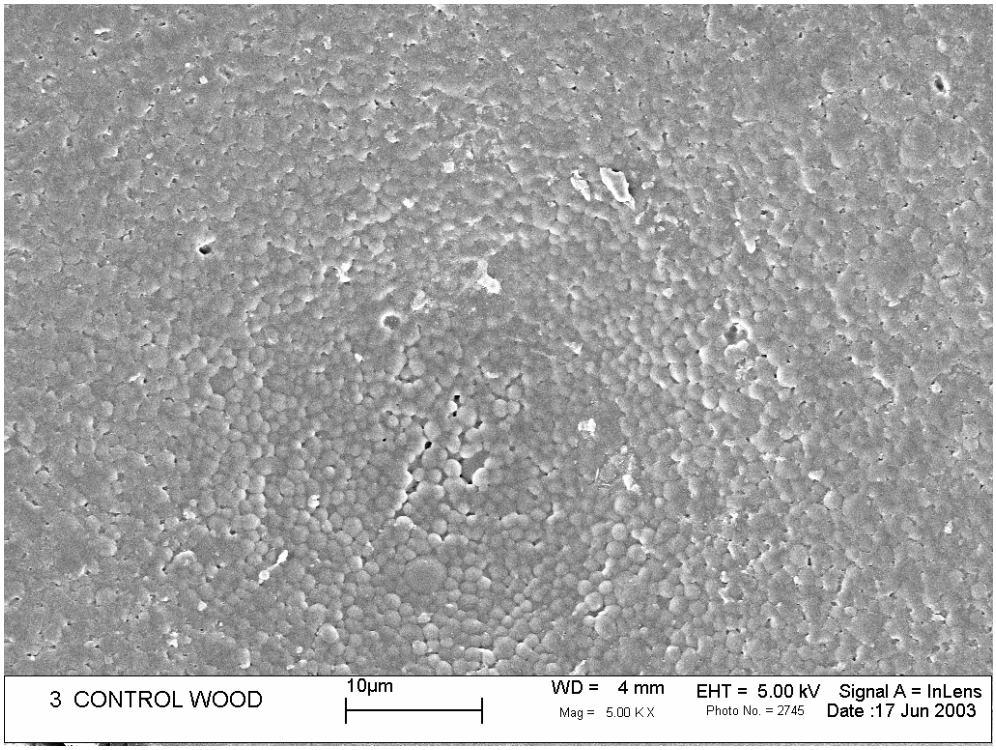

Figure 4-69: Latex 2 catalyzed (5% w/w) applied to wood, oven dried 24hrs, 5,000 x.

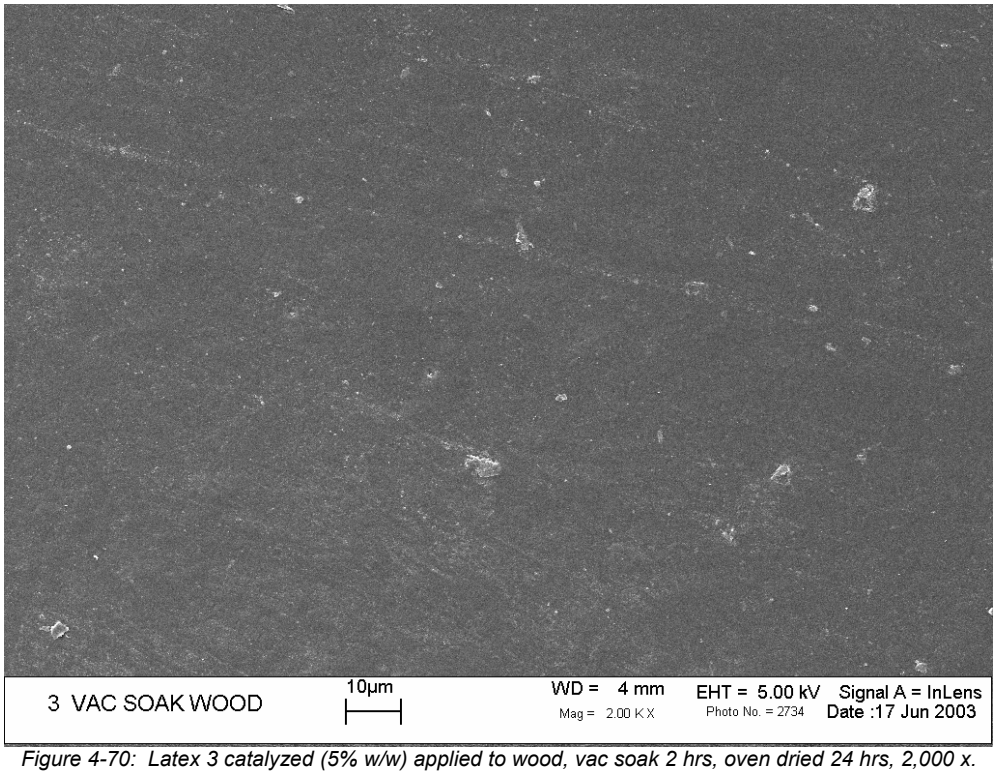

Figure 4-70: Latex 3 catalyzed (5% w/w) applied to wood, vac soak 2 hrs, oven dried 24 hrs, 2,000 x.

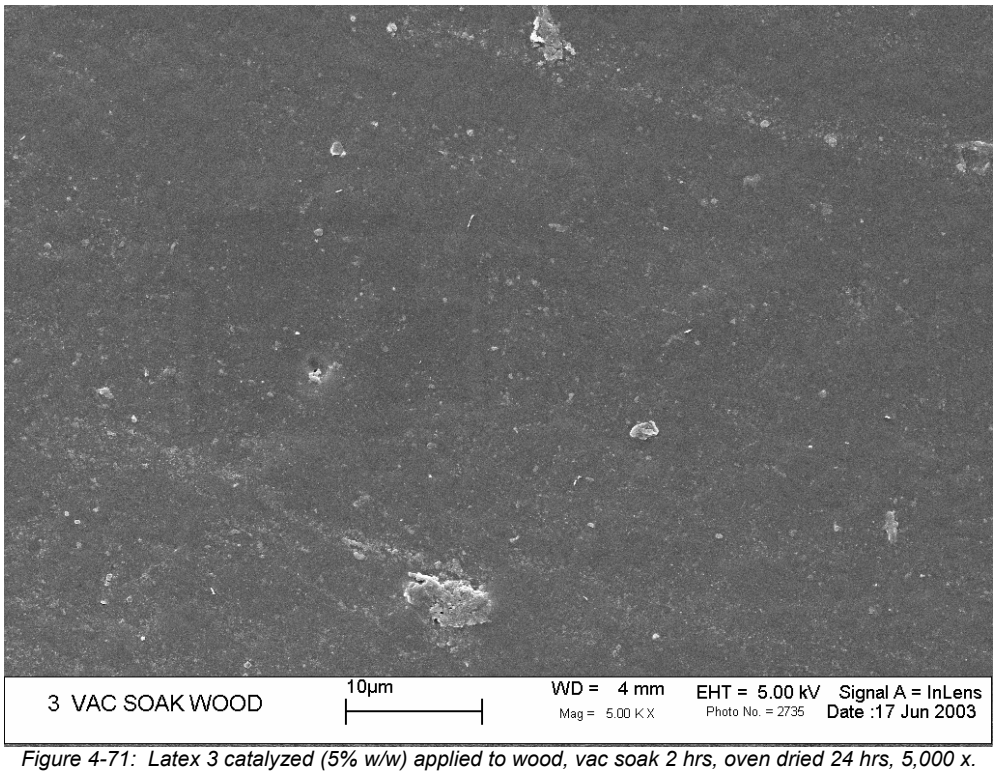

Figure 4-71: Latex 3 catalyzed (5% w/w) applied to wood, vac soak 2 hrs, oven dried 24 hrs, 5,000 x.

Chapter 5: Determining the Distribution of NMA

5.1 Introduction

One of the specific objectives of this project was to identify the distribution of polymerized NMA units within poly(vinyl acetate) latexes. This chapter will focus on the methods used to identify NMA distribution and the results of these analyses. The three latex adhesives whose synthesis and characterization were described in Chapter 4 are the subjects of this study. Recall that different monomer addition strategies were used to manipulate NMA distribution. The following chapter will explore adhesive durability; correlations between NMA distribution and performance will then be discussed.

The method for detecting NMA distribution relies on solution NMR spectroscopy. Previously, in Chapter 3, some of the fundamental aspects of the solution NMR experiment were discussed. Particular attention was given to spin-spin coupling and chemical shifts, which are diagnostic in interpreting the structure of molecules. Here, a different aspect of the solution NMR experiment is of interest. NMR experiments were conducted at different temperatures to investigate effects relating to polymer dynamics. The method will be described below following some background on relaxation mechanisms in the NMR experiment.

5.1.1 Solution NMR Spectroscopy and Mobility

There are several possible mechanisms by which nuclear spins relax. For ^{13}C-NMR, the most predominant means is through magnetic dipole-dipole interactions with surrounding nuclei (Levy and Lichter 1979). Other relaxation mechanisms include chemical shift anisotropy, spin rotation interaction, scalar interactions, quadrupolar interaction, and paramagnetic interaction (Traficante 1996). For ^{15}N-NMR, many of these mechanisms can play an important role in the observed relaxation, but the dipole-dipole interactions continue to dominate the behavior in the case of protonated nitrogen atoms (Levy and Lichter 1979) Two important parameters describe the characteristic relaxation times of nuclear spins. The first is referred to as the spin lattice (T_1) relaxation time, where the lattice is the collection of molecules (solute or solvent) surrounding the nuclear spin(s) of interest. The other is the spin-spin relaxation time (T_2).

The solution NMR method used to determine NMA distribution has been published by Bonardi et al., who applied the approach to acrylic latices containing NMA (Bonardi, Christou et al. 1991). Three phases of the latex are considered as possible locations of polymerized NMA units: 1. the water phase; 2. the surface of the polymer particles; and 3. the core of the polymer particles. These three locations are illustrated in a simplistic representation shown in Figure 5-1. This figure is not meant to suggest that only oligomeric NMA chains are possible. To clarify, NMA units could exist in random or blocked segments along a poly(vinyl acetate) chain. On the other hand, it is also possible that homopolymeric chains of NMA could exist. The copolymer composition is governed by the availability of NMA present in the reactor because NMA is much more reactive than vinyl acetate (reactivity ratios are 2.45 (NMA) and 0.45 (VAc), respectively) (Niyazova and Kulagina 1972).

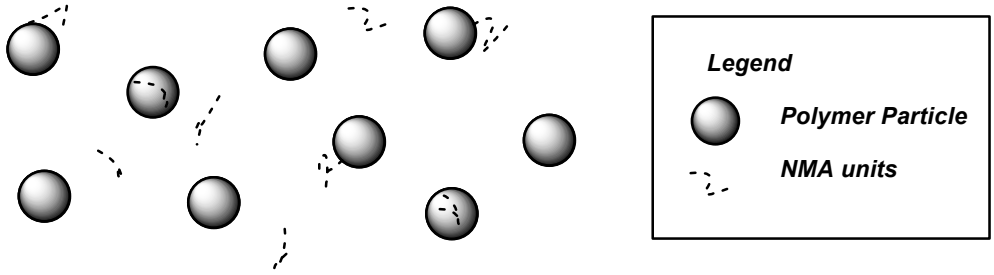

Figure 5-1: Diagram illustrating the three possible locations of NMA units in a latex. The dashed line represents NMA units.

To investigate NMA distribution in the latex, Bonardi et al. took advantage of one of the constraints of the solution NMR experiment: mobility. In most cases, sufficient mobility in solution NMR spectroscopy corresponds to a solute being well dissolved in some solvent. However, this is not always necessary. In the case of polymers, mobility can be achieved by several different means. These include dissolution in a good solvent, as well as raising the temperature sufficiently above the melting point of a semicrystalline material or above the glass transition temperature of an amorphous polymer (Howarth 1993). The reason for this mobility requirement in solution NMR is that the solute molecules must be able to average out dipolar interactions with the lattice, and similarly must average out any anisotropies in the magnetic field. If the solute is not sufficiently mobile, local secondary interactions will dominate the

relaxation of the nuclear spins, and the spins will experience local anisotropies in the applied magnetic field. In these cases, no peaks, or greatly broadened peaks will be observed.

Here, the sample is a high molecular weight, branched polymer. The bulk of the sample is not dissolved in an isotropic solution; instead, it is heterogeneous. Polymer spheres, on the order of 1 micron diameter, are dispersed in an aqueous phase. The poly(vinyl acetate) repeat units which comprise 94% of the system do not have a high affinity for water. Therefore, it is likely that only the exterior portions of the polymer particle are significantly plasticized by the surrounding aqueous phase. These plasticized portions of the sample would relax normally in a solution NMR experiment, as would any dissolved species, because they would have sufficient mobility to overcome any fixed interactions (dipolar couplings or chemical shift anisotropy) by rapid isotropic motion. It is interesting to point out that the "surface" region that is considered here is actually defined by the extent to which water is able to plasticize the particle surface layer. Little can be said about the dimension of this surface layer , or shell, in discrete terms.

The mobility of the unplasticized portion in the interior of the polymer particles is restricted. At room temperature, the interior of the polymer particle is solid-like. There is not enough thermal energy for the chain segments in the particle core to undergo large scale molecular motions; they are below the T_g. In a room temperature NMR experiment, we would not see any "core" material. However, when the temperature is increased substantially above the glass transition temperature (in our work, to 92°C), segmental motions of the polymer chain can occur, thereby allowing the anisotropies to be overcome by motional averaging (Bonardi, Christou et al. 1991). The result is that the high temperature spectrum would contain peaks from all three phases of the latex: the core, the surface, and the water-phase.

Figure 5-2 contains a stacked plot of the ^{13}C NMR spectra of a poly(vinyl acetate) latex adhesive in D_2O. The lower spectrum was obtained at room temperature, while the upper spectrum was obtained at high temperature. Peak assignments are provided later. Noticeable here are the additional signals at ~170 ppm, ~67 ppm, ~38 pm, and ~18 ppm in the high temperature spectrum. These peaks all correspond to poly(vinyl acetate) within the core of the particles.

While these peaks are not visible at room temperature, at high temperature they are clearly detected.

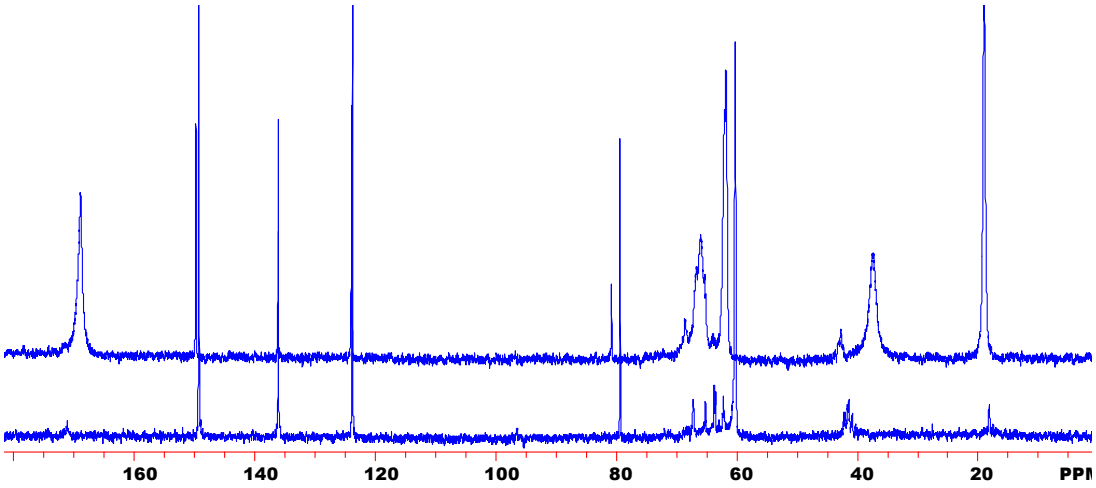

Figure 5-2: ^{13}C-NMR spectra demonstrating the effects of increased molecular mobility due to temperature increase. This latex was made with ^{13}C-NMA. The lower spectrum was obtained at room temperature whereas the upper spectrum was obtained at high temperature (22°C and 92°C, respectively)

The relative amount of a given species can be determined via peak integration, provided that the effects of differential relaxation are eliminated (this will be discussed later). By subtracting the integral of the NMA signal from the room temperature analysis (where only surface-bound and dissolved NMA would be measured) from the integral for the high temperature analysis, we obtain the relative amount of NMA in the core of the latex. However, determination of the water-phase NMA and surface-NMA requires another operation; the latex must be cleansed or washed.

5.1.2 Latex Washing Methods

Washing a latex involves replacing the existing aqueous phase with pure water. Two different washing techniques were used here: membrane dialysis and ultracentrifugation. Other techniques that have been mentioned in the literature which accomplish the same result are ion-exchange and ultrafiltration (Ahmed, El-Aasser et al. 1980).

Ultracentrifugation

In an ultracentrifugation washing method, the latex is loaded into a centrifuge and spun very rapidly. Latex particles separate from the water-phase and pack on the bottom of the centrifuge tube. To wash the latex, we simply remove the supernatant material and replace it with pure water. The sample is then resuspended via mechanical agitation, and the cycle is repeated until the water-phase is pure. This washing method was applied by Bonardi et al. in their study of acrylic latexes having some NMA functionality (Bonardi, Christou et al. 1991).

Dialysis

In this washing technique, a membrane is filled with latex. The membrane is sealed at both ends and placed in a bath of pure water. As time passes, the water from the bath diffuses into the membrane; the nascent water-phase including the polymeric material small enough to pass the membrane is eventually replaced by a fresh water phase. The water bath must be changed periodically, and the water in the bath should be circulated for optimum results.

5.1.3 Distinguishing between water-soluble and surface-bound NMA

Washing the latex eliminates all species that were dissolved in the water phase. At high temperature, the washed sample would have substantial mobility, so all remaining NMA (surface and core) should be detected (Bonardi, Christou et al. 1991). At room temperature, the washed sample indicates only surface-NMA. By subtraction, the amount of NMA in the water-phase is obtained. Figure 5-3 shows the effects of washing the latex via centrifugation. Notice how the intensity of the NMA peak (62 ppm) diminishes after centrifugation. This indicates a large portion of the NMA had been in the water-phase.

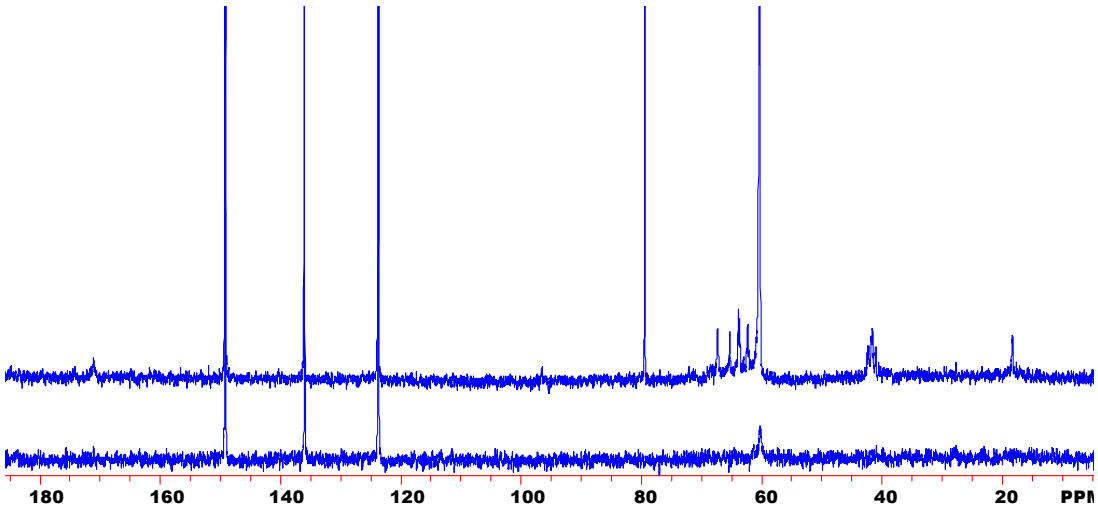

Figure 5-3: Two ^{13}C-NMR spectra of a latex labeled with ^{13}C-NMA in D_2O. Top spectrum shows the untreated spectrum at room temperature (22°C), while the lower spectrum is the centrifuged spectrum at room temperature (22°C). Pyridine standard peaks are evident between 120 and 160 ppm.

5.1.4 Quantitative NMR

In a proton spectrum, the area under a given peak usually corresponds to the number of nuclei present. However, quantitative integrations for ^{13}C and ^{15}N NMR require careful experimental setup. First, nuclear Overhouser effects (NOE) must be negated, and second, the pulse sequence must be set to accommodate the relaxation of all nuclei of interest.

NOE

NOE is a complex mechanism that can result in signal enhancement or signal loss. These effects are not consistent for all nuclei in a spectrum, so NOE effects must be negated for quantitative studies. To eliminate NOE, an inverse gated decoupling pulse sequence should be used. In this mode, the proton decoupler is turned off during the relaxation delay (this negates NOE) and is turned on during acquisition (eliminating the effects of coupling).

Other important parameters for ensuring quantitative spectra include: equal excitation across the spectral width, a well-digitized spectrum, and proper relaxation (Sotak, Dumoulin et al. 1984). Most modern instruments allow equal excitation over the desired range of frequencies. With modern instrumentation it is also easy to obtain a properly digitized spectrum, although zero filling the FID produces more intermediate data points via extrapolation, and often results in less

error during integration. Setting up the pulse sequence to allow proper delays is the second critical component of obtaining a quantitative spectrum.

Setting the relaxation delay

The NMR pulse sequence must allow ample time for all signals of interest to relax. This part of the pulse sequence is known as the relaxation delay. Obtaining proper delays is most readily accomplished by measuring the T_1 for all signals of interest via an inversion-recovery NMR experiment. The quantitative pulse sequence settings are dependent upon the longest T_1; the relaxation delay should be set to at least five times the maximum T_1. This gives all nuclei the chance to fully relax before another pulse is applied. If the pulse sequence is not modified to allow for slow relaxing species, the resulting spectrum will show larger peak areas for species with shorter relaxation times. This would lead to erroneous integrations.

5.2 Materials and Methods

5.2.1 Adhesives

Three poly(vinyl acetate)/NMA latex adhesives were produced for this study. Due to the low concentration of NMA in the system, these adhesives were made with either ^{15}N-NMA or ^{13}C, ^{15}N-NMA. The synthesis of the isotopically labeled monomers was described previously in Chapter 3. The synthesis and characterization of the latex adhesives was presented in Chapter 4.

5.2.2 Washing Methods

Centrifugation

For the ultracentrifugation method, samples of the labeled copolymer were diluted to 35% solids content and loaded into centrifuge tubes. Each sample was equilibrated at 4°C for 15 minutes, then centrifuged for 30 minutes at 4°C in a Sorvall SS-34 rotor at 13,000 rpm (20,200 x g). Afterwards, the supernatent fluid was removed from the sample with a pipette, and a corresponding amount of distilled water was added to maintain the solids content. Particles which had sedimented during centrifugation were resuspended in the fresh water phase via mechanical agitation, followed by an ultrasonic treatment. The ultrasonic treatment was performed with a Tekmar ultrasonicator equipped with a microtip probe. The treatment lasted

five minutes, and the instrument was set so that the sonicator cycled on and off every second with a duty cycle of 40% (ultrasonic pulses lasted 0.4 seconds followed by a 0.6 second delay). The centrifugation cycle was repeated so that the latex was washed and resuspended 6 times prior to NMR analysis. Two samples from each latex were subjected to the centrifugation method. After the final centrifugation cycle, the sedimented particles were stored in the refrigerator.

Dialysis

Dialysis membrane was obtained from Spectra/Por®. The poly(vinylidene difluoride) membrane had a molecular weight cutoff of one million Daltons. The tubing was cut into 6" strips and cleansed according to manufacturer directions. Latex was loaded into the tubing, which was clamped shut with universal closures. Samples were stirred in a reservoir of distilled water for a period of one week. The reservoir water was changed every 12 hours. Samples were then removed from the reservoir and analyzed. Two samples of each latex were dialyzed. After dialysis, samples were stored at room temperature in vials.

5.2.3 NMR

Sample preparation. Samples were diluted to 20% solids content with D_2O (Cambridge Isotope Labs). After being well mixed, 3.3 grams of this solution were loaded into a clean sample vial. A fixed amount (0.45 grams) of poly(vinyl alcohol) solution (7% Celvol™ 840 in water) was added to enhance latex stability. The sample mixture was then loaded into a 10 mm NMR tube to achieve a sample height of 54 mm. This required approximately 3.27 grams of the sample mixture. Samples were analyzed one hour after they were prepared.

An external standard comprised of a ~0.1 M solution of chromium acetylacetonate (Aldrich) in ^{15}N-aniline (Cambridge Isotope Labs) was prepared. The solution was syringed into two microcapillary tubes which were flame-sealed. One of the reference tubes was inserted in each 10 mm NMR tube prior to analysis. For all of the ^{15}N studies, the same microcapillary tube was used. During the ^{13}C studies this tube broke, so the second tube was used. The microcapillary provided a chemical shift reference and a standard for integration.

NMR Conditions. (^{15}N NMR). All spectra were recorded on a Varian Unity 400 MHz spectrometer equipped with a 10 mm probe tuned to an observation frequency of 40.531 MHz. The spectrometer was locked on the deuterium resonance of D_2O. Spinning was not necessary due to the heterogeneous nature of the sample. Prior to each experiment, the pulse width was calibrated, and the T_1s were measured via an inversion recovery experiment. Relaxation delays for the pulse widths were always set to $5*T_1$ in an inverse gated decoupling pulse sequence. One thousand scans were accumulated. High temperature studies were conducted at 92°C. Temperature was calibrated by observing the difference between peaks in a proton spectrum of ethylene glycol. For high temperature work, the sample was allowed to equilibrate in the spectrometer for 15 minutes prior to analysis. Room temperature studies were always completed before the high temperature studies.

(^{13}C NMR). Conditions were the same as ^{15}N NMR with the following exceptions. The probe was tuned to 100.578 MHz. The pulse width (15.5 μs) and relaxation delay (15 s) were set after a series of preliminary experiments. Five hundred scans were acquired.

5.3 Results and Discussion

5.3.1 Setting up the pulse sequence

The first step in the analysis of a particular sample was to calibrate the pulse width and measure the T_1 of the two signals of interest (the ^{15}N-amide peak from NMA and the ^{15}N-aniline peak from the reference microcapillary). Differences in pulse widths were minor (50 to 55 μs). However, the observed T_1 measurements were very different. Comparing the aniline peak and the polymerized NMA peak, aniline always exhibited the longer T_1. In room temperature ^{15}N NMR experiments, the measured T_1 values varied between 0.45 and 0.76 seconds, leading to delay periods of 2.1 to 3.8 seconds. For the 92°C experiments, T_1 values increased, ranging from 2.78 to 3.88 seconds. This led to relaxation delay periods of 13.9 to 19.4 seconds. The reason for the appreciable differences in the T_1 measurements at a given temperature condition are unclear. The aniline solution was of a fixed composition. In fact, the same microcapillary tube was used in all of the ^{15}N-NMR studies. It is well known that sensitivity in NMR decreases as

temperature increases. This could be having an effect. Slight differences in viscosities among the samples could also have led to some variability in T_1.

For the ^{13}C studies, the measured T_1s were considerably shorter. It was decided that instead of measuring the T_1 of each individual sample, a conservative relaxation delay would be applied to each of the spectra. For this study, the relaxation delay was set to 3 seconds (room temperature) or to 15 seconds (high temperature), and the pulse width was set to 15.5 μs. These settings were based on the analysis of several preliminary samples.

5.3.2 Peak assignments in ^{15}N-NMR and ^{13}C-NMR of poly(vinyl acetate) adhesives

^{15}N-NMR

A room temperature ^{15}N-NMR spectrum of Latex 1 (unwashed) is shown in Figure 5-4. Two peaks are present. The peak at 59 ppm corresponds to ^{15}N-aniline (Lambert, Binsch et al. 1964). All ^{15}N-NMR spectra are referenced to this chemical shift. The broader peak occurring at approximately 140 ppm is due to ^{15}N-NMA. Figure 5-5 illustrates a high temperature ^{15}N NMR spectrum of the unwashed latex. Differences between the room temperature and high temperature spectra of the untreated latices are not appreciable, except for the peak integrals.

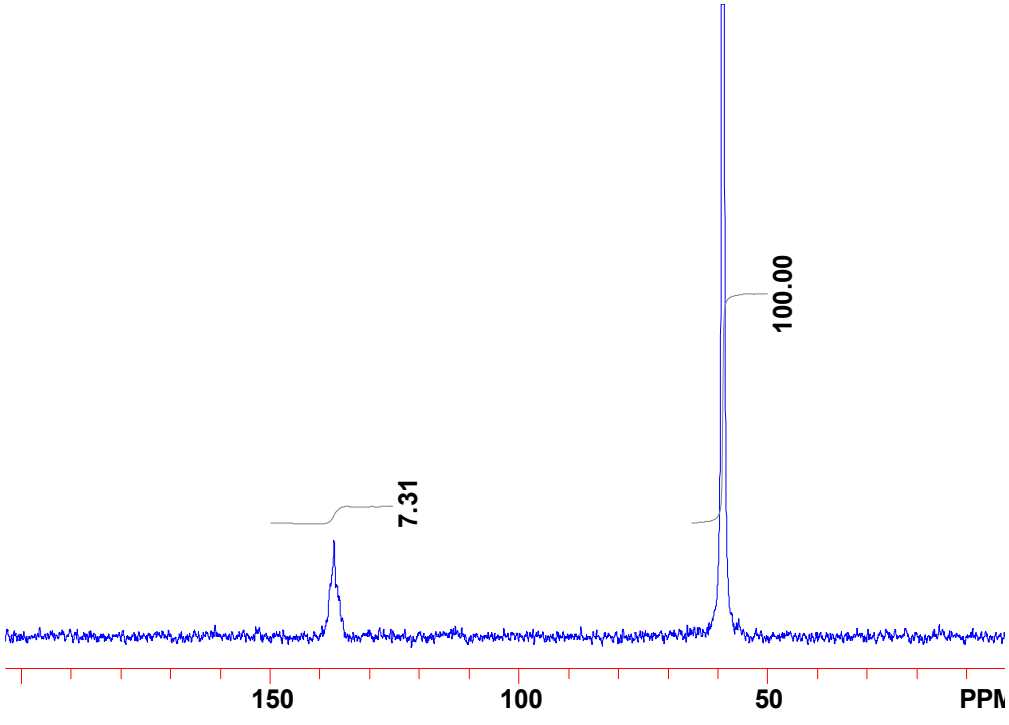

Figure 5-4: Latex 1 room temperature ^{15}N-NMR.

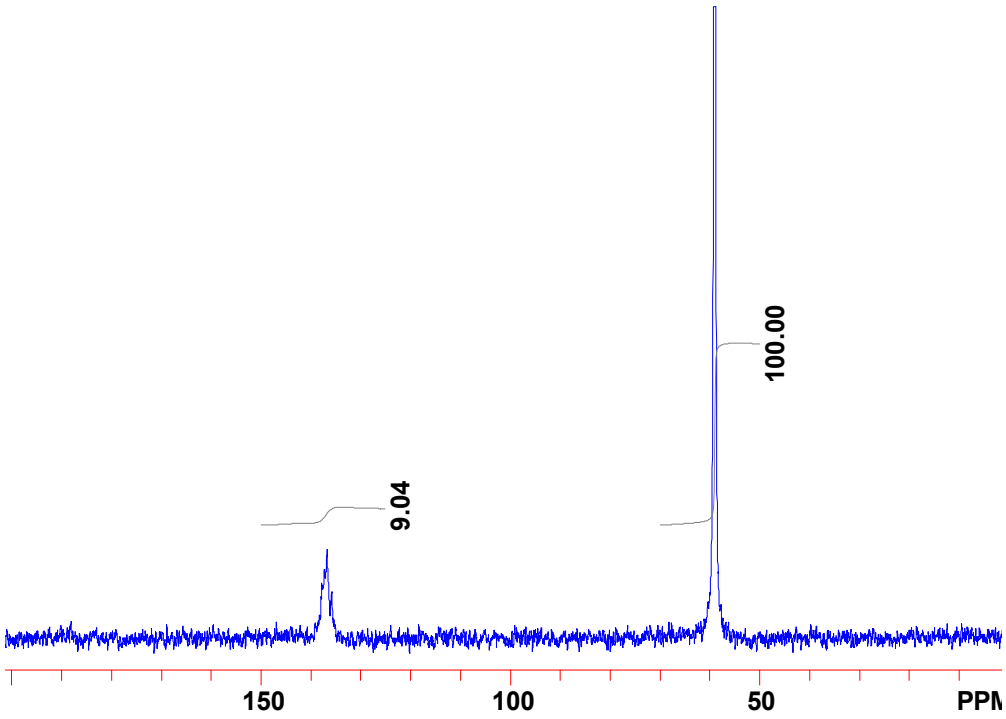

Figure 5-5: ^{15}N-NMR spectrum of a Latex 1 sample at 92°C.

^{13}C-NMR

Representative room temperature and high temperature spectra of Latex 3 are included in Figure 5-6 and Figure 5-7. In the room temperature spectrum, the four peaks occurring between 100 and 150 ppm correspond to the four carbon atoms of the ^{15}N-aniline reference in the microcapillary tube. The C_1 carbon of aniline is split by ^{15}N, causing a doublet that is centered at 147.98 ppm (Hansen and Jakobsen 1972). The C_2 and C_3 carbons also show splitting from ^{15}N. They occur at 114.28 ppm and 129.87 ppm, respectively (Hansen and Jakobsen 1972). Finally, the C_4 carbon appears as a singlet 117.45 ppm (Hansen and Jakobsen 1972). All ^{13}C spectra were referenced to the chemical shift of the aniline C_1 peak. Integration was performed relative to the C_3 carbon of aniline.

By comparing the room temperature and high temperature carbon spectra (Figure 5-6 vs Figure 5-7), we can see the effect that is caused by increased temperature. Material that is in the core of the particles [poly(vinyl acetate)] becomes evident at high temperature. Downfield, at ~172 ppm, the carbonyl carbon peak appears. At the other end of the spectrum, the methyl group appears (20 ppm). Two broad peaks at 44 (methylene) and 67 ppm (methine) correspond to the two backbone carbons.

In the room temperature spectrum, the poly(vinyl acetate) signals are not noticeable. Peaks in the room temperature spectrum correspond to the aniline standard (discussed previously), the poly(vinyl alcohol) colloid stabilizer, surface and or water-phase NMA (~62 ppm) and free formaldehyde (~82 ppm). Peaks between 64 and 70 ppm are due to poly(vinyl alcohol). This is confirmed by comparing the spectra shown in Figure 5-8 (methine region of poly(vinyl alcohol) ^{13}C spectrum) and Figure 5-9 (untreated room temperature spectrum of Latex 3). Additional peaks corresponding to poly(vinyl alcohol) (see Figure 5-2) include the small peaks at 173 ppm and ~ 20 ppm (these are residual acetate groups due to incomplete saponification) and the methylene carbons, which appear between 38-45 ppm.

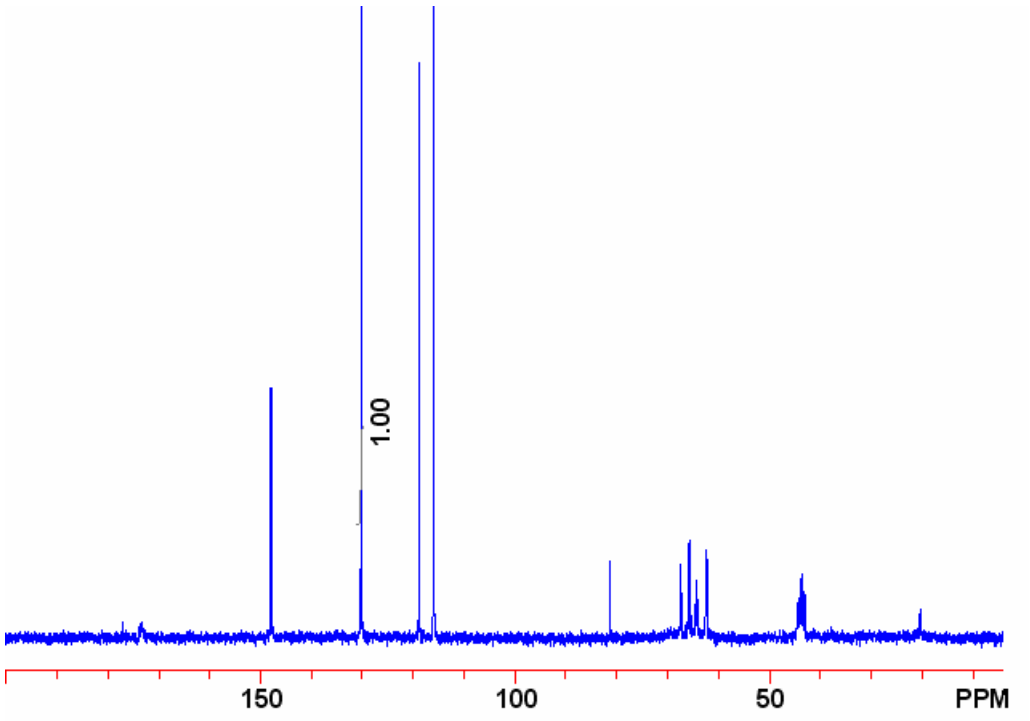

Figure 5-6: ^{13}C-NMR spectrum of Latex 3 untreated specimen analyzed at room temperature.

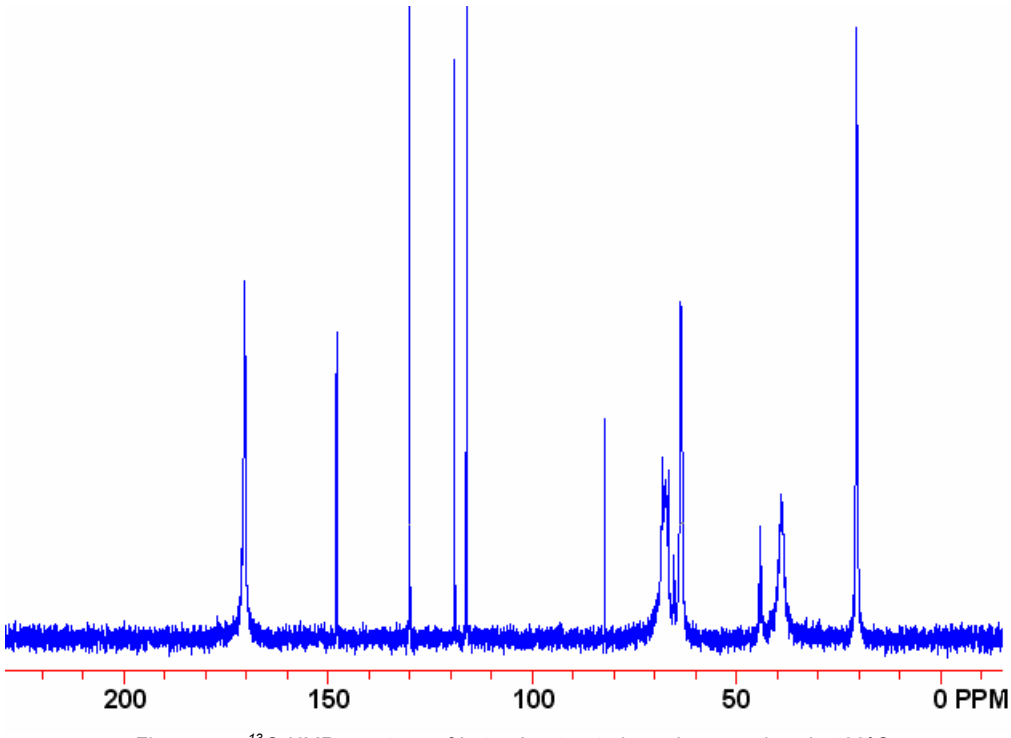

Figure 5-7: ^{13}C-NMR spectrum of Latex 3 untreated specimen analyzed at 92°C.

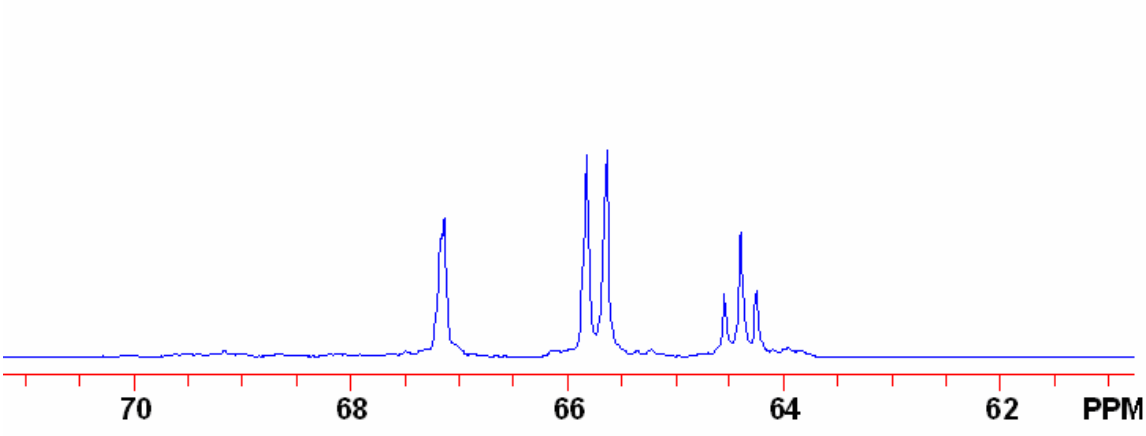

Figure 5-8: Enlarged region of the ^{13}C-NMR spectrum of poly(vinyl alcohol) in D_2O.

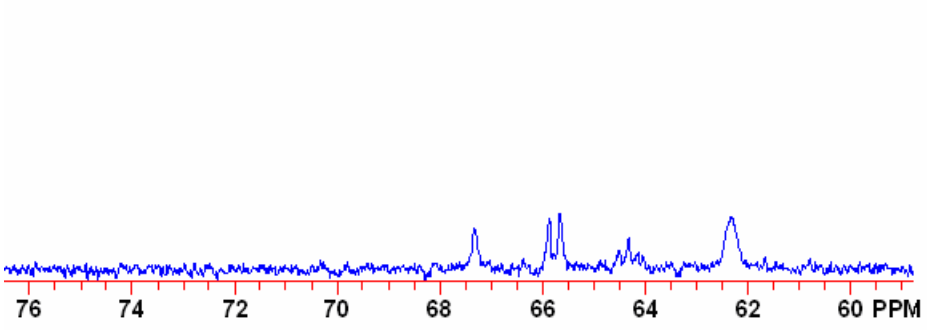

Figure 5-9: Enlarged view of ^{13}C-NMR spectrum of untreated Latex 3 at room temperature in D_2O.

5.3.3 The two washing methods; dialysis and centrifugation

In preliminary studies, it was concluded that the centrifugation method was shearing away the surface of the latex particles. The high shear forces during the centrifugation experiment are more than enough to pull away the adsorbed material at the particle interface (Davis 2000). Evidence for this claim was found in NMR spectra of the supernatant material (refer to the upper spectrum in Figure 5-3), which revealed the presence of the poly(vinyl alcohol) colloid stabilizer (peaks at 65-70 ppm, and ~40 ppm, plus peaks due to incomplete saponification appearing at ~170 and ~18 ppm). The bottom spectrum in Figure 5-3 is the latex after centrifugation, which indicates all poly(vinyl alcohol) has been removed.

The conclusion is that the centrifugation washing method limits the amount of information that can be gleaned about the true distribution of surface and water-phase NMA. The method was not dropped from the study because other reports in the literature are based on this approach. Instead, a complementary washing technique, membrane dialysis, was added. It is expected that the two washing methods will provide different pictures of NMA distribution in a latex. Comparing the results and considering the limitations of each approach will provide a better understanding of NMA distribution.

5.3.4 Calculating the Relative Distribution of NMA

The relative amount of NMA in these spectra can be obtained by either integration or by line fitting. For the ^{15}N-NMR studies, a 25 ppm region around the NMA peak (125 to 150 ppm) was integrated relative to a 20 ppm region around the aniline peak (50 to 70 ppm). For the ^{13}C-NMR studies, line fitting was used. Integration requires adequate baseline on both sides of a peak. The ^{13}C-NMA peak at high temperature was too close to the poly(vinyl alcohol) peaks for reliable integration (see Figure 5-10). It is clear that the NMA peak (62 ppm) does not return to the baseline, therefore, integration overestimates the amount of NMA present (compare 3.27 obtained by integration to 2.90 obtained by line fitting). Only in the case of the room temperature centrifuged latices was integration used. For those samples the observed peak was not large enough for the line fitting approach. Adequate baseline around the NMA peak was available for the centrifuged samples since the poly(vinyl alcohol) had been removed during the treatment. Integration and line fitting were performed relative to the C_3 carbon of aniline.

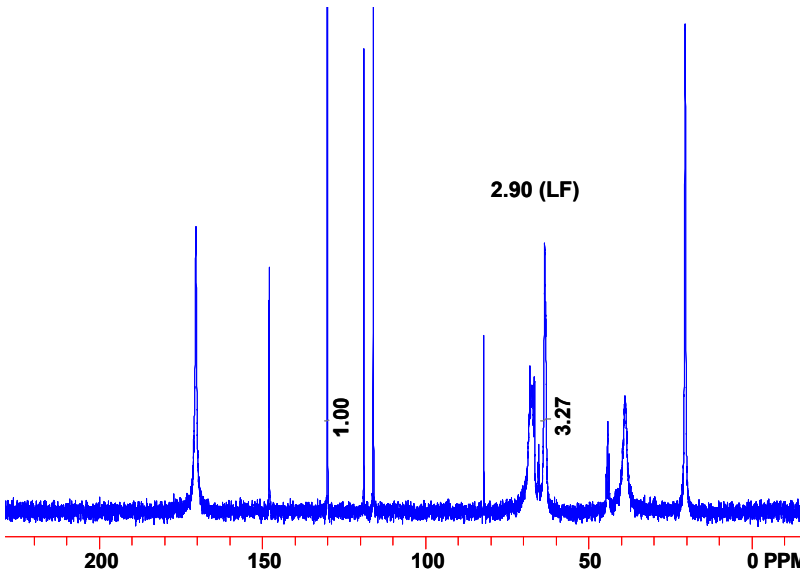

Figure 5-10: Latex 3 evaluated at 92°C in D_2O via ^{13}C-NMR.

The distribution of NMA in a latex can be calculated in a number of ways. For each latex and washing method, we have a set of data which can be expressed as 4 equations (shown below). With just 3 unknowns (water, surface, and core-NMA), there are several ways to compute the proportion of NMA in a given location.

NMA in Untreated, Room Temp Spectra = Surface + Water-phase
NMA in Untreated, High Temp Spectra = Surface + Water-phase + Core
NMA in Washed, Room Temp Spectra = Surface
NMA in Washed, High Temp Spectra = Surface + Core

Ideally, the four experimental conditions should give consistent indications of the NMA distribution. However, discrepancies are evident depending upon the calculation method. An illustration of how the calculation method affects NMA distribution is included in the Appendix. A single approach was always used to determine NMA distribution. Furthermore, this

calculation method was based on the data points that were considered the most reliable: the room-temperature and untreated results. The approach is defined as follows:

1. Surface-NMA will be given by the result of the room temperature washed experiment.
2. Water-phase NMA will be determined by subtracting surface-NMA from the untreated, room temperature spectra.
3. Core NMA will be determined by subtracting the room temperature untreated spectra from the high temperature untreated spectra.
4. Total NMA will be defined as the sum of these three quantities. This is equivalent to the result of the high temperature untreated sample.

This approach relies heavily on *room temperature* results. Reactions of NMA can occur at high temperature, which can impact the integrals obtained (this will be discussed later). Additionally, the results from the *untreated* specimens are preferred over the washed specimens. Nothing has been done to interfere with these samples, so they most accurately represent the true nature of the latex. The least reliable experimental condition is the high temperature washed latex. Applying the suggested calculation method allows us to ignore data from this experimental condition.

5.3.5 Results

Table 5-1 shows the integral values obtained from each ^{15}N-NMR analysis. All NMR spectra are included in the Appendix. For each latex/treatment/temperature grouping, at least 2 samples were analyzed. Averages were computed for each latex/treatment/temperature grouping. Average integral values had to be greater than or equal to 0.28 (this was the minimum detectable amount of NMA) to be included in the analysis; otherwise, they were considered to be zero. Zeroes were recorded for individual sample readings if no NMA peak was evident between 130 and 140 ppm in the spectrum. In the Appendix, spectra exhibiting no peaks are clearly labeled.

Judging whether or not a peak exists is subjective, but it appears to be the best method of interpreting the data. Integrating a blank region of the spectra was found to give integrals

ranging from -1.68 to +1.00; therefore, it is not appropriate to blindly accept an integral value. Clearly, integral values are affected by the noise in the spectrum. Integration results were only accepted if some indication of a peak existed between 130 and 140 ppm. In most cases, a peak was evident when integral values were greater than 1.0. A small "peak" was evident even with integrals of less than 1.0 in three of the samples. In one instance, no peak was evident even though the integral value was slightly greater than 1.0. Note that only three of the seven room temperature centrifuged samples exhibited a peak.

Table 5-1: Summary of findings for ^{15}N-NMR experiments . Room temperature and high temperature integral values are reported for each sample. The averages and standard deviations are also given.

Adhesive	*Treatment*	*Temperature*	*Sample 1*	*Sample 2*	*Sample 3*	*Average*	*St.Dev.*
Latex 1	*Untreated*	*22°C*	*7.82*	*9.59*	*7.31*	**8.24**	± 1.20
		92°C	*9.04*	*10.70*	-	**9.87**	± 1.17
	Centrifuged	*22°C*	*0*	*0*	*0.29*	**0**	-
		92°C	*0*	*0*	-	**0**	-
	Dialyzed	*22°C*	*6.45*	*6.59*	*5.52*	**6.19**	± 0.58
		92°C	*0.84*	-	*1.30*	**1.07**	± 0.32
Latex 2	*Untreated*	*22°C*	*6.26*	*6.15*	*6.50*	**6.30**	± 0.18
		92°C	*6.67*	*7.43*	-	**7.05**	± 0.54
	Centrifuged	*22°C*	*0.28*	*0*	-	**0**	-
		92°C	*1.62*	*1.62*	-	**1.62**	± 0.000
	Dialyzed	*22°C*	*5.70*	*5.90*	-	**5.80**	± 0.14
		92°C	*3.69*	*2.48*	*2.39*	**2.85**	± 0.73
Latex 3	*Untreated*	*22°C*	*1.00*	*1.68*	*1.20*	**1.29**	± 0.35
		92°C	-	*8.14*	*8.69*	**8.42**	± 0.39
	Centrifuged	*22°C*	*0*	*0.62*	-	**0.31**	± 0.44
		92°C	*8.26*	*5.37*	-	**6.82**	± 2.04
	Dialyzed	*22°C*	*0.67*	*1.58*	-	**1.13**	± 0.64
		92°C	*10.57*	*6.36*	-	**8.47**	± 2.98

Relative distributions of NMA are computed based on the average values in Table 5-1, and in Table 5-2, which includes the ^{13}C-NMR results. Recall that Latex 3 was synthesized with ^{13}C, ^{15}N-NMA, so it can be analyzed by both ^{13}C and ^{15}N-NMR. ^{13}C-NMR has much greater sensitivity than ^{15}N-NMR. Peaks were evident for all samples—even the centrifuged room temperature samples.

Table 5-2: Peak areas for ^{13}C-NMR spectra of Latex 3 where values were determined by line fitting, with the exception of the room temperature centrifugation results; those were determined via integration.

Adhesive	*Treatment*	*Temperature*	*Sample 1*	*Sample 2*	*Sample 3*	*Average*	*St.Dev.*
Latex 3	*Untreated*	*22°C*	*0.33*	*0.32*	-	**0.32**	± 0.01
		92°C	*2.9*	*2.89*	*2.78*	**2.90**	± 0.01
	Centrifuged	*22°C*	*0.15*	*0.13*	-	**0.14**	± 0.01
		92°C	*2.25*	*1.78*	-	**2.01**	± 0.33
	Dialyzed	*22°C*	*0.27*	*0.27*	-	**0.27**	± 0.00
		92°C	*3.06*	*2.98*	-	**3.02**	± 0.06

Several of the latex/temperature/treatment groups in the ^{15}N-NMR analysis showed significant variability among samples. These included the high temperature dialysis and centrifugation samples from Latex 3. This discrepancy could be due to aging of the samples. Latex aging could be manifested in various physical changes (such as poorer stability), or even chemical changes, due to crosslinking or other hydrolysis reactions that might occur over time. Such changes could impact the results of this NMR analysis. All samples were analyzed over a period of 45 days. Approximately half of the data was collected between days 1 and 20, while the other half was collected between days 38 and 45. In most cases, sample age did not seem to affect the results. However, the two dialysis and centrifuged samples were analyzed 26 days apart, and the time delay corresponds with a noticeable drop in the amount of NMA that was detected at high temperature. It is not clear what other reason would exist for this variability, yet the aging theory is not consistent with other data points. The room temperature centrifuged and dialyzed samples had the same age discrepancy, yet gave very reproducible results.

5.3.6 The Distribution of NMA in Latex 3

^{15}N-NMR. The relative amount of NMA on the surface is given directly by the average of the room temperature centrifuged samples (0.31). By subtracting this result from the room temperature untreated sample (1.29), the relative amount of NMA in the water phase can be calculated (0.98). High temperature results are required to determine the amount of NMA in the core region. The integral of the untreated high temperature latex (which includes water-phase, surface, and core NMA) is 8.42. Subtraction of the previously obtained surface and water-phase NMA integrals gives the relative amount of NMA in the core (7.13). Based on this method, the distribution of NMA is: 3.7 % surface-NMA, 11.6% water-phase NMA, and 84.7% core-NMA.

The dialysis method gives another means of establishing NMA distribution. Using the same approach as described above, results are: 13.4% surface-NMA, 1.90% water-phase NMA, and 84.7% core NMA.

In comparing the dialysis method with the centrifugation method (see Figure 5-11), we observe that the dialysis method indicates a higher proportion of surface-NMA. This was expected because the centrifugation method removes surface-NMA. For the same reason, the centrifugation method overestimates the amount of water-phase NMA. Identical proportions of core-NMA are found because core-NMA is independent of the washing method (i.e., it is computed based upon the same untreated samples).

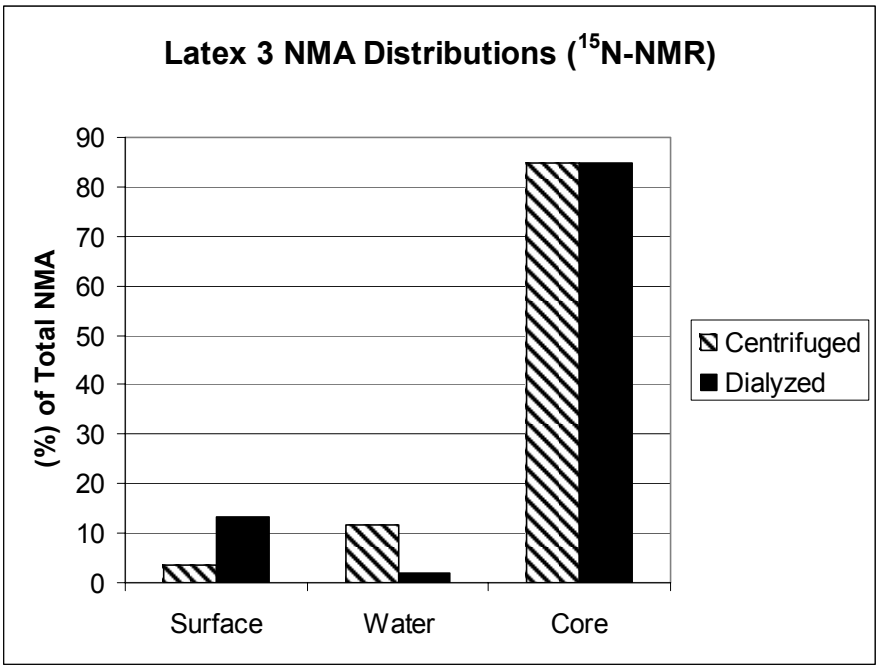

Figure 5-11: NMA distributions in Latex 3 as calculated from the two different washing methods.

^{13}C-NMR

NMA distribution in Latex 3 was also studied using ^{13}C-NMR. This analysis was possible because Latex 3 was made with ^{13}C, ^{15}N-NMA. Results are shown in Figure 5-12.

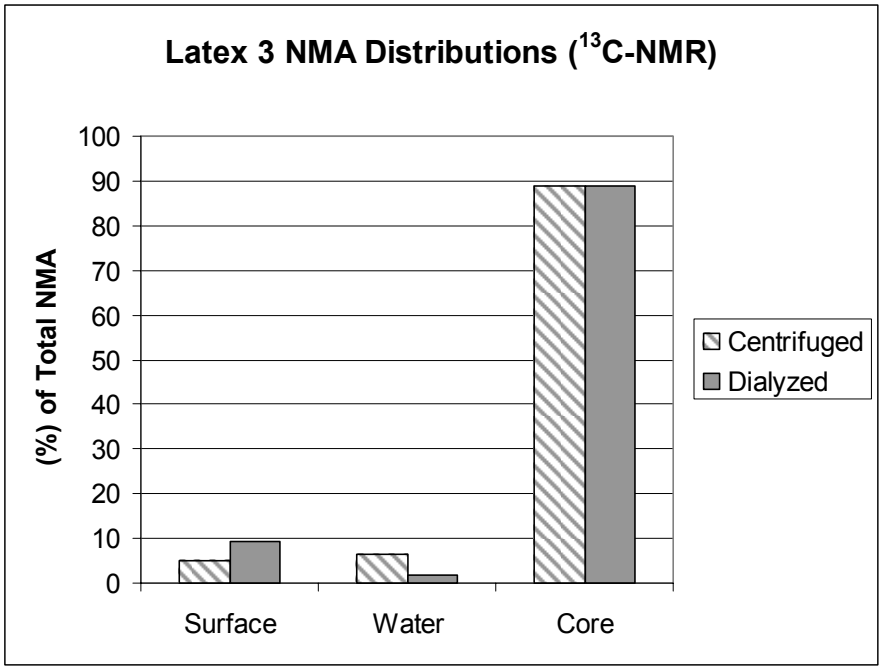

Figure 5-12: NMA distribution via ^{13}C-NMR for Latex 3 as calculated from the two different washing methods.

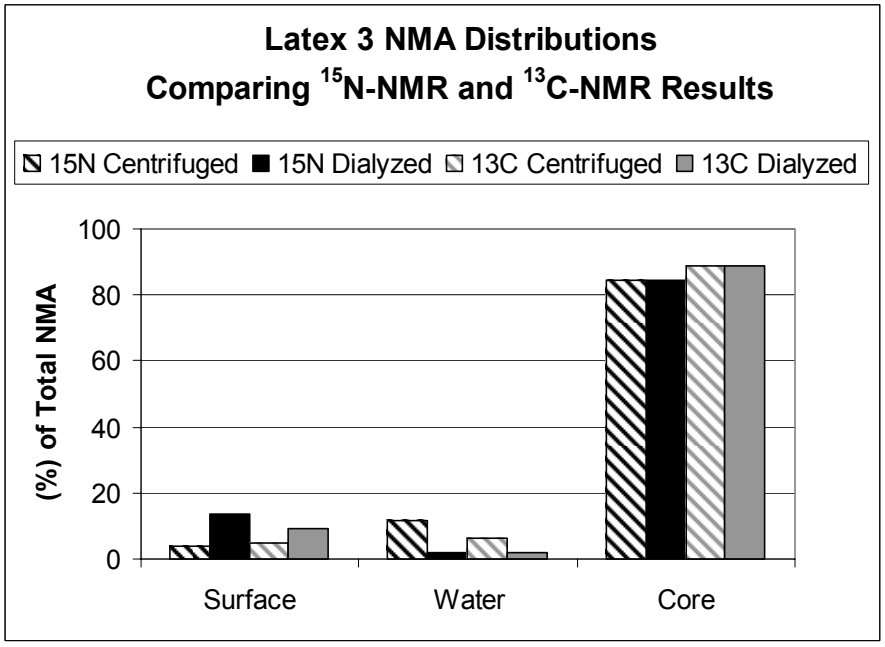

Figure 5-13: A comparison of ^{13}C, and ^{15}N NMR results for determining NMA distribution.

A comparison of the ^{13}C and ^{15}N results for Latex 3 is available in Figure 5-13. Here we observe very good agreement between the four results. For a given washing treatment, ^{13}C and ^{15}N NMR

give nearly identical results. Dialysis indicates that more NMA is on the surface than in the water phase, while centrifugation indicates the opposite trend. Most (80+%) of the NMA exists in the core, in this case for Latex 3.

Recall that preliminary studies had indicated that hydrolysis of the ^{13}C-methylol group was occurring. There were concerns that hydrolysis would deplete the ^{13}C label and interfere with the ability to detect NMA. Here, we continue to see evidence of hydrolysis in the ^{13}C-spectra. The peak at 82 ppm is that of ^{13}C-methylene glycol, which is hydrated formaldehyde. However, the results from the ^{13}C-NMR analysis correspond very well to the ^{15}N-NMR studies.

5.3.7 Interpreting Data from Latex 1 and 2

The interpretation of the NMA distribution in Latex 1 and 2 is more complicated. The average integral values for the dialyzed samples are plotted in Figure 5-14. Here we observe that the room temperature results are *higher* than the 92° results for Latex 1 and Latex 2. Clearly, NMA present at room temperature should also be evident in the high temperature spectrum. Therefore, something must be occurring in these samples to obscure the ^{15}N-NMA signals at 92°C.

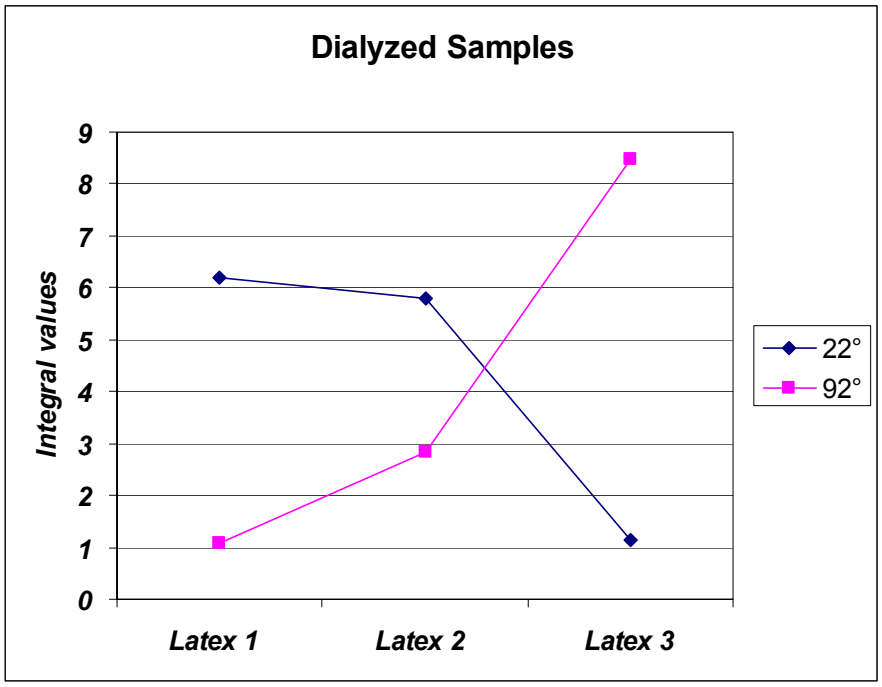

Figure 5-14: The effect of temperature on the integral values obtained from dialyzed samples.

Hypotheses for the aberrant data

Several possibilities could account for the lower integral values at high temperatures. First, one could rationalize that instability of the particles at high temperature could lead to agglomerates dropping to the bottom of the NMR tube, and thus out of the coil region. However, there was only limited evidence of particle settling after the NMR experiments. This settling behavior was uniform among the latices and accelerated aging conditions. Furthermore, the issue of particle stability was addressed in preliminary studies, where settling was a problem. It was decided at that point that some poly(vinyl alcohol) should be added to each sample prior to analysis. This was found to noticeably improve the stability. Therefore, the observed findings are not likely due to particle settling.

A second possibility would be reaction of the ^{15}N-NMA units. This could lead to the formation of new ^{15}N-species which would appear in a different region of the spectrum. Reactions of NMA are certainly a possibility. Condensations could occur, leading to methylol bridges or methylene bridges. However, these products would likely have very similar ^{15}N chemical shifts. This prediction is based on a series of model compounds showing monomethylol, N, N'-dimethylol and N, N, N' trimethylol-ureas, which exhibit ^{15}N-NMR signals within 30 ppm of one another (Andreis and Koenig 1995). New peaks would easily be detected due to the presence of the ^{15}N label; however, such peaks were not detected. While the presence of a few crosslinks would not likely affect mobility of the polymer chains, extensive crosslinking might limit mobility. Crosslinking could happen on the surface of distinct polymer particles (creating a "shell" around the particles), or could happen between two particles after a collision. In either case, if the extent of crosslinking is high enough, hindered mobility would result, which could obscure NMR signals.

If crosslinking occurred, it had to happen during the 92° NMR scan. Otherwise, the large NMA signals at room temperature would not be present. Long relaxation delays at high temperature caused the analysis to last for approximately 6 hours. This extended high temperature exposure could certainly promote crosslinking. This hypothesis could explain the dialysis findings. However, it introduces a new question: why is a similar trend not observed for the untreated

samples? A similar extent of crosslinking could also occur in an untreated latex having a high proportion of surface or water-phase NMA.

It is possible that the dialysis method could actually change the distribution of NMA by promoting a reorientation of hydrophilic moieties at the particle surfaces. NMA units are much more hydrophilic than vinyl acetate units. Homopolymeric chains of NMA, or NMA-rich blocks of a copolymer chain would be ideally suited for stabilizing the particle interface. In the dialyzed samples, this reorientation could occur as a response to the changing nature of the dispersing phase. Initially the serum of the latex is full of ionic species based on initiator and redox fragments, as well as oligomers and low molecular weight polymers. All of these can stabilize the particle-water interface. However, as the latex is dialyzed, these species are being removed, which has a destabilizing effect on the particles. To maintain stability, it becomes energetically favorable for more hydrophilic compounds to orient themselves towards the surface. NMA migration to the interface would make crosslinking even more likely, simply due to the higher local concentration of NMA. For the untreated latex, which remains in a matrix full of surface active species, there is no perturbation that would promote such surface reorientations. Data from the untreated latex samples indicates that a large amount of surface or water-phase NMA is present. However, it could be much more evenly distributed within the surface region. If crosslinking did occur, the distance between crosslinks would be much higher, so the mobility would not suffer as greatly.

If this hypothesis is correct, then the implications are interesting. Considering the difference between room temperature and high temperature dialysis results, one could say that Latex 1 has the greatest extent of crosslinking. In terms of molecular architecture, this could be indicative of significant proportions of either homopolymeric NMA or NMA-rich blocks along copolymer chains, which are able to migrate to the surface of the particles. Recent work by O'Rourke et al. confirmed that a series of adjacent functional groups (as opposed to two adjacent groups of opposing character) provides the best opportunity of surface "segregation". Furthermore, these authors pointed out that the optimal case for minimizing the surface energy at an interface would result if the stabilizing species occurred at chain ends, because this affords additional degrees of freedom for migration to the interface (O'Rourke-Muisener, Koberstein et al. 2003). Latex 2 also

exhibits crosslinking, but to a lesser extent, indicating that migration to the surface may be impeded. This could be due to a more random distribution of NMA units along poly(vinyl acetate) chains, or due to lower proportions of homopolymeric NMA, etc.

It should be stated that there is no evidence to prove that crosslinking is occurring. There are indications, though, that the high temperature experiment causes the sample to react. The ^{13}C-NMR spectra of Latex 3 (Figures 5-61 through 5-73, Appendix) provide some insight. Three of the four washed samples show no ^{13}C-methylene glycol at room temperature, but do show the product at high temperature. Recall that ^{13}C-methylene glycol is formed when ^{13}C-formaldehyde is released. Hydrolysis of ^{13}C, ^{15}N-NMA can release ^{13}C-formaldehyde. Also, crosslinking of ^{13}C, ^{15}N-NMA can release ^{13}C-formaldehyde. These results indicate that even for Latex 3, which had mostly core NMA, the high temperature experiment is causing NMA to react. In Latex 3, the amount of hydrolysis/crosslinking did not affect the overall interpretation of the NMR results. This mechanism must have occurred to a far greater extent in both Latex 1 and Latex 2.

If hydrolysis were responsible for the signal loss in the Latex 1 and Latex 2 data, then it had to be due to the hydrolysis of acrylamide. While hydrolysis of the methylol group of NMA is relatively easy to achieve under neutral conditions, acrylamide is more resistant to hydrolysis. In cases where strong bases are present, acrylamide can be hydrolyzed to acrylic acid (Yasuda, Okajima et al. 1988). However, the conditions here are far different. It is unlikely that the loss of signal in Latex 1 and Latex 2 is due a significant amount of hydrolysis of NMA, followed by the hydrolysis of acrylamide. Crosslinking seems to be a more feasible explanation.

This "crosslinking hypothesis" can be easily confirmed. A solid state NMR experiment could be performed on Latex 1 and Latex 2 samples after they were exposed high temperature to look for signals due to immobilized regions. This experiment was not conducted in this work, but it will be in the future.

5.3.8 NMA Distribution in Latex 1 and Latex 2

Results (shown in Figure 5-15 and Figure 5-16) indicate that the NMA distributions for Latex 1 and Latex 2 are dependent upon the washing method. This was not true for Latex 3, where most

of the NMA was in the core. The effect due to the washing methods is more prominent in Latex 1 and 2 because more NMA is present in either the surface or the water-phase. Based on the dialysis results (which are probably more accurate than the centrifugation results in evaluating surface/water-phase NMA), Latex 1 had more water-phase NMA than Latex 2 (20% to 7%), while Latex 2 had a higher proportion of surface-NMA (82% to 62%). This is also an interesting finding. Latex 1 showed more indications of crosslinking, yet a lot of the NMA had been eliminated by the dialysis treatment. Perhaps this is another indication that the NMA in Latex 1 was very blocky, or in the case of the water-phase NMA, homopolymeric. If this is the case, the particle surface was probably also covered with blocky NMA functional groups, which could easily crosslink.

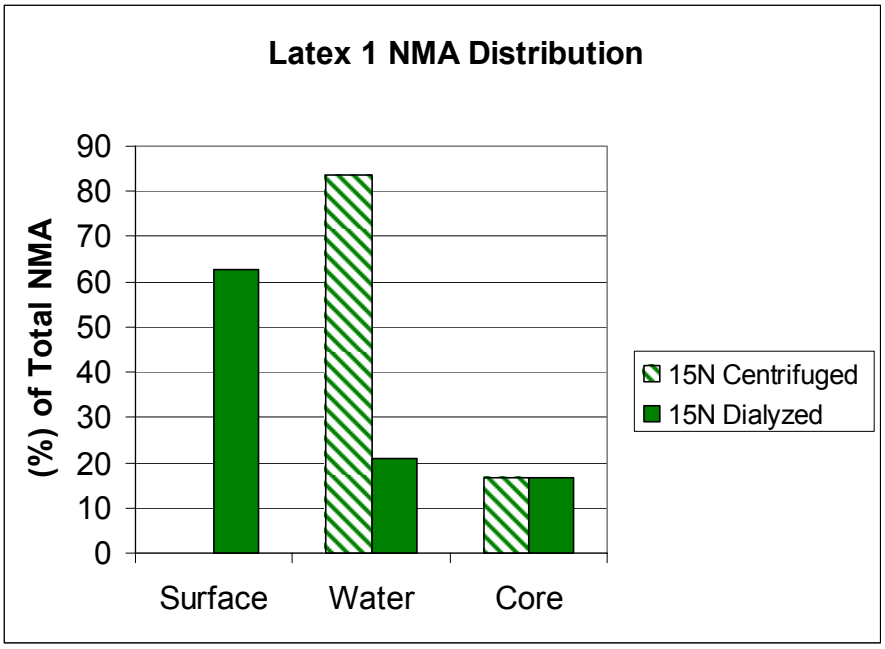

Figure 5-15: NMA distribution in Latex 1.

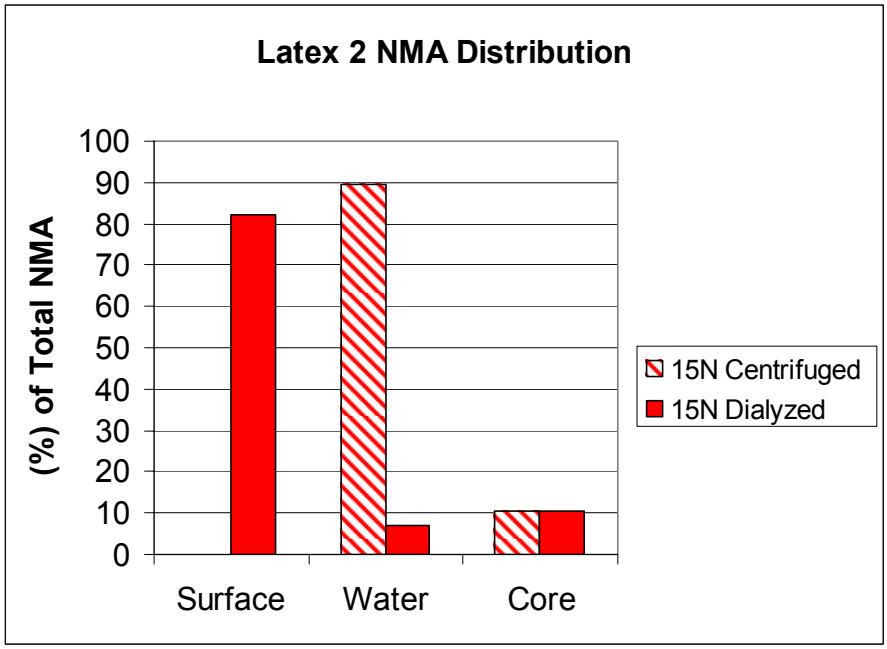

Figure 5-16: NMA Distribution in Latex 2.

In Figure 5-17 and Figure 5-18, NMA distributions (computed by the original method) are compared among the three latices for a given washing method. The centrifugation results for Latex 1 and 2 show a bias towards the water-phase because of the washing treatment. Since the surface is being removed, we cannot really distinguish between surface and water-phase NMA. The dialysis method is more reliable. Latex two has most of its NMA at the particle surface (~80%). Latex 1 also has most of its NMA at the surface (~60%), but maintains a significant amount of NMA in both the water-phase (~20%) and the core (~20%). Latex 3 has mostly core-NMA (80+%).

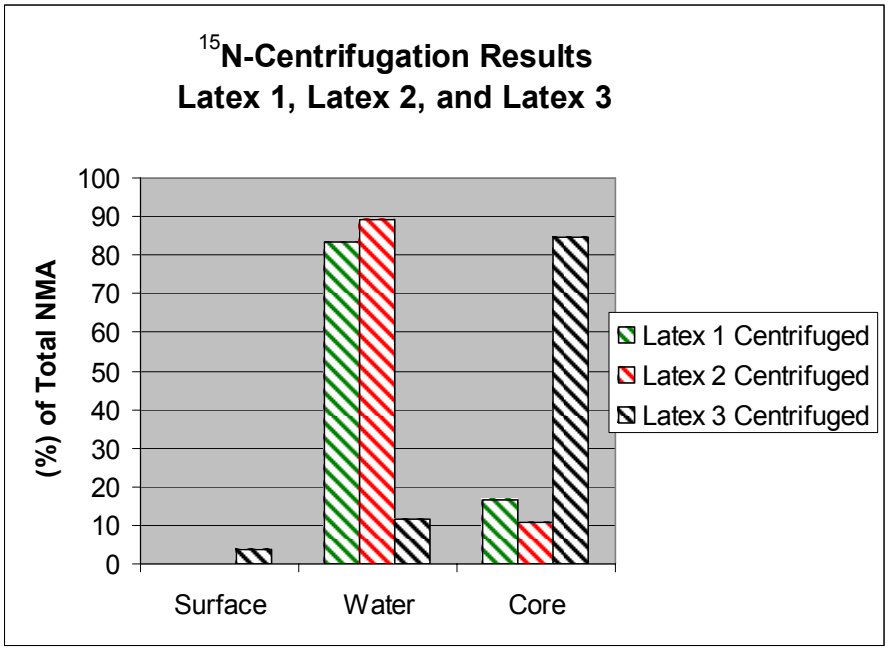

Figure 5-17: NMA distribution of all three latexes based on the centrifugation washing method.

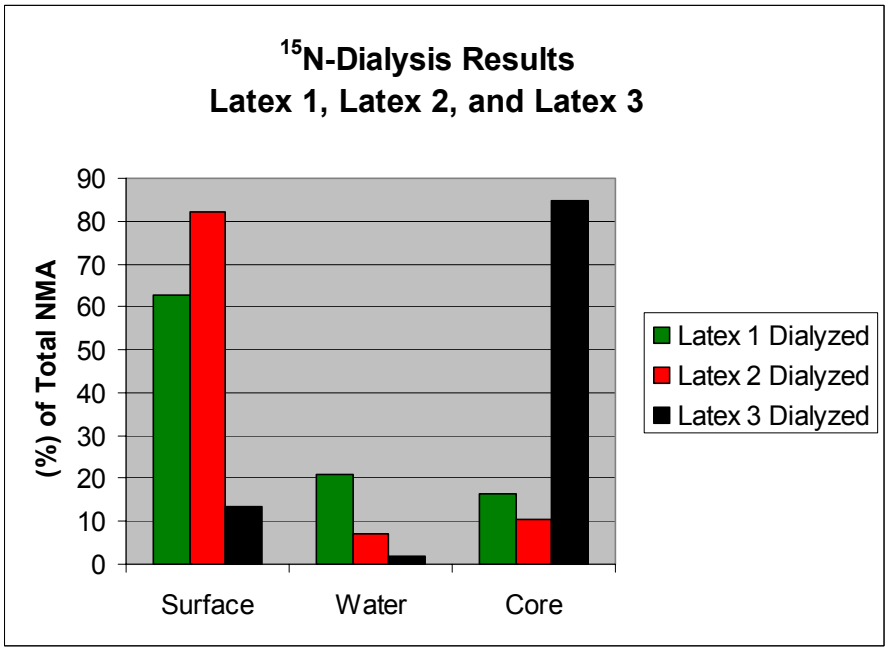

Figure 5-18: NMA distribution of all three latexes based on the dialysis washing method.

Based on these results, it appears that the polymerization attempts were moderately successful in achieving different NMA distributions. Recall that the three copolymerizations were conducted with varying NMA feed strategies. In Latex 1, NMA was injected into the reactor, beginning at

0% conversion. For Latex 2, the NMA injections were delayed until ~50% conversion. For Latex 3, NMA was pumped continuously into the reactor.

Of these polymerization strategies, we would expect Latex 3 to have the most random copolymer composition. In Latex 3, the NMA was pumped continuously into the reactor. A random copolymer composition would mean that NMA units comprise the copolymer chains in the core of the polymer particles. The expectation of a greater random copolymer microstructure is consistent with most of the NMA being located within the particle core, as found in this study.

In Latex 1 and Latex 2, NMA was injected according to a set profile. Injections lead to a blockier microstructure, or possibly to homopolymer chains of NMA, because a quantity of the monomer is injected suddenly. The primary difference between Latex 1 and Latex 2 is that the NMA feed began immediately in Latex 1. In Latex 2, NMA injections were delayed. Dialysis results indicate that most of the NMA is on or within the surface region in both Latex 1 and Latex 2. For Latex 1, the NMA is more evenly distributed among the three phases. Latex 1 has the highest amount of water-phase NMA (~20%).

The fracture results (in the following chapter) may provide insight as to whether these differences in distribution correlate with performance.

5.4 Conclusions

To summarize, taking advantage of the mobility constraint in solution NMR spectroscopy provides a valuable tool for analyzing the distribution of surface and water-phase NMA. The method requires the use of a washing technique. Here, centrifugation and dialysis methods were employed. Since NMA is present in very small quantities, isotopic enrichment was required for detection.

Latex 3 included ^{13}C, ^{15}N-NMA, so the monomer distribution study was conducted for both ^{15}N and ^{13}C-NMA. For latexes 1 and 2, the distribution was determined based on ^{15}N NMR. The ^{13}C and ^{15}N methods gave very similar findings. Hydrolysis of the ^{13}C label did not limit

detection of the NMA. For Latex 3, most of the NMA (~85%) existed in the core. Centrifugation and dialysis washing methods led to very similar NMA distributions for Latex 3.

Latex 1 and Latex 2 had very different NMA distributions from Latex 3. Most of the NMA was detected either at the surface or in the water phase, depending on the washing method used. The centrifugation treatment was very harsh, and sheared off particle surfaces. Therefore, it overestimated the amount of water-phase NMA. The dialysis method was less damaging and resulted in more surface-NMA. Latex 1 dialysis results indicated that it had the highest amount of water-phase NMA. In general, Latex 1 showed the most even distribution of NMA among the three possible locations. Latex 2 had the highest proportion of surface NMA.

The high temperature analyses of the Latex 1 and Latex 2 dialyzed samples resulted in less NMA than the room temperature analyses. This finding is thought to be due to crosslinking occurring during the high temperature analysis. It is hypothesized that the dialysis treatment causes the migration of NMA to the surface.

Overall, the solution NMR method provides insight regarding the distribution of NMA in the latex. Results depend on the calculation method. Here a standard procedure was adopted. The procedure focused on the most reliable data points (the untreated and room temperature samples). The measured NMA distributions were consistent with the copolymer microstructures that would be expected to arise from the three NMA addition methods.

5.5 Acknowledgements

The author gratefully acknowledges Tom Glass of the Virginia Tech NMR Facility for his assistance in setting up these experiments, and for his willingness to designate long blocks of spectrometer time for this study. Dr. Rick Davis of the Chemical Engineering Department also provided valuable insights towards this work, in addition to the use of his ultrasonicator. Dr. Robert White and Dr. Eugene Gregory graciously provided access to their centrifuge.

5.6 References

Ahmed, S. M., M. S. El-Aasser, et al. (1980). "Cleaning Latexes for Surface Characterization by Serum Replacement." Journal of Colloid and Interface Science **73**(2): 388-405.

Andreis, M. and J. L. Koenig (1995). "Application of Nitrogen-15 NMR to Polymers." Advances in Polymer Science **124**: 191-237.

Bonardi, C., P. H. Christou, et al. (1991). "Acrylic Latexes Functionalized by N-Methylolacrylamide and Crosslinked Films from these Latexes." New Polymeric Materials **2**(4): 295-.

Davis, R. (2000). Personal Communication. Blacksburg.

Hansen, M. and H. J. Jakobsen (1972). "^{13}C-^{15}N Spin-Spin Coupling Constants in [^{15}N]-Aniline from ^{13}C NMR Spectra." Acta Chem. Scand. **26**(5): 2151-2153.

Howarth, O. W. (1993). Liquid state NMR studies of polymer dynamics and conformation. NMR Spectroscopy of Polymers. R. N. Ibbett. London, Blackie Academic and Professional**:** 125-160.

Lambert, J. B., G. Binsch, et al. (1964). "Nitrogen-15 Magnetic Resonance Spectroscopy, I. Chemical Shifts." Proceedings of the National Academy of Sciences of the United States of America **51**(5): 735-737.

Levy, G. C. and R. L. Lichter (1979). Nitrogen-15 Nuclear Magnetic Resonance Spectroscopy. New York, John Wiley and Sons.

Niyazova, Z. M. and T. G. Kulagina (1972). "Copolymerization of N-alkylolacrylamides with vinyl acetate in a suspension." Sin. Vysokomol. Soedin.: 14-17.

O'Rourke-Muisener, P. A., J. T. Koberstein, et al. (2003). "Optimal Chain Architectures for the Molecular Design of Functional Polymer Surfaces." Macromolecules **36**(3): 771-781.

Sotak, C. H., C. L. Dumoulin, et al. (1984). High-Accuracy Quantitative Analysis by 13C Fourier Transform NMR Spectroscopy. Topics in Carbon-13 NMR Spectroscopy. G. C. Levy. New York, John Wiley and Sons. **4:** 91-121.

Traficante, D. D. (1996). Relaxation: An Introduction. Encyclopedia of Nuclear Magnetic Resonance. D. M. Grant and R. K. Harris. Chichester, John Wiley and Sons. **6:** 3988-4003.

Yasuda, K., K. Okajima, et al. (1988). "Study on alkaline hydrolysis of polyacrylamide by carbon-13 NMR." Polymer Journal (Tokyo) **20**(12): 1101-7.

5.7 Appendix

5.7.1 Effect of the calculation method on the NMA Distribution

It was stated previously that the calculation methods can lead to different interpretations of NMA distribution. As an example, we consider the Latex 3 data.

Table 5-3: Review of Latex 3 centrifuged results

Latex 3 Data	*(1)*	*Untreated 22°*	*Surface + Water*	*1.29*
	(2)	*Untreated 92°C*	*Surface+ Water+ Core*	*8.42*
	(3)	*Centrifuged 22°C*	*Surface*	*0.31*
	(4)	*Centrifuged 92°C*	*Surface + Core*	*6.82*

Consider data from the centrifuge washing technique. The amount of core-NMA can be obtained in two ways: (2) – (1); or (4) – (3). We obtain different answers for each method (6.51 vs. 7.13). Similarly, water-phase NMA can be determined in different ways: (2) – (4), or (1) – (3). This gives results of 1.60 vs. 0.98. In some cases, the results of these calculations are inconsistent with experimental data. Consider the value of 1.60 for water-phase NMA, when (1) indicates that the amount of surface and water-phase NMA is only 1.29.

Including the high temperature washed results seemed to lead to more inconsistencies in the data. Evidence shows that reactions may be occurring in that data, so it is preferable to rely on the room temperature results. The calculation method that is the basis for the data analysis ignores the high temperature washed results. All data obtained by this method were reasonable.

5.7.2 ^{15}N-NMR Spectroscopy Results

All samples were in D_2O. The caption indicates pertinent information about the samples. Integral values are shown. Sample numbers in the captions correspond to the entries in Table 5-1.

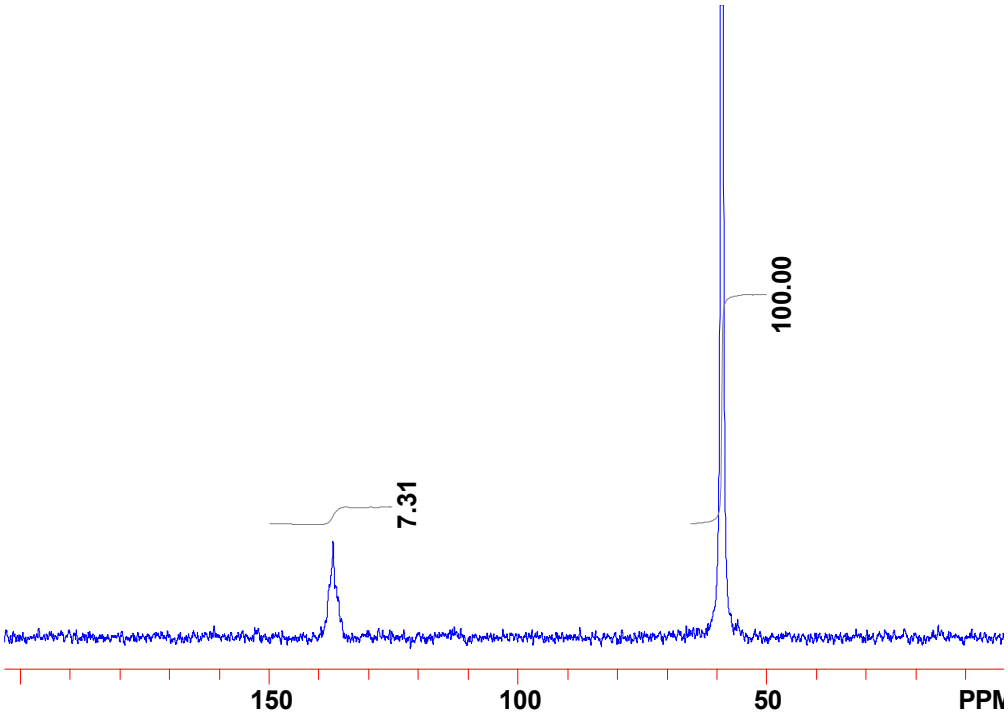

Figure 5-19: Latex 1, Untreated Sample #3—22°C.

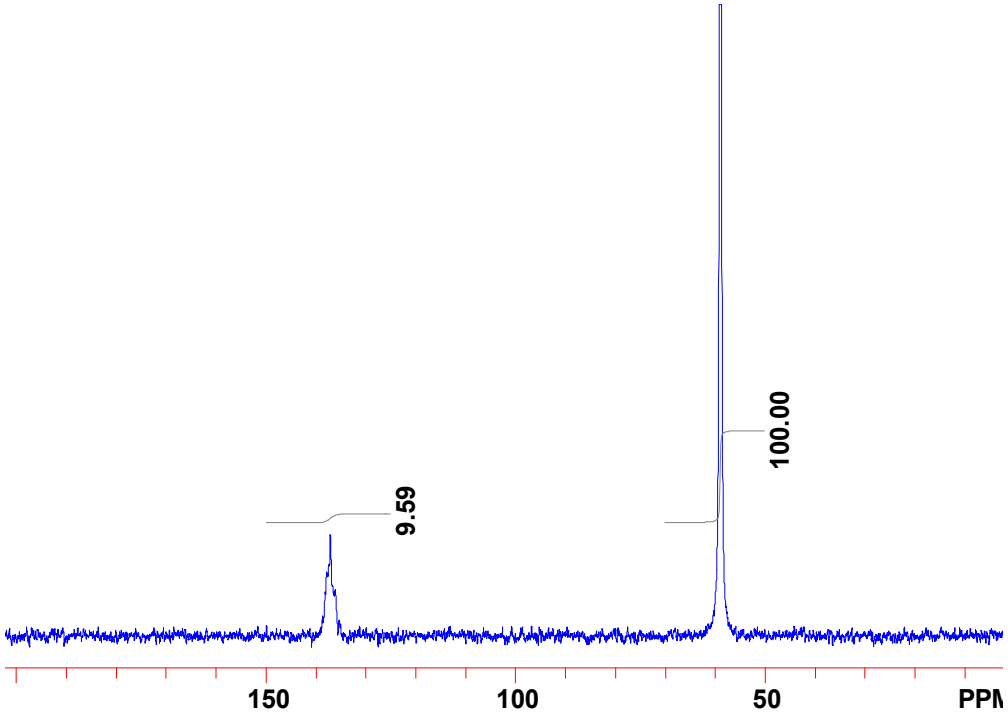

Figure 5-20: Latex 1, Untreated Sample #2—22°C.

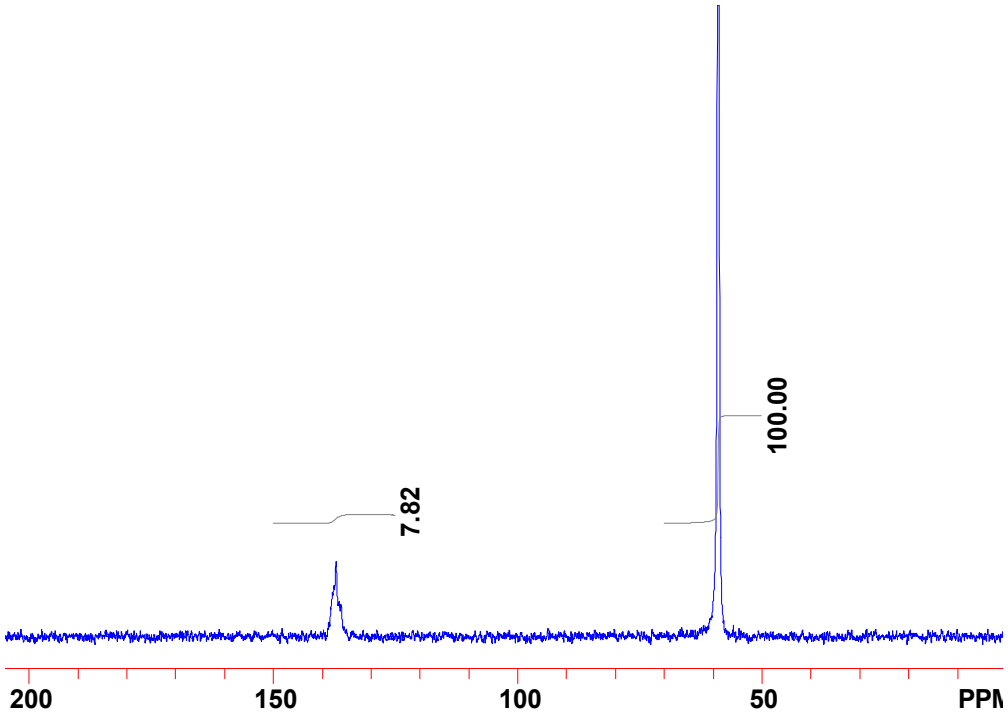

Figure 5-21: Latex 1, Untreated Sample #1—22°C.

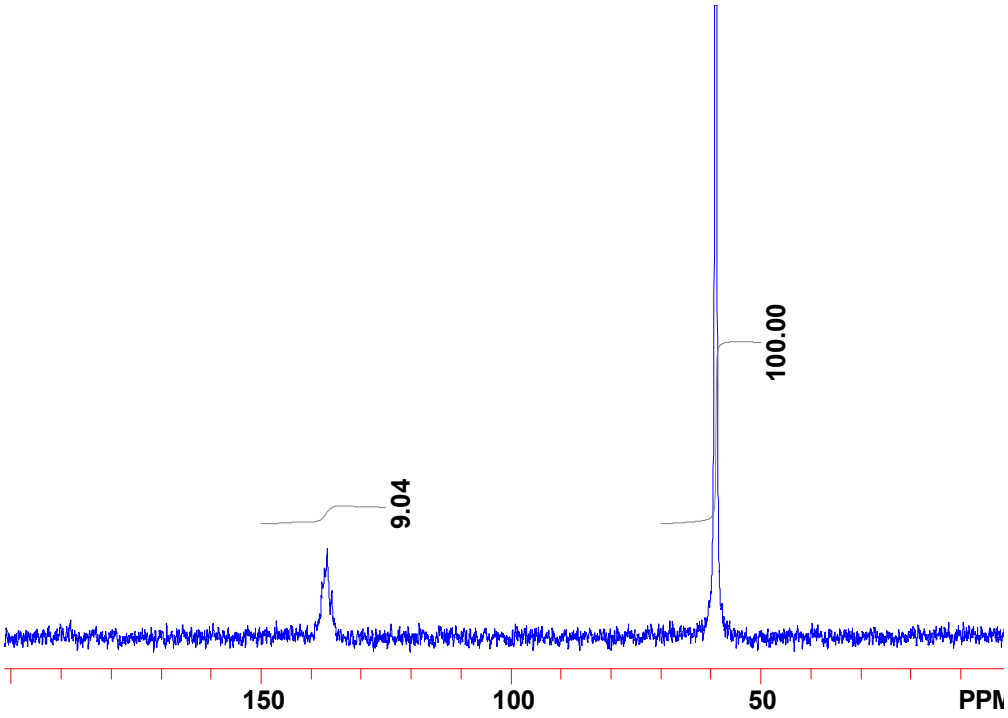

Figure 5-22: Latex 1, Untreated Sample #1—92°C.

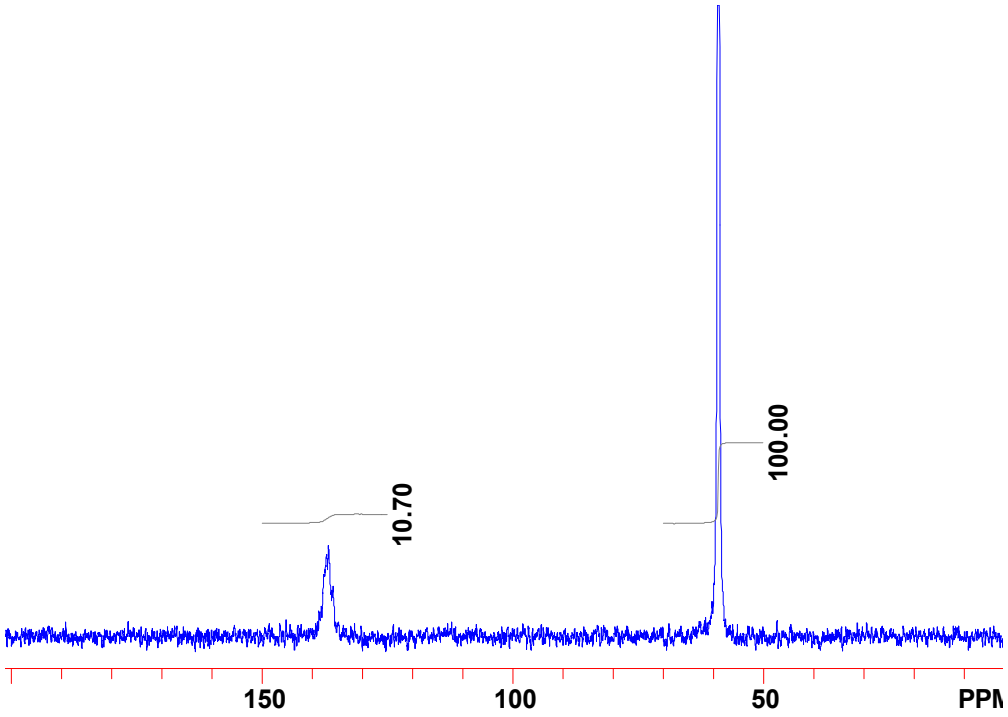

Figure 5-23: Latex 1, Untreated Sample #2—92°C.

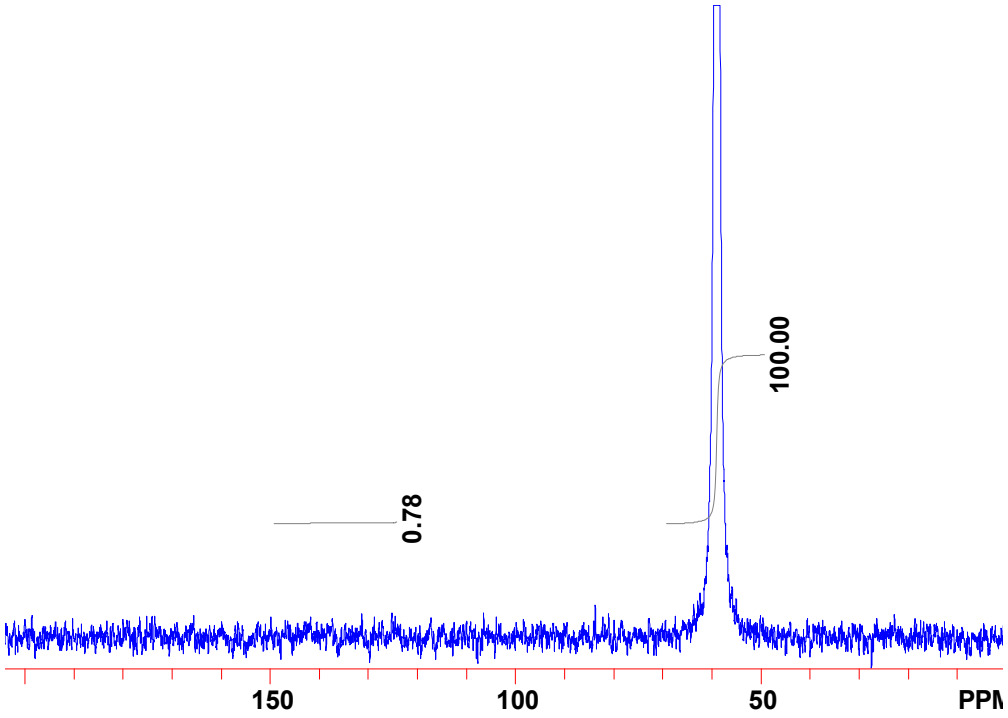

Figure 5-24: Latex 1, Centrifuged Sample #1—22°C. (NO PEAK EVIDENT)

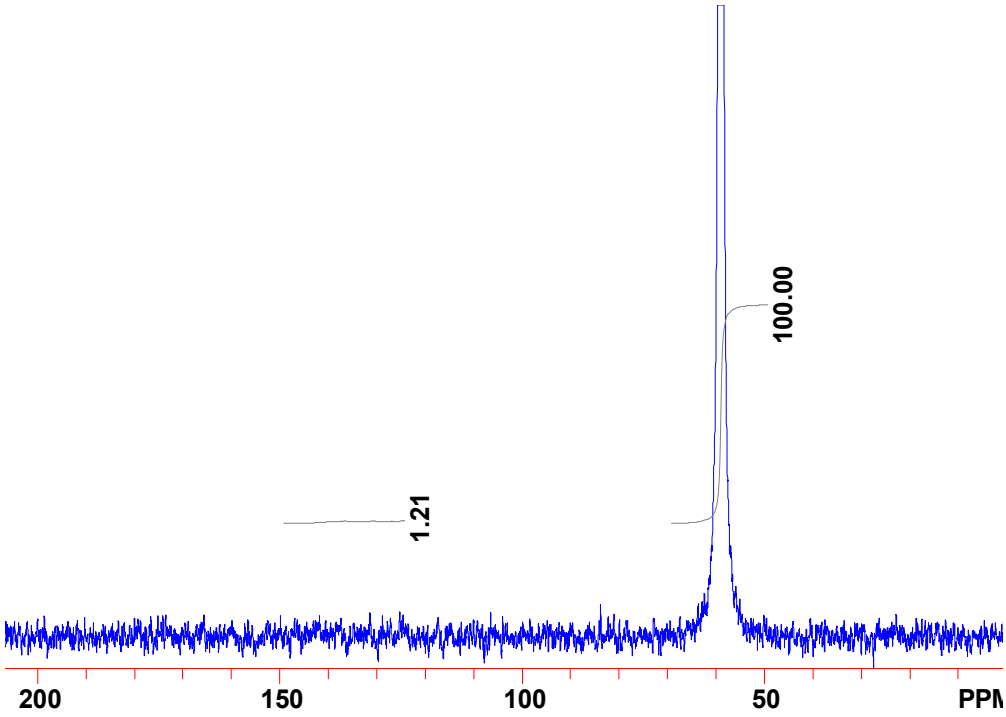

Figure 5-25: Latex 1, Centrifuged Sample #2—22°C. (NO PEAK EVIDENT)

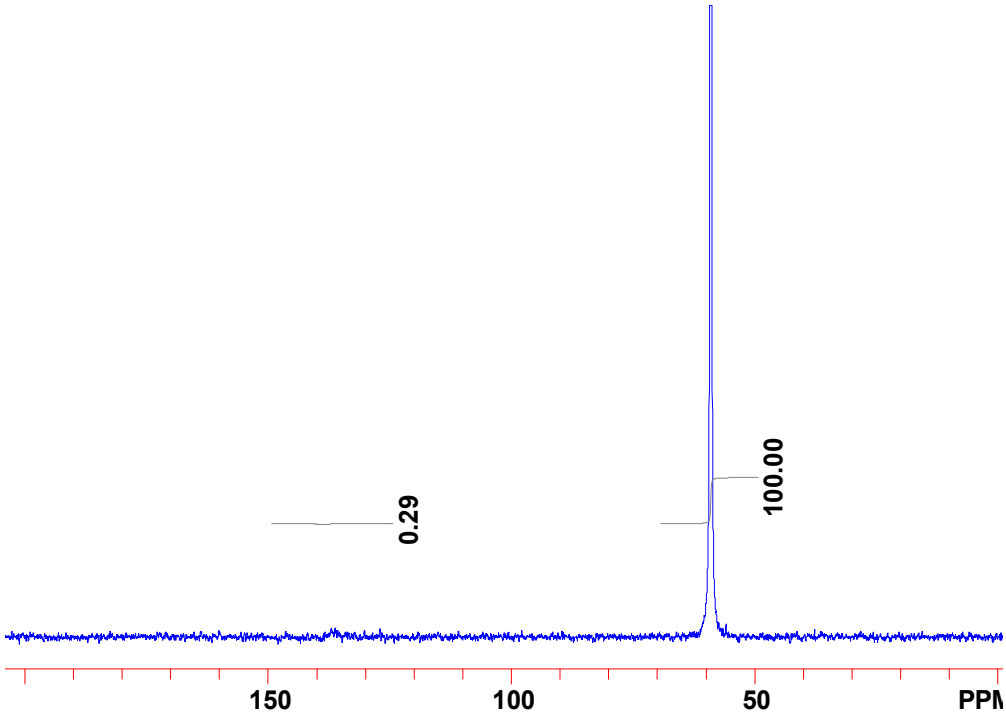

Figure 5-26: Latex 1, Centrifuged Sample #3—22°C.

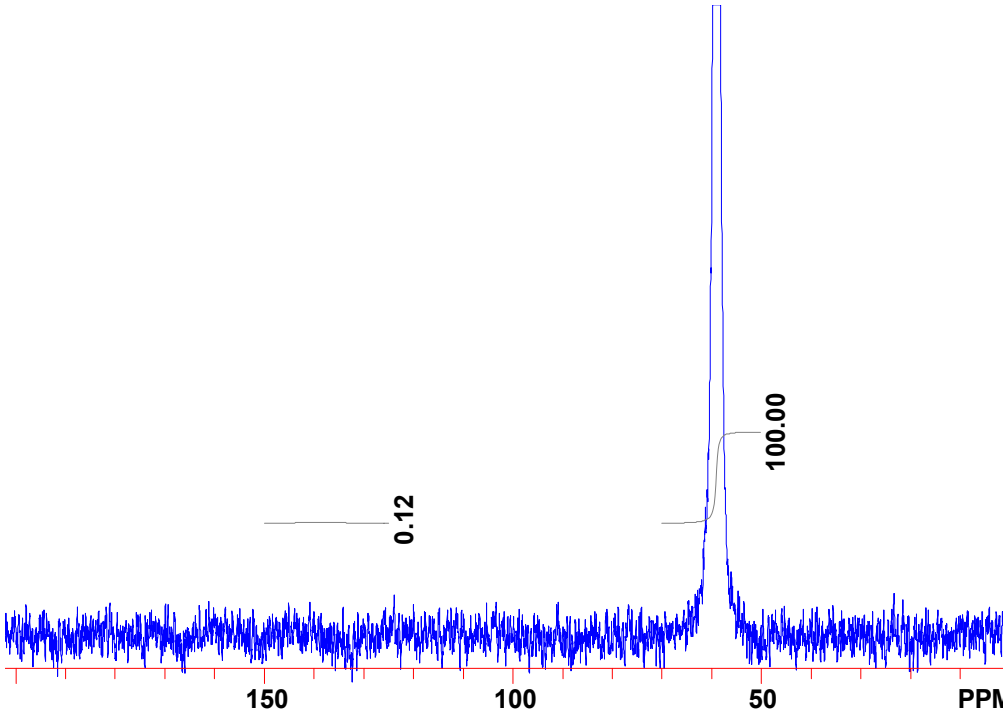

Figure 5-27: Latex 1, Centrifuged Sample #1—92°C. (NO PEAK EVIDENT)

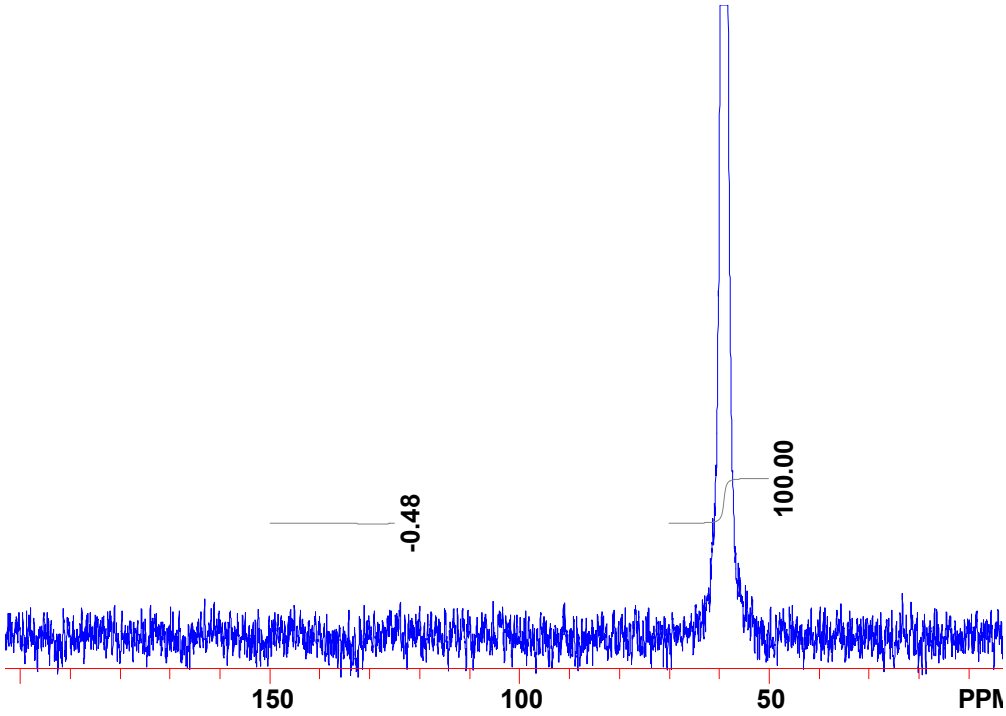

Figure 5-28: Latex 1, Centrifuged Sample #2—92°C. (NO PEAK EVIDENT)

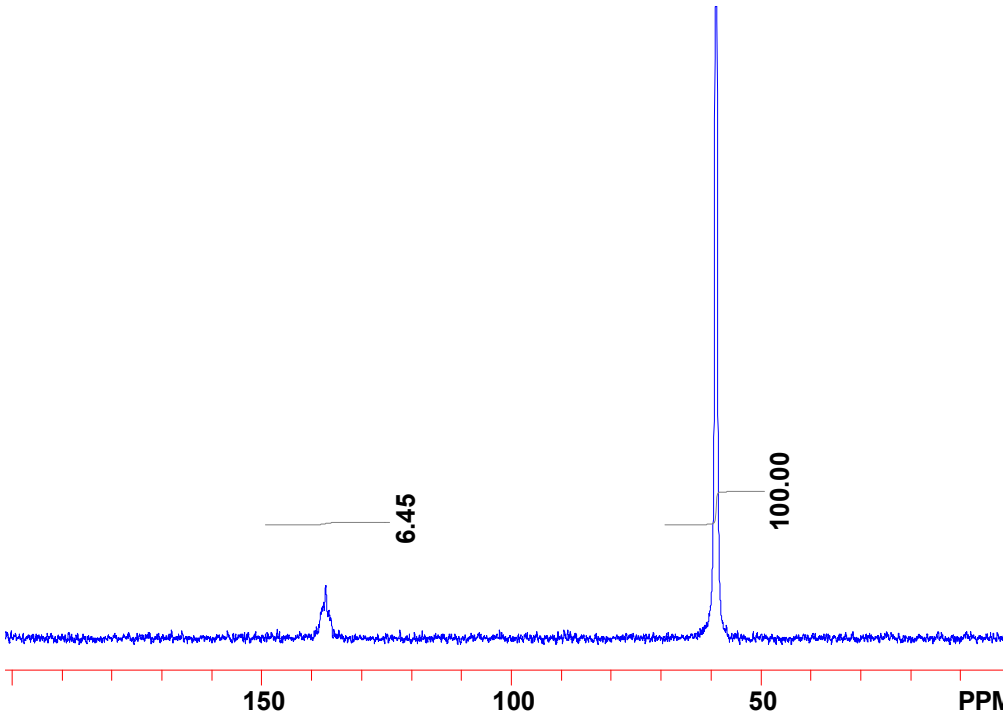

Figure 5-29: Latex 1, Dialyzed Sample #1—22°C.

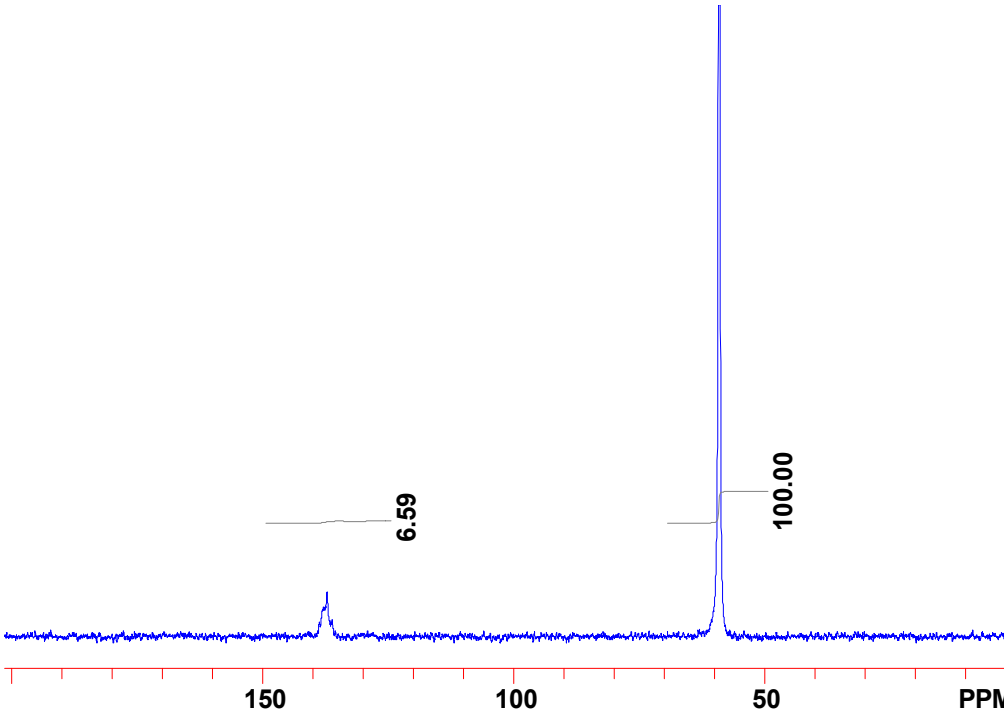

Figure 5-30: Latex 1, Dialyzed Sample #2—22°C.

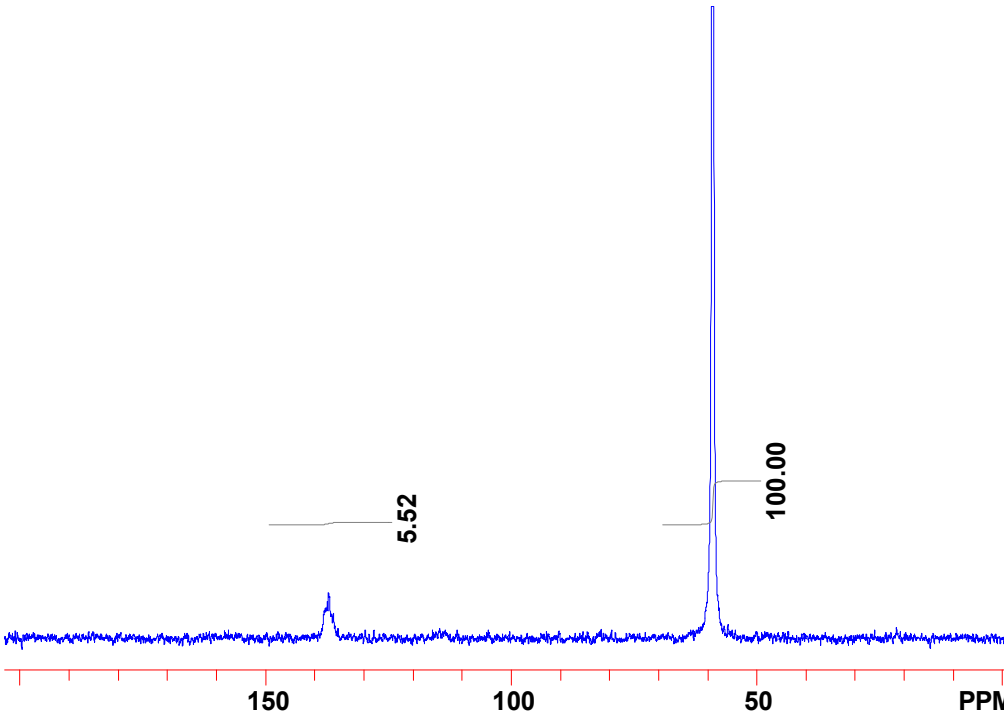

Figure 5-31: Latex 1, Dialyzed Sample #3—22°C.

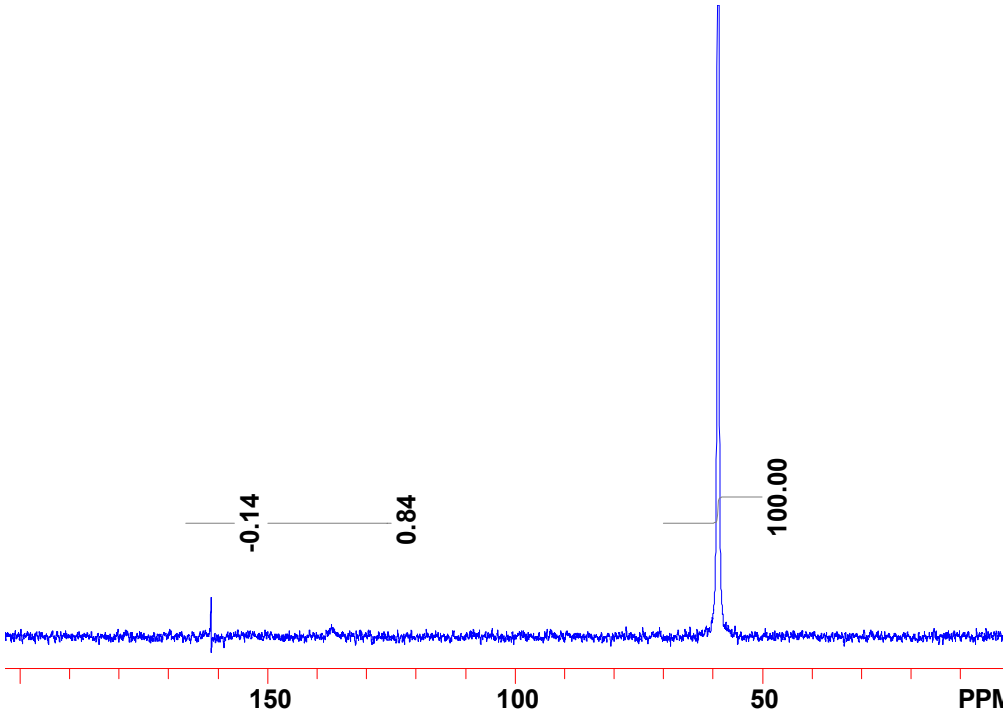

Figure 5-32: Latex 1, Dialyzed Sample #1—92°C. (Transmitter glitch at ~160 ppm, this is not a real peak).

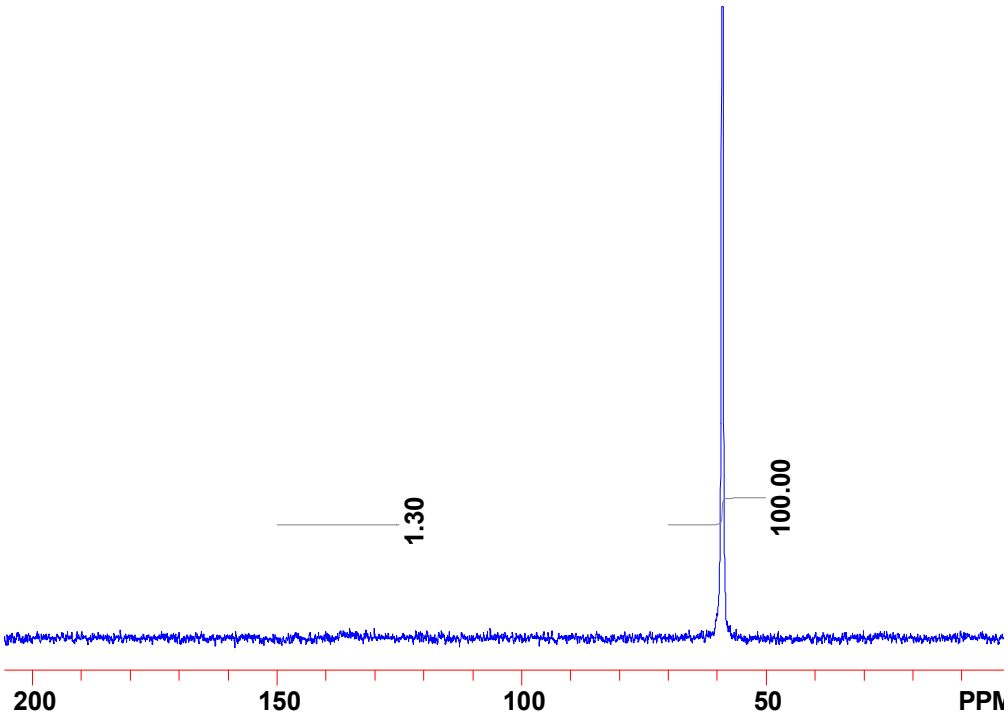

Figure 5-33: Latex 1, Dialyzed Sample #3—92°C.

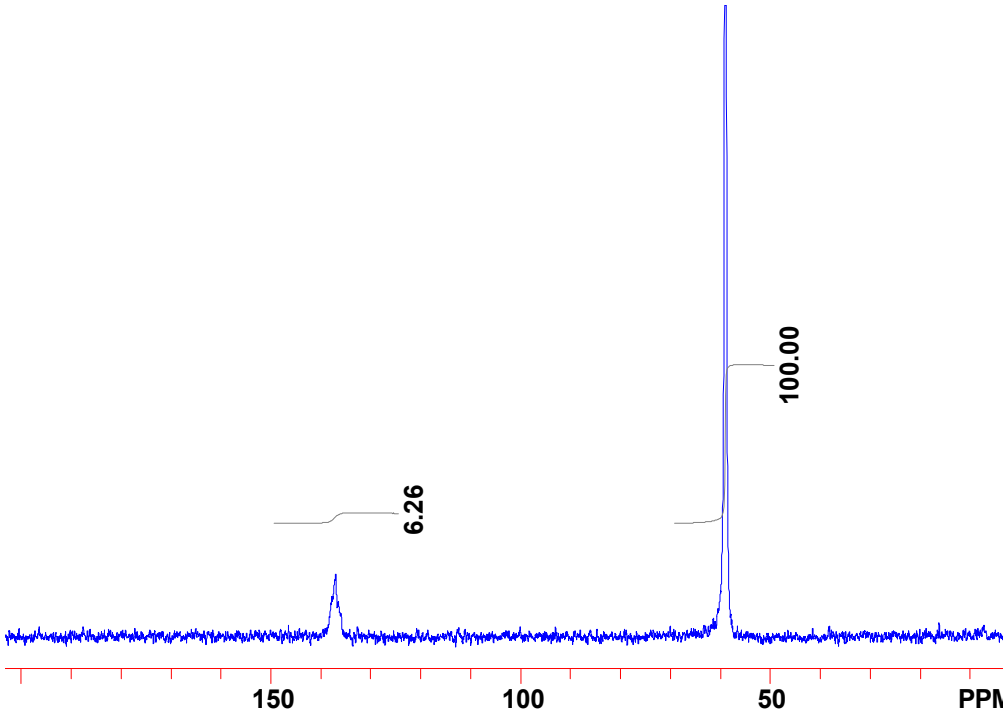

Figure 5-34: Latex 2, Untreated Sample #1—22°C.

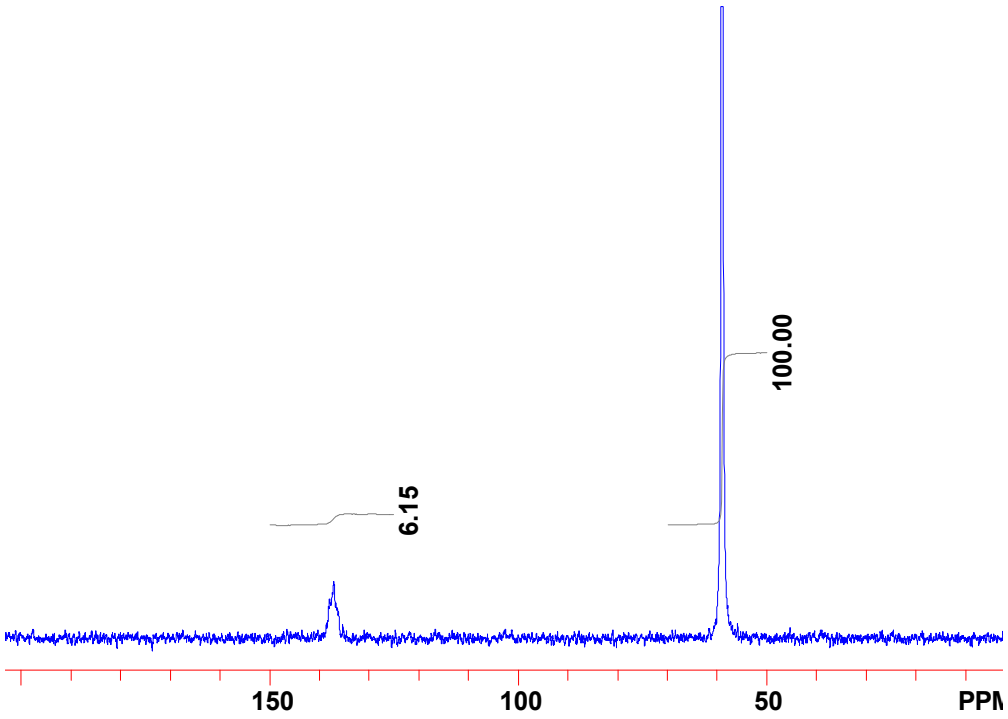

Figure 5-35: Latex 2, Untreated Sample #2—22°C.

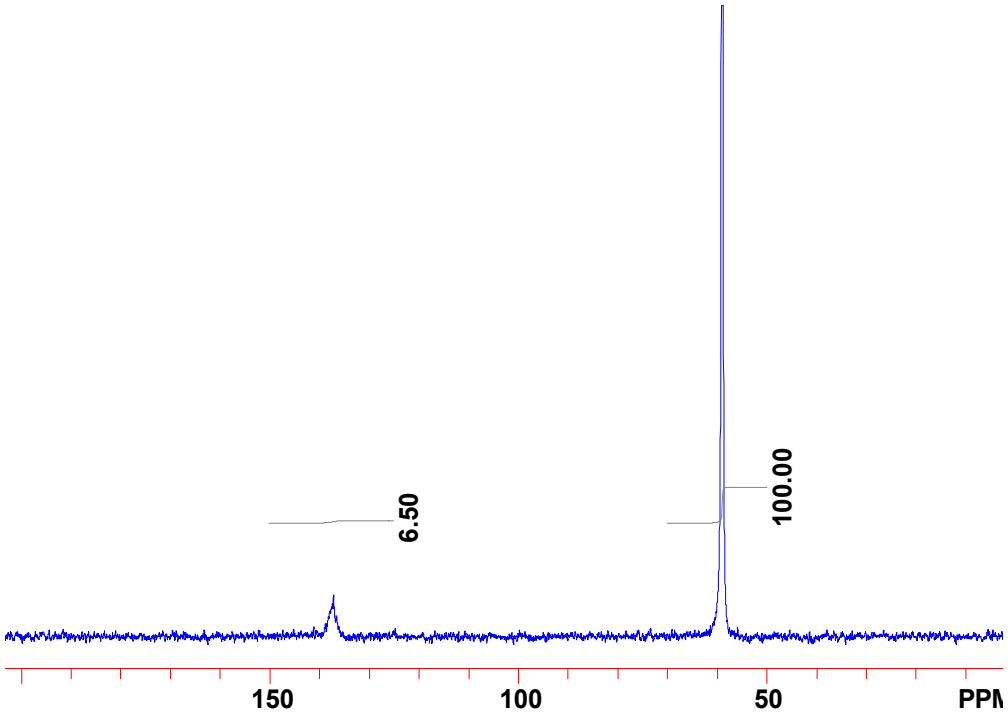

Figure 5-36: Latex 2, Untreated Sample #3—22°C.

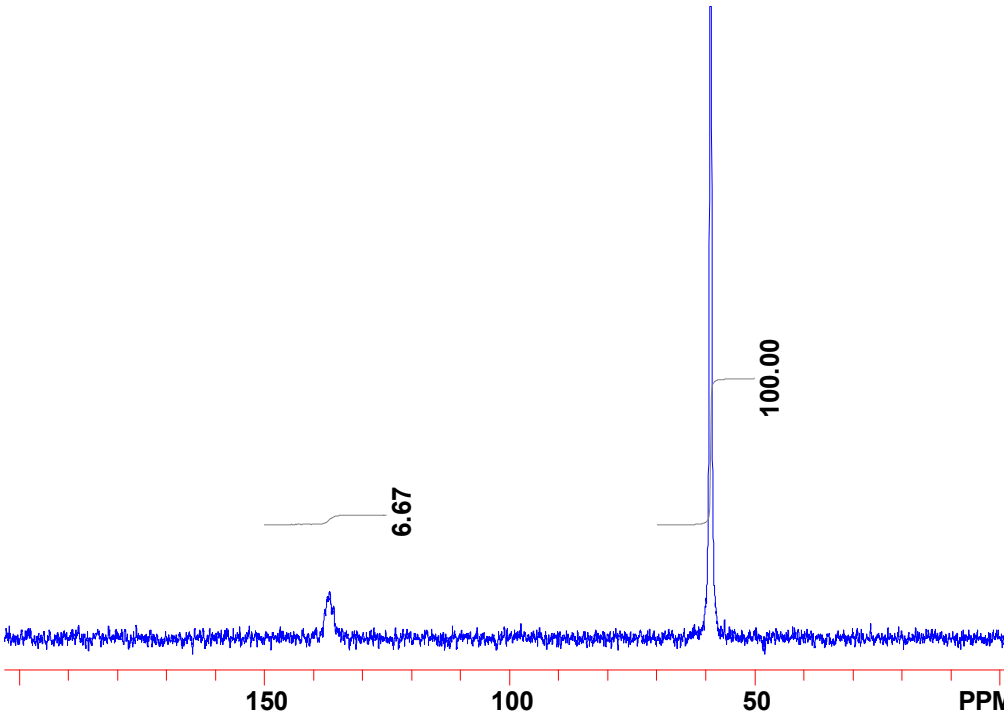

Figure 5-37: Latex 2, Untreated Sample #1—92°C.

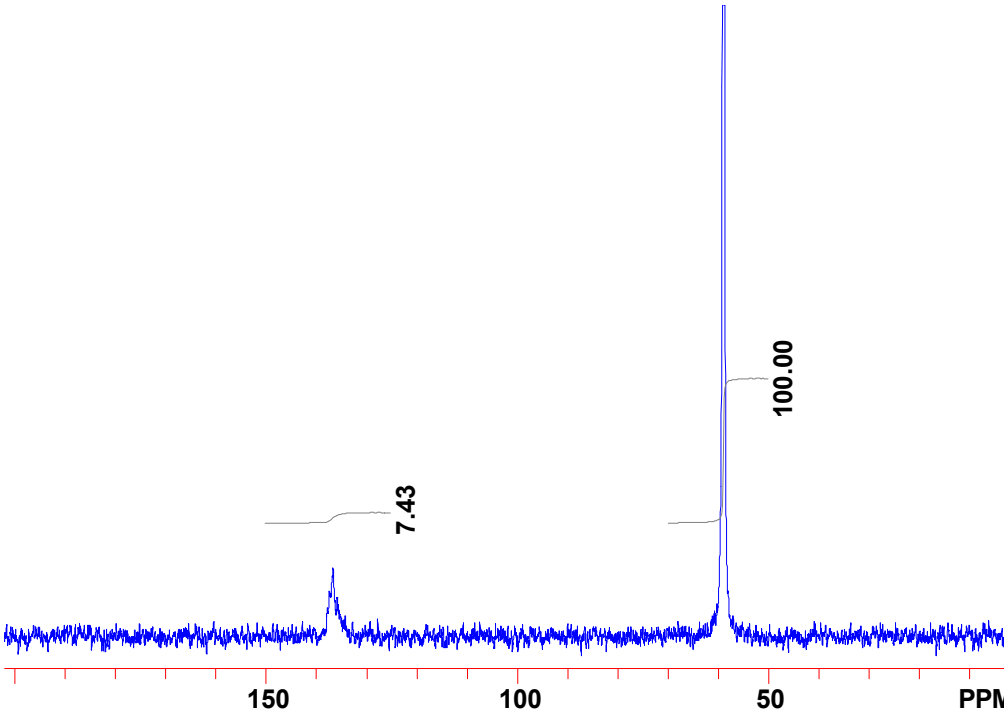

Figure 5-38: Latex 2, Untreated Sample #2—92°C.

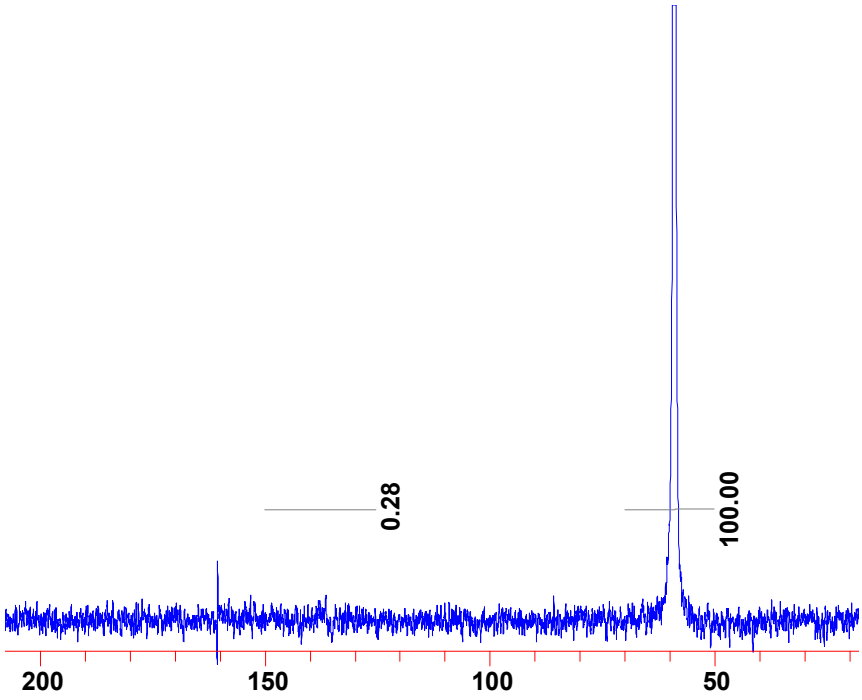

Figure 5-39: Latex 2, Centrifuged Sample #1—22°C. (Transmitter glitch at 160 ppm).

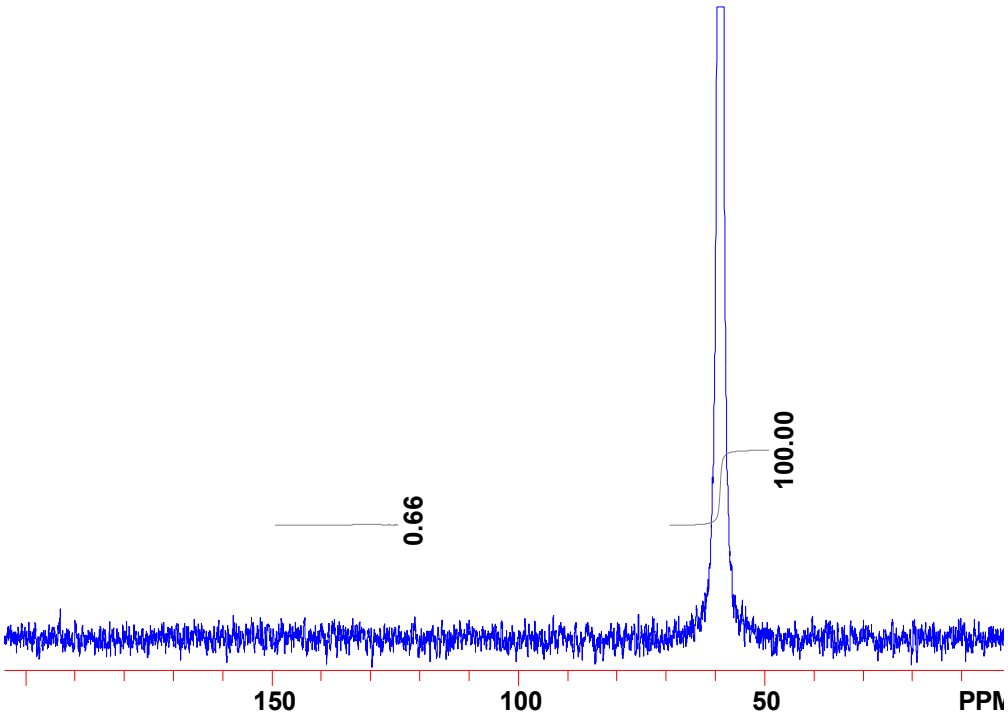

Figure 5-40: Latex 2, Centrifuged Sample #2—22°C. (NO PEAK EVIDENT)

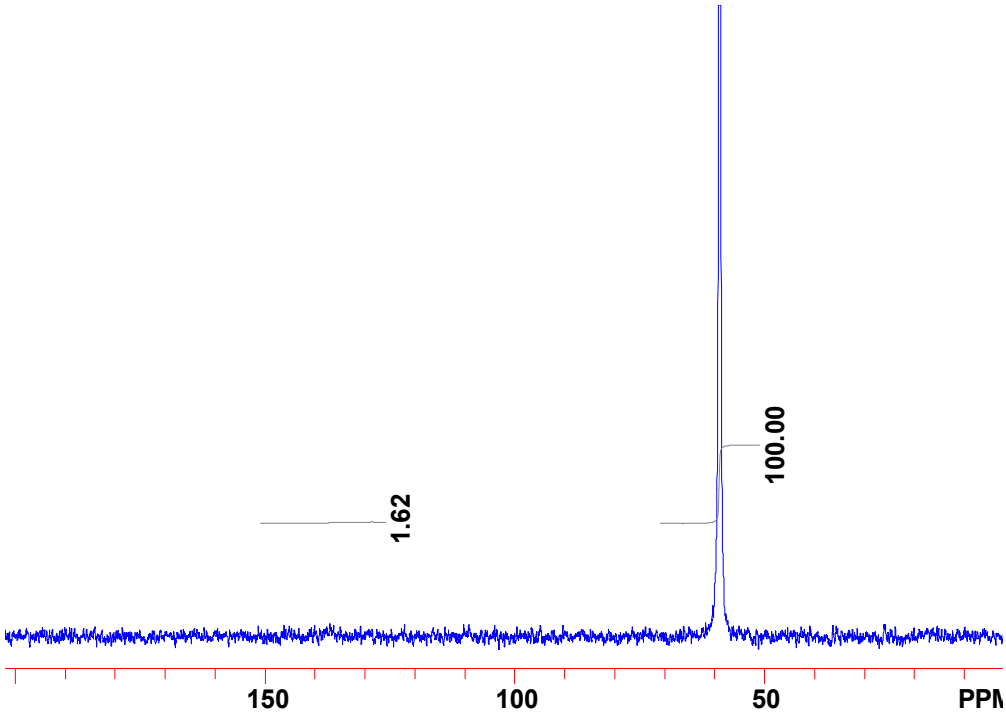

Figure 5-41: Latex 2, Centrifuged Sample #1—92°C.

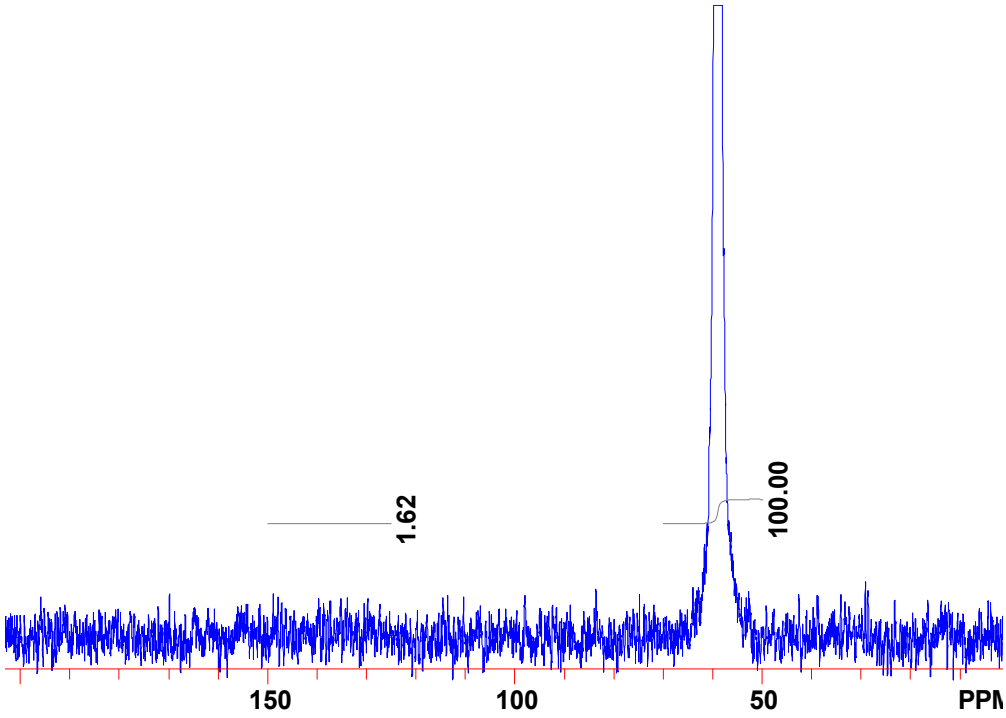

Figure 5-42: Latex 2, Centrifuged Sample #2—92°C.

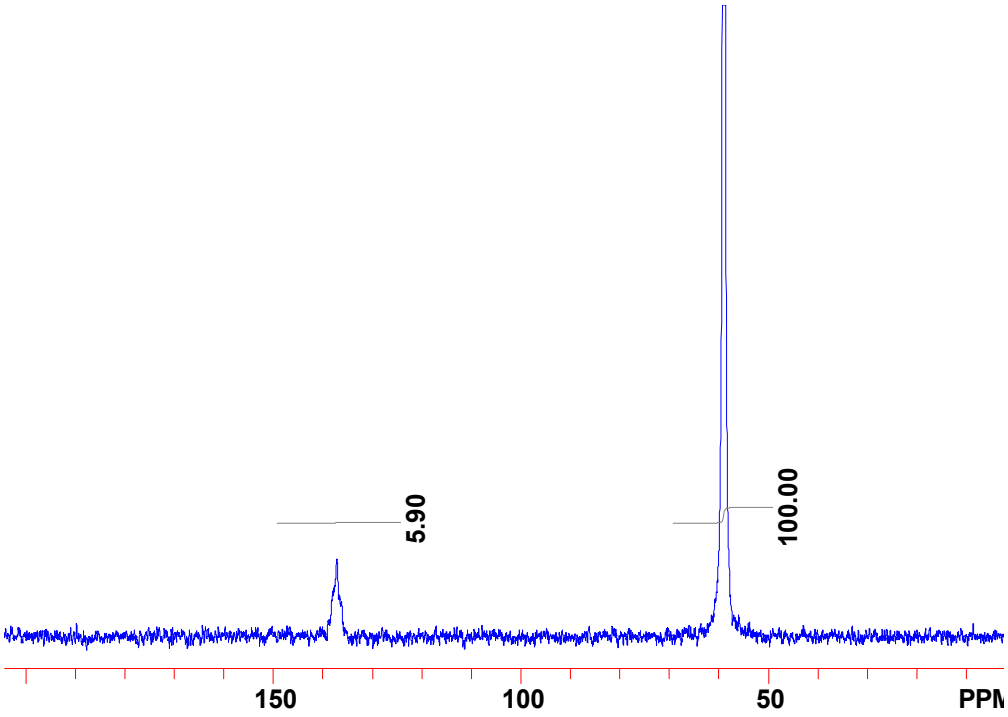

Figure 5-43: Latex 2, Dialyzed Sample #2—22°C.

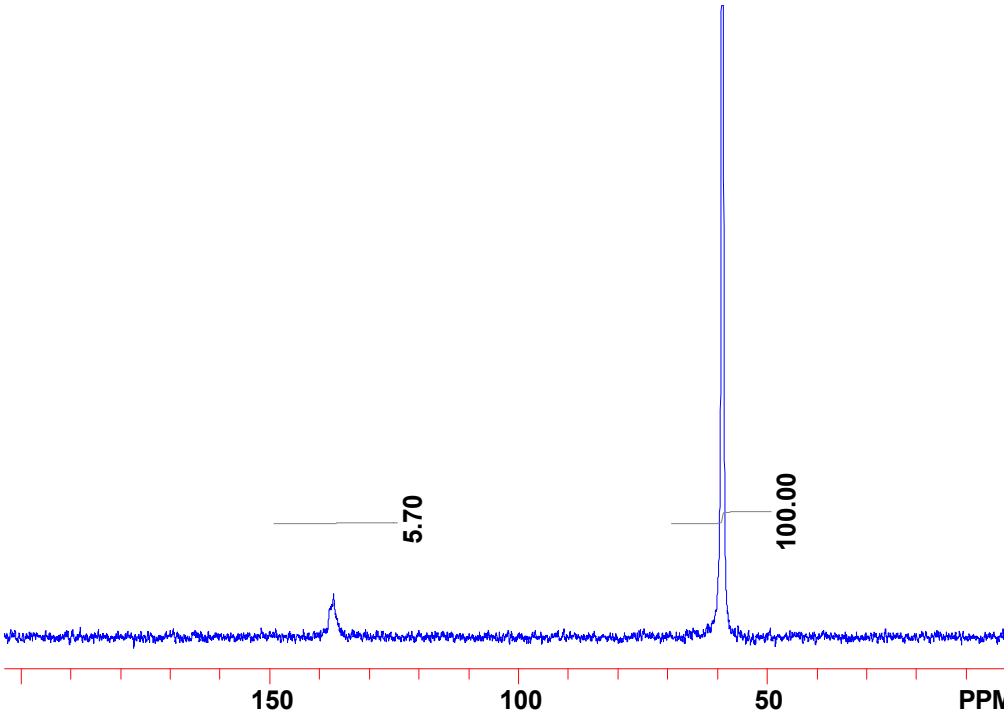

Figure 5-44: Latex 2, Dialyzed Sample #1—22°C.

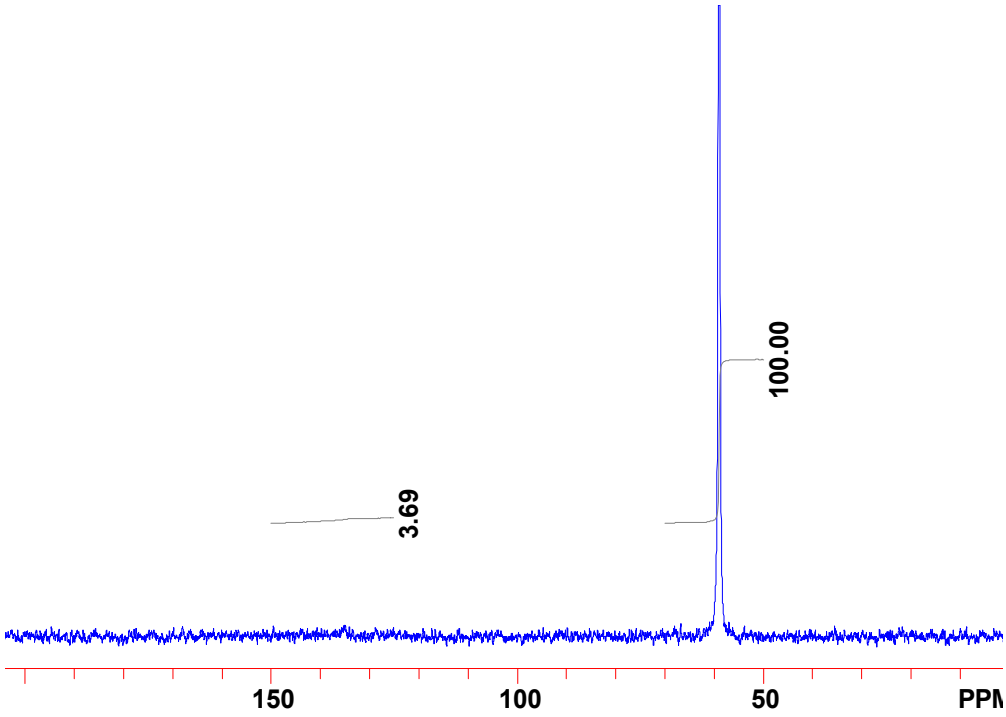

Figure 5-45: Latex 2, Dialyzed Sample #1—92°C.

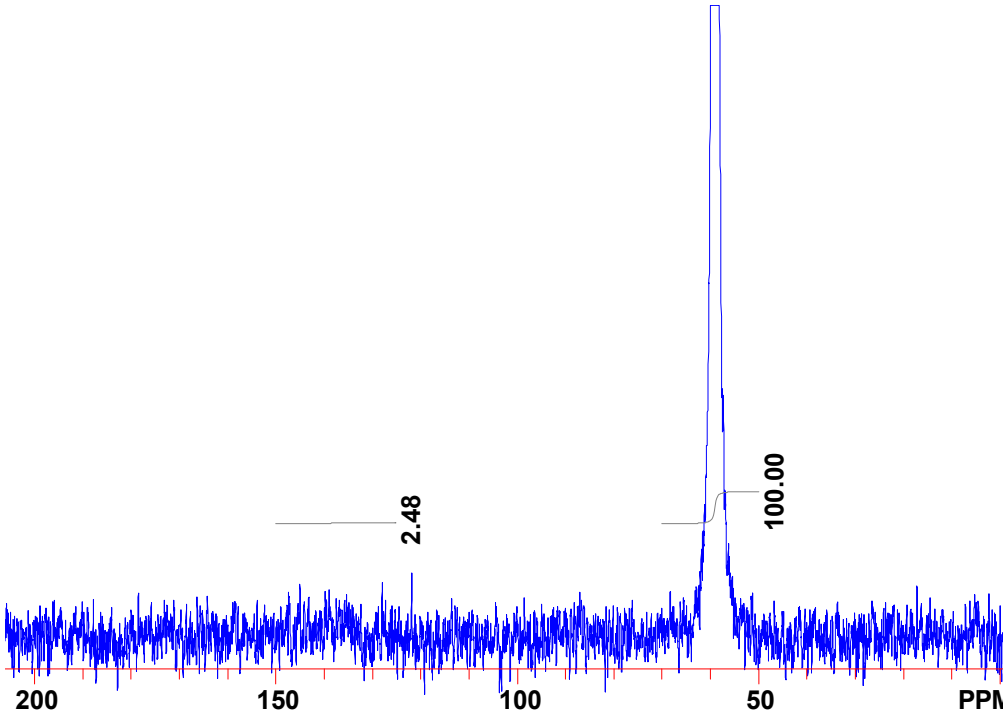

Figure 5-46: Latex 2, Dialyzed Sample #2—92°C.

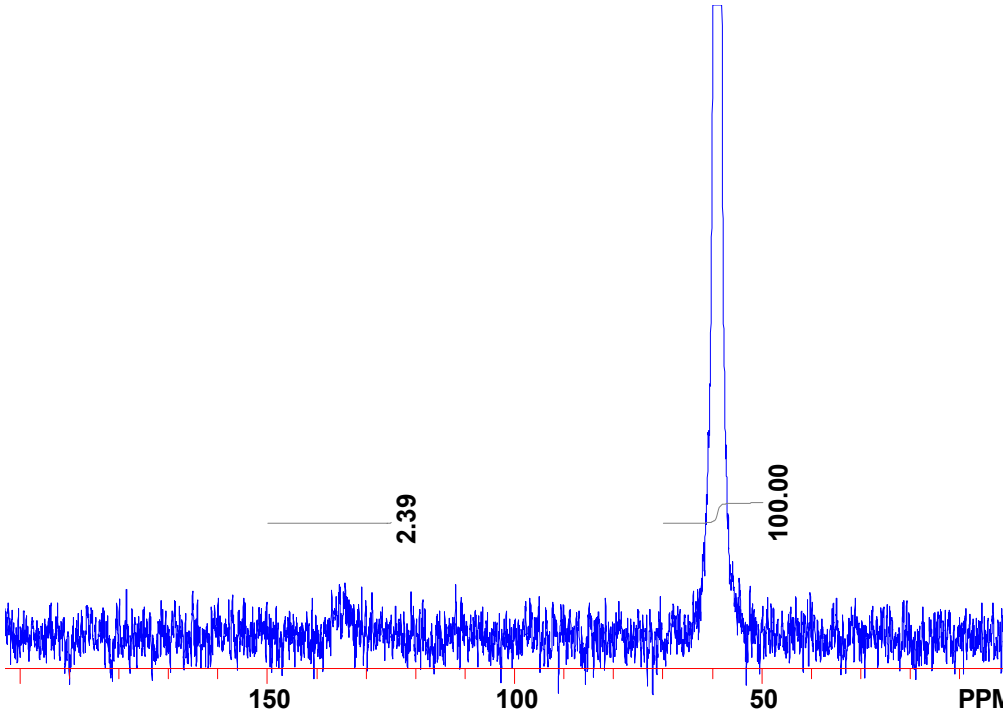

Figure 5-47: Latex 2, Dialyzed Sample #3—92°C.

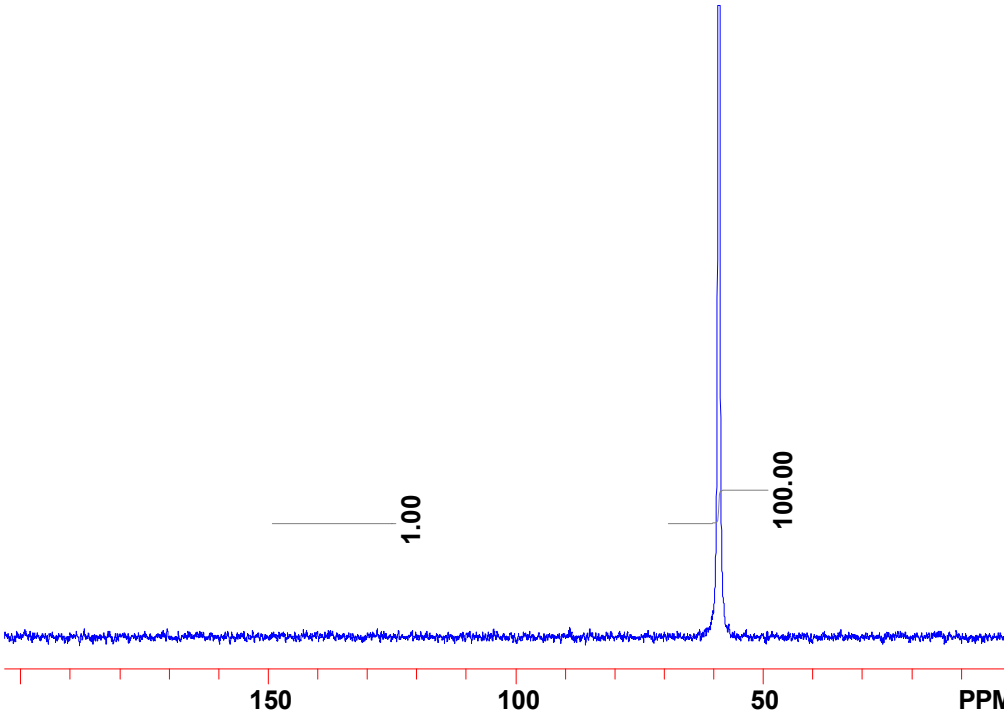

Figure 5-48: Latex 3, Untreated Sample #1—22°C.

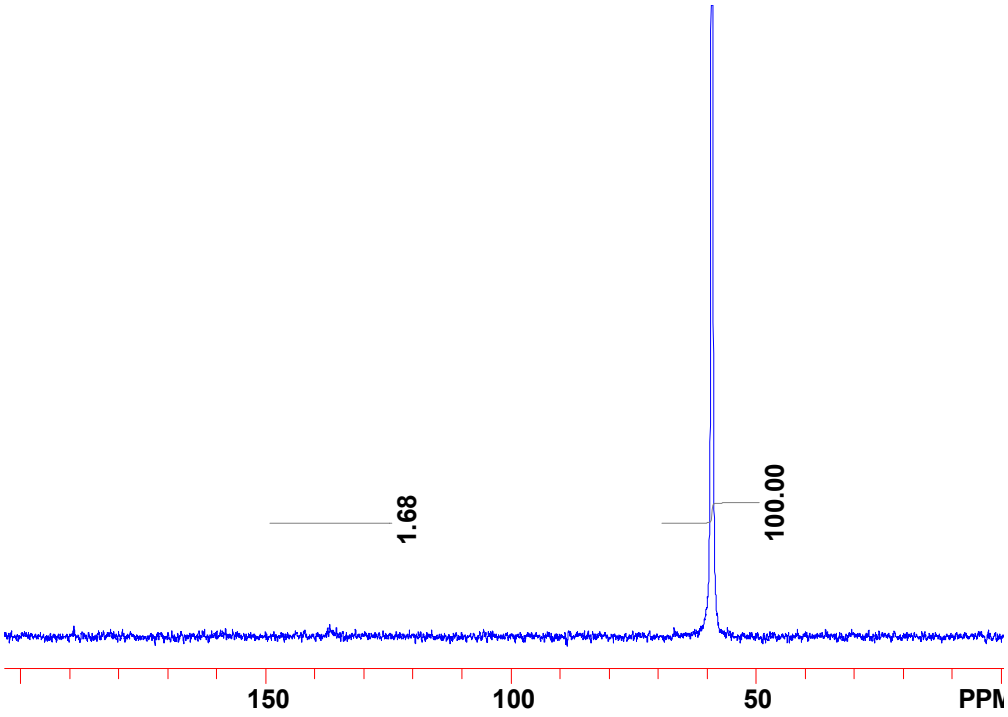

Figure 5-49: Latex 3, Untreated Sample #2—22°C.

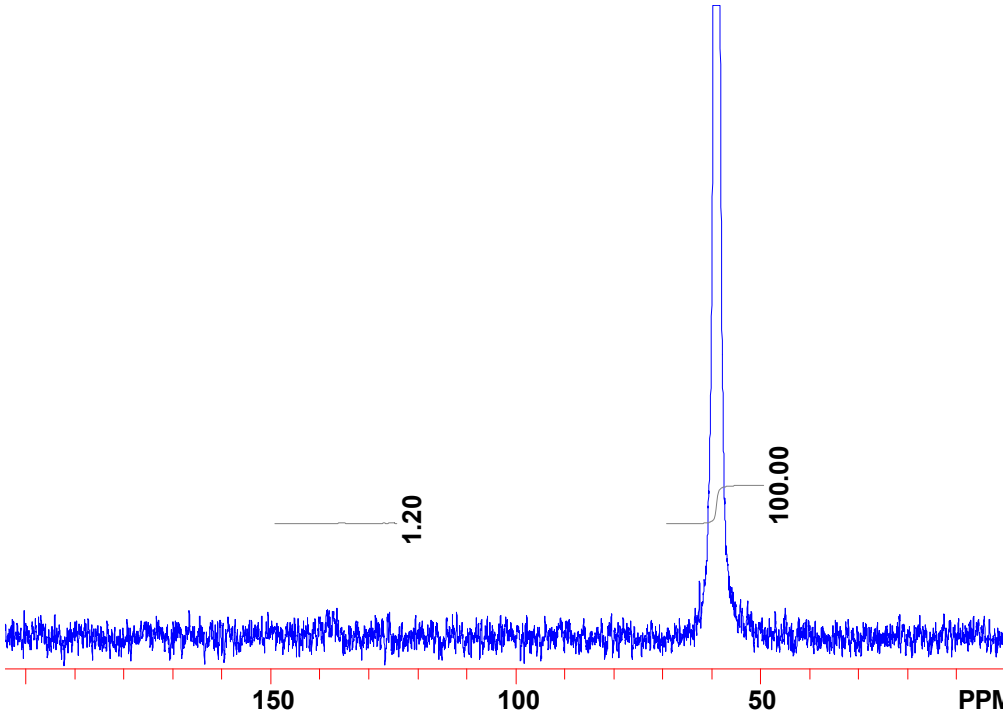

Figure 5-50: Latex 3, Untreated Sample #3—22°C.

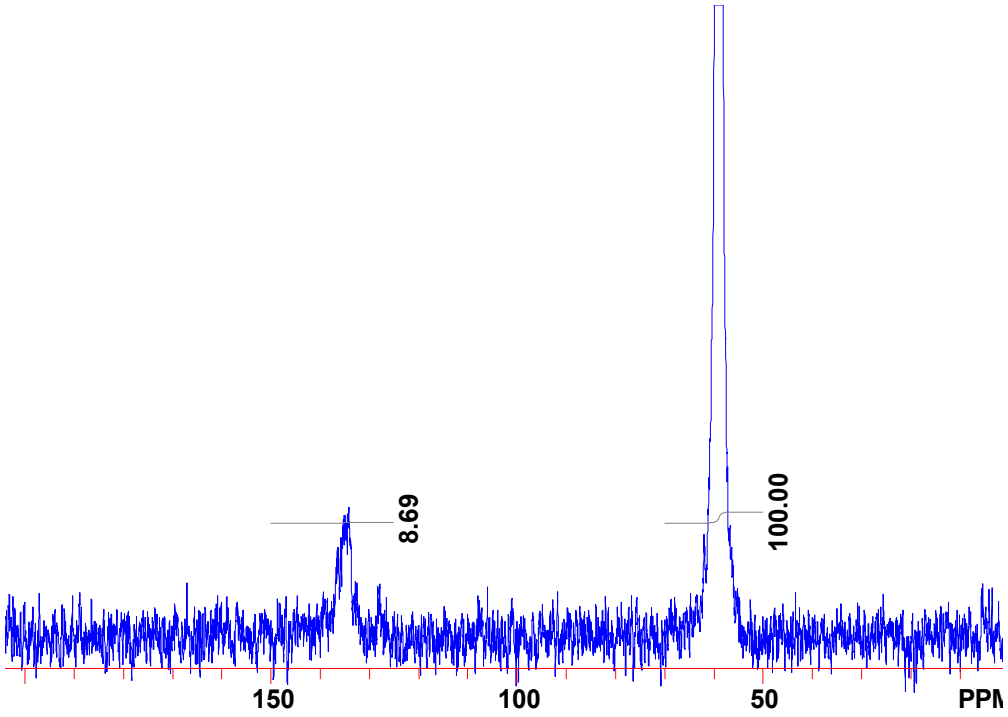

Figure 5-51: Latex 3, Untreated Sample #3—92°C.

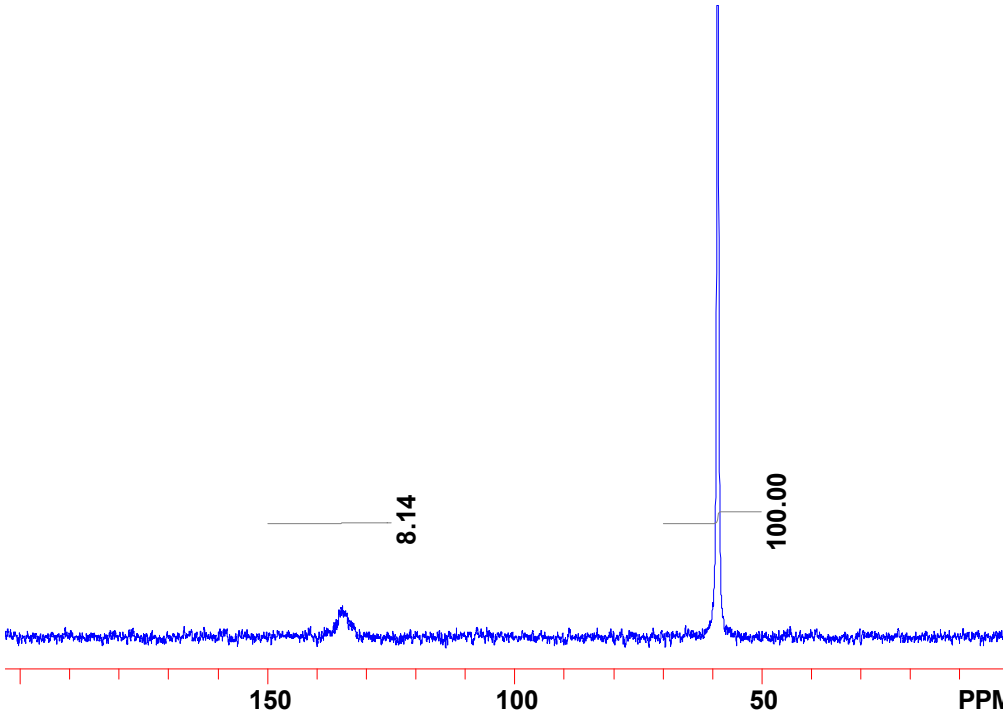

Figure 5-52: Latex 3, Untreated Sample #2—92°C.

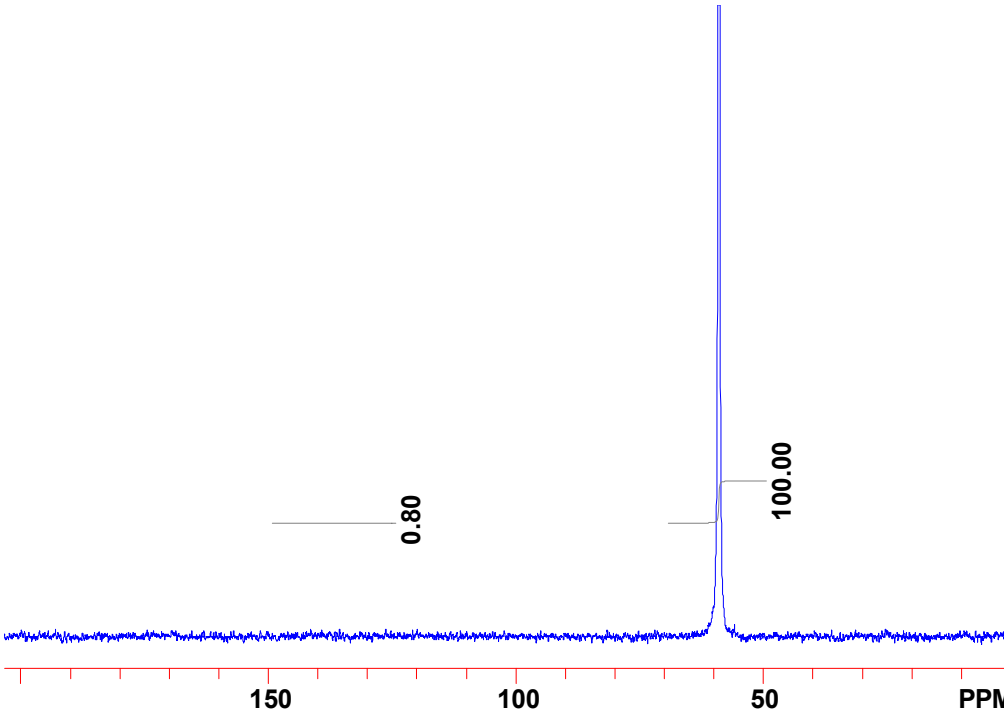

Figure 5-53: Latex 3, Centrifuged Sample #1—22°C. (NO PEAK EVIDENT)

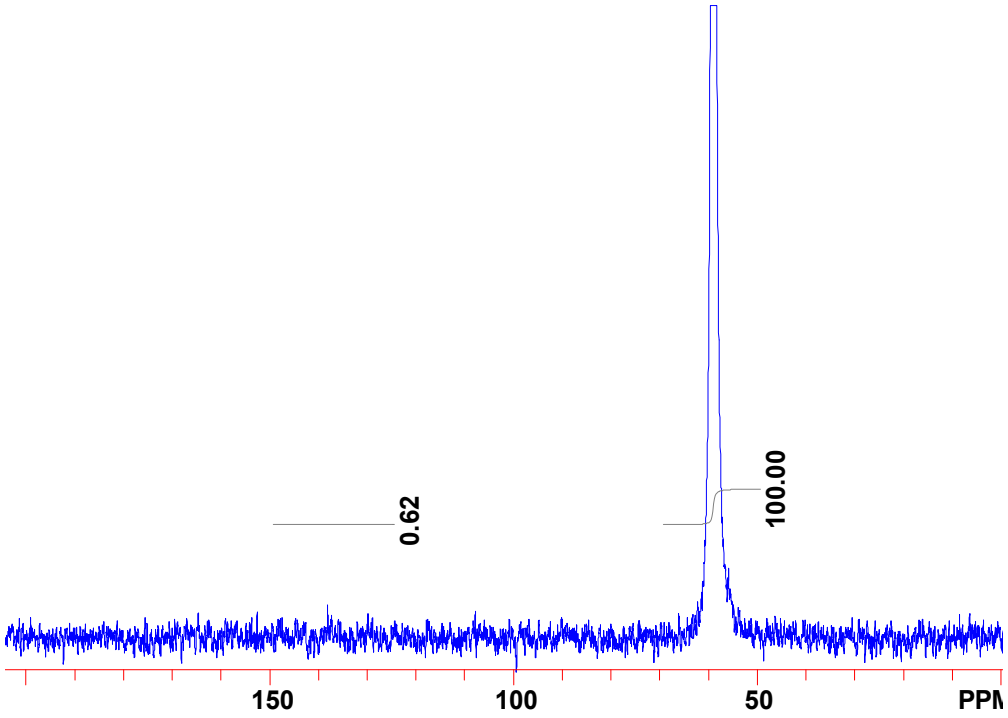

Figure 5-54: Latex 3, Centrifuged Sample #2—22°C.

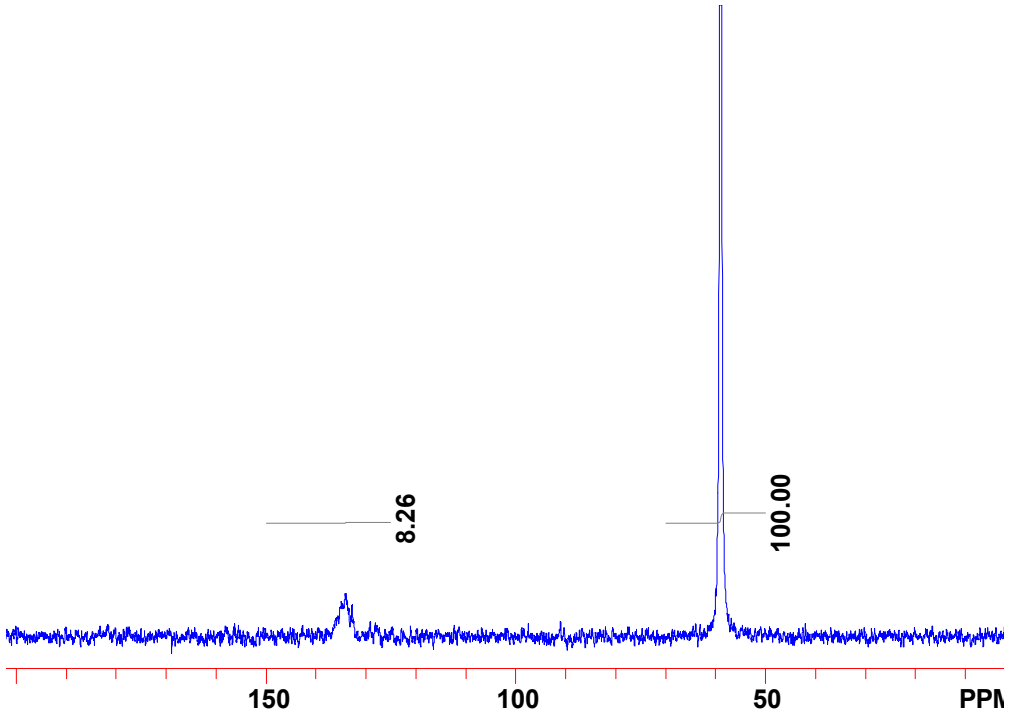

Figure 5-55: Latex 3, Centrifuged Sample #1—92°C.

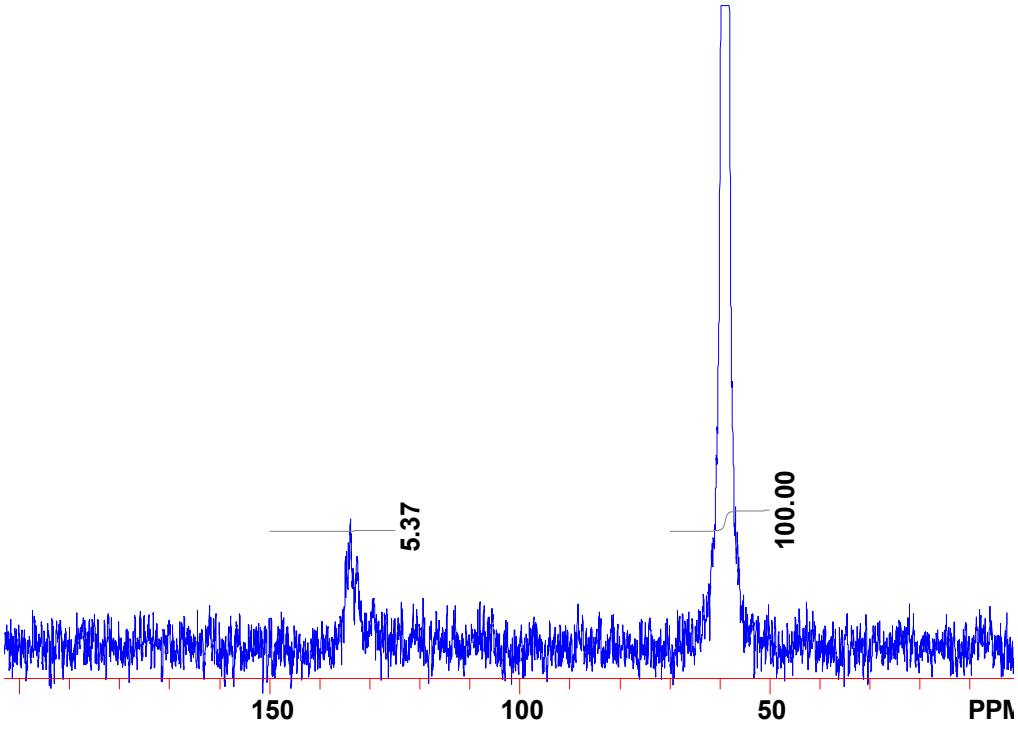

Figure 5-56: Latex 3, Centrifuged Sample #2—92°C.

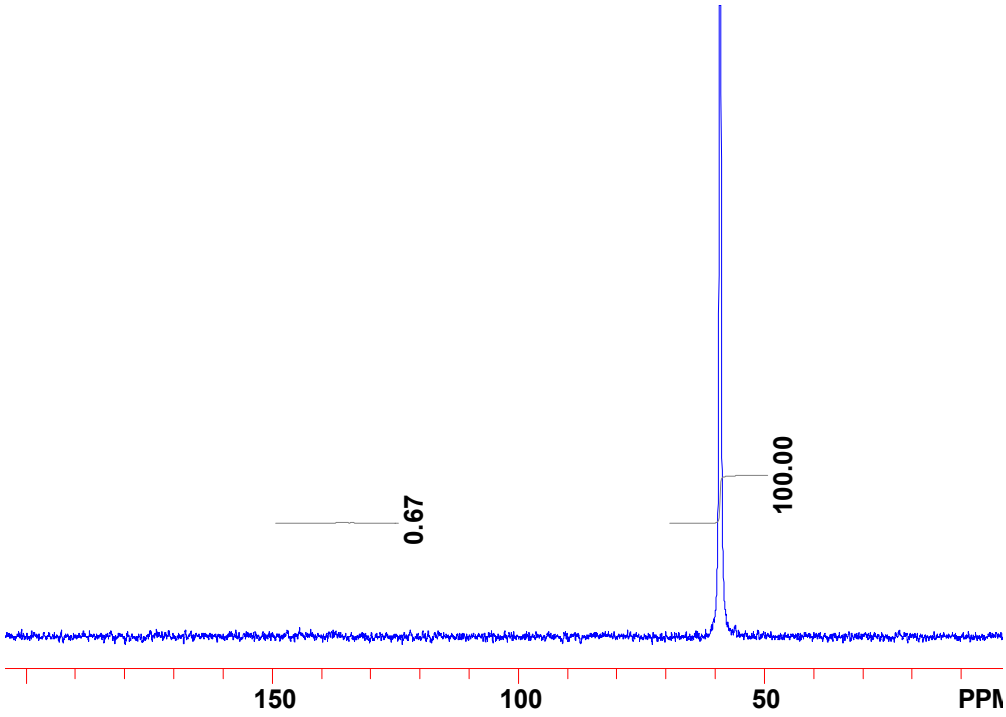

Figure 5-57: Latex 3, Dialyzed Sample #1—22°C.

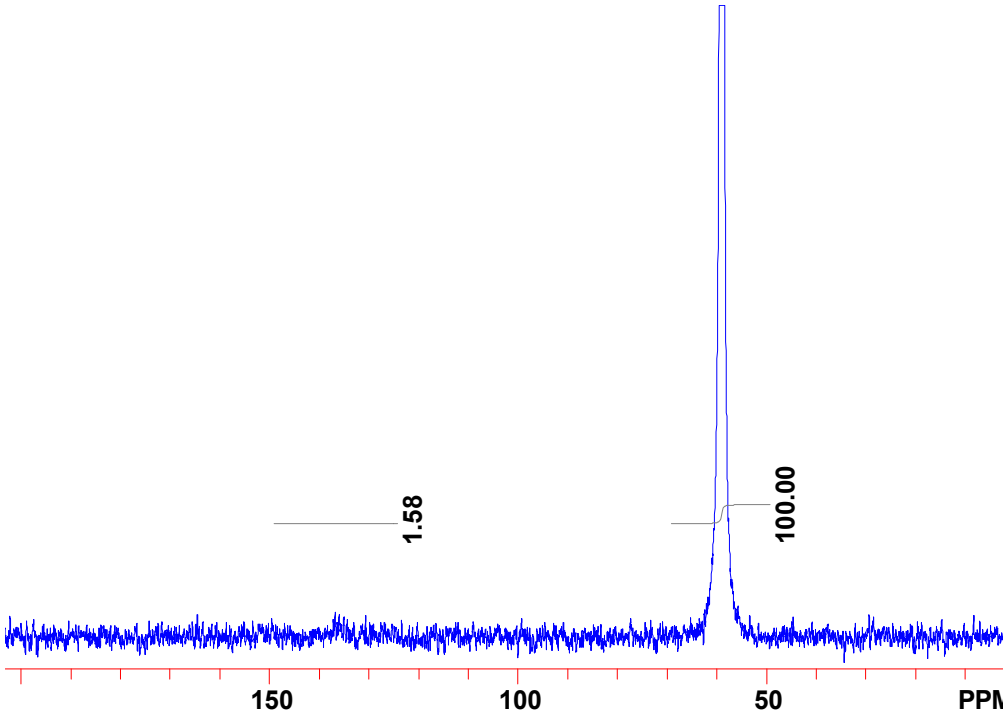

Figure 5-58: Latex 3, Dialyzed Sample #2—22°C.

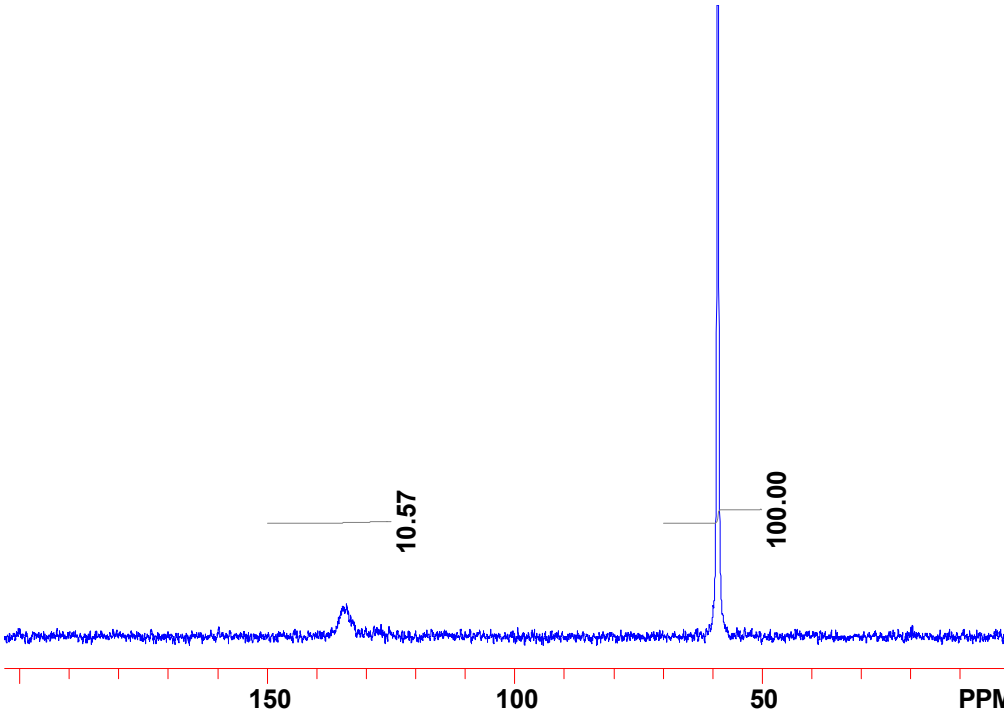

Figure 5-59: Latex 3, Dialyzed Sample #1—92°C.

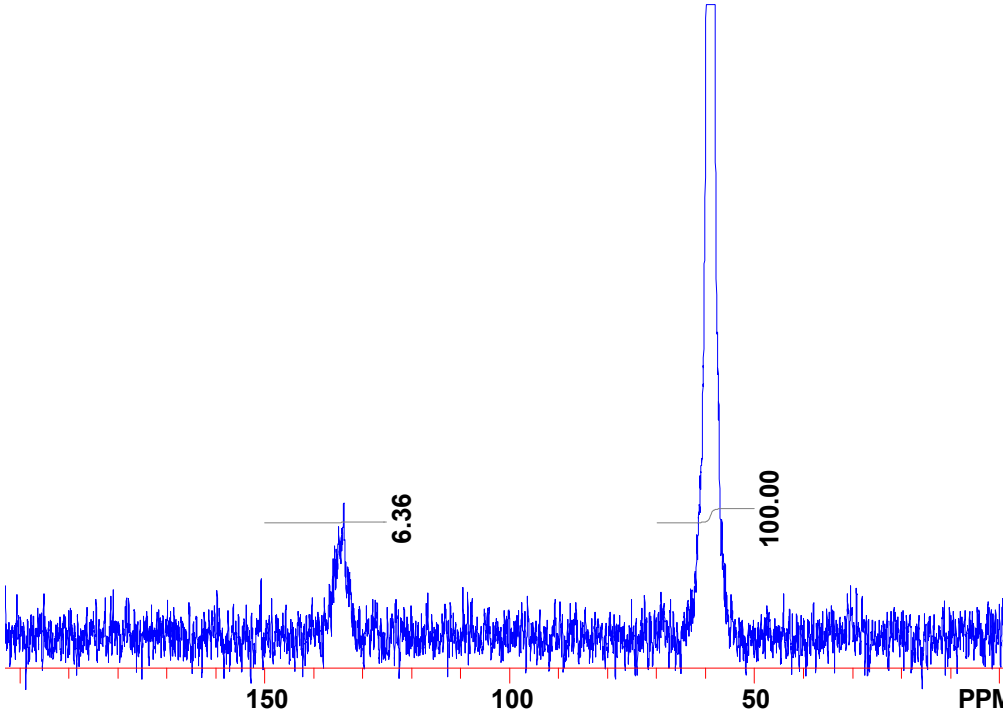

Figure 5-60: Latex 3, Dialyzed Sample #2—92°C.

5.7.3 ^{13}C-NMR Results

All samples in D_2O. Pertinent information regarding each sample is listed in the caption. Sample numbers correspond with data in Table 5-2.

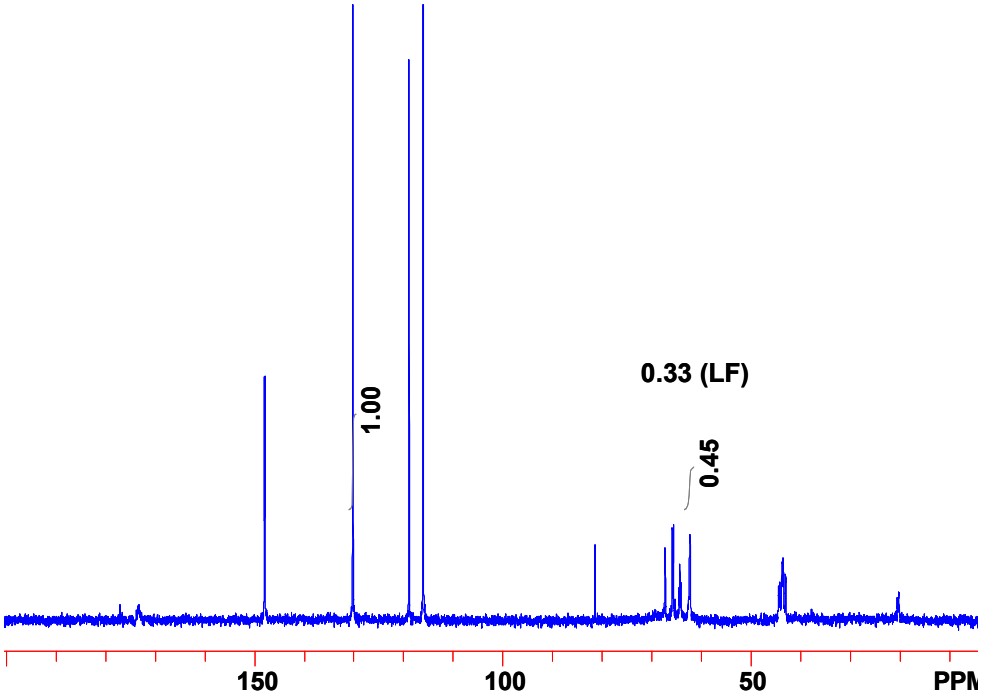

Figure 5-61: ^{13}C-NMR Latex 3, Untreated Sample #1—22°C.

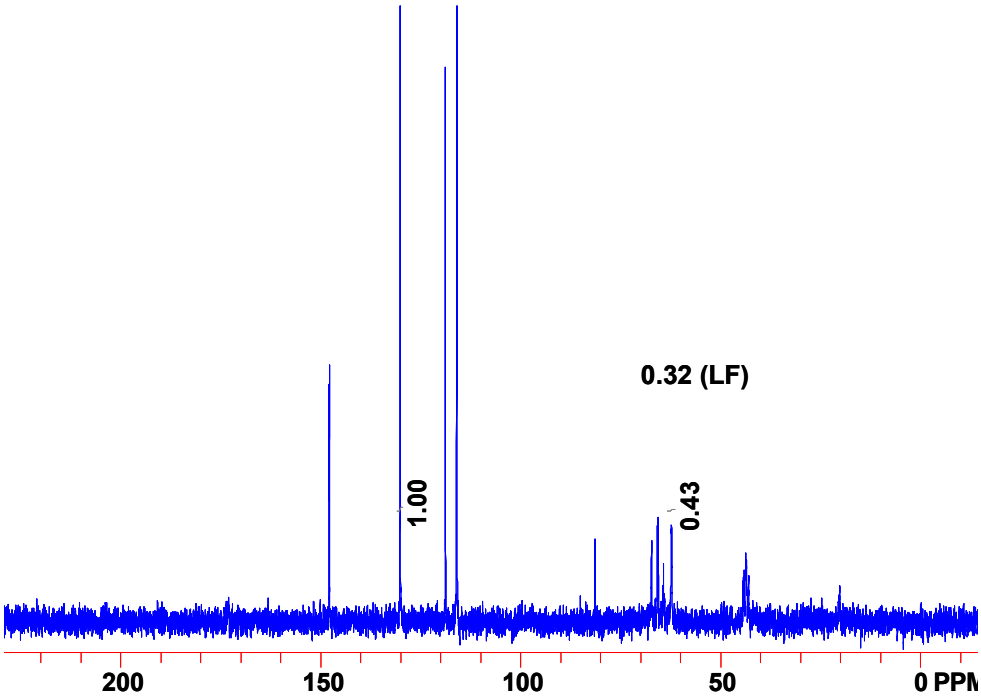

Figure 5-62: ^{13}C-NMR Latex 3, Untreated Sample #2—22°C.

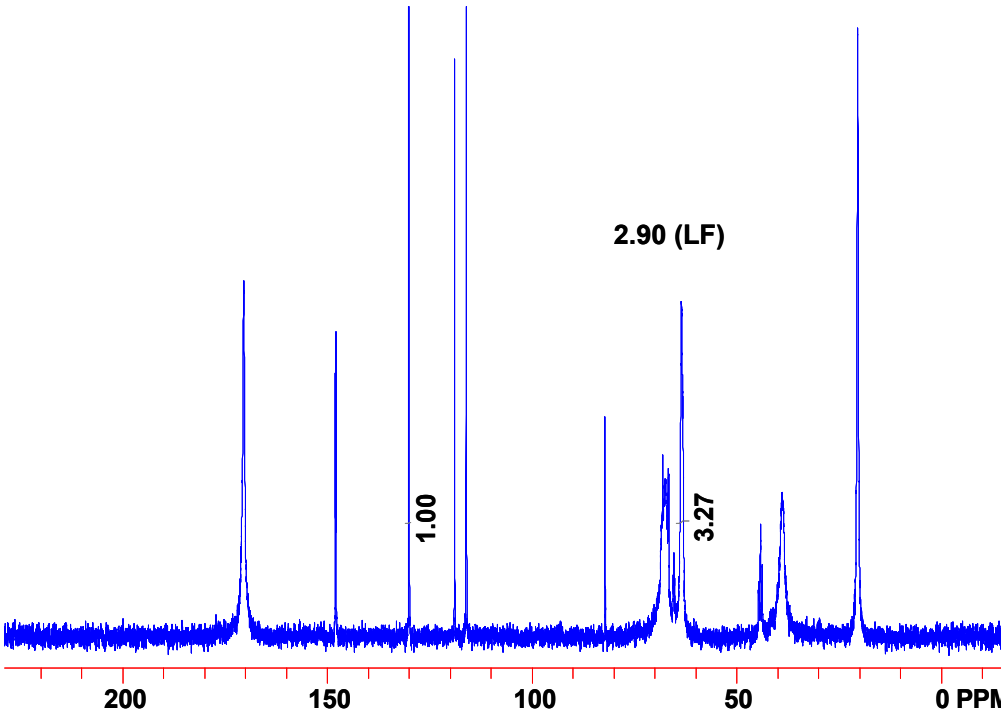

Figure 5-63: ^{13}C-NMR Latex 3, Untreated Sample #1—92°C.

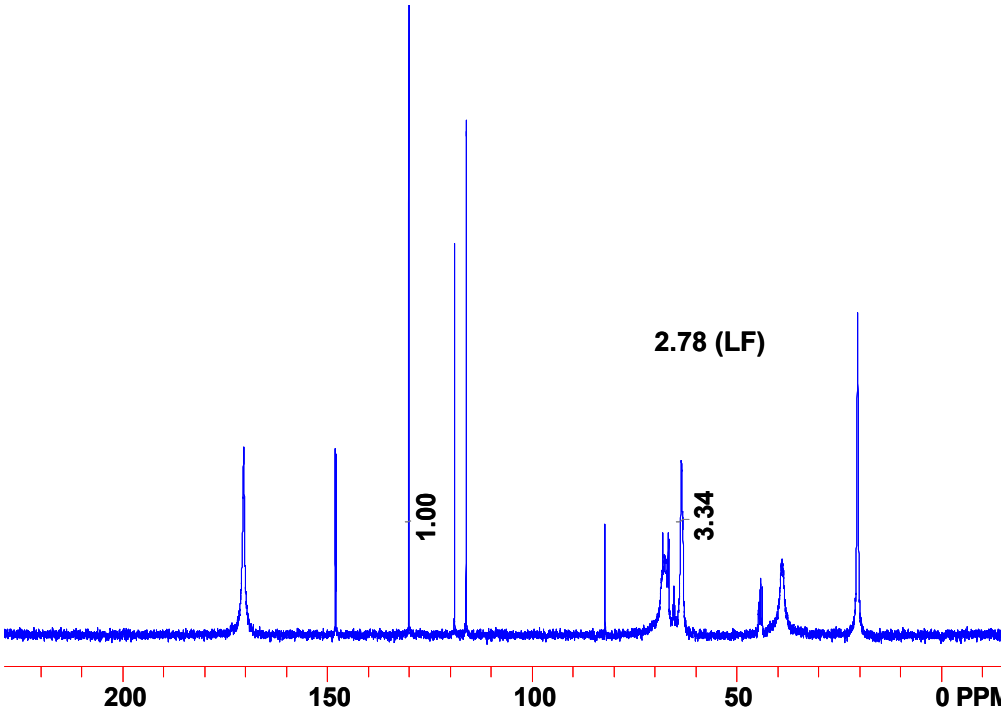

Figure 5-64: ^{13}C-NMR Latex 3, Untreated Sample #3—92°C.

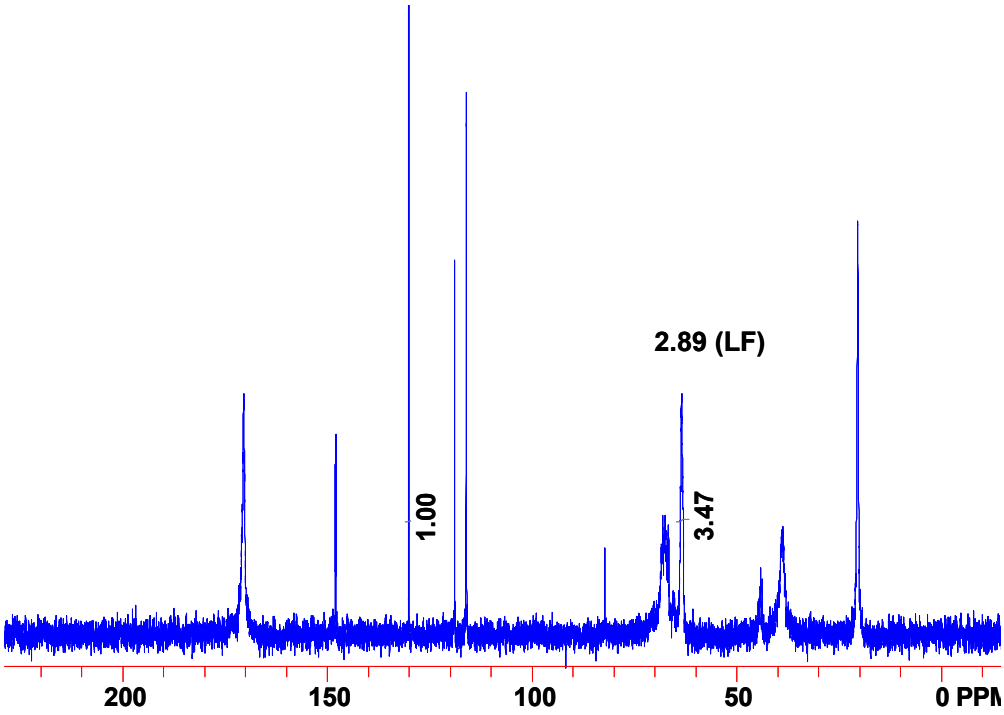

Figure 5-65: ^{13}C-NMR Latex 3, Untreated Sample #2—92°C.

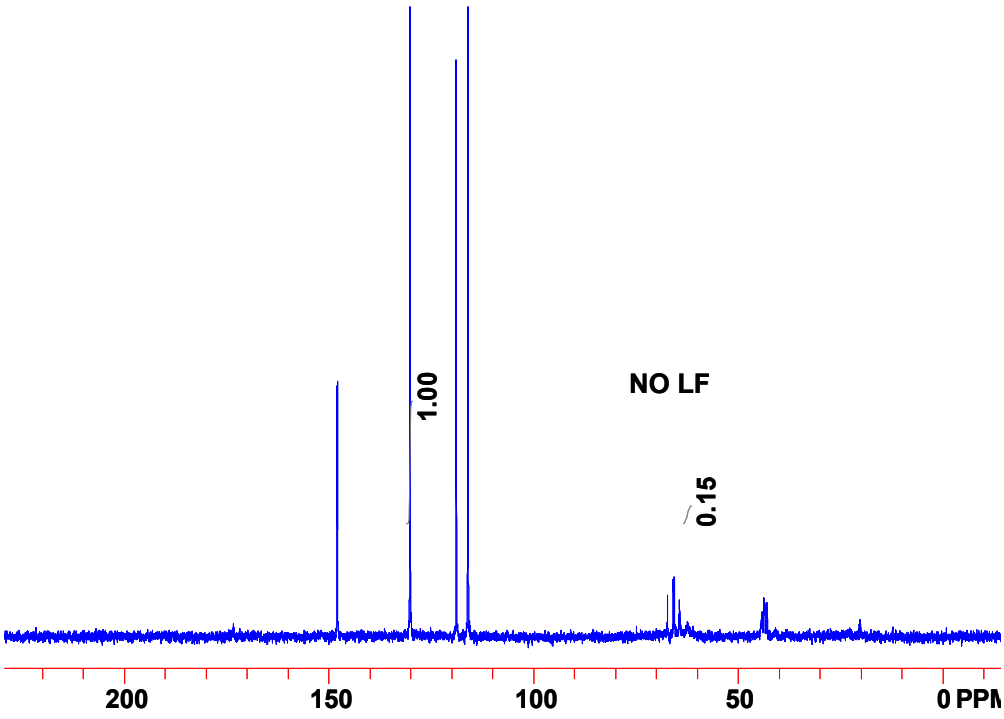

Figure 5-66: ^{13}C-NMR Latex 3, Centrifuged Sample #1—22°C.

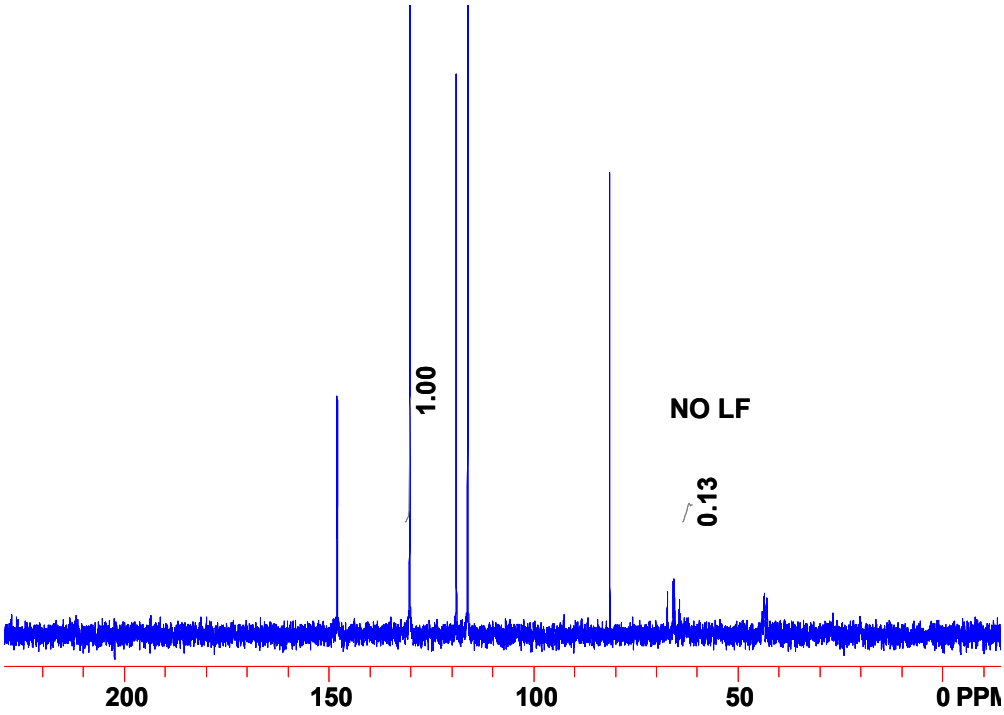

Figure 5-67: ^{13}C-NMR Latex 3, Centrifuged Sample #2—22°C.

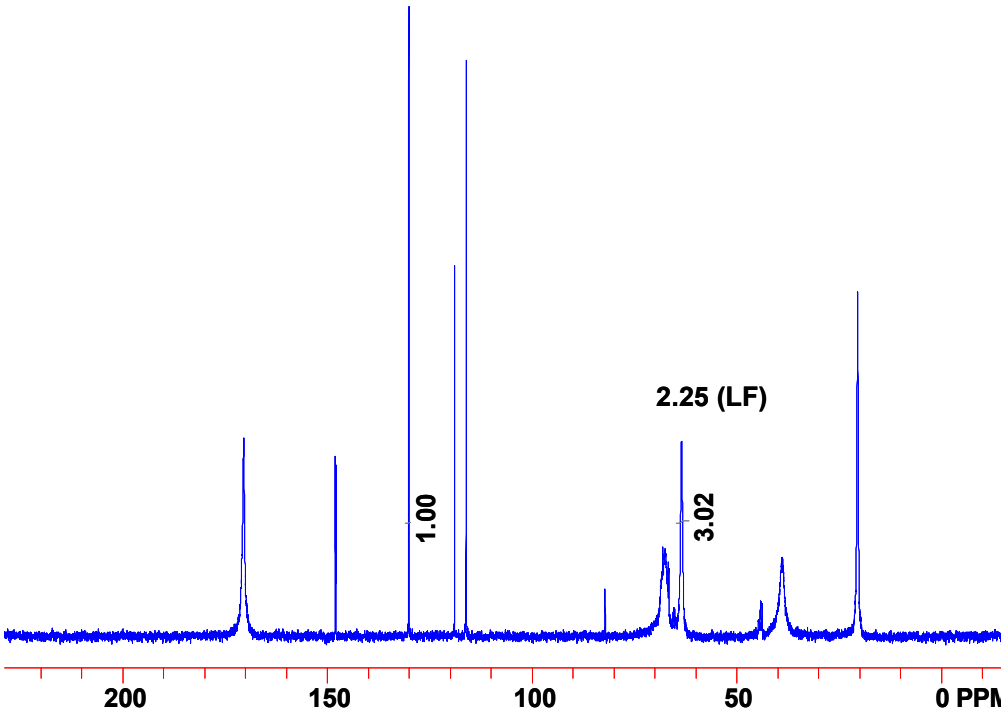

Figure 5-68: ^{13}C-NMR Latex 3, Centrifuged Sample #1—92°C.

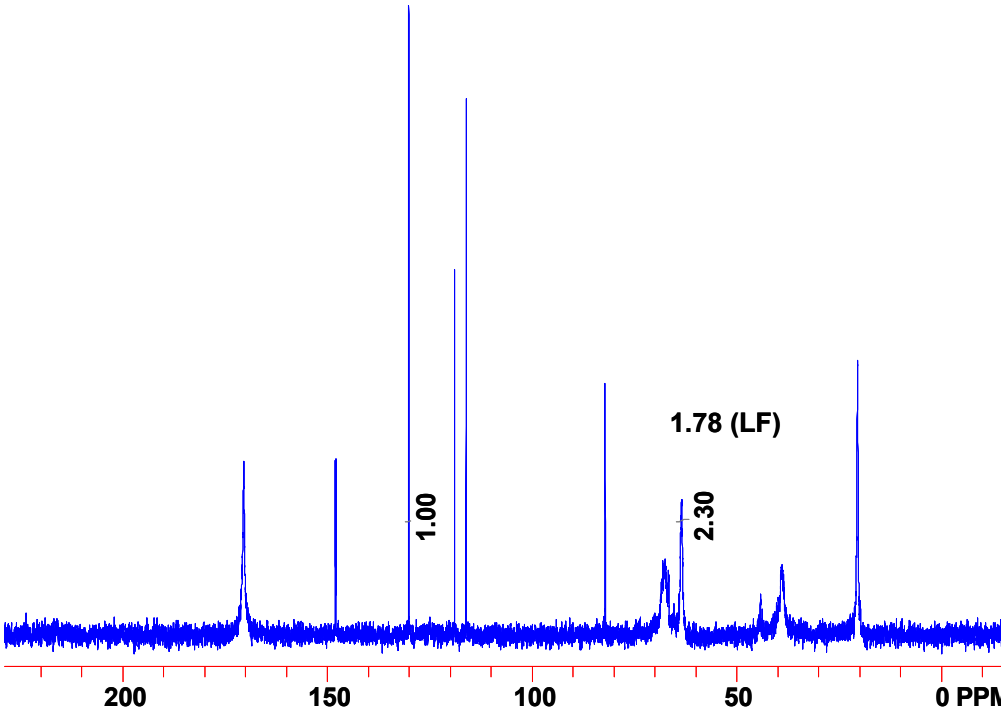

Figure 5-69: ^{13}C-NMR Latex 3, Centrifuged Sample #2—92°C.

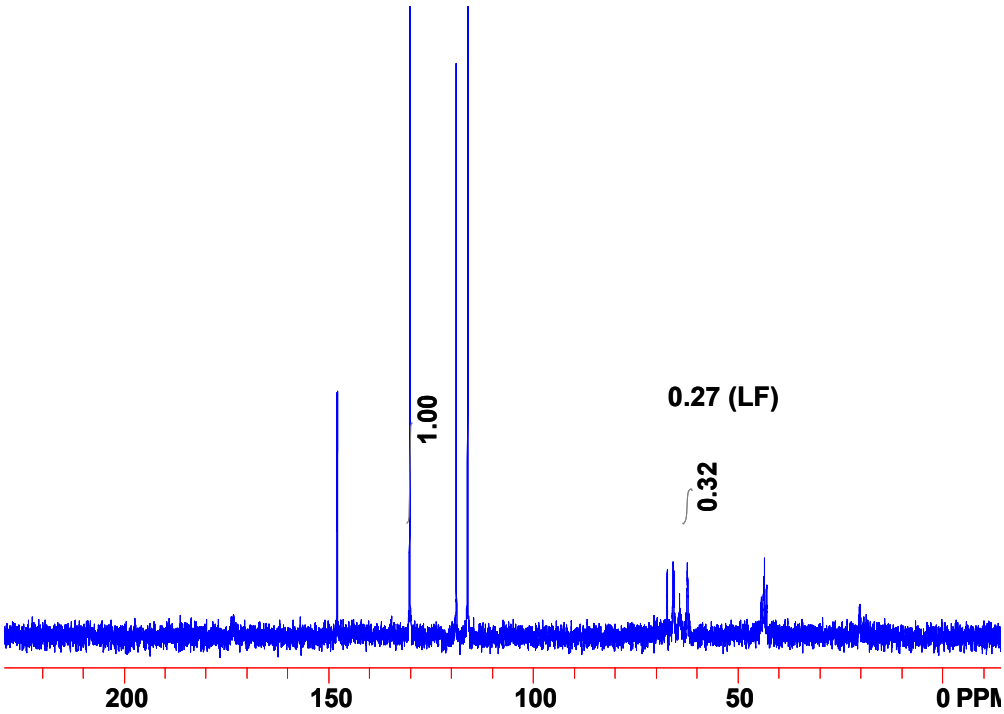

Figure 5-70: ^{13}C-NMR Latex 3, Dialyzed Sample #1—22°C.

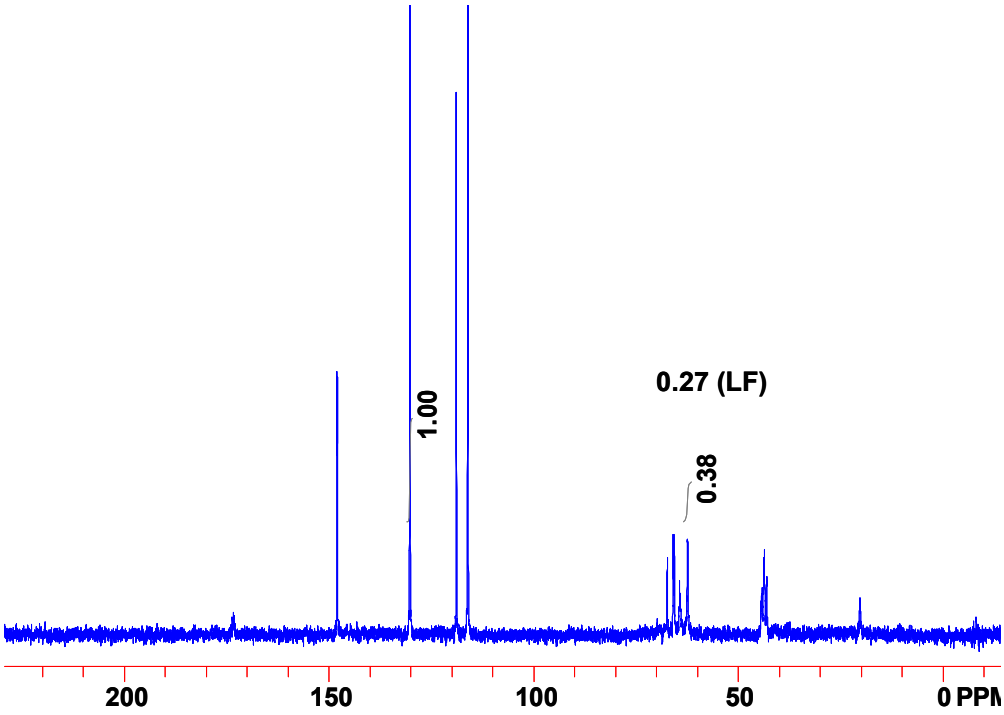

Figure 5-71: ^{13}C-NMR Latex 3, Dialyzed Sample #2—22°C.

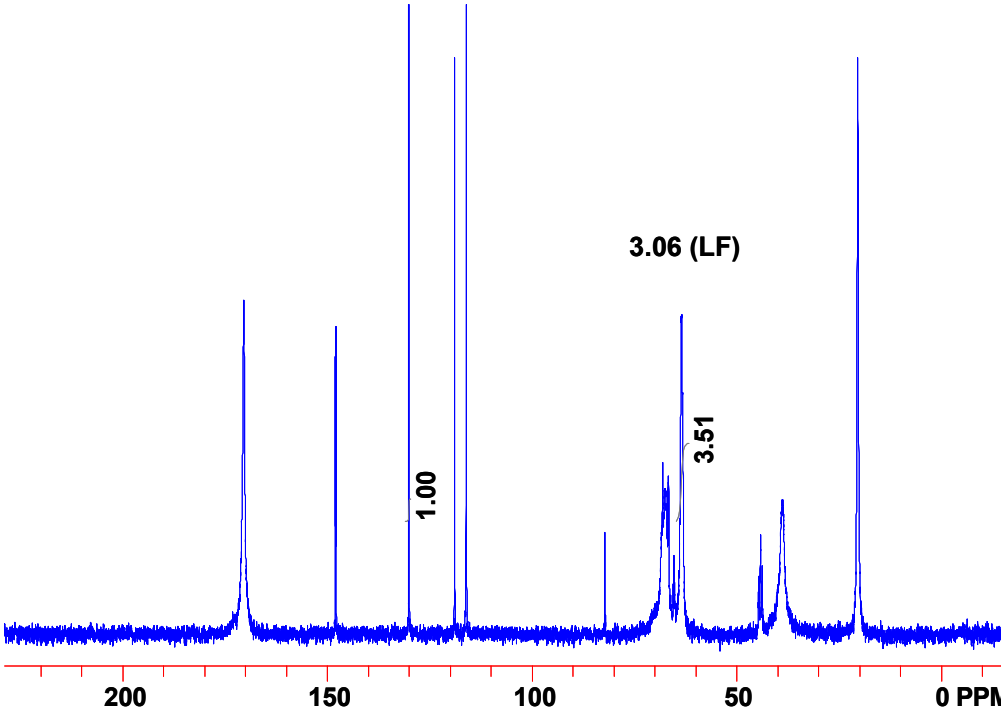

Figure 5-72: ^{13}C-NMR Latex 3, Dialyzed Sample #1—92°C.

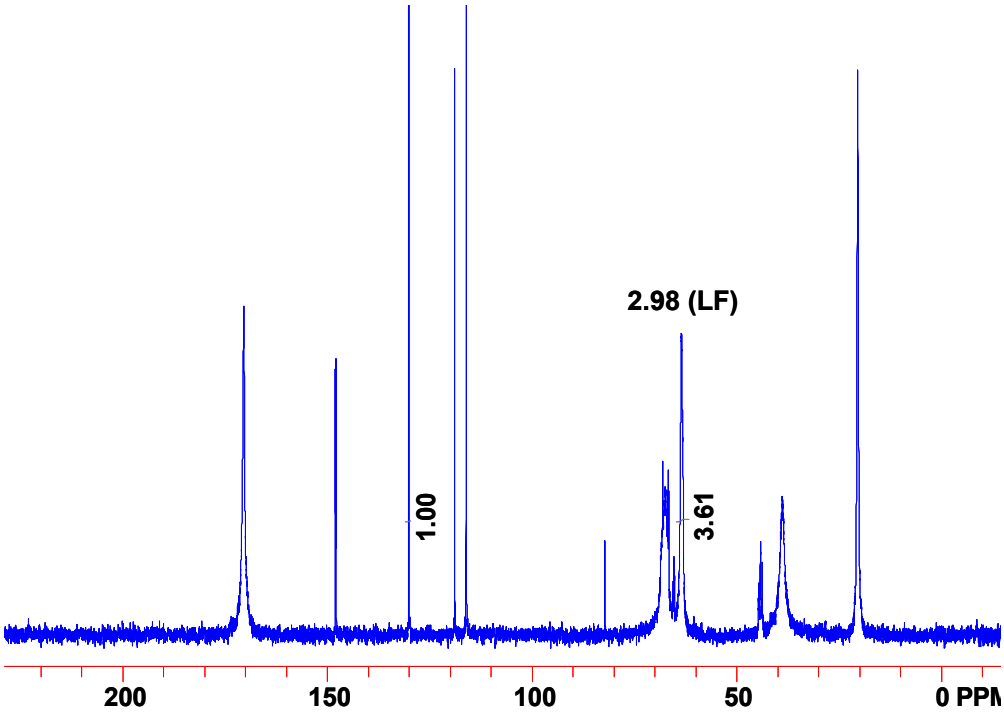

Figure 5-73: ^{13}C-NMR Latex 3, Dialyzed Sample #2—92°C.

Chapter 6: Performance of Latex Adhesives Evaluated by Mode-I Fracture Mechanics

6.1 Introduction

One of the overall objectives of this project is to evaluate adhesive joints and determine if any correlation between NMA distribution and performance exists. Of particular interest is the durability-related performance of the adhesives, since the inclusion of NMA typically results in enhanced durability. Several testing methods could be used to evaluate the performance of the wood-adhesive bondline. Here, the approach is mode I cleavage or fracture toughness tests. The more traditional method is the compression shear block test. Each method will be briefly described, and the advantages of the fracture approach will be discussed.

6.1.1 Compression Shear Block Testing

For years, the industry standard for evaluating interior-grade glued lumber products has been the compression shear block test (1994). In this test, specimens having a step-like geometry (specimen shown in Figure 6-1) are loaded into a testing fixture and a compressive load is applied. The other side of the specimen is held in place, which imposes a shear force along the bondline. Loading continues at a designated rate until the specimen fails. Load at failure is recorded, as is the percentage of wood failure observed along the failure surfaces. In order for an adhesive to pass the test and be certified for interior or exterior use, designated benchmarks for performance—including both critical load and percentage of wood failure—must be met or exceeded.

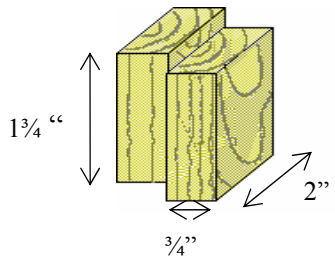

Figure 6-1: Diagram of a compression shear block specimen.

There are several key problems with the compression shear block test. The bulk of the load is applied in shear parallel to the grain. In addition, there is always some degree of rotation which introduces tension perpendicular to the grain. Consequently, the wood specimen is loaded in its two weakest modes. Another problem with the compression shear block test is its sensitivity to

the inherent variability of wood. The density of the wood substrates, their initial position within the log, species, moisture content, and the presence of juvenile or reaction wood are all factors that can impact the critical loads obtained and also the percentage of wood failure that is observed. This type of variability can obscure test results and limit the amount of information gleaned about the true performance of an adhesive. Finally, the percentage of wood failure is a very important criterion for whether or not the adhesive meets required specifications, yet this quantity is obtained via visual observation and is highly subjective. To summarize, the compression shear block test can be informative if the method is conducted appropriately, but there are many factors that make reproducible results difficult to obtain. In terms of learning about the ultimate performance of an adhesive, the compression shear block test is an unsatisfactory probe when the result is 100% wood failure because the test is limited by the strength of the substrate. Typical in-service adhesive failures involve delamination, not wood failure. Therefore, the mode I fracture mechanics approach was conducted.

6.1.2 Fracture Mechanics Approach

Mode I fracture mechanics analyses are a possible alternative to compression shear block testing. This test eliminates visual observation of wood failure, limits the impact of wood variability (by factoring out bulk wood properties), and, most importantly, tests the intrinsic properties of the adhesive bondline (Gagliano and Frazier 2001).

Early applications of the fracture mechanics (or cleavage) testing approach to the wood-adhesive bondline required arduous calibrations of tapered cantilever beams and extensive machining of specimens (Ebewele, River et al. 1979; Ebewele, River et al. 1980; Ebewele, River et al. 1986). However, the most current method replaces the contoured beams with simple beam geometry, thereby eliminating complex calibrations and also reducing specimen preparation time. Developments involving the application of fracture mechanics to wood specimens are noted in a literature review by Gagliano (Gagliano 2001). Additionally, Gagliano and Frazier applied the shear-corrected compliance method to wood specimens and noted that this method provided the best results (Gagliano and Frazier 2001). It is this method which will be utilized in this work.

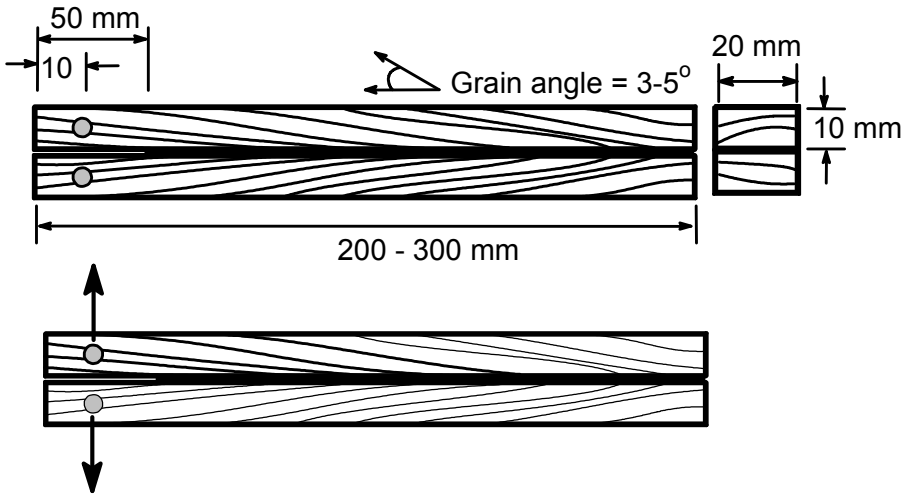

Figure 6-2: Dimensions of a fracture mechanics specimen.

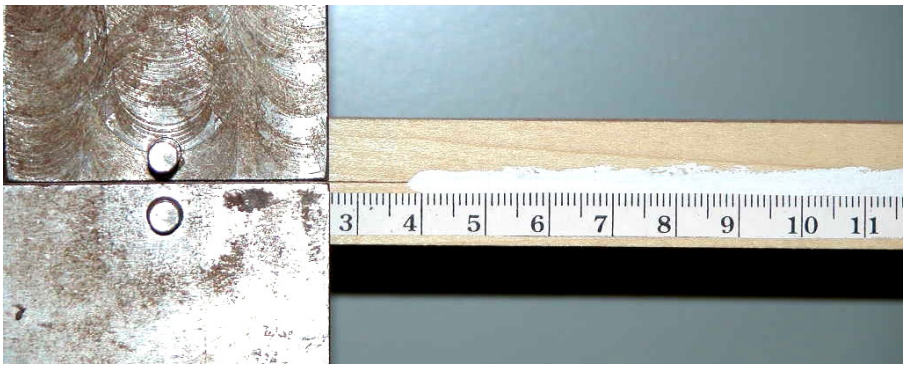

Figure 6-3: Photo of actual specimen loaded in grips.

Simply stated, the fracture mechanics approach is an energy balance. Energy is input to the system as the specimen is loaded in mode I cleavage. This energy is initially stored in the system as potential energy, but above a critical point some of this energy is released by the system in the form of a debond and crack growth. It is important to recognize that the fracture approach assumes linear elasticity—that all energy input to the specimen is recovered, or is released by crack formation. From a different perspective, the fracture energy can be considered as the amount of energy required to create two new surfaces. This critical fracture energy is assigned the symbol G_c and is also referred to as the strain energy release rate (*SERR*). Some

researchers in the field have used the term G_{max} instead of G_c, where G_{max} refers to the strain energy release rate where the applied load is at its maximum. In an ideal case, G_{max} would equal G_c.

A typical loading/unloading cycle during a fracture test is shown in Figure 6-4. The plot indicates the increase in applied load as a function of the crosshead displacement. After the specimen is fixed into the grips of the testing machine, the crosshead travels at a fixed rate, which increases the tensile load applied to the specimen (*A*). The loading continues until a crack begins to grow. The "break" criterion is defined as a 3% drop in the applied load. At this point, the crosshead is stopped and held at a fixed position as crack growth is monitored (*B*). During the period of crack growth the load decreases because energy is being released into the crack. The crosshead is held in the fixed position for 45 seconds, which is ample time for the crack to stop growing. Once the hold time expires, the crosshead returns to its initial position (*C*), and a new loading cycle commences. Figure 6-5 illustrates that a number of loading and unloading cycles can be performed on each test specimen. The number of test cycles conducted on any one specimen was found to vary from 3 to 20 during this study. From each testing cycle one critical strain energy release rate (G_c) is obtained. This makes the fracture mechanics test a powerful means of obtaining data since a series of data points are obtained from each specimen.

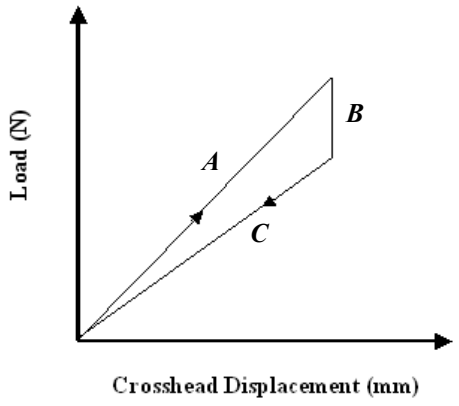

Figure 6-4: Representation of a loading/unloading cycle during a mode I fracture mechanics test.

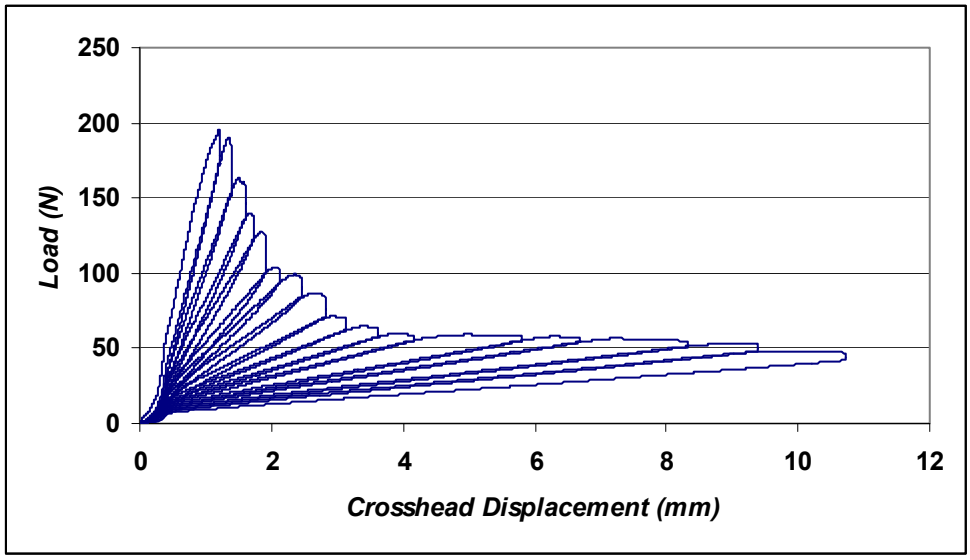

Figure 6-5: Actual loading/unloading data from one test specimen during a mode I fracture test. Sixteen test cycles were conducted on this single specimen.

Mathematically, the G_C value can be computed according to several different methods. Some of the theories that have been developed include the area, compliance, load, and displacement methods. Blackman et al. (Blackman, Dear et al. 1991) and Hashemi, Kinloch and Williams (Hashimi, Kinloch et al. 1990) reviewed the methods available for calculating G_C, and demonstrated that results can differ significantly among the different analysis methods. For this work, the shear-corrected compliance method will be used to analyze the data. Previously, Gagliano and Frazier compared analysis methods and found that the shear-corrected compliance method was most appropriate for adhesively-bonded wood double cantilever beam specimens (Gagliano and Frazier 2001). In adherends with a low shear modulus (wood), it is important to account for shear and crack-tip rotation effects, which is precisely the advantage of the shear-correction method.

The equation for calculating the critical strain energy release rate according to the shear-corrected compliance method is given below.

$$G_{IC} = \frac{P_C{}^2 (a+x)^2}{B(EI)_{eff}} \tag{6-1}$$

In this equation, P_C is the load at the critical point, B is the width of the specimen, a is the length of the crack, x is the correction factor, and EI_{eff} is the effective rigidity (effective modulus times the moment of inertia) of the specimen. Of these variables, P and a are recorded directly, B is measured *a-priori*, while both x and EI_{eff} require further explanation.

As the specimen is being loaded, the slope of the linear portion of the load-displacement curve reveals the effective modulus of the adherends. The inverse of this quantity is the effective compliance of the adherends. Simple beam theory gives the following relationship between compliance and crack length:

$$C = \frac{2a^3}{3EI} = k a^3 \qquad (6\text{-}2)$$

The relationship between the cube root of compliance, C, and crack length, a, is linear. A line fit applied to a plot of these experimental quantities ($C^{1/3}$ vs. a) gives a y-intercept (b) and a slope (m). The shear-correction factor, x, is simply the ratio of b/m. Similarly, the effective rigidity (EI_{eff}), is $2/(3m^3)$.

An example plot showing the cube root of compliance versus crack length is shown in Figure 6-6. This plot is from one of the specimens bonded with Latex 1. Notice that there are 13 data points plotted. This corresponds to 13 loading-unloading cycles. However, not all of these data points will be used for the analysis. Data points from the first 45 mm of the sample, the last 45 mm of the specimen, as well as cycles where the crack jumps significantly into the wood will all be discarded. Data from the specimen shown in Figure 6-6 were used to calculate 10 G_c values. Those values are plotted as a function of crack length in Figure 6-7. Theoretically, the G_c values are a material property of the system, and thus, should not change as a function of position along the length of the specimen. However, variation does exist. Histograms showing all G_c values for a given adhesive and accelerated aging condition are found in the Appendix at the end of the chapter.

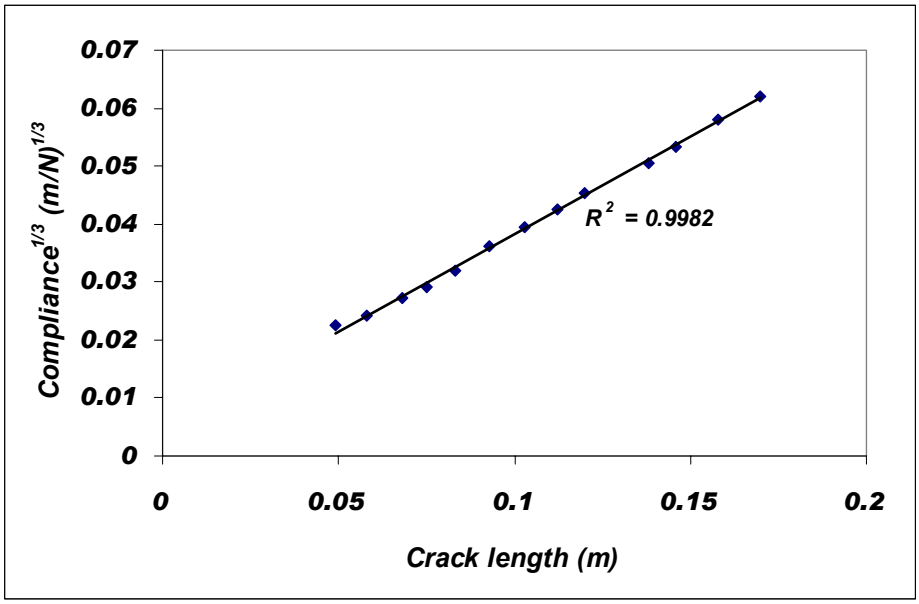

Figure 6-6: Cube root of compliance verses crack length. All data points obtained on one specimen.

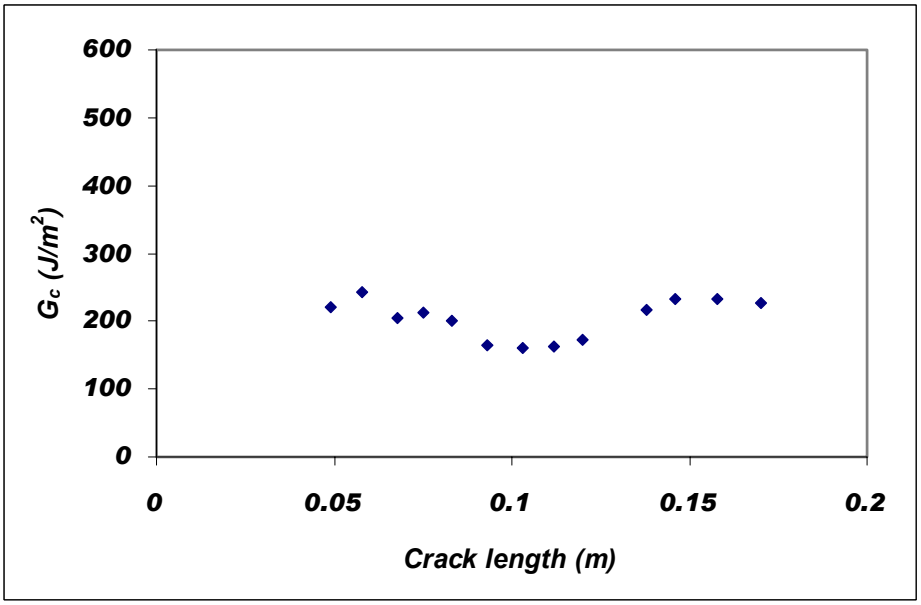

Figure 6-7: Critical strain energy release rates (G_cs) obtained as a function of crack length for a single specimen.

6.2 Materials and Methods

6.2.1 Sample Preparation

Boards of yellow-poplar (*Liriodendron tulipifera*) having minimal defects and consisting of primarily sapwood were purchased from Ideal Building Supply. The boards were of varying lengths and widths, but they had to be at least two inches thick (eight-quarter) to accommodate the desired grain angle. Once received, the boards were cut into sections measuring approximately 250 mm in length. Each of these sections was marked to include one or two 18-20 mm thick planar sections (later referred to as "lamina" or "laminae") having a 3° grain angle. The laminae were then cut from each section using a band saw. Next the laminae were planed down to a thickness of approximately 12 mm and trimmed to uniform dimensions of 114 x 231 mm. They were stored in an environmental chamber at 20°C (± 1°C) and 65% (± 1%) relative humidity for several months.

Two days before bonding, the boards were planed to a final thickness of 10 mm. Surfaces to be bonded were immediately stacked face-to-face to prevent contamination and were stored for 48 hours in the environmental chamber (conditions noted above). Bonding surfaces were paired so that the grain angles converged at the bondline (see Figure 6-3).

Adhesives 1-3, synthesis described elsewhere, were diluted to similar solids contents (see details in Chapter 4), then were hand mixed with 5% (w/w) catalyst (MultiBond®) just prior to application. To produce a pre-crack, the first 40 mm of each board was lightly covered by Crayon® paraffin wax. Adhesive was applied just below the wax-covered area and it was spread evenly on the face of each laminae with a plastic spreader. The amount of adhesive to be spread on each face was calculated so as to achieve identical bondline solids. Table 6-1 shows the amount of adhesive that was applied to each face for each of the three adhesives, as well as the open time before consolidation. In all cases, the total bondline solids were ~5 grams, where the surface dimensions were 4.5" x 9.1" (114 mm x 231 mm).

Table 6-1: Amount of adhesive applied to each face and open times (as a function of adhesive solids content)

	Adhesive 1	Adhesive 2	Adhesive 3
Solids content (%)	35.27	42.50	49.67
Total Adhesive per face (grams)	6.9	5.8	4.9
Adhesive Solids (grams) per face	2.4	2.5	2.4
Open time (minutes)	10	7	5

After the specific open time had been met, the specimen was consolidated under a 50 lb weight (a pressure of 1.2 psi, or 0.008 N/mm^2) for 24 hours at ambient conditions. Limited squeeze-out was observed during the first 5-10 minutes of consolidation. Twenty four hours later the weight was removed and a ½" section was trimmed and discarded from the long edges of the bonded laminae. Four specimens, each 20mm wide, were machined from each bonded laminum. Individual specimens were allowed to sit at ambient conditions for two additional days prior to exposure to the aging treatments. A total of 108 specimens were tested. For each of the three latices, 36 samples were tested, and 12 samples were designated to each of the three accelerated aging treatments. Statistically, the design was completely randomized with repeated measures.

6.2.2 Accelerated Aging of the Specimens

Specimens were randomly assigned to one of three groups: 1. a two cycle boil; 2. a one cycle vacuum soak; and 3. a control group. The boil exposure included submerging the specimens in boiling water for 4 hours, drying them completely in an oven at 104°C, then repeating the cycle. For the vacuum-soak treatment, vacuum was applied to specimens submerged in water inside a glass desiccator. After 10 minutes, the desiccator was sealed with ultimate pressure readings varying between 0.05 and 0.1 mm Hg (measured with a McLeod gauge). The specimens remained under vacuum for 1 hour then the chamber was opened to atmospheric pressure. Specimens soaked for an additional hour under atmospheric pressure, then were removed and oven dried. All specimens, including the control group, were dried at 104°C in a Lindberg Blue/M oven until completely dry (determined gravimetrically by weight change of less than 0.1 grams). Drying typically required 48 to 72 hours. Control specimens dried faster than the boiled and vacuum soak specimens. Dry specimens were sealed in a glass desiccator over drierite at room temperature until tested (7-10 days).

Prior to testing, holes were drilled 10 mm from the end of the specimen to accommodate pins that affix the specimen to the test grips (see Figure 6-3). Also, white typographic correction fluid was applied to the bondline to facilitate crack length measurements. Since the solvent for the correction fluid (toluene) could plasticize the poly(vinyl acetate) adhesive, it was applied more than 24 hours prior to testing to ensure appropriate time for drying. Immediately prior to testing, each specimen was removed from the desiccators and a small paper scale was bonded to the specimen with a glue-stick to facilitate measurements of crack length.

6.2.3 Test Method

Mode I opening fracture mechanics tests were conducted on a screw driven Materials Test System (MTS) Syntech 10/GL test frame equipped with a 1000 N load cell. A CCD camera with 10x magnification was set up on a movable track just in front of the grips, providing real time output to a video monitor. Specimens were loaded into the grips, supported on the free end (to prevent rotation), and leveled before testing began. Crosshead position was zeroed prior to each test and the load cell was calibrated at the beginning of each testing session. No pre-load was applied to the specimens, as had been done by earlier researchers because precise control over the preload force was difficult to achieve (Schmidt 1998; Gagliano 2001; Sernek 2002).

As the test commenced, the crosshead began traveling at a rate of 1 mm/minute. The TestWorks™ software used to control the testing frame was configured so that the crosshead would stop when a 3% drop in load was detected. Once the drop was detected, the crosshead was held fixed for a period of 45 seconds. During this time, the CCD camera was manually positioned along the track so as to watch the crack grow. Near the end of the 45 second hold time, an arrest load was recorded and the crack length was manually noted by the operator. After the hold time had expired, the crosshead returned to the zero position and a new loading cycle began. The ASTM standard requires incremental increases in the loading rate so that crack initiation begins within one minute of loading (1999). New loading rates for each cycle were calculated by observing the opening displacement during the previous hold cycle and dividing this value (in millimeters) by one minute. Each specimen was tested repeatedly until the specimen failed in its entirety, the crack grew deeply (> 3mm) into the the wood substrate, or

until the crack length exceeded the usable data range (the first 45 and last 45 mm of the specimen cannot be used because the stress state becomes complex) (Gagliano 2001).

Bondline Images

One inch sections were cut from untested fracture specimens. These specimens were prepared exactly as the fracture specimens were. The cross sectional face was microtomed, then stained with a 0.05% Saffranin dye. Samples were dried in a Blue/M oven overnight at 104°C. An epi-fluorescence microscope (Zeiss Axioskop) fitted with a Spot Camera was used to record images of the specimens.

6.3 Results and Discussion

6.3.1 Sample Preparation and Test Methodology

Yellow-poplar (*Liriodendron tulipifera*) was selected for this study because it is recognized as being relatively easy to machine, and is locally available. Selected boards were required to be predominantly sapwood, and relatively free of defects so as not to influence penetration and other characteristics of the bondline. Boards had to be of 8/4 or greater thickness to accommodate the 3° grain angle on the laminae. Previous work has shown that machining the laminae with this grain angle limits irreversible crack growth into the wood substrates (Schmidt 1998). This controlled-grain angle method allows the scientist to learn about the toughness of the adhesive and wood-adhesive interphase instead of merely the bulk properties of wood, which are already well-established (Porter 1964).

Developing a sharp crack tip is important for this analysis. Previously, researchers have machined a blunt crack along the interface using a band saw, or have hammered a razor blade into the machined crack. Gagliano applied a novel approach of coating the first 50 mm of the specimen with paraffin wax, then applying the adhesive below the wax-coated section (Gagliano 2001). This creates a "natural" pre-crack. This approach was also used here.

In making the specimens, different amounts of adhesive were applied to the faces of the laminae to achieve the same adhesive solids per bondline (refer to Table 7-1). For Latex 1, the solids content of the latex was 35.27%; whereas solids for Latex 2 and 3 were 42.50% and 49.67%,

respectively. Therefore, more of Latex 1 had to be applied to each face to achieve the same solids per bondline. Since more adhesive was present and its solids content was lower, it took longer for the extra water in Latex 1 to penetrate the wood or evaporate. Therefore, Latex 1 required longer open times than either Latex 2 or 3. Open times were determined by trial and error so that a limited amount of squeeze out was achieved.

Previous researchers applied the adhesive to freshly planed laminae. In this work it was more convenient to store the samples for 48 hours between planing and adhesive application. While it is generally accepted that surface deactivation can result in poorer wetting and penetration, work by Sernek showed that yellow-poplar does not exhibit much surface deactivation, even when heated in excess of 150°C (Sernek 2002). Furthermore, he found that poly(vinyl acetate) adhesives are relatively insensitive to surface effects as compared to other wood resins (Sernek 2002).

Samples were consolidated under relatively low pressure (1.2 psi, or 0.008 N/mm^2) for 24 hours. This is considerably lower consolidation pressure than that used by Gagliano (690 kPa or 100 psi), and Sernek (0.1 N/mm^2) (Gagliano 2001; Sernek 2002). However, Gagliano and Sernek only applied the consolidation pressure for 1 hour. Manufacturers typically recommend clamping joints bonded with PVAc adhesives for 24 hours, so this extended low-pressure consolidation meets their recommendations.

Accelerated aging conditions were selected to be similar in nature to those imposed on specimens in the ASTM standards for wood adhesive testing. This includes the standards for the compression shear block (1989; 1990; 1994), as well as the newer standards for finger jointed lumber and plywood (1995; 1999; 1999) . In these standards it is typical to expose samples to cyclic boil and soak conditions. Here, the accelerated aging conditions were more rigorous because they included drying until oven dry at 104°C whereas the standards incorporate lower drying temperatures and only dry the specimens to 8-12% moisture content. For this work, specimens were tested when completely dry. In other work, specimens attained an equilibrium moisture content ranging from 8-12% (Schmidt 1998; Gagliano 2001; Sernek 2002). Since the wood was bonded at 12% moisture content but tested dry, internal stresses could be an issue.

The compliant nature of the adhesive (the T_g is slightly above room temperature) may compensate this effect.

The test method was very similar to that described by Gagliano, Sernek, and others. There were several notable differences. First, no preload was applied to the specimens. The means of applying the preload to the specimens was not found to be reproducible, so it was abandoned for this work. Instead, a sharp crack tip was generated by the "natural" pre-crack, and by subsequent loading and unloading cycles. Data from the first 45 mm of the sample were discarded due to the presence of shear forces and data from the last 45 mm of the sample were also discarded because the assumption of beam on elastic foundation breaks down (Gagliano 2001). If the first loading cycle resulted in a crack beyond the 45 mm limit, that loading cycle was included in the experimental data.

The second major change in the test method was to verify that appropriate data points were included when the slope of the load vs. crosshead displacement curve was determined. Specifically, points included in the slope determination had to be located within the linear region. The slope value is important because it is used in the calculations for G_c. Previously, researchers relied upon a software program to select valid points for this determination. However, it was discovered that the slope data was in some cases based on data points that were outside the linear region of the loading curve. Such points were discarded and more appropriate ones were selected by the operator.

There is some question regarding the sensitivity of the "break" criterion used in this approach. Sometimes the crack began growing before the system detected a 3% drop in the applied load. This peculiarity seems to be associated with poly(vinyl acetate) adhesives. When this occurred, the amount of energy input to the specimen was actually *greater* than the true critical energy. This is recognized as a potential source of error in the results.

The designation "G_c" is given to the strain energy release rates. Other authors have used the designation "G_{max}". G_c is a material property of the system being investigated, and is widely reported in the scientific literature. This is the information we are interested in obtaining. It is

true that values obtained here may offer an approximation to the true G_c. This limitation is recognized.

6.3.2 Preliminary Analysis of the Data

Twelve specimens were tested for each adhesive/treatment combination, yielding 108 total test specimens. All specimens were intact following the accelerating aging treatments. After testing, some data points had to be excluded from the analysis. When test specimens failed before three loading cycles could be completed, insufficient data were available to obtain a reliable slope from a plot of $C^{1/3}$ vs a. Therefore these specimens were discarded from the analysis. The other occasion where data was excluded occurred when the crack tip propagated significantly (> 2 mm) into one of the wood substrates. In certain cases, wood failure led to the discard of an entire specimen, while in other cases, data from some of the loading cycles were omitted. The number of specimens that provided adequate data after these two criterion were considered is shown in Table 6-2.

Table 6-2: Number of G_c data points for a given adhesive and aging condition.

Latex	Treatment	Usable specimens	Proportion of Usable Specimens
1	Control	12/12	1.000
1	Boil	9/12	0.750
1	Vacuum Soak	5/12	0.417
2	Control	12/12	1.000
2	Boil	11/12	0.917
2	Vacuum Soak	12/12	1.000
3	Control	11/12	0.917
3	Boil	12/12	1.000
3	Vacuum Soak	11/12	0.917

Previous researchers used an additional criterion for inclusion; the goodness of fit for the $C^{1/3}$ vs a plot. Using a linear regression, this plot had to result in R^2 values greater than or equal to 0.98 for a specimen to be included. This criterion was completely arbitrary, but was considered sensible because the results of the analysis are highly dependent upon the slope of the compliance plot and the associated shear correction factor. Here, this additional criterion will

not be used. If it were imposed, four specimens would have to be discarded—all of them from the Latex 3 control group. Of those four specimens, three gave R^2 values above 0.95. By evaluating the average G_c value of the Latex 3 control group with and without the specimens in question, it was decided that there was no reason to discard the specimens having lower R^2 values. The average G_c only shifted from 167 to 170 J/m^2 when data from the four questionable samples were included.

From Table 6-2, one can observe the proportion of usable test specimens as a function of the adhesive and the applied accelerated aging treatment. Accelerated aging treatments decreased the likelihood that a given specimen would be included. Of the 36 specimens exposed to the control treatment, 35 (97.2%) were acceptable. For the boil treatment, the percentage of acceptable specimens dropped to 88.9% (32/36 specimens included) and for the vacuum soak, it fell to 77.8% (28/36 specimens included). The interaction between latex type and the accelerated aging treatment also seemed to play a role in whether or not specimens were included. In particular, the accelerated aging treatments resulted in fewer acceptable Latex 1 specimens.

Determining Outliers

The next step in evaluating the data was to determine whether any of the data points were outliers. Box plots are one way of evaluating a distribution of data points and determining outliers. Box plots are based on a statistical concept known as the interquartile range (IQR). To determine the IQR, data points are ranked numerically in ascending order and divided into quadrants. For the case of *n* data points, the first *n*/4 data points represent the lower outer quartile. Similarly, the last *n*/4 data points represent the higher outer quartile. The inner *n*/2 data points define the IQR. The IQR is illustrated as a gray rectangular box (see Figure 6-8), hence the name "box plot". The central horizontal line dividing the box represents the median value, while the '⊕' in the center of each rectangular box marks the mean G_c value. Data points in the outer quartiles (higher and lower) are represented by dashed vertical lines (here the dashes overlap and appear as a solid line) that extend some distance from the upper and lower hinges (these are the upper and lower boundaries of the IQR). These vertical dashes are typically known as "whiskers". Mild outliers (represented by *) are those values that extend more than

1.5 times IQR from one of the hinges. Extreme outliers (o) are those data points that are located more than 3 times IQR from a hinge. There were no extreme outliers in the experimental data.

When a data point is designated as an outlier, it should not be immediately discarded from the data set. Some justification for exclusion must be given. A possibility warranting exclusion in fracture mechanics testing might be a "bad" specimen (a result of uneven adhesive coverage, etc.). Here it was decided that if most of the data points from one test specimen are outliers, then the entire specimen should be excluded from the analysis.

Box plots including data from all three latices are shown in Figure 6-8. A single mild outlier exists in the Latex 1 boil set, as well as in the Latex 3 boil and Latex 3 control data sets. These individual outliers do not warrant exclusion from the data set. However, the Latex 1 control condition reveals a number of outliers (10), as does the Latex 2 vacuum soak condition (8). These outliers result in the exclusion of two specimens—one from Latex 1 control (6 of the 9 data points from one specimen were outliers), and one from the Latex 2 vacuum soak treatment (8 of the 15 data points from that specimen were outliers).

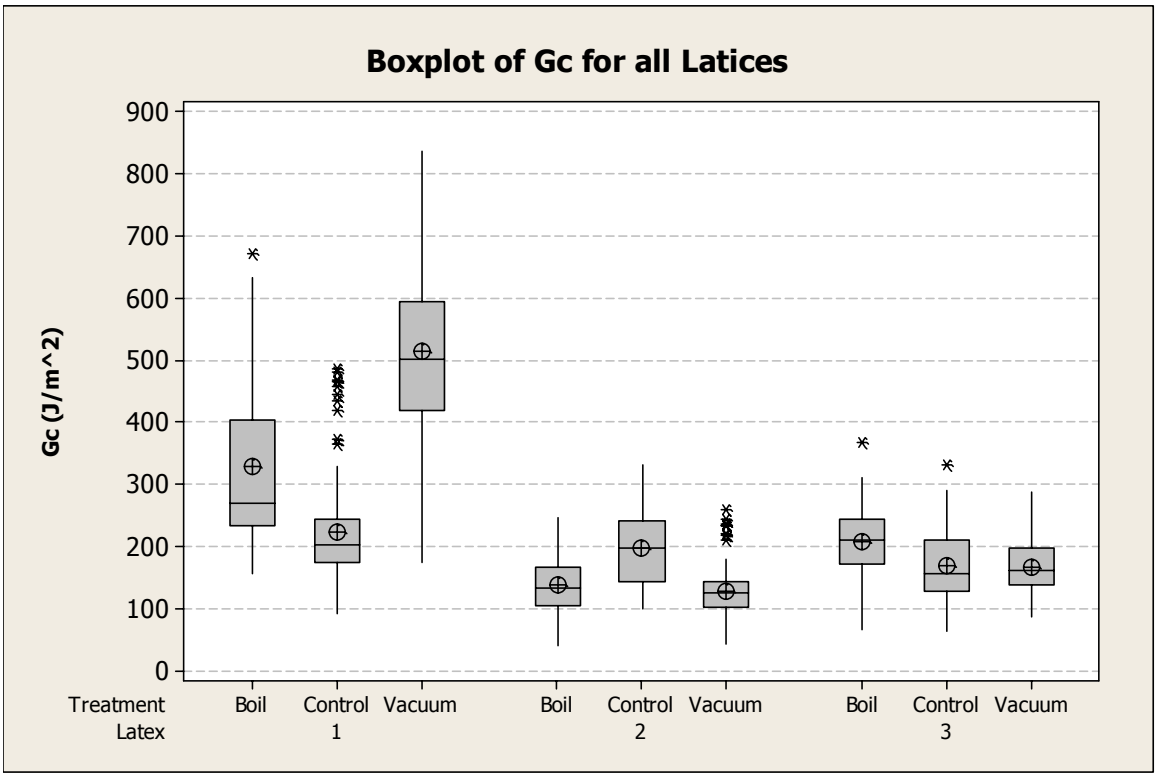

Figure 6-8: Box plots showing raw G_c data for all Latices as a function of accelerated aging treatment (Boil, Control, or Vacuum Soak).

A new box plot, shown in Figure 6-9, reveals the distribution of data points after the exclusion of the two bad specimens. Notice that the Latex 2 vacuum soak data now has no outliers, and that the Latex 1 control data has only 4 outliers. These four points come from the same specimen, but do not warrant the exclusion of the specimen, since it also contained 7 good data points. Excluding the two outlier specimens shifted the mean G_c value for Latex 1 control from 224.2 to 213.3 J/m^2, and the mean Latex 2 vacuum soak G_c from 129.1 to 118.0 J/m^2. Also, the standard deviation for each group drops when the outliers are excluded. For Latex 1 control, it changes from 79.0 to 64.9 J/m^2, and for Latex 2 vacuum soak it is reduced from 38.5 to 23.9 J/m^2.

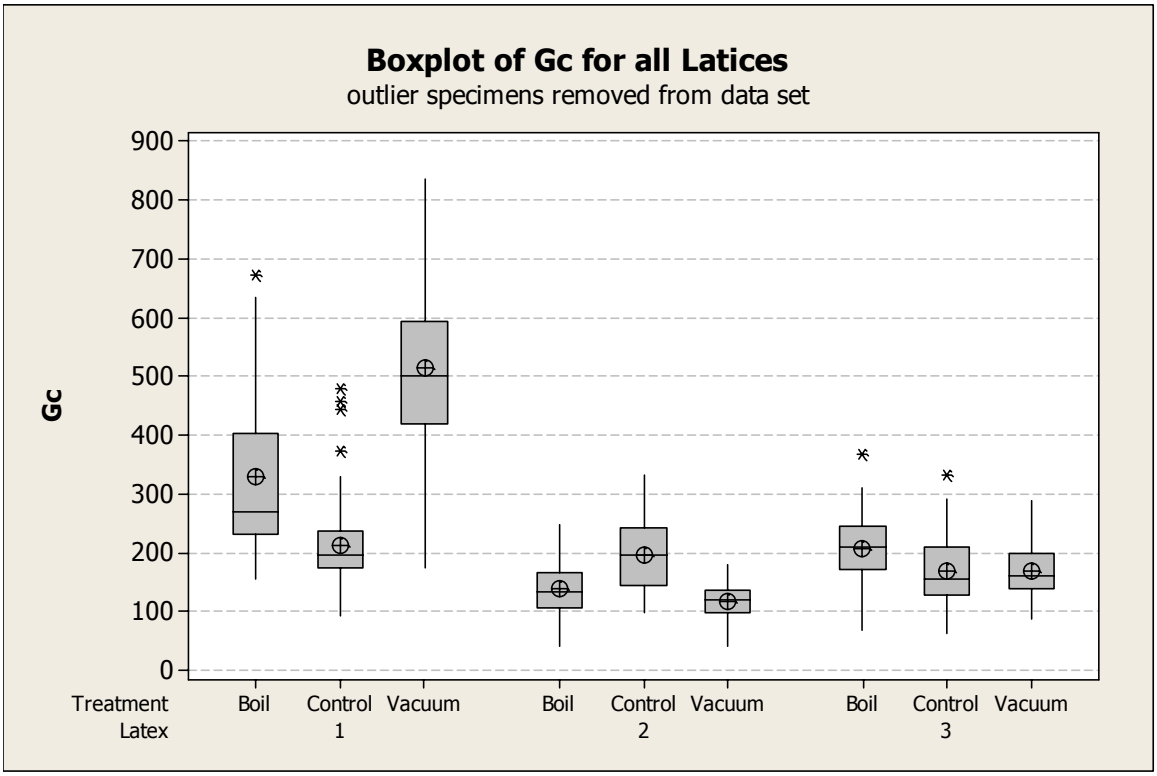

Figure 6-9: Boxplots showing G_c data after outlier specimens have been removed.

After excluding bad specimens, the descriptive statistics about the data set can be evaluated. The number of G_c values for a given latex and accelerated aging condition can be found in Table 6-3. There are over 200 data points for each of the three latices, and over 700 total data points. As stated previously, the control treatment was least likely to lead to specimens being excluded from the data set while both the boil and vacuum soak treatments increase the likelihood that a given sample will have to be excluded. This finding was anticipated to some extent since both the boil and the vacuum soak treatments expose the specimen to considerable stress through shrinking and swelling. Of all the latices and conditions, the vacuum soak for Latex 1 resulted in the fewest usable specimens. Only five of the twelve met the criteria for being a "good" sample.

Table 6-3: Number of G_c data points for a given adhesive and accelerated aging condition after outlier specimens are excluded.

Latex	Treatment	Proportion of Usable Specimens	Total # Data Points
1	Control	0.917	123
1	Boil	0.750	74
1	Vacuum Soak	0.417	43
			Subtotal: 240
2	Control	1.000	130
2	Boil	0.917	49
2	Vacuum Soak	0.917	90
			Subtotal: 269
3	Control	0.917	91
3	Boil	1.000	55
3	Vacuum Soak	0.917	65
			Subtotal: 211
			Total: 720

6.3.3 Statistical analyses

Several different approaches exist for making multiple comparisons within a sample population. Here, any differences in performance among the three latex adhesives are of interest. Also, the effect of the accelerated aging conditions on the performance of each adhesive will be investigated. Statistically, it would be possible to investigate differences between any two of these populations (i.e., Latex 1 and Latex 2) via pair-wise comparisons, using t-tests. However, multiple t-tests would be necessary to make comparisons among the three latices and the three accelerated aging conditions. Using a series of t-tests to compare means is a dangerous approach. The probability of falsely rejecting at least one of the hypotheses increases with the number of pair-wise comparisons performed. In other words, it is relatively easy to overestimate the differences among means using this approach. While each individual decision might be made at the $\alpha = 0.05$ level (meaning the Type I error is fixed at $\alpha = 0.05$), the effect of conducting multiple t-tests increases the Type I error considerably above 0.05. Multiple comparisons can be achieved more rapidly, and with less error, using an analysis of variance (ANOVA).

Performing an ANOVA for this data set was complicated by several factors. First, G_c values from a given test specimen cannot be assumed to be independent. The first loading cycle could have an effect on the second loading cycle, the third loading cycle, or even the tenth loading cycle. Statistically, this phenomenon is described by saying that G_c values could exhibit some covariance with loading cycle. A second complicating factor was that the data set was highly

unbalanced. While only three loading cycles could be completed on some specimens, fifteen loading cycles were possible on others.

The first step, then, was to obtain a balanced data set. Table 6-4 shows the number of fracture specimens available for each adhesive and aging combination if N consecutive loading cycles are included. Notice that beyond 5 consecutive loading cycles some latex/aging combinations would only include two fracture specimens. This severely limits sample size. Therefore, the data set was limited to include only specimens containing G_c values from five consecutive loading cycles. That allows at least four specimens (20 G_c values) for each latex/aging combination.

Table 6-4: Number of specimens for each latex and treatment combination that contain N consecutive loading cycles.

Latex	Accelerated Aging Condition	N									
		3	4	5	6	7	8	9	10	11	12
1	Boil	7	6	6	6	5	5	4	4	4	3
	Control	12	12	12	12	12	12	11	10	7	4
	Vacuum Soak	5	5	5	4	3	3	3	3	2	1
2	Boil	9	7	5	2	2	-	-	-	-	-
	Control	12	12	12	12	12	12	12	11	9	4
	Vacuum Soak	11	11	10	8	8	8	8	4	4	4
3	Boil	12	9	5	2	1	1	1	1	-	-
	Control	8	8	8	8	7	7	7	7	5	2
	Vacuum Soak	10	10	8	6	3	2	2	1	-	-

Before the covariance with loading cycle was investigated, the balanced data set (where N=5) was analyzed to determine the best fitting linear model. The linear model includes terms that have a fixed effect on mean G_c values. SAS® statistical software was used to evaluate the models. In particular, the "proc mixed" procedure was used. Initially, the most complex model was evaluated, where G_c means were said to be due to various levels of the following fixed effects (and interactions of fixed effects): latex, accelerated aging treatment (referred to as "treatment" for short), loading cycle, latex*treatment (the asterisk indicates interaction between the terms), treatment*loading cycle, and latex*treatment*loading cycle. Terms were rejected from the model (one at a time) based on the p-values (shown in parentheses) associated with the F statistic. The most complex terms (interactions) were eliminated first. Initially, the three way interaction of latex, treatment, and loading cycle was eliminated from the model since the p-

value was highly insignificant (p-value 0.9999). This indicates that the levels of that three way interaction do not have a significant effect on means of G_c. The new model was then analyzed, and the interaction of treatment with loading cycle was removed (p-value 0.8361). Next, loading cycle was eliminated from the model (p-value 0.3963). This produced the reduced model where G_c was based on latex, treatment, and latex*treatment. The F-statistic for the interaction of latex*treatment was 87.65 (p-value of < 0.0001) and had 4(numerator) and 418(denominator) degrees of freedom. The p-values for latex and treatment were each < 0.0001. This model indicates that the "levels" of latex (i.e., the three different adhesives), treatment, and the interactions between those two variables all have a significant effect on the means of the G_c subsets. All that remains at this juncture is to investigate the covariance of G_c with loading cycle.

As was stated previously, the G_c observations within a fracture specimen cannot be assumed to be independent. Therefore, the reduced model that we obtained might not account for all sources of variability among our observations. To investigate whether covariance with loading cycle was important, we included covariance structures in the general linear model. Two different covariance matrices were selected, and the fit of the model including these covariance structures were compared with the model bearing no covariance matrix. In the first covariance structure, compound symmetry was assumed, while in the second, the effect of loading cycle was predicted to follow a first order autoregressive structure. These two covariance matrices are best described pictorially. Table 6-5 and Table 6-6 show the regression matrices where σ is the fixed effect (considering only random variability) and ρ is the estimate for the covariance with loading cycle. Notice that in the compound symmetry model, the covariance between any two non-equivalent loading cycles is the same. This indicates that the first, third, and 5th loading cycles would have an identical correlation with the G_c obtained from the 2nd loading cycle. So, regardless of the distance of separation, the covariance with loading cycle would be considered constant. In the first order autoregressive model, the correlation between subsequent loading cycles is much more important than the correlation between distant cycles. This is illustrated by the higher order terms in the model (since ρ is always between 0 and 1, higher order terms actually predict a decay in the covariance matrix).

Table 6-5: Matrix showing compound symmetry covariance structure for correlation between different loading cycles

N	***1***	***2***	***3***	***4***	***5***
1	σ	ρ	ρ	ρ	ρ
2	ρ	σ	ρ	ρ	ρ
3	ρ	ρ	σ	ρ	ρ
4	ρ	ρ	ρ	σ	ρ
5	ρ	ρ	ρ	ρ	σ

Table 6-6: Matrix showing autoregressive covariance structure for correlation between different loading cycles

N	***1***	***2***	***3***	***4***	***5***
1	σ	ρ	ρ^2	ρ^3	ρ^4
2	ρ	σ	ρ	ρ^2	ρ^3
3	ρ^2	ρ	σ	ρ	ρ^2
4	ρ^3	ρ^2	ρ	σ	ρ
5	ρ^4	ρ^3	ρ^2	ρ	σ

The covariance structures were included in the best fitting model, and the models were evaluated based on AIC (Akaike's Information Criterion) and BIC (Bayesian Information Criterion) fit statistics, where smaller fit statistics indicated a better model. Ignoring covariance (assuming G_c values are independent), the AIC and BIC fit statistics were 4873.1 and 4877.2 respectively. When the compound symmetry covariance matrix was applied to the model, the fit statistics improved to 4539.9 and 4545.0 (AIC and BIC, respectively). This indicates that it is correct to assume some type of covariance between loading cycle and G_c. The first order autoregressive covariance matrix led to the lowest AIC and BIC values, 4515.5 and 4520.6, indicating it is the most appropriate way to account for covariance with loading cycle. This indicates that the covariance is most pronounced for subsequent loading cycles.

One last check to be sure that the model and covariance structure were valid was produce plots of the residuals. These plots are not included. They showed that the residuals were randomly

distributed. This verified that the model was sufficient in accounting for all important sources of variability. Any trend in a residual plot indicates that an important term has been left out of the model.

Determining that G_c values have some covariance with loading cycle is an interesting finding. It is not surprising that results from a given loading cycle depend on the previous crack cycle, or that any given loading cycle will have an effect on the subsequent cycle. This could be due to the nature of the crack tip (blunt vs. sharp) at a particular point, which could easily affect the subsequent G_c value. It could also be due to the zone of plastic deformation that extends in front of a given crack tip. Another possibility is that the location of the crack tip within the wood-adhesive bondline could influence the subsequent G_c value.

After the appropriate model for the data was obtained, the analysis of variance (ANOVA) was performed and comparisons were made among the three adhesives and the accelerated aging conditions. Within the ANOVA, pairwise comparisons are completed using the Tukey-Kramer adjustment. This adjustment reduces the likelihood of mistaking an insignificant difference between means for a significant difference. In other words, the Tukey-Kramer adjustment controls the type I error.

Figure 6-10 shows how the treatments affect the mean G_c for each adhesive. The figure is an interaction plot showing how the different levels of latex (i.e., Latex 1, Latex 2, and Latex 3) interact with the levels of the treatments (boil, control, and vacuum soak exposures for accelerated aging). Least squares (LS) mean G_c values are plotted. Statistically, the LS means represent mean G_c values after all sources of variability (due to random and other effects, like covariance) have been removed from the data. Therefore, the LS means shown in the interaction plot are not the sample means, but rather are means that have been adjusted to remove external sources of variability. P-values will be reported in parentheses throughout the discussion as a criterion for significance between two means. Low p-values ($\leq$ 0.10) indicate significant differences between the means.

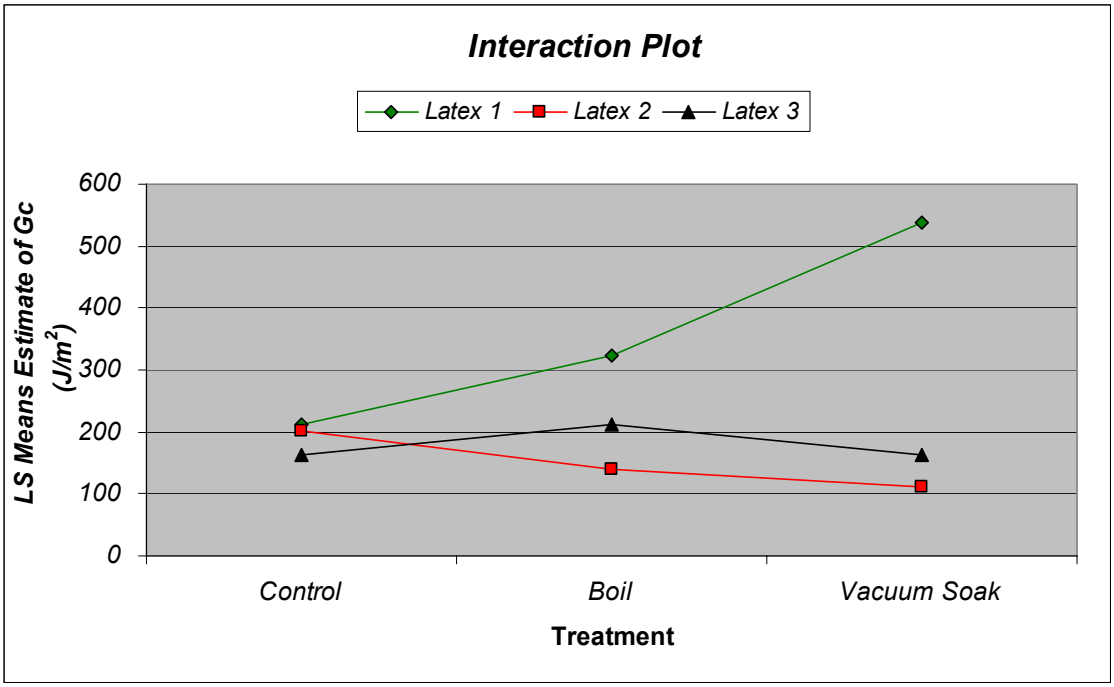

Figure 6-10: Plot showing the interaction between the three latices and the three accelerated aging treatments.

A surprising finding is that Latex 1 exhibits *better* performance after aging. There is a statistically significant increase in the G_c from the control treatment and the boil treatment (0.0207). Similarly, specimens exposed to the vacuum soak treatment had significantly higher G_c*s* than both the control (< 0.0001) and the boil treatment groups (<0.0001). While this finding is puzzling, it is not the first time that accelerated aging exposures have resulted in enhanced fracture toughness values. Previous work using isocyanate resins also indicated that moisture exposures increased the fracture toughness (Schmidt 1998; Zheng 2002). It was thought that this behavior may be due to the relaxation (during the accelerated aging treatment) of cure stresses in the bondline. However, for latex adhesives, we would expect less stress to occur on the bondline prior to the accelerated aging treatments. Unlike isocyanates, no thermal treatment is required during consolidation of latex adhesives. Here the mechanism for improved behavior after aging treatments could be entirely different, especially considering the thermoplastic nature of poly(vinyl acetate) adhesives. Perhaps the additional moisture allows the polymer chains to achieve greater stages of coalescence. Perhaps more even coverage of the bondline was possible after the aging treatments, or perhaps the treatments somehow resulted in greater penetration into

the wood microstructure. However, any of these effects would likely occur in the other two latices as well, and that does not occur.

The trend for Latex 2 G_c values as a function of accelerated aging exposure seems to indicate that the fracture toughness diminishes with treatment. Statistically, there is no significant difference between the LS Mean G_c of the control and the boil groups (0.5078). However, the vacuum soaked specimens have a significantly lower mean G_c than the control group (0.0806). There is no significant difference between the Latex 2 boil and vacuum soak values (0.9933). Latex 3 G_c values also do not change due to the applied treatment conditions (control vs. boil 0.7558, control vs. vacuum soak 1.0000, boil vs. vaccum soak 0.7488).

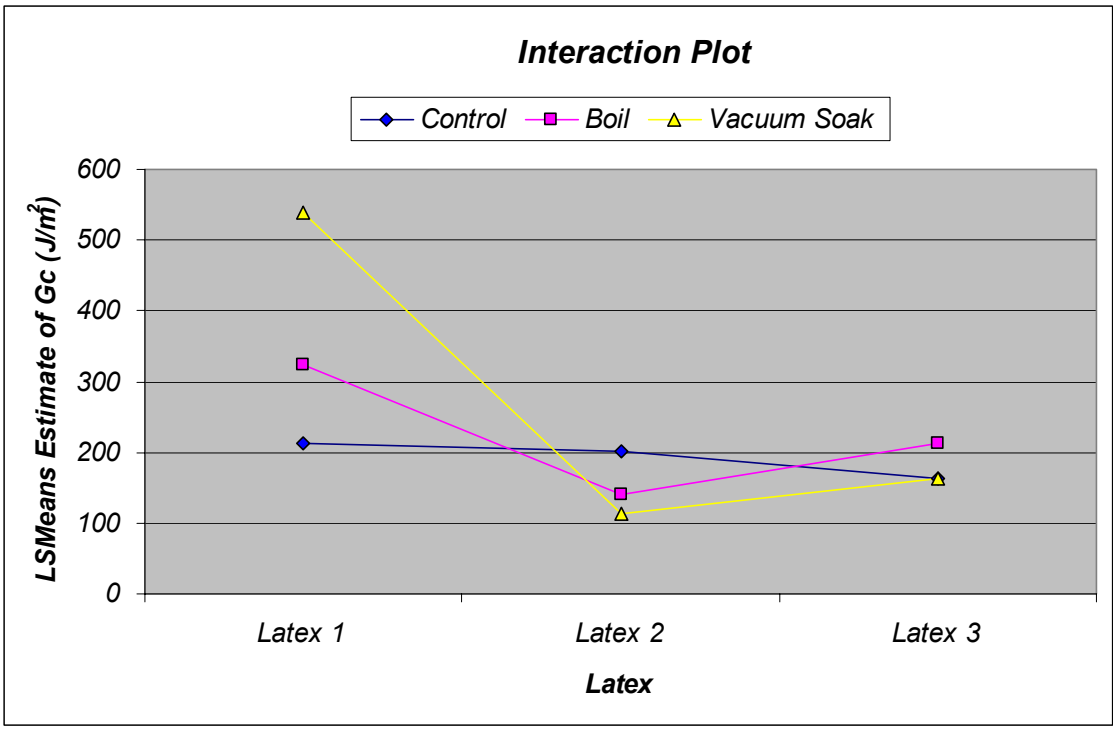

Figure 6-11: Least Squared Means for the three accelerated aging treatments plotted as a function of adhesive.

Figure 6-11 shows the same LS means, but the effect due to the adhesive is more apparent. No differences exist among the three adhesives when only the control treatment is considered (Latex 1 vs Latex 2: 1.000, Latex 1 vs. Latex 3: 0.7829, Latex 2 vs. Latex 3: 0.9270). The boil treatment resulted in significantly different fracture toughness values for Latex 1 and Latex 2

(<.0001), and for Latex 1 and Latex 3 (0.0219). No differences were evident between the boiled Latex 2 and Latex 3 groups (0.2872). Vacuum soaking appeared to differentiate the performance of Latex 1, just as the boil treatment did. Here clear differences exist between Latex 1 and Latex 2 (< 0.0001) as well as between Latex 1 and Latex 3 (< 0.0001). Latex 2 and 3 show no difference (0.7823).

The differences among the means among all latex-treatment groups can be illustrated in the table below. Within the table, the groups with the highest mean G_c values are listed at the top. To distinguish between statistically significant groups, each group is assigned a letter. When two adjacent groups are assigned the same letter, the two groups are not significantly different. Different letters indicate significant differences. In a series of bearing the same letter designation, consecutive means will not be significantly different, but sometimes there will be a significant difference between the n^{th} mean and the first mean, for example. In such cases, sub-groupings are created. Observations that are statistically identical are joined by a line. In Table 6-7, the last mean (Latex 2 Vacuum Soak) is the same as Latex 2 Boil, thus giving it a grouping of C. However, it is significantly different from Latex 1 Control. Therefore, the lines illustrating the groupings are employed.

Table 6-7: Statistically significant groupings of G_c's

Adhesive and Condition	***LS Mean G_c***	***Grouping***
Latex 1 Vacuum Soak	538.08	A
Latex 1 Boil	324.13	B
Latex 3 Boil	212.95	C
Latex 1 Control	211.82	C
Latex 2 Control	201.03	C
Latex 3 Control	162.36	C
Latex 3 Vacuum Soak	161.92	C
Latex 2 Boil	139.3	C
Latex 2 Vacuum Soak	112.12	C

To summarize, the accelerated aging treatments had a dramatic effect on the performance of Latex 1. Instead of resulting in diminished performance, Latex 1 actually exhibited greater fracture toughness values following the aging treatments. Both boiling and vacuum soaking conditions yielded higher G_c values than the control condition; and the vacuum soak conditions

resulted in higher G_c values than the boil condition. On the other hand, Latex 3 was completely insensitive to the applied accelerating aging conditions. Latex 2 control specimens had higher G_cs than the vacuum soak specimens, but there was no difference between the control and the boil specimens, or between the boil and the vacuum soak specimens. Exposure to control conditions resulted in all latices behaving similarly.

The LS mean G_c values (discussed above) are illustrated in Figure 6-12. Standard deviation is indicated by the error bars.

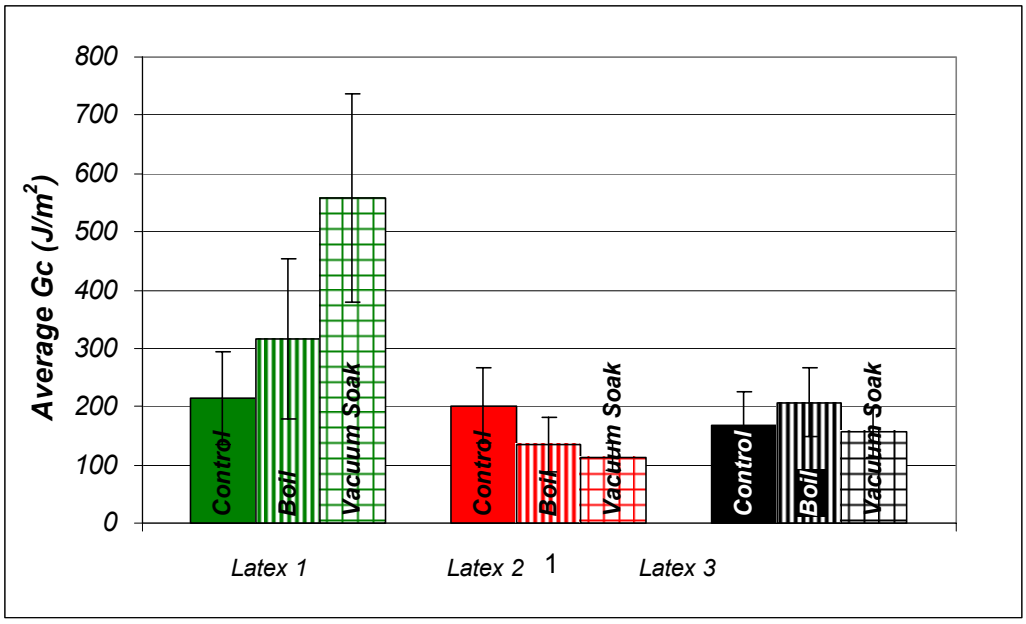

Figure 6-12: Average fracture energies (standard deviations indicated by error bars) for each of the three latices and treatment conditions.

Table 6-8 shows the mean values and standard deviations for the data set where the first five loading cycles are included. This is the same data that is depicted in Figure 6-12. Recall that the first five loading cycles were selected to provide a more balanced data set.

Table 6-8: Chart showing the average fracture energies, standard deviations, and the number of G_c datapoints for each adhesive-treatment combination.

		G_c (J/m^2)		
		Average	**St. Dev.**	**# of Observations**
	Control	214.2	80.6	55
Latex 1	*Boil*	315.7	136.9	39
	Vac Soak	558.8	178.5	24
	Control	202.0	65.2	60
Latex 2	*Boil*	135.6	47.2	45
	Vac Soak	112.9	23.5	52
	Control	168.1	56.7	52
Latex 3	*Boil*	206.9	59.3	49
	Vac Soak	155.9	42.2	51

Table 6-9 provides the mean and standard deviation for *all* loading cycles. By comparing Tables 6-8 and 6-9, it is clear that the smaller data set (where the first five loading cycles are considered) provides a good representation of the overall data.

Table 6-9: Chart showing the average fracture energies, standard deviations,and the number of G_c datapoints for each adhesive-treatment combination.

		G_c (J/m^2)		
		Average	**St. Dev.**	**# of Observations**
	Control	213.3	64.9	123
Latex 1	*Boil*	329.1	136.4	74
	Vac Soak	514.1	155.5	43
	Control	197.5	60.8	130
Latex 2	*Boil*	139.2	47.0	49
	Vac Soak	118.0	23.9	90
	Control	170.1	51.2	91
Latex 3	*Boil*	208.8	56.2	55
	Vac Soak	168.1	46.9	65

Poly(vinyl acetate) adhesives have been tested in previous fracture toughness studies. Sernek and Gagliano both performed these tests using commercially available PVAc formulations (Gagliano 2001; Sernek 2002). Here, the specimens were tested in the dry state. Gagliano and

Sernek each tested their specimens after conditioning to 8-10% moisture content. Also, recall that an extended low pressure consolidation was applied here, whereas Gagliano and Sernek each applied higher consolidation pressures for one hour. The amount of adhesive applied per face was approximately the same. Neither Gagliano nor Sernek applied accelerated aging treatments to investigate the durability of the adhesive, although Sernek did apply different heat treatments to the substrates before bonding. The only test condition that would be similar to these previous experiments would be the control groups. Sernek found a G_{max} value of 313.9 J/m^2, whereas Gagliano reported a G_{max} of 400 J/m^2. In this study the G_c values for the three adhesives exposed to the control condition were statistically the same, with mean values ranging from 162 to 212 J/m^2. Each of the latices tested exhibited much lower fracture toughness values than the latices tested by Gagliano and Sernek.

Physically, differences were observed between specimens that received the control treatment and those that were submitted to boiling or vacuum soaking. For the control group, the color of the bondline became dark brown after oven drying. This was not the case for the weathered specimens, although they also underwent oven drying. A possible reason for the darker color is increased crosslinking. The catalyst could have leached out of the system during the accelerated aging exposures, and therefore less crosslinking might have occurred in those specimens.

Another difference was the uniformity of adhesive coverage across the bondline. For the control specimens, the adhesive appeared as a thin, dark layer between two flat adherends. However, for the other two treatments, some cupping was evident, and the adhesive appeared to be stretching between the adherends, resulting in a much thicker bondline region and a much less uniform bondline. Images of the samples were captured under magnification via a fluorescence microscope. Results are shown in Figures 6-13 through 6-19.

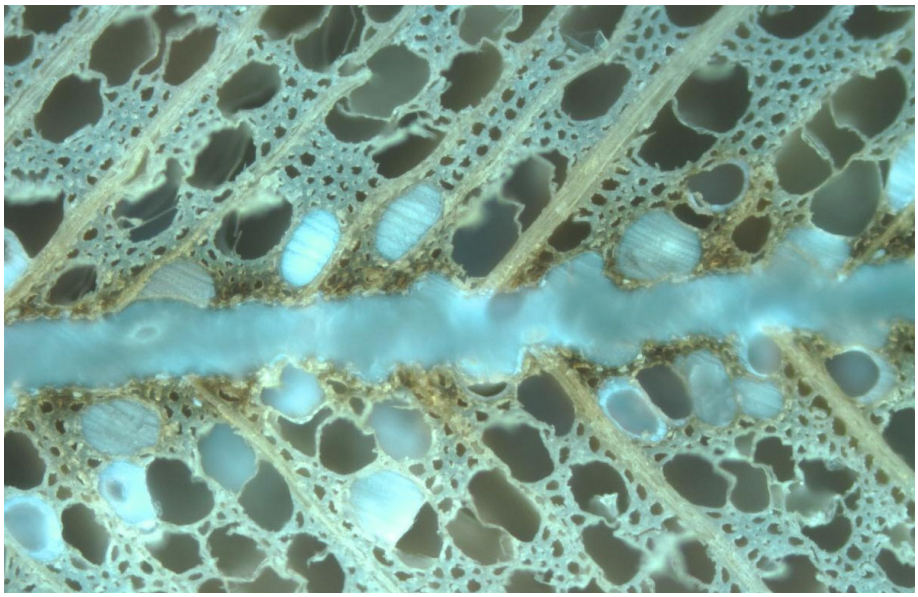

Figure 6-13: Control specimen of Latex 2, 5x. This is image is also representative of Latex 1 and 3 control specimens.

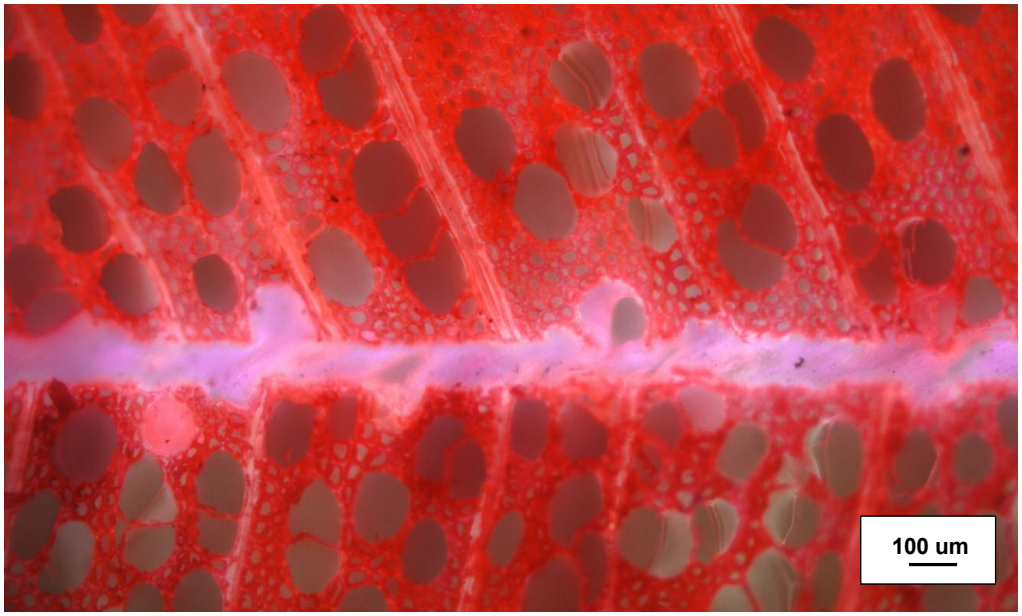

Figure 6-14: Latex 1 Boil, 5x.

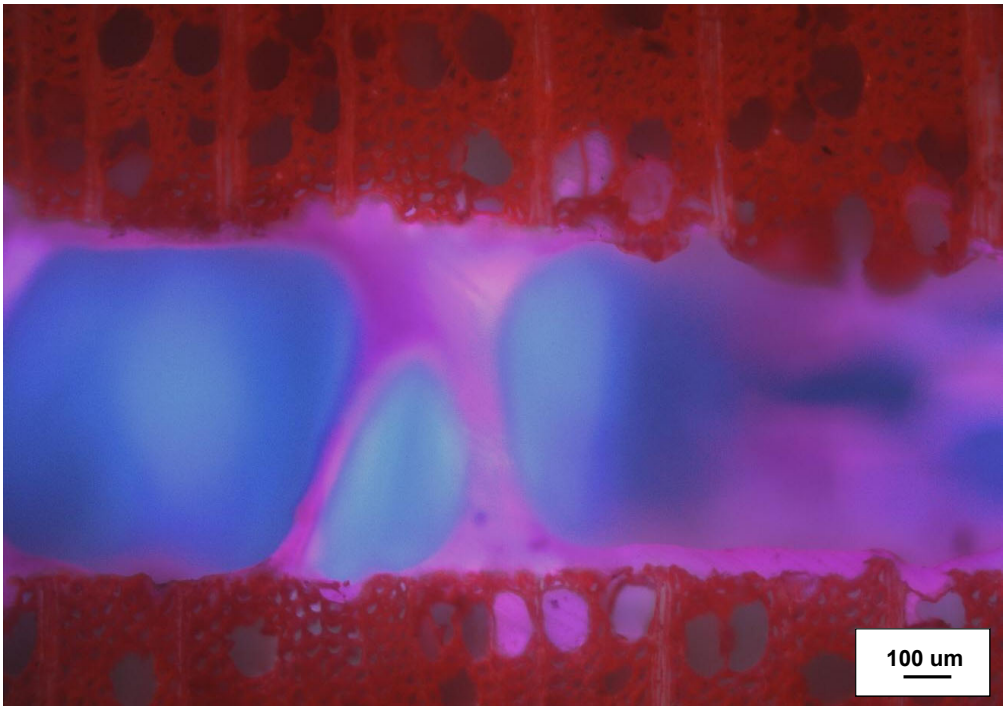

Figure 6-15: Latex 2 Boil, 5x.

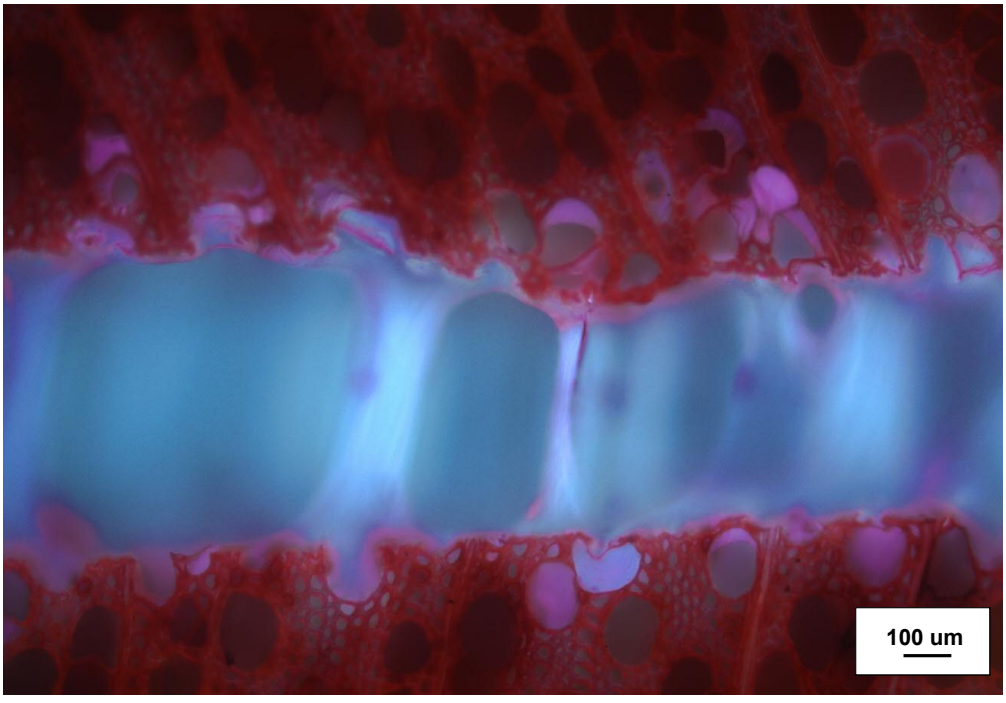

Figure 6-16: Latex 3 Boil, 5x.

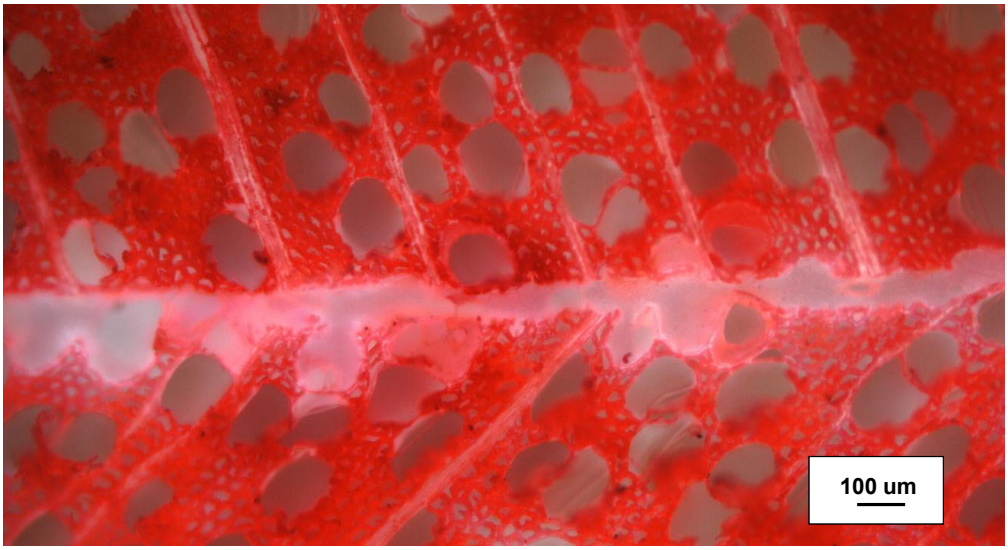

Figure 6-17: Latex 1, Vacuum Soak, 5x.

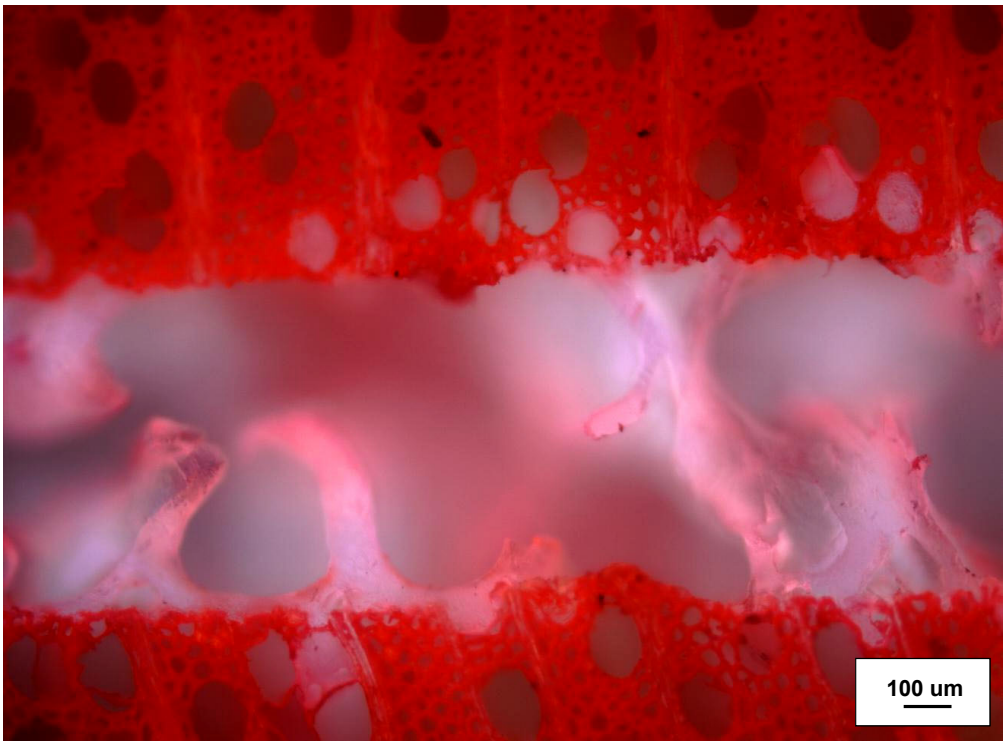

Figure 6-18: Latex 2 Vacuum Soak, 5x.

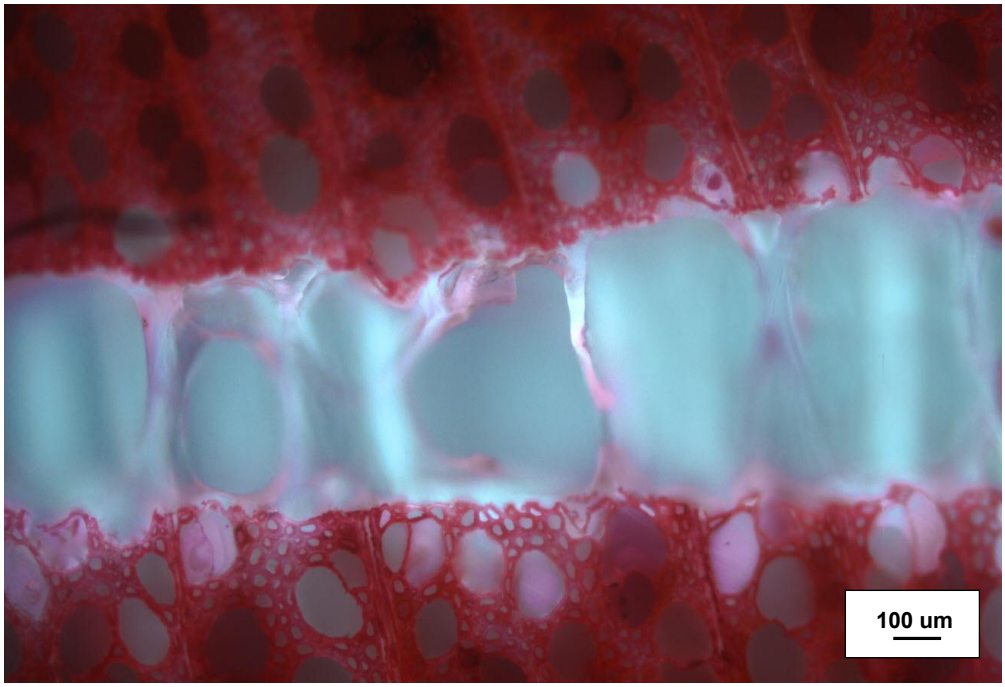

Figure 6-19: Latex 3 Vacuum Soak

All control specimens appeared similar to that shown in Figure 6-13, so only one representative control specimen is shown. Notice the dark brown regions in the wood surrounding the bondline. This is likely due to staining by the acidic catalyst. Solutions of Lewis acids discolor wood. The control samples from all three adhesives showed this staining phenomenon. The only difference between the control specimens among the three adhesives was that the Latex 1 samples appeared to have slightly thinner bondlines.

After the accelerated aging treatments, the Latex 1 samples were clearly different from the Latex 2 and Latex 3 samples. All weathered samples were stained with saffranin dye to help distinguish the adhesive from the wood. Notice that the Latex 2 and Latex 3 samples show evidence of adhesive stretching and bridging after the boil and vacuum soak treatments. Latex 1 samples do not. The greater integrity of the Latex 1 bondlines after treatment may explain why they were so much tougher than the Latex 2 and 3 samples weathered samples. The bondline images do not explain why the treatments for Latex 1 increased the fracture toughness over the Latex 1 control specimens. Similarly they do not explain why the adhesive stretching and

bridging did not cause a significant decrease in the fracture toughness of the weathered Latex 2 and 3 samples.

To summarize, Latex 1 exhibited unique fracture results. The fracture toughness increased after exposure to weathering conditions. Fluorescence microscopy of fracture specimens revealed that all Latex 1 samples had uniform bondline thicknesses. This was not the case for Latex 2 and 3, which showed adhesive bridging and voids along the bondline after accelerated aging exposures. Recall that Latex 1 also exhibited unique morphological features when characterized via SEM (see Chapter 4). In particular, the latex films showed variations in depth, and also seemed to have a thick polymeric serum coating the particles. When applied to wood, and subjected to the accelerated aging treatments, Latex 1 never formed a film, while Latex 2 and 3 did. This confirms that Latex 1 is more resistant to the imposed accelerated aging treatments.

Although Latex 1 exhibited better durability, it must also be noted that fewer of the Latex 1 samples were included in the analysis (see Table 6-2). This could introduce a bias into the data. The proportion of usable specimens could be an indication of durability as well, especially in cases of catastrophic delamination. Here, all of the specimens survived the accelerated aging treatments intact. Unusable specimens were due to either wood failure, or to having less than 3 loading cycles per specimen. For Latex 1 boil samples, 75% of the samples were included in the analysis (9 of 12). Three specimens were eliminated because of an insufficient number of loading cycles. Latex 1 vacuum soak samples had an inclusion rate of only 42% (5 of 12). Two specimens were unusable because of wood failure, while the other 5 had an insufficient number of loading cycles. The reason for this high proportion of discards among Latex 1 accelerated aging samples is unclear. Other indications point to the Latex 1 having more durability than its counterparts.

According to the solution NMR results (Chapter 5), Latex 1 had the highest proportion of water-phase NMA (~20%). The unusual behavior of Latex 1 could be related to its NMA distribution. It is possible that NMA-rich portions of the adhesive, or water-soluble poly-NMA chains achieved greater penetration into wood during the accelerated aging exposures. As discussed in the introduction, the methylol groups of NMA are capable of forming crosslinks with wood

polymers. However, other factors could be responsible for the fracture results as well. The unique morphology in itself could be the key to the performance of Latex 1. If the polymer particles were protected in a polymeric serum (as the SEM micrographs suggested), that could play an important role. In a similar fashion, the degree of particle aggregation observed in the Latex could be a key factor.

Realistically, many different factors could be influencing the fracture toughness of the three adhesives. Differences in the fracture behavior among the adhesive and accelerated aging conditions may or may not be related to differences in the NMA distribution.

6.4 Conclusions

Fracture mechanics testing is a method useful in probing the wood-adhesive interphase. Here yellow-poplar specimens were bonded with three different PVAc latex adhesives. The specimens were assigned to one of three accelerated aging conditions (control, boil, vacuum soak) in a completely randomized design. Specimens were dried completely and stored in dessicators until tested.

G_c values were found to exhibit a first order autoregressive covariance with loading cycle. This indicates that any given G_c value is related to the previous G_c value, and has an effect on the subsequent G_c value. This is probably due to the zone of plastic deformation that exists in front of a crack tip, or due to the location of the crack tip within the wood-adhesive interphase.

For each adhesive, the effect of the accelerated aging conditions was investigated by comparing each of the accelerated aging treatments to the control treatment. Test results showed that Latex 1 behaved in a fashion that was substantially different than Latex 2 and Latex 3. For Latex 1, exposure to both the boil and vacuum soak conditions resulted in statistically significant increases in the G_c. The vacuum soak exposure caused higher fracture toughness values than the boil exposure. Latex 3 specimens showed no difference in G_c when the control treatments were compared with the accelerated aging treatments. For Latex 2, the vacuum soaked specimens gave lower fracture toughness values than the control specimens.

Comparisons of the three adhesives were also made as a function of the aging exposure. The control treatment resulted in no significant differences among the three adhesives. After boiling, Latex 1 specimens exhibited significantly higher G_c values than both Latex 2 and Latex 3 boil specimens. There was no significant difference between the Latex 2 boil and the Latex 3 boil G_c results. The vacuum soak treatment for specimens bonded with Latex 1 resulted in very large (and highly significant) G_c values. Differences between Latex 2 and Latex 3 vacuum soak results were not significant.

Bondline images revealed that all control specimens had similar bond thicknesses. In the control specimens, the adhesive appeared to be dark brown, and the wood surrounding the bondline was stained. The brown color is likely due to a discoloration associated with wood staining by Lewis acids. After accelerated aging treatments, Latex 2 and 3 specimens showed that the adhesive stretched significantly, causing voids and leading to much thicker bondlines. Latex 1 did not show the same behavior as Latex 2 and Latex 3; after aging exposures, the bondline thicknesses remained constant and there was no indication of the stretching behavior.

Results of the fracture tests reveal that all three of the latices exhibit good durability related performance. A clear distinction must be made between Latex 1 and Latices 2 and 3. Latex 1 actually performed better after exposure to the aging conditions. The mechanism for this behavior is not known. SEM micrographs of Latex 1 indicated that the particle boundaries always remained intact, even after accelerated aging exposures. Solution NMR studies revealed that Latex 1 had the most water-phase NMA of the three latices (20%). It is possible that the reason for the enhanced durability is due to NMA distribution, but it could also be due to particle morphology, or many other factors. It should also be noted that fewer Latex 1 samples were included in the analysis due to either wood failure or too few loading cycles per specimen.

6.5 Acknowledgements

The author would like to acknowledge the assistance of several individuals for their help with this study. First, special thanks go to other graduate students who helped train me on the fracture testing approach, and to those who shared their thoughts, ideas and testing experience with me. These include Rob Schmidt, Mike Malmberg, Jerone Gagliano, Jun Zheng, Jonathan Williams,

Brian Liswell, and Milan Sernek. A special thanks also goes to Steve Brown, who helped conduct the testing. Also acknowledged are the efforts of David Jones, who helped machine the wood specimens, and the support of the staff members of the Brooks Forest Products Laboratory, including Rick Caudill, Kenny Albert, Carlile Price, and Butch Sizemore. Finally, the author acknowledges the assistance of KB Boomer at the Statistical Consulting Center at the Pennsylvania State University.

6.6 References

(1989). Standard Test Method for Strength Properties of Adhesive Bonds in Shear by Compression Loading. American Society for Testing and Materials. **ASTM D905:** 27-30.

(1990). Standard Specification for Adhesives Used in Nonstructural Glued Lumber Products. ASTM. **D3110-90:** 184-192.

(1995). Standard Specification for Adhesives Used for Finger Joints in Nonstructural Lumber Products. ASTM. **D5572-95:** 459-475.

(1999). Standard Specifications for Adhesives Used for Laminate Joints in Nonstructural Lumber Products. ASTM. **D5751-99:** 503-512.

(1999). Standard Test Method for Fracture Strength in Cleavage of Adhesives in Bonded Metal Joints. ASTM. **D3433-99:** 228-234.

Blackman, B., J. P. Dear, et al. (1991). "The calculation of adhesive fracture energies from double-cantilever beam test specimens." Journal of Materials Science Letters **10**: 253-256.

Ebewele, R. O., B. H. River, et al. (1979). "Tapered Double Cantilever Beam Fracture Tests of Phenolic-Wood Adhesive Joints." Wood and Fiber Science **11**(3): 197-213.

Ebewele, R. O., B. H. River, et al. (1980). "Tapered double cantilever beam fracture tests of phenolic-wood adhesive joints. Part II. Effects of surface roughness, the nature of surface roughness, and surface aging on joint fracture energy." Wood and Fiber Science **12**(1): 40-65.

Ebewele, R. O., B. H. River, et al. (1986). "Wood Processing Variables and Adhesive Joint Performance." Journal of Applied Polymer Science **32**: 2979-2988.

Gagliano, J. M. (2001). An Improved Method for the Fracture Cleavage Testing of Adhesively-Bonded Wood. Materials Science Engineering. Blacksburg, Virginia Polytechnic Institute and State University**:** 87.

Gagliano, J. M. and C. E. Frazier (2001). "Improvements in the Fracture Cleavage Testing of Adhesively-Bonded Wood." Wood and Fiber Science **3**(3): 377-385.

Hashimi, S., A. J. Kinloch, et al. (1990). "The Analysis of Interlaminar Fracture in Uniaxial Fibre-Polymer Composites." Proceedings of the Royal Society of London. Series A, Mathematical and Physical Sciences **427**(1872): 173-199.

Malmberg, M. (2003). Species Dependence of pMDI/Wood Adhesion. Wood Science and Forest Products. Blacksburg, Virginia Polytechnic Institute and State University.

Porter, A. W. (1964). "On the Mechanics of Fracture in Wood." Forest Products Journal **14**(8): 325-331.

Schmidt, R. G. (1998). Aspects of Wood Adhesion: Applications of ^{13}C CP/MAS NMR and Fracture Testing. Wood Science and Forest Products. Blacksburg, Virginia Polytechnic Institute and State University**:** 150.

Sernek, M. (2002). Comparative Analysis of Inactivated Wood Surfaces. Wood Science and Forest Products. Blacksburg, Virginia Polytechnic Institute and State University**:** 193.

Zheng, J. (2002). Studies of PF Resole/Isocyanate Hybrid Adhesives. Wood Science and Forest Products. Blacksburg, Virginia Polytechnic Institute and State University**:** 198.

6.7 Appendix

Histograms and statistical summaries are included for each latex and accelerated aging condition. These plots illustrate the number of individual G_c values falling within a specified range. The number of data points are given, as is the mean value and the standard deviation within that adhesive and accelerated aging condition.

The second plot on each page includes plots showing G_c as a function of crack length for all "good" specimens for that adhesive and treatment combination.

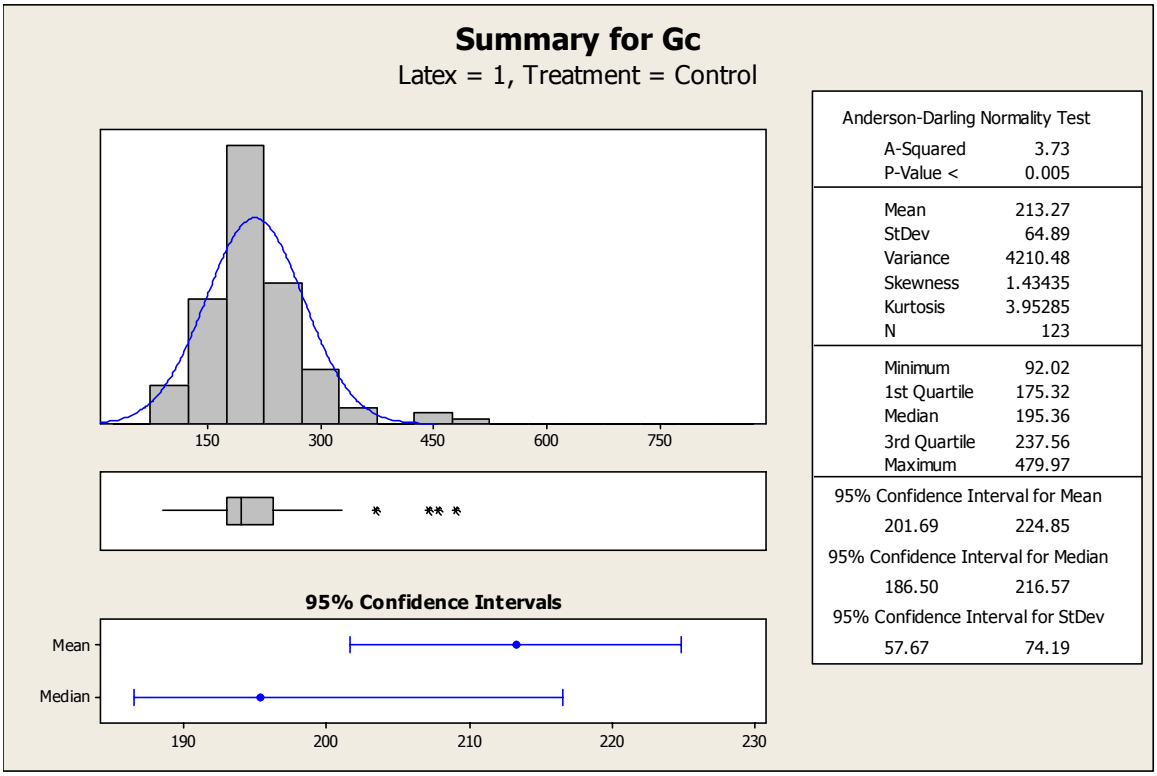
Summary for Gc
Latex = 1, Treatment = Control
150
300
450
600
750
95% Confidence Intervals
Mean
Median
190
200
210
220
230
Anderson-Darling Normality Test
A-Squared 3.73
P-Value < 0.005
Mean 213.27
StDev 64.89
Variance 4210.48
Skewness 1.43435
Kurtosis 3.95285
N 123
Minimum 92.02
1st Quartile 175.32
Median 195.36
3rd Quartile 237.56
Maximum 479.97
95% Confidence Interval for Mean
201.69 224.85
95% Confidence Interval for Median
186.50 216.57
95% Confidence Interval for StDev
57.67 74.19

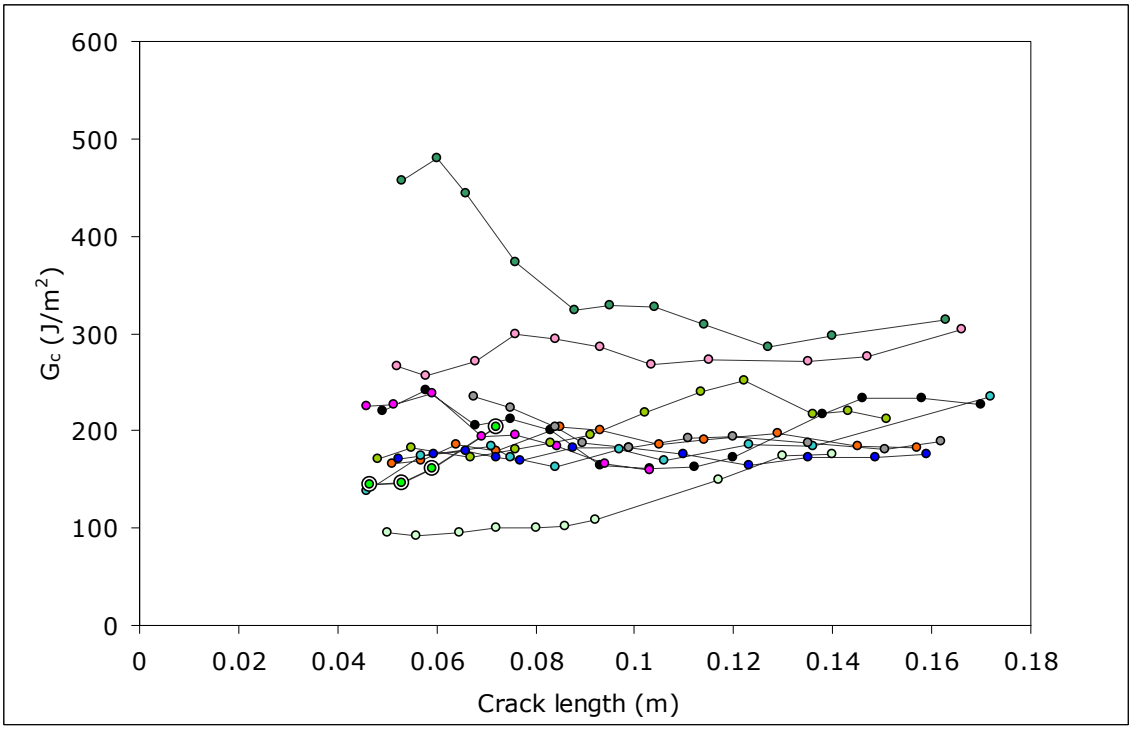
600
500
400
300
200
100
0
Gc (J/m2)
0
0.02
0.04
0.06
0.08
0.1
0.12
0.14
0.16
0.18
Crack length (m)

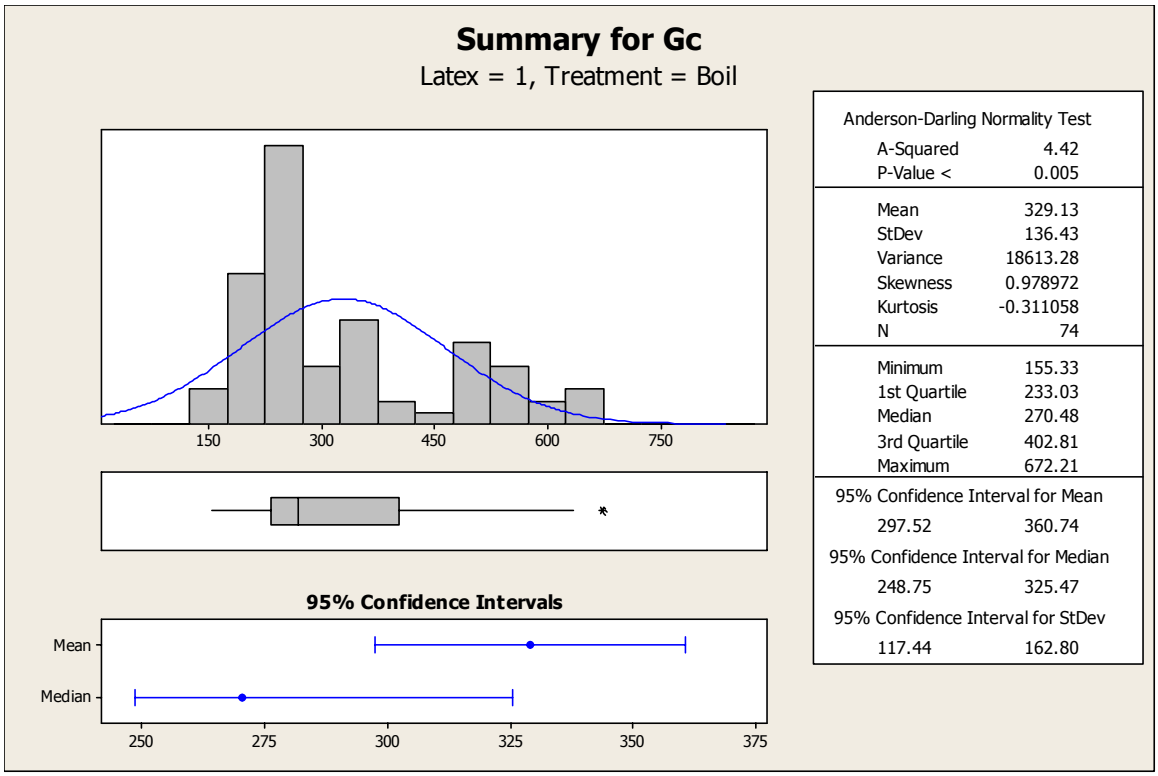
Summary for Gc
Latex = 1, Treatment = Boil
150
300
450
600
750
95% Confidence Intervals
Mean
Median
250
275
300
325
350
375
Anderson-Darling Normality Test
A-Squared 4.42
P-Value < 0.005
Mean 329.13
StDev 136.43
Variance 18613.28
Skewness 0.978972
Kurtosis -0.311058
N 74
Minimum 155.33
1st Quartile 233.03
Median 270.48
3rd Quartile 402.81
Maximum 672.21
95% Confidence Interval for Mean
297.52 360.74
95% Confidence Interval for Median
248.75 325.47
95% Confidence Interval for StDev
117.44 162.80

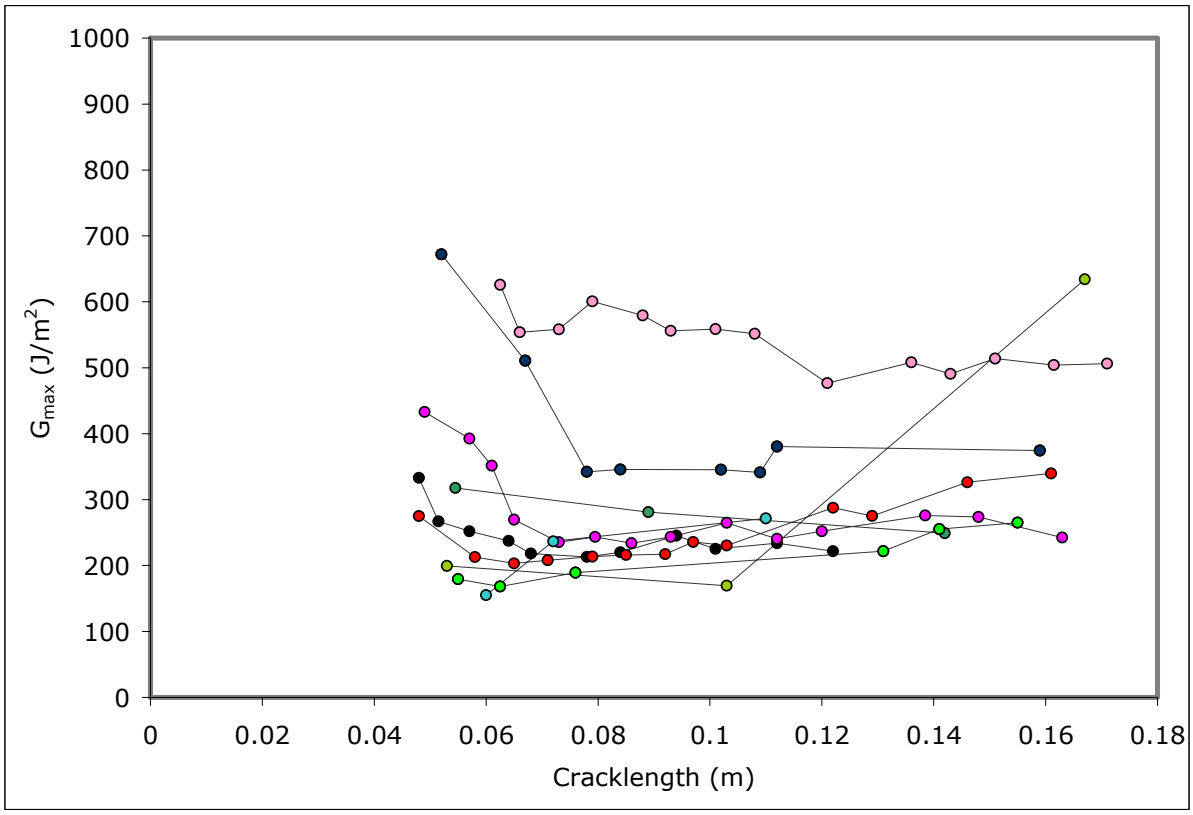
1000
900
800
700
600
500
400
300
200
100
0
G_{max} (J/m^2)
0
0.02
0.04
0.06
0.08
0.1
0.12
0.14
0.16
0.18
Cracklength (m)

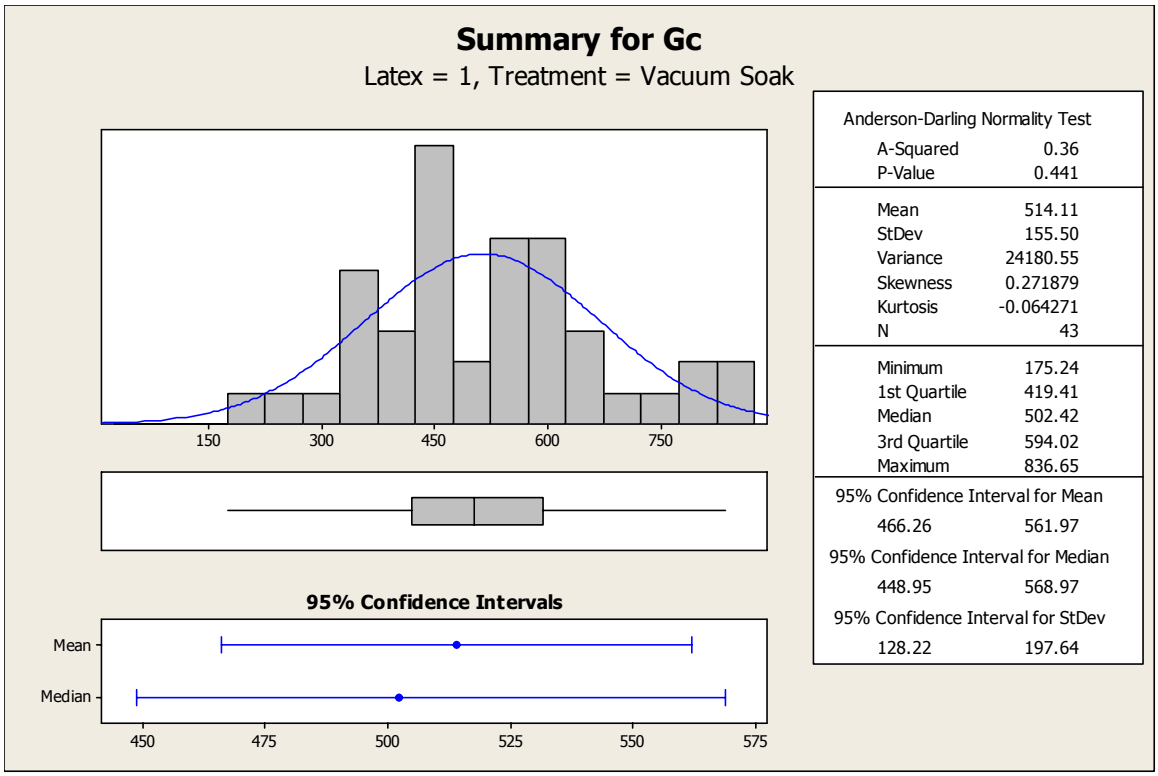
Summary for Gc
Latex = 1, Treatment = Vacuum Soak
150
300
450
600
750
95% Confidence Intervals
Mean
Median
450
475
500
525
550
575
Anderson-Darling Normality Test
A-Squared 0.36
P-Value 0.441
Mean 514.11
StDev 155.50
Variance 24180.55
Skewness 0.271879
Kurtosis -0.064271
N 43
Minimum 175.24
1st Quartile 419.41
Median 502.42
3rd Quartile 594.02
Maximum 836.65
95% Confidence Interval for Mean
466.26 561.97
95% Confidence Interval for Median
448.95 568.97
95% Confidence Interval for StDev
128.22 197.64

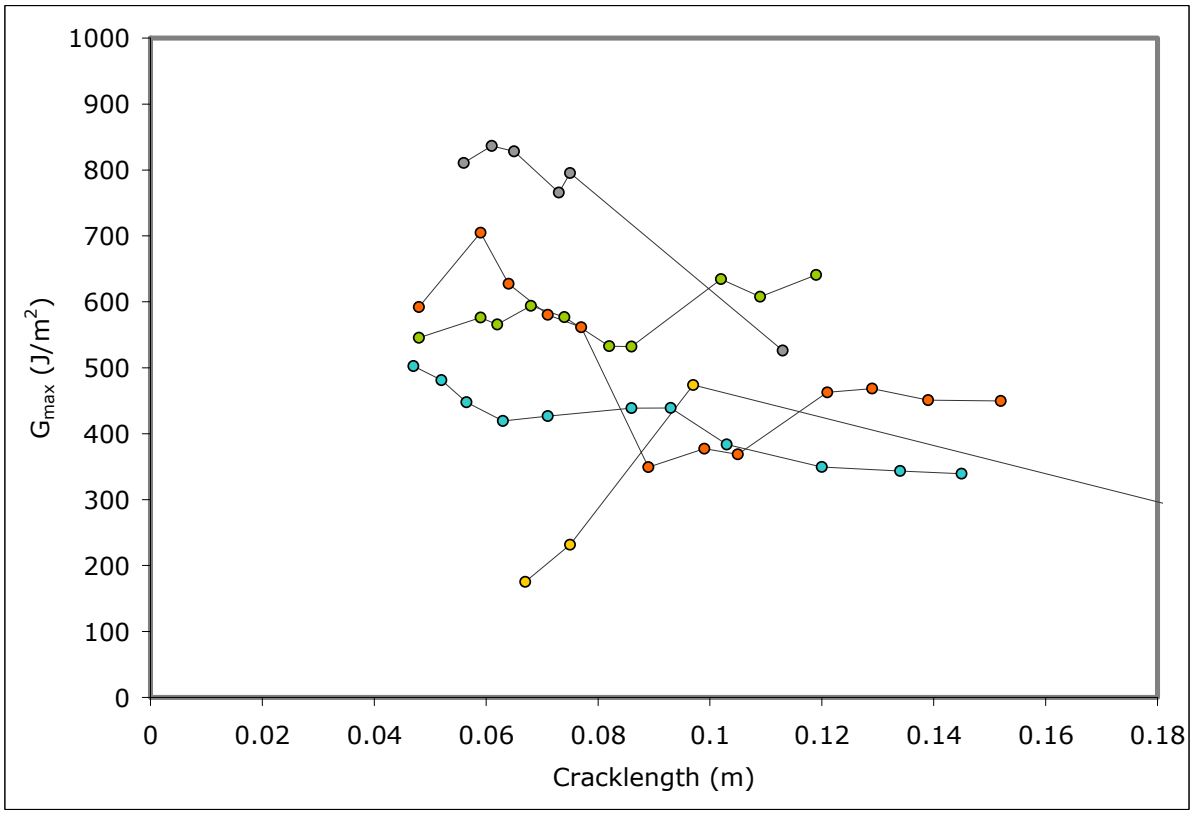
1000
900
800
700
600
500
400
300
200
100
0
G_{max} (J/m^2)
0
0.02
0.04
0.06
0.08
0.1
0.12
0.14
0.16
0.18
Cracklength (m)

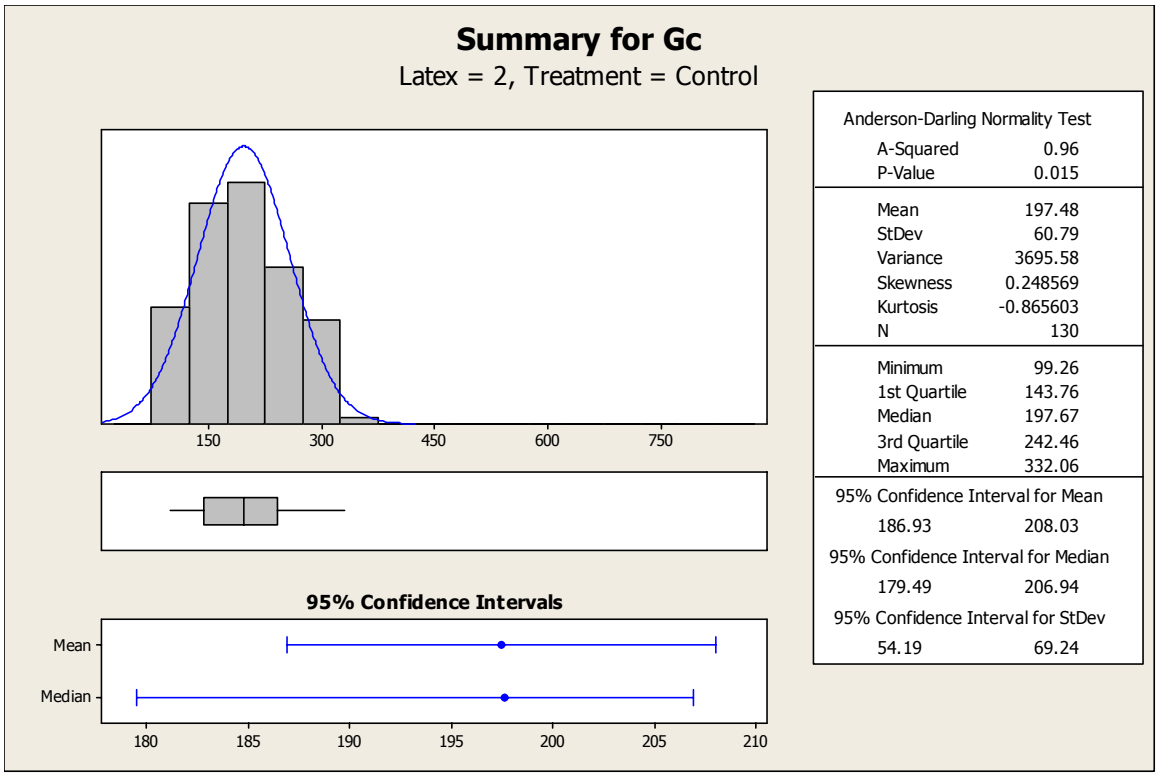
Summary for Gc
Latex = 2, Treatment = Control
150
300
450
600
750
95% Confidence Intervals
Mean
Median
180
185
190
195
200
205
210
Anderson-Darling Normality Test
A-Squared 0.96
P-Value 0.015
Mean 197.48
StDev 60.79
Variance 3695.58
Skewness 0.248569
Kurtosis -0.865603
N 130
Minimum 99.26
1st Quartile 143.76
Median 197.67
3rd Quartile 242.46
Maximum 332.06
95% Confidence Interval for Mean
186.93 208.03
95% Confidence Interval for Median
179.49 206.94
95% Confidence Interval for StDev
54.19 69.24

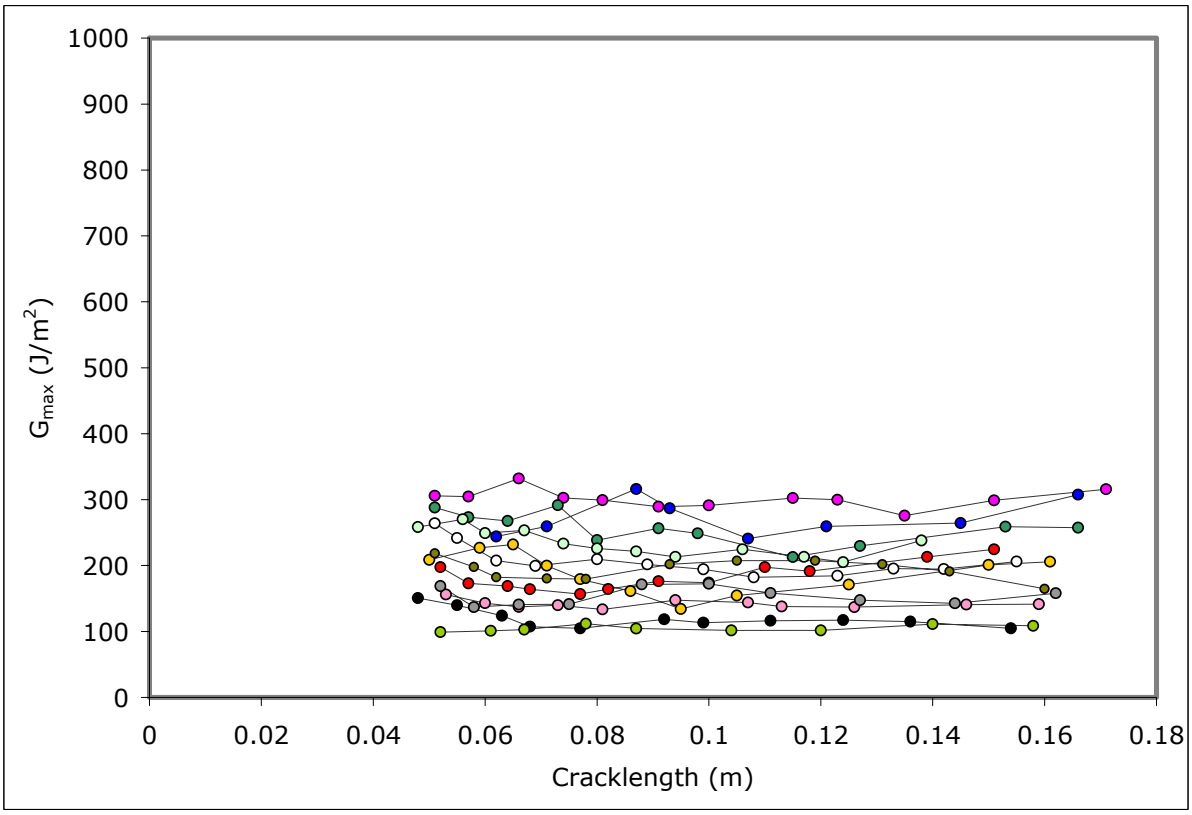
1000
900
800
700
600
500
400
300
200
100
0
G_{max} (J/m^2)
0
0.02
0.04
0.06
0.08
0.1
0.12
0.14
0.16
0.18
Cracklength (m)

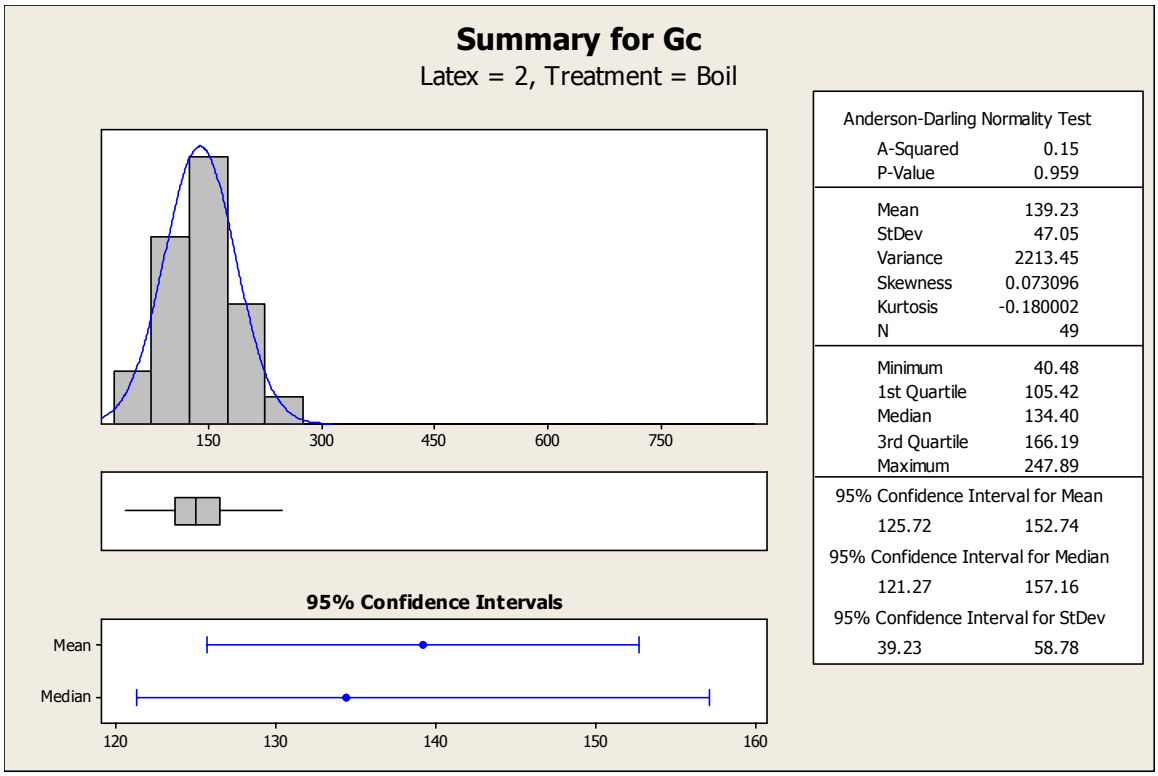
Summary for Gc
Latex = 2, Treatment = Boil
150
300
450
600
750
95% Confidence Intervals
Mean
Median
120
130
140
150
160
Anderson-Darling Normality Test
A-Squared 0.15
P-Value 0.959
Mean 139.23
StDev 47.05
Variance 2213.45
Skewness 0.073096
Kurtosis -0.180002
N 49
Minimum 40.48
1st Quartile 105.42
Median 134.40
3rd Quartile 166.19
Maximum 247.89
95% Confidence Interval for Mean
125.72 152.74
95% Confidence Interval for Median
121.27 157.16
95% Confidence Interval for StDev
39.23 58.78

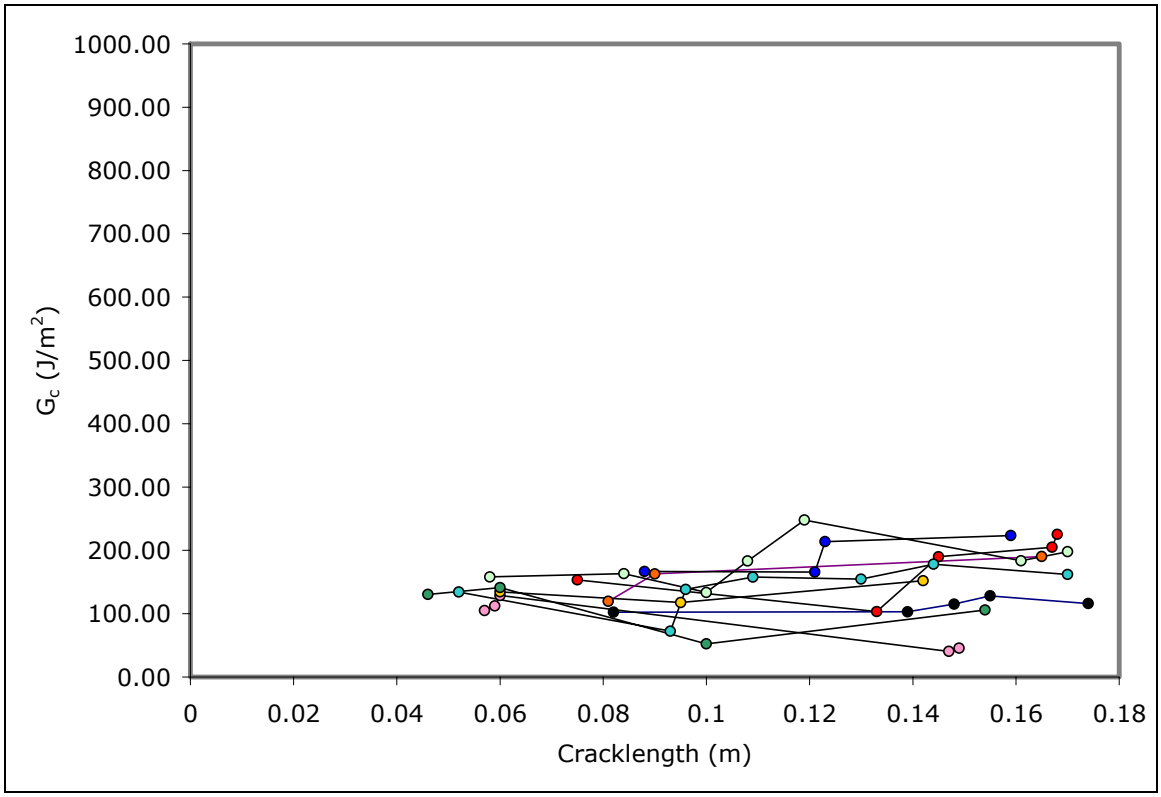
1000.00
900.00
800.00
700.00
600.00
500.00
400.00
300.00
200.00
100.00
0.00
Gc (J/m2)
0
0.02
0.04
0.06
0.08
0.1
0.12
0.14
0.16
0.18
Cracklength (m)

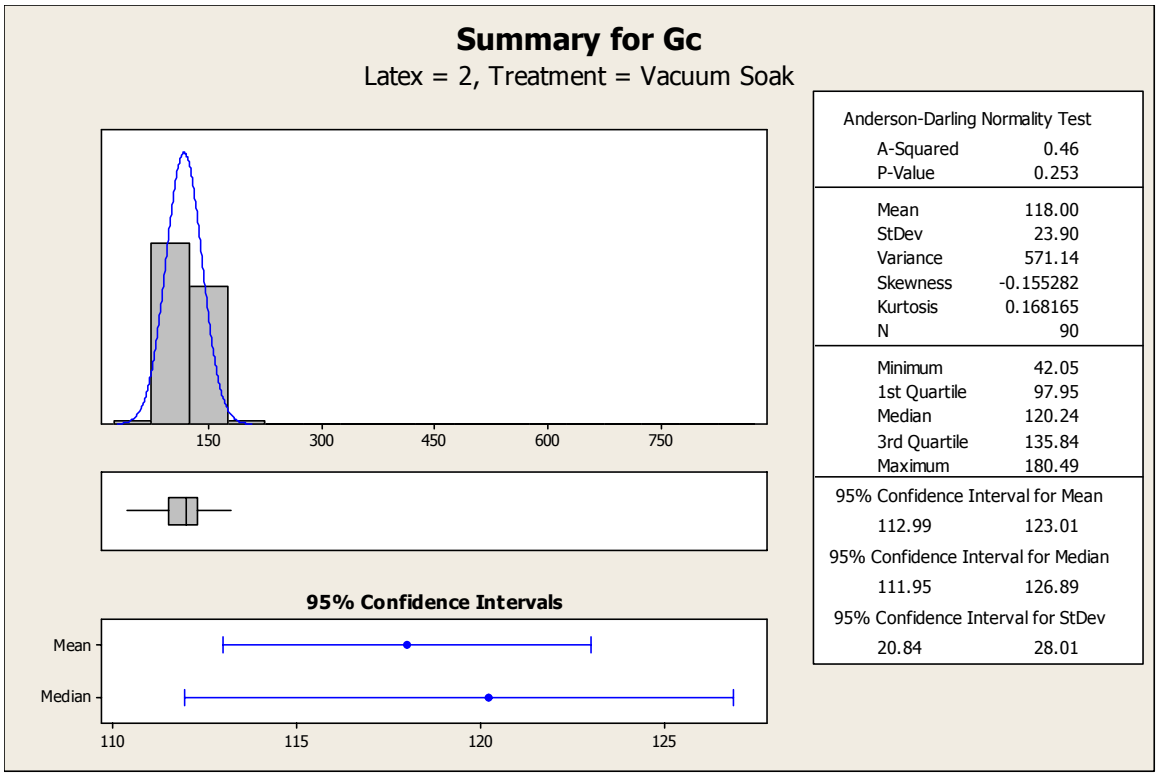
Summary for Gc
Latex = 2, Treatment = Vacuum Soak
150
300
450
600
750
95% Confidence Intervals
Mean
Median
110
115
120
125
Anderson-Darling Normality Test
A-Squared 0.46
P-Value 0.253
Mean 118.00
StDev 23.90
Variance 571.14
Skewness -0.155282
Kurtosis 0.168165
N 90
Minimum 42.05
1st Quartile 97.95
Median 120.24
3rd Quartile 135.84
Maximum 180.49
95% Confidence Interval for Mean
112.99 123.01
95% Confidence Interval for Median
111.95 126.89
95% Confidence Interval for StDev
20.84 28.01

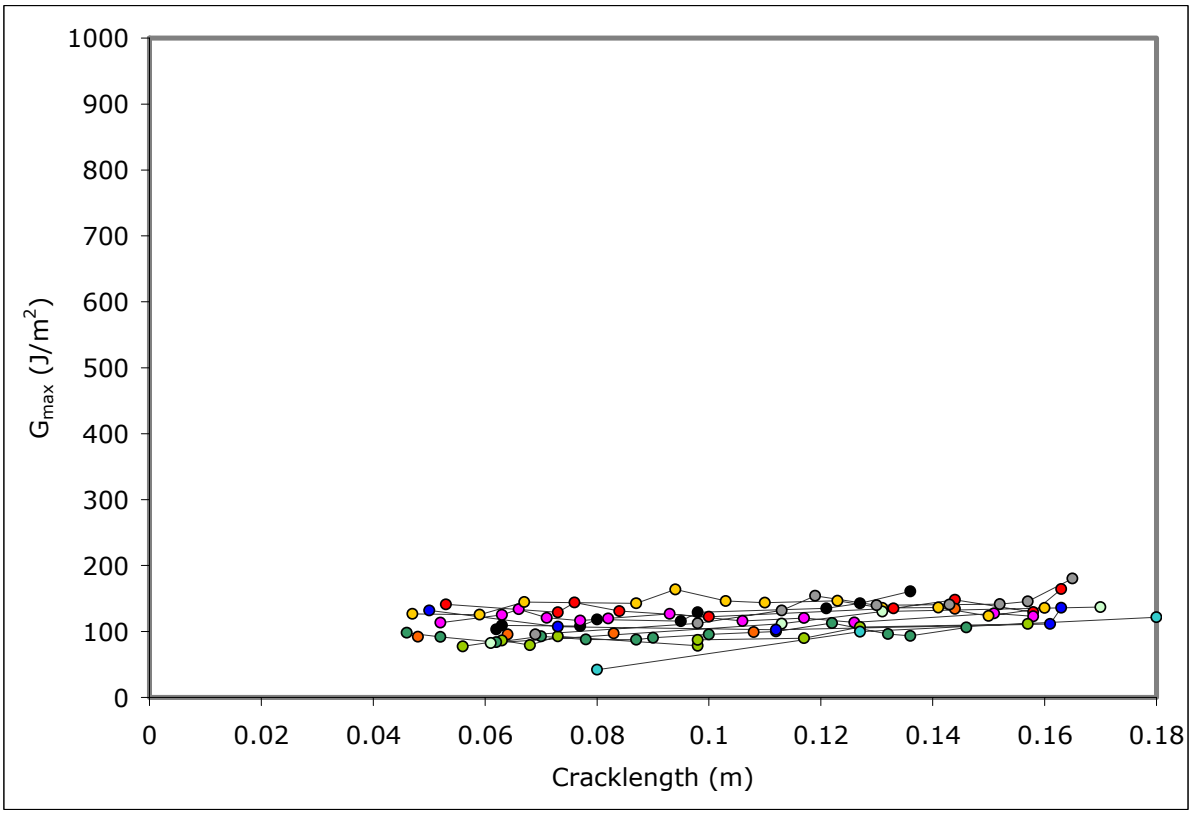
1000
900
800
700
600
500
400
300
200
100
0
G_{max} (J/m^2)
0
0.02
0.04
0.06
0.08
0.1
0.12
0.14
0.16
0.18
Cracklength (m)

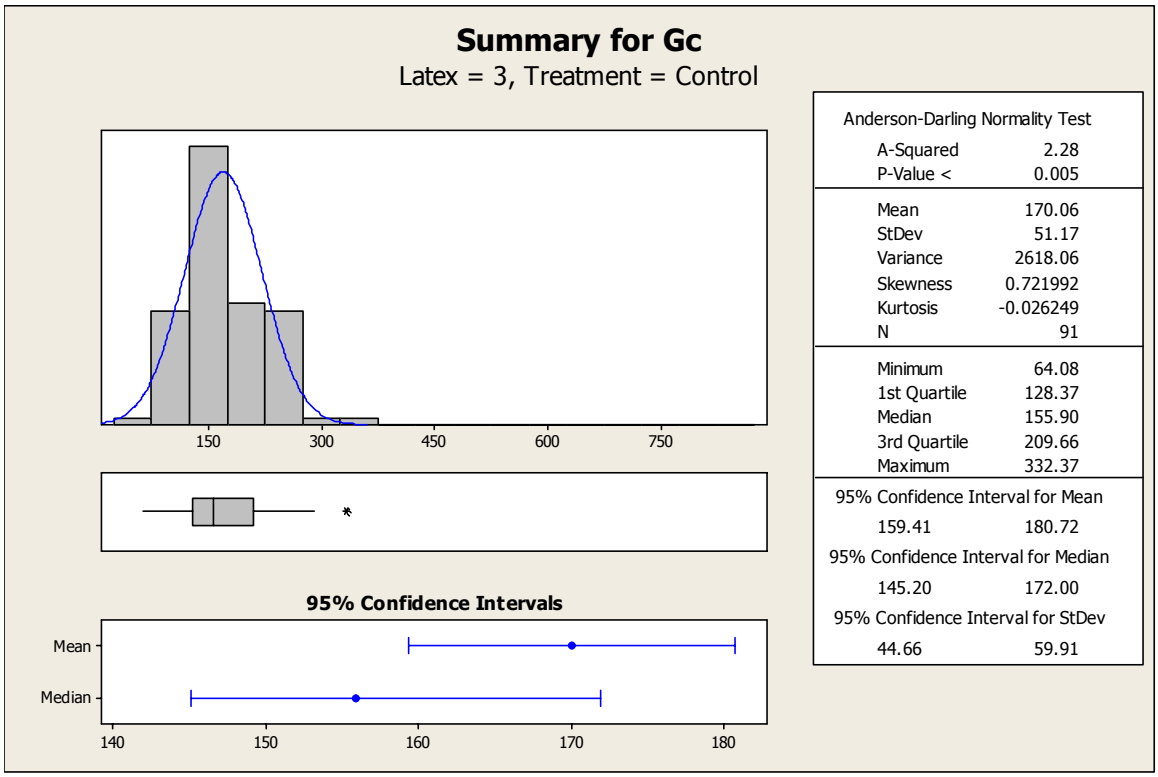
Summary for Gc
Latex = 3, Treatment = Control
150
300
450
600
750
95% Confidence Intervals
Mean
Median
140
150
160
170
180
Anderson-Darling Normality Test
A-Squared 2.28
P-Value < 0.005
Mean 170.06
StDev 51.17
Variance 2618.06
Skewness 0.721992
Kurtosis -0.026249
N 91
Minimum 64.08
1st Quartile 128.37
Median 155.90
3rd Quartile 209.66
Maximum 332.37
95% Confidence Interval for Mean
159.41 180.72
95% Confidence Interval for Median
145.20 172.00
95% Confidence Interval for StDev
44.66 59.91

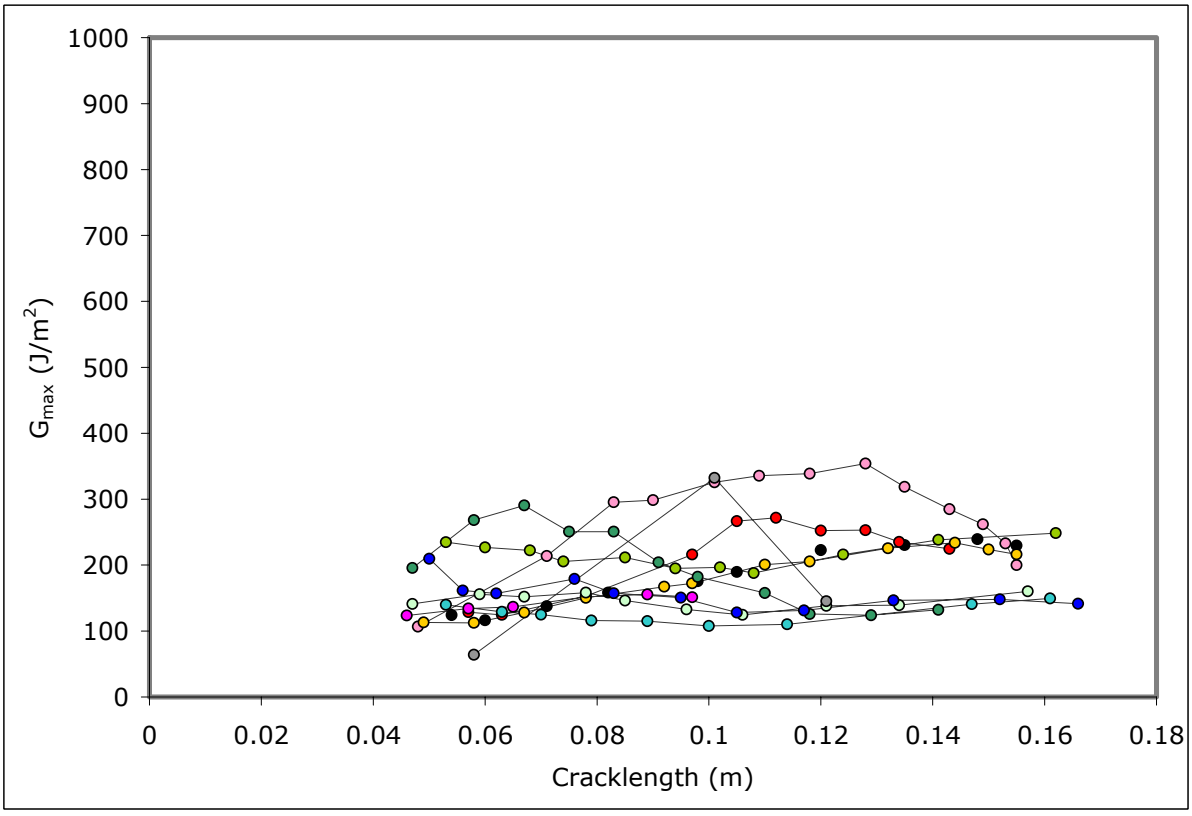
1000
900
800
700
600
500
400
300
200
100
0
G_{max} (J/m^2)
0
0.02
0.04
0.06
0.08
0.1
0.12
0.14
0.16
0.18
Cracklength (m)

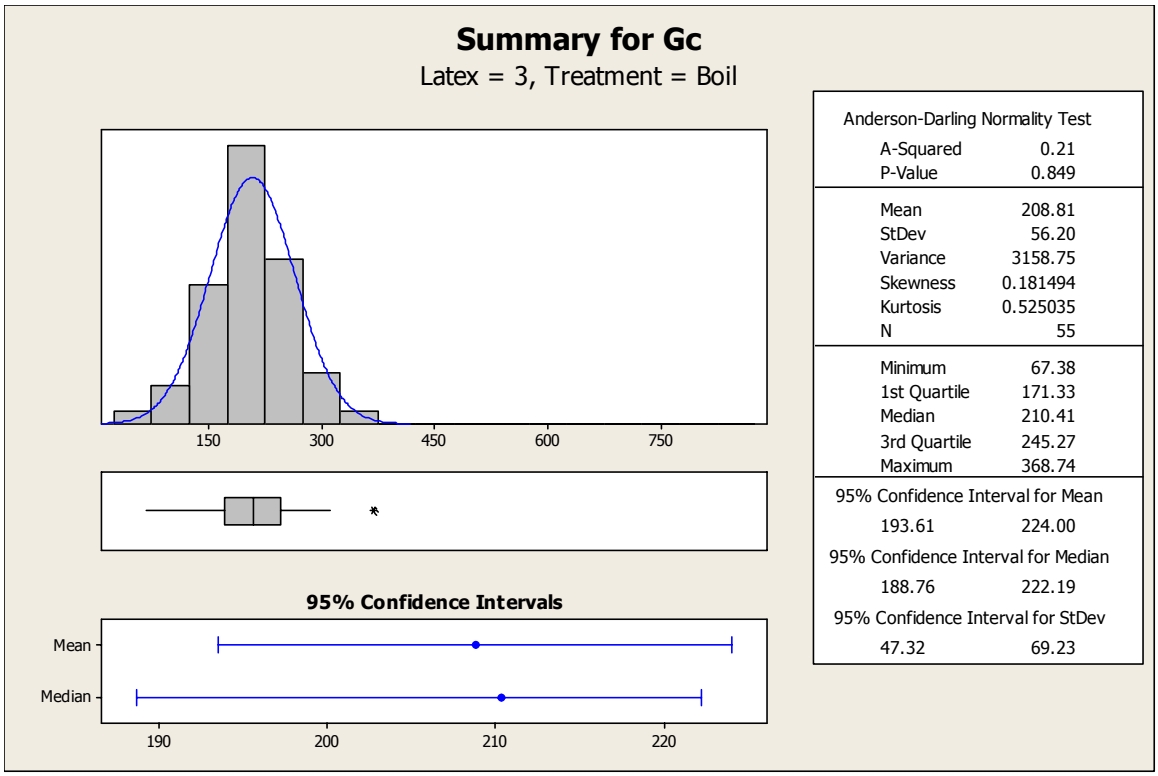
Summary for Gc
Latex = 3, Treatment = Boil
150
300
450
600
750
95% Confidence Intervals
Mean
Median
190
200
210
220
Anderson-Darling Normality Test
A-Squared 0.21
P-Value 0.849
Mean 208.81
StDev 56.20
Variance 3158.75
Skewness 0.181494
Kurtosis 0.525035
N 55
Minimum 67.38
1st Quartile 171.33
Median 210.41
3rd Quartile 245.27
Maximum 368.74
95% Confidence Interval for Mean
193.61 224.00
95% Confidence Interval for Median
188.76 222.19
95% Confidence Interval for StDev
47.32 69.23

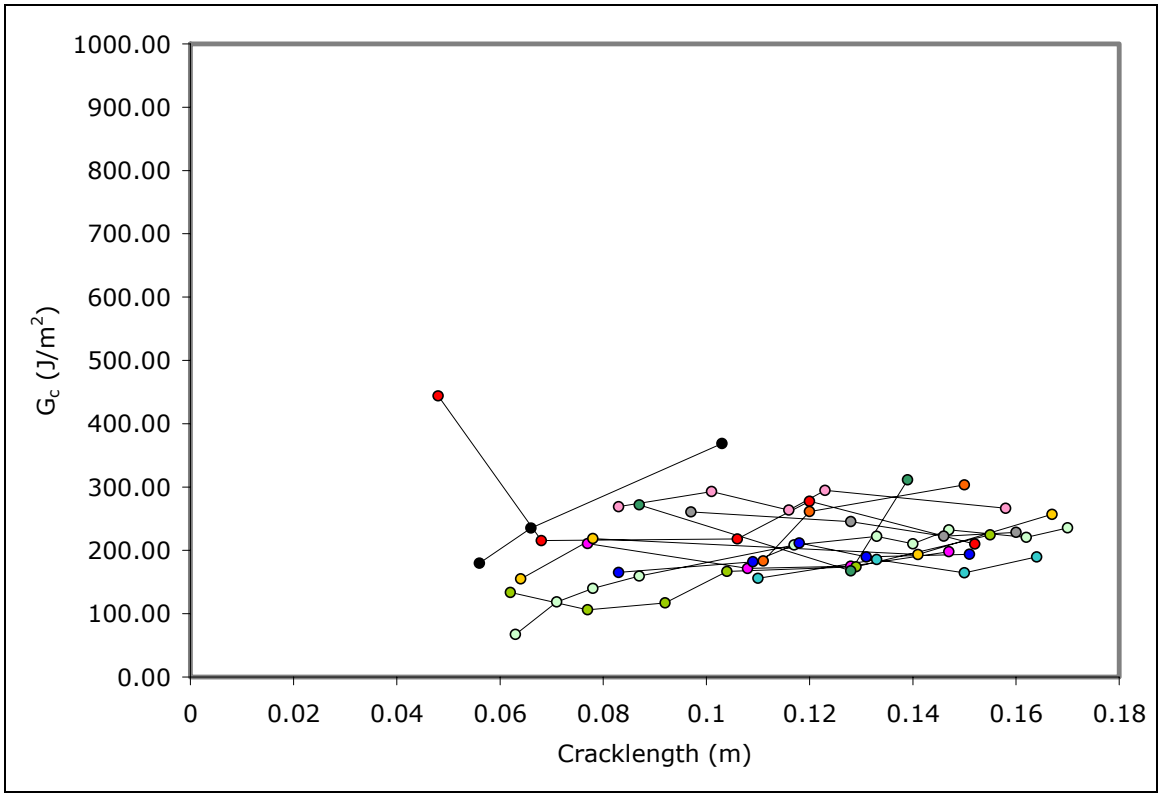
1000.00
900.00
800.00
700.00
600.00
500.00
400.00
300.00
200.00
100.00
0.00
Gc (J/m2)
0
0.02
0.04
0.06
0.08
0.1
0.12
0.14
0.16
0.18
Cracklength (m)

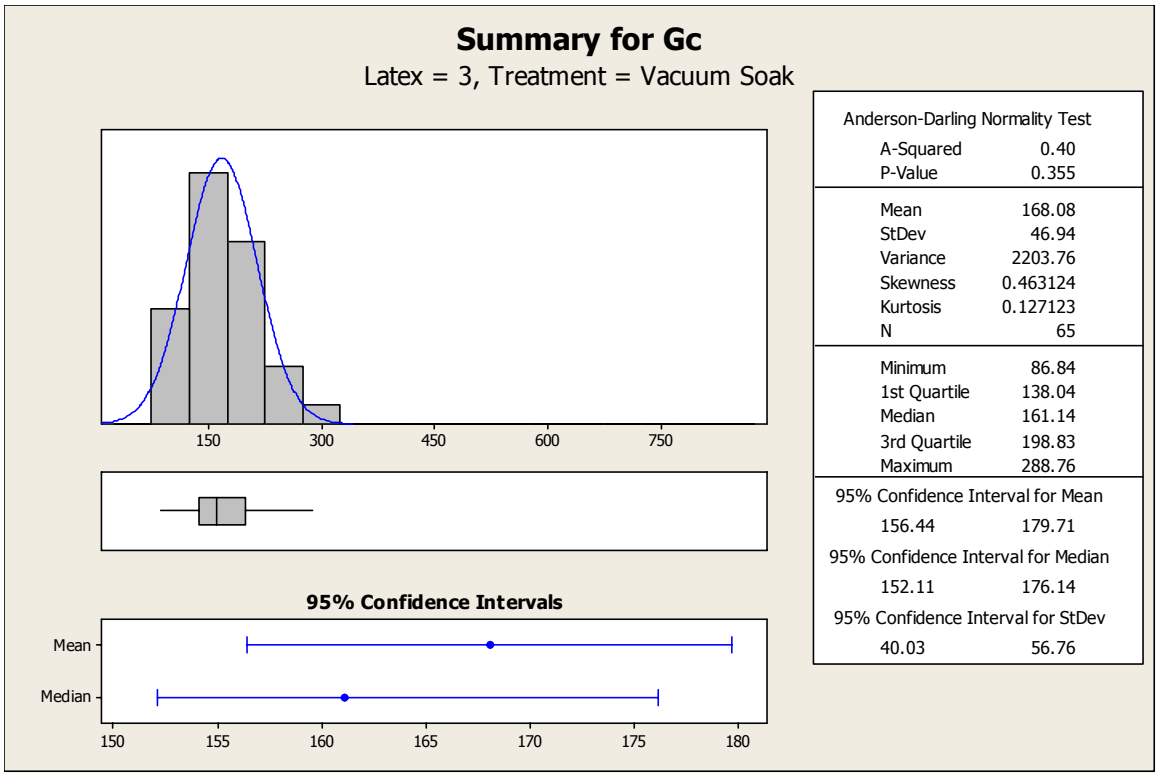
Summary for Gc
Latex = 3, Treatment = Vacuum Soak
150
300
450
600
750
95% Confidence Intervals
Mean
Median
150
155
160
165
170
175
180
Anderson-Darling Normality Test
A-Squared 0.40
P-Value 0.355
Mean 168.08
StDev 46.94
Variance 2203.76
Skewness 0.463124
Kurtosis 0.127123
N 65
Minimum 86.84
1st Quartile 138.04
Median 161.14
3rd Quartile 198.83
Maximum 288.76
95% Confidence Interval for Mean
156.44 179.71
95% Confidence Interval for Median
152.11 176.14
95% Confidence Interval for StDev
40.03 56.76

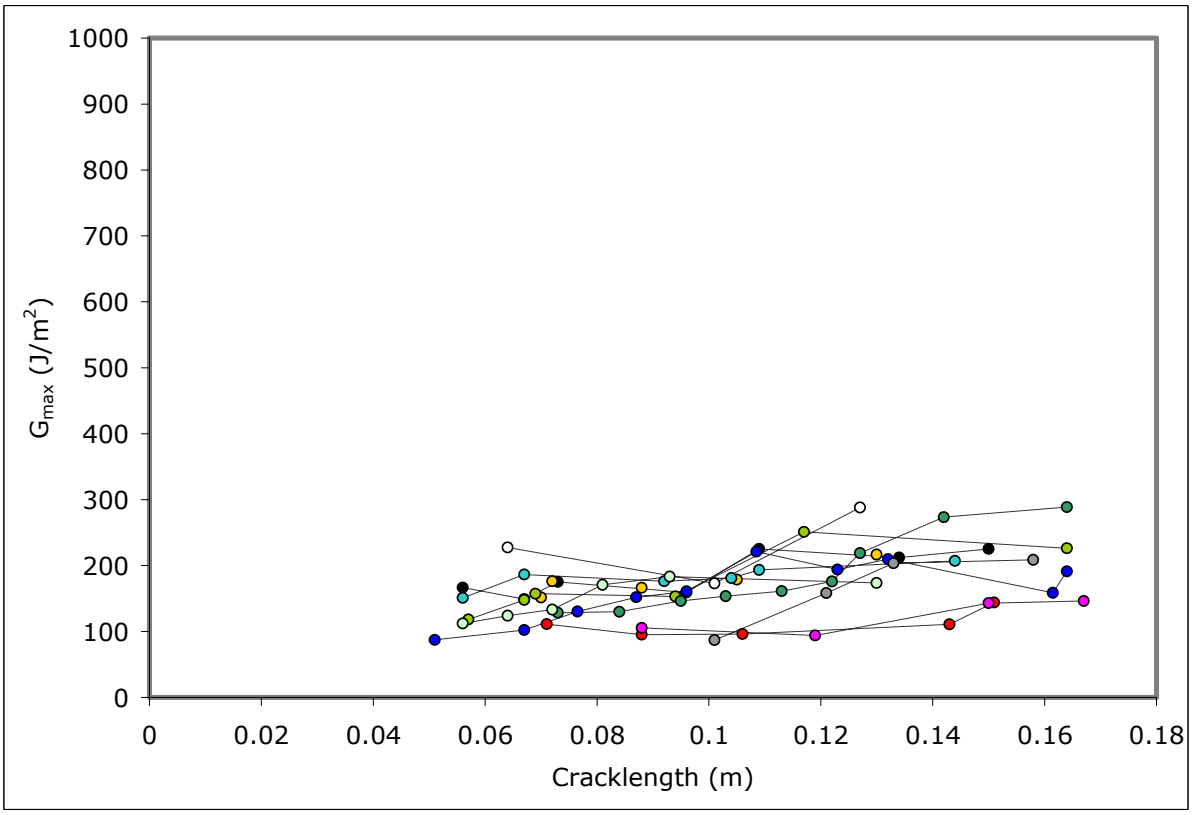
1000
900
800
700
600
500
400
300
200
100
0
G_{max} (J/m^2)
0
0.02
0.04
0.06
0.08
0.1
0.12
0.14
0.16
0.18
Cracklength (m)

Chapter 7: Conclusions

7.1 Summary

A solution NMR approach was successfully utilized to study NMA distribution in poly(vinyl acetate) latex adhesives. Isotopically labeled NMA was synthesized to allow detection of the comonomer. Both ^{15}N-NMA and ^{13}C, ^{15}N-NMA were prepared and copolymerized into three latices. During the copolymerizations the comonomer addition profile was intentionally altered to create three latices with different NMA distributions. The different NMA feed strategies successfully produced latices with different properties. Differences in adhesive viscosity and film morphology were clear. Slight differences in glass transition temperatures of latex films (after exposure to various treatments) were also observed, although it is difficult to say whether they were significant. The goal of achieving different NMA distributions among the three latices was also successfully achieved. Measured NMA distributions correlated with the expected copolymer microstructures, based on the various NMA feed strategies. For example, Latex 3 had a very high proportion of core-NMA (80+%) which was expected since the NMA addition method promoted relative NMA starvation and a more randomized copolymer microstructure. The synthesis methods for Latices 1 and 2, on the other hand, were expected to produce more blocky NMA segments, or even homopolymeric (water-phase) NMA. These hypotheses were also proven true (see results below).

The distinction between surface and water-phase NMA was possible by analyzing washed latices. Two washing methods were utilized: centrifugation and membrane dialysis. The centrifugation treatment changes the nature of the particle surface. It shears away the colloid stabilizer and other surface groups. Dialysis is a less destructive technique, and therefore probably gives a more reliable means of differentiating between surface and water-phase NMA. According to the dialysis results, NMA distribution for the latices was as follows:

Latex 1	63% surface	20% water-phase	17% core
Latex 2	82% surface	7% water-phase	11% core
Latex 3	13% surface	2% water-phase	85% core

Latex 3 was made with ^{13}C, ^{15}N-NMA, which allowed NMA distribution to be measured independently by both carbon and nitrogen NMR spectroscopy. The NMA distributions from the two nuclei were found to be in excellent agreement (based on the dialysis washing method). This indicates that hydrolysis of the ^{13}C-methylol group of NMA was not a factor.

The three latices were also characterized by a series of analytical techniques. Films of the latices were studied by DSC and SEM. The films were exposed to accelerated aging treatments to simulate the fracture mechanics aging exposures. The bulk T_g was relatively insensitive to the aging treatments. SEM showed interesting differences among the latices. Catalysis limited the extent of the film formation process for all latex films. Uncatalyzed adhesives were able to achieve different degrees of film formation. Latex 3 produced a continuous film. Latex 2 retained some particle boundaries, and Latex 1 never formed a continuous film. SEM was also used to evaluate the morphology of the latices when applied to wood. After accelerated aging, Latex 1 samples showed discrete particles, while Latex 2 and 3 samples formed continuous films. The particle size analysis results indicated that Latex 1 had the largest particles with an average diameter of ~9 microns. The average diameter of the particles in Latex 2 was 3.3 microns, while for Latex 3 the average diameter was 2.6 microns. SEM results contradicted the particle size analysis results for Latex 1, indicating that Latex 1 was composed of smaller particles (similar to those of Latex 2 and 3). However, SEM showed extensive agglomeration in Latex 1, and the agglomerates could have biased the particle size analysis result. The rheology work showed that the untreated latices had drastically different viscosities. After dilution, the viscosities were comparable. All of the latices except Latex 2 showed a peak in viscosity with increasing shear rates. This is thought to be due to the formation of aggregates, which are then disrupted at higher shear rates.

The performance of the latex adhesives was evaluated via mode I fracture toughness tests. Samples were exposed to one of three accelerated aging treatments prior to analysis: control, boil, or vacuum soak. All samples were tested in the oven dry state. A series of statistical tests were conducted to identify and exclude poor specimens. Individual G_c values demonstrated a first order autoregressive covariance with loading cycle; that is, within a given specimen, each G_c value is affected by the previous G_c value, and each G_c value influences the subsequent value.

This finding could be due to the location of the crack tip within the wood adhesive interphase. An ANOVA was performed to evaluate differences among the adhesive and accelerated aging treatments. The Tukey-Kramer adjustment allowed pairwise comparisons without inflating Type I error. At the α=0.10 level of significance, the G_c values were relatively insensitive to the adhesive and treatment conditions—except Latex 1. Results indicated that Latex 1 had *enhanced* fracture toughness after exposure to the boil and vacuum soak exposures. SEM micrographs confirmed that Latex 1 films retained their morphologies after the selected exposures, whereas Latex 2 and 3 did not.

Bondline images of the fracture samples were captured under magnification using a fluorescence microscope. All control samples exhibited a relatively uniform bond line thickness. After aging, the Latex 2 and Latex 3 samples show significant stretching of the adhesive between the two substrates. Also, large regions of the samples showed voids. Latex 1 samples maintained bond line integrity after the aging treatments.

It is clear that Latex 1 exhibited a unique resistance to the accelerated aging conditions. This is noted in the fracture results, as well as the bondline images and the SEM micrographs. The mechanism for the behavior *could* be tied to NMA distribution. Latex 1 had the highest proportion of water-phase NMA. Such NMA was likely polymeric. It is possible that the moisture-rich environment during the accelerated aging treatments could have facilitated greater polyNMA penetration into wood, and ultimately even NMA-wood crosslinks. There is no conclusive evidence to prove this hypothesis at this point. The unique morphology of Latex 1 could itself be responsible for the enhanced toughness.

7.2 Limitations

Copolymerization strategies were not repeated to determine the reproducibility of the polymerization method.

The interpretation of the ^{15}N-solution NMR spectra of the latices was subjective. However, it was based on a conservative criterion. Integral values were only accepted if some evidence of a peak appeared in the appropriate chemical shift region.

The distribution of NMA is dependent upon the calculation method that is employed. Ideally, all methods would yield the same results. Here, reactions of NMA at high temperature may be introducing error to the analysis. A calculation method was defined to interpret the distribution of NMA in the latex. The method was based on room temperature and untreated results, since these experimental conditions were deemed to be the most reliable.

Solution NMR results showed an anomaly for the Latex 1 and Latex 2 dialyzed samples. The amount of NMA observed actually decreased from the room temperature experiment to the high temperature experiment. This result was rationalized as being due to crosslinking of NMA units. There is little evidence to support this claim. In the near future a solid state NMR experiment will be conducted on a dialyzed latex sample after it has been exposed to high temperature. The presence of signals in the solid state NMR will confirm the hypothesis.

References

(Excluding Literature Review References)

(1989). Standard Test Method for Strength Properties of Adhesive Bonds in Shear by Compression Loading. American Society for Testing and Materials. **ASTM D905:** 27-30.

(1990). Standard Specification for Adhesives Used in Nonstructural Glued Lumber Products. ASTM. **D3110-90:** 184-192.

(1994). American Society for Testing and Materials. **ASTM D905:** 21-24.

(1995). Standard Specification for Adhesives Used for Finger Joints in Nonstructural Lumber Products. ASTM. **D5572-95:** 459-475.

(1999). Standard Specifications for Adhesives Used for Laminate Joints in Nonstructural Lumber Products. ASTM. **D5751-99:** 503-512.

(1999). Standard Test Method for Fracture Strength in Cleavage of Adhesives in Bonded Metal Joints. ASTM. **D3433-99:** 228-234.

Ahmed, S. M., M. S. El-Aasser, et al. (1980). "Cleaning Latexes for Surface Characterization by Serum Replacement." Journal of Colloid and Interface Science **73**(2): 388-405.

Andreis, M. and J. L. Koenig (1995). "Application of Nitrogen-15 NMR to Polymers." Advances in Polymer Science **124**: 191-237.

Armour, W. B. (1962). N-Methylolacrylamide -Vinyl Acetate Copolymer Emulsions. U.S.A.

Armour, W. B. (1969). Water Resistant Polyvinyl Acetate Adhesive Compositions.

Blackman, B., J. P. Dear, et al. (1991). "The calculation of adhesive fracture energies from double-cantilever beam test specimens." Journal of Materials Science Letters **10**: 253-256.

Bonardi, C., P. H. Christou, et al. (1991). "Acrylic Latexes Functionalized by N-Methylolacrylamide and Crosslinked Films from these Latexes." New Polymeric Materials **2**(4): 295.

Bufkin, B. G. and J. R. Grawe (1978). "Survey of the Applications, Properties, and Technology of Crosslinking Emulsions, Part I." Journal of Coatings Technology **50**(641): 41-55.

Carpenter, E. L. and H. S. Davis (1957). "Acrylamide. Its Preparation and Properties." Journal of Applied Chemistry **7**: 671-6.

Chan, G. Y. N., A. G. Jhingran, et al. (1998). "Approaches to the controlled formation of network polymers. 1. Synthesis and evaluation of monomers with vinyl differentiation." Polymer **39**(23): 5781-87.

Crews, P., J. Rodriguez, et al. (1998). Organic Structure Analysis. New York, Oxford University Press.

Davis, R. (2000). Personal Communication. Blacksburg.

Ebewele, R. O., B. H. River, et al. (1979). "Tapered Double Cantilever Beam Fracture Tests of Phenolic-Wood Adhesive Joints." Wood and Fiber Science **11**(3): 197-213.

Ebewele, R. O., B. H. River, et al. (1980). "Tapered double cantilever beam fracture tests of phenolic-wood adhesive joints. Part II. Effects of surface roughness, the nature of surface roughness, and surface aging on joint fracture energy." Wood and Fiber Science **12**(1): 40-65.

Ebewele, R. O., B. H. River, et al. (1986). "Wood Processing Variables and Adhesive Joint Performance." Journal of Applied Polymer Science **32**: 2979-2988.

Feuer, H. and U. E. Lynch (1953). "The Synthesis and Reactions of Unsaturated N-Methylolamides." Journal of the American Chemical Society **75**: 5027-9.

Gagliano, J. M. (2001). An Improved Method for the Fracture Cleavage Testing of Adhesively-Bonded Wood. Materials Science Engineering. Blacksburg, Virginia Polytechnic Institute and State University**:** 87.

Gagliano, J. M. and C. E. Frazier (2001). "Improvements in the Fracture Cleavage Testing of Adhesively-Bonded Wood." Wood and Fiber Science **3**(3): 377-385.

Goldberg, A. I. and V. Jasinski (1967). N-Methylolacrylamide-Vinyl Acetate Copolymer Emulsions Containing Polyvinyl Alcohol. U.S.A.

Griffifths, D. (2002). Horiba Information. N. Brown. Blacksburg.

Habermann, C. E. (1991). Acrylamide. Encyclopedia of Chemical Technology. New York, John Wiley and Sons. **1:** 251-266.

Hansen, M. and H. J. Jakobsen (1972). "^{13}C-^{15}N Spin-Spin Coupling Constants in [^{15}N]-Aniline from ^{13}C NMR Spectra." Acta Chem. Scand. **26**(5): 2151-2153.

Hashimi, S., A. J. Kinloch, et al. (1990). "The Analysis of Interlaminar Fracture in Uniaxial Fibre-Polymer Composites." Proceedings of the Royal Society of London. Series A, Mathematical and Physical Sciences **427**(1872): 173-199.

Howarth, O. W. (1993). Liquid state NMR studies of polymer dynamics and conformation. NMR Spectroscopy of Polymers. R. N. Ibbett. London, Blackie Academic and Professional**:** 125-160.

Jones, G. D., J. Zomlefer, et al. (1944). "Attempted Preparation of Polyvinylamine." Journal of Organic Chemistry **9**: 500-512.

Lambert, J. B., G. Binsch, et al. (1964). "Nitrogen-15 Magnetic Resonance Spectroscopy, I. Chemical Shifts." Proceedings of the National Academy of Sciences of the United States of America **51**(5): 735-737.

Lauterbur, P. C. (1957). "C13 Nuclear Magnetic Resonance Spectra." Journal of Chemical Physics **26**(1): 217-218.

Le Botlan, D. J., B. G. Mechin, et al. (1983). "Proton and Carbon-13 Nuclear Magnetic Resonance Spectroscopy of Formaldehyde in Water." Analytical Chemistry **55**: 587-91.

Levy, G. C. and R. L. Lichter (1979). Nitrogen-15 Nuclear Magnetic Resonance Spectroscopy. New York, John Wiley and Sons.

Malmberg, M. (2003). Species Dependence of pMDI/Wood Adhesion. Wood Science and Forest Products. Blacksburg, Virginia Polytechnic Institute and State University.

Matejicek, A. and J. Cerny (1986). "Synthesis of N-hydroxymethylacrylamide in an Aqueous Solution." Collection Czechoslovak Chem. Commun. **51**: 1656-64.

Moureau, C. and U. E. Lynch (1893). Bull. Soc. Chim. Fr. **3**(9): 417.

Niyazova, Z. M. and T. G. Kulagina (1972). "Copolymerization of N-alkylolacrylamides with vinyl acetate in a suspension." Sin. Vysokomol. Soedin.: 14-17.

Odian, G. (1991). Principles of Polymerization. New York, John Wiley & Sons.

O'Rourke-Muisener, P. A., J. T. Koberstein, et al. (2003). "Optimal Chain Architectures for the Molecular Design of Functional Polymer Surfaces." Macromolecules **36**(3): 771-781.

Porter, A. W. (1964). "On the Mechanics of Fracture in Wood." Forest Products Journal **14**(8): 325-331.

Schmidt, R. G. (1998). Aspects of Wood Adhesion: Applications of ^{13}C CP/MAS NMR and Fracture Testing. Wood Science and Forest Products. Blacksburg, Virginia Polytechnic Institute and State University**:** 150.

Schmidt, R. G., M.-P. Laborie, et al. (2000). "Lab-Scale Synthesis of Isotopically Labeled Formaldehyde for the Production of Formaldehyde-Based Wood Adhesives." Holzforschung **54**(1): 98.

Sernek, M. (2002). Comparative Analysis of Inactivated Wood Surfaces. Wood Science and Forest Products. Blacksburg, Virginia Polytechnic Institute and State University**:** 193.

Silverstein, R. M., G. C. Bassler, et al. (1974). Spetrometric Identification of Organic Compounds. New York, John Wiley and Sons.

Sotak, C. H., C. L. Dumoulin, et al. (1984). High-Accuracy Quantitative Analysis by 13C Fourier Transform NMR Spectroscopy. Topics in Carbon-13 NMR Spectroscopy. G. C. Levy. New York, John Wiley and Sons. **4:** 91-121.

Traficante, D. D. (1996). Relaxation: An Introduction. Encyclopedia of Nuclear Magnetic Resonance. D. M. Grant and R. K. Harris. Chichester, John Wiley and Sons. **6:** 3988-4003.

Ugelstad, J. and J. de Jonge (1957). "A Kinetical Investigation of the Reaction between Amides and Formaldehyde." Recueil des Travaux Chimiques des Pays-Bas **76**: 919-945.

Warson, H. (1990). "Preparation of Derivatives of Acrylamide." Paint and Resin **60**(3): 26-9.

Werstler, D. D. (1986). "Quantitative 13C n.m.r. characterization of aqueous formaldehyde resins: 2. Resorcinol-formaldehyde resins." Polymer **27**: 757-64.

Wojcik, J., S. Szymanski, et al. (1980). "Conformational Analysis of Some Acrylamide Homologues." Bulletin de l'Academie Polonaise Des Sciences. Serie des sciences chimiques. **28**(9-10): 613-619.

Yasuda, K., K. Okajima, et al. (1988). "Study on alkaline hydrolysis of polyacrylamide by carbon-13 NMR." Polymer Journal (Tokyo) **20**(12): 1101-7.

Zheng, J. (2002). Studies of PF Resole/Isocyanate Hybrid Adhesives. Wood Science and Forest Products. Blacksburg, Virginia Polytechnic Institute and State University**:** 198.

Vita

Nicole was born in Portsmouth, Virginia, in 1975, to parents Paul and Nancy Robitaille. In her childhood, she enjoyed playing sports in the backyard with her three younger brothers, Mike, Joe, and Marc. She attended South Carroll High School and graduated at the top of her class in 1993. After high school she enrolled at Virginia Polytechnic Institute and State University, where she completed her Bachelor of Science degree in Forestry and Wildlife with a minor in Chemistry. During her undergraduate studies, she had the opportunity to join the Center for Adhesive and Sealant Science (CASS). In conjunction with CASS she participated in the 1,2-Think Glue program, which allowed her to work on an undergraduate research project and to intern with the industrial sponsor—National Starch and Chemical Company—in Bridgewater, New Jersey. After completing her B.S. in 1997, Nicole decided to pursue a Ph.D. in the area of wood adhesion with Dr. Charles E. "Chip" Frazier. It was during this time that she met and married Stephen Brown. Her doctoral studies finally concluded in 2003. She is currently employed as an Assistant Professor of Wood Chemistry at the Pennsylvania State University.